Gesellschaft für Anlagen- und Reaktorsicherheit (GRS) mbH

Reactor Safety Issues Resolved by the 2D/3D Program

GRS - 101

Gesellschaft für Anlagen- und Reaktorsicherheit (GRS) mbH

Reactor Safety Issues Resolved by the 2D/3D Program

Prepared jointly by:
Japan Atomic Energy Research Institute,
Gesellschaft für Anlagen- und Reaktorsicherheit (GRS) mbH,
Siemens AG, UB KWU,
U.S. Nuclear Regulatory Commission,
Los Alamos National Laboratory,
MPR Associates, Inc.

Edited by
Paul S. Damerell and
John W. Simons,
MPR Associates, Inc.

September 1993

GRS - 101
ISBN 3-923875-51-7

NOTICE:

This Report was prepared as an account of work prepared in the international 2D/3D Program which was jointly conducted by the German Federal Minister for Research and Technology (BMFT), the Japan Atomic Energy Research Institute (JAERI) and the United States Nuclear Regulatory Commission (USNRC). The Responsibility for the content of this report rests with the authors.

The Authors make no warranty or assume any legal liability for the correctness, completeness or applicability of information compiled in this report.

Keywords

DWR, internationale Zusammenarbeit, Reaktorsicherheitsforschung, Thermohydraulik, Versuchsprogramm

ABSTRACT

The 2D/3D Program studied multidimensional thermal-hydraulics in a PWR core and primary system during the end-of-blowdown and post-blowdown phases of a large-break LOCA (LBLOCA), and during selected small-break LOCA (SBLOCA) transients. The program included tests at the Cylindrical Core Test Facility (CCTF), the Slab Core Test Facility (SCTF), and the Upper Plenum Test Facility (UPTF), and computer analyses using TRAC. Tests at CCTF investigated core thermal-hydraulics and overall system behavior while tests at SCTF concentrated on multidimensional core thermal-hydraulics. The UPTF tests investigated two-phase flow behavior in the downcomer, upper plenum, tie plate region, and primary loops. TRAC analyses evaluated thermal-hydraulic behavior throughout the primary system in tests as well as in PWRs. This report summarizes the test and analysis results in each of the main areas where improved information was obtained in the 2D/3D Program. The discussion is organized in terms of the reactor safety issues investigated.

ZUSAMMENFASSUNG

Das 2D/3D-Programm wurde von Deutschland, Japan und den Vereinigten Staaten von Amerika durchgeführt, um die Thermohydraulik von Kühlmittelverluststörfällen mit großen Brüchen der druckführenden Umschließung von Druckwasserreaktoren zu erforschen. Es wurde eine Durchführungsform gewählt, in der jedes Land einen beträchtlichen Beitrag zum Gesamtprogramm leistete und alle drei Länder gleichermaßen teil hatten an den erzielten Ergebnissen. Deutschland baute und betrieb die Großversuchsanlage **U**pper **P**lenum **T**est **F**acility (UPTF), während Japan Bau und Betrieb der Versuchsanlagen **C**ylindrical **C**ore **T**est **F**acility (CCTF) und **S**lab **C**ore **T**est **F**acility (SCTF) beitrug. Der Beitrag der USA bestand aus der Bereitstellung fortschrittlicher Instumentierung für die drei Versuchsanlagen sowie aus der Überprüfung des Rechenprogramms TRAC anhand der Versuchsergebnisse. Versuchsauswertungen wurden in allen drei Ländern durchgeführt. Der vorliegende Bericht faßt das 2D/3D-Programm zusammen, in dem die beigesteuerten Leistungen der drei beteiligten Länder beschrieben werden.

TABLE OF CONTENTS

TABLE OF CONTENTS (Cont'd)

TABLE OF CONTENTS (Cont'd)

LIST OF FIGURES

LIST OF TABLES

EXECUTIVE SUMMARY

Thermal-hydraulic behavior in a PWR during a loss-of-coolant accident (LOCA) has been investigated for over 20 years. The 2D/3D Program was a combined experimental and analytical research program on PWR end-of-blowdown and post-blowdown phenomena conducted by the countries of Germany, Japan, and the United States. The program utilized a "contributory" approach in which each country contributed significant effort to the program and all three countries shared the research results. Germany constructed and operated the Upper Plenum Test Facility (UPTF), and Japan constructed and operated the Cylindrical Core Test Facility (CCTF) and the Slab Core Test Facility (SCTF). The US contribution consisted of provision of advanced instrumentation to each of the three test facilities, and assessment of the Transient Reactor Analysis Code (TRAC). Evaluations of the test results were carried out in all three countries. The total cost of the program was approximately $500,000,000 (US).

The objective of the 2D/3D Program was to study the multidimensional thermal-hydraulic behavior in a heated core and throughout the primary system during the end-of-blowdown, refill and reflood phases of a large-break LOCA (LBLOCA), and selected small-break LOCA (SBLOCA) transients. Tests at CCTF investigated core thermal-hydraulics and overall system behavior while tests at SCTF concentrated on multidimensional core thermal-hydraulics. The UPTF tests investigated two-phase flow behavior in the downcomer, upper plenum, tie plate region, and loops of the primary system. TRAC analyses evaluated thermal-hydraulic behavior throughout the primary system in the tests as well as in PWRs. The tests and analyses covered the following emergency core cooling systems (ECCS): cold leg injection, combined injection, upper plenum injection, and downcomer injection (with and without vent valves).

The experimental and analytical results of the 2D/3D Program resolved nine reactor safety issues which were addressed in the program.

- ECC Delivery to Lower Plenum during Depressurization. Delivery of ECC injected in the cold legs and downcomer initiates during blowdown and is multidimensional. Specifically ECC injected in the loops or nozzle adjacent to the broken cold leg is almost completely bypassed, while ECC injected away from the break mostly penetrates to the lower plenum. For each ECCS considered, the lower plenum is filled to the bottom of the core barrel prior to the completion of depressurization. This result means that a potential core heatup of 100 K during refill is eliminated.

- Entrainment in Downcomer during Reflood. With cold leg ECC injection or downcomer ECC injection with vent valves, the downcomer water level during late reflood is reduced up to 1 m below the cold leg elevation by the combination of wall boiling and water entrainment in the downcomer steam flow. The increase in the reflood peak clad temperature (PCT) due to the reduction in downcomer driving head is estimated to be 15 K.

- Steam/ECC Interactions in Loops. With cold leg or hot leg ECC injection, stratified flow always occurs when the condensation potential of the ECC is less than the steam flow. Plug flow occurs only when the condensation potential of the ECC exceeds the steam flow. Regardless of flow regime, a substantial amount of steam is condensed in the loops, and almost all ECC is delivered to the reactor vessel.

- Effect of Accumulator Nitrogen. The discharge of nitrogen from accumulators connected to the cold legs or downcomer causes a sudden high flow of nitrogen into the primary system which pressurizes the top of the downcomer causing a surge of water into the core. Although core heat transfer was not covered in the 2D/3D tests, TRAC analyses predict the hottest parts of the core are quenched by the surge in core water level.

- Thermal Mixing of ECC and Primary Coolant. For ECC injection into the cold legs while the loops are stagnated, ECC entering the downcomer is significantly warmed by mixing in the cold leg and the resultant plume of cooler water in the downcomer decays quickly. These results suggest that ECC injection into water-filled cold legs does not cause severe local changes in fluid temperature at the vessel wall which could lead to pressurized thermal shock.

- Core Thermal-hydraulic Behavior. Core cooling is adequate for the ECCS types investigated. Behavior in the core during reflood is influenced by two-phase and multidimensional flow phenomena.

  -- In the bottom flooding case, water is quickly carried to the upper regions of the core with the steam flow. This two-phase flow establishes good core cooling above the quench front. Also, the lateral water distribution is nearly uniform due to efficient lateral redistribution.

-- With top injection (i.e., hot leg or upper plenum injection), water flows down through the core in local regions while a two-phase steam/water mixture flows up to the upper plenum in the remainder of the core. Core cooling is enhanced in the water downflow regions relative to the two-phase upflow (i.e., bottom flooding) region. Note that, since water downflow to the core initiates during end-of-blowdown/refill, core cooling in the downflow regions actually initiates prior to reflood.

- Water Delivery and Distribution in the Upper Plenum. For hot leg or upper plenum injection, downflow of ECC from the upper plenum to the core occurs in local regions below the injection locations, and is not limited by countercurrent flow at the tie plate. Also, most of the steam upflow from the core is condensed in the upper plenum or hot legs, and returned to the core with the water downflow.

- Water Carryover and Steam Binding with Cold Leg Injection. With cold leg ECC injection, water carryover to the steam generator tube regions is delayed about 20 to 30 seconds by de-entrainment and accumulation in the upper plenum, hot legs, and steam generator inlet plena. It is estimated that de-entrainment upstream of the tube regions reduces the reflood PCT by about 180 K relative to the situation where no de-entrainment occurs.

- Hot Leg Countercurrent Flow. Uninhibited water runback in the hot legs is expected for reflux-condenser conditions of an SBLOCA.

Tests and analyses from the 2D/3D Program have allowed a relatively complete understanding of ECCS performance during the end-of-blowdown, refill, and reflood phases of an LBLOCA to be developed. The adequacy of existing systems has been confirmed, and the margin associated with traditional, conservative evaluation approaches has been quantified.

DEDICATION/FOREWORD

In the mid-seventies experiments and analytical evaluations revealed that multidimensional thermal-hydraulic phenomena could have significant impact on loss-of-coolant accident (LOCA) transients in PWRs. But even the largest test facilities in operation at that time (e.g., LOFT, LOBI, or PKL) were scaled down geometrically by two or three orders of magnitude. Therefore these facilities could not resolve the issues associated with multidimensional effects on emergency core cooling.

In addition, safety evaluations in the framework of licensing procedures for nuclear power plants employed conservative assumptions and calculational models to envelope the key parameters of principal safety significance. But in the late seventies the need for best-estimate evaluation of core damage to be expected during a LOCA was recognized. Such analyses were needed for risk assessment studies.

To meet these needs, comprehensive thermal-hydraulic investigations in a single, full-scale test facility were evaluated, but this approach was found to be too expensive and technically impractical. In searching for more practical solutions, the authors and other scientists engaged in reactor safety research in Germany, Japan and the US, developed a vision to resolve this problem by combining and adjusting the reactor safety research programs conducted in the three respective countries. They proposed to couple the Japanese 1/20-scale heated core experimental programs CCTF and SCTF, with the German full-scale Upper Plenum Test Facility. The Japanese heated-core facilities would concentrate on one-dimensional and two-dimensional effects while the UPTF would test full-scale multidimensional effects using a core simulator. Each of the facilities would be outfitted with advanced instrumentation for evaluating local two-phase flow phenomena. The connecting link would be the multidimensional computer code TRAC. Both TRAC and the instrumentation were to be developed and supplied by the US. The authors proposed this approach to government representatives who were responsible for reactor safety research in their respective countries. The governments eventually approved the proposed approach and the trilateral 2D/3D Program was brought to reality.

The 2D/3D Program lasted about 15 years and cost approximately $500 million (US) in total. It is the largest research program ever conducted in the field of reactor safety. Today, the excellent results justify the time and funds expended upon this extraordinary program. All major questions which arose concerning the influence multidimensional thermal-hydraulic effects may have on emergency core cooling processes during design basis accidents have been answered. The technical results and the experience gained by the 2D/3D Program enable us today to close the issues about design basis accidents and concentrate in the future on issues arising from beyond design basis events and accident management. Work on these issues will further improve the safety of nuclear energy production.

F. Mayinger L. S. Tong M. Nozawa

ACKNOWLEDGEMENTS

This report summarizes the efforts of countless engineers, scientists, technicians, and support personnel in each of the three participating countries. The Project Leaders would like to thank each of these individuals for their contribution to the overall success of the 2D/3D Program.

"Reactor Safety Issues Resolved by the 2D/3D Program" was prepared jointly by personnel from the three participating countries. Specific people who have contributed in the preparation and review of this report are summarized below by organization.

GRS	Siemens	TUM	JAERI
R. Zipper	P. Weiss	F. Mayinger	Y. Murao
K. Liesch	F. Depisch		T. Iguchi
B. Riegel	R. Emmerling		H. Akimoto
I. Vojtek	J. Liebert		T. Iwamura
			T. Okubo
			A. Ohnuki
			Y. Abe

USNRC	INEL	LANL	MPR
G. Rhee	S. Naff	D. Siebe	P. Damerell
L. Shotkin			J. Simons
			K. Cardany
			E. Claude
			A. Russell
			M. Smith
			R. Vollmer
			K. Wolfe

The editors would like to thank Ms. C. M. Christakos of MPR for her assistance in preparing this report.

Section 1

INTRODUCTION

1.1 BACKGROUND

Historical Perspective

The thermal-hydraulic response of a PWR primary coolant system to a Loss-of-Coolant Accident (LOCA) and the performance of the Emergency Core Cooling System (ECCS) have been areas of research interest for two decades. The primary objective of LOCA/ECCS research has been to improve the understanding and modeling of the phenomena so that safety margins can be better quantified and more realistic evaluation approaches can be utilized. Initially, the focus of the research was the depressurization (blowdown) transient. Later the focus shifted to include the post-blowdown phases (refill and reflood).

The 2D/3D Program was the major program on PWR end-of-blowdown and post-blowdown phenomena for the countries of Germany, Japan, and the United States. The formal program name is "The International Program on the Thermal-Hydraulic Behavior of ECC during the Refill and Reflood Phases of a LOCA in a PWR". The common name became "2D/3D Program" because refill/reflood phenomena are strongly influenced by multidimensional (2D and 3D) effects.

Participants in 2D/3D Program

The participants in the 2D/3D Program were the governments of the Federal Republic of Germany (FRG), Japan, and the United States of America (US) as represented by the following agencies:

- The Federal Ministry for Research and Technology (BMFT) in FRG.
- The Japan Atomic Energy Research Institute (JAERI) in Japan.
- The US Nuclear Regulatory Commission (USNRC) in the US.

The 2D/3D Program used a "contributory" approach. Each of the three participants contributed significant effort to the program and all three countries shared the research results. There was no exchange of funds between the participants. This approach fostered technical cooperation among the three countries.

Scope of 2D/3D Program

In general terms, the scope of the 2D/3D Program was PWR LOCA post-blowdown phenomena. Sections 1.2 and 1.3 present a more detailed discussion of the specific objectives and approach of the program. The major facilities in the 2D/3D Program constituted some of the largest and most sophisticated thermal-hydraulic facilities ever employed. This is reflected in the combined financial commitment of the three participants which exceeded the equivalent of US $500,000,000.

Purpose and Scope of this Report

This report presents a summary of the 2D/3D Program in terms of the reactor safety issues investigated. The major issues are discussed individually and the findings, conclusions, and resolutions based on all of the relevant tests and analyses are presented. This report is a companion to another report entitled "2D/3D Program Work Summary Report," which summarizes the principal test and analysis results of the program in terms of the contributing efforts of the participants.

Availability of Results from 2D/3D Program

Numerous reports document the detailed results from the 2D/3D Program; many are cited in this report. Most of these reports have a restricted availability per the 2D/3D Program International Agreement. The detailed reports have been made available to users in the three host countries for the purposes of improving reactor safety.

1.2 OBJECTIVES of 2D/3D PROGRAM

As previously discussed, the overall objective of the 2D/3D Program was to study the post-blowdown phases of a PWR LOCA, and to provide improved experimental data and analysis tools for this transient. The detailed objectives of the 2D/3D Program are summarized below.

1. Study the effectiveness of ECC systems (including cold leg injection, combined injection, upper plenum injection, and downcomer injection) during the end-of-blowdown and refill phases of a large, cold leg break LOCA by evaluating:

- Penetration of ECC to the lower plenum during high flows that exist at end-of-blowdown.
- Condensation of steam by ECC.
- Liquid storage in cold legs, downcomer, upper plenum, and hot legs.
- The liquid flow pattern through the core (for hot leg and upper plenum injection) and resultant core cooling.

2. Study the effectiveness of several types of ECC systems during the reflood phase of a large break LOCA by evaluating:
   - Entrainment, storage, and transport of liquid water in the upper core, upper plenum, hot legs, and steam generators.
   - Vaporization of entrained water in steam generators.
   - Steam condensation by ECC near injection points.
   - Steam/ECC interaction and flow patterns, particularly in regions between the ECC injectors and the core.
   - ECC flow rate to the core.
   - Convective flow patterns and heat transfer in the core.
   - Downcomer driving head and loop pressure drop.
3. Study selected phenomena from other transients; e.g., hot leg steam/water countercurrent flow during a small break LOCA (SBLOCA), fluid/fluid mixing during a pressurized thermal shock event, and high pressure ECC injection into the hot legs during an SBLOCA in which the core uncovers.

1.3 OVERVIEW OF 2D/3D PROGRAM

The objectives of the 2D/3D Program were addressed using a combined experimental/analytical approach. Three major facilities were designed, fabricated, and operated within the 2D/3D Program.

- Cylindrical Core Test Facility (CCTF) in Japan
- Slab Core Test Facility (SCTF) in Japan
- Upper Plenum Test Facility (UPTF) in FRG

The design of each facility involved input from all three countries. Advanced instruments were designed and fabricated by the US for use in all three facilities.

Evaluations of the experimental data were carried out in all three countries. A major analysis program involving the assessment and use of a best-estimate computer code was carried out in the US. The computer code is the Transient Reactor Analysis Code (TRAC).

1.4 ORGANIZATION OF REPORT

The main body of this report is in Sections 3 and 4. Section 3 covers PWR LOCA behavior based on the results of the 2D/3D Program. Several types of PWR ECCS configurations are covered individually in Section 3. Section 4 covers the reactor safety issues individually. For each issue, the phenomena and their importance are defined, the tests and analyses related to the issue are identified, and the conclusions and applications to PWRs are discussed.

Section 2

SUMMARY AND SAFETY IMPLICATIONS

As discussed in Section 1, the objectives of the 2D/3D Program were to study thermal-hydraulic phenomena occurring during the end-of-blowdown, refill, and reflood phases of a large break LOCA and selected other transients. In Section 4 of this report, the program results are discussed in the form of nine separate "issues". An "issue" refers to a set of phenomena occurring in a specific location or region during a specific time frame. A summary of key program results and their implications for safety is discussed below for each of the nine issues. Within each issue, the types of ECC injection affected by the issue are identified.

2.1 ECC DELIVERY TO LOWER PLENUM DURING DEPRESSURIZATION

A key issue with regard to core cooling during a large, cold leg break LOCA is the extent to which ECC can be delivered to, and accumulated in, the lower plenum during the end-of-blowdown (ECC bypass issue). In large-scale tests in the 2D/3D Program (UPTF), multidimensional behavior was observed in the downcomer which strongly affected ECC delivery. Specifically, ECC injected into the cold leg adjacent to the broken cold leg is almost completely bypassed during end-of-blowdown. ECC injected to cold legs away from the broken cold leg has a greater tendency to be delivered, and complete delivery of this water occurs prior to the completion of blowdown.

For ECC injected into the downcomer with vent valves between the upper plenum and downcomer, the ECC delivery behavior was similar to that described above for cold leg injection. However, this was the result of two offsetting phenomena. First, downcomer ECC injection tended to promote bypass, apparently due to ECC being more finely distributed in the upper region of the downcomer because of high velocity injection jets. Separate effects tests with downcomer injection but without vent valves confirmed strong bypass throughout end-of-blowdown, although it appears nozzle configuration details may significantly influence the results. When the vent valves were unlocked, significant delivery of water from the nozzle away from the break was observed because the flow through the vent valves changed the flow rate and flow pattern in the downcomer.

For combined ECC injection, ECC injected in the hot leg passes through the core to the lower plenum. During the end-of-blowdown, lower plenum refill is initiated by hot leg ECC. Shortly thereafter, the ECC injected to the cold legs away from the break

is delivered to the lower plenum, but the ECC injected to the cold leg adjacent to the break continues to be almost completely bypassed.

For all three ECC injection modes, refill of the lower plenum up to the lower edge of the core barrel occurred by end-of-blowdown. This result significantly shortens the portion of the refill phase where core cooling is very low and significant core heat up could occur. Past safety analyses usually assumed that ECC injected prior to conclusion of blowdown is totally lost. The large-scale test results from the 2D/3D Program have demonstrated this assumption to be conservative.

2.2 ENTRAINMENT IN DOWNCOMER DURING REFLOOD

During reflood, steam flows via the intact loops to the downcomer and out the broken cold leg. Water entrainment from the downcomer can occur in the steam flow out the break. Further, steam generation on hot downcomer walls can create voiding in the downcomer. The combination of downcomer wall boiling and entrainment can reduce the downcomer collapsed water level which affects the driving head for core flooding.

These phenomena were observed and studied in small- and large-scale tests in the 2D/3D Program. One important observation, supported by analysis, is that for full-height facilities where the vertical flow area in the downcomer is scaled by the scale factor, water entrainment in the steam flow and attendant level reduction increased with scale. This is due to increases in the steam velocity in the downcomer and at the broken cold leg nozzle at large-scale.

For US/J PWRs cold leg injection, the downcomer behavior is affected by the interaction of steam and ECC in the cold legs. During accumulator injection, all of the intact loop steam flow is condensed. Consequently, there is no steam flow out the broken cold leg and entrainment does not occur. Further, subcooled water is delivered to the downcomer and boiling on the downcomer walls is suppressed. As a result, the downcomer fills to the cold leg (i.e., spillover) elevation. During LPCI, the intact loop steam flow is partially condensed and the ECC delivered to the downcomer is essentially saturated. The uncondensed steam entrains water from the downcomer out the break. As the saturated water gradually replaces subcooled water in the downcomer, wall boiling begins to create voiding in the downcomer. These two effects are calculated to reduce the downcomer level by up to 1.0 m during reflood.

For downcomer injection with vent valves, the overall behavior is similar to cold leg injection although there are some phenomenological differences. ECC injected in the downcomer nozzle nearest the broken cold leg was almost fully swept out the break during LPCI, but ECC injected to the other nozzle was delivered to the downcomer with minimal entrainment when the vent valves were open. With the vent valves closed entrainment increased and the observed level reduction was more severe than for cold

leg injection, although the phenomena in this case appear to be strongly related to nozzle configuration details (e.g., elevation and azimuthal spacing relative to cold legs).

GPWRs with combined injection are not affected by downcomer entrainment during reflood since most of the steam generated in the core is condensed by subcooled ECC injected to the hot legs. Any remaining intact loop steam flow is completely condensed by ECC injected in the cold legs, and there is no steam flow out the broken cold leg to entrain water.

Downcomer entrainment and wall boiling lead to a downcomer level reduction during reflood for PWRs with cold leg or downcomer injection. The assumption usually made in past safety analyses that the downcomer is full to the spillover level is appropriate for combined injection plants and slightly nonconservative for cold leg and downcomer injection plants. The extent of nonconservatism is estimated to be about 15 K in clad temperature for typical PWR conditions.

2.3 STEAM/ECC INTERACTIONS IN LOOPS

Interaction of steam and ECC in the loops affects ECC delivery to the reactor pressure vessel. These phenomena were investigated by several integral and separate effects tests in the 2D/3D Program. A variety of flow regimes were observed, depending primarily on steam flow, ECC flow, and ECC subcooling. A key correlation parameter proved to be the thermodynamic ratio (R_T) which is the ratio of steam condensation potential to steam flow. Three basic flow regimes were identified, as follows:

- stratified flow
- stable plug flow
- unstable plug flow

Regardless of scale, stratified flow was always observed for $R_T < 1$; i.e., the condensation potential of the ECC was less than the steam flow. In these cases saturated (or nearly saturated) water flows at the bottom of the pipe while steam flows at the top of the pipe. Note that the loop steam flow and ECC injection are cocurrent in the cold leg and countercurrent in the hot leg. Plug flow only occurred for $R_T > 1$; i.e., the loop steam flow is less than that needed to heat the ECC flow to saturation temperature. The transition from stratified to plug flow in the cold legs was only slightly dependent on scale and injection configuration. Analyses indicated stable plug flow was established when the momentum of the loop steam flow exceeded the hydrostatic force at the plug end, which is dependent on pipe diameter. Otherwise unstable plug flow occurs; i.e., plugs form and decay periodically. Plug formation can occur rapidly and produce strong condensation events.

For all flow regimes, a substantial amount of steam is consumed by condensation. In general, condensation tends to be near the maximum possible amount; either the ECC is heated to saturation or the entire steam flow is condensed. ECC delivery to the reactor vessel fluctuates during plug flow and either fluctuates or occurs steadily during stratified flow. Regardless of the flow regime, ECC is completely delivered to the pressure vessel.

2.4 EFFECT OF ACCUMULATOR NITROGEN

In some PWRs nitrogen would be discharged into the primary coolant system after the accumulator water has been delivered. This occurs for US/J PWR designs whereas in GPWRs the accumulators are designed not to empty completely.

When nitrogen enters the cold legs and downcomer, condensation is almost totally suppressed and the downcomer is pressurized by the high flow of noncondensible gas. This causes a surge of water into the core which has a beneficial effect on core cooling. During this in-surge, the downcomer water level is decreased and ECC is swept out the broken cold leg by nitrogen flow. The surge of water into the core resulted in increased steam generation in the core and water carryover to the upper plenum. Increased steam generation and the reduced downcomer water head subsequently lead to a water out-surge to the downcomer, which removes the beneficial core cooling effect. Hence, the effect is temporary. Tests in the 2D/3D Program confirmed the phenomena discussed above. Due to limitations of test facilities used in the program, quantification of the effect of accumulator nitrogen discharge on core temperatures was not covered.

2.5 THERMAL MIXING OF ECC AND PRIMARY COOLANT

During some transients or small break LOCAs, ECC is injected at high pressure (HPCI) into the primary system. If subcooled ECC is injected into water-filled cold legs while the loops are stagnated, the extent to which cold water could potentially cause local cooldown of the primary vessel wall is an important issue (Pressurized Thermal Shock Issue).

Prior to the 2D/3D Program, analyses and small-scale tests showed effective thermal mixing of cold ECC and primary coolant would occur at the injection location and in the downcomer, thus mitigating temperature reductions at the vessel wall. In UPTF tests, mixing of subcooled ECC and primary coolant occurred at the injection location. Thermal stratification developed in the cold leg. Cold water flowed at the bottom of the cold leg towards the downcomer while warm water flowed at the top of the pipe from the downcomer to the injection location where it mixed with the ECC. The temperature of the subcooled water stream at the bottom of the cold leg was significantly higher than that of the ECC.

Another mixing process occurred at the cold leg-to-downcomer junction. Due to this additional mixing, the subcooling rapidly decayed in a plume in the downcomer. Overall mixing of ECC and primary coolant was found to be very effective so that cold ECC does not appear to cause severe local changes of fluid temperature at the vessel wall which could lead to pressurized thermal shock.

2.6 CORE THERMAL-HYDRAULIC BEHAVIOR

Core thermal-hydraulic behavior determines the fuel rod temperature history during an LBLOCA and is sensitive to the boundary conditions at the core created by ECC system effectiveness and overall system response. The core behavior during reflood was studied extensively in the 2D/3D Program in tests at CCTF and SCTF while core behavior during end-of-blowdown was investigated in previous tests outside the 2D/3D Program.

During end-of-blowdown, a two-phase mixture flows through the core providing core cooling. In addition, in PWRs with combined hot and cold leg ECC injection, hot leg injected ECC is delivered to the core in local regions below the hot legs. Portions of the core in these downflow regions are expected to be quenched prior to the completion of blowdown.

In the brief period after blowdown and before the lower plenum refills to the bottom of the core, the core heats up almost adiabatically in plants with cold leg or downcomer injection. In combined injection and upper plenum injection plants, ECC water is delivered to the core during this period. The majority of this water flows down through the core in areas located below the injectors, providing local core cooling.

When the water level increases to the bottom of the core, reflood begins and extensive steam generation initiates. Some of the bottom flood water is entrained by steam flow, and two-phase flow is quickly established over the entire core. This process re-establishes core cooling at all axial locations. The principal quench front on the rods advances steadily up the core. In cold leg or downcomer injection systems, ECC flows down the downcomer and enters the core from the bottom. For ECC injected in hot legs or the upper plenum, water flows down the core in local regions and contributes to the global core reflood process described above. In these local regions, cooling is enhanced and the fuel rods are quenched sooner than those in the non-downflow region. In fact, for hot leg injection, most fuel rods in the water downflow regions are quenched prior to reflood.

2.7 WATER DELIVERY AND DISTRIBUTION IN THE UPPER PLENUM

Some PWRs inject ECC directly to the upper plenum. Also, PWRs with combined injection inject ECC into the hot and cold legs simultaneously. In these cases, the ECC delivery to, and distribution in, the upper plenum create specific boundary

conditions for core cooling. In the end-of-blowdown and refill phases, the ECC injected into the upper plenum or hot legs is delivered to the upper plenum and flows down through the core in local areas adjacent to the injectors. Steam condensation by subcooled ECC supports rapid depressurization of the primary system.

During reflood, steam and entrained water are flowing from the core to the upper plenum and toward the hot legs. Water delivery and distribution in the upper plenum are strongly affected by interaction between steam and subcooled ECC. With upper plenum injection, extensive condensation occurs in the upper plenum which reduces steam flow to the hot legs and adds to the water available for downflow to the core. Under typical conditions, the ECC flow condenses about 70% of the steam flow. About 90% of the available water flows to the core in a local region below the injector; the water downflow is only slightly subcooled. With combined injection, condensation in the hot legs near the ECC injectors creates subcooled ECC plugs which are intermittently delivered to the upper plenum. Although extensive condensation occurs in the upper plenum, water flows to the core in local regions with substantial subcooling. Steam generated in the core is almost entirely consumed by condensation in the core, upper plenum, and hot legs. Nearly all of the available water is delivered to the core.

For both upper plenum injection and combined injection, liquid accumulation in the upper plenum was not extensive at large-scale (UPTF). Specifically, upper plenum liquid fractions were about 10%. This result is in contrast with small-scale tests (e.g., CCTF and SCTF) which showed significant upper plenum accumulation. Finally, at large-scale the liquid distribution was observed to be two-dimensional; i.e., higher liquid accumulation above ECC downflow regions.

2.8 WATER CARRYOVER AND STEAM BINDING WITH COLD LEG INJECTION

During reflood, steam generated in the core flows through the upper plenum and hot legs toward the break. Some of the water carried by the steam flow evaporates due to heat transfer from hot surfaces, principally the steam generator tubes. This additional steam flow inhibits core venting and can degrade core cooling. This phenomenon is referred to as steam binding and was investigated in several tests in the 2D/3D Program. For cold leg or downcomer injection, CCTF and SCTF tests showed that liquid carryover from the core started almost immediately after reflood initiation. The extent of carryover was time-dependent and also dependent on the test conditions, but tended to be about 10% to 40% of the core inlet flow.

Water carried out of the core in the steam flow de-entrained mainly in the upper plenum and steam generator inlet plena. This de-entrainment produced a delay of about 20 to 30 seconds in the delivery of water to the tube regions of the steam generators. At large-scale, water accumulation and (in some cases) runback in the hot legs initiated after the delay, which reduced the amount of water carried to the

steam generators. The increased hot leg water storage was the principal effect of scale. The overall effect of de-entrainment is to reduce the peak clad temperature. Specifically, it is estimated that de-entrainment upstream of the steam generator tube regions reduces the peak clad temperature by about 180 K compared to the situation where no de-entrainment would occur.

PWRs with upper plenum or combined ECC injection are not sensitive to steam binding due to interaction of steam and ECC (i.e., condensation in the upper plenum and hot legs) as discussed in Section 2.7.

2.9 HOT LEG COUNTERCURRENT FLOW

In some small break LOCA scenarios, the primary coolant inventory decreases to the extent that heat removal is achieved by the reflux condenser mode. In this mode, steam flows from the reactor vessel through the hot legs to the steam generators countercurrent to condensate flowing back from the steam generators to the upper plenum.

Countercurrent flow in the hot leg was examined in large-scale UPTF tests. Comparison of the UPTF results to the results of previous small-scale tests indicated that increased scale favors water runback. Analyses showed that uninhibited water runback is expected during reflux condenser conditions of a PWR small break LOCA scenario.

Section 3

OVERALL SYSTEM BEHAVIOR DURING A LOCA

This section describes overall system behavior of a PWR during a LOCA based on tests and analyses performed within the 2D/3D Program. The discussion addresses only a large, cold leg break LOCA (LBLOCA) transient, which was the principal focus of the 2D/3D Program. Detailed information on the various reactor safety issues associated with an LBLOCA is contained in Section 4 of this report. Section 4 also covers certain non-LBLOCA safety issues investigated in the 2D/3D Program; specifically, reflux condenser mode of a small-break LOCA (see Section 4.9), high pressure injection into the hot legs during an SBLOCA in which the core uncovers (see Section 4.7.2), and pressurized thermal shock (see Section 4.5).

The experimental and analytical programs of the 2D/3D Program provided expanded insights into the complex two-phase thermal-hydraulic behavior of a heated core and the primary system during the end-of-blowdown, refill, and reflood phases of a LOCA. Tests at CCTF investigated core thermal-hydraulics and overall system behavior while tests at SCTF concentrated on multidimensional core thermal-hydraulics. The UPTF tests included integral tests and separate effects tests for the investigation of multidimensional two-phase flow behavior in the downcomer, the upper plenum, the tie plate region, and the loops of the primary system. The descriptions of PWR behavior in this section reflect the results of TRAC analyses and tests from the 2D/3D Program.

The descriptions of overall system behavior during an LBLOCA for PWRs with different ECCS configurations are covered in separate subsections. The subsections and corresponding ECCS types are listed below.

- 3.1 Cold Leg Injection Plant
- 3.2 Combined Injection Plant
- 3.3 Downcomer Injection Plants
  - -- 3.3.1 US Downcomer Injection Plant
  - -- 3.3.2 FRG Downcomer Injection Plant
  - -- 3.3.3 Japanese Downcomer Injection Plant
- 3.4 Upper Plenum Injection Plant

3.1 COLD LEG INJECTION PLANT

PWRs are equipped with safety systems which inject emergency core coolant (ECC) in the event of a LOCA. ECC systems typically consist of three types of coolant injection systems: accumulator (ACC) injection, low pressure coolant injection (LPCI), and high pressure coolant injection (HPCI). The ACC system provides high flow rate, short duration injection from pressurized accumulator tanks, while the LPCI system provides low flow rate, long duration flow. The HPCI system provides long duration, high pressure flow at an even lower flow rate. For most PWRs in the US and Japan, all ECC systems inject water into the primary system through nozzles in the cold legs.

During an LBLOCA, water from the pressurized accumulators is automatically injected into the reactor vessel when the reactor pressure drops below the accumulator tank pressure. HPCI flow is also injected into the vessel with the accumulator flow, but the HPCI flow is small in comparison to the accumulator flow. The accumulator tanks are sized so that when emptied, the lower plenum is filled and core reflood has begun. At low pressures, LPCI flow begins and continues indefinitely. HPCI normally continues throughout the LPCI injection phase, but the flow rate is dominated by the LPCI system. Design parameters for ECC systems of PWRs with cold leg injection are tabulated for three different PWR designs in Table 3.1-1.

Thermal-hydraulic behavior in the reactor coolant system during an LBLOCA is described below. The discussion is divided chronologically into the following time periods: blowdown, end-of-blowdown/refill, early reflood, accumulator nitrogen discharge, and late reflood. The sequence of events is indicated on Figures 3.1-1 and 3.1-2 which show the pressure and rod temperature transients, respectively, from TRAC calculations for US/J PWRs with cold leg injection.

Blowdown

The 2D/3D Program did not investigate system behavior during the blowdown portion of an LBLOCA. Based on results from other reactor safety research programs, it is known that during blowdown, most of the initial contents of the reactor coolant system are rapidly expelled through the break. A significant fraction of the water initially present in the reactor coolant system flashes to steam, which drives the flow out the broken cold leg. The pressure in the primary system decreases as the blowdown progresses. After approximately 25 seconds, the reactor coolant system and containment equalize at a pressure of about 350 kPa.

End-of-Blowdown/Refill (see Figure 3.1-3)

During the end-of-blowdown, the reactor coolant system is filled with steam except for the lower plenum which still contains some water. The steam is vented to containment by either flowing around the bottom of the core barrel and up the downcomer to the

break or through the loops to the break. The water inventory in the lower plenum continues to decrease from entrainment by the steam flow around the core barrel and from flashing due to decreasing system pressure. The reverse steam flow in the core provides limited core cooling, which reduces to almost zero as the flow stops at the end-of-blowdown.

When the system pressure has decreased below the accumulator pressure (1,400 to 4,600 kPa, depending on plant design), the accumulators automatically inject ECC into the cold legs. Water plugs form in the cold legs, as the steam flow through the loops is condensed by the high flow of subcooled ECC. Plug formation consumes a few seconds of ECC delivery and thus slightly delays ECC delivery to the downcomer. This delay is not detrimental because the system is at a pressure where significant ECC bypass could occur if ECC reached the downcomer. The water plugs in the cold legs oscillate, causing fluctuations in the flow of ECC into the downcomer.

In the downcomer, the two-phase (i.e., steam and entrained water) upflow initially entrains the ECC flow directly out the broken cold leg (i.e., ECC bypass) thereby preventing ECC from refilling the lower plenum. However, as blowdown proceeds and the upflow decreases, the bypass also decreases and ECC is delivered to the lower plenum. Based on the UPTF tests, ECC delivery to the lower plenum initiates at the loops away from the break at a pressure of about 800 kPa. Delivery from the loop near the break initiates later in the end-of-blowdown when the steam upflow is lower.

By the completion of blowdown, the lower plenum is filled almost to the bottom of the core barrel. Within a few seconds of the end of depressurization, the vessel fills to the core inlet and refill is complete. Hence, refill and blowdown are overlapping rather than consecutive. Overlapping blowdown and refill reduces the time to core reflood, and therefore the adiabatic heat-up period, by about 10 seconds over consecutive blowdown and refill. Reference U-455 estimates the reduction in cladding temperatures at reflood initiation for overlapping, rather than consecutive, blowdown and refill is 100 K (see Section 4.1.1).

Early Reflood (Accumulator Injection) (see Figure 3.1-4)

In the early portion of reflood, the downcomer water level increases rapidly due to the high ECC flow from the accumulators. Based on CCTF and UPTF tests, the downcomer water level stabilizes at the cold leg elevation due to water spillover out the broken cold leg. Heat release from the vessel wall initiates as the downcomer fills. Tests and analyses show that this heat release heats up the downcomer water inventory but does not result in vaporization because the subcooling of the water delivered to the vessel is sufficient to suppress boiling.

The increase in downcomer water level forces water into the core. Steam generation in the core initiates first at the bottom of the core as water enters the core from the lower plenum. However, within a few seconds, water entrained by the boiling process is present throughout the core and core cooling is occurring at all elevations. The entrained water is evenly distributed across the core (i.e., horizontal or radial direction) regardless of the initial power and temperature profiles in the core. The steam generated in the core is vented to containment via the upper plenum and reactor coolant loops. Some of the water in the upper region of the core is carried by the steam flow out of the core; the average quality for the net flow at the core exit is 40% for this part of the transient.

Initially, the core flooding rate is high and the collapsed water level in the core increases rapidly. When the downcomer water level reaches the cold leg elevation and water spills out the break, the core flooding rate decreases quickly. However, since the core steam generation is essentially the same as during early reflood, the reduction in the core flooding rate results in lower rates of water accumulation in the core and water carryover out of the core.

Water carried out of the core is either de-entrained in the upper plenum or carried over with the steam to the reactor coolant loops. In the upper plenum, the water which de-entrains either accumulates as a two-phase mixture or falls back to the core. The water carried over to the loops de-entrains and accumulates in the steam generator (SG) inlet plena. Entrained water does not reach the steam generator tube regions during the accumulator injection portion of reflood.

In the intact cold legs, the steam flow toward the downcomer is completely condensed by the subcooled ECC. Due to the high ECC flows, the condensation results in the maintenance of water plugs in the cold legs which oscillate upstream and downstream from the injection nozzle location. Consequently ECC delivery to the pressure vessel fluctuates.

Once the downcomer has filled to the cold leg elevation, flow out the broken cold leg is primarily single-phase water flow since the intact loop steam flow is completely condensed and vaporization in the downcomer is suppressed.

Accumulator Nitrogen Discharge

When the water in the accumulators is depleted, the nitrogen that pressurizes the tanks escapes through the ECC piping. The nitrogen quickly pushes ECC water from the intact cold legs into the reactor vessel downcomer. Also, water in the top of the downcomer and in the broken cold leg is pushed toward the break. The primary system (particularly the region into which the nitrogen is injected) is pressurized for a short period until the nitrogen can leave the system.

System pressure is further increased by suppression of steam condensation. As nitrogen mixes with and displaces steam, the rate of condensation becomes much lower than when pure steam was in contact with the subcooled water. The accumulation of uncondensed steam contributes to the temporary pressurization of the downcomer and cold leg regions of the primary system.

Before the nitrogen discharge begins, the pressure above the core exceeds the pressure in the downcomer due to the pressure drop of steam flowing from the upper plenum around the intact loops. This pressure difference keeps the water level in the core lower than in the downcomer. The nitrogen pressurization of the downcomer disrupts the existing pressure distribution and forces a portion of the water in the downcomer into the lower plenum, displacing lower plenum water into the core (see Figure 3.1-5). TRAC analyses predict that core water inventory increases from a volume fraction of 0% to 20% before nitrogen discharge to a maximum of 60% to 70% (see Section 4.4).

The lower plenum water is subcooled, in part due to the rise in pressure. As the water surges into the core, heat is absorbed until, after a brief delay during which the water is heated to saturation, additional steam is produced. The increased steam production in the core increases the pressure above the core. The pressure increase, coupled with a decreasing nitrogen discharge rate, eventually stops the rise in core water level and then forces some of the water to flow out of the core and back into the lower plenum (see Figure 3.1-6). TRAC analyses predict that the core water inventory following the out flow from the core to downcomer is greater than the inventory before nitrogen discharge (30 - 40% volume fraction versus 0 - 20% -- see Section 4.4).

As discussed in Section 4.4, the 2D/3D test data regarding the effect of nitrogen discharge are limited. Specifically, the 2D/3D tests did not simulate the peak magnitude and duration of the core level surge, the long-term effects of the nitrogen discharge, or the effect of these phenomena on core cooling; however, TRAC analyses predict that the core water level surge quenches the hottest portion of the hottest rod.

Late Reflood (LPCI) (see Figure 3.1-7)

As previously indicated, water carryover out of the core decreases prior to termination of accumulator injection when the downcomer water level reaches the cold leg elevation. Later in reflood, however, water carryover out of the core increases as the quench front reaches the upper regions of the core. Reflood ends when the entire core is quenched. The quality for the net flow out of the core is about 90% when accumulator injection terminates but decreases to less than 45% just prior to whole core quench.

The upper plenum and SG inlet plenum inventories, which had been increasing during early reflood, decrease due to the reduction in water carryover from the core. The decrease in SG inlet plenum inventory initiates accumulation in the hot legs as some of the water from the inlet plenum drains into the hot legs. The flow regime in the hot leg is stratified with the two-phase mixture from the upper plenum flowing over a layer of water on the bottom of the hot leg.

Water carryover to the SG tubes also initiates when water carryover from the core decreases and the SG inlet plenum inventory decreases (i.e., about 25 seconds after BOCREC -- see Section 4.8). Heat transfer from the hot water on the secondary side of the SG vaporizes water entrained into tubes and superheats the steam. Vaporization of water in the SGs contributes to steam binding and degrades core cooling. Specifically, vaporization increases the volumetric flow, and therefore pressure drop, through the reactor coolant loops. The resulting increase in upper plenum pressure reduces the core flooding rate.

Based on UPTF test results, a significant portion of water carryover from the core de-entrains upstream of the SG tubes, particularly in the initial portion of reflood, and therefore does not contribute to steam binding. As discussed in Section 4.8, Reference U-456 estimated the effect of steam binding from the predicted carryover to the SG U-tubes assuming complete vaporization. The evaluations showed that if all the water carried out of the core reaches the SG U-tubes, PCT increases by about 240K (430°F). However, due to de-entrainment upstream of the SG U-tubes, the increase in PCT from carryover to the SG U-tubes is only about 65K (120°F).

In the intact cold legs, steam is condensed by subcooled ECC. However, due to the lower ECC flow, only a portion of the steam flow is condensed. The resultant flow regime in the intact cold legs is stratified with steam flowing over the ECC flow to the downcomer. The condensation efficiency is nearly 100%. The uncondensed steam vents to containment via the downcomer and broken cold leg.

The steam flow around the downcomer reduces the water level in the downcomer by entraining water out the break. Voiding due to heat release from the walls also reduces the collapsed water level in the downcomer. The reduction of downcomer collapsed water level reduces the driving head for core reflood and therefore the core flooding rate. However, as discussed in Section 4.2.1, calculations show that the effect of the level reduction on cladding temperatures is small (about 10 - 13K--see Reference U-455).

During the LPCI portion of reflood, a two-phase mixture of steam with entrained water flows out the break. The pressure drop associated with this flow pressurizes the downcomer relative to containment and increases the system pressure. Tests at CCTF and SCTF indicate increasing system pressure improves core cooling (see Section 4.6.1).

Table 3.1-1

ECC SYSTEM DESIGN PARAMETERS FOR PWRS WITH COLD LEG INJECTION

PWR Vendor/Class	Accumulators			HPCI		LPCI	
	Quantity	Pressure kPa (psia)	Water Volume per Accumulator m^3 (ft^3)	Number of Pumps	Pump Flow Design/Maximum m^3/hr (gpm)	Number of Pumps	Pump Flow Design/Maximum m^3/hr (gpm)
Combustion Engineering/System 80[1]	4	4310 (625)	53 (1860)	2	185/225 (815)/(1130)	2	955/1135 (4200)/(5000)
Westinghouse/3400 MWt[2]	4	4580 (665)	24 (850)	2 2	95/150 (425)/(650) 35/125 (150)/(550)	2	680/1025 (3000)/(4500)
Japanese/3400 MWt[3]	4	4500	27	2	NA/320	2	NA/1020

NOTES:

1. Design parameters for the Combustion Engineering System 80 PWR obtained from Reference E-511.

2. The reference reactor for a 3400 MWt class Westinghouse PWR is the reactor at Trojan Nuclear Generating Station operated by Portland Gas and Electric; design parameters obtained from Reference E-512.

3. The reference reactors for a 3400 MWt class Japanese PWR are the reactors at Genkai Nuclear Plant Units 3 and 4; design parameters obtained from Reference E-514. Note that the design flow rates of the HPCI and LPCI pumps are not available.

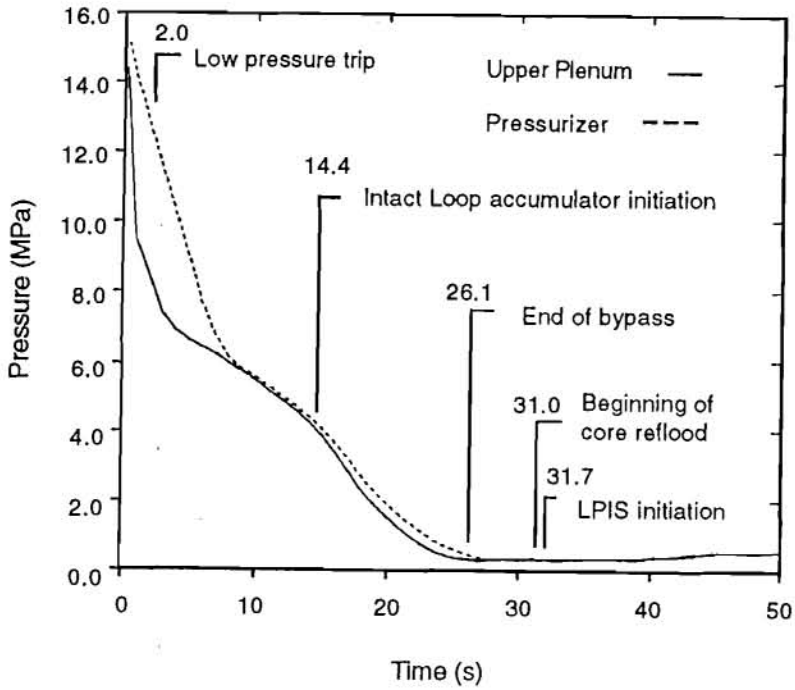

CALCULATED PRESSURE TRANSIENT FOR
US/J PWR WITH COLD LEG INJECTION

FIGURE 3.1-1

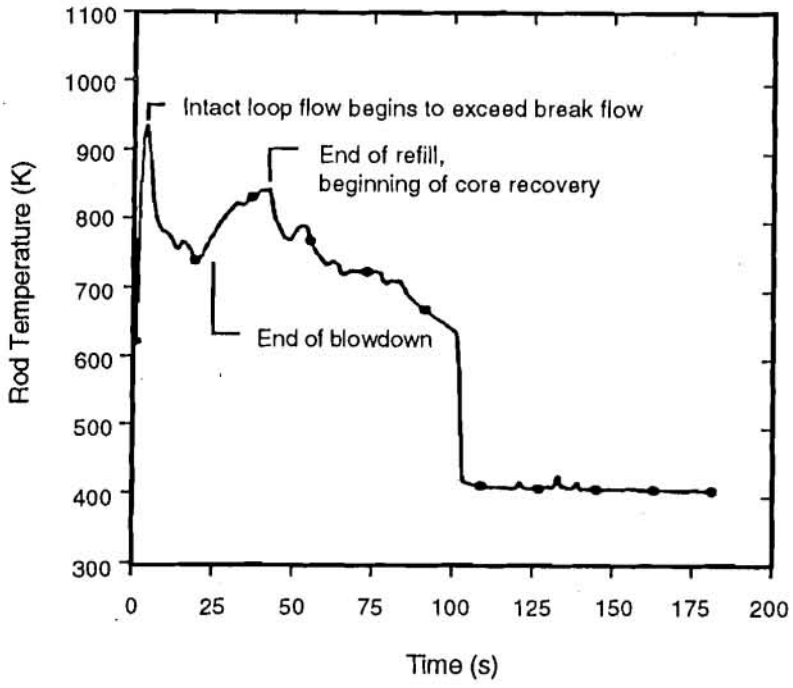

Maximum BE Rod Temperature

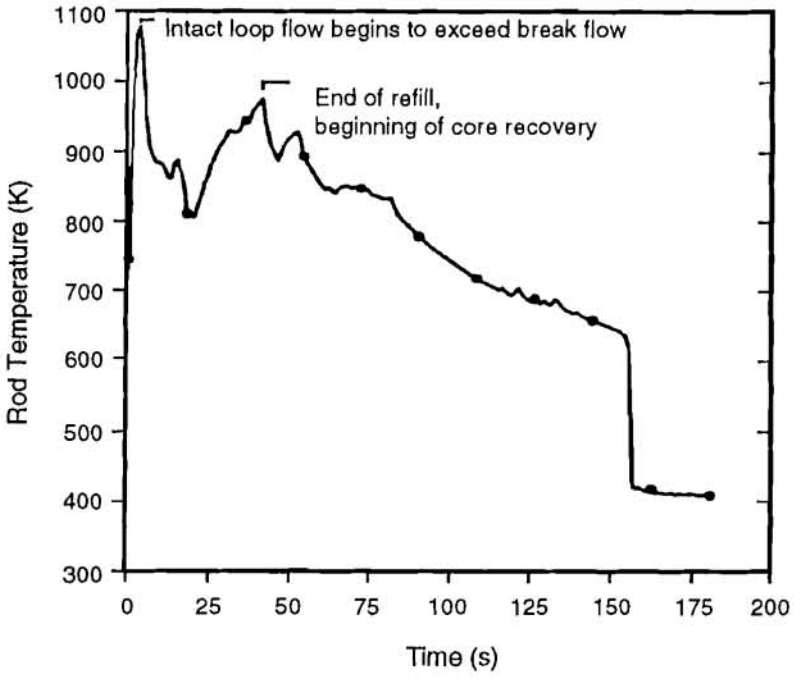

Maximum EM Rod Temperature

CALCULATED ROD TEMPERATURE TRANSIENT FOR US/J PWR WITH COLD LEG INJECTION

FIGURE 3.1-2

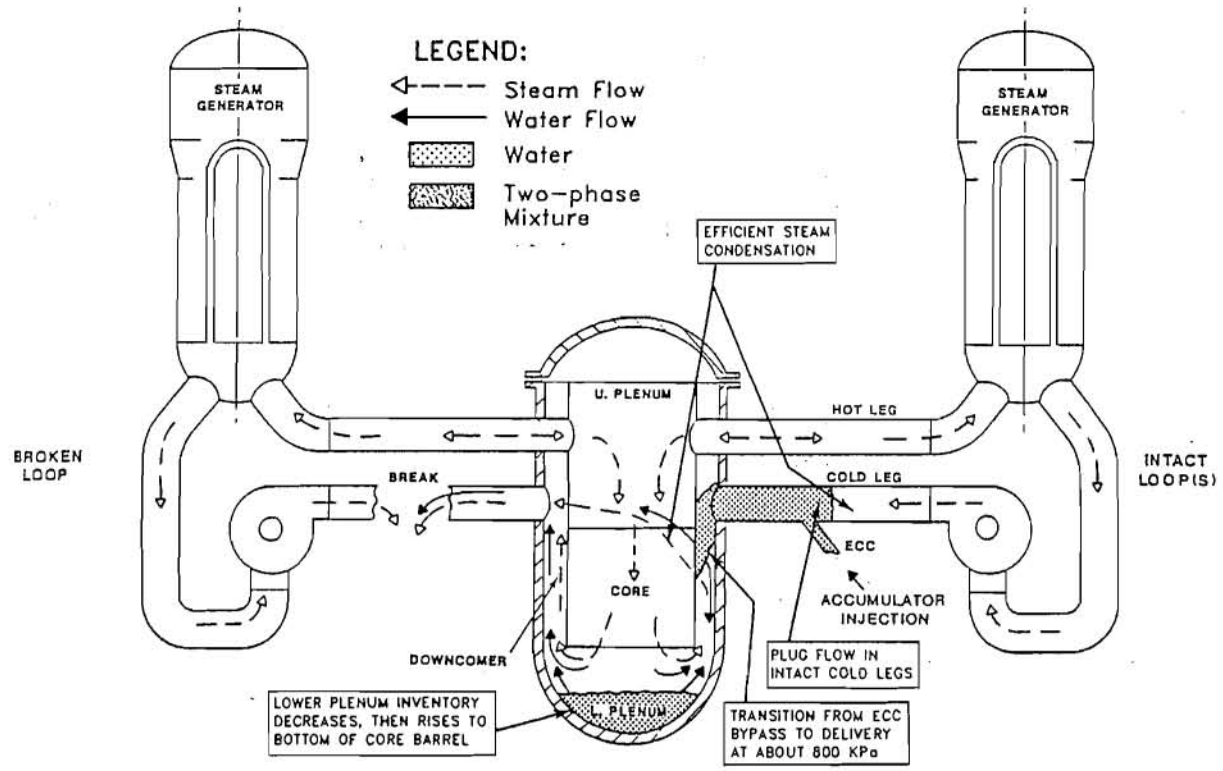

SUMMARY OF LBLOCA BEHAVIOR IN A COLD LEG INJECTION PWR END-OF-BLOWDOWN/REFILL PHASE

FIGURE 3.1-3

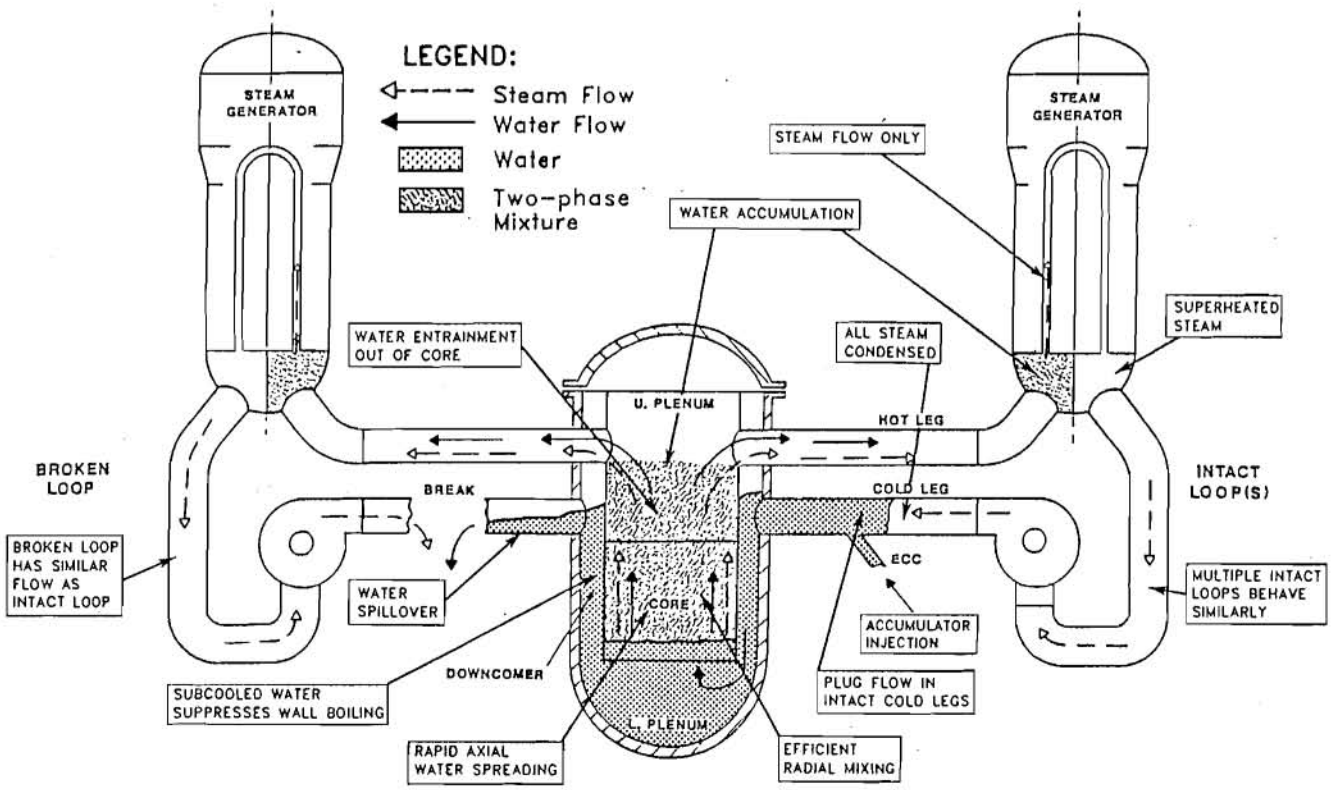

SUMMARY OF LBLOCA BEHAVIOR IN A COLD LEG INJECTION PWR EARLY REFLOOD (ACCUMULATOR INJECTION)

FIGURE 3.1-4

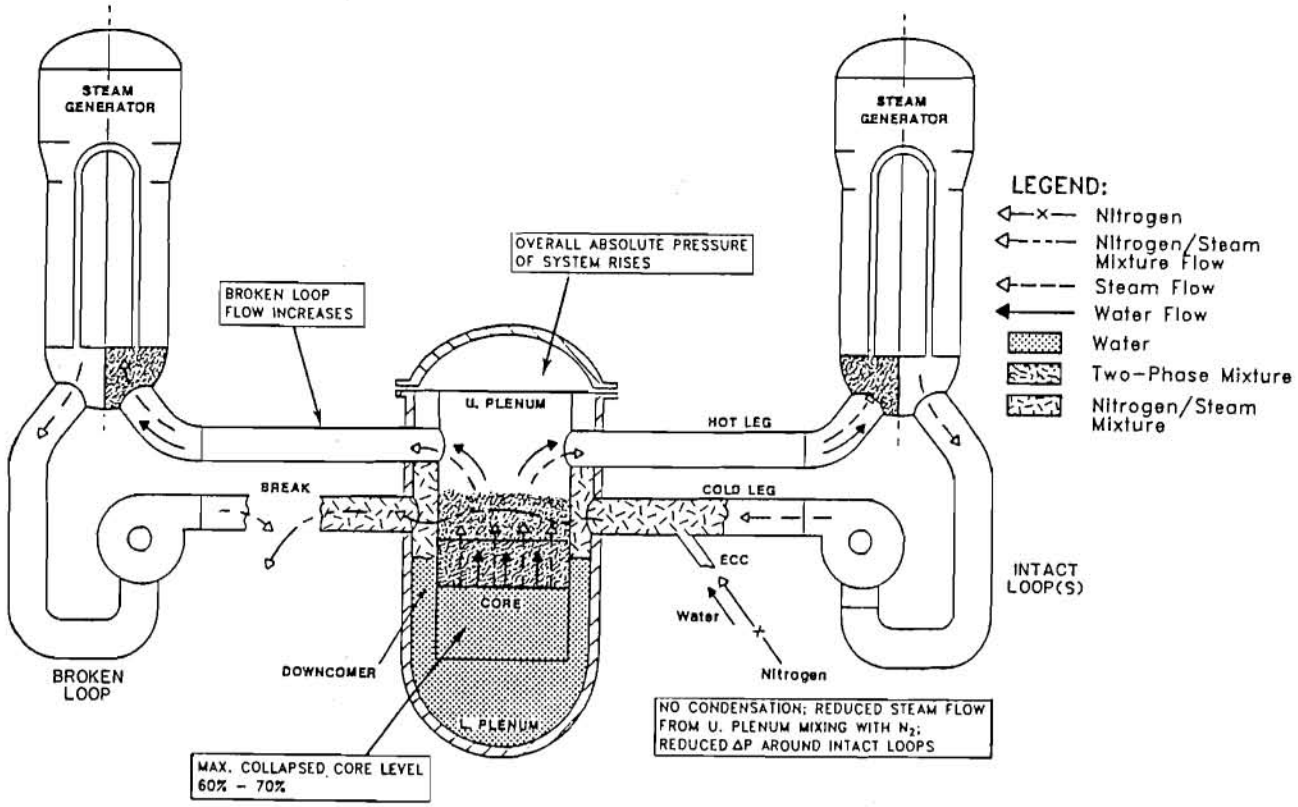

SUMMARY OF LBLOCA BEHAVIOR IN A COLD LEG INJECTION PWR SHORTLY AFTER N_2 INJECTION STARTS

FIGURE 3.1-5

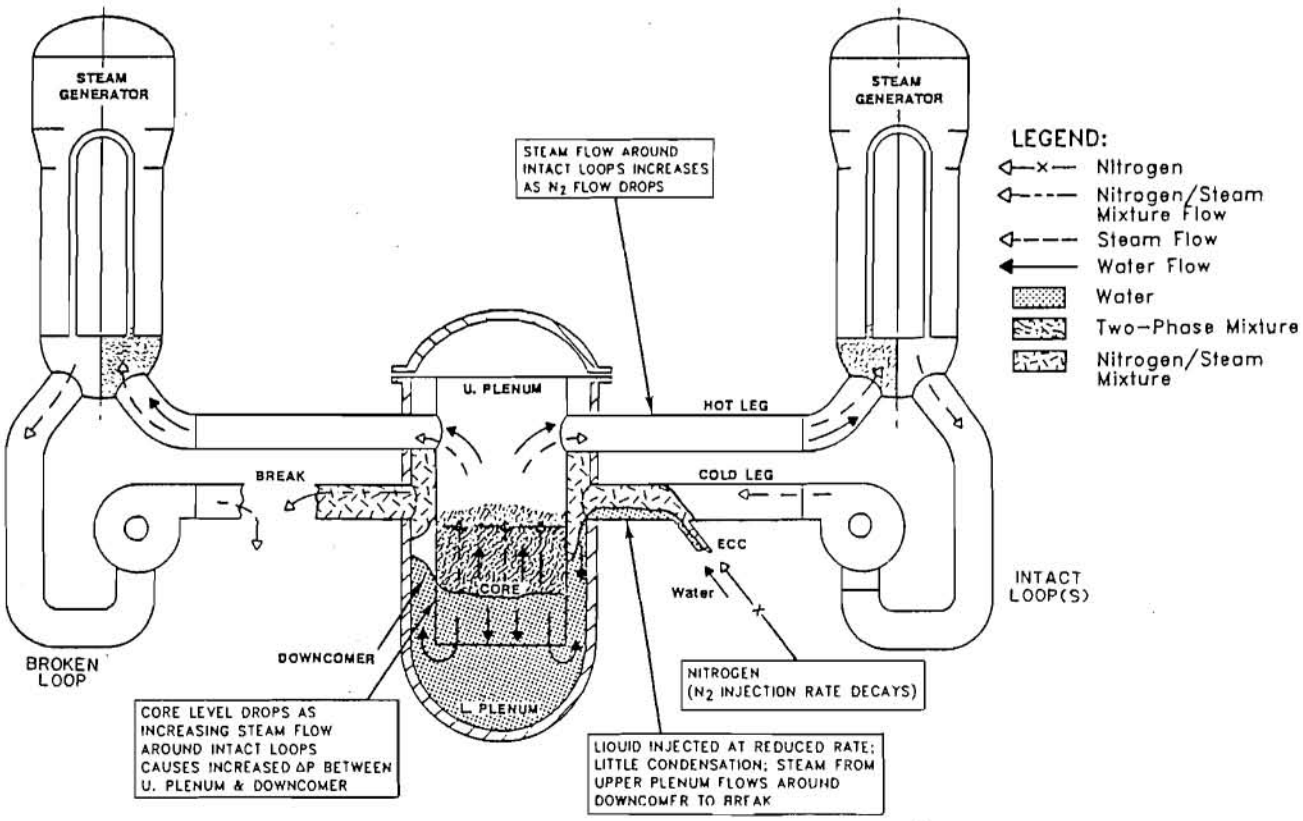

SUMMARY OF LBLOCA BEHAVIOR IN A COLD LEG INJECTION PWR DURING N_2 INJECTION

FIGURE 3.1-6

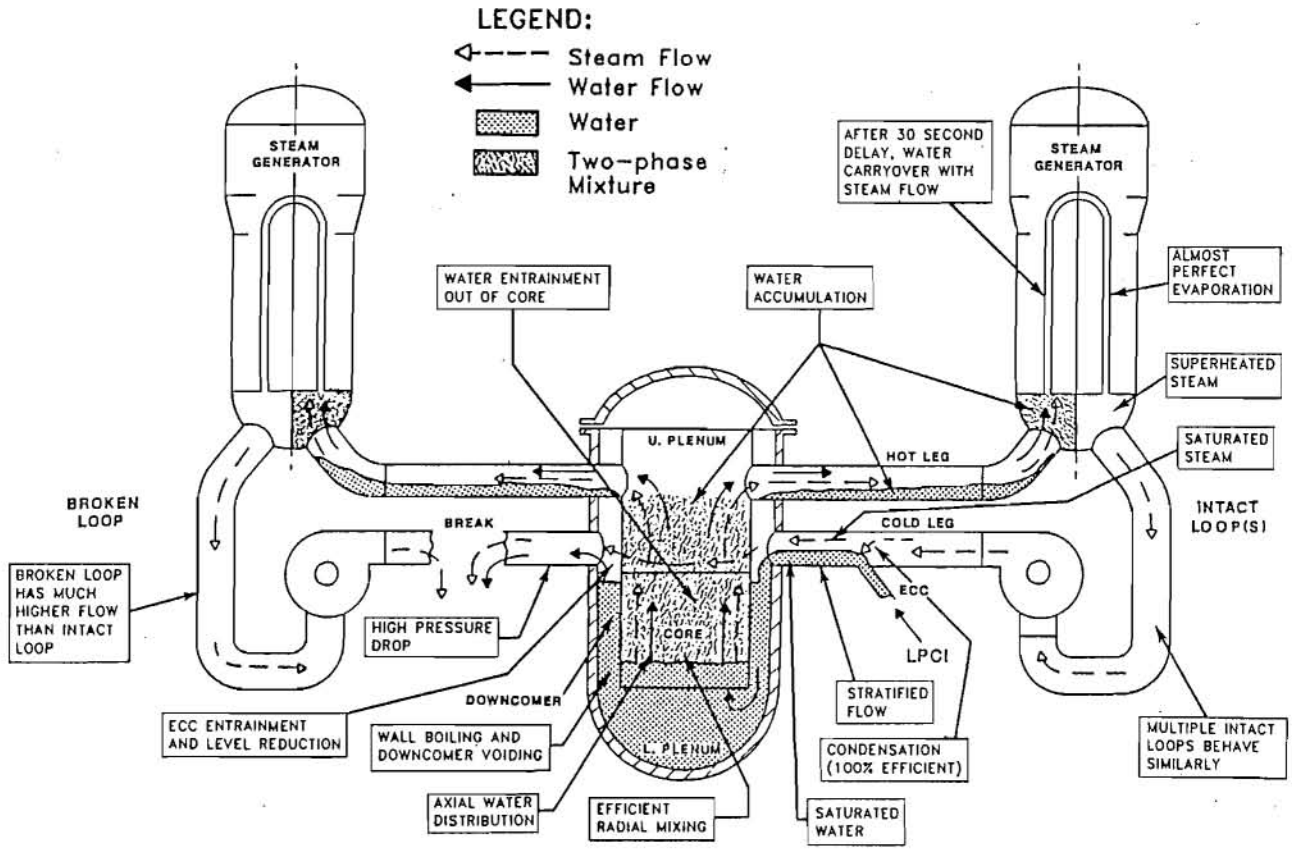

SUMMARY OF LBLOCA BEHAVIOR IN A COLD LEG INJECTION PWR LATE REFLOOD (LPCI)

FIGURE 3.1-7

3.2 COMBINED INJECTION PLANT

The ECC systems in four-loop German (Siemens/KWU; 1300 MWe) PWRs consist of three types of coolant injection systems, namely: high pressure coolant injection (HPCI), accumulator (ACC) injection, and low pressure coolant injection (LPCI). A unique feature of the GPWR design is that each of the ECC systems injects coolant into the primary system through nozzles in the hot legs as well as through nozzles in the cold legs. This type of injection scheme is termed "combined injection."

During an LBLOCA, the HPCI system is actuated at a primary system pressure of about 11,000 kPa. When the pressure in the primary system has decreased to 2,600 kPa, the ACCs automatically start to inject ECC. When the primary system pressure reaches about 1,100 kPa, injection by the LPCI system commences. HPCI continues throughout the ACC and LPCI phases, but ECC flow rate is dominated by the ACC and LPCI flows.

Overall system behavior in a combined injection PWR during an LBLOCA is described below based on findings from 2D/3D tests and the results of a TRAC-PF1/MOD1 calculation with 5/8 injection (Reference G-661). Schematics depicting system behavior at several times in a UPTF test are shown in Figure 3.2-1. The discussion below is divided into the following time periods: blowdown, end-of-blowdown/refill, and reflood.

Blowdown

System behavior during blowdown was not investigated within the 2D/3D Program. This discussion is based on test results from other safety research programs, and the results of code analyses. Overall, system behavior during blowdown is independent of the ECCS configuration until ACC injection starts.

During blowdown, the initial contents of the primary system are expelled through the break to containment as the system depressurizes. The net flow in the reactor vessel is from the core to the lower plenum and up the downcomer to the broken cold leg. The rate at which primary coolant is discharged is controlled by the critical flow at the break. For a 200% cold leg break, the pressures in the primary system and the containment equalize approximately 35 seconds after break initiation at a pressure of about 400 kPa.

End-of-Blowdown/Refill (see Figure 3.2-2)

When the primary system pressure has decreased below 2,600 kPa, the ACCs automatically start to inject ECC into the hot and cold legs. A few seconds later highly subcooled ECC from the hot legs is delivered to the upper plenum and penetrates through the tie plate to the core. Water penetration to the core occurs only within

defined areas (20-40% of the total core area, depending on the number of activated hot leg ECC systems--see Figure 4.7-7) located in front of the delivering hot legs. While a significant portion of the steam in the hot legs and the upper plenum is condensed by ECC injected into the hot legs, UPTF tests indicate that ECC which penetrates through the tie plate is still highly subcooled (~70 K).

Water downflow from the upper plenum initiates core cooling during end-of-blowdown. SCTF tests indicate the portions of the core in the downflow regions are immediately quenched. CCTF tests indicate that heat transfer in the remainder of the core is slightly enhanced by the water downflow. Some of the water downflow is vaporized and steam flows out the top and bottom of the core; however, most of the water downflow is heated to near saturation and flows to the lower plenum. When the steam flow around the bottom of the core barrel is high, a substantial part of the water downflow which reaches the lower plenum is entrained out the break; the remainder of the water downflow is accumulated in the lower plenum. As the steam flow around the bottom of the core barrel decreases, entrainment decreases and the rate of water accumulation to the lower plenum increases.

UPTF tests (References G-018 and G-218) and a TRAC analysis (Reference G-661) indicate that the lower plenum inventory starts to increase about ten seconds before the end of depressurization at a system pressure of 1,000 kPa. This level increase is primarily due to hot leg ECC injection which penetrates through the tie plate and core because most of the ECC injected in the cold legs is entrained out the break by the upflow in the downcomer. However, as blowdown progresses and the upflow decreases, bypass also decreases and ECC penetrates down the downcomer to the lower plenum. Based on UPTF tests, delivery of ECC injected into the cold legs initiates at the cold legs away from the break when the system pressure decreases below 800 kPa.

In the end-of-blowdown phase, water plugs form in the cold legs as steam is condensed by the high flow of subcooled ECC. These plugs oscillate upstream and downstream from the injection nozzle location resulting in fluctuations in ECC delivery to the downcomer. In the hot legs, water plugs form and collapse periodically; consequently, ECC delivery to the upper plenum also fluctuates.

By the completion of blowdown, the lower plenum is filled to the bottom of the core barrel. A few seconds later, the vessel fills to the core inlet and refill is complete. Hence, the end-of-blowdown and refill are overlapping rather than consecutive. This reduces the time to core reflood and therefore the heat-up period of the non-downflow regions of the core; consequently, cladding temperatures in the non-downflow regions at reflood initiation are lower than for consecutive end-of-blowdown and refill. As indicated in Section 4.1.3, the reduction in cladding temperatures at reflood initiation is about 80 - 100 K.

Reflood

Initially, the downcomer water level increases rapidly as ECC injected into the cold legs is delivered to the downcomer and ECC injected into the hot legs penetrates through the core to the lower plenum and flows into the downcomer. When the downcomer water level reaches the cold leg elevation, water spills out the broken cold leg and the water level stabilizes.

Core thermal-hydraulic behavior during reflood is strongly heterogeneous (see Figure 3.2-3). Specifically, the core is separated into two regions. Within the water downflow region, the core is mainly quenched from the top down by the water downflow from the upper plenum. Outside the water downflow region, core cooling initiates at the bottom of the core as water entering the core from the lower plenum is vaporized. Water entrained by the boiling process is carried to the upper regions of the core initiating core cooling at all elevations.

UPTF tests indicate more than 80% of the steam generated in the core is condensed in the upper plenum and hot legs. The uncondensed steam flows through the loops. However, since most of the steam is condensed in the upper plenum and hot legs, the loop steam flows are minimal and the flow pressure drop is small. Consequently, the core flooding rate is high (0.15 - 0.25 m/s per SCTF tests).

The steam flow in the intact loops is completely condensed in the cold legs and no steam enters the downcomer; consequently, there is no reduction in downcomer water level due to entrainment out the break.

Water plugs form in both the hot and cold legs due to condensation of steam by the high flow of subcooled water. UPTF tests indicate the hot leg plugs are unsteady and the cold leg plugs oscillate. In both cases, delivery to the reactor vessel fluctuates. The fluctuating nature of ECC delivery does not adversely affect core heat transfer and quench times.

In a TRAC calculation of an LBLOCA, the average powered rods were quenched 90 seconds after break initiation. Whole core quench occurred within 130 seconds of break initiation (Reference G-661).

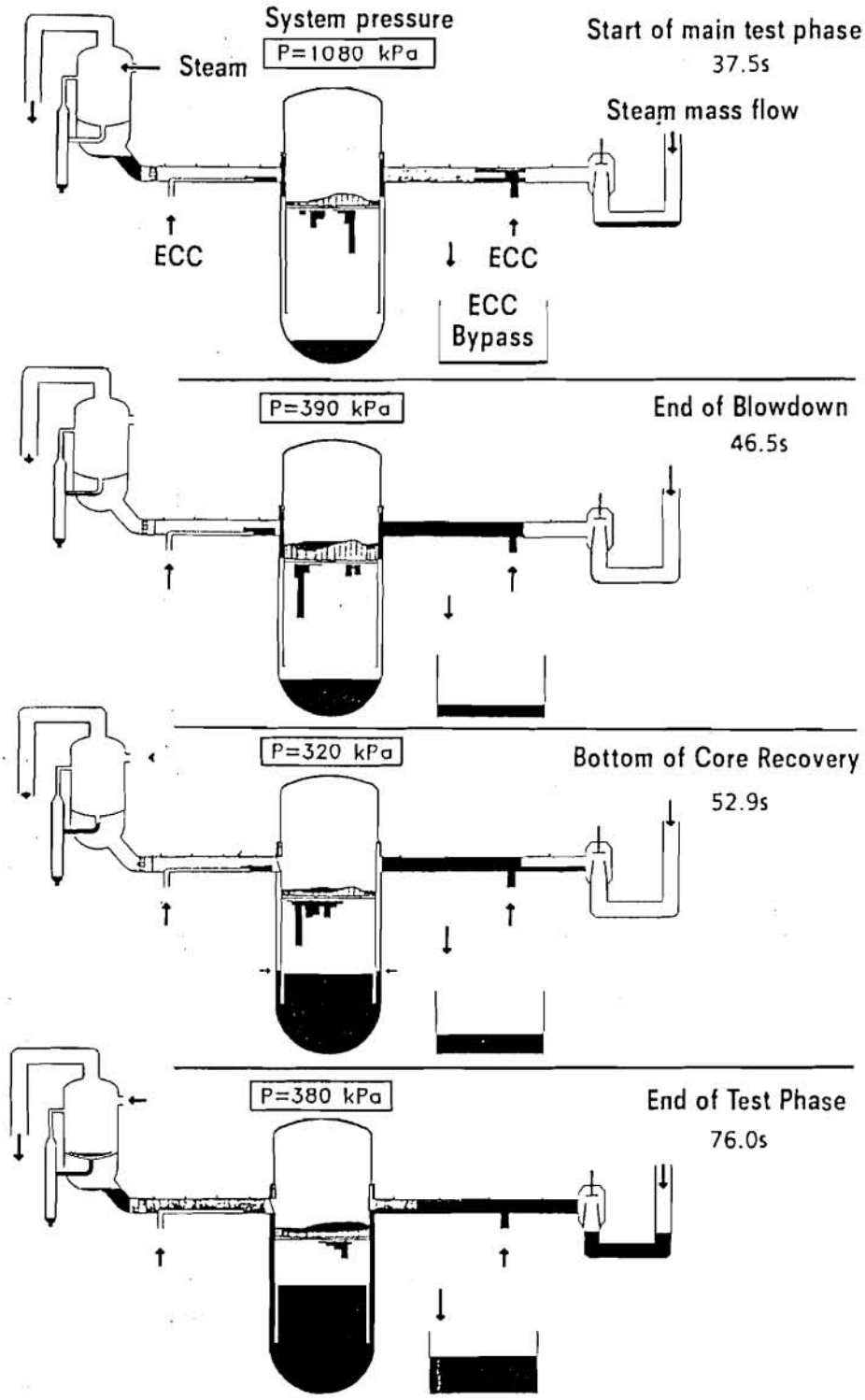

OVERALL SYSTEM BEHAVIOR IN A COMBINED INJECTION INTEGRAL TEST AT UPTF (TEST NO.18)

FIGURE 3.2-1

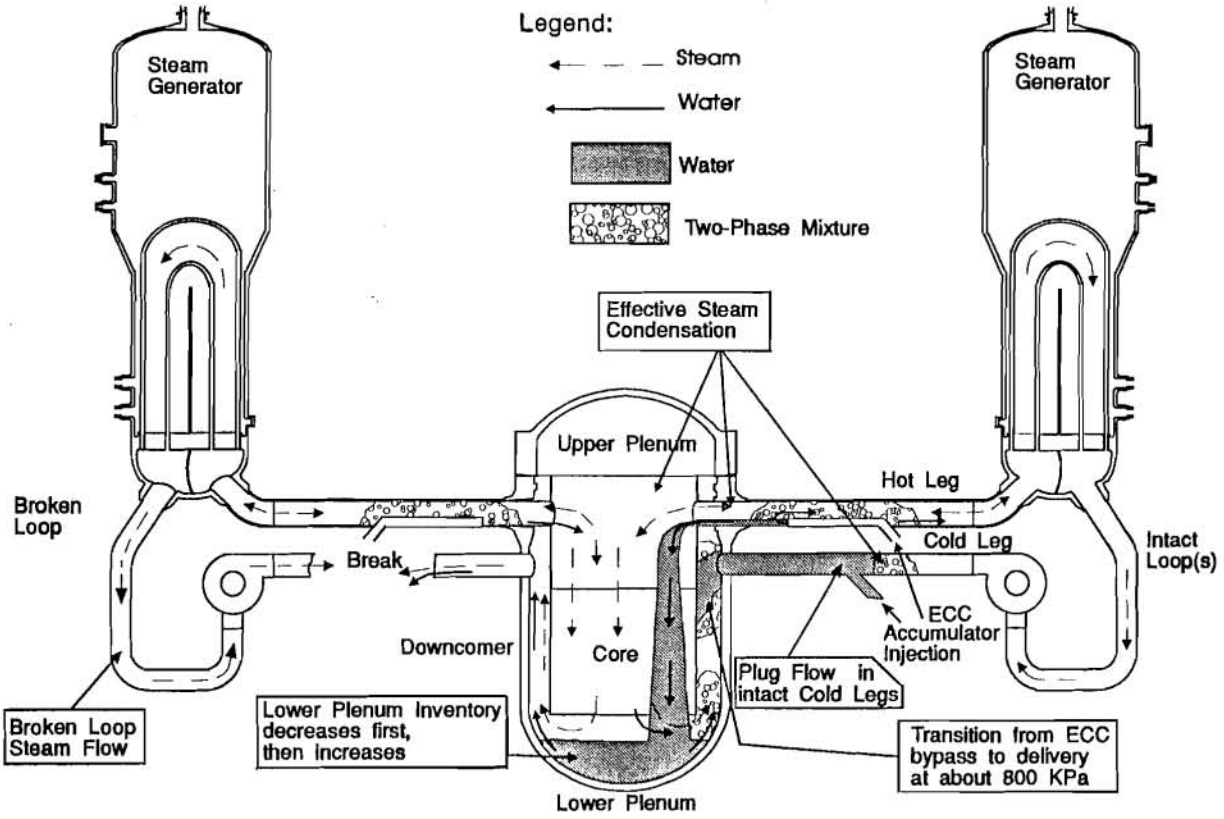

SUMMARY OF LBLOCA BEHAVIOR IN A COMBINED INJECTION PWR
END-OF BLOWDOWN/REFILL PHASE

FIGURE 3.2-2

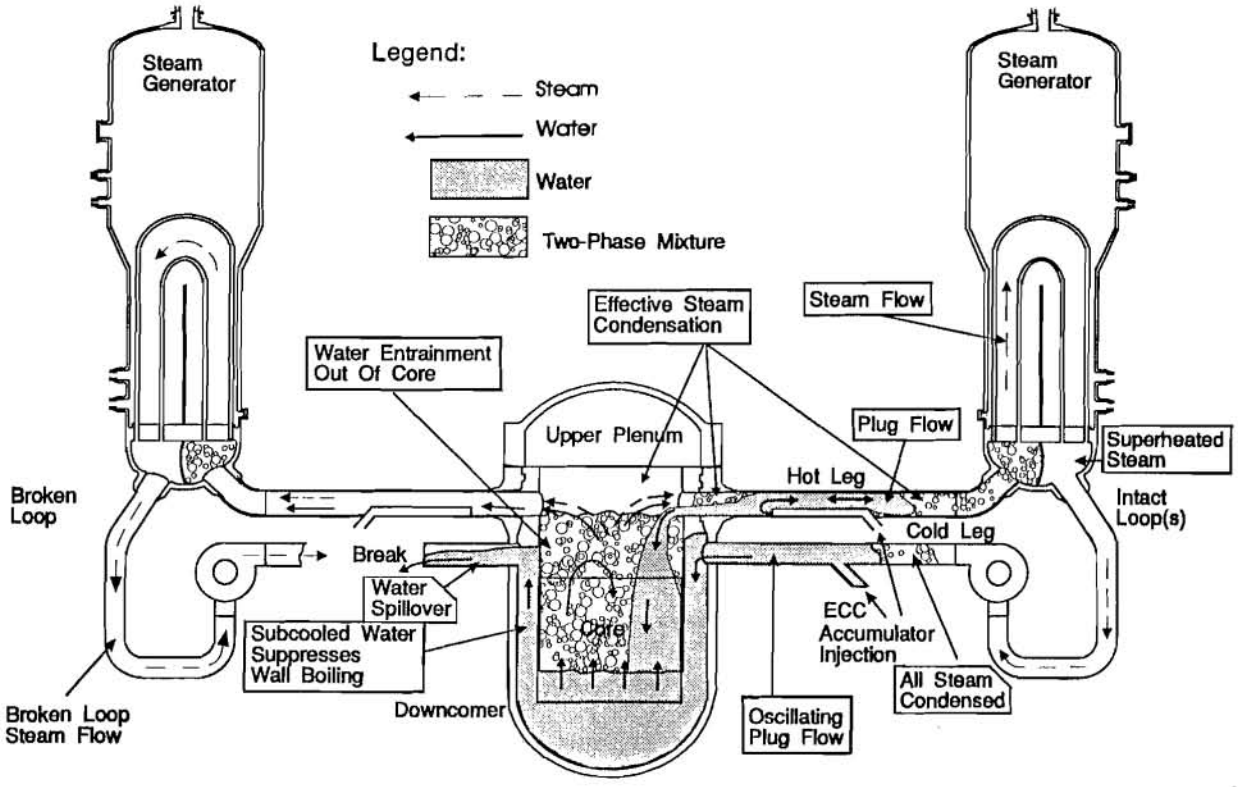

SUMMARY OF LBLOCA BEHAVIOR IN A COMBINED INJECTION PWR
REFLOOD PHASE

FIGURE 3.2-3

3.3 DOWNCOMER INJECTION PLANTS

The ECCS configuration of PWRs with downcomer injection varies considerably among the three countries participating in the 2D/3D Program; consequently, overall system behavior during an LBLOCA is described in a separate subsection for each PWR. The subsection and corresponding PWR are listed below.

- 3.3.1 US Downcomer Injection Plant
- 3.3.2 FRG Downcomer Injection Plant
- 3.3.3 Japanese Downcomer Injection Plant

3.3.1 US Downcomer Injection Plant

Babcock & Wilcox (B&W) PWRs are 2 x 4 loop designs with once-through steam generators. It has been conservatively postulated that, during an LBLOCA in a lowered loop B&W PWR, stable water plugs can form in the portions of the cold legs upstream of the pumps and thereby prevent steam flow through the loops. To provide an alternative flow path for steam to vent to containment, vent valves are installed in the reactor vessel core barrel. There are eight vent valves located around the core barrel approximately 1 m above the cold leg centerline (see Figure 4.1-11). ECC systems for B&W PWRs consist of three types of coolant injection systems: accumulator (ACC) injection, low pressure coolant injection (LPCI), and high pressure coolant injection (HPCI). For B&W PWRs, the ACC and LPCI systems inject ECC into the primary system through nozzles located in the downcomer and the HPCI system injects ECC through nozzles in the cold legs.

During an LBLOCA, water from the pressurized accumulators is automatically injected into the reactor vessel downcomer when the reactor pressure drops below the accumulator tank pressure. HPCI flow is simultaneously injected into the cold legs, but the HPCI flow is small compared to the accumulator flow. The accumulator tanks are sized so that when emptied, the lower plenum is filled and core reflood has begun. At low pressures, LPCI flow begins and continues indefinitely. HPCI normally continues throughout the LPCI injection phase, but the flow rate is dominated by the LPCI system. Design parameters for ECC systems of B&W PWRs are tabulated in Table 3.3.1-1.

Thermal-hydraulic behavior in the reactor coolant system during an LBLOCA is described below. The discussion is divided chronologically into the following time periods: blowdown, end-of-blowdown/refill, early reflood, accumulator nitrogen discharge, and late reflood.

Blowdown

The 2D/3D Program did not investigate system behavior during the blowdown portion of an LBLOCA. Based on results from other reactor safety research programs, it is known that during blowdown, most of the initial contents of the reactor coolant system are rapidly expelled through the break. A significant fraction of the water initially present in the reactor coolant system flashes to steam, which drives the flow out the broken cold leg. The pressure in the primary system decreases as the blowdown progresses.

End-of-Blowdown/Refill (see Figure 3.3.1-1)

During the end-of-blowdown, the reactor coolant system is filled with steam except for a small amount of water in the lower plenum. Vent valves located in the core barrel above the cold leg centerline provide a steam path from the upper plenum directly to the downcomer. Steam is vented to containment by flowing around the bottom of the core barrel and up the downcomer to the break and by flowing through the vent valves and around the downcomer to the break. The water inventory in the lower plenum continues to decrease from entrainment by the steam flow around the core barrel and from flashing due to decreasing system pressure. Steam flow in the core provides limited core cooling which is eliminated as the flow stops at the end-of-blowdown.

When the system pressure has decreased below the accumulator pressure (4,200 kPa), the accumulators automatically inject ECC into the downcomer. There is a small amount of HPCI injection to the cold legs, but this flow is negligible relative to the ACC injection. In the downcomer, the steam upflow initially entrains the injected ECC directly out the broken cold leg (ECC bypass) thereby preventing ECC from refilling the lower plenum. However, as blowdown proceeds and the steam flow decreases, bypass also decreases and ECC is delivered to the lower plenum. In UPTF tests for cold leg injection, ECC delivery to the lower plenum from the loops away from the break begins at a pressure of about 800 kPa. As discussed in Section 4.1.2, there were no transient full-scale tests which simulated B&W PWRs. However, because the steady-state full-scale test results for downcomer injection (with vent valves) were similar to the test results for cold leg injection, ECC delivery to the lower plenum for downcomer injection is expected to begin at approximately the same pressure. Thus, delivery to the lower plenum from the nozzle opposite the break begins at approximately 800 kPa. Delivery from the nozzle adjacent to the break begins later in the end-of-blowdown when the steam upflow is significantly reduced.

At the completion of blowdown, the lower plenum is filled almost to the bottom of the core barrel. Within a few seconds of the end of depressurization, the vessel is filled to the core inlet and refill is complete. Hence, refill and blowdown are overlapping rather than consecutive. Overlapping blowdown and refill reduces the time to core reflood, and therefore the adiabatic heat-up period. It was estimated in Reference U-460 that the reduction in cladding temperature at reflood initiation for overlapping blowdown and refill versus consecutive blowdown and refill is approximately 100 K (see Section 4.1.2).

Early Reflood (Accumulator Injection)

In the early portion of reflood, the downcomer water level increases rapidly due to the high ECC flow from the accumulators. Based on CCTF test results, the downcomer water level reaches the cold leg elevation resulting in water spillover out the broken cold leg. Heat release from the vessel wall is initiated as the downcomer fills. Tests and analyses show that this heat release does not cause vaporization of the downcomer water inventory because the subcooling of the water delivered to the vessel is sufficient to suppress boiling.

The downcomer water level increase drives water into the core. Steam generation in the core begins first at the bottom of the core as water enters the core from the lower plenum. However, within a few seconds, water entrained by the boiling process is distributed throughout the core and core cooling occurs at all elevations. In B&W lowered loop plants, stable water plugs can form in the intact cold legs which prevent steam flow through the intact loops. Thus, all of the steam generated in the core is vented through the vent valves to the downcomer and then out the break to containment. Some of the water in the upper core is carried by steam flow out of the core to the vent valves.

Initially, the core flooding rate is high and the collapsed water level in the core increases rapidly. When the downcomer water level reaches the cold leg elevation and water spills out the break, the core flooding rate decreases quickly. However, since the core steam generation is essentially the same as during early reflood, the reduction in the core flooding rate results in lower rates of water accumulation in the core and water carryover out of the core.

Water carried out of the core is either de-entrained in the upper plenum or carried with the steam through the vent valves to the downcomer. Water which is de-entrained in the upper plenum either accumulates as a two-phase mixture or falls back to the core.

Accumulator Nitrogen Discharge

When the water in the accumulators is depleted, the nitrogen that pressurizes the accumulators escapes through the ECC piping. Water in the top of the downcomer is pushed toward the break. The primary system (particularly the region into which the nitrogen is injected) is pressurized for a short time until the nitrogen escapes to containment. System pressure is further increased due to the suppression of steam condensation by the presence of the non-condensible nitrogen. The accumulation of uncondensed steam contributes to the temporary pressurization of the downcomer and cold leg regions of the primary system.

There were no full-scale nitrogen discharge tests with downcomer injection and vent valves; however, the phenomena discussed in Section 3.1 for PWRs with cold leg injection are applicable to B&W PWRs. Before the nitrogen discharge begins, the pressure above the core is higher than the pressure in the downcomer due to the steam flow through the vent valves. From tests without vent valves, it is known that the nitrogen discharge tends to pressurize the downcomer relative to the upper plenum. It is possible that the pressurization of the downcomer due to the nitrogen discharge temporarily closes the vent valves, although data in this regard are not available. Regardless of vent valve position, it appears that a portion of the water in the downcomer is forced into the lower plenum, displacing lower plenum water into the core. The magnitude of core water level increase with vent valves is not known.

Water in the lower plenum is subcooled, in part due to the rise in pressure. As the water surges into the core, heat is absorbed until, after a brief delay during which the water is heated to saturation, additional steam is produced. The increased steam production in the core increases the upper plenum pressure such that the upper plenum-to-downcomer pressure difference is re-established, and steam flow through the vent valves resumes. When this occurs, the core level decreases.

Late Reflood (LPCI) (see Figure 3.3.1-2)

As previously indicated, water carryover out of the core decreases prior to the termination of accumulator injection when the downcomer water level reaches the cold leg elevations. Later in reflood, however, water carryover out of the core increases as the quench front reaches the upper regions of the core. Reflood ends when the entire core is quenched.

The upper plenum water inventory, which was increasing during early reflood, decreases due to the reduction in water carryover from the core. In the downcomer, steam is condensed by subcooled ECC; however, due to the lower ECC flow (LPCI flow only), only a portion of the steam flow is condensed. The condensation efficiency is nearly 100%. The uncondensed steam vents to containment via the broken cold leg.

The steam flow around the downcomer reduces the water level in the downcomer by entraining water out the break. In UPTF, almost all of the water injected into the ECC nozzle adjacent to the broken cold leg was directly entrained out the break. (This phenomenon may be strongly dependent on nozzle position relative to the break and it is not clear that this will occur to the same extent in B&W PWRs.) Water injected into the ECC nozzle opposite the break penetrates into the downcomer and contributes to downcomer inventory; entrainment of this water is limited. Overall, the downcomer water level is similar to cold leg injection. Voiding due to heat release from the walls also reduces the downcomer water level. This reduction in downcomer level reduces the driving head for core reflood and therefore the core flooding rate.

However, as discussed in Section 4.2.2, calculations show that the increase in cladding temperature due to the level reduction is small (about 13 - 18 K--see Reference U-460).

Table 3.3.1-1

ECC SYSTEM DESIGN PARAMETERS FOR B&W PWRS

PWR Vendor/Class	Accumulators			HPCI		LPCI	
	Quantity	Pressure kPa (psia)	Water Volume per Accumulator m^3 (ft^3)	Number of Pumps	Pump Flow m^3/hr (gpm)	Number of Pumps	Pump Flow m^3/hr (gpm)
Babcock & Wilcox/2600 MWt[1]	2	4200 (615)	30 (1040)	3	114 (500)	2	680 (3000)

NOTE:

1. The reference reactor for a 2600 MWt B&W PWR is Crystal River Unit 3 operated by Florida Power Corporation; design parameters obtained from Reference E-513.

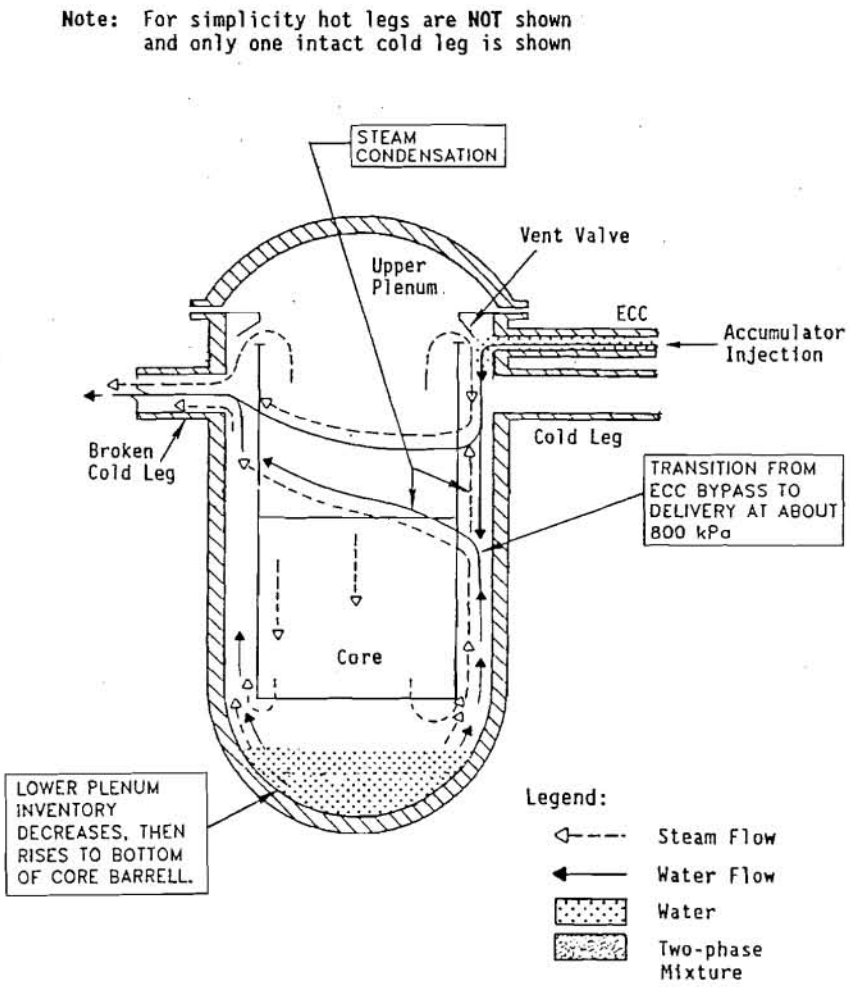

SUMMARY OF LBLOCA BEHAVIOR IN A B&W PWR END-OF-BLOWDOWN/REFILL

FIGURE 3.3.1-1

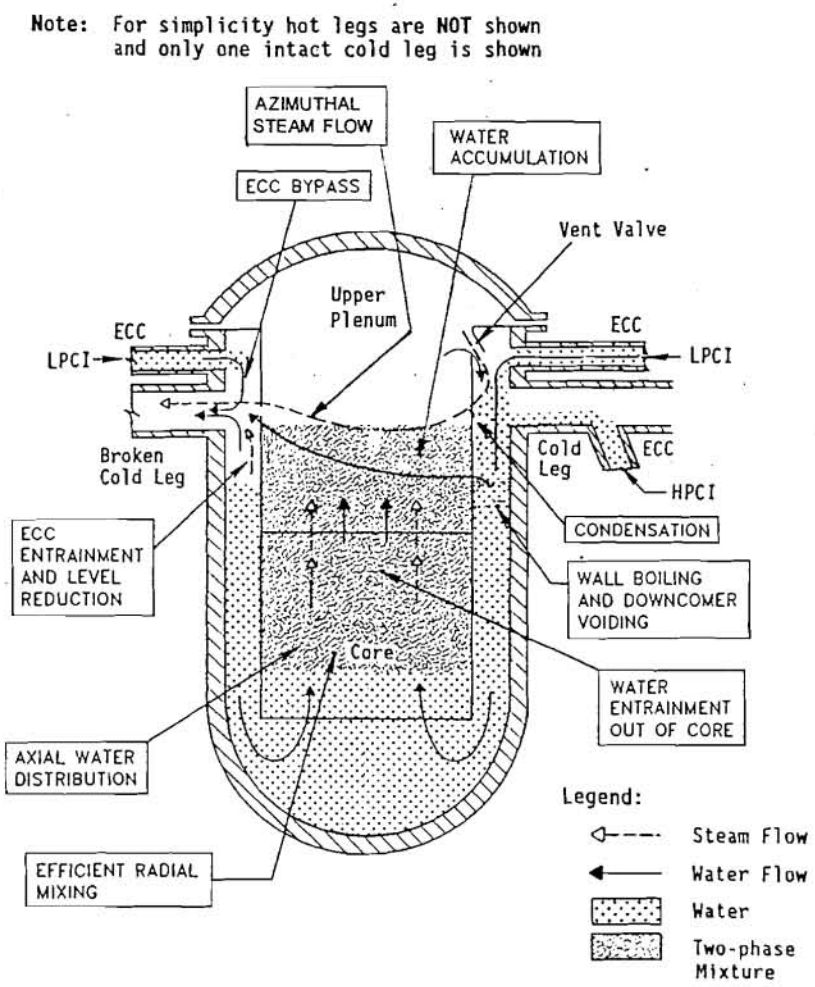

SUMMARY OF LBLOCA BEHAVIOR IN A B&W PWR REFLOOD

FIGURE 3.3.1-2

3.3.2 FRG Downcomer Injection Plant

The Muelheim-Kaerlich (MK) plant in the FRG, which was built by Brown Boveri Reactor (BBR--now Asea Brown Boveri or ABB), is a 2 x 4 loop PWR similar in design to a raised loop Babcock & Wilcox (B&W) PWR. Like B&W PWRs, the MK reactor vessel is equipped with vent valves in the core barrel to allow steam to vent directly from the upper plenum to the downcomer during a LOCA. The vent valves are located approximately 1 m above the hot leg nozzles.

The configuration of ECC system of the MK PWR is shown in Figure 3.3.2-1. The ECCS has four separate systems. Two of the systems inject ECC directly into the downcomer and two systems inject ECC into the loops. For each loop, ECC is injected into only one of the two cold legs. Each system consists of three types of injection; namely, high pressure coolant injection (HPCI), accumulator (ACC) injection, and low pressure coolant injection (LPCI). The primary system pressure at which the different types of injection initiate are listed below.

- HPCI 12,750 kPa
- ACC 4,200 kPa
- LPCI 1,300 kPa

Overall behavior in an ABB/BBR PWR during an LBLOCA is described below based on findings from 2D/3D tests and the results of a TRAC-PF1/MOD1 calculation for the MK PWR (Reference G-662). The discussion below is divided into the following time periods: blowdown, end-of-blowdown/refill, and reflood.

Blowdown

System behavior during blowdown was not investigated within the 2D/3D Program. This discussion is based on the results of other safety research programs, and the results of code analyses.

Upon initiation of the break, the pressure in the primary system decreases rapidly as the water inventory expands and fluid is discharged out the break. When the system pressure reaches saturation pressure (12,500 kPa), steam is produced by flashing and heat transfer in the core, and the rate of depressurization decreases. Steam produced in the core vents to containment by flowing through the vent valves to the downcomer and out the break. As the primary system inventory decreases, the lower plenum water seal is lost. This allows some of the steam in the core to flow around the bottom of the core barrel and up the downcomer to the break.

End-of-Blowdown/Refill (see Figure 3.3.2-2)

During the end-of-blowdown, the primary system is filled with steam except for the lower plenum which still contains some water. Steam in the reactor vents out the broken cold leg by flowing through the vent valves and around the downcomer to the break, and by flowing around the bottom of the core barrel and up the downcomer to the break. Based on UPTF tests, the steam flow through the vent valves constitutes 30-40% of the total steam flow (see Section 4.1.2).

When the primary system pressure decreases below 4,200 kPa the ACCs automatically start to inject ECC into the downcomer and cold legs. Steam condenses on the high flow of highly subcooled ECC. The high condensation rate reduces the system pressure and accelerates system depressurization. At the end of blowdown, the primary system pressure is actually lower than containment pressure; therefore steam flows into the primary system from containment.

The upflow in the downcomer initially entrains all the ECC flow directly out the broken cold leg (ECC bypass); however, as blowdown proceeds and the upflow decreases, bypass also decreases and ECC is delivered to the lower plenum. Per the UPTF tests, ECC injected adjacent to the break is largely bypassed during blowdown. Consequently, lower plenum refill is primarily due to delivery of ECC injected away from the break (see Section 4.1.2).

By the completion of blowdown, the lower plenum is filled to the bottom of the core barrel. A few seconds later, the vessel fills to the core inlet and refill is complete. Hence, the end-of-blowdown and refill are overlapping rather than consecutive. This reduces the time to core reflood and therefore the core heatup period. Consequently, cladding temperatures at reflood initiation are lower than for consecutive end-of-blowdown and refill. As indicated in Section 4.1.2, the reduction in cladding temperatures at reflood initiation is about 100 K.

Reflood (see Figure 3.3.2-3)

ECC flows down the downcomer to the lower plenum and into the core. Steam generation initiates at the bottom of the core as water enters the core. Quench propagation is therefore from the bottom up. Water entrained by the boiling process is carried to the upper regions of the core providing core cooling above the quench front. Overall, thermal-hydraulic behavior in the core is similar to that described in Section 3.1 for cold leg injection PWRs. However, the core flooding rate is higher than in cold leg injection PWRs because, as discussed below, the back pressure for venting steam from the core is lower.

Steam generated in the core is vented to containment via the upper plenum and either the vent valves or reactor coolant loops. Since the flow resistance of the reactor coolant pumps is large compared to the vent valves, most of the steam flows through the vent valves and only a small amount flows through the loops. Due to the low flow through the loops, the flow pressure drop for the steam venting from the core (i.e., system back pressure) is lower than for cold leg injection PWRs.

In the upper plenum, some of the water carried out of the core de-entrains and either falls back to the core or accumulates. The remainder of the water is either entrained by the steam flow through the vent valves or carried over to the loops. However, since the steam flow through the loops is small, carryover to the hot legs and steam generators is low.

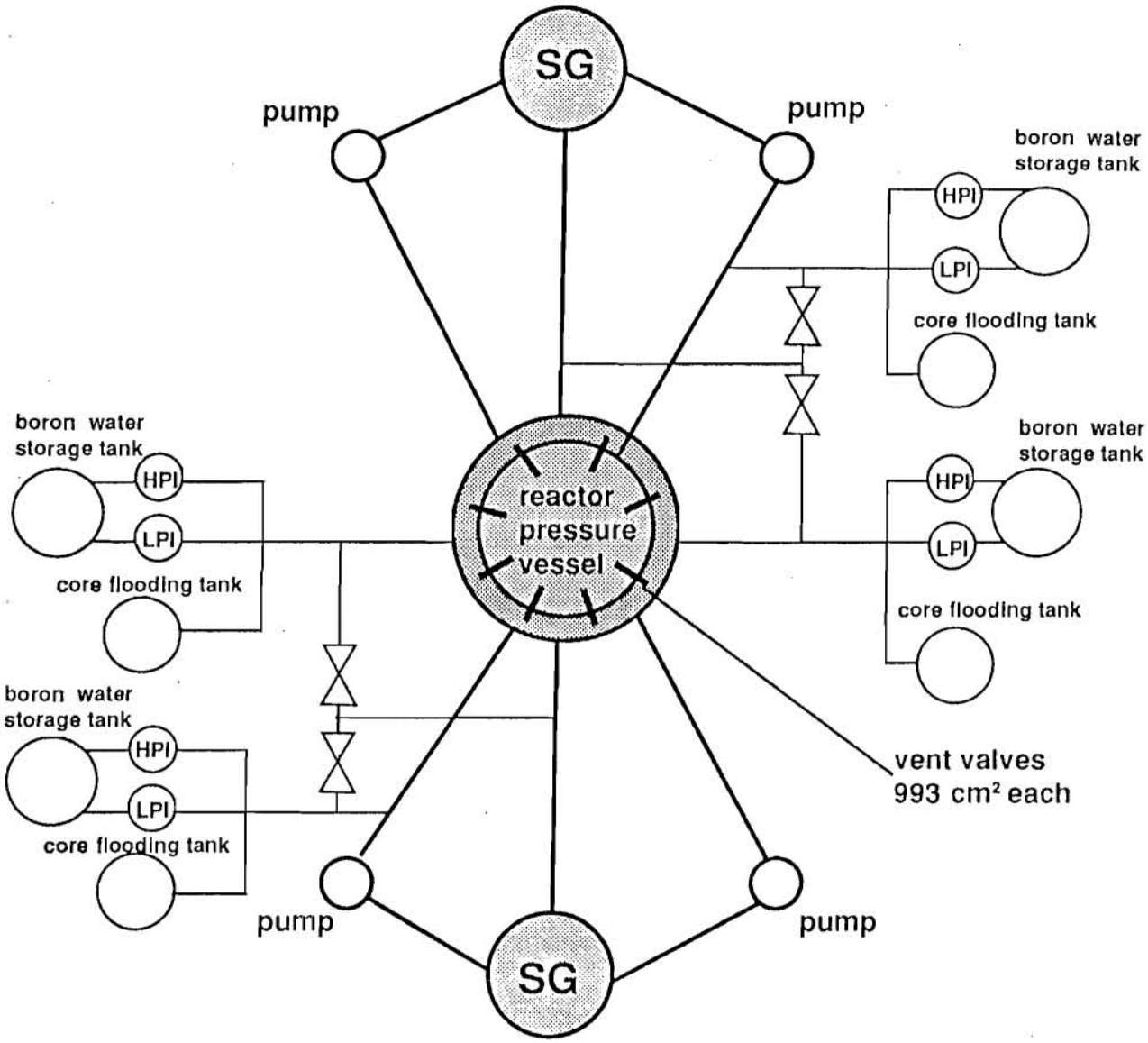

ECCS CONFIGURATION FOR MK PWR

FIGURE 3.3.2-1

Note: For simplicity hot legs are NOT shown
and only one intact cold leg is shown

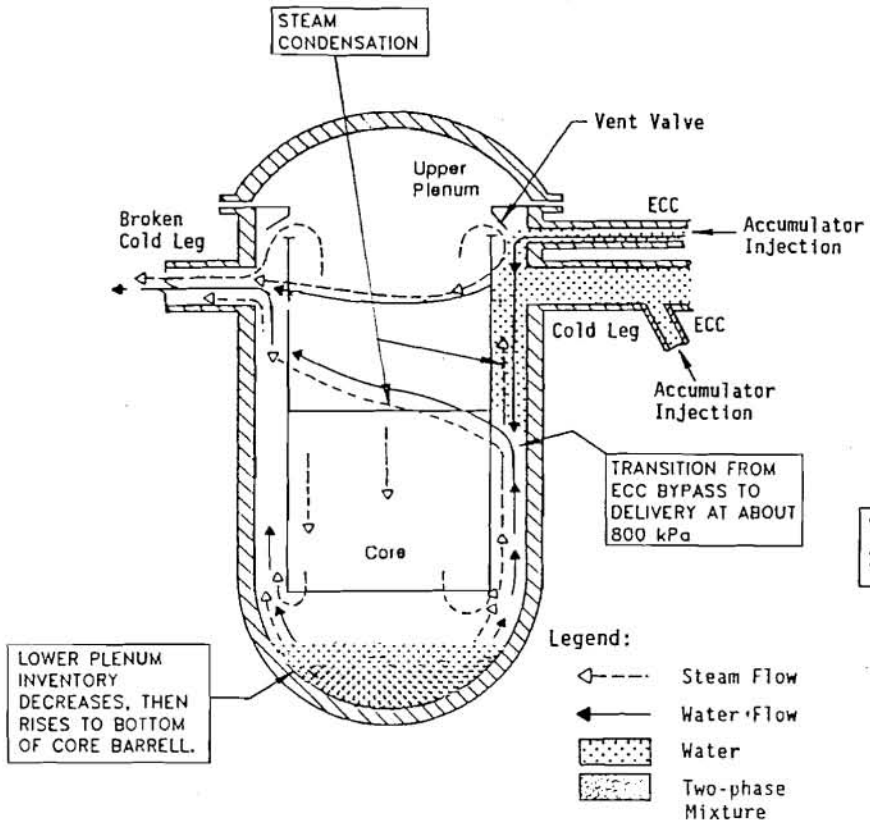

SUMMARY OF LBLOCA BEHAVIOR IN THE MK PWR
END-OF-BLOWDOWN/REFILL

FIGURE 3.3.2-2

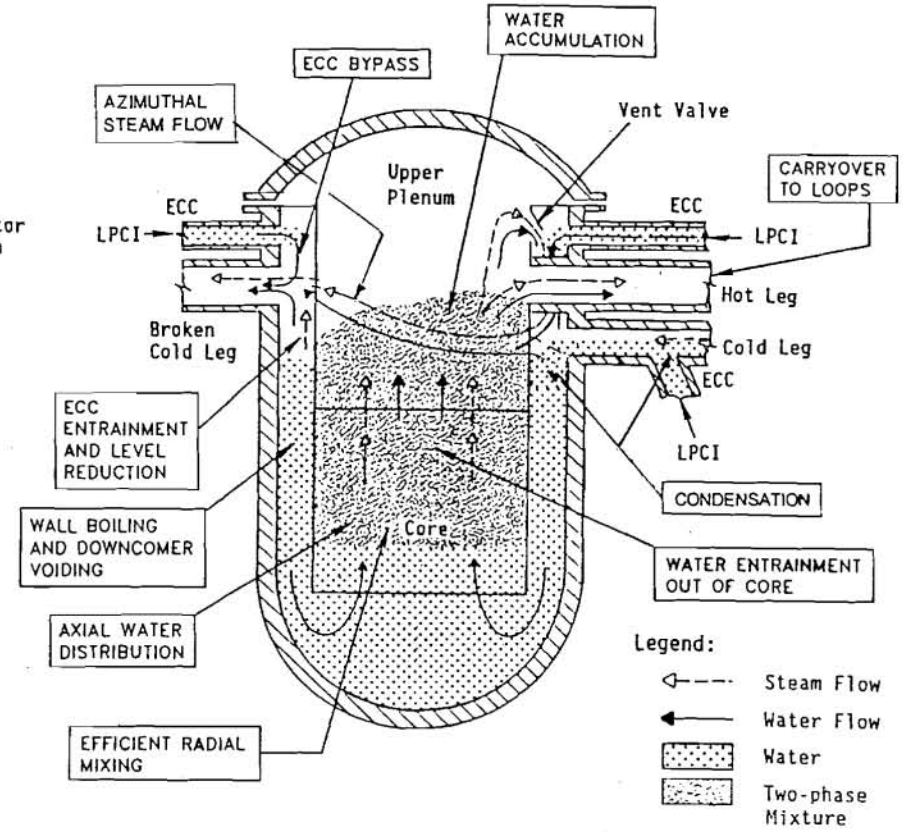

SUMMARY OF LBLOCA BEHAVIOR IN THE MK PWR
REFLOOD

FIGURE 3.3.2-3

3.3.3 Japanese Downcomer Injection Plant

Some Japanese PWRs with a power rating of about 500 MWe are equipped with downcomer injection-type ECCS. These PWRs have two reactor coolant loops with one hot leg and one cold leg per loop. Unlike the B&W and ABB/BBR PWRs with downcomer injection, these PWRs do not have vent valves in the core barrel.

As shown in Figure 3.3.3-1, the ECCS for these two-loop PWRs consists of accumulators, high pressure injection (HPI) pumps, and low pressure injection (LPI) pumps. The design parameters for each part of the ECCS are listed in Table 3.3.3-1. The LPI pumps inject water directly into the downcomer. The two injection nozzles are located on the side wall of the downcomer at about the cold leg elevation. Since each of the two LPI pumps are connected to both injection nozzles, ECC is injected symmetrically in both the no-LPI-pump failure case and the single-failure case. The ratio of the effective LPI flow rate to core power is approximately 20% higher than in four-loop PWRs.

The ACCs and HPI pumps inject ECC through nozzles in the cold legs. Each of the two ACCs is connected to both cold legs. Similarly, both HPI pumps inject ECC into both of the cold legs. The ratio of the effective ACC water volume to core power is approximately the same as in the four-loop PWRs.

The cold leg diameter and downcomer gap for these two-loop PWRs with downcomer injection are comparable to those of four loop PWRs. However, since the primary system volume is about half that of four-loop plants, the break area relative to system volume is larger in the two-loop PWRs.

System behavior in a two-loop PWR with downcomer injection is described briefly below. The description is divided into the following time periods: blowdown, end-of-blowdown/refill, early reflood, accumulator nitrogen discharge, and late reflood. The description of late reflood includes both evaluation model (EM) and best-estimate (BE) conditions.

Blowdown

System behavior during the blowdown portion of an LBLOCA for the two-loop downcomer injection PWR should be essentially the same as that for the four-loop cold leg injection PWR (see Section 3.1). However, as indicated above, the break area relative to the system volume is larger for the two-loop PWR. Consequently, the primary system pressure is expected to decrease faster in the two-loop, downcomer injection PWRs than in larger four-loop PWRs (i.e., blowdown is shorter).

End-of-Blowdown/Refill

When the primary system pressure has decreased below the ACC pressure, the ACCs automatically start to inject ECC into the cold legs. A water plug forms in the intact cold leg as the steam flow through the loop is condensed by the high flow of subcooled ECC. The water plug oscillates in the cold leg causing fluctuations in the flow of ECC into the downcomer. Shortly after the start of ACC injection when the primary system pressure has decreased further, the LPI system starts to inject ECC directly into the downcomer.

Initially, the two-phase (steam with entrained water) upflow in the downcomer entrains the ECC out the broken cold leg (i.e., ECC bypass); however, as blowdown proceeds and the upflow decreases, the bypass also decreases and ECC is delivered to the lower plenum. Lower plenum refill is initiated primarily by ACC injection into the intact cold leg. Since the LPI flow rate into the downcomer is small in comparison to the ACC injection into the intact cold leg, lower plenum refill behavior should be comparable to that for cold leg injection PWRs (see Section 3.1).

By the completion of blowdown, the lower plenum is filled almost to the bottom of the core barrel. Within a few seconds of the end of depressurization, the lower plenum water level reaches the core and refill is complete. Hence, refill and blowdown are overlapping rather than consecutive. This limits the cladding temperatures at reflood initiation by reducing the duration of the adiabatic heat-up period.

Early Reflood (Accumulator Injection)

In the early portion of reflood, the downcomer fills rapidly with subcooled water. The water level in the downcomer stabilizes at the cold leg elevation as water spills out the broken cold leg. This increase in downcomer water level forces water into the core. Steam generation initiates at the bottom of the core as water enters the core from the lower plenum; however, within a few seconds, water entrained by the boiling process is present throughout the core and core cooling is occurring at all elevations.

Steam and entrained water from the core enter the upper plenum where part of the water de-entrains and accumulates. Steam exits the upper plenum via the intact and broken loop hot legs. The steam which flows through the intact loop is completely condensed in the cold leg by the subcooled ECC injection.

Accumulator Nitrogen Discharge

Thermal-hydraulic behavior during ACC nitrogen discharge is expected to be the same as that described in Section 3.1 for cold leg injection PWRs. Specifically, the flow of nitrogen into the downcomer pressurizes the downcomer and suppresses condensation in the intact cold leg until the nitrogen is vented out the break. The

increase in downcomer pressure forces water from the downcomer into the core; however, this insurge of water increases steam generation in the core which pressurizes the upper plenum and forces water back into the downcomer.

Late Reflood (LPCI)

ECC injected into the cold leg and downcomer flows down the downcomer to the lower plenum and into the core. Due to the downcomer water level oscillations described below, the core flooding rate is oscillatory. The average core flooding rate, however, is nearly constant for the duration of the transient. Overall, thermal-hydraulic behavior in the core is similar to that described in Section 3.1 for cold leg injection PWRs.

Some of the water carried out of the core de-entrains and either falls back to the core or accumulates in the upper plenum, hot legs, and steam generator inlet plena. The remainder of the water carryover from the core is carried over to the steam generator U-tubes. Heat transfer from the secondary side vaporizes entrained water in the U-tubes; hence, flow in cold legs consists of single-phase, superheated steam.

In the intact cold leg, steam is condensed by the subcooled ECC injection; however, due to the reduction in ECC injection into the cold leg (HPCI versus ACC and HPCI), only a portion of the steam flow is condensed. The resultant flow regime in the intact cold leg is stratified with steam flow over the ECC flow to the downcomer.

The steam flow from the intact loop enters the downcomer where some of the steam is condensed by the ECC injection into the downcomer. Condensation is intermittent as U-tube oscillations of the core and downcomer water levels occur. When the downcomer water level is below the ECC injection nozzle, steam condensation increases due to good steam access to the ECC injection stream and subcooled water on top of the downcomer water column. Increased condensation reduces the pressure in the downcomer relative to the core pressure which forces water out of the core and into the downcomer. The increase in steam condensation also warms the top portion of the downcomer water column to near saturation. As the downcomer water level rises, steam access to the ECC injection stream is blocked by saturated water and condensation is reduced. The reduction in condensation increases the downcomer pressure which forces water from the downcomer back into the core and starts the cycle again (Reference J-973). The character of this oscillation is influenced by the vertical position of the downcomer injection nozzles slightly below the cold leg nozzles.

Overall, condensation in the two-loop downcomer injection PWRs is low because contact between steam and the LPCI flow is limited; consequently, ECC accumulating in the downcomer is still subcooled. The subcooling is sufficient to suppress downcomer voiding.

The downcomer water level and condensation oscillations described above are expected to occur only for the single-failure case. In the no-failure case, complete condensation of the steam flow from the intact cold leg into the downcomer is expected.

Table 3.3.3-1

ECC SYSTEM DESIGN PARAMETERS FOR JAPANESE PWRS WITH DOWNCOMER INJECTION

Accumulators			HPCI		LPCI	
Quantity	Pressure kPa	Water Volume per Accumulator m^3	Number of Pumps	Pump Flow m^3/hr	Number of Pumps	Pump Flow m^3/hr
2	5000	35.4	2	160	2	454

NOTE:

1. The reference PWRs are the reactors at Tomari Nuclear Plant Units 1 and 2; design parameters obtained from Reference E-515.

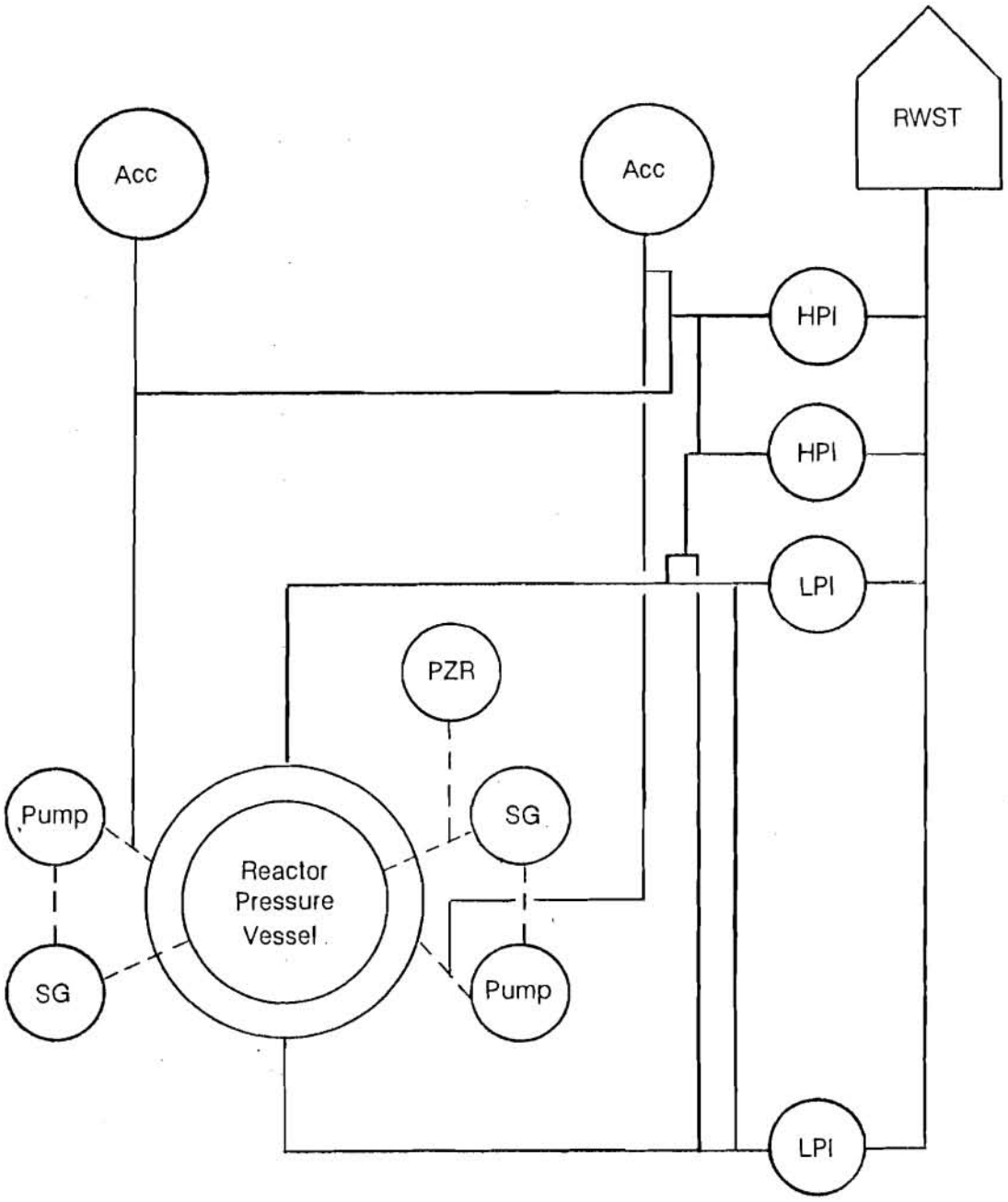

SG	Steam Generator
PZR	Pressurizer
RWST	Refueling Water Storage Tank
Acc	Accumulator
HPI	High Pressure Injection Pump
LPI	Low Pressure Injection Pump

ECCS CONFIGURATION FOR JAPANESE PWR'S
WITH DOWNCOMER INJECTION

FIGURE 3.3.3-1

3.4 UPPER PLENUM INJECTION (UPI) PLANT

In some two-loop PWRs in the US and Japan, low pressure coolant injection (LPCI) is into the upper plenum, rather than into the cold legs as in three- and four-loop plants. Except for the LPCI injection location, the ECC system configuration and injection sequence at these PWRs are similar to that described in Section 3.1 for cold leg injection PWRs.

Blowdown, Refill, Early Reflood and Accumulator Nitrogen Discharge

Early in the LBLOCA transient, until the accumulator (ACC) water inventory is depleted, system behavior in an upper plenum injection (UPI) PWR is similar to that for a cold leg injection PWR. This is because ACC injection is into the cold legs in both types of plants, and the ACC injection rate is much higher than the LPCI flow rate. Accordingly, the behavior during the blowdown, end-of-blowdown/refill, and early reflood phases is similar to that described in Section 3.1. The only significant difference is that some upper plenum accumulation and cooling of the rods near the top of the core occurs due to the LPCI flow into the upper plenum during refill and early reflood. The effects of accumulator nitrogen discharge in a UPI plant are also expected to be the same as those in a cold leg injection plant (see Section 3.1), since the locations, timing, and relative amounts of nitrogen discharge are similar.

Late Reflood

The late reflood (LPCI) period, after depletion of accumulator inventory, is qualitatively different in a UPI PWR. Figure 3.4-1 shows the hydraulic behavior in a UPI plant during the late reflood period. The most notable characteristic is that ECC enters the core from the top and the net flow rate at the bottom of the core is negative (toward the downcomer). A positive flow rate (flow from the downcomer to the core) is the flooding mechanism for plants with cold leg injection. Even though flow directions are different for the two types of injection, there is similar liquid accumulation in the core which provides global core cooling; i.e. the net core flooding rate is similar to that for cold leg injection.

ECC water flows from the upper plenum down to the core in a local region, covering about 10% of the core. The size of the downflow region in a UPI plant is determined by interpolating between CCTF (subscale) and UPTF (above full-scale). UPTF results show there is a small amount of subcooling (10 - 15 K) in the downflow. The downflow region is beneath the ECC injection nozzle and does not change during the transient. CCTF results show that the initial downflow partially quenches the rods in the downflow region so that less steam is generated in that region for the remainder

of the transient, and, consequently, there is less resistance to water downflow. Near the top of the core in the downflow region, core cooling is enhanced by the downflowing water. In other core regions, an upflowing steam/water mixture provides cooling, comparable to that in cold leg injection PWRs.

Subcooled injection water and steam generated in the core mix completely in the upper plenum and the top of the core, leading to significant steam condensation. Based on UPTF data with an extensive network of thermocouples, it appears most or all of the mixing occurs in the upper plenum. As discussed above, this means that water delivered to the core has a small amount of subcooling. The major result is that the amount of steam which needs to be vented through the loops to containment is decreased by condensation. For a single-failure LPCI assumption, the injected water condenses about 40% of the steam produced in the core at the beginning of reflood, and a higher fraction as the core heat release decays. For a no-failure LPCI assumption, the steam flow is entirely condensed.

In the upper plenum, accumulation of water to a steady-state inventory occurs quickly; i.e., within several seconds after start of reflood. UPTF results show that the water distribution across the flow area is uniform except at the breakthrough region where more water accumulates. The differential pressure resulting from water accumulation is a small fraction of the total loop differential pressure.

In a UPI plant, a larger fraction of the injected water is carried over to the hot legs and steam generators, in comparison to a cold leg injection plant. The result is that more water is vaporized in the steam generators, contributing to the steam binding effect which degrades core cooling. Thus, the UPI configuration has two opposing effects on steam binding; condensation in the upper plenum (discussed above) reduces the amount of steam flowing through the loops, while liquid carryover to the steam generators increases the steam flow rate. CCTF results indicate the net effect is a benefit (less resistance to steam venting) compared to a cold leg injection configuration. In the PWR, the carryover rate is expected to be less, and the condensation rate the same, as in CCTF (based on scaling effects as deduced from comparison of CCTF and UPTF results) so the net effect of UPI in a PWR should be less steam binding.

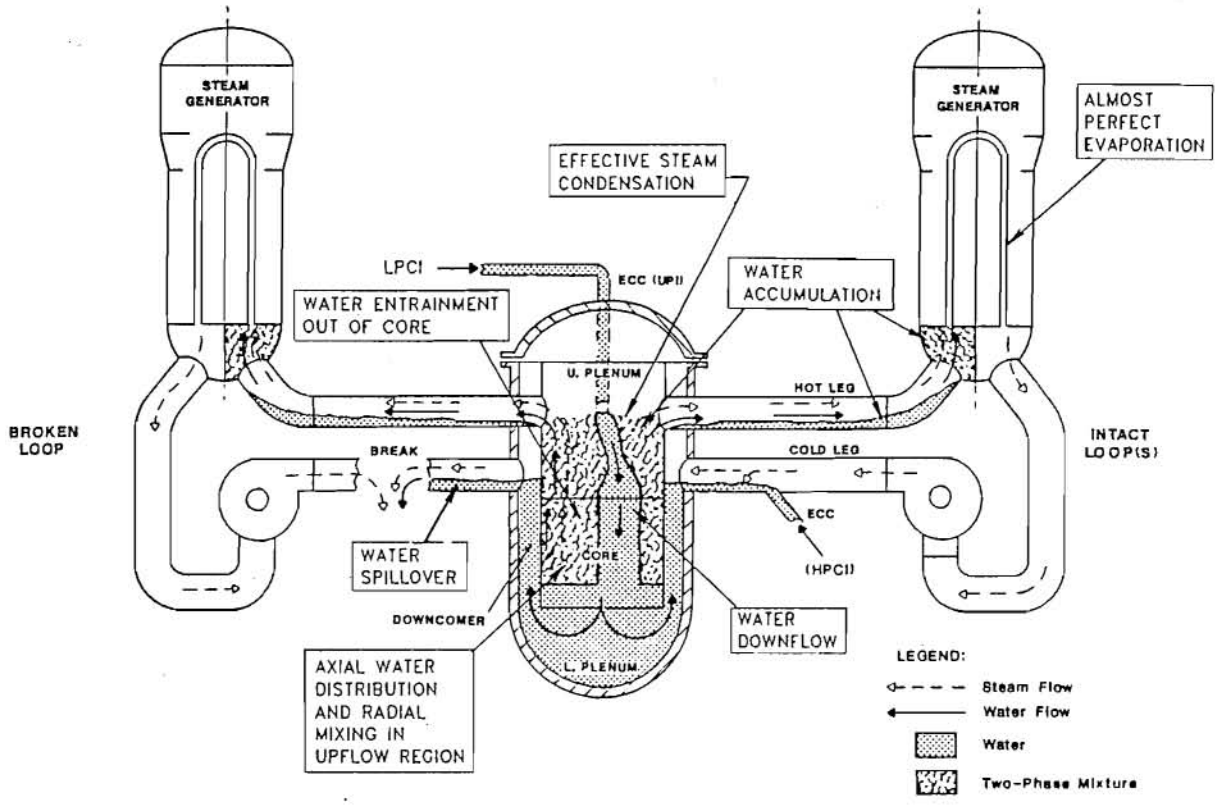

SUMMARY OF LBLOCA BEHAVIOR IN A UPI PWR LATE REFLOOD

FIGURE 3.4-1

Section 4

EVALUATION OF TESTS AND ANALYSES TO ADDRESS KEY REACTOR SAFETY ISSUES

This section summarizes the evaluations of the experimental and analytical results of the 2D/3D Program to address various reactor safety issues. Each issue is covered individually in the manner shown in Figure 4-1. For each issue the phenomena and their importance are defined, tests and analyses related to the issue are identified, and the conclusions and applications to the PWRs are discussed. Each issue is discussed in a separate section. For issues relevant to PWRs with different ECCS configurations, the application of the test and analysis results to PWRs are covered in separate subsections by ECCS configuration. These separate subsections also include technical findings and conclusions which are specific to a given ECCS configuration.

4.1 ECC DELIVERY TO LOWER PLENUM DURING DEPRESSURIZATION

Definition of Issue and Description of Phenomena

In a large, cold leg break LOCA at a PWR, most of the initial contents of the reactor coolant system are rapidly expelled through the break. A two-phase mixture of flashing and entrained fluid is forced up the downcomer and out the broken cold leg, as the pressure in the primary system decreases from its initial value of 15,500 kPa to an "equilibrium" value of 200 - 400 kPa, which represents the equilibrium pressure between the primary system and containment. When the pressure has decreased to a predetermined value in the range of 1,400 - 4,600 kPa, depending on plant design, the accumulators begin to automatically inject ECC into the reactor coolant system. The purpose of this ECC is to rapidly refill the reactor vessel lower plenum and start reflooding the reactor core.

When the accumulator ECC (which is highly subcooled) is first injected, the system is still blowing down. During the end-of-blowdown (EOB), the steam/water flow path is up the downcomer and out the broken cold leg nozzle (see Figure 4.1-1). The two-phase upflow may entrain some or all of the ECC injected into the cold legs and/or downcomer directly out the broken cold leg. This is referred to as "ECC bypass". As blowdown proceeds and the downcomer upflow decreases, the bypass also decreases and ECC can be delivered, allowing some initial filling of the lower plenum.

In PWRs with combined injection, ECC injected into the hot legs is delivered to the lower plenum via the upper plenum and core. When the steam flow around the bottom of the core barrel to the downcomer is high, a substantial part of the water downflow which reaches the lower plenum is entrained out the break. However, as the steam flow decreases, entrainment decreases and delivery increases. The water downflow through the core initiates core cooling during end-of-blowdown (see Section 4.6.3).

The "refill" phase of the LOCA starts with the initiation of ECC accumulation in the lower plenum and lasts until the reactor vessel water level reaches the bottom of the core. During this phase, the reactor vessel average wall temperature tends to be near its full power value of 560 K; hence, steam generation on the hot walls can contribute to the overall steam flow up the downcomer.

Importance of Issue to PWR LOCA

The rapid depressurization of the reactor vessel and the resulting two-phase flow in the lower plenum and downcomer tend to prevent the accumulation of ECC in the lower plenum. The interaction of the steam/water flow in the lower plenum and downcomer is important since it affects how quickly the reactor vessel refills. Specifically, for cold leg or downcomer injection, ECC delivery to the lower plenum is

controlled by the countercurrent flow limitation in the downcomer. However, for hot leg injection, ECC accumulation in the lower plenum is controlled by entrainment by the steam flow around the bottom of the core barrel. Higher ECC delivery and accumulation during the blowdown phase reduces the duration of the refill phase, limiting the clad temperature at the beginning of reflood.

Tests and Analyses that Relate to the Issue

ECC delivery to the lower plenum during blowdown has been investigated in numerous transient and quasi-steady tests both in the 2D/3D Program and elsewhere. The transient tests evaluated the transient progression of phenomena under typical PWR conditions at the EOB and the quasi-steady tests evaluated downcomer countercurrent flow under controlled conditions. Table 4.1-1 lists only the tests considered in this report. In the 2D/3D Program, tests were performed at UPTF and CCTF to investigate ECC delivery at large-scale. The UPTF tests included tests with cold leg ECC injection, downcomer ECC injection, and combined ECC injection. The cold leg ECC injection tests consisted of Tests 4A and 5A which were transient EOB simulations, and Tests 5B, 6, and 7 which were quasi-steady tests. The downcomer ECC injection tests consisted of Tests 21A, 21B, and 22 which were quasi-steady tests, and Test 24 which was a transient test. The combined injection tests included Tests 3, 18, 19, and 28 which were transient tests. In CCTF, three cold leg injection transient tests (C2-11, C2-14, and C2-17) and three combined injection transient tests (C2-19, C2-20, and C2-21) simulated EOB/refill conditions.

Outside the 2D/3D Program, several small-scale tests with various geometries and flow conditions have been performed (see Reference E-401). Table 4.1-1 lists the facilities that are included in the scale comparisons presented in this report.

The evaluations of the UPTF cold leg injection tests and downcomer injection tests, including comparisons to subscale tests are provided in References U-455 and U-460, respectively. Evaluation of the UPTF combined injection tests is covered in Reference G-411. The major results of these evaluations and comparisons are summarized below.

Several post-test TRAC calculations of the UPTF tests have also been performed (References U-711 and U-715). These have included TRAC-PF1/MOD1 calculations of all UPTF Test 6 runs (Reference E-611), and TRAC-PF1/MOD2 calculations of UPTF Test 4A; Test 5A; Test 6, Run 133; and Test 7, Runs 200 and 201; Test 21A; and Test 22A (see Appendix B).

Summary of Key Results and Conclusions from Tests and Analyses

The following discussion focuses on the tests and analyses in which ECC was injected into only the cold legs and is applicable to PWRs with cold leg injection, cold

leg/downcomer injection, and combined injection. Application of these results to PWRs are covered in the following subsections by ECCS configuration. The subsections on downcomer injection (Subsection 4.1.2) and combined injection (Subsection 4.1.3) also cover tests and analysis results specific to these ECCS configurations.

The results of the full-scale UPTF tests have shown multidimensional phenomena in the downcomer not previously observed in small-scale tests. The steam upflow and the calculated ECC delivery to the lower plenum for the quasi-steady UPTF tests with cold leg injection are plotted in Figure 4.1-2. This plot shows that delivery characteristics are very different between the loop near the break (Loop 1) and the loops away from the break (Loops 2 and 3). Specifically, ECC injected into the loop near the break was mainly bypassed while ECC injected in the loops away from the break was delivered to the lower plenum. Contour plots of fluid temperature measurements (i.e., subcooling) in the downcomer are consistent with these observations (see Figure 4.1-3). Based on the delivery data in Figure 4.1-2 and fluid temperature contour plots, Siemens identified the following flow regimes for ECC delivery in UPTF (Reference G-907).

- Complete bypass from Loop 1 with partial delivery from Loops 2 and 3 for high steam flows (>320 kg/s).

- Complete bypass from Loop 1 and nearly complete delivery from Loops 2 and 3 for intermediate steam flows ($\geq$100 kg/s and $\leq$320 kg/s).

- Partial delivery from Loop 1 and complete delivery from Loops 2 and 3 for low steam flows (<100 kg/s).

Several methods have been proposed to correlate these UPTF flooding data. Each method is discussed briefly below.

- The Siemens analysis (Reference G-907), discussed above, identified three different flow regimes for countercurrent flow in the downcomer. These analyses indicated that ECC delivery from Loops 2 and 3 appears to be injection limited for steam flows up to 320 kg/s. This suggests that the UPTF data do not reveal the true countercurrent flow limitation at steam flows less than 320 kg/s and leads to a representation of UPTF flooding characteristics as a three-region curve (see Figure 4.1-2).

- The correlation proposed by H. Glaeser includes a term for the proximity of each ECC injection location to the broken cold leg to account for the multidimensional behavior observed in the tests (see References G-415 and G-915). This term is applied to steam flow (K^*_g) for each cold leg, resulting in a lower effective, dimensionless steam upflow at the loops away from the break, and therefore

higher ECC delivery from these loops. Similarly, for the cold leg near the break, the effective steam flow is higher, and ECC is more easily bypassed. The correlation is plotted in Figure 4.1-4.

- MPR calculated a simple best-fit correlation of the UPTF data using the j^* parameter (Reference U-455). Separate correlations were done for runs with Loop 1 injection only and runs with uniform injection to all three loops. The resulting curves are shown on Figure 4.1-5. Since some of the data are injection-limited, the correlation is not a CCFL correlation; however, the correlation is considered a useful tool for the comparison and application evaluations discussed in Reference U-455.

Although UPTF has provided the only full-scale test data on this issue, a large body of data has been obtained from small-scale tests, particularly from the Creare and Battelle Columbus Laboratory facilities (References E-417, E-001 through E-004, E-414, and E-420). The principal effort of these small-scale tests was to evaluate the effect of various downcomer flooding parameters on countercurrent flow limitation (CCFL) curves, at different facility scales. CCFL curves determined from the Battelle and Creare facilities were presented in RIL-128 (Reference E-412).

The previous evaluation of the small-scale data from Creare and Battelle Columbus Laboratory (Reference E-412) recommended using momentum flux scaling (i.e., using the Kutateladze parameter or K^*, to scale the complete bypass point) for applying small-scale results to full-scale. However, the full-scale UPTF data indicate that Wallis parameter (j^*) scaling may be more appropriate. The calculated steam velocity, j^*_g at a given delivery rate, j^*_f is plotted versus the scale factor for UPTF and the five Creare and Battelle subscale facilities on Figure 4.1-6. The two plots show the calculated steam upflow (j^*_g) that would allow delivery rates (j^*_f) of 0.0125 (500 kg/s at full-scale) and 0.025 (1000 kg/s at full-scale) for a given injection rate ($j^*_{f,in}$ of 0.037, or 1500 kg/s at full-scale). The calculated j^*_g's for the subscale facilities were obtained using the correlation and constants from Reference E-412; the UPTF values were calculated using the best-fit correlation shown in Figure 4.1-5. Note that the j^*_g value for 500 kg/s delivery at UPTF is from the CCFL-limited portion of the data, while that for 1000 kg/s delivery may be artificially low because delivery may have been injection-limited. As shown in the figure, the steam flow at full-scale for the given delivery rates is better predicted by constant j^* scaling than constant momentum flux scaling; hence, j^* scaling may be more appropriate for predicting ECC delivery at full-scale (Reference U-455).

UPTF Test 4A was a transient test which simulated the EOB and refill phases of a LOCA. The pressure and lower plenum mass inventory transients for this test are shown in Figure 4.1-7. In terms of ECC delivery and bypass, two important characteristics of the transient were identified. First, ECC delivery behavior occurred in two distinct phases: an initial period of very high two-phase downcomer upflow with

little ECC delivery and rapidly decreasing lower plenum inventory, then quickly changing to a period of high, probably injection-limited, ECC delivery. The transition between these periods occurred at a relatively high pressure (about 800 to 1200 kPa), well before the end of the blowdown phase). Second, the lower plenum inventory deficit was rapidly recovered, and by the time blowdown was complete, the lower plenum was filled almost to the bottom of the core barrel. The liquid level could not be higher than the bottom of the core barrel since a flow path from the core to the downcomer is required during blowdown.

Figure 4.1-7 also compares UPTF Test 4A with EOB/refill transients for open loop tests at CCTF (CCTF Tests C2-14 and C2-17). The lower plenum mass is scaled up to UPTF using the lower plenum volume scale factor. Note that although the initial pressure for the tests is different, blowdown is completed for all tests at approximately the same time (19 to 24 seconds). More importantly, however, the location of the mass turnaround point (the time at minimum lower plenum inventory) relative to the pressure transient is very different for UPTF and the CCTF tests. Specifically, this point occurs high on the pressure transient curve in UPTF (about 800 kPa), but almost at the end of the transient at CCTF (about 200 to 300 kPa). This key difference was also observed in comparisons of blocked loop tests (including UPTF Test 5A with Creare 1/5-scale Test 9066, and CCTF Test C2-11--Reference U-455).

Although the mass turnaround point occurs earlier in UPTF, the general shape of the inventory transient is similar for all tests: before the turnaround, mass is lost from the lower plenum very quickly, but after, ECC delivery increases rapidly and may even be injection limited. This indicates that the period of partial delivery of ECC may be very brief (for the loops away from the break) and that large uncertainties in the flooding curve may have little effect on the rate of water accumulation in the lower plenum when applied to estimating the EOB/refill transient. However, predicting the detailed time history of lower plenum refill (e.g., initiation of delivery) depends on the accuracy of the flooding curve.

Post-test TRAC calculations of the quasi-steady UPTF tests were performed using both MOD1 and MOD2. The MOD2 calculations predicted the multidimensional behavior observed in the tests when adequate model noding was used. Specifically, a model with eight azimuthal sectors, rather than four, was required to suitably predict multi-dimensional behavior. In the MOD2 calculations, the predicted delivery was greatly improved over MOD1 calculations. This improvement in the prediction of ECC delivery with MOD2 is shown in Figure 4.1-8 which compares the ECC delivery rates calculated with MOD1 and MOD2 with the UPTF test data.

Post-test TRAC-PF1/MOD2 calculations of the transient UPTF tests predicted the key characteristics of these transients. Specifically, TRAC predicted an initial period of high downcomer upflow with little ECC delivery and decreasing lower plenum inventory which quickly changed to a period of high ECC delivery. Also, TRAC predicted that

the lower plenum was filled by the end of depressurization, which is consistent with the test data.

4.1.1 Cold Leg Injection

Two important implications for US/J PWRs arise from the UPTF countercurrent flow test results. Delivery occurs first at loops away from the break and, a short time later, from the loop near the break. The transition from very low to very high ECC delivery also occurs quickly (for the loops away from the break), and little time is spent on the partial delivery portion of the CCFL curve. Thus it appears knowledge of the full-scale CCFL curve with a high degree of certainty is not a requirement for accurate, best-estimate, EOB/refill predictions. In addition, the full-scale results appear to be better predicted by j^*, rather than K^*, scaling from small-scale results, which gives a more favorable full-scale ECC delivery (Reference U-455).

Second, the mass turnaround point (i.e., the beginning of refill) during the EOB/refill transient occurs well before the primary system is completely depressurized. Because of this, UPTF test results indicate that the lower plenum was essentially refilled to the bottom of the core barrel by the time the primary system pressure equalized with containment. In a PWR best-estimate calculation, allowing the lower plenum to be refilled by the end of the blowdown phase reduces the core adiabatic heat-up time before the beginning of the reflood phase. Assuming an overlapping blowdown and refill reduces the time to core reflood by about 10 seconds over a consecutive blowdown and refill. This reduces clad temperatures at the beginning of reflood by about 100K (Reference U-455). Similar reductions in the overall peak clad temperature would also be expected. This indicates the conservatism in the assumption that refill is not initiated until blowdown is complete.

Several key differences, however, may have an effect on the applicability of these UPTF results to PWRs. These differences include:

- Cold Leg Arrangement - Wider cold leg spacing than in UPTF (which has loops spaced at 45° and 135° intervals like a Westinghouse plant) may result in different bypass/delivery behavior from the loop near the break. With wider spacing (such as in the reference Combustion Engineering plant with 60° x 120° spacing), delivery from the loop near the break may be enhanced.

- Thermal Shield - No thermal shield was present in the UPTF downcomer. A "pad" type shield is estimated to reduce the downcomer flow area by about 10%, increasing superficial velocities by a similar amount. For a cylindrical shield, however the flow area blockage and superficial velocity increase is about 30%. While such an increase in velocity could reduce ECC delivery, the cylindrical shield could also create two flow channels, separating the upward and downward flows, and possibly improving delivery.

- ECC Flow Rate - In the UPTF tests with ECC injection to three loops, the flow rate was about 500 kg/s per loop. However, the typical ECC injection rate at the end of the accumulator discharge period is about 700 kg/s per loop for 3400 MWt class Westinghouse PWRs and about 970 kg/s per loop for Combustion Engineering System 80 PWRs. Because more steam can be condensed at the higher ECC flow rates, delivery would be higher, and the UPTF results are conservative.

The conclusion is that the UPTF results are representative of PWR behavior, although downcomer configuration differences (such as cylindrical thermal shield) must be considered in applying these results (Reference U-455).

The ability of TRAC-PF1/MOD1 to predict ECC delivery to the lower plenum for cold leg injection PWRs was evaluated as part of the USNRC's Code Scaling, Applicability, and Uncertainty (CSAU) study. The evaluation was based largely on the analyses of UPTF tests. While MOD1 significantly underpredicts delivery to the lower plenum (see Section 4.1), the CSAU study determined that the impact of the poor prediction of delivery on the prediction of PCT was small. Specifically, it was estimated that TRAC-PF1/MOD1 overpredicts PCT by as much as 19 K due to underpredicting ECC delivery to the lower plenum (Reference E-611).

4.1.2 Downcomer Injection

The results of the UPTF tests with downcomer injection revealed multidimensional characteristics of ECC delivery similar to that observed in the cold leg injection tests. The core simulator steam injection rate and calculated ECC penetration rate for the downcomer injection tests are plotted in Figure 4.1-9. The plots show that ECC injected through the nozzle near the break (Nozzle 1) was largely bypassed while ECC injected through the nozzle away from the break (Nozzle 2) penetrated down the downcomer. For example, in an open vent valve test with a steam flow of 100 kg/s and an ECC injection rate of 900 kg/s, the penetration rate for injection into Nozzle 1 was near zero while the penetration rate for injection into Nozzle 2 was 750 kg/s. Fluid temperature contour plots also show this multidimensional behavior (see Figure 4.1-10).

For downcomer injection with the vent valves open, the delivery rate was essentially constant for all steam flows tested, indicating that countercurrent flow limitation (CCFL) conditions were not reached during the tests (see Figure 4.1-9). The delivery rate for injection to Nozzle 2 only was similar to the delivery rate for injection to both nozzles, again confirming that ECC injected adjacent to the break was bypassed and ECC injected opposite the break was delivered. Highly subcooled ECC injection had little effect on the ECC delivery rate, for two reasons: (1) the vent valves provided a noncountercurrent flow path for steam, reducing the potential for condensation; (2) CCFL conditions were apparently not reached, so any reduction in steam upflow had little effect on ECC delivery. Finally, increased ECC injection velocity (due to the installation of thermal sleeves in the downcomer injection nozzles) had no appreciable effect on ECC delivery.

For downcomer injection with the vent valves locked shut, the ECC delivery rate was substantially affected by the steam injection rate, indicating that CCFL conditions were reached during these tests (see Figure 4.1-9). As shown in Figure 4.1-9, ECC delivery with closed vent valves was lower than with open vent valves. This difference in ECC delivery is due to differences in the amount of steam upflow in the downcomer and the steam flow pattern in the top of the downcomer. Specifically, with the vent valves open, the steam upflow was lower because about 1/3 of the steam injection flowed through the vent valves. The vent valve steam flow created a circumferential flow in the downcomer which appeared to reduce/redirect downcomer upflow and facilitate ECC delivery. Finally, Figure 4.1-9 indicates that, for closed vent valves, highly subcooled ECC injection produced much higher delivery than saturated ECC.

Figure 4.1-9 includes the results of the UPTF downcomer countercurrent flow tests with cold leg injection. Comparison of the cold leg injection tests to the downcomer injection tests indicates that ECC delivery for downcomer injection with closed vent valves was significantly less than for cold leg injection. However, delivery for

downcomer injection with open vent valves was comparable to cold leg injection over the range of conditions tested.

Post-test analyses of the quasi-steady UPTF tests with downcomer injection were performed using TRAC-PF1/MOD2. The tests analyzed included tests with closed vent valves (Test 21A) and open vent valves (Test 22A). ECC delivery to the lower plenum was significantly underpredicted for Test 21A (closed vent valves) and well predicted for Test 22A (open vent valves); however, since countercurrent flow conditions exist for only a short period of time, poor prediction of ECC downflow does not significantly affect the overall prediction of the EOB transient (Reference U-715).

Transient behavior during end-of-blowdown (EOB)/refill was investigated in an integral test at UPTF (Test 24). This test simulated an ABB/BBR PWR with accumulator injection into the downcomer and cold legs. The test results indicate that the lower plenum was filled to the bottom of the core barrel by the completion of blowdown; i.e., blowdown and refill overlapped. This is a beneficial result with respect to core cooling. Specifically, relative to a consecutive blowdown and refill, an overlapping blowdown and refill reduces the core adiabatic heat-up time before reflood initiation and therefore the cladding temperatures at reflood initiation. Comparison of the test results with a TRAC analysis of an ABB/BBR PWR indicates that the reduction in cladding temperatures at reflood initiation is about 100 K.

The UPTF tests did not investigate transient EOB/refill behavior in a Babcock & Wilcox (B&W) PWR with accumulator into only the downcomer. However, as indicated above, downcomer injection with vent valves provided ECC delivery comparable to cold leg injection. This suggests that transient behavior with downcomer (only) injection and vent valves would be similar to that observed in the transient EOB/refill tests with cold leg injection. As previously discussed, the lower plenum was filled to the bottom of the core barrel prior to the end of depressurization in the cold leg injection tests. Reference U-460 estimated the reduction in cladding temperature for an overlapping EOB and refill relative to a consecutive EOB and refill to be 100 K for a B&W PWR.

Two differences between UPTF and ABB/BBR and B&W PWRs may influence the applicability of the full-scale test results (Figure 4.1-11):

- Cold Leg Arrangement - The UPTF cold legs are spaced in a 45° x 135° arrangement around the downcomer circumference while the ABB/BBR and B&W cold legs are spaced in a 60° x 120° arrangement. In both configurations, the ECC injection nozzles are located between adjacent cold legs, so one ECC nozzle is always in close proximity to the broken cold leg; however, the nozzle is closer in UPTF than in ABB/BBR and B&W PWRs. Delivery from the nozzle near the break could be enhanced somewhat in PWRs relative to UPTF.

- Vent Valve Flow Area - While the vent valves in UPTF and ABB/BBR and B&W PWRs are identical in size and number, the two vent valves in UPTF opposite the ECC injection nozzles were locked shut throughout the UPTF tests. Thus, the vent valve flow area in the UPTF tests was 6/8 or 75% of the B&W vent valve flow area, reducing the benefit of vent valve steam flow in UPTF (relative to PWRs). The larger flow area available in PWRs for vent valve steam flow could produce higher ECC delivery rates than were found in the UPTF tests.

The UPTF results are considered to be representative of ABB/BBR and B&W PWR behavior, provided that the above differences are considered in applying the results.

4.1.3 Combined Injection

ECC delivery to the lower plenum for combined injection ECC systems was investigated in transient tests at UPTF (see Table 4.1-1). These tests included depressurization transients for simulation of the end-of-blowdown (EOB)/refill phase. The UPTF tests were open loop tests; that is, steam from the test vessel was vented to containment through the intact loops and broken loop hot leg, as well as around the bottom of the core barrel and up the downcomer to the broken cold leg. The results of the UPTF tests are summarized below.

After a brief delay for accumulation in the cold legs, ECC injected into the cold legs entered the downcomer. As previously discussed, the steam upflow in the downcomer initially entrained almost all ECC delivered to the downcomer out the broken leg; however, as the upflow decreased, bypass decreased and cold leg ECC injection penetrated to the lower plenum. The transition from complete bypass to partial delivery and to essentially complete delivery was very rapid.

ECC injected in the hot legs flowed toward the upper plenum, counter to the steam flow through the loops. The interaction of steam and ECC in the loops resulted in the formation of water plugs and fluctuations in ECC delivery to the upper plenum (see Section 4.3.2). In the hot legs and upper plenum, steam was condensed by the ECC injected in the hot legs.

ECC delivered to the upper plenum flowed down through the tie plate and core to the lower plenum. In the UPTF tests, the steam upflow through the tie plate was small since most of the steam in the test vessel vented to containment by flowing around the bottom of the core barrel and up the downcomer to the break; consequently, almost all ECC delivered to the upper plenum penetrated through the tie plate to the lower plenum. Tests at CCTF and SCTF showed that water downflow through the core initiated core cooling in the downflow region. In SCTF tests, rods in the downflow region were almost quenched before blowdown was complete. Analyses and code calculations indicate that, for the GPWR case, the fuel rods in the downflow regions are quenched prior to reflood (see Section 4.6.3).

In the UPTF tests, lower plenum refill was initiated at a system pressure of 1000 kPa by the downflow of ECC injected in the hot legs. Shortly later, at a system pressure of 800 kPa, ECC injected in the cold legs penetrated to the lower plenum. The lower plenum was filled to the bottom of the core barrel prior to the end of depressurization (i.e., the equilibration of primary system and containment pressures).

A TRAC calculation of a best-estimate LOCA transient in a GPWR indicated that the lower plenum mass turnaround point (i.e., initiation of lower plenum refill) occurred about 10 seconds before the end of depressurization at a system pressure of 1000 kPa. The lower plenum liquid fraction at that time was 10%. Like the UPTF

tests, lower plenum refill was complete prior to the end of depressurization (Reference G-661).

In conclusion, the test results demonstrated that hot leg ECC injection contributed significantly to lower plenum refill during the end-of-blowdown phase of an LBLOCA. With combined hot leg and cold leg injection, the lower plenum inventory increased rapidly and reached the bottom of the core barrel before depressurization was complete. Rapid filling of the lower plenum reduces the period for core heat-up thereby limiting clad temperatures at the beginning of reflood. For a GPWR with five of the eight injection locations active, calculations indicate that refilling the lower plenum during the end-of-blowdown reduces the core heat-up period by about ten seconds and the cladding temperatures at reflood initiation by 80 - 100 K relative to the case where the lower plenum is assumed to be empty at the completion of blowdown. Within the water downflow regions of the core, most of the fuel rods are quenched during EOB by the flow of ECC from the upper plenum through the core to the lower plenum.

Table 4.1-1

SUMMARY OF TESTS RELATED TO ECC DELIVERY DURING DEPRESSURIZATION

Facility	ECC Injection Type	Type of Tests	Scale[1]	Downcomer		References
				OD mm (in)	Gap mm (in)	
UPTF	Cold Leg	Quasi-steady; Transient	1	4870 (192)	250 (9.8)	G-004, G-005, G-006, G-007, G-204, G-205, G-206, G-207, G-411, U-455
	Downcomer[2]	Quasi-steady; Transient	1	4870 (192)	250 (9.8)	G-021, G-022, G-024, G-221, G-222, G-224, G-411, U-460
	Combined	Integral	1	4870 (192)	250 (9.8)	G-003, G-018, G-019, G-028, G-203, G-218, G-219, G-228, G-411
CCTF	Cold Leg	Transient	0.22	1085 (43)	61.5 (2.4)	J-059, J-062, J-065, J-257, J-260, J-263
Creare 1/5 Scale	Cold Leg	Quasi-steady; Transient	0.18	892 (35)	38 (1.5)	E-001, E-417
Creare 1/15 Scale	Cold Leg	Quasi-steady; Transient	0.060	292 (11.5)	12.7, 25.4 (0.5, 1.0)	E-002, E-003, E-414
Creare 1/30 Scale	Cold Leg	Quasi-steady; Transient	0.032	152 (6.0)	6.4 (0.25)	E-002, E-003, E-414
Battelle Columbus 2/15 Scale	Cold Leg	Quasi-steady	0.13	618 (24)	31.2 (1.2)	E-420
Battelle Columbus 1/15 Scale	Cold Leg	Quasi-steady	0.063	307 (12)	15, 25.4 (0.6, 1.0)	E-004

Table 4.1-1

NOTES:

1. Scale is relative to the UPTF downcomer diameter (OD) (4870 mm or 192 in). For comparison, the downcomer diameters for typical cold leg injection PWRs are: 4630 mm (182 in) for a Combustion Engineering System 80 PWR; and 4390 mm (173 in) for a Westinghouse or Japanese 3400 MWt PWR. The downcomer diameter of a 3900 MWt Siemens/KWU PWR with combined injection is 5000mm.

2. The UPTF tests with downcomer ECC injection were performed both with the vent valves locked closed and with the vent valves free to open.

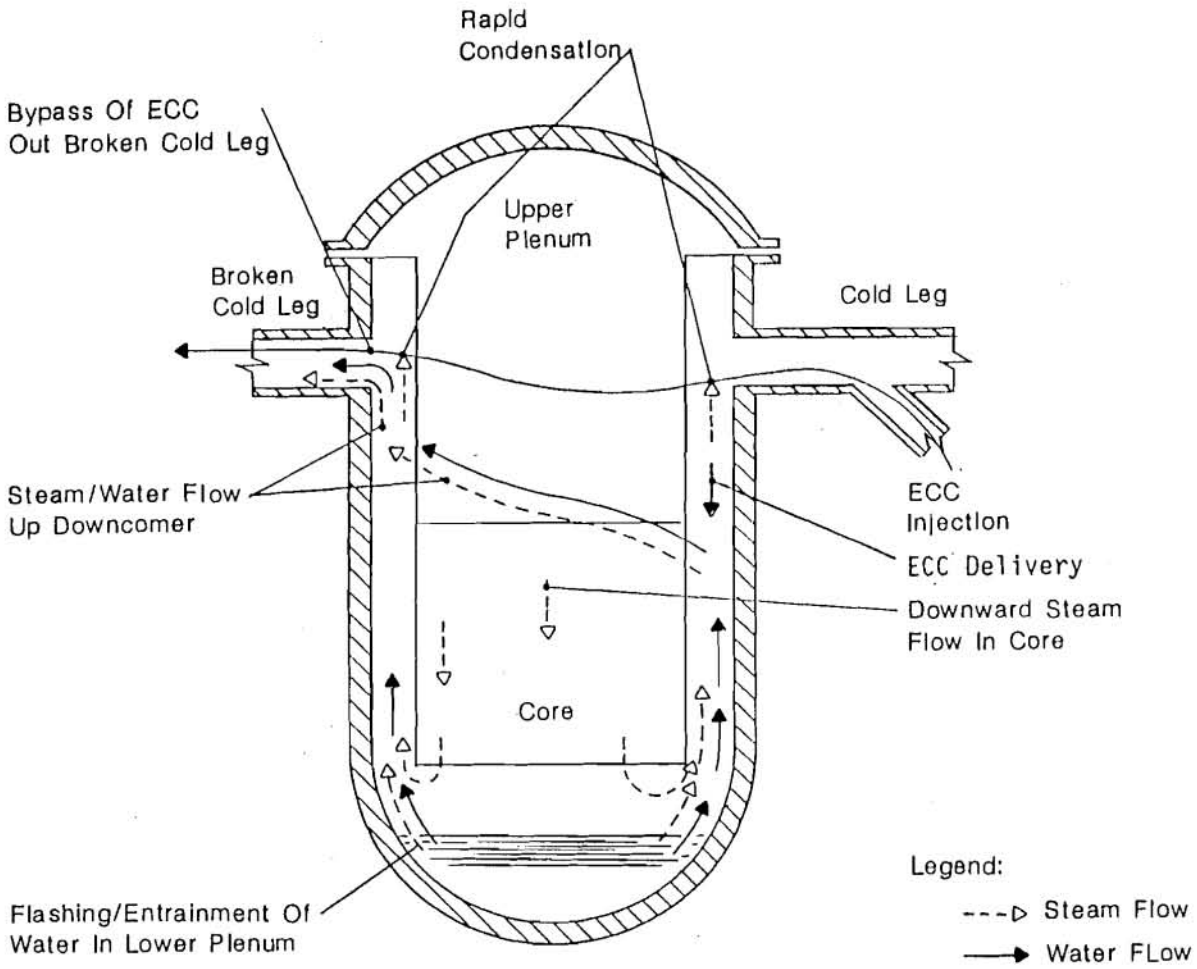

Notes: 1. This figure shows end-of-blowdown phenomena for PWRs which inject ECC into the cold legs and, therefore, is applicable to PWRs with either cold leg or combined injection systems. With combined injection, ECC is also injected into the hot legs (not shown).

2. For downcomer ECC injection (or direct vessel injection), ECC is injected through nozzles in the downcomer rather than the cold legs. The phenomena are essentially the same as shown in this figure.

PWR END-OF-BLOWDOWN PHENOMENA
IN THE DOWNCOMER

FIGURE 4.1-1

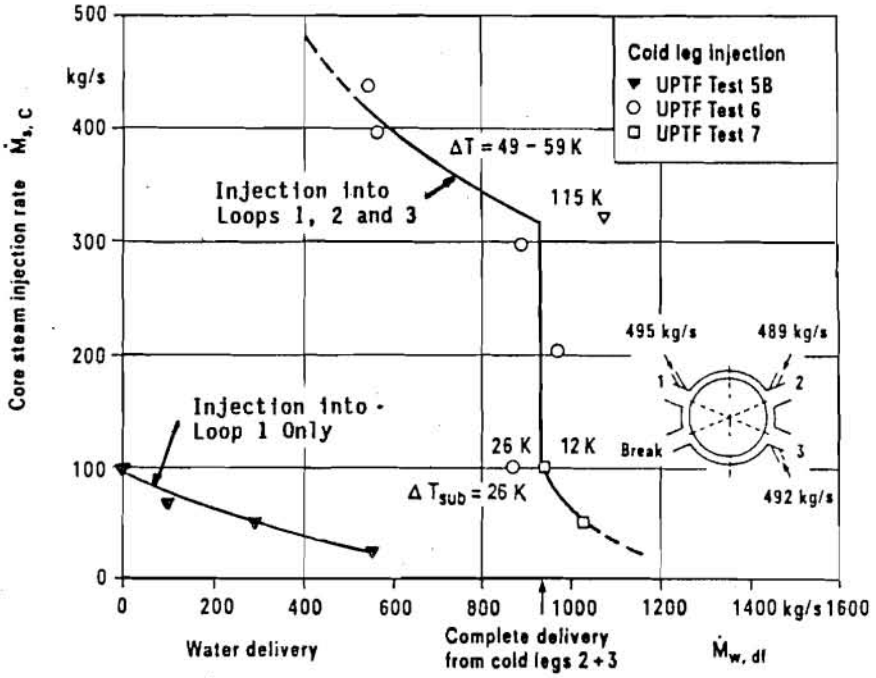

STEAM INJECTION AND ECC DELIVERY RATES FOR UPTF COLD LEG INJECTION TESTS

FIGURE 4.1-2

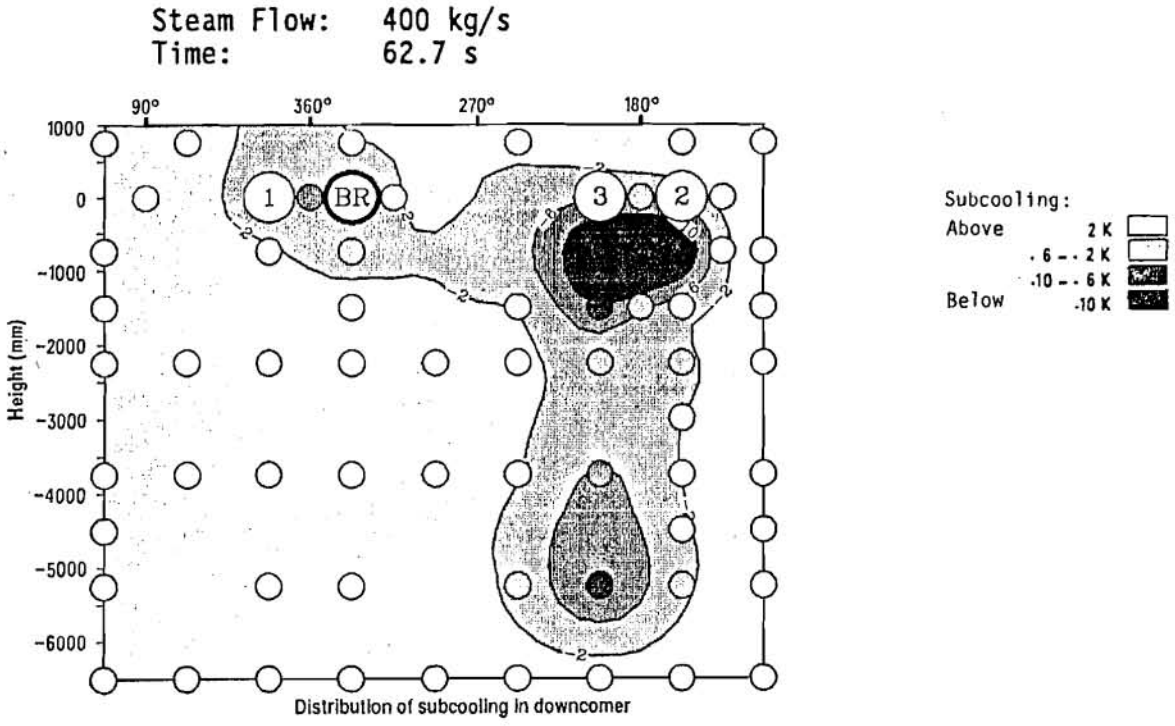

UPTF Test 6, Run 131

EXAMPLE SUBCOOLING CONTOUR PLOT FOR UPTF COLD LEG INJECTION TESTS (REFERENCE G-907)

FIGURE 4.1-3

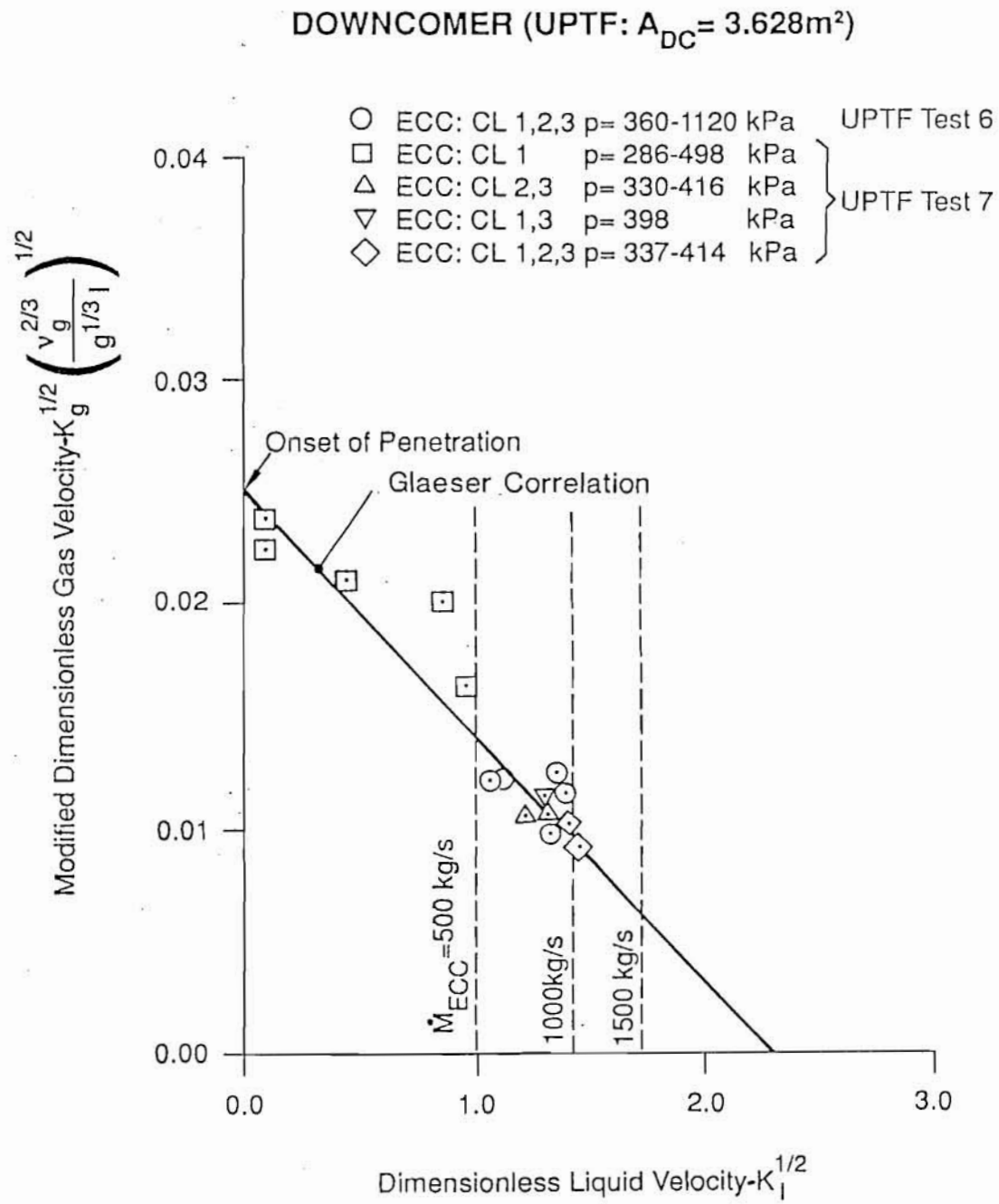

GLAESER CORRELATION OF ECC DELIVERY
IN UPTF COLD LEG INJECTION TESTS
(REFERENCE G-415)

FIGURE 4.1-4

Legend:

- ○ ECC Injection to Loops 1, 2 and 3
- ▲ ECC Injection to Loops 2 and 3 or Loops 1 and 3
- □ ECC Injection to Loop 1 Only

$$j^{*1/2}_{g,eff} = C + m \cdot j^{*1/2}_{f}$$

	f	C	m
Curve 1	0.80	0.819	-4.193
Curve 2	0.80	0.214	-0.769

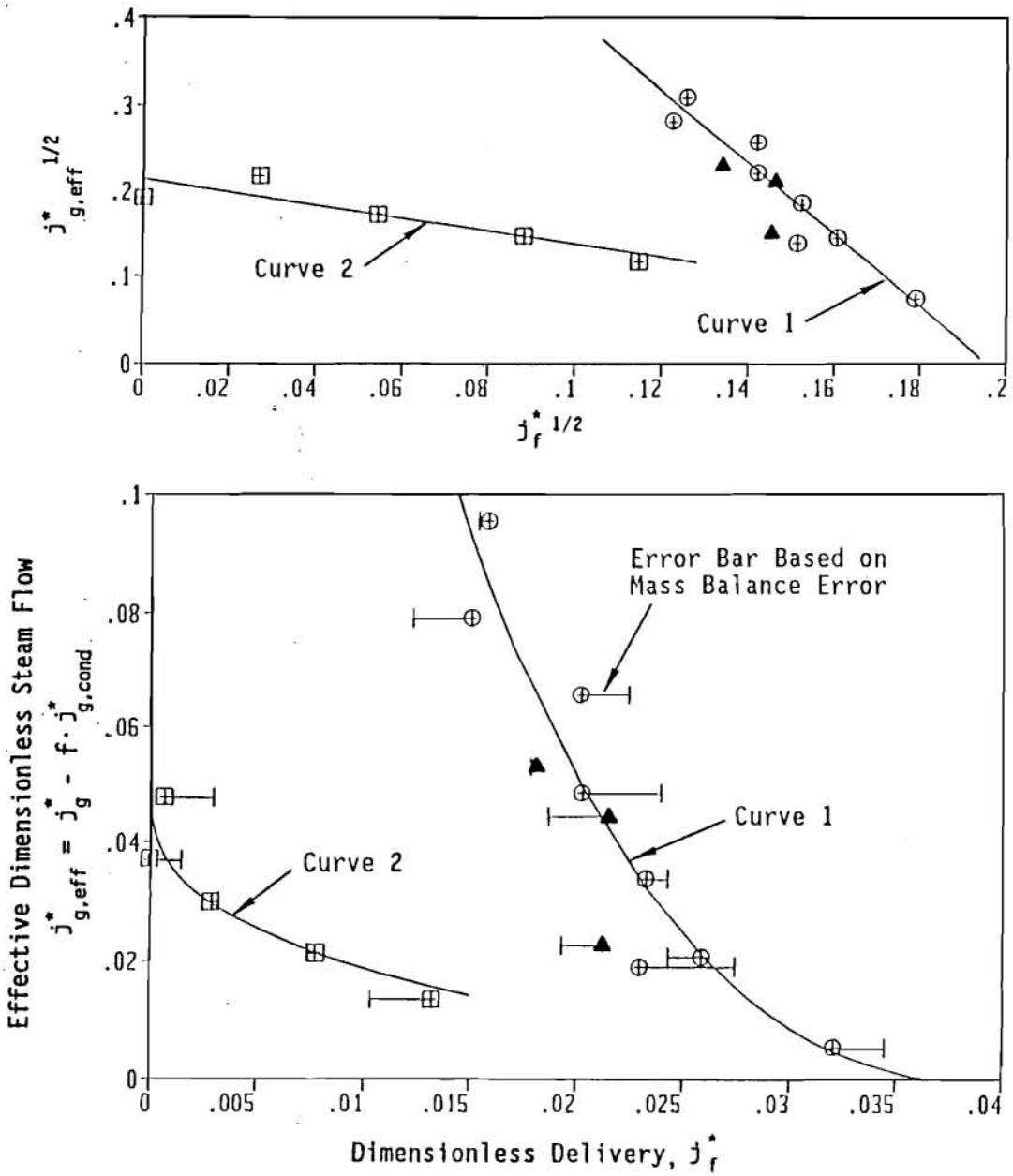

BEST-FIT OF DIMENSIONLESS STEAM AND DELIVERY RATES
FOR UPTF COLD LEG INJECTION TESTS
(REFERENCE U-455)

FIGURE 4.1-5

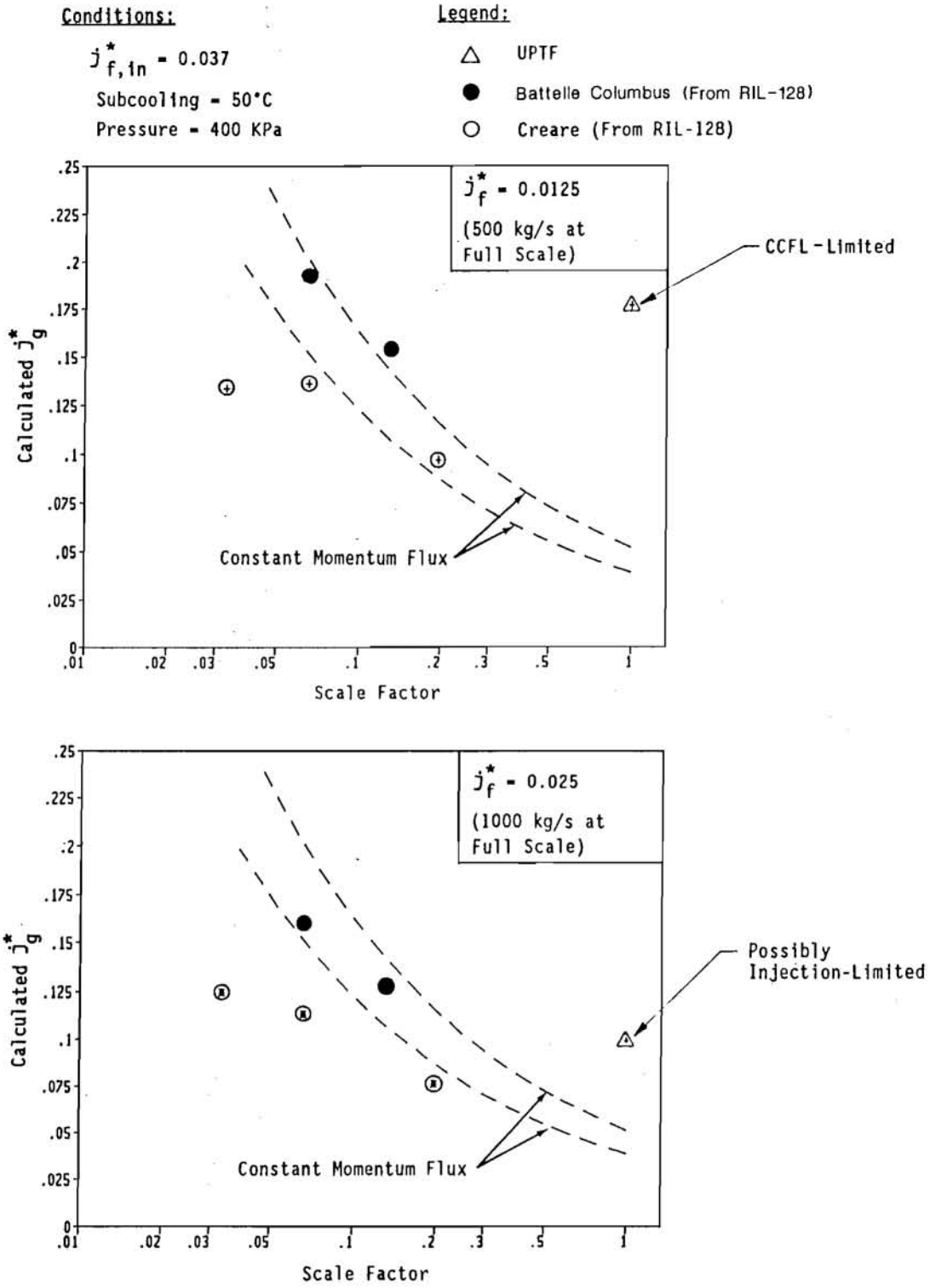

Note: The dimensionless gas velocities were calculated from correlations of countercurrent flow data. The values for UPTF were calculated from the correlation shown in Figure 4.1-5. The calculated j_g^* for the subscale facilities were obtained using the correlations and constants from Reference E-412.

EFFECT OF SCALE FACTOR ON CALCULATED j_g^*
FOR ECC INJECTION TO ALL COLD LEGS
(REFERENCE U-455)

FIGURE 4.1-6

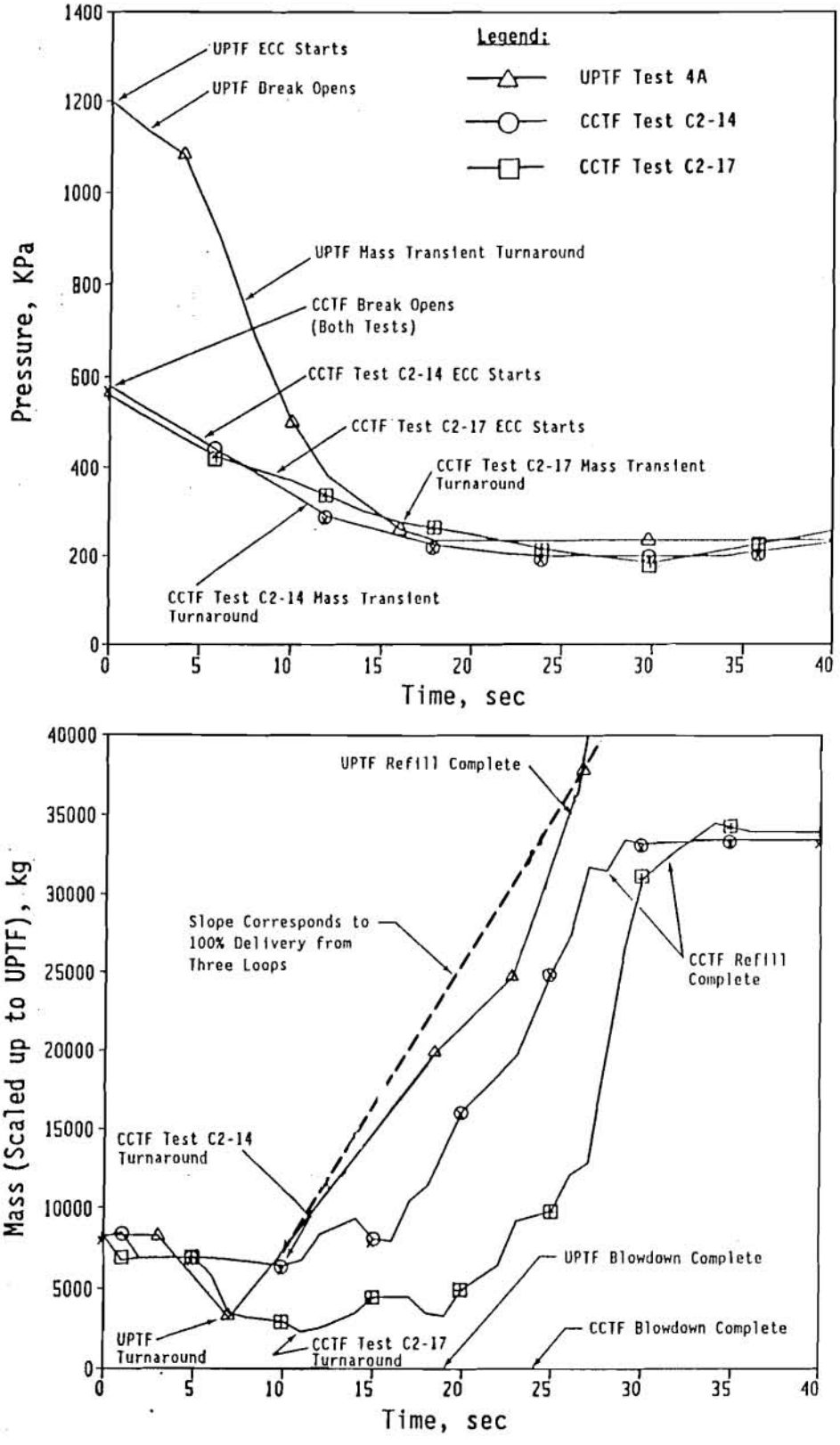

Note: All tests shown in this figure were performed with the loops open.

COMPARISON OF END-OF-BLOWDOWN/REFILL TRANSIENTS IN THE COLD LEG INJECTION TESTS AT UPTF AND CCTF (REFERENCE U-455)

FIGURE 4.1-7

LEGEND:

ECC Injection Location	Data	TRAC MOD2	TRAC MOD1
Loops 1, 2 & 3	○	●	◑
Loops 2 & 3	△	▲	- - -
Loop 1 only	✳	■	- - -

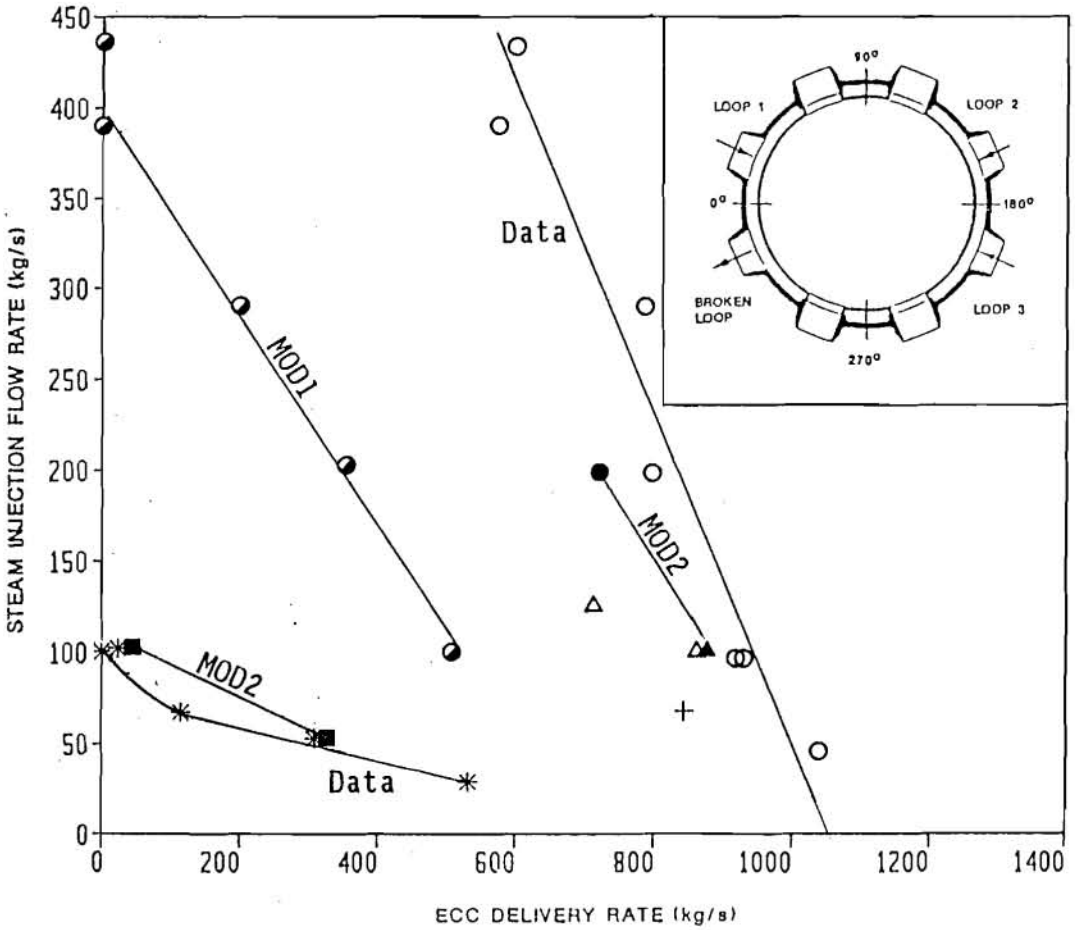

Notes: 1. The UPTF data were obtained from Reference U-455.
2. The TRAC results were obtained from Reference U-711.

TRAC/DATA COMPARISON OF DELIVERY RATES
FOR UPTF COLD LEG INJECTION TESTS

FIGURE 4.1-8

LEGEND:

- ● Cold leg ECC injection to Loops 1, 2 and 3
- ○ Cold leg ECC injection to Loop 1 only
- ■ Downcomer ECC injection to Nozzles 1 and 2; vent valves free to open
- ▬ Downcomer ECC injection to Nozzle 2 only; vent valves free to open
- ▬ Downcomer ECC injection to Nozzle 1 only; vent valves free to open
- ◆ Downcomer ECC injection to Nozzles 1 and 2; vent valves closed
- ◆ Downcomer ECC injection to Nozzle 1 only; vent valves closed

Note: Nozzle 1 and Loop 1 are adjacent to the broken cold leg, and Nozzle 2 and Loops 2 and 3 are opposite the broken cold leg.

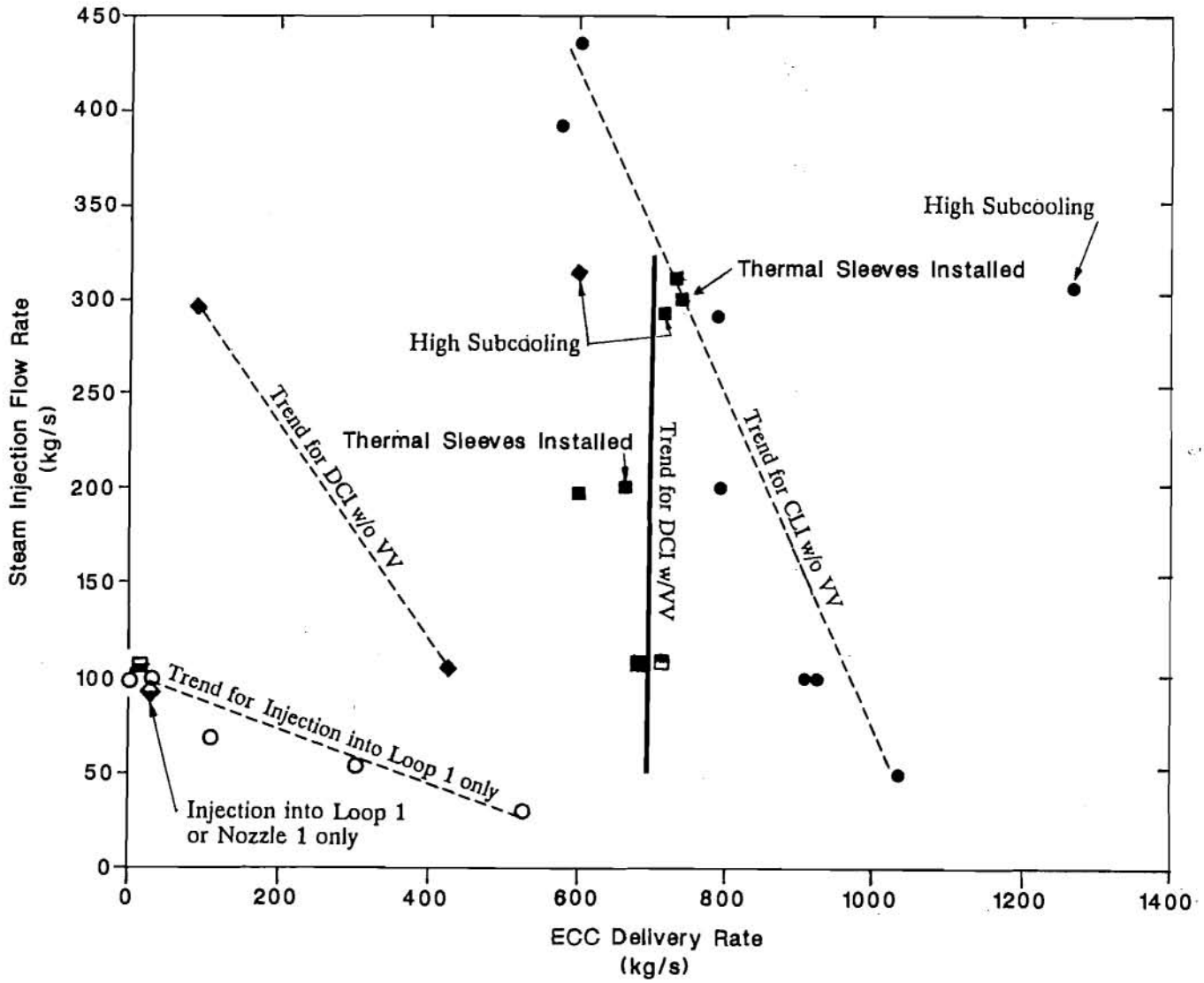

STEAM INJECTION AND DELIVERY RATES
FOR UPTF DOWNCOMER INJECTION TESTS

FIGURE 4.1-9

Steam Flow: 316 kg/s
Time: 74.4 s
Vent Valves: Closed

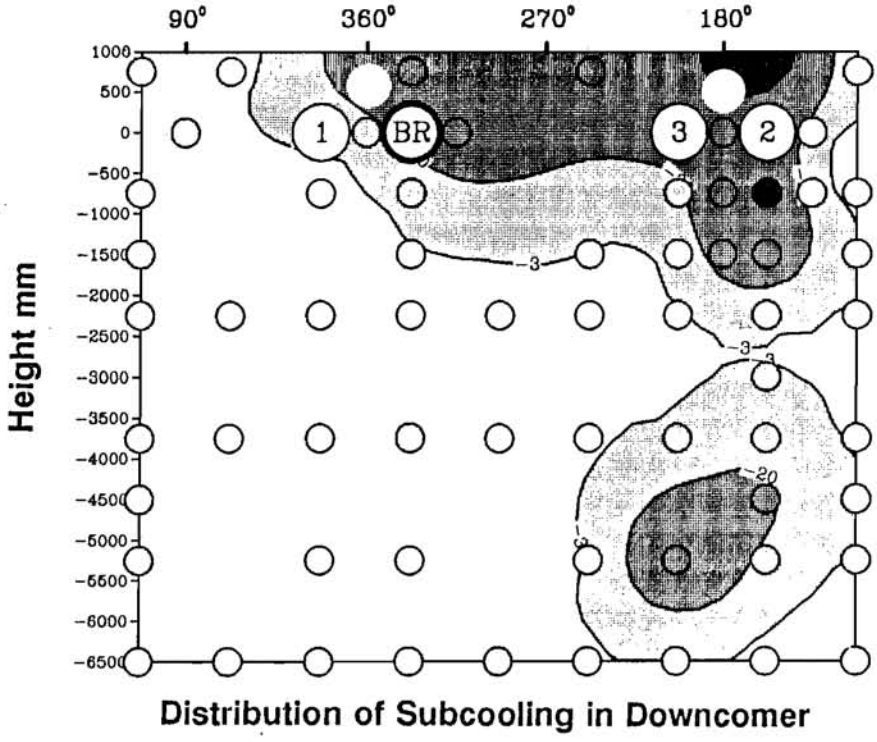

UPTF Test 21A, Run 272

Temp. Difference, K

	Above - 3	Saturated/Superheated
	-20 - - 3	Subcooled
	-70 - -20	
	Below -70	

EXAMPLE SUBCOOLING CONTOUR PLOT FOR
UPTF DOWNCOMER INJECTION TESTS
(REFERENCE G-221)

FIGURE 4.1-10

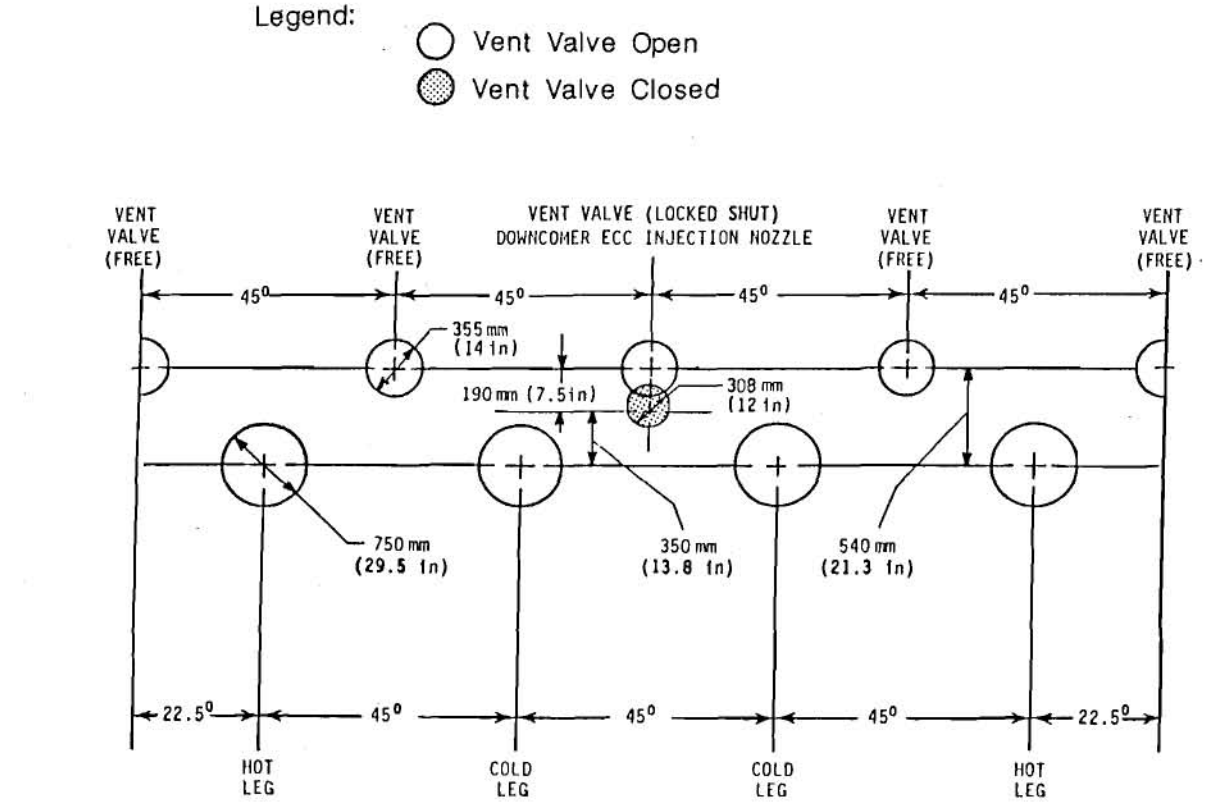

UPTF

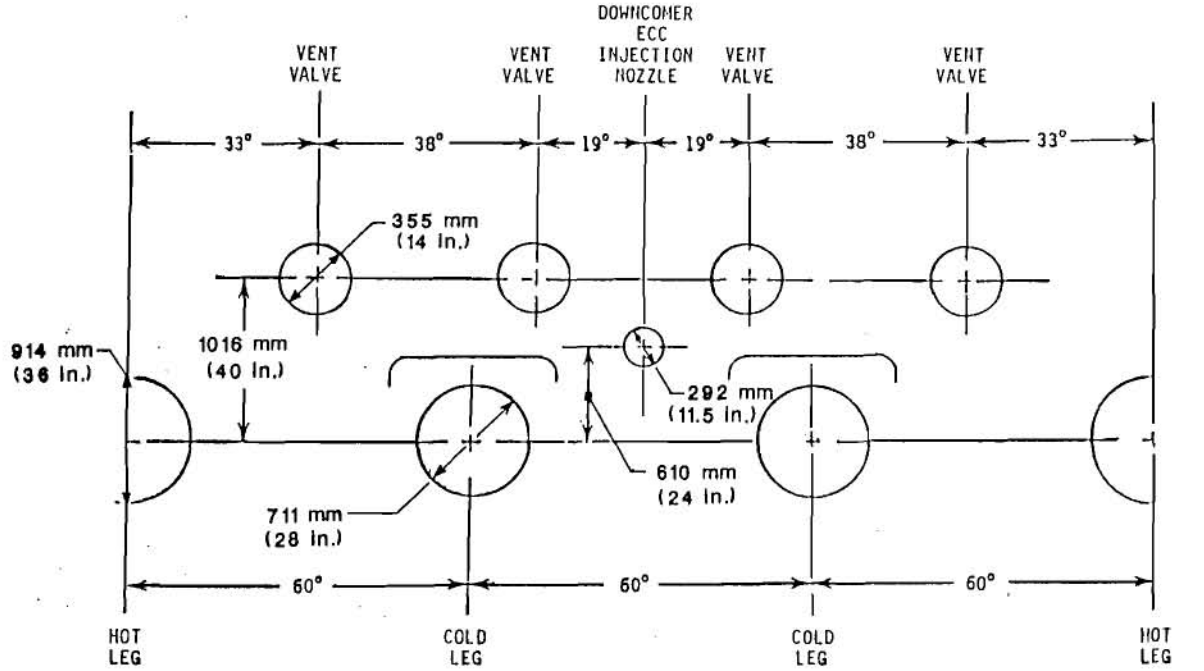

B&W PWR

COMPARISON OF UPTF AND TYPICAL B&W PWR HOT/COLD LEG, AND DOWNCOMER INJECTION NOZZLE ARRANGEMENT

FIGURE 4.1-11

4.2 ENTRAINMENT IN DOWNCOMER DURING REFLOOD

Definition of Issue and Description of Phenomena

In a cold leg break LOCA, the beginning of the "reflood" phase occurs when the reactor vessel water level reaches the bottom of the core. This creates a seal between the core and the downcomer, and further ECC injection tends to fill the downcomer to near the cold leg elevation. The difference in water level between the downcomer and the core provides the driving head for core flooding. This driving head also creates a pressure difference from the top of the core to the top of the downcomer which tends to cause core steam generation to flow out of the core and through the loops to the downcomer. In combined injection PWRs, essentially all of the steam flow is condensed by hot leg and/or cold leg ECC and there is no steam flow into the downcomer. In cold leg injection or downcomer injection PWRs, steam flows to the downcomer via intact loops or vent valves. Some of the steam is condensed by ECC injected in the cold legs or in the downcomer. Any steam not condensed, along with steam generated in the downcomer due to superheated walls, flows circumferentially around the downcomer and out the broken cold leg, potentially entraining and carrying away a portion of the ECC. These reflood phenomena are illustrated in Figure 4.2-1.

Importance of Issue to PWR LOCA Behavior

The circumferential flow of steam around the downcomer and the generation of steam on superheated downcomer walls tend to entrain ECC in the downcomer region. The interaction of steam flow, wall boiling, and ECC entrainment is important since it affects the water level in the downcomer. Reduction of the downcomer liquid level below the spillover level (which is at the bottom of the cold leg nozzles) reduces the available driving head and tends to reduce the core flooding rate. This prolongs quench times and potentially allows higher clad temperatures in the core.

Tests and Analyses that Relate to the Issue

The steam/water interaction and entrainment in the downcomer have been investigated in separate effects tests at UPTF and integral tests at UPTF and CCTF. The separate effects tests evaluated the influence of steam flow and downcomer wall superheat on downcomer water level and entrainment, and the integral tests provided information on the transient characteristics of these phenomena. The tests included tests with cold leg ECC injection, downcomer ECC injection, and combined ECC injection. Table 4.2-1 lists the tests considered in this evaluation.

The evaluations of the UPTF cold leg injection tests and downcomer injection tests, including comparisons to the CCTF tests, are provided in References U-455 and U-460, respectively. Evaluation of the UPTF combined injection tests is covered in Reference G-411. The major results of these evaluations and comparisons are summarized below.

Post-test TRAC calculations have been performed for tests at both CCTF and UPTF. These analyses include TRAC-PF1/MOD1 calculations of several CCTF tests (References U-621 through U-628, and U-631) and of UPTF Test 2 (Reference U-714). TRAC-PF1/MOD2 calculations have been performed for CCTF Test C2-4 (Reference U-714), and UPTF Tests 23 and 25 (References U-715 and U-714, respectively).

Summary of Key Results and Conclusions from Tests and Analyses

The UPTF separate effects tests were designed to create a steady-state equilibrium among the downcomer water level, steam flow rate, ECC entrainment rate, and vessel drainage. Steam entered the downcomer from either the intact cold legs or the vent valves, and ECC was injected into either the cold legs or downcomer. The vessel was simultaneously drained to simulate the loss of water inventory from the vaporization of ECC in the core that would occur in an actual PWR. The intent was to hold these conditions constant long enough for the downcomer water level and entrainment rate to reach equilibrium. Similar flow conditions were created with cold leg injection, downcomer injection with vent valves, and downcomer injection without vent valves.

The results of the separate effects tests indicate that as the steam flow increased, liquid entrainment out the broken cold leg increased which tended to reduce the downcomer water level. As the ECC injection rate increased, the downcomer water level increased due to the combination of reduced steam flow from increased condensation and the higher rate of excess ECC supply to the downcomer. Correlations which relate the "void height" (reduction in the collapsed water level below the cold legs) to the steam and entrainment flow rates were independently developed by Siemens and MPR. Both correlations are based on the results of the UPTF tests with cold leg injection. While the assumptions and approaches of the two correlations are different, both correlations are consistent with the test data and predict about the same level reduction for given flow conditions. Each correlation is described below.

- The Siemens correlation assumes that entrainment primarily occurs in front of the broken cold leg nozzle because the steam flow and water level are highest at that location. This correlation is based on fundamental hydraulic equations, while the shear stress coefficient and constants in the correlation were

determined from UPTF tests. The steam flow in the correlation is the total steam flow out the break, which includes steam generation in the downcomer. Figure 4.2-2 is a plot of the correlation with the test data. The development of this correlation is discussed in detail in Reference G-411.

- The MPR correlation assumes entrainment can occur throughout the downcomer due to the azimuthal steam flow, and that the level reductions due to entrainment and steam generation are separate and additive. Wall steam generation is taken into account by correcting the measured void height for the voiding due to the steam generation. The void height due to wall boiling (or bottom void height) is based on the steam generation rate corresponding to the calculated downcomer wall heat release, and a void fraction correlation developed by JAERI for vertical steam flow in a column of liquid. As shown in Figure 4.2-3, the "top" void height (level reduction due to entrainment) was plotted as a function of the ratio of the effective steam flow and the entrainment rate. The effective steam flow is defined as the injected steam flow less condensation. A detailed description of the development of this correlation is provided in Reference U-455.

Detailed discussions of the 2D/3D Program results are provided in Subsections 4.2.1, 4.2.2, and 4.2.3 for cold leg injection, downcomer injection, and combined injection, respectively.

4.2.1 Cold Leg Injection

The preceding discussion of test results covered UPTF Test 25 which evaluated the effect of parametric variations in the loop steam flow and cold leg ECC injection rates on entrainment and level reduction in the downcomer. The following discussion covers the results of integral tests and the effect of wall boiling on the downcomer water level reduction.

In integral tests at UPTF and CCTF, the downcomer water level (and therefore the driving head available for core flooding) was reduced below the cold leg elevation by ECC entrainment in the steam flow and by boiling on superheated downcomer walls. Note that while water spillover out the break due to water level oscillations can also contribute to the downcomer water level reduction, entrainment and wall boiling are considered the dominant phenomena.

Figure 4.2-3, the plot of the MPR void height correlation, includes data points from CCTF Test C2-4 and UPTF Test 2. These integral tests were counterpart tests. As shown on Figure 4.2-3, the dimensionless steam flow and top void height were much lower in CCTF Test C2-4 than in UPTF Test 2. This is a result of scale effects which greatly reduced the top void height in the scaled CCTF. This reduction was due to the relatively enlarged circumferential flow area in the subscale facility. Figure 4.2-4 illustrates how these geometric differences affect dimensionless velocities. It also shows that the UPTF and CCTF results bound the behavior expected in a PWR (i.e., $j^*_{CCTF} < j^*_{PWR} < j^*_{UPTF}$).

In the UPTF tests with wall superheat, the initial downcomer liquid inventory was saturated water and ECC delivered to the top of the downcomer was warmed to nearly saturation by condensation in the cold legs. Accordingly, essentially all of the downcomer wall heat release contributed to steam generation. However, in CCTF tests, the steam generation was temporarily suppressed because the downcomer inventory was initially subcooled. Although it was not observed in CCTF tests, it appears there could be situations where LPCI water is not fully heated to saturation in the cold legs. The delivery of subcooled water to the downcomer can suppress wall boiling and downcomer voiding.

CCTF tests also displayed a transient wall boiling effect which was not observed in the UPTF tests, but which is likely to occur in a PWR. The top diagram of Figure 4.2-5 shows the calculated heat release and estimated steam generation rate for CCTF Test C2-4. With the high flow of subcooled ECC during accumulator injection, the initial downcomer inventory was highly subcooled (by as much as 100 K) and most of the energy initially released by the superheated walls simply heated the downcomer inventory. Steam generation began to occur after accumulator injection was terminated, when ECC entering the downcomer was saturated, not subcooled. As saturated water slowly replaced the subcooled water

at the top of the downcomer, steam generation increased to a maximum, but then fell off as the total wall heat content and heat release rate decreased.

Also shown in Figure 4.2-5 is the collapsed downcomer water level for Test C2-4. This figure illustrates the influence of the wall steam generation on the downcomer level/entrainment behavior observed in most CCTF Core-II reflood tests. As steam generation increased in the first 150 seconds after the downcomer was filled, voiding due to steam generation (bottom voiding) increased, corresponding to the decrease in the collapsed water liquid level. After about 200 seconds, the steam generation rate dropped, decreasing bottom voiding and corresponding to the increase in the collapsed water level. Thus the variation in the downcomer water level appears to be mostly due to bottom voiding, while the void height created by ECC entrainment in the loop steam flow (the top void height) remains fairly constant at a small value.

Comparisons to the TRAC analyses showed that the TRAC-PF1/MOD2 analysis of CCTF Test C2-4 did not show the observed level reduction transient due to downcomer wall steam generation. Instead, the calculated downcomer level was at the spillover elevation throughout the transient. It appears the code did not correctly calculate steam condensation in the cold legs which allowed saturated water to be delivered to the downcomer in the tests. Instead, subcooled water was delivered to the downcomer, which suppressed steam generation from wall heat release.

The TRAC-PF1/MOD2 analysis of UPTF Test 25 generally underpredicted downcomer water level. Since it is unclear as to why TRAC underpredicted the downcomer water level, the accuracy of the code in predicting local downcomer phenomena could not be evaluated. Reference E-609 concluded that, since the impact of downcomer entrainment and wall boiling on PCT is small, the underprediction of downcomer level is not a significant contributor to code uncertainty.

Using the test results and evaluations described above, the best-estimate driving head available in a Westinghouse PWR during the reflood period was calculated. The void height contribution due to entrainment in the loop steam flow was based on the loop steam flow rate and the core inlet mass flow rate from best-estimate CCTF tests. The ECC entrainment rate was calculated from the ECC injection rate and the core inlet flow rate, assuming a steady downcomer level. Using the MPR entrainment correlation, the top void height was estimated as essentially zero to 0.25 m. The higher value (0.25 m) corresponds to the single-LPCI-pump failure ECC flow rate of 240 kg/s, while the zero void height corresponds to the no-failure ECC flow rate of 420 kg/s. In the no-failure case, all of the intact loop steam flow is condensed, so there is no steam flow out the broken cold leg and no level depression due to entrainment.

The contribution to the total void height resulting from wall boiling was estimated based on conduction-limited wall heat release and the fraction of that available for steam generation. For the no-failure LPCI case, steam generation was suppressed throughout the transient. For the single-failure case, ECC delivered to the downcomer was assumed to be saturated as observed in CCTF, and steam generation gradually increased as the saturated water replaced subcooled water in the downcomer. Steam generation in the PWR (for single-failure LPCI case) would be about five percent of the total loop steam flow.

With an effective downcomer length of 5 m, the PWR bottom void height was calculated to range from 0.3 m initially to 0.7 m for the majority of reflood. The total maximum estimated void height in the PWR was therefore 0.95 m. The resulting downcomer liquid level is shown on Figure 4.2-6. Assuming the core liquid level measured in CCTF Test C2-4 is representative of that for a PWR, the downcomer driving head would be about 2.6 m of water. Note that since the bottom of the cold legs are at an elevation of 4.95 m in the Westinghouse PWR, the maximum downcomer driving head would be about 3.5 m. Based on the calculated driving head, it was estimated that, relative to no downcomer voiding (i.e., the full 3.5 m driving head), the overall increase in PCT during reflood would be 13 K (Reference U-455). Thus, while assuming the downcomer remains completely filled (to the bottom of the cold leg nozzles) is a nonconservative assumption, the overall influence of downcomer voiding on the reflood PCT is estimated to be relatively small.

4.2.2 Downcomer Injection

As previously indicated the separate effects tests at UPTF were intended to maintain constant flow conditions long enough for the downcomer water level and entrainment rate to reach equilibrium. However, in the tests with downcomer ECC injection, the downcomer water level did not always reach steady state in the time allowed. This was apparently due to the fact that a large fraction (40 - 50%) of the ECC bypassed the downcomer entirely and traveled directly out the break, meaning less ECC was delivered to the vessel than expected. Direct bypass of about half of the injected ECC appeared to be a result of the close proximity of one of the ECC injection nozzles to the break at UPTF (see Figure 4.1-11). Accordingly, this result is not necessarily directly applicable to B&W and ABB/BBR plant configurations.

The results of the UPTF separate effects tests with downcomer injection are shown in Figure 4.2-7, a plot of void height versus steam flow. For comparison, Figure 4.2-7 also includes data from the cold leg injection tests. The steam and ECC flow rates were similar for all the tests. Note that the circled data points were the only ones which achieved equilibrium, so the other data points would be expected to move to a lesser void height as they approached equilibrium.

As shown in Figure 4.2-7, the void height for downcomer injection without vent valves was significantly higher than for cold leg injection. This difference was attributed to the location of the downcomer injection nozzles above the cold legs (where steam enters the downcomer). This configuration favored bypass (Reference U-460).

Figure 4.2-7 also shows that the void height for downcomer injection with vent valves was lower than for downcomer injection without vent valves because the steam entered the downcomer via the vent valves rather than the cold legs. With the vent valves open, steam entered the downcomer at a higher elevation which favored flow stratification and reduced entrainment. This reduction in entrainment compensated for direct ECC bypass. Consequently, as shown in Figure 4.2-7, the void height for downcomer injection with vent valves was comparable to cold leg injection (Reference U-460).

The UPTF tests with open vent valves simulated both single-phase steam flow and two-phase steam/water flow through the vent valves. Test results indicate that, for the same steam flow, the void height with two-phase flow through the vent valves was higher than with single-phase flow (see Figure 4.2-7). Apparently, entrainment out the break increased due to the higher momentum flux in the downcomer (Reference U-460).

The UPTF data are plotted in Figure 4.2-8 to show the downcomer top void height versus the ratio of the dimensionless steam flow and entrainment rates. The amount of direct bypass was subtracted from the total break water outflow to obtain an "entrainment" outflow comparable to that evaluated in cold leg injection tests. Note, for the test with two-phase flow through the vent valves (i.e., Test 23C), j_g^* was calculated based on the two-phase flow and not just the steam flow; hence the data points are shifted to the right relative to the single-phase data points. Most of the UPTF downcomer injection data were out of the range of the cold leg injection correlation (Reference U-455) because the high ECC bypass caused the entrainment rates to be much lower than in the cold leg injection tests. The downcomer injection data indicate that the downcomer water level will approach a lower asymptote (i.e., maximum void height) with high steam flows. This suggests that the cold leg correlation should not be extrapolated beyond the range of cold leg data (i.e., beyond dimensionless steam flow/entrainment ratio of 2).

Two downcomer injection tests, one with vent valves and one without vent valves, were performed at CCTF. In the test without vent valves, the downcomer water level periodically exceeded the cold leg elevation as the downcomer and core water levels oscillated. These oscillations were attributed to the location of the downcomer injection nozzles slightly below the cold leg elevation (see References J-973 and U-414).

For comparison with the UPTF tests, data from the two CCTF tests are included on Figure 4.2-8. The vertical bars indicate the magnitude of the significant water level oscillations that occurred during these tests. The entrainment rates were determined assuming direct bypass of the ECC injected in the nozzle near the break. For the test with open vent valves, j_g^* was calculated based on the estimated steam flow through the vent valves because the two-phase flow could not be readily determined. If j_g^* was calculated for the two-phase flow, the data points would be shifted to the right. Review of Figure 4.2-8 indicates that the top void height for the CCTF tests was small compared to that in the UPTF tests (less than 0.75 m versus greater than 0.85 m). This is consistent with the scale effect observed in cold leg injection tests (see Section 4.2.1). Also, due to two-phase flow through the vent valves, the top void height was larger with vent valves than without vent valves.

A post-test analysis of UPTF Test 23B was performed using TRAC-PF1/MOD2 (Reference U-715). The analysis results indicate that TRAC can predict downcomer level/entrainment phenomena for downcomer injection with vent valves. Specifically, TRAC predictions of the collapsed water level in the downcomer and ECC entrainment out the broken cold leg were in reasonable agreement with the test data.

To determine what effect entrainment and downcomer voiding may have on an actual PWR with downcomer ECC injection, the increase in PCT for a B&W 2600 MWt plant was estimated. The assumption was made that half of the injected ECC was bypassed (as in the UPTF tests), and the cold leg injection correlation was used to estimate the void height due to entrainment. Use of the cold leg correlation is reasonable since the UPTF data in Figure 4.2-7 indicate similar void heights in the downcomer injection/vent valve and cold leg injection tests; also, the expected PWR flow conditions are within the range of the cold leg injection data. The increase in PCT due to the bypass and entrainment phenomena was estimated to be in the range of 13 - 18 K at a B&W plant, indicating that the overall influence of downcomer voiding on reflood PCT is relatively small (Reference U-460). Note that this estimate is based on the downcomer water level reaching steady-state early in the reflood period. If ECC bypass occurs in the B&W plant as in the UPTF tests, the attainment of steady-state downcomer water level could be delayed such that an additional increase in reflood PCT could result (Reference U-460).

4.2.3 Combined Injection

The results of combined injection integral tests at CCTF and SCTF indicate that most of the downcomer wall heat transfer was to subcooled water which was present in the downcomer due to high ECC injection rates. The presence of significant subcooling was confirmed in UPTF tests. The subcooling was sufficient to completely suppress wall boiling; therefore no voiding due to wall heat release is expected in combined injection PWRs.

In the UPTF tests with combined ECC injection into cold leg and hot leg, the ECC flows were sufficiently high (about 400 kg/s per injection port) to condense all of the loop steam flow during reflood; consequently, there was no downcomer water level reduction due to entrainment flow out the broken cold leg.

In conclusion, downcomer level reductions due to wall boiling or entrainment are not expected in a PWR with combined cold and hot leg ECC injection.

Table 4.2-1

SUMMARY OF TESTS RELATED TO
DOWNCOMER ENTRAINMENT DURING REFLOOD

Type of Test	Facility and Test	Facility Scale	References
Cold Leg Injection Separate Effects Tests	UPTF: Test 25A Test 25B	1 [2,3]	U-455, G-411 G-025, G-225 G-025, G-225
Cold Leg Injection Integral Tests	UPTF: Test 2	1 [2,3]	U-455, G-411 G-002, G-202
	CCTF-II: Test C2-4	1/21 [3]	U-414 J-052, J-250, J-448
Downcomer Injection Separate Effects Tests	UPTF: Test 21D Test 23B Test 23C [(6)]	1.5 [2,4]	U-460, G-411 G-021, G-221 G-023, G-223 G-022, G-222
Downcomer Injection Integral Tests	CCTF-II: Test C2-AA2 Test C2-10	1/16 [4]	U-414 J-048, J-246, J-446 J-058, J-256
Combined Injection Integral Tests	UPTF: Test 3 Test 18 Test 28	1 [2,5]	G-411 G-003, G-203 G-018, G-218 G-028, G-228

NOTES:

1. Facility scale is based on core thermal power.

2. The scale of UPTF is based on the thermal power of its reference PWR - 3900 MWt.

3. Relative to a 3400 MWt Westinghouse or Japanese PWR.

4. Relative to a 2600 MWt Babcock & Wilcox PWR.

5. Relative to a 3900 MWt Siemens/KWU PWR.

6. UPTF Test 23C was actually the second portion of Test 22A.

Note: For simplicity hot legs are not shown.

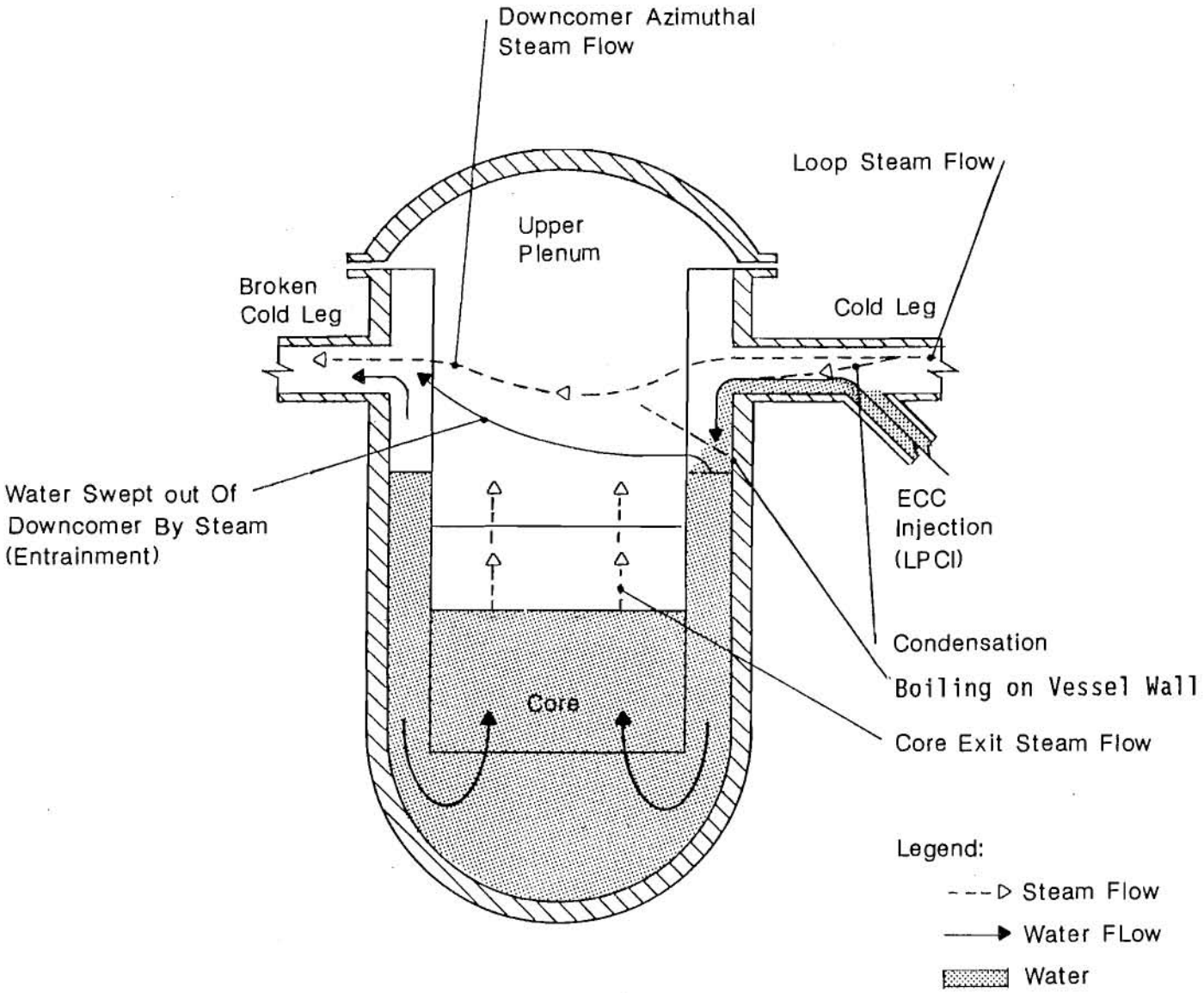

Notes:

1. This figure shows reflood phenomena for PWRs which inject ECC into the cold legs.
2. For combined injection, ECC is also injected into the hot legs.
3. For downcomer injection, ECC is injected through nozzles in the downcomer rather than the cold legs, and the phenomena are similar to that shown in this figure.
4. For PWRs with vent valves, steam flows directly from the upper plenum to the downcomer through vent valves (not shown).

PWR REFLOOD PHENOMENA
IN THE COLD LEG/DOWNCOMER REGION

FIGURE 4.2-1

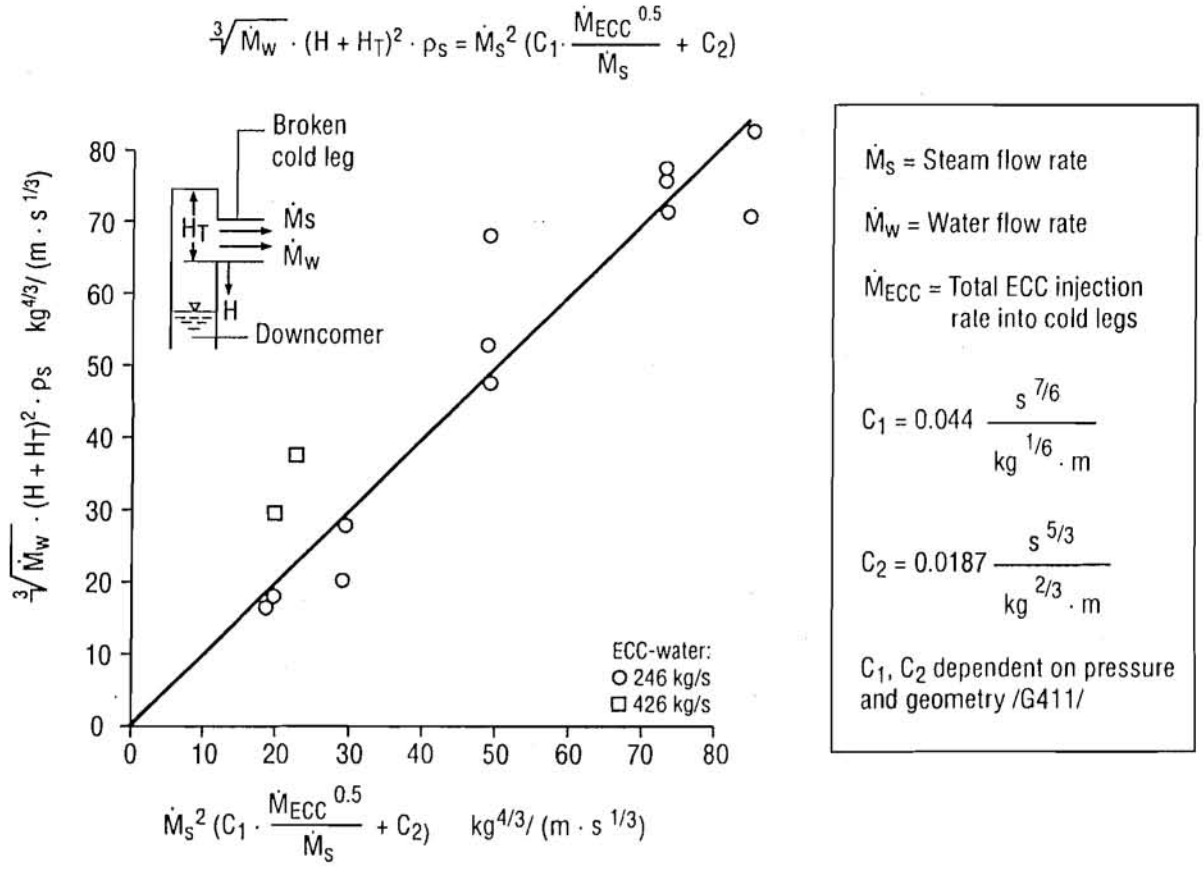

$\dot{M}_S$ = Steam flow rate

$\dot{M}_w$ = Water flow rate

$\dot{M}_{ECC}$ = Total ECC injection rate into cold legs

$$C_1 = 0.044 \frac{s^{7/6}}{kg^{1/6} \cdot m}$$

$$C_2 = 0.0187 \frac{s^{5/3}}{kg^{2/3} \cdot m}$$

C_1, C_2 dependent on pressure and geometry /G411/

SIEMENS DOWNCOMER LEVEL/ENTRAINMENT CORRELATION FOR UPTF COLD LEG INJECTION TESTS (REFERENCE G-411)

FIGURE 4.2-2

Legend:
- ○ UPTF Test 25, Phase A (Hot Walls)
- ✱ UPTF Test 25, Phase B (No Hot Walls)
- △ UPTF Test 2 (Hot Walls)
- ◇ CCTF Test C2-4 (Hot Walls)

$$H_{v,top} = 0.35 \left(j^*_{g,eff} / j^{*\,1/4}_{f,ent}\right)^2$$

$$j^*_{g,eff} = j^*_g - 0.8 \cdot j^*_{g,cond}$$

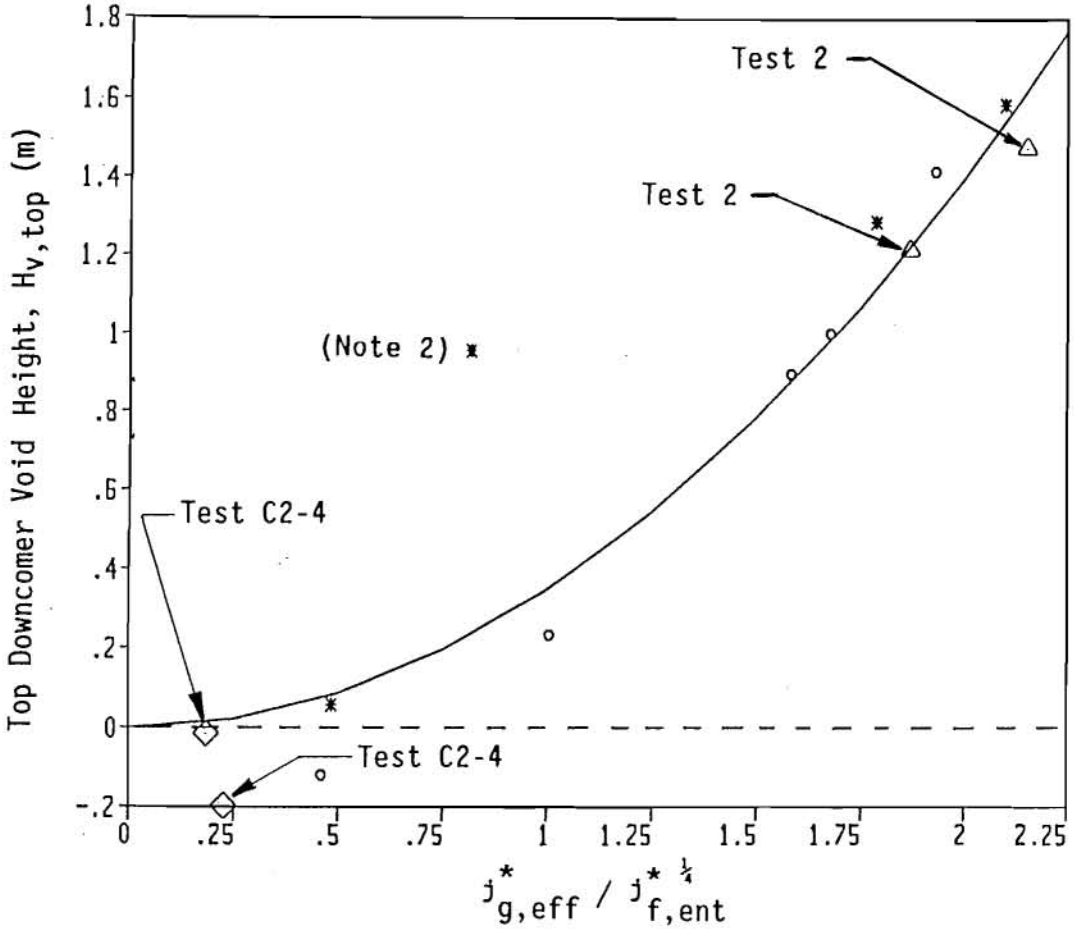

Notes:
1. The correlation is based on the UTPF Test 25 data.
2. Time averaged value is shown for 25-B-II data point. Downcomer level fluctuations, however, were approximately ± 0.9 m. Typical level fluctuations for other points were ± 0.2 m.

MPR DOWNCOMER LEVEL/ENTRAINMENT CORRELATION FOR UPTF COLD LEG INJECTION TESTS (REFERENCE U-455)

FIGURE 4.2-3

DOWNCOMER AZIMUTHAL STEAM FLOW:

$$\frac{V_1}{V_2} = \left[\frac{\dot{M}_1}{\dot{M}_2}\right]\left[\frac{\rho_2}{\rho_1}\right]\left[\frac{L_2}{L_1}\right]\left[\frac{Gap_2}{Gap_1}\right]$$

$$\frac{V_{UPTF}}{V_{CCTF}} = 7.7 \qquad \frac{V_{UPTF}}{V_{PWR}} = 1.9$$

$$\frac{j_1^*}{j_2^*} = \left[\frac{V_1}{V_2}\right]\left[\frac{L_2}{L_1}\right]^{1/2}$$

$$\frac{j^*_{UPTF}}{j^*_{CCTF}} = 8.2 \qquad \frac{j^*_{UPTF}}{j^*_{PWR}} = 2.4$$

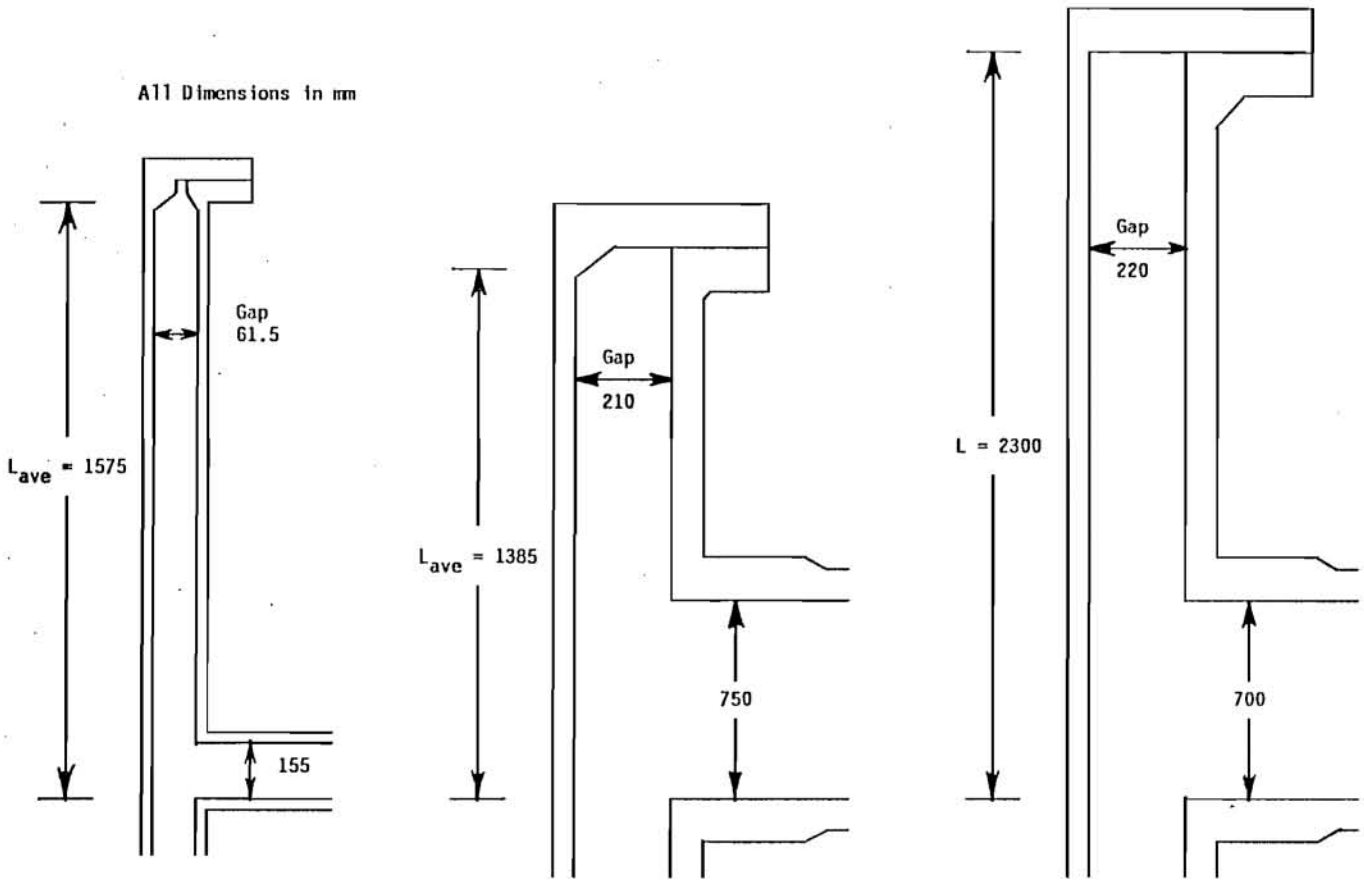

CCTF (1/21) UPTF (1.1/1) WESTINGHOUSE PWR (1/1)

Note: Facility scale is based on the downcomer flow area.

COMPARISON OF UPPER DOWNCOMER DIMENSIONS AND EFFECT ON DIMENSIONLESS VELOCITY

FIGURE 4.2-4

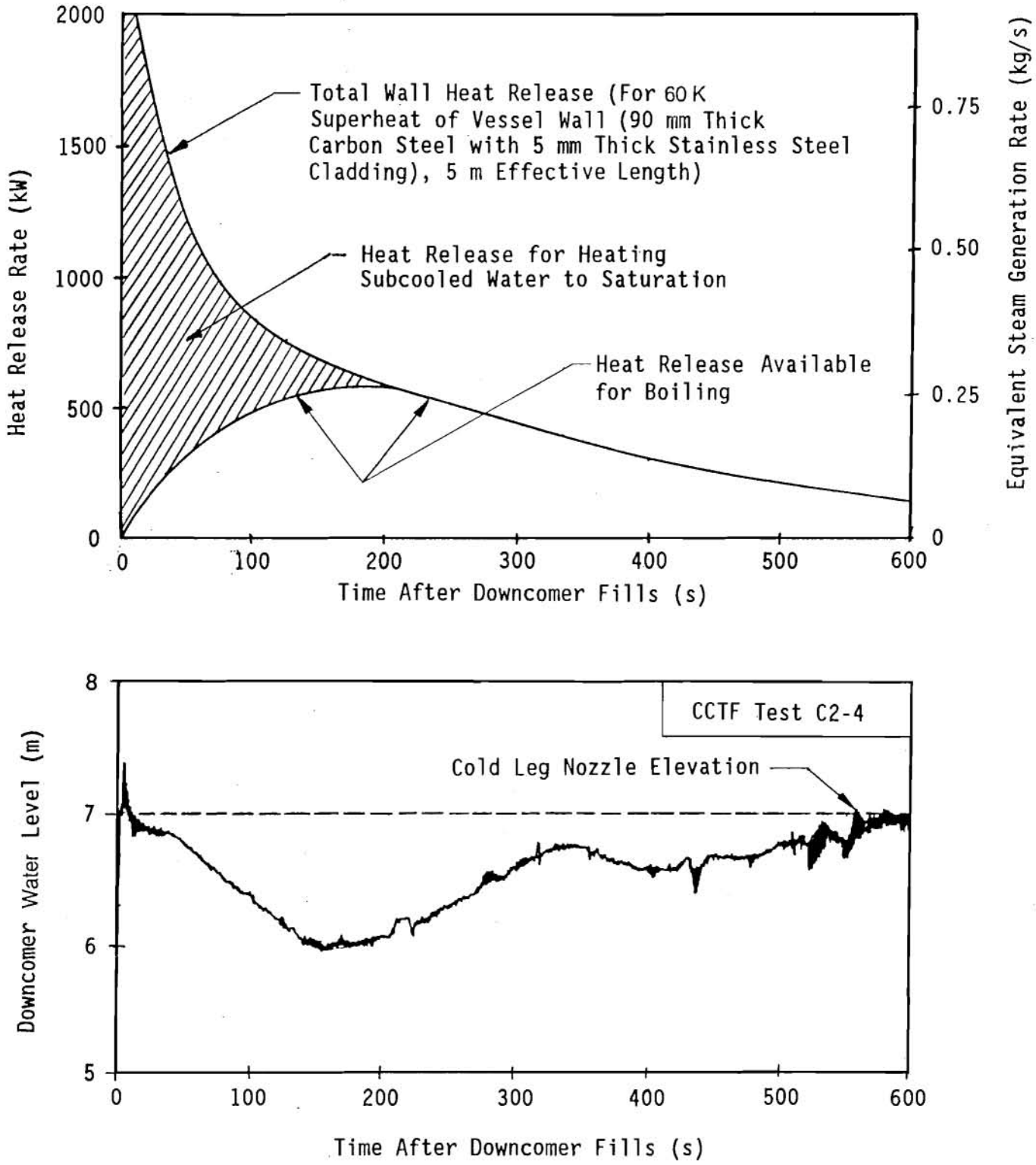

DOWNCOMER WALL STEAM GENERATION AND EFFECT ON DOWNCOMER WATER LEVEL IN CCTF COLD LEG INJECTION TEST (REFERENCE U-455)

FIGURE 4.2-5

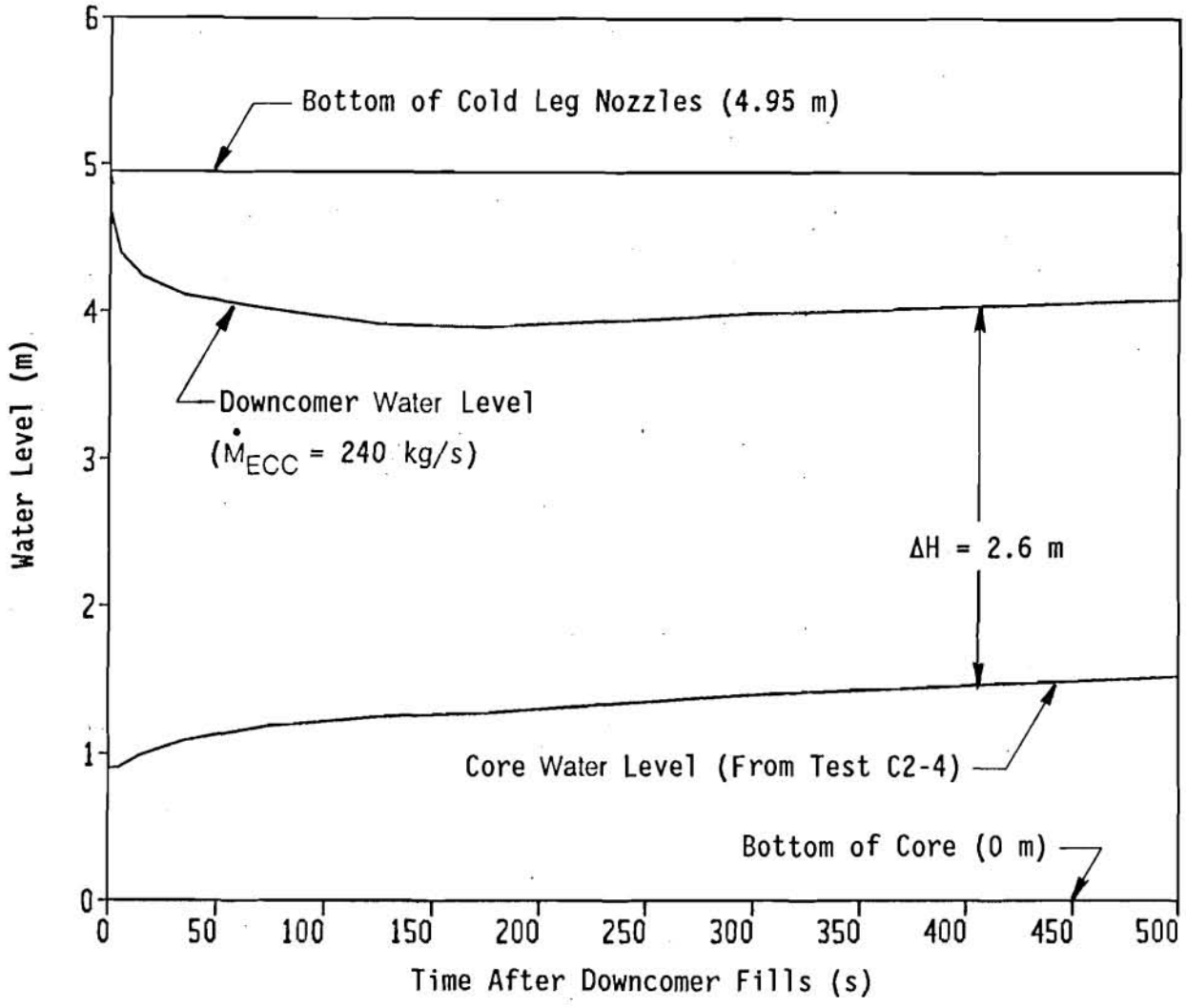

Notes:

1. Core water level is from CCTF Test C2-4.
2. PWR Geometry is for Westinghouse four-loop 3400 MWt plant.
3. Wall boiling rate is based on 150 K initial wall superheat and 5 m effective length for heat transfer.
4. The effective steam flow for entrainment is based on a total intact loop steam flow of 100 kg/s, an ECC injection rate of 240 kg/s and a condensation efficiency of 80%.
5. The core inlet mass flow rate is 100 kg/s.

ESTIMATED DOWNCOMER WATER LEVEL
IN A COLD LEG INJECTION PWR DURING REFLOOD
(REFERENCE U-455)

FIGURE 4.2-6

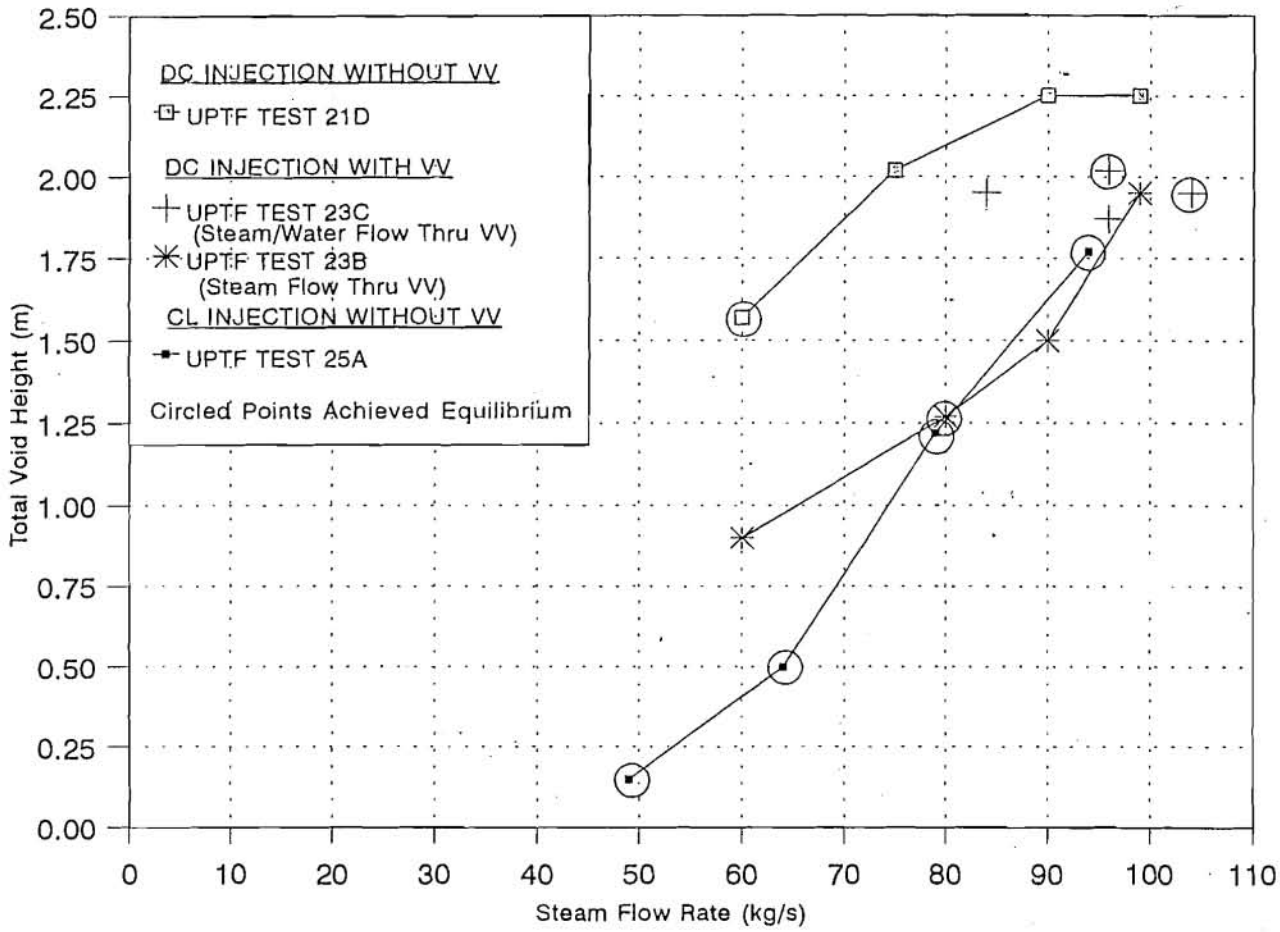

DOWNCOMER VOID HEIGHT VERSUS STEAM FLOW
FOR UPTF DOWNCOMER INJECTION TESTS
(REFERENCE U-460)

FIGURE 4.2-7

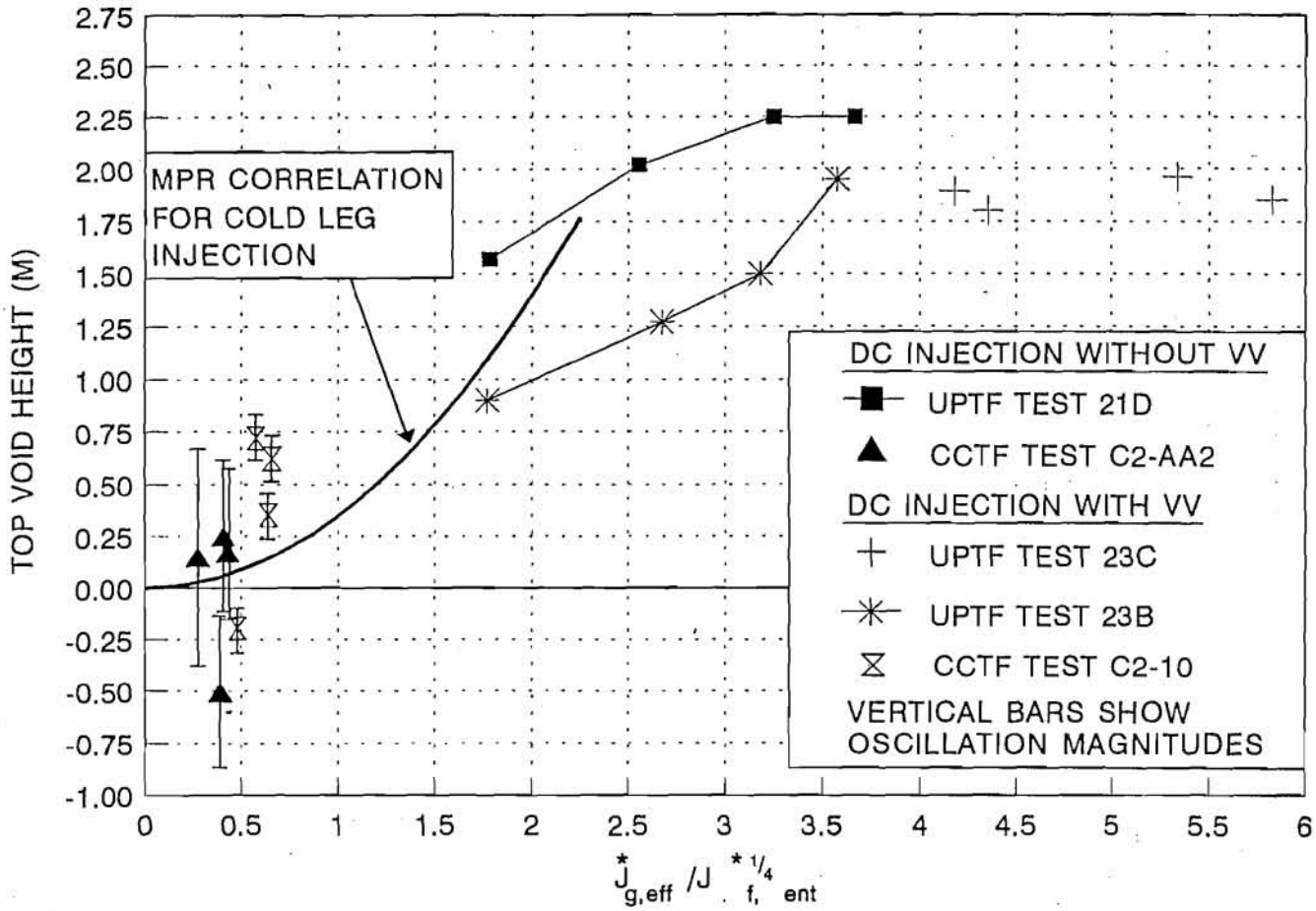

COMPARISON OF UPTF AND CCTF RESULTS
FOR DOWNCOMER INJECTION
WITH DOWNCOMER ENTRAINMENT CORRELATION
FOR COLD LEG INJECTION
(REFERENCE U-460)

FIGURE 4.2-8

4.3 STEAM/ECC INTERACTIONS IN LOOPS

Definition of Issue and Description of Phenomena

During an LBLOCA, ECC is injected into the reactor coolant system to refill the lower plenum and reflood the core. For most PWRs, the ECC is injected through nozzles in the reactor coolant piping; i.e., cold legs and/or hot legs. The interaction of the loop steam flow with subcooled ECC results in either a plug flow regime or a separated flow regime depending on the steam flow rate, ECC flow rate, ECC subcooling, and ECC injection configuration.

- Plug flow regimes are characterized by the formation of a water plug which fills the pipe cross section. In plug flow, the plug can either remain stationary or oscillate relative to the injection nozzle location.

- Separated flow is typically stratified flow. The steam and water flows can be cocurrent (e.g., cold leg ECC injection) or countercurrent (e.g., hot leg ECC injection).

Because the steam and ECC flow rates change with time during the course of a LOCA, changes in flow regime also occur. In some cases an "intermediate" flow regime can occur, in which the flow switches between plug and separated regimes, even for relatively constant conditions; this regime is called unstable plug flow.

With cold leg injection, both the ECC and steam flows are toward the downcomer (i.e., cocurrent). In this case, plug formation is determined by steam condensation. Oscillatory plug flow occurs at high ECC flows due to condensation oscillations. When the plug/steam interface is downstream of the ECC nozzle, the steam condenses on the plug interface which is continuously supplied with subcooled ECC. This strong condensation causes a reduction in steam pressure in the cold leg which draws the plug upstream. When the plug/steam interface is upstream of the ECC nozzle, the interface becomes saturated and condensation reduces significantly. Steam pressure increases and pushes the plug downstream until the interface is exposed to the ECC nozzle and the process repeats. As the ECC flow decreases, the magnitude of the oscillations decreases. At low ECC flows, the plug breaks down into the cocurrent stratified flow regime (see Figure 4.3-1).

For hot leg injection, the ECC and steam flows are countercurrent rather than cocurrent. In this case, the steam/ECC interaction involves both condensation and the countercurrent flow limitation (CCFL). Flow in the hot legs can be stratified flow or plug flow. Plug formation occurs at high steam flows due to the reversal of the ECC flow by the momentum of the steam. The plug grows toward the steam generator (SG) as water accumulates in the hot leg. Water which reaches the SG U-tubes is evaporated by heat transfer from the secondary side. The plug is discharged

into the upper plenum when either the hydrostatic head of the plug, or the pressure increase due to the evaporation in the U-tubes exceeds the loop differential pressure.

In combined injection PWRs, the phenomena described above occur simultaneously in the hot legs and cold legs. Also, the steam/ECC interaction in the hot leg can influence behavior in the cold leg and vice versa.

Overall, the steam/ECC interaction in the loops and the resultant flow regime affect the steam condensation rate, the steam flow in the loops, and the rate and temperature of ECC delivery to the reactor vessel.

Importance of Issue to PWR LOCA Behavior

The steam/ECC interaction in the loops and the resultant flow regime determine the steam condensation rate, and the temperature and rate of ECC delivery to the reactor vessel. Plug formation in the loops could block steam flow in the loops and thereby impair venting of steam generated in the core. These phenomena affect the overall system LOCA response, including core flooding rate and core cooling. The plug flow regime can also result in large oscillations of steam flow, water delivery to the reactor vessel, and system and loop pressures which may impact the time that reflood initiates and may excite downcomer-core manometer oscillations during reflood.

Tests and Analyses that Relate to Issue

The steam/ECC interaction in the loops and associated flow regimes have been investigated in several tests and analyses within the 2D/3D Program and elsewhere. Table 4.3-1 lists the tests which are considered in this evaluation. Within the 2D/3D Program, separate effects tests at UPTF investigated flow regime, condensation effects and countercurrent flow effects under controlled conditions. These tests covered cold leg injection, hot leg injection, and combined injection. Also, integral tests at CCTF and UPTF provided information on steam/ECC interactions during simulated transients. Outside the 2D/3D Program, numerous separate effects tests were performed at small-scale facilities. The small-scale tests included tests with cold leg injection and tests with hot leg injection.

The evaluation of the UPTF separate effects with cold leg injection including comparisons to the applicable integral tests at CCTF and UPTF, and the separate effects tests at small-scale facilities is provided in Reference U-458. Evaluation of the UPTF separate effects tests with hot leg injection is provided in References G-411 and G-911. Reference G-411 also covers the evaluation of the combined injection integral tests. The major results of these evaluations and comparisons are discussed below.

Post-test TRAC calculations have been performed for several of the UPTF and CCTF tests. These analyses include TRAC-PF1/MOD1 calculations of UPTF Tests 8 and 9 (References G-641 and G-642, respectively) and TRAC-PF1/MOD2 calculations of UPTF Tests 8A, 25, 2 and 17B, and several CCTF tests (Reference U-714). In addition, a post-test analysis of UPTF Test 26A was performed using ATHLET (Reference G-646).

Summary of Key Results and Conclusions from Tests and Analyses

The test results indicate that the loop flow regime depends strongly on the thermodynamic ratio (R_T) which is the ratio of the potential condensation rate to the steam flow. A thermodynamic ratio of one indicates that the ECC can fully condense the steam.

$$R_T = \frac{\dot{M}_{ECC} C_P (T_{sat} - T_{ECC})}{\dot{M}_{STM} (h_{STM} - h_f)}$$

In general, stratified flow occurred when the condensation potential of the ECC was less than the steam flow ($R_T < 1$), and plug flow occurred when the condensation potential of the ECC exceeded the steam flow ($R_T > 1$). Whether plug flow was stable or unstable was determined by the momentum flux of the loop steam flow. Detailed discussions of the results are provided in Subsections 4.3.1, 4.3.2, and 4.3.3 for cold leg injection, hot leg injection, and combined injection, respectively.

4.3.1 Cold Leg Injection

The results of the UPTF separate effects tests with cold leg injection are plotted in Figure 4.3-2. This figure indicates that plug flow only occurred when the condensation potential of the ECC exceeded the steam flow (i.e., thermodynamic ratio greater than one). At low steam flows plug flow was unstable because the momentum of the steam flow was not sufficient to maintain the plug. The cyclic formation and decay of water plugs in unstable plug flow resulted in large pressure and flow oscillations.

Figure 4.3-2 also indicates that stratified flow always occurred when the steam flow exceeded the ECC condensation potential (i.e., a thermodynamic ratio less than one). Stratified flow also occurred at thermodynamic ratios slightly greater than one. In these cases, thermal stratification of the water layer in the bottom of the cold leg limited condensation to less than its maximum value and prevented total consumption of steam. The highest thermodynamic ratio for which stratified flow was observed was about 1.3.

For comparison, Figure 4.3-2 includes data from UPTF integral test results covering flow conditions from end-of-blowdown through reflood. As shown in the figure, the integral test data were consistent with the separate effects test data.

As indicated above, for stratified flow conditions, the steam was only partially condensed. Condensation in this case was evaluated in terms of condensation efficiency, defined as the ratio of the measured condensation rate to the condensation rate needed to heat the ECC to saturation. The condensation efficiency for the UPTF separate effects tests was found to be 80-100% with saturated and slightly superheated steam as shown by the circle data on Figure 4.3-3. UPTF integral test results, where stratified flow conditions existed (the triangle data points in Figure 4.3-3), were consistent with the separate effects test results.

The flow regime results from subscale tests were found to be consistent with the UPTF results in that the transition from stratified flow to plug flow occurred at a thermodynamic ratio somewhat greater than one. A summary of the flow regime transition boundary vs. scale is shown in Figure 4.3-4. Scale appears to have a small influence on flow regime, whereas the nozzle orientation appears to have a more significant influence. The flow regime transition thermodynamic ratio tended to decrease slightly towards 1.0 with increasing scale for tests with top ECC injection nozzles. Results for tests with side ECC injection nozzles indicate that flow regime transition occurs at thermodynamic ratios around 1.3 instead of about 1.0 for top ECC injection. The thermodynamic ratio for the transition to plug flow was higher for side injection than top injection because side injection tends to result in thermal stratification of the water layer in the cold leg which, as indicated above, limits steam condensation and prevents plug formation. The condensation efficiencies determined from the scaled tests were close to 100%.

Post-test runs of the TRAC-PF1/MOD2 code (Versions 5.3 and 5.4) were used to assess the code's ability to predict cold leg flow phenomena for UPTF Tests 8A, 25, 2A, and 17B, and CCTF Tests C2-SH2 and C2-4 (Reference U-714). Results indicated that the code predicts the flow regime and the transition point between plug flow and stratified flow. For plug flow, the code predicted the frequency of the flow and pressure oscillations but slightly underpredicted the amplitude of the oscillations. Condensation during plug flow conditions was also underpredicted. For stratified flow conditions, code predictions of condensation rate and the temperature of ECC delivered to the downcomer were in good agreement with the test results.

Typically, cold leg injection PWRs use top injection for the ECC; hence, plug flow is expected to occur when the ECC flow is high enough to cause the thermodynamic ratio to exceed 1.0. During an LBLOCA, the high ECC flow from accumulator injection is sufficient to cause plug flow. Accumulator injection occurs during the end-of-blowdown, refill, and early reflood phases of the LBLOCA. The plug does not prevent steam flow through the cold leg as has sometimes been conservatively assumed; instead condensation on the plug interface induces a steam flow. The late reflood phase is characterized by lower ECC flow rates from the pumped low pressure coolant injection system. For this phase, stratified flow is expected except for selected combinations of conditions like low steam flow coupled with flow from both low pressure injection pumps (i.e., no-LPCI-failure case). Condensation efficiency during the stratified flow regime is expected to be near 100%.

4.3.2 Hot Leg Injection

In the UPTF tests with hot leg injection, three different flow regimes were observed; specifically, stable plug flow, unstable plug flow, and stratified flow. Each of these flow regimes is described below.

- In stable plug flow, a water plug formed adjacent to the injection nozzle. The plug grew toward the steam generator as ECC accumulated in the hot leg. For tests in which steam was injected in the steam generator simulator (SGS) to simulate vaporization of the plug in the steam generator U-tubes, the plug was discharged into the upper plenum when the combination of the increase in SGS pressure and the hydrostatic head of the plug exceeded the momentum flux of the steam flow. For tests in which steam was not injected in the SGS, the plug was discharged into the upper plenum when the hydrostatic head of the plug exceeded the momentum flux of the steam flow into the hot leg. In both cases, ECC delivery to the upper plenum fluctuated over time.

- In unstable plug flow, water plugs alternately formed and decayed. The cyclic formation and decay of water plugs resulted in pressure and flow oscillations, and fluctuations in ECC delivery to the upper plenum.

- In stratified flow, steam flowed toward the steam generator in the top portion of the hot leg while ECC flowed toward the upper plenum in the bottom portion of the hot leg. In some cases, the water layer was thermally stratified. At high steam flows, the ECC flow was partially reversed resulting in temporary water accumulation (or hold-up) and fluctuations in ECC delivery. However, at low steam flows, there was no significant hold-up and ECC delivery fluctuated only slightly.

Regardless of whether water delivery to the upper plenum fluctuated or was nearly steady, almost all of the ECC injected into the hot legs was delivered to the upper plenum.

Figure 4.3-5 is a plot of the steam flow versus condensation potential of the ECC which indicates the flow regime established under different conditions. Included in the figure is a line which shows the condensation potential and steam flow are equal (i.e., thermodynamic ratio, R_T, of one). Figure 4.3-5 shows that when the condensation potential was less than the steam flow (i.e., $R_T < 1$), flow in the hot leg was stratified to provide a vent path for the uncondensed steam flow.

Figure 4.3-5 shows that plug flow, either stable or unstable, occurred only when the condensation potential of the ECC exceeded the steam flow (i.e., $R_T > 1$). The UPTF data also show that, for a given condensation potential, unstable plug flow occurred at low steam flows.

Siemens calculated the minimum steam flow for stable plug flow assuming that the plug does not decay when the flow force acting on the end of the plug balances or exceeds the hydrostatic pressure on the plug end and the momentum flux of the ECC (Reference G-411). The calculations predict that the minimum steam flow for stable plug flow in the hot legs is dependent on the pressure, the pipe diameter, and the condensation potential of the ECC (Reference G-911). The results of these calculations are compared to the UPTF data in Figure 4.3-5 and to the Creare data in Figure 4.3-6. As shown in these figures, the calculated minimum steam flow for stable plug flow is consistent with the data.

Post-test calculations of the UPTF tests were performed using both TRAC-PF1/MOD1 and ATHLET. The momentum interaction between the steam and ECC was well predicted by the codes. Specifically, the code predictions of flow parameters such as mass flow rates, liquid levels, entrainment, and countercurrent flow limitation were in good agreement with the test data. However, the code predictions of interfacial heat transfer were deficient (References G-641 and G-646).

Based on the full-scale UPTF tests, the following conclusions can be made regarding LBLOCA behavior in PWRs with hot leg ECC injection.

- For typical core exit steam flows (i.e., 50 kg/s to 100 kg/s) and ECC flow rates up to 150 kg/s, the flow regime in the hot leg is stratified countercurrent flow and ECC delivery to the upper plenum is steady. However, for ECC flow rates higher than 150 kg/s, the flow regime is plug flow and delivery of subcooled ECC to the upper plenum fluctuates.

- Regardless of the hot leg flow regime, almost all ECC injected into the hot legs is delivered to the upper plenum. In the case of plug flow, a small amount of water is evaporated if the water plug enters the SG U-tubes.

4.3.3 Combined Injection

In the UPTF separate effects test with combined injection (Test 9), stratified flow was observed in both the hot and cold legs for ECC injection rates less than 100 kg/s. However, for ECC flows greater than 200 kg/s, plugs formed in both the hot leg and cold leg. Formation of the plugs was affected by changes in the pressure of the steam volume between the plugs (i.e., between the steam generator simulator [SGS] and the pump simulator). Specifically, condensation on the pump simulator side of the cold leg plug and the SGS side of the hot leg plug reduced the pressure in the steam volume between the plugs. Consequently, the plugs grew toward each other. When the hot leg plug entered the SGS tube region, steam was injected into the top of the SGS to simulate vaporization of water in steam generator U-tubes. This pressurized the steam volume between the plugs and pushed the hot leg plug to the upper plenum and the cold leg plug to the downcomer. After the hot leg plug was discharged into the upper plenum, another cycle of plug formation started.

A post-test analysis of UPTF Test 9 was performed using TRAC-PF1/MOD1 to assess the code's ability to predict flow phenomena in the intact loops (Reference G-632). The results of the analysis are summarized briefly below.

- Overall, the TRAC predictions were in good agreement with the test. Specifically, plug movement was dependent on the pressure history in the steam volume between the hot leg plug and the cold leg plug, and delivery of ECC to the upper plenum was intermittent.

- TRAC correctly calculated the cold leg liquid temperatures on both sides of the ECC injection nozzle. This indicates that heat transfer from the vapor to the subcooled liquid by direct contact condensation is adequately modeled in the code.

- TRAC correctly calculated the formation of a plug in the hot leg between the injection pipe (Hutze) and the SGS. While the calculated temperature in the water plug behind the injection nozzle was too low, the calculated temperature of the ECC stream between the injection nozzle and upper plenum was too high.

For ECC injection rates typical of combined injection PWRs (i.e., >200 kg/s per injection nozzle), the following conclusions can be made.

- The flow regime in both the hot and cold legs is plug flow and delivery to the reactor vessel (upper plenum and downcomer) fluctuates.

- Essentially all ECC injected into the intact loops is delivered to the reactor vessel.
- The steam flow in the intact loops is completely condensed in the loops.

Table 4.3-1

SUMMARY OF TESTS RELATED TO STEAM/ECC INTERACTION IN THE LOOPS

Type of Test	Facility	Facility Scale[1]	References
Cold Leg Injection Separate Effects Tests	UPTF: Test 8 Test 25	1	U-458, G-411 G-008, G-208 G-025, G-225
Cold Leg Injection Integral Tests	UPTF: Test 2 Test 4 Test 17	1	U-458, G-411 G-002, G-202 G-004, G-204 G-017, G-217
	CCTF-II: Test C2-2 Test C2-4 Test C2-12 Test C2-14	1/5	U-414 J-046, J-244 J-052, J-250 J-060, J-258 J-062, J-260
Cold Leg Hydraulic Resistance Tests	Westinghouse	1/14	E-435
	Westinghouse	1/3	E-435
	Combustion Engineering	1/5	E-431
	Combustion Engineering	1/3	E-432
Cold Leg Flow Regime Tests	Creare	1/20	E-433
	Tokyo Institute of Technology	1/25	E-911 J-936

Table 4.3-1

SUMMARY OF TESTS RELATED TO STEAM/ECC INTERACTION IN THE LOOPS

Type of Test	Facility	Facility Scale[1]	References
Hot Leg Injection Separate Effects Tests	UPTF: Test 8 Test 26	1	G-411, G-911 G-008, G-208 G-026, G-226
Hot Leg Flow Regime Tests	Creare	1/5	E-434
	Creare	1/10	E-434
Combined Injection Separate Effects Tests	UPTF: Test 9	1	G-411 G-009, G-209
Combined Injection Integral Tests	UPTF: Test 3 Test 14 Test 18 Test 19	1	G-411 G-003, G-203 G-014, G-214 G-018, G-218 G-019, G-219
	CCTF-II: Test C2-19 Test C2-20 Test-C2-21	1/5	J-067, J-454, J-455 J-068, J-456 J-069, J-456

NOTE:

1. The facility scale is based on the loop diameter and is relative to a typical PWR.

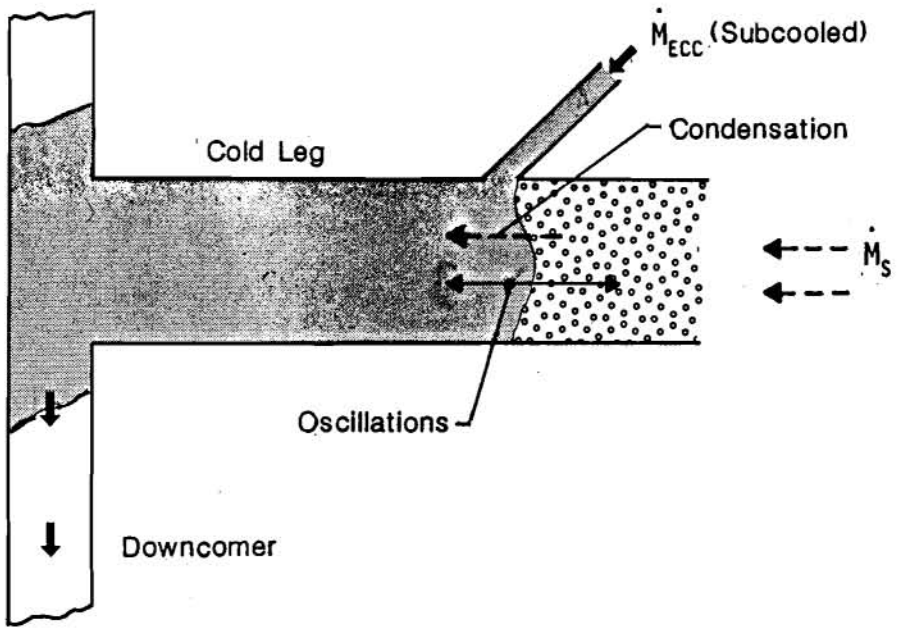

PLUG FLOW

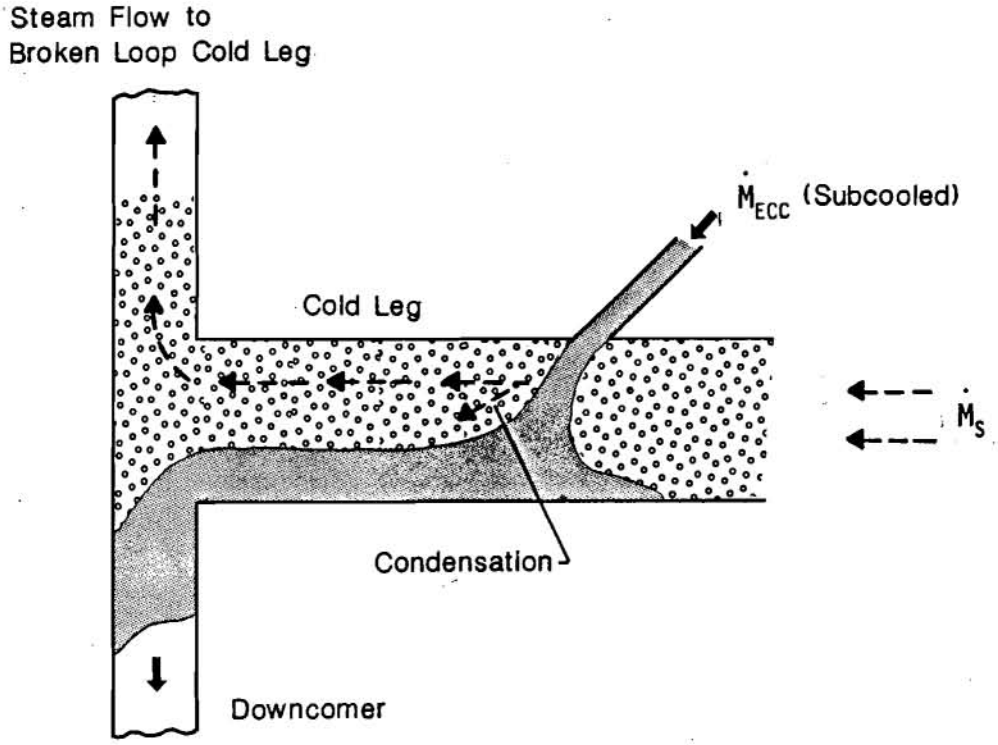

STRATIFIED FLOW

COLD LEG FLOW REGIMES

FIGURE 4.3-1

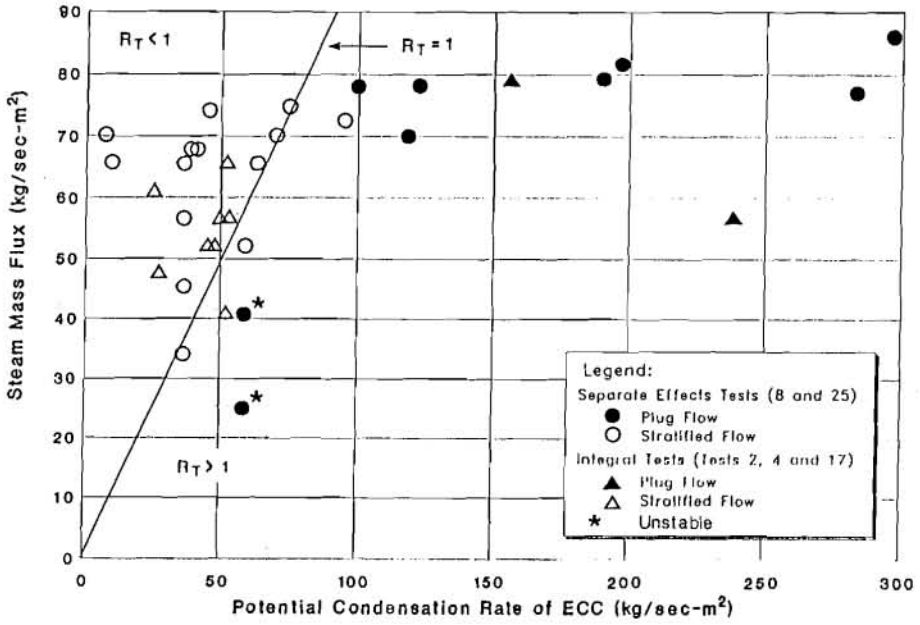

COLD LEG FLOW REGIME DATA
FROM UPTF COLD LEG INJECTION TESTS
(REFERENCE U-458)

FIGURE 4.3-2

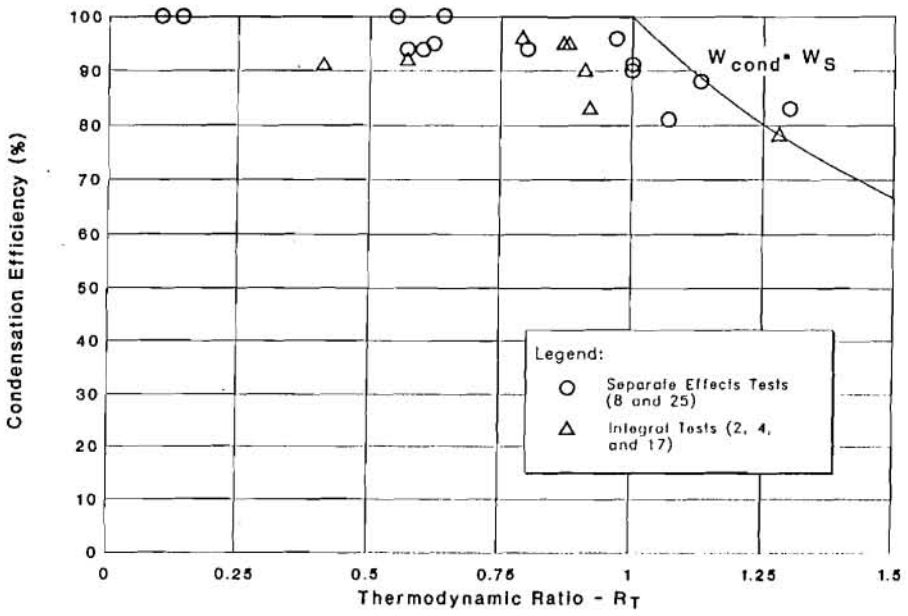

CONDENSATION EFFICIENCY FOR STRATIFIED FLOW CONDITIONS
IN UPTF COLD LEG INJECTION TESTS
(REFERENCE U-458)

FIGURE 4.3-3

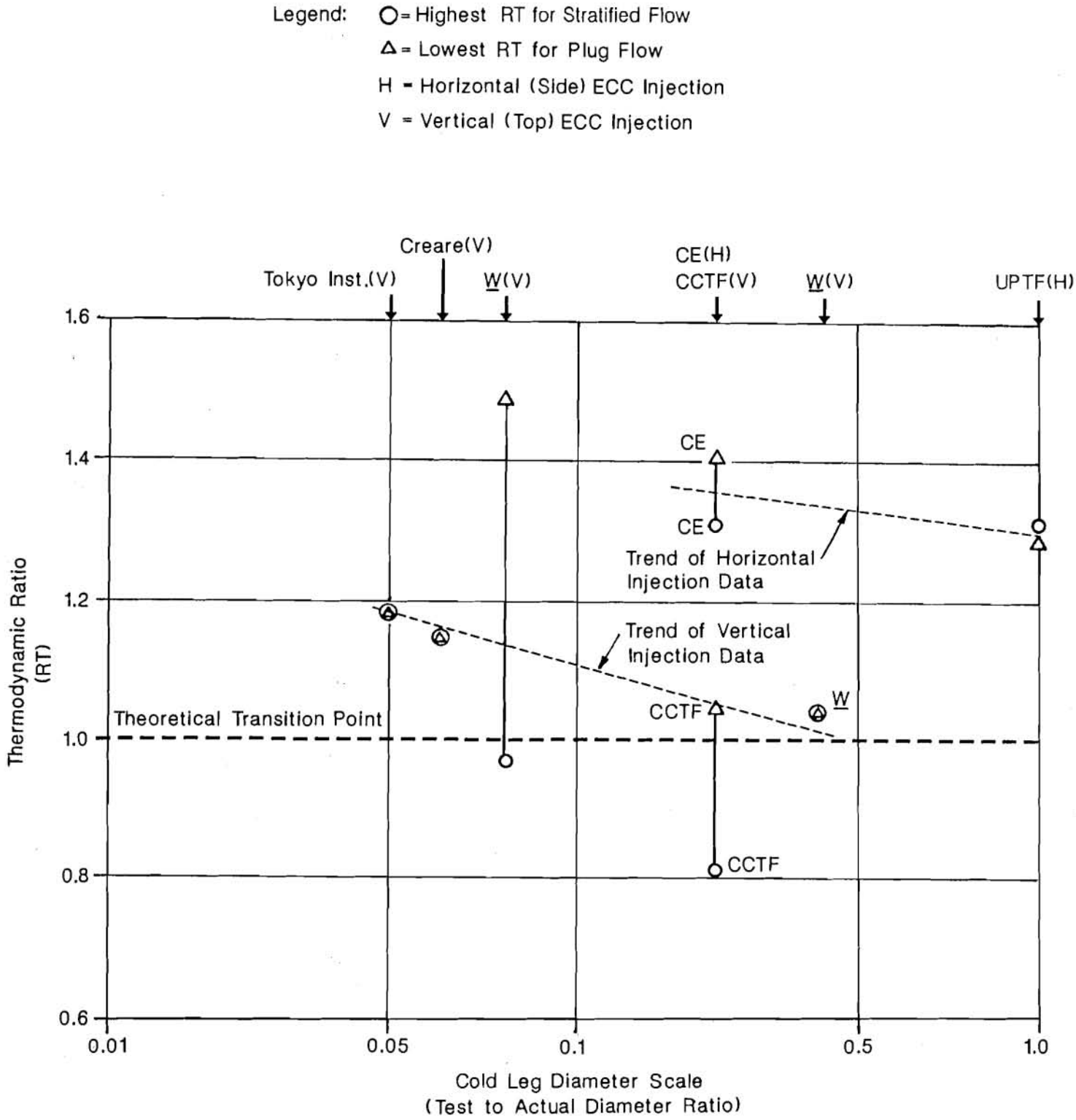

EFFECT OF SCALE AND NOZZLE ORIENTATION ON THE TRANSITION FROM PLUG TO STRATIFIED FLOW IN THE COLD LEGS (REFERENCE U-458)

FIGURE 4.3-4

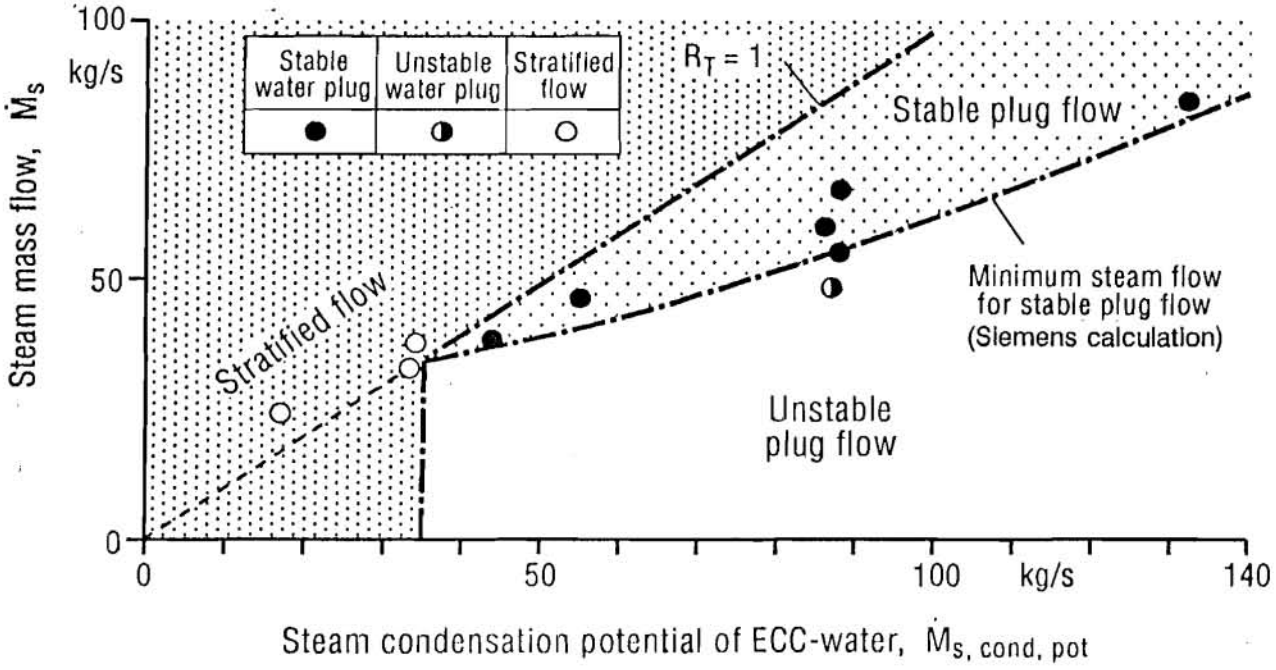

HOT LEG FLOW REGIME DATA
FROM UPTF HOT LEG INJECTION TESTS
(REFERENCE G-411)

FIGURE 4.3-5

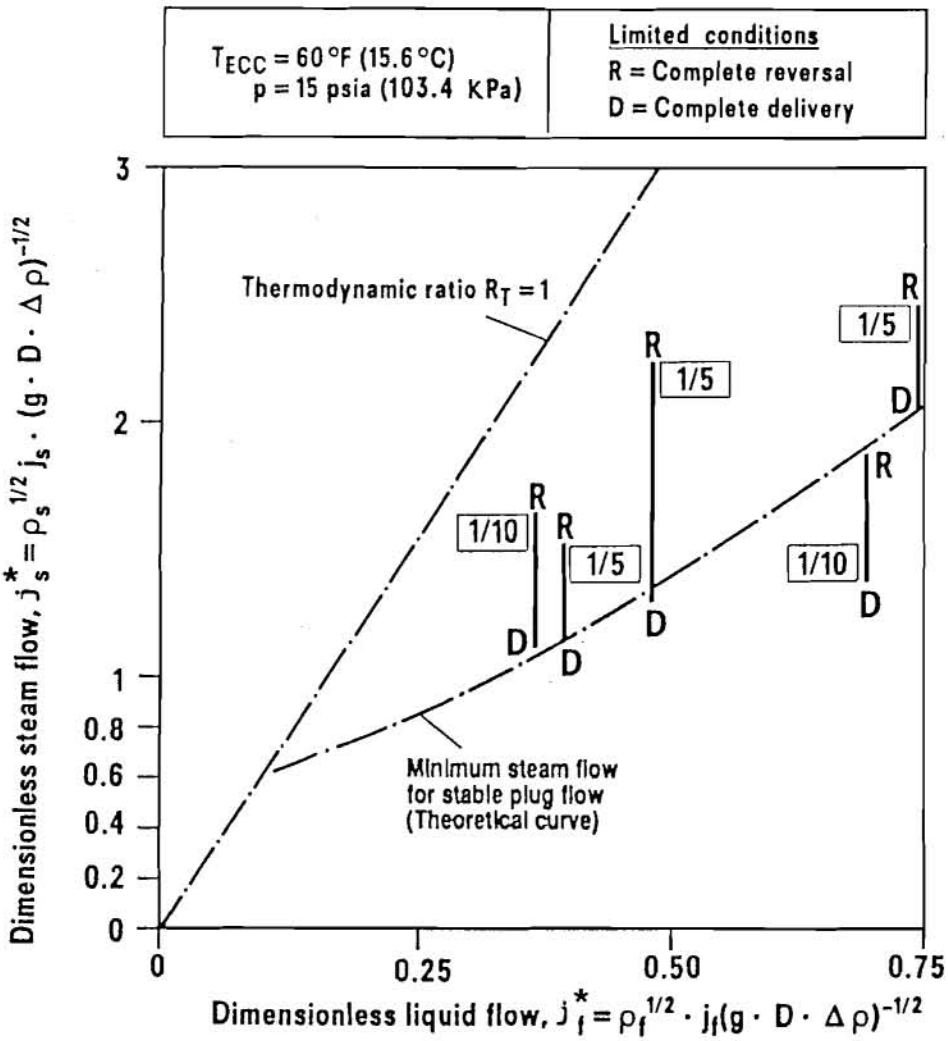

1/10 , 1/5 = Creare measurement data for scaled tests 1/10, 1/5 (Original: UPTF)

COMPARISON OF RESULTS FROM CREARE HOT LEG COUNTERCURRENT FLOW TESTS WITH THEORETICAL CURVE FOR STABLE PLUG FLOW (REFERENCE G-411)

FIGURE 4.3-6

4.4 EFFECT OF ACCUMULATOR NITROGEN DISCHARGE

Definition of Issue and Description of Phenomena

In some PWRs, depending on accumulator design, the discharge of nitrogen from ECC accumulator tanks into the primary system occurs shortly after the start of the reflood phase of the LOCA transient. When the water in the accumulator tank attached to the cold leg of each coolant loop is depleted, the nitrogen that pressurizes the tanks escapes through the ECC piping (see Figure 4.4-1). The nitrogen flows at a much higher volumetric rate than the preceding water because the pressure losses in the piping are less for the lower density gas. The effects of the nitrogen flow transient have been discussed previously in Reference U-911, a summary of TRAC analyses of the phenomenon.

The nitrogen quickly pushes ECC water from the intact cold legs into the reactor vessel downcomer. Also, water in the top of the downcomer and in the broken cold leg is pushed toward the break. The primary system (particularly the region into which the nitrogen is injected) is pressurized for a short period until the nitrogen can leave the system.

System pressure is further increased by suppression of steam condensation. As nitrogen mixes with or displaces steam, the rate of condensation becomes much lower than when pure steam was in contact with the subcooled water (see Figure 4.4-1). The accumulation of uncondensed steam contributes to the temporary pressurization of the downcomer and cold leg regions of the primary system.

Note that just before the nitrogen discharge begins, the pressure above the core exceeds the pressure in the downcomer due to the pressure drop of steam flowing from the upper plenum around the intact loops. The pressure difference keeps the water level in the core lower than in the downcomer (see Figure 4.4-2). The nitrogen pressurization of the downcomer disrupts the existing pressure distribution and forces a portion of the water in the downcomer into the lower plenum, displacing lower plenum water into the core (see Figure 4.4-3). The lower plenum water is subcooled, in part due to the rise in pressure. As the water surges into the core, heat is absorbed until, after a brief delay during which the water is heated to saturation, additional steam is produced.

The increased steam production in the core increases the pressure above the core. The pressure increase, coupled with a decreasing nitrogen discharge rate, eventually stops the rise in core water (see Figure 4.4-4) and then forces some of the water to flow out of the core and back into the lower plenum (see Figure 4.4-5). More water may remain in the core than was present before the nitrogen-induced surge.

Importance of Issue to PWR LOCA Phenomena

Proper understanding and characterization of the nitrogen discharge transient is important because the reflood turnaround in clad temperatures can be significantly affected. Specifically, the volume and duration of the water surge into the core may be sufficient to quench some portions of the core and to temporarily arrest the temperature rise in other portions. The ensuing reflood would begin with lower clad temperatures.

The goals of the 2D/3D tests and analyses discussed in this section were to confirm the occurrence of, and quantify the magnitude and duration of, the following phenomena:

- The dilution or displacement of steam in the downcomer and cold leg regions by nitrogen,
- The rapid increase in core water inventory,
- The subsequent drop in core water inventory, and
- The quench or cooling of the fuel rods and the reduction in clad temperatures.

Note that the issue of the effect of accumulator nitrogen discharge is not applicable to GPWRs with combined injection because the accumulators are designed not to empty completely during an LBLOCA.

Tests and Analyses that Relate to the Issue

Tests and analyses related to accumulator nitrogen discharge, which are evaluated in this report, are listed in Table 4.4.-1. Within the 2D/3D Program, one CCTF test (Test C1-15) and one UPTF test (Test 27A) simulated the nitrogen discharge. Outside the 2D/3D Program, a nitrogen discharge test was conducted at Achilles. Three TRAC PWR calculations included accumulator nitrogen discharge as part of the LBLOCA transient. The results of the 2D/3D tests and TRAC PWR analyses are summarized in Tables 4.4-2 and 4.4-3, respectively.

CCTF Test C1-15 apparently was not successful in simulating the nitrogen discharge. In the test, ECC water was injected into the intact cold legs from a single accumulator tank pressurized by nitrogen. The water inventory and valve timing for the tank allowed the nitrogen to flow out of the tank for 10 seconds after the water was depleted. However, test measurements indicate that most or all of the nitrogen apparently was expended in clearing out the lengthy ECC piping between the tank and the loop nozzles. Water was still passing through the cold leg injection nozzles until just before the accumulator tank outlet valve was closed. Observed effects on the

downcomer and core water levels were minimal, and no nitrogen was detected by calculations of the steam partial pressure in the cold legs and reactor vessel. Accordingly, the test did not yield detailed insight into effects of the nitrogen discharge in the primary system.

UPTF Test 27 Phase A was successful in injecting nitrogen into the primary system and induced measurable effects, but the duration of the nitrogen discharge was much shorter than planned. Due to facility limitations, the test injected nitrogen directly into the upper downcomer rather than through each cold leg ECC nozzle. Downcomer injection was judged to have an equivalent effect on core and downcomer water levels. Unfortunately, less than one second after the nitrogen discharge initiated, automatic shutdown of the test occurred due to an excessive indicated water level rise of over four meters in the core region. In all, about 11 m^3 (40% of the downcomer volume) of nitrogen was injected before the test ended.

The three TRAC PWR analyses modelled core cooling following a large-break LOCA in four-loop reactor plants. The analyses are summarized in References U-724, U-726, and U-727. As shown in Table 4.4-3, the assumptions in one analysis varied slightly from assumptions in the others, but the results were very similar. In addition to the PWR analyses, a post-test TRAC analysis of UPTF Test 27A, which simulated nitrogen discharge, was performed.

The reviews of the results of the TRAC evaluation and the analyses of the CCTF and UPTF tests are detailed in Reference U-459. The Achilles test is discussed in Reference E-031.

Summary of Key Results and Conclusions from Tests and Analyses

The results of the evaluation of UPTF Test 27A are summarized in Table 4.4-2. Evaluation of the UPTF test results revealed that the large indicated core water level increase and downcomer water level decrease were not representative of true level changes. The fluid in each region was displaced so rapidly that inertial and flow velocity pressure gradients in the fluid distorted level indications that were based on differential pressure. The pressure gradients and corrected water levels were calculated using a simplified hydraulic model of the regions (Reference U-459). The corrected core and downcomer water levels during the transient are plotted in Figure 4.4-6. The beginning of nitrogen injection and the end of the test are indicated in the figure. In the short time that the test ran during the nitrogen injection, the corrected core level rose by about 1.5 meters from 20% of the core height to 60% of the core height. The test was terminated before the peak level occurred. The UPTF test did not simulate the peak magnitude and duration of the core level surge, the long-term effects of the nitrogen, or the effect of the level surge on core cooling.

Evaluation of UPTF Test 27A also showed that steam in the downcomer and cold legs was significantly diluted by nitrogen. The composition of the steam/nitrogen mixture in the downcomer and one intact cold leg is plotted in Figure 4.4-7. Pressure and

temperature measurements at three locations around the top of the downcomer and in a cold leg between the ECC injection nozzle and the pump simulator were used to determine the local partial pressures of steam and nitrogen and the relative composition of the mixture. Figure 4.4-7 shows the mass fraction of steam in the downcomer was reduced to less than 10% within 0.3 seconds. The steam in the cold leg was diluted to a similar concentration a short time later. (Note, the delay between the downcomer and cold legs is not anticipated to occur in actual PWRs where the nitrogen discharges into the cold legs.) Dilution of the steam with nitrogen suppresses steam condensation in the cold legs and downcomer which contributes to pressurization of the downcomer; however, the effect of this dilution on the rate of steam condensation was not measured in the UPTF test.

In the Achilles test, the surge of water into the core enhanced core cooling and temporarily increased steam generation. Also, water carryover to the upper plenum increased, resulting in a decrease in the core/downcomer inventory. The surge of water back into the downcomer from the core resulted in manometer oscillations and water spillover out the broken cold leg, which further decreased the downcomer/core inventory. Core cooling was degraded for about 50 seconds until the inventory decrease was recovered by accumulation of ECC (Reference E-031).

The results of the TRAC PWR analyses are summarized in Table 4.4-3. The water inventory in the core just prior to the nitrogen discharge was low--the volume fraction of only 0% to 20%. During the nitrogen release, the core water inventory peaked at a volume fraction of 60% to 70%. All three analyses predicted that the surge would quench the hottest portion of the hottest rod, with a sustained turnaround in the cladding temperatures. Within 10-15 seconds of the initial nitrogen surge, the rising pressure above the core drove water from the core back into the downcomer. The minimum core inventory after nitrogen discharge was 30% to 40% (which is greater than the inventory before nitrogen discharge).

In addition to the PWR analyses, with nitrogen discharge, a post-test TRAC analysis of UPTF Test 27A was performed. As shown in Figure 4.4-8, TRAC predicted the pressure trends in the upper plenum and downcomer during nitrogen discharge. However, because TRAC overpredicted the rate of condensation in the downcomer, the calculated downcomer pressure did not exceed the upper plenum pressure; consequently, TRAC underpredicted the core level surge.

In summary, the UPTF test confirmed some phenomena related to accumulator nitrogen discharge which were predicted in TRAC PWR analyses; namely, the pressurization of the downcomer, the dilution of steam in the downcomer and cold legs, and the surge in the core water level. While the UPTF test did not simulate the effects of nitrogen discharge on core cooling, TRAC PWR analyses suggest that accumulator nitrogen discharge and the resulting surge in the core water level are

beneficial to core cooling. Specifically, TRAC predicts that the hottest portion of the hottest rod is quenched by the level surge.

Table 4.4-1

SUMMARY OF TESTS AND ANALYSES ADDRESSING
THE EFFECT OF NITROGEN DISCHARGED FROM ECC ACCUMULATORS

Type of Test or Analysis	Facility	References
End-of Blowdown, Refill & Reflood Test	UPTF Test 27A	U-459 G-027 G-227 G-411
Refill & Reflood Test	CCTF Test C1-15	U-459 J-020 J-218 J-407
Reflood Test	Achilles	E-031
TRAC-PF1/MOD2 Post-test Analysis of UPTF Test 27A	---	U-716
TRAC-PF1/MOD1 PWR Analyses	--- --- ---	U-724 U-726 U-727

Table 4.4-2

SUMMARY OF RESULTS FROM 2D/3D TESTS THAT INVESTIGATED THE EFFECT OF THE DISCHARGE OF NITROGEN FROM ECC ACCUMULATORS

Facility	Test	Scale[1]	Conditions	Limitations	Results
CCTF	C1-15	Core: 1/21.0 Downcomer: 1/17.0	· Refill & reflood · Subcooled ECC into cold legs · N_2 into cold legs	· N_2 depleted in injection piping before reaching cold legs	· Minimal effect on system--see limitations
UPTF	27 Phase A	Core: 1.05 Downcomer: 1.08	· End-of-blowdown, refill & reflood · Subcooled ECC into cold legs · N_2 into downcomer	· Test terminated <1 sec after start of N_2 · Core, downcomer levels corrected for flow and inertial effects	· Core water inventory increased from ~20% before N_2 to ~60% at end of test · Steam in downcomer diluted to mass fraction of less than 10% after 0.3 sec.

NOTE:

1. Scale based on ratio of facility flow area (core or downcomer) to flow area in 3400 MWt Westinghouse or Japanese plant.

Table 4.4-3

SUMMARY OF RESULTS FROM TRAC PWR ANALYSES THAT INVESTIGATED THE EFFECT OF THE DISCHARGE OF NITROGEN FROM ECC ACCUMULATORS

Year	Performed By	Model	Core Water Inventory (Liquid Volume Fraction)		
			Just Before N_2	Peak During N_2 (Duration)	Minimum After N_2
1986	LANL (Ref. U-724)	W 4-Loop, 1 Intact Loop Accumulator Inoperable	~20%	~60% (~10 sec)	~35%
1987	LANL (Ref. U-726)	Generic US/J 4-Loop, All Accumulators Operable	0%	~70% (~15 sec)	~35%
1987	INEL (Ref. U-727)	Generic US/J 4-Loop, All Accumulators Operable	0%	~70% (~10 sec)	~35%

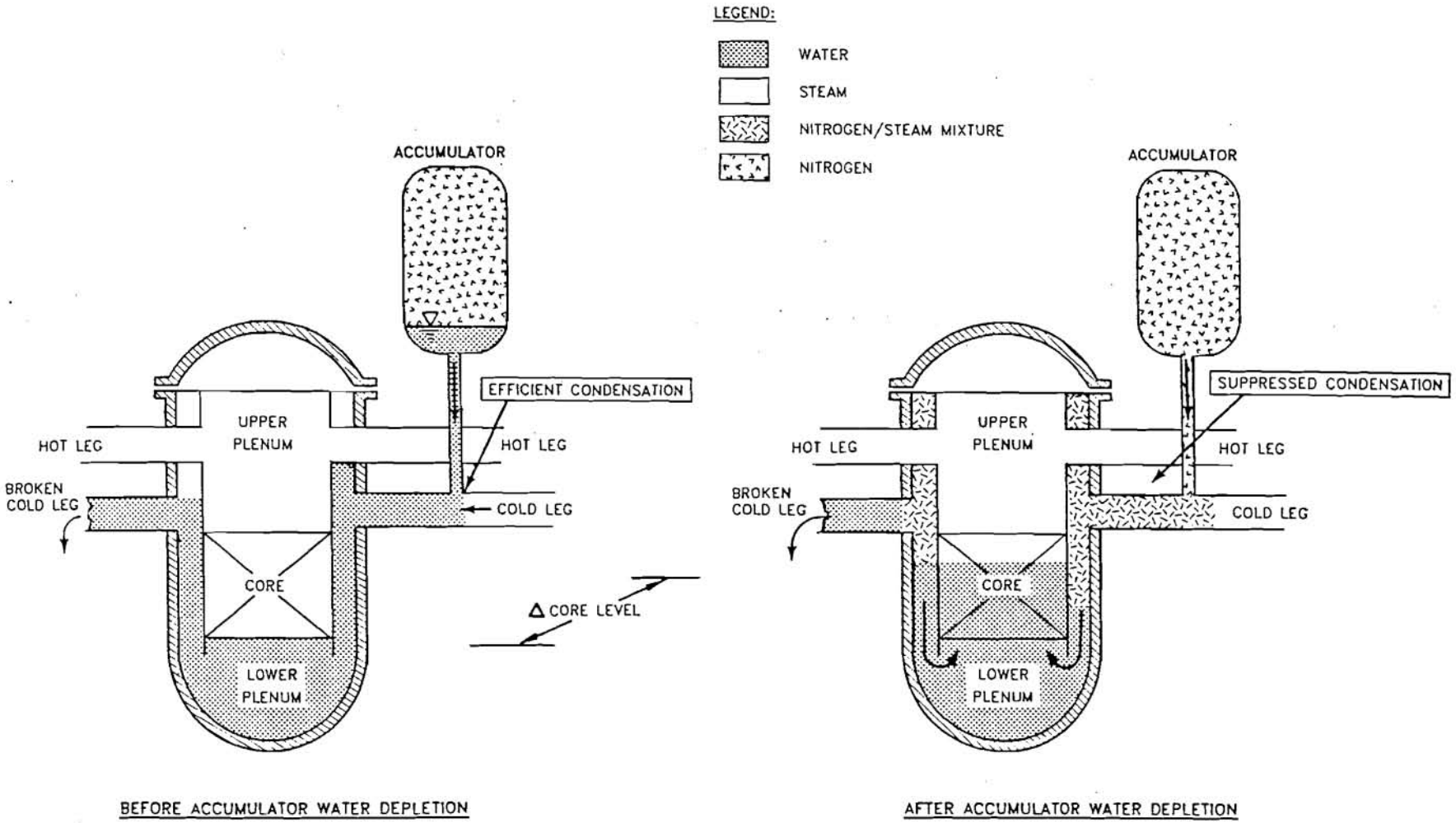

INITIAL CHANGES IN CORE AND DOWNCOMER WATER LEVELS AND SUPPRESSION OF STEAM CONDENSATION DUE TO ACCUMULATOR N_2 PRESSURIZATION OF DOWNCOMER

FIGURE 4.4-1

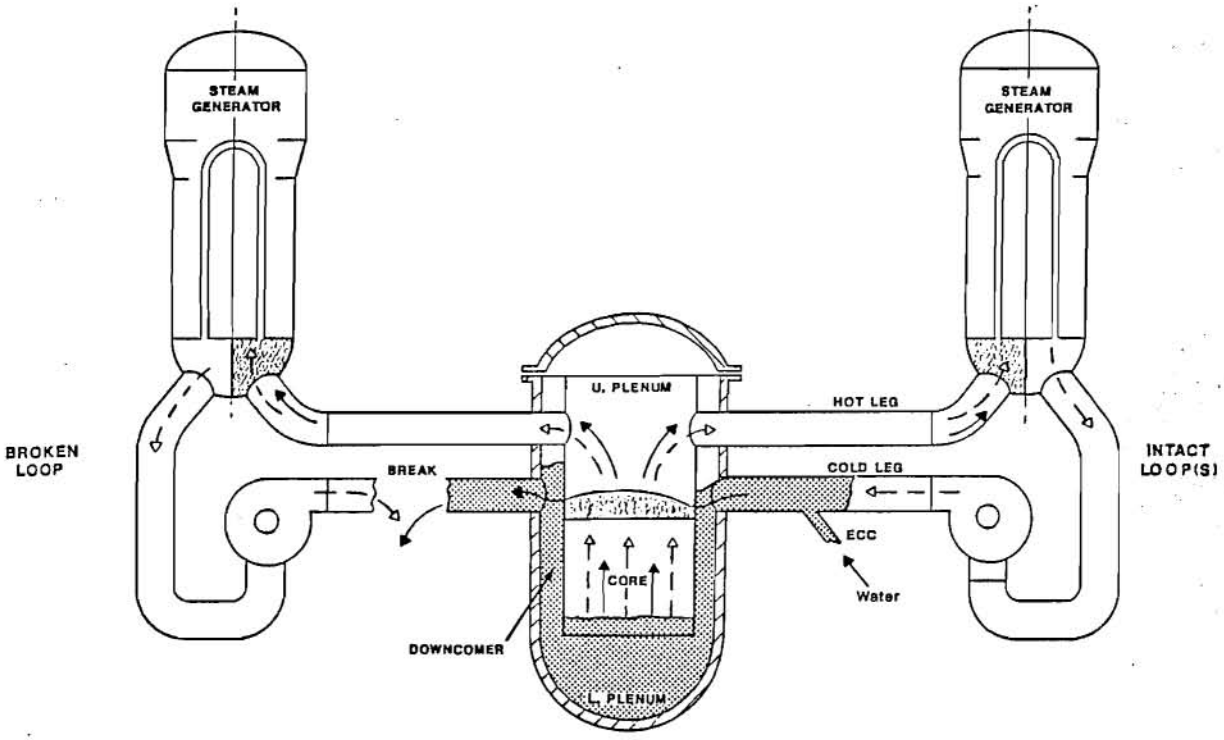

PWR LOCA CONDITIONS
JUST BEFORE ACCUMULATOR WATER INJECTION ENDS
AND N_2 DISCHARGE BEGINS

FIGURE 4.4-2

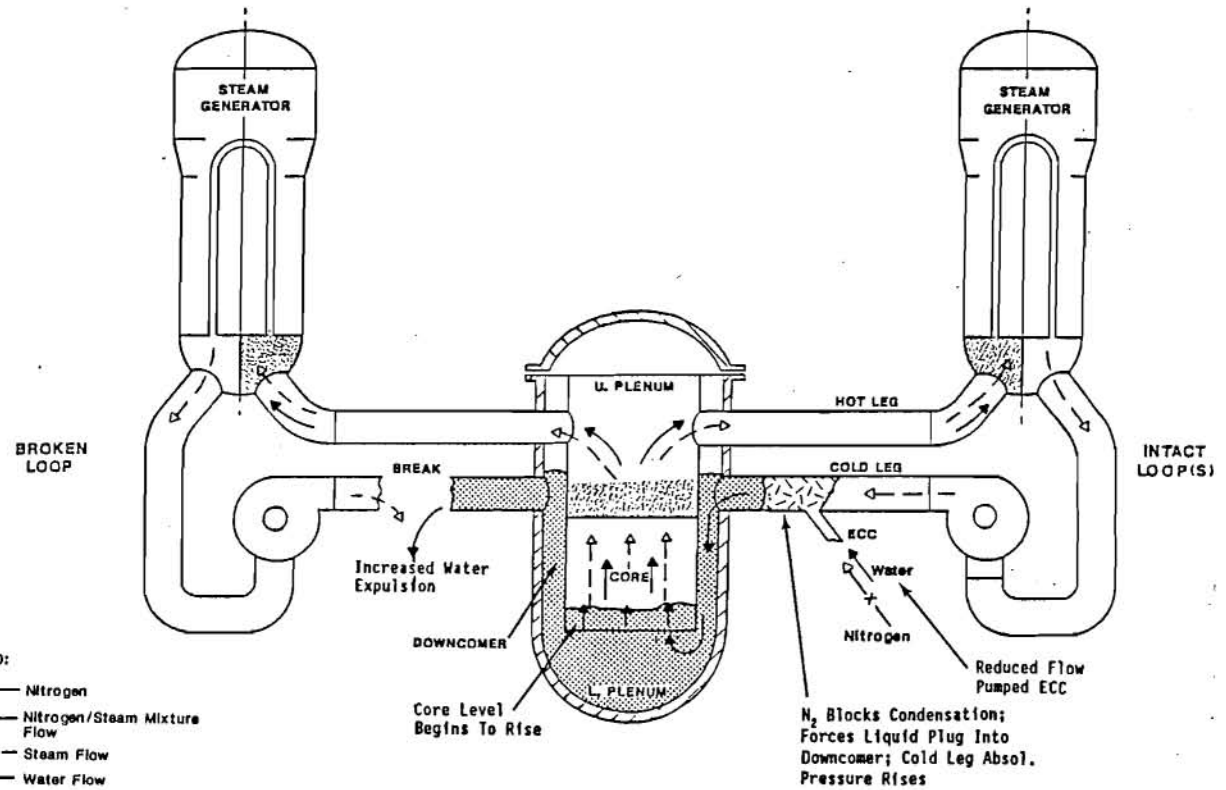

PWR LOCA CONDITIONS
JUST AFTER N_2 DISCHARGE BEGINS

FIGURE 4.4-3

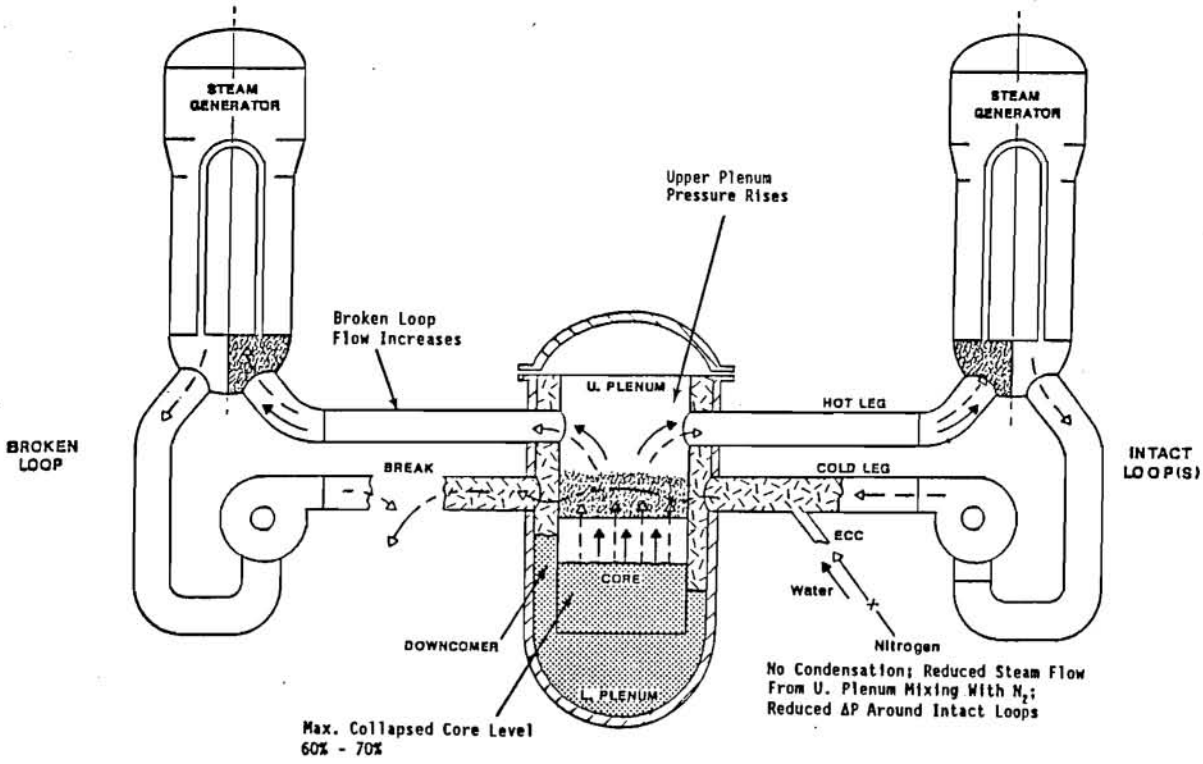

PWR LOCA CONDITIONS
MAXIMUM CORE LEVEL DURING N_2 DISCHARGE

FIGURE 4.4-4

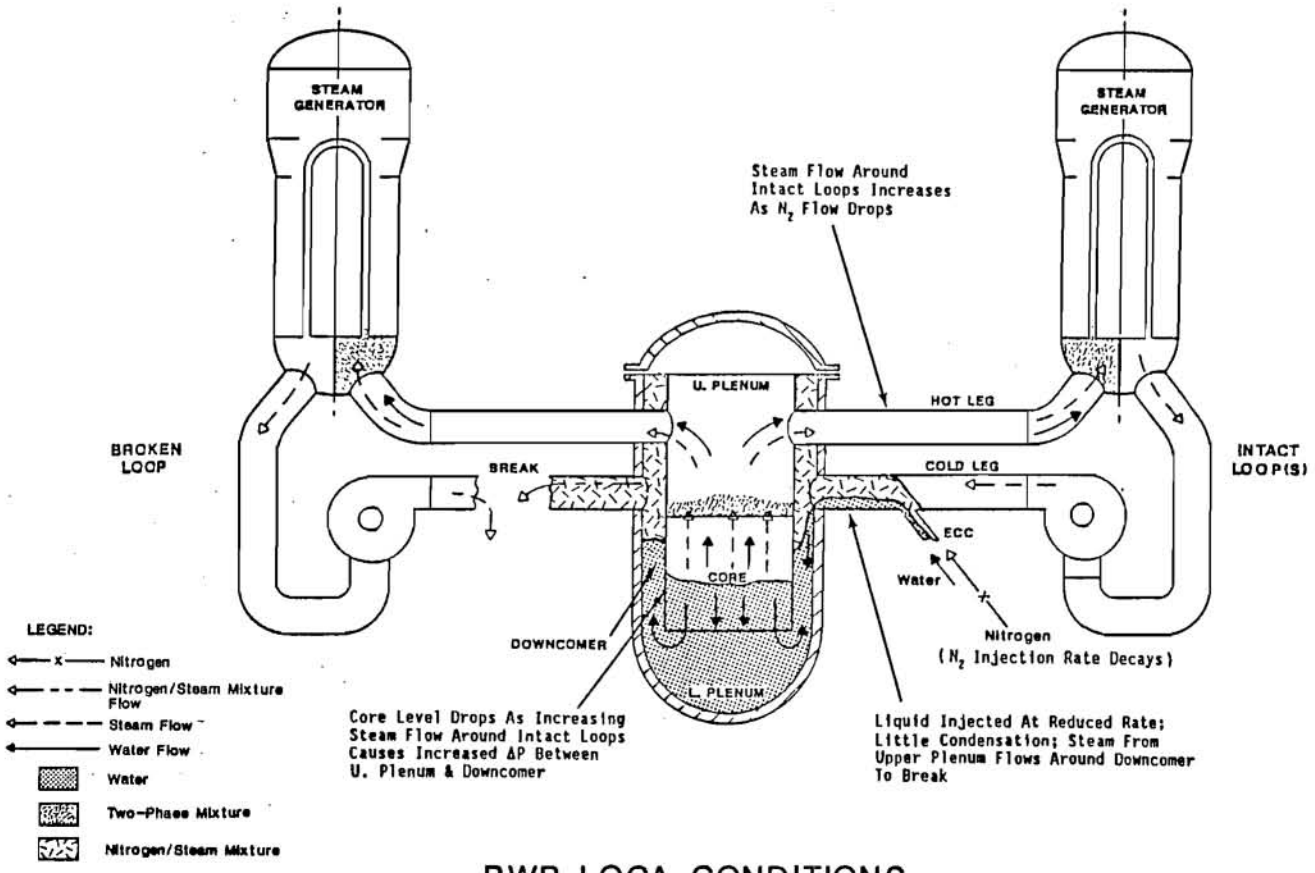

PWR LOCA CONDITIONS
NEAR END OF N_2 DISCHARGE

FIGURE 4.4-5

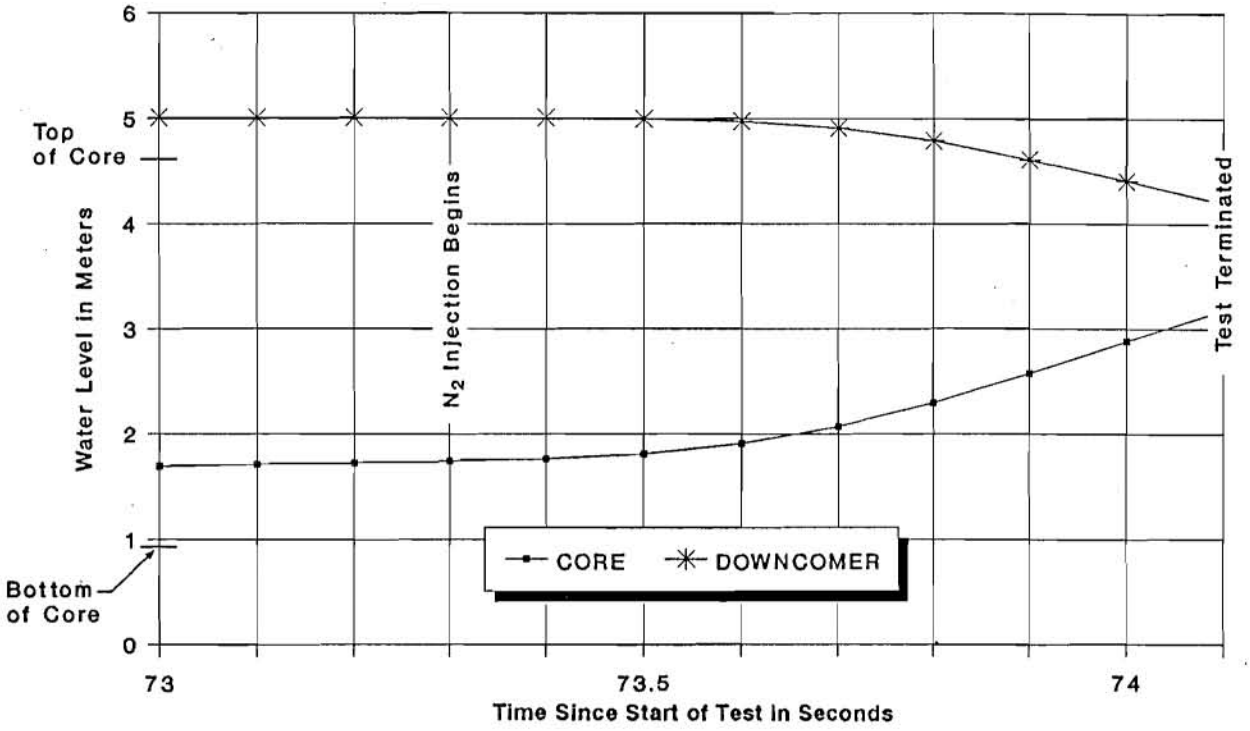

CORRECTED CORE AND DOWNCOMER WATER LEVELS
FOR UPTF TEST 27A
(REFERENCE U-459)

FIGURE 4.4-6

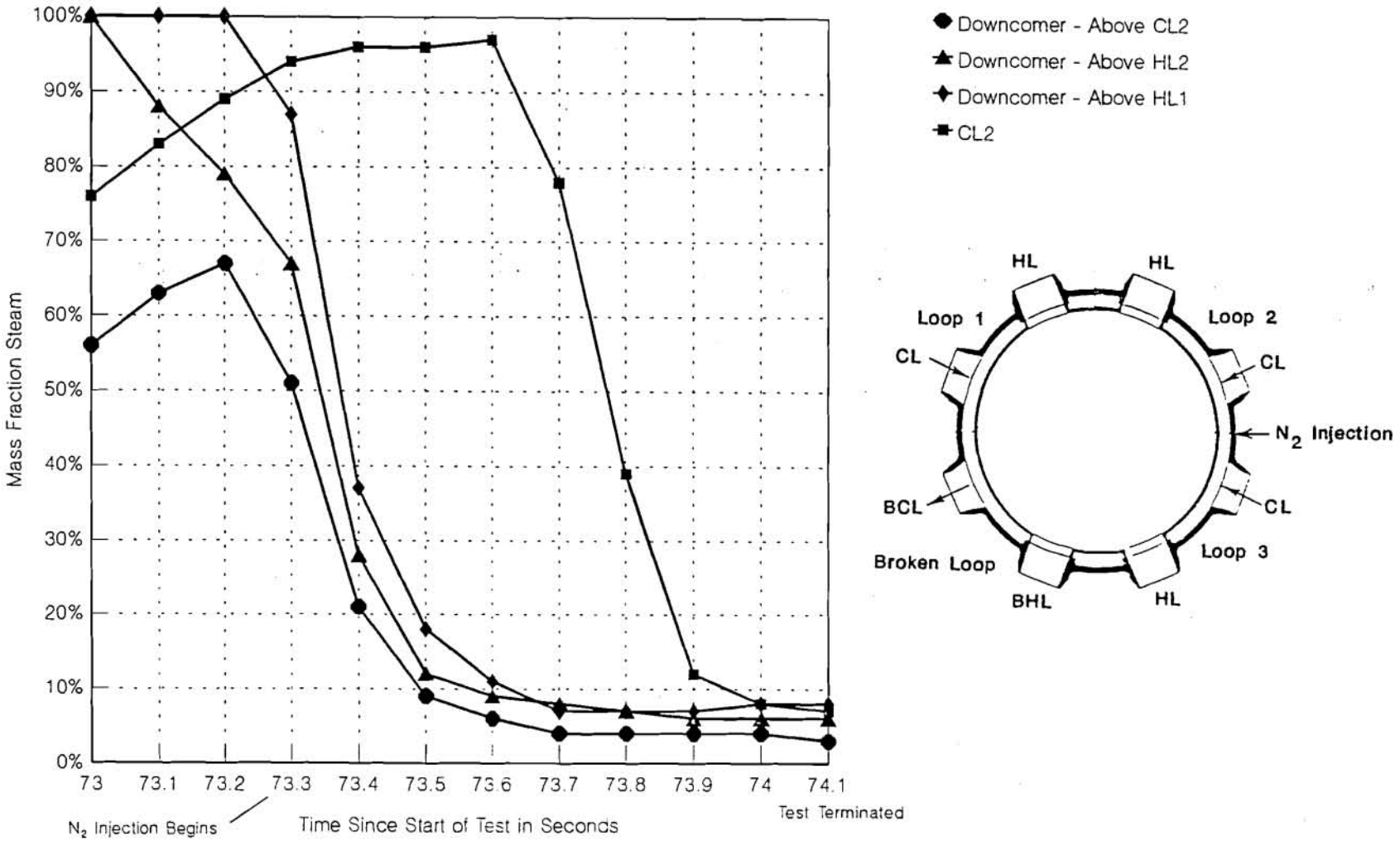

Composition of Steam/Nitrogen Mixture in Downcomer and Cold Leg During UPTF Test 27A
(Reference U-459)
Figure 4.4-7

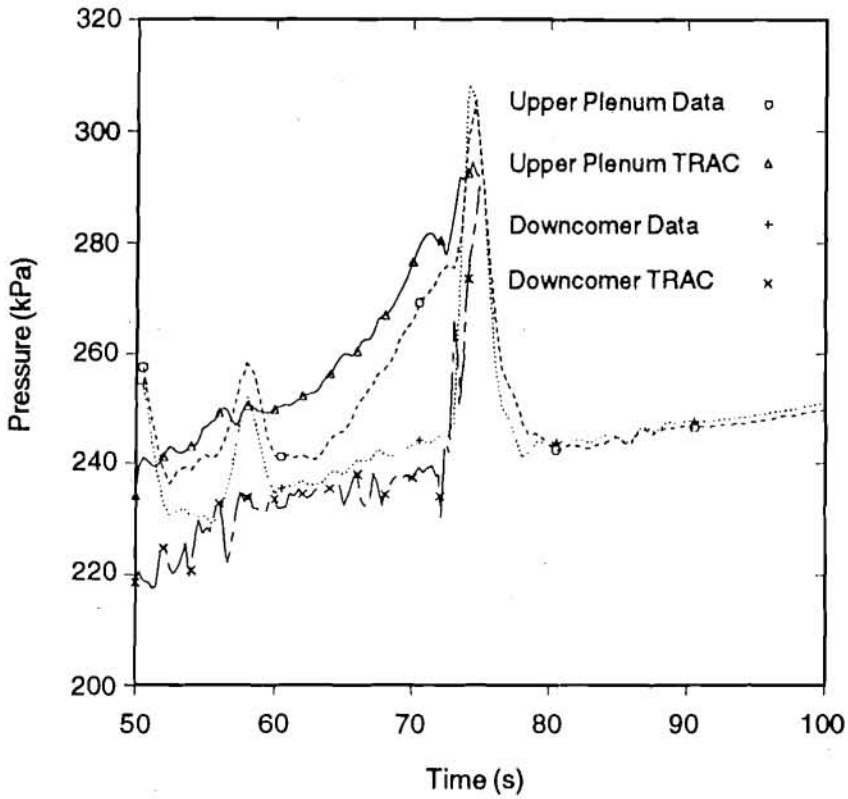

TRAC/DATA COMPARISON OF VESSEL PRESSURES
DURING NITROGEN DISCHARGE
FOR UPTF TEST 27A
(REFERENCE U-716)

FIGURE 4.4-8

4.5 THERMAL MIXING OF ECC AND PRIMARY COOLANT

Definition of Issue and Description of Phenomena

Thermal mixing of ECC and primary coolant refers to the mixing phenomena which occur in the cold legs and downcomer of a PWR as a result of high pressure coolant injection (HPCI) into the cold legs at a time when the reactor coolant system is at an elevated temperature. This mixing relates to the overall reactor safety issue of pressurized thermal shock (PTS). In PTS, the concern is that simultaneous occurrence of the following conditions could result in brittle crack growth in the vessel wall and possibly even vessel failure.

- High pressure
- Sudden, localized reduction of reactor vessel wall temperature
- Reduced reactor vessel metal ductility due to prolonged irradiation
- Existing flaw in weld metal of reactor vessel

Hypothesized scenarios by which these conditions could occur simultaneously include inadvertent HPCI actuation and an SBLOCA with HPCI. For these scenarios the key concern is how the ECC mixes with the primary coolant. If mixing is good, a slow and drawn-out cooldown occurs, which provides sufficient time to prevent the development of significant temperature gradients in the vessel wall. However, if mixing is poor, the ECC can "stream" through the cold leg and into the downcomer (see Figure 4.5-1). This stream of ECC could possibly cool local regions of the vessel wall, leading to wall temperature gradients and to a localized reduction of wall temperature.

Importance of Issue

Typically, if there is flow through the cold legs, either forced flow (i.e., reactor coolant pumps running) or natural circulation, good mixing is obtained in the cold legs. Hence, thermal mixing is of interest only in SBLOCA's where the flow in one or all cold legs has stagnated. Thermal mixing in the cold legs and downcomer determines the temperature transient to which the vessel wall is subjected.

Tests and Analyses that Relate to Issue

Within the 2D/3D Program, one test related to thermal mixing in the cold leg and downcomer was performed at UPTF (Test No. 1). Test No. 1 consisted of five separate test phases. In each phase, the primary system was initially filled with hot water and cold ECC was injected into a single cold leg; the cold leg with ECC injection was blocked at the pump simulator. Since there was no heating during the test, each

phase was a gradual cooldown of the entire system. Due to facility design limitations, the initial primary system temperature was significantly lower than the primary system temperature in a PWR during a PTS-related transient.

Pre-test evaluation of the side-mounted ECC injection pipe in UPTF and GPWRs showed that mixing was poor and not typical of US/J PWRs which inject ECC into the top of the cold leg. To simulate mixing phenomena more typical of US/J PWRs, a modified ECC injection nozzle was used in UPTF. The design of the modified nozzle was developed by the USNRC (Reference U-913).

Outside the 2D/3D Program, numerous subscale tests investigated mixing in the cold leg and downcomer. These tests were used to characterize the mixing phenomena and develop computer codes (e.g., REMIX and NEWMIX). The results of these tests are not discussed in detail in this report. Evaluation of the UPTF and subscale tests, and comparison to REMIX and NEWMIX predictions are documented in Reference U-457. The data and quick-look reports for the UPTF test are provided in References G-001 and G-201, respectively. References E-441 and E-921 through E-926 discuss the results of some of the subscale tests as well as comparisons to code predictions.

Summary of Key Results and Conclusions from Tests and Analyses

The flow regime associated with mixing in the cold leg and downcomer were characterized based on the subscale tests. The phenomena are shown in Figure 4.5-1. The following description is taken from Reference U-457.

> "...A 'cold stream' originates with the HPI plume at the point of injection, continues toward both ends of the cold leg, and decays away as the resulting plumes fall into the downcomer and pump/loop-seal regions. A 'hot stream' flows counter to this 'cold stream' as indicated, supplying the flow necessary for mixing (entrainment) at each location. This mixing is most intensive in certain locations identified as mixing regions (MRs). MR1 indicates the mixing associated with the highly buoyant, nearly axisymmetric HPI plume. MR3 and MR5 are regions where mixing occurs because of the transitions (jumps) from horizontal layers into falling plumes. MR4 is the region of final decay of the downcomer (planar) plume. The cold streams have special significance since they induce a global recirculating flow pattern with flow rates significantly higher than the net flow through-put (Q_{HPI})...."

The UPTF test results were consistent with the subscale results described above. Figure 4.5-2 shows the fluid and wall temperatures measured in the cold leg for two phases of Test 1. These measurements show that flow in the cold leg was thermally stratified between the injection nozzle and the downcomer. Specifically, a cold stream flowed along the bottom of the cold leg from the injection nozzle to the downcomer and a hot stream flowed along the top of the cold leg countercurrent to the cold

stream. The cooldown of fluid in the cold leg between the injection nozzle and the pump simulator followed a "well mixed" transient; i.e., the vertical fluid temperature distribution was relatively uniform.

Figure 4.5-2 also shows the temperature difference between the hot and cold streams increased with increasing ECC injection. Due to mixing in the cold leg, the cold stream entering the downcomer was significantly warmer than the ECC injection for all ECC flows tested.

The cold stream from the cold leg penetrated down the downcomer as a plume. Temperature measurements in the downcomer indicate that, due to mixing in the cold legs and at the cold leg/downcomer interface, the temperature of the plume was significantly higher than the temperature of the ECC injection. Also, the plume decayed within approximately four to five cold leg diameters (see Figure 4.5-3).

A post-test REMIX calculation was performed to investigate the code's ability to predict system behavior and decay of the downcomer plume at full-scale. The calculation of entrainment and stratification in the cold leg was artificially altered to account for the modified ECC injection nozzle used in the UPTF test. The predicted fluid temperatures at various locations in the downcomer were in close agreement with the measured temperatures; hence, REMIX can accurately predict downcomer plume decay at full-scale (Reference U-457).

Post-test calculations have also been performed for many subscale tests. These calculations include REMIX calculations for tests with ECC injection into the top of the cold leg and NEWMIX calculations for tests with high Froude number injection on the side of the inclined portion of the cold leg. Both the REMIX and NEWMIX accurately predicted the mixing phenomena (Reference U-457).

REMIX calculations for PWRs with low Froude number top injection (i.e., Combustion Engineering PWRs and Westinghouse PWRs) indicate that a recirculation flow involving the lower plenum, downcomer, cold leg, and pump seal is established even though the degree of stratification is small. Due to the small degree of stratification, the downcomer plume is weak and decays rapidly (i.e., within about five cold leg diameters--Reference E-922). Similarly, NEWMIX calculations for PWRs with high Froude number side injection (i.e., Babcock & Wilcox PWRs), predict a small degree of thermal stratification in the cold leg and a weak downcomer plume which decays rapidly (Reference E-923).

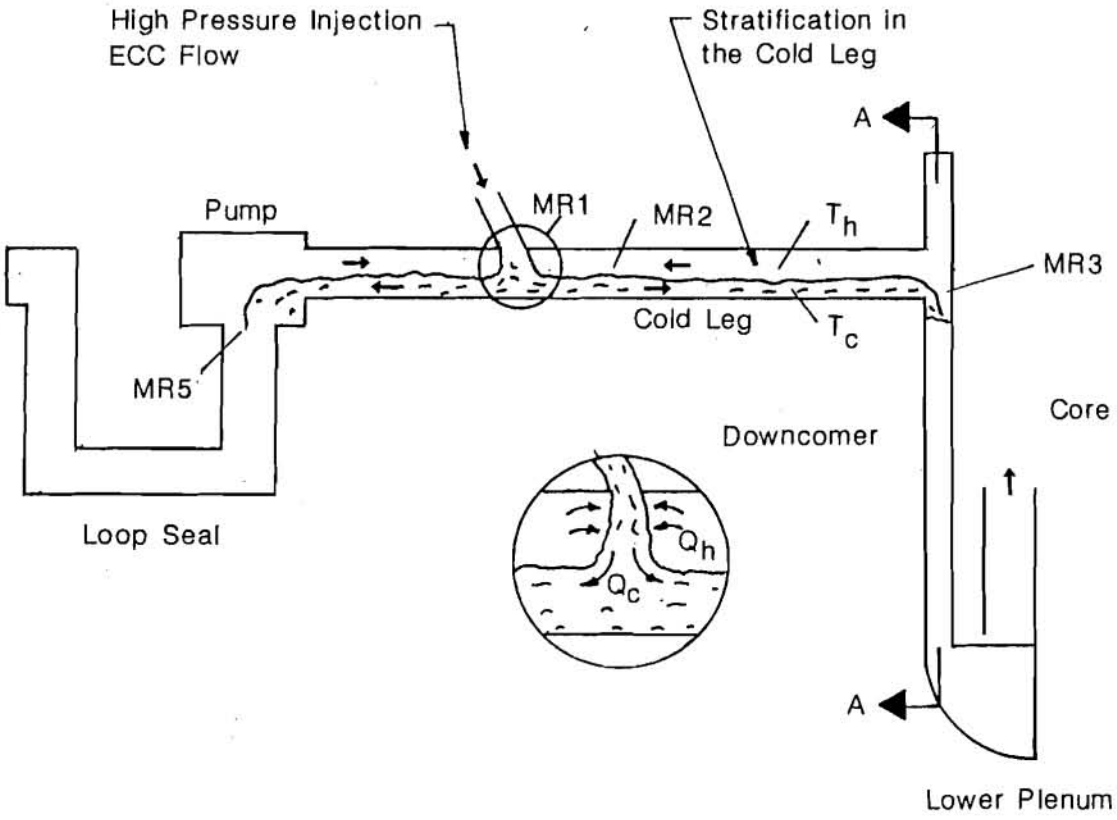

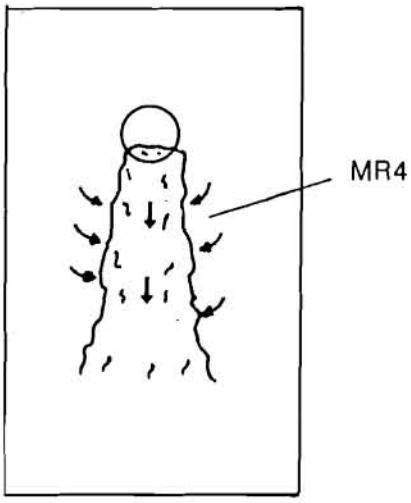

View A-A

Stratification in the Downcomer

DIAGRAM OF ECC STRATIFICATION IN COLD LEG AND DOWNCOMER OF A PWR

FIGURE 4.5-1

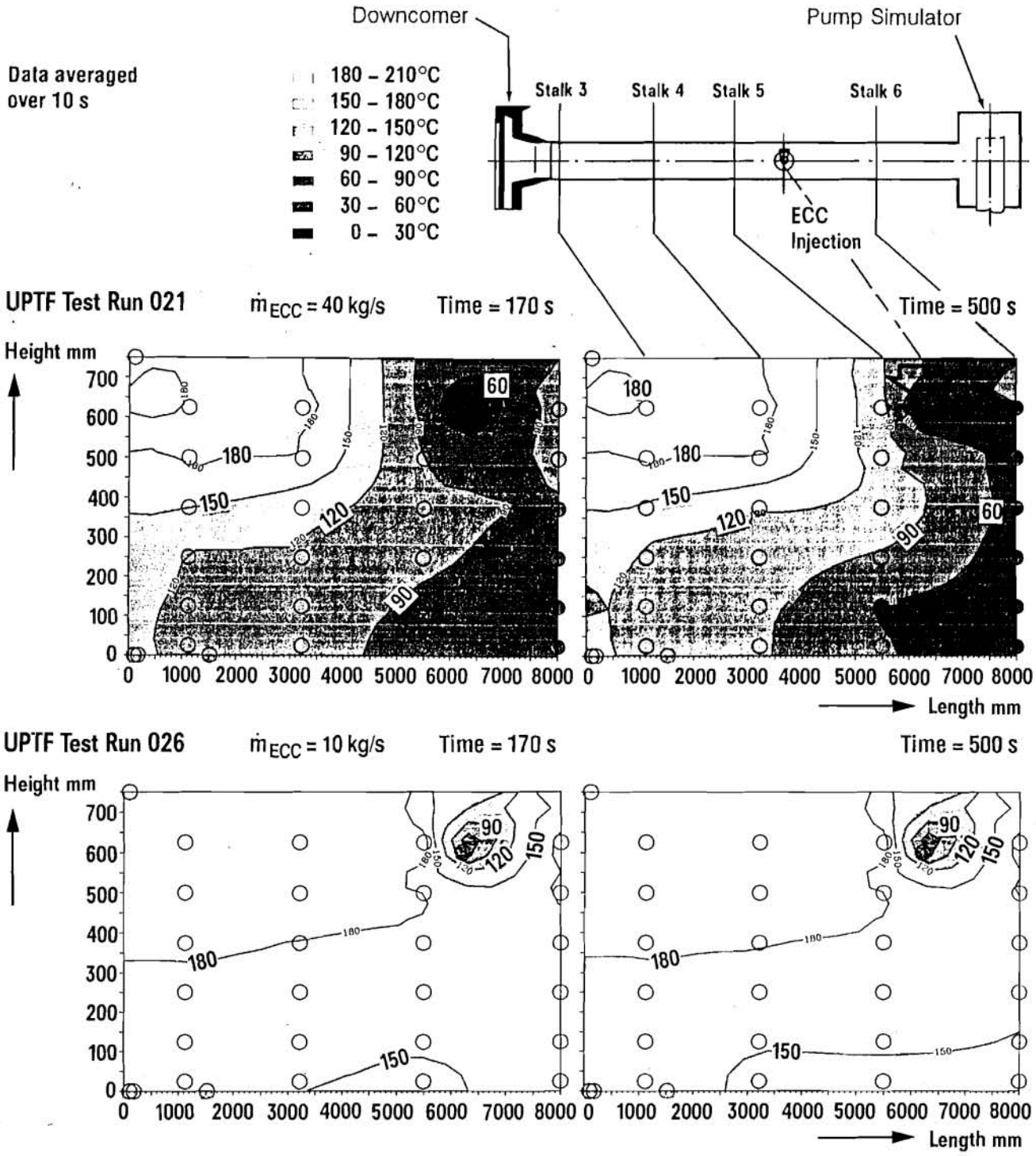

VERTICAL FLUID TEMPERATURE DISTRIBUTION IN COLD LEG FOR UPTF TEST 1

FIGURE 4.5-2

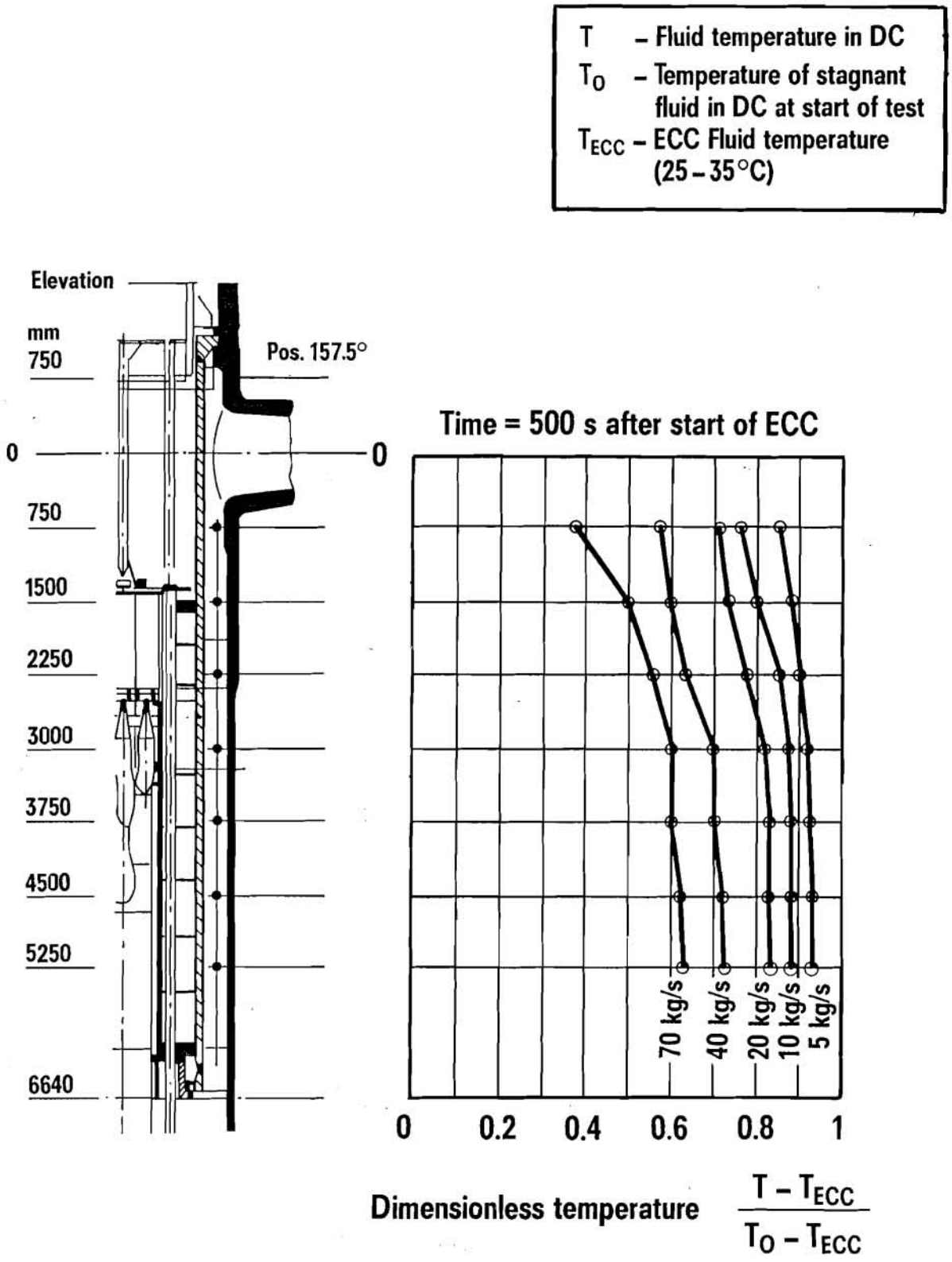

DIMENSIONLESS FLUID TEMPERATURE ALONG DOWNCOMER CENTERLINE 500 SECONDS AFTER START OF ECC INJECTION FOR UPTF TEST 1

FIGURE 4.5-3

4.6 CORE THERMAL-HYDRAULIC BEHAVIOR

Definition of Issue and Description of Phenomena

During the reflood phase of a LOCA, water enters the core and can be vaporized, accumulated in the core, or transported out of the core. Water transport out of the core can occur with the steam upflow out the top of the core or by downflow of excess water out the bottom of the core (for combined injection or UPI).

Water accumulation and vaporization and the resulting two-phase flow provide cooling to remove stored energy and decay heat from the fuel rods. During the post-blowdown LOCA transient, the progression of cladding temperatures and heat transfer mechanisms is typically as follows:

- During the refill phase, cladding temperatures increase almost adiabatically, except for regions with water downflow due to top injection ECC (combined injection or UPI). Water downflow provides core cooling and can quench fuel rods in local regions.

- After core reflood begins when the lower plenum water level reaches the bottom of the core, global core cooling initiates. A variety of heat transfer mechanisms exist simultaneously in different parts of the core including steam/droplet convective cooling, film boiling, transition boiling, nucleate boiling, and convection to subcooled water. As this phase progresses, typical cladding temperatures rise slowly, turn around and then decrease. Regions quenched by water downflow during the refill phase continue to be cooled effectively.

- Quenching occurs when nucleate boiling initiates at a particular location and is characterized by the cladding temperature rapidly decreasing to near the saturation temperature. Quenching occurs first where the liquid fraction is high and the heat flux is low.

Core thermal-hydraulic behavior is influenced by the axial and radial distributions of stored energy and decay power within the core. These distributions can result in multidimensional flow, void, and temperature effects.

In a PWR with cold leg or downcomer ECC injection, flooding of the reactor core is initiated from the bottom. After core reflooding is initiated, a variety of heat transfer modes exist simultaneously. At a particular axial location, the progression is from steam/droplet convective cooling, through film and transition boiling to nucleate boiling as the local liquid fraction of the steam-water mixture increases. These modes are illustrated on Figure 4.6-1. Quench front propagation is predominantly

from the bottom upward. A more detailed description of the heat transfer modes which exist during both reflood and blowdown is provided in Reference E-401.

In PWRs with upper plenum injection or combined injection, almost all of the ECC delivered to the upper plenum flows downward through the core toward the lower plenum. The water downflow initiates during end-of-blowdown providing core cooling prior to reflood. During reflood, the water delivered to the lower plenum either flows up the downcomer to the break, or back up into the core accelerating bottom reflood. The fuel rods are cooled either directly by water downflow or by two-phase upflow from the lower part of the core. Quench front propagation is mainly from the top downward in the water downflow regions and from the bottom upward in the two-phase upflow regions.

Importance of Issue to PWR LOCA Behavior

Core thermal-hydraulic behavior directly affects core heat transfer, since the rate of heat transfer is determined by the rod cladding temperature and by the local temperature, quality, flow rate, and flow pattern of the steam-water mixture surrounding the rods. The peak cladding temperature and cladding temperature history during a postulated LOCA transient are key factors in evaluating the performance of ECC systems.

Test and Analyses that Relate to the Issue

An extensive database on core thermal-hydraulics and heat transfer exists, and includes results of tests performed both within the 2D/3D Program and in other facilities. The majority of the large-scale tests related to core heat transfer during the reflood phase of a LOCA have been performed within the 2D/3D Program at the Cylindrical Core Test Facility (CCTF) and the Slab Core Test Facility (SCTF). Outside the 2D/3D Program, much of the relevant test data has been obtained from the Westinghouse FLECHT and FLECHT-SEASET facilities. Other data relevant to core reflood thermal-hydraulics have been obtained from tests at many small-scale facilities, including: Semiscale, the UCLA facility, JAERI's small-scale facility, LOBI, PKL, and REBEKA. Table 4.6-1 provides a comparison of these test facilities. (Reference E-401 includes an extensive list of references.)

The CCTF and SCTF tests investigated core thermal-hydraulic behavior for bottom reflood conditions and top injection conditions. Bottom reflood tests included gravity flooding tests with cold leg or downcomer ECC injection, and forced flooding tests with lower plenum injection. Top injection tests covered UPI and combined injection. For both bottom reflood and top injection conditions, the tests addressed a wide variety of parameter effects with respect to core thermal-hydraulic behavior. Also, tests were performed under both EM and BE conditions. Table A.1-1 in Appendix A of this report summarizes the CCTF and SCTF test

matrices according to ECCS configurations and phenomena investigated. The JAERI data, quick look and evaluation reports for the CCTF and SCTF tests are listed in the bibliography (Section 5) by test series.

A typical test sequence for simulating reflood conditions involved first preheating the core and then injecting ECC into appropriate locations (one or a combination of cold legs, hot legs, upper plenum, downcomer, or lower plenum). Throughout the test, the core power was controlled to simulate decay heat. Parameters which were varied in these tests included the ECC injection rate, ECC subcooling, system pressure, core power magnitude and distribution (axial and radial), and core initial temperature level and distribution. System configuration parameters which have been varied include the pump simulator resistance, and the use of vent valves.

Predictive models for core thermal-hydraulics have been incorporated in many computer codes including: TRAC, RELAP, COBRA/TRAC, ATHLET, and REFLA. TRAC calculations have been completed for many of the CCTF and SCTF tests. Detailed discussions of these TRAC analyses and comparisons of measured and predicted results are contained in References U-601, U-621, U-622, U-641, U-661 and U-681. ATHLET calculations of a CCTF and an SCTF test are documented in References G-611 and G-622, respectively. Calculations of CCTF and SCTF tests using REFLA are documented in References J-984 and J-995.

Summary of Key Results and Conclusions from Tests and Analyses

CCTF and SCTF are the largest scale, heated-core test facilities which have been used to provide thermal-hydraulic and heat transfer data for reflood conditions. These facilities closely simulated the major PWR core and ECC parameters which influence the core heat transfer process; such as, core height and geometry, core power and temperature, ECC injection rate, and ECC subcooling. Accordingly, the results are judged to be closely representative of the behavior which would result in a PWR core under reflood conditions. It should be noted that the heated rods used in CCTF and SCTF have different thermal characteristics than nuclear fuel rods in terms of heat capacity, gap conductance, thermal conductivity, and cladding material. For example, the heated rods in CCTF and SCTF had heat capacities 30 to 40% higher than that of nuclear fuel rods. Hence, the temperature rise in PWR fuel rods would be expected to be slightly higher than observed in CCTF and SCTF tests. Results of the CCTF and SCTF bottom flooding tests are discussed and evaluated in detail in References U-401, U-414, U-421, U-431, and U-441. Reference U-412 summarizes the evaluation of the CCTF Core-II UPI tests. For combined ECC injection, the CCTF and SCTF results are evaluated in References G-401, J-455, J-553, J-555, and J-557.

The results of the tests and analyses and major conclusions related to core thermal-hydraulic behavior are summarized by ECCS type in the following subsections. Specifically, Section 4.6.1 covers cold leg injection/downcomer injection with and without vent valves, Section 4.6.2 covers upper plenum injection, and Section 4.6.3 covers combined injection.

4.6.1 Cold Leg Injection/Downcomer Injection with and without Vent Valves

One of the major findings of the CCTF and SCTF tests was that liquid which accumulated in the core was distributed quickly throughout the core. Figure 4.6-2 shows the measured void fraction in six axial regions of the core for a typical CCTF test. The figure indicates that some liquid was present at high elevations in the core very soon after the beginning of reflood, and that the liquid inventory at these high elevations slowly increased over time. The rapid distribution of liquid was measured in both high flooding cases and low flooding cases.

Rapid distribution of liquid throughout the core was also observed in small-scale visual tests conducted by JAERI (References J-928 and J-975). In the visual tests, the flow regime in the portion of the core above the quench front appeared to be dominated by the "flow transition regime," as defined in Figure 4.6-1 (Reference E-462). It is reasonable to assume that in the CCTF and SCTF tests, flow in portions of the core above the quench front was also dominated by the flow transition regime.

Heat transfer began to increase shortly after reflood since film boiling occurred at all elevations. Typical CCTF tests showed that the heat transfer coefficient at middle elevations in the core increased from about 10 $W/m^2 K$ to over 50 $W/m^2 K$ only five seconds after the beginning of reflood. Heat transfer coefficients reached about 200 $W/m^2 K$ just above the quench front. The heat transfer coefficients are expected to be typical of PWR behavior because of the realistic fuel geometry simulation in CCTF and SCTF. The temperature rise during reflood in CCTF and SCTF tests was typically limited to about 100 K or less. (Note, the temperature rise for nuclear fuel rods is expected to be slightly higher than observed in the tests--see discussion on p. 4.6-3.)

Another important finding was that, for a given core power and initial core energy, the rate of the quench front propagation was determined by the core liquid head, the amount of cooling above the quench front by the two-phase upflow, and axial heat conduction in the fuel rods. Phenomena which reduced the core liquid head (e.g., increased steam binding) retarded the quench front propagation. Figure 4.6-3 shows the propagation of the bottom quench front for a typical CCTF test. Also shown on the figure is the core collapsed liquid level. Note that the flooding rate was less than 0.025 m/s which was typical of most tests during the LPCI phase. Also note that although an initial offset developed between the low power and high power bundles, the quench front speed was nearly identical in all regions. This suggests preferential cooling of the high powered region, a result confirmed by SCTF tests.

Comparison of the FLECHT-SEASET tests and the CCTF and SCTF tests showed similar overall behavior, including similar core liquid inventories. Multidimensional

effects, such as the core heat transfer enhancement due to radial power distribution could not be evaluated in FLECHT-SEASET because of the small cross-sectional area. Other differences in hydraulic behavior occurred which were the result of the larger scaled upper plenum flow area and volume and smaller core flow area in FLECHT-SEASET.

The typical CCTF and SCTF results have compared favorably with void fraction and heat transfer coefficient correlations developed by JAERI (References J-906 and J-910). These correlations were developed based on the results of small-scale JAERI tests, and were incorporated in the REFLA code, which was able to predict reflood transient cladding temperatures.

A significant number of tests were conducted in CCTF and SCTF to determine the separate effects of various parameters on core thermal-hydraulics. The effects of varying several parameters are shown in Figures 4.6-4(a) and 4.6-4(b). Major parameter effects which were observed to influence typical test behavior are summarized on Table 4.6-2 and are discussed below.

- System Pressure. Decreasing the system pressure resulted in a significant decrease in core heat transfer. Figure 4.6-4(a) shows the resulting increase in the cladding temperature rise and peak cladding temperature. The effect of system pressure on heat transfer was related to the change in steam density. Decreasing system pressure reduced the steam density which increased the void fraction in the core. The decrease in steam density also enhanced steam binding, which reduced core liquid inventory. The increased void fraction and enhanced steam binding allowed core temperatures to increase.

- Core Power. Higher core power increased the adiabatic rod heat-up prior to reflood and the rate of steam generation during reflood. Higher core power increased core temperatures at the beginning of reflood and the overall temperature rise, even for the same initial temperature. The higher steam generation rate increased the core void fraction and reduced core liquid inventory, thereby slowing quench front propagation, and increasing the quench time.

- Initial Cladding Temperatures. Lower cladding temperatures at the beginning of reflood reduced the overall peak cladding temperature, but core heat transfer was somewhat degraded since the temperature difference between the rods and the fluid was smaller. The temperature rise during reflood, therefore, increased. For CCTF tests with initial cladding temperatures 200 K less than the typical tests, the temperature rise was about 50 to 100 K greater.

- Core Power and Initial Cladding Temperature Distribution. The effects of stored energy and power distribution have been evaluated by comparing results of

tests with the same total core power and the same core heat-up time, but with different radial power profiles. In steep radial power profile tests, peak cladding temperatures were consistently higher (by about 120 K) than in flat power profile tests. This difference was primarily due to the higher adiabatic heating (before reflood) in the high-powered bundles. The maximum temperature rise appeared to be only slightly dependent on power profile and was generally less for steep power profile tests. This behavior represents a two-dimensional coolant redistribution phenomenon, whereby water flow was increased to higher powered regions due to greater steam generation in these regions. This coolant redistribution keeps the core liquid inventory profile essentially flat. The void fraction, therefore, is principally a function of elevation and time, as shown in Figure 4.6-1. The enhanced cooling in high-powered regions is due to both the higher temperature difference and higher heat transfer coefficients. The higher heat transfer coefficients are the result of the coolant redistribution effect, and the degree of heat transfer enhancement is governed mainly by the bundle power ratio. Figure 4.6-5 shows the difference in heat transfer coefficients resulting from different radial peak power profiles.

The distribution of power and stored energy does not have a strong effect on reflood behavior outside the core. Comparisons of key differential pressures as well as core pressures for tests with different power profiles show little difference, and it is concluded that system performance is dominated by the total core power and stored energy and not by their distribution.

- ECC Injection Rate. The effect of increasing the accumulator injection rate was to rapidly increase the core flooding driving head, causing a sudden increase in steam generation and rapid core cooling. This can reduce the peak cladding temperature. However, once the downcomer water level stabilizes at the cold leg elevation, prolonging the duration of the accumulator injection can adversely affect core heat transfer. This is because increased condensation of steam in the intact loops lowered the system pressure, reducing core heat transfer. Increasing the ECC injection rate during the LPCI phase (for example, no-LPCI-pump-failure case versus single-pump-failure case) can also adversely affect core heat transfer for the same reason. Figure 4.6-4(b) shows that cladding temperatures at the same location can actually increase slightly with the higher LPCI flow rate.

- ECC Subcooling. In integral tests, the ECC subcooling at the core inlet depended on heat release from structures (e.g., vessel wall) and condensation of steam in the cold legs and downcomer. Based on forced flooding tests at SCTF, increased core inlet subcooling tends to reduce the amount of ECC needed and the length of time needed to quench the core. Core inventory also increased.

- Loop Flow Resistance. As shown of Figure 4.6-4(a), the net effect of increasing the loop resistance was to slightly increase the peak cladding temperature and to prolong the core quench time. The higher loop resistance increases the loop pressure drop and reduces the core flooding rate.

- Evaluation Model versus Best-Estimate Conditions. Tests conducted in CCTF and SCTF with "best-estimate" conditions had significantly lower core power and initial cladding temperatures, and higher containment pressure and LPCI flow rates, relative to the typical (evaluation model type) tests. Because of the higher system pressure and lower core power, core cooling was improved and the temperature rise and quench time were reduced. In the CCTF BE test, system-wide hydraulic oscillations occurred due to intermittent water carryover to the steam generators. A brief core re-dryout with a small heat-up prior to re-quench occurred during these oscillations. (See Reference U-413 for a detailed discussion of the oscillations.)

- Core Blockage. Results of SCTF-I tests showed that the effect of 60% coplanar core blockage on core heat transfer was negligible. A small effect on peak cladding temperatures was observed, and only a slight effect on quench times was noted (see Figure 4.6-4(b)).

Comparisons of tests with cold leg and downcomer injection revealed that the overall differences in core thermal-hydraulics were relatively minor (see Figure 4.6-4(b)). For downcomer injection, reduced interaction of steam and ECC occurred; consequently, less steam was condensed and ECC subcooling remained higher in the downcomer. The effects of vent valves were also relatively minor. In tests with open vent valves, steam binding was reduced, allowing increased core flooding rates, and better core cooling. The peak cladding temperature reduction was about 20 K (36°F) in CCTF tests. (Reference U-414).

Calculations of CCTF and SCTF tests using the TRAC-PF1/MOD1 code showed overall reasonable agreement with the test results. TRAC-PF1/MOD1 used a generalized boiling curve for heat transfer. The predicted heat transfer in the core is closely tied to the prediction of liquid distribution in the core. In TRAC-PF1/MOD1 calculations, entrainment of liquid in the core was generally underpredicted, resulting in deficiencies in predicting the axial void fraction distribution. Specifically, the liquid inventory in the core above the quench front was underpredicted (see Figure 4.6-6). This typically resulted in an overprediction of core temperatures in the upper half of the core; however, as shown in Figure 4.6-7, overall peak cladding temperatures were generally in reasonable agreement with the test data. A detailed statistical evaluation comparing predicted and measured temperatures was carried out for eight SCTF-III tests (see Figure 4.6-8). Turnaround temperature comparisons were made for three elevations (quarter-height, mid-height, and three-quarter height) in four bundles yielding 12

comparisons per test. The mean bias was -19.4 K and the standard deviation was 59.8 K, which reflects the generally favorable comparison. Rod quench times and turnaround times were predicted with reasonable agreement as well.

Post-test analyses of three CCTF and SCTF tests have also been performed using TRAC-PF1/MOD2. MOD2 has a new reflood model which is based on post-critical heat flux flow regime descriptions developed by DeJarlais and Ishii (Reference E-455). These flow regimes are shown in Figure 4.6-1. The models and correlations developed for MOD2 mechanistically address the key phenomena in each flow regime. The PCT prediction accuracy of MOD2 is similar to MOD1. The deficiency in core liquid distribution discussed earlier for MOD1 was also observed for MOD2. Figure 4.6-9 shows the measured and calculated collapsed liquid levels in the core upper half for a CCTF test. The measured value considerably exceeds the predicted value.

The CCTF and SCTF results confirmed that assumptions used in PWR safety systems evaluations are generally conservative. The single-LPCI-pump-failure assumption was found to have an adverse but minor effect on core cooling. With regard to core heat transfer, the 2D/3D results showed that, for a core flooding velocity of 2 cm/s, core cooling was not degraded.

4.6.2 Upper Plenum Injection

While tests with upper plenum injection (UPI) were performed at CCTF, SCTF, and UPTF, only the CCTF tests simulated thermal-hydraulic behavior in the core. The SCTF and UPTF tests focused on water delivery and distribution in the upper plenum which is discussed in Section 4.7.1. The CCTF tests consisted of a series of five integral tests which evaluated core behavior with UPI. These tests simulated both evaluation model (EM) and best-estimate (BE) conditions. The tests also evaluated the effect of parametric variations in UPI flow rate, injection configuration, core power, and initial core stored energy on thermal-hydraulic behavior in the core. Results of the CCTF UPI tests are described in detail in Reference U-412. Key results related to core thermal-hydraulic behavior are summarized below.

During reflood in the CCTF UPI tests, water penetrated to the core from the upper plenum. Flow exited the core at both the top (steam and water) and at the bottom (water only). In the UPI base case test (C2-16), about 55% of the water which penetrated from the upper plenum to the core continued to the lower plenum, up the downcomer, and out the break.

Rod cladding temperature measurements indicated water downflow occurred only in a limited region of the core. Specifically, rod temperatures near the top of the core, over an area covering about 1/3 to 1/2 of the core, dropped sharply at the beginning of the test, indicating water downflow. Rod temperatures in the remainder of the core indicated no water downflow. In tests with injection into only one of the two UPI ports, the downflow occurred under the injection port; however, the asymmetric downflow occurred in tests with injection into both UPI ports as well as in tests with one port injection. The location of the downflow region did not shift as the test progressed. Figure 4.6-10 shows the downflow region for the CCTF UPI base case test (Test C2-16; one port injection).

In the remainder of the core, rod temperatures were comparable to those in bottom flooding tests with similar conditions. This result indicates that these regions were cooled by water which flowed down through the core to the lower plenum and back up into the core; i.e., bottom flooding behavior (see Section 4.6.1). In this portion of the core, a two-phase mixture of steam and water flowed upward through the core to the upper plenum.

Core cooling near the top of the core was enhanced in the water downflow region. Specifically, peak cladding temperatures were lower and quench times earlier compared to those in the two-phase upflow region and also compared to those in bottom flooding tests. Figure 4.6-11 shows quench times at the 3.05 m (10 ft) elevation in the CCTF UPI base case test (Test C2-16) and a bottom flooding (i.e., cold leg injection) test with comparable conditions (Test C2-SH2). Quench times

are significantly shorter in the UPI test between about the 90° and 240° azimuths--the water downflow region. At lower elevations, including the mid-core elevation where peak cladding temperatures are highest, there appeared to be very little direct cooling from the water downflow. This indicates the effects of local water downflow were evened out, perhaps by cross-flow or by vaporization of the water, before the downflow reaches the mid-core elevation. Quench times in the two-phase upflow region were similar to those for the bottom flooding test.

The effects of various parameters on core thermal-hydraulics were investigated in the CCTF UPI tests. The results of these tests are discussed below.

- UPI Distribution. For comparable injection rates, injecting ECC through both UPI nozzles versus only one nozzle had little effect on core thermal-hydraulic behavior.

- UPI Flow. Increasing the UPI flow from the single-LPCI-pump-failure case to the no LPCI-pump-failure case significantly reduced the cladding temperatures and quench times throughout the core. This effect was more pronounced in the water downflow region.

- Evaluation Model versus Best-Estimate Conditions. The test conducted with "best-estimate" conditions had significantly lower core power and initial cladding temperatures, and higher containment pressure relative to the evaluation model (or base case) test; however, both tests simulated the single-LPCI-pump-failure case. Due to the lower core power and initial cladding temperatures, the peak cladding temperatures and quench times were significantly reduced.

LANL analyzed the CCTF UPI tests using the TRAC-PF1/MOD1 computer code. Reference U-622 summarizes the results. In general, the code predicted multidimensional core reflood conditions, negative core inlet flow, location of the liquid downflow, and average values for fuel rod temperatures. However, the code overpredicted the amount of UPI downflow to the core while also not predicting the core void distribution accurately. Overall, the TRAC predictions were in reasonable agreement with the test results.

It is expected that the same core phenomena observed in CCTF will occur in the full-size PWR. Specifically:

- The delivery of UPI water to the core region should occur in an asymmetric manner. Core cooling in the water downflow region should be enhanced relative to a cold leg injection plant.

- Heat transfer in the two-phase upflow region should be comparable to PWRs with bottom flooding as a result of the following flow mechanisms:

-- Accumulation of water in the lower plenum and lower core region and cooling as a result of bottom reflood.

-- Limited interaction between water downflow and two-phase upflow in the upper portion of the core.

4.6.3 Combined Injection

During tests simulating the end-of-blowdown/refill phase with combined injection, ECC entered the upper plenum and flowed downward through the tie plate to the core in distinct regions located adjacent to the loops with ECC injection. Core cooling was initiated in these downflow regions (top quenching) while the remainder of the core heated up. Evaluation of SCTF and CCTF data reveals that, during the EOB/refill phase, heat transfer coefficients were high (200 $W/m^2 K$) in the water downflow regions and low (less than 50 $W/m^2 K$) in the remainder of the core. Water flowing down through the core in conjunction with ECC injected in the cold legs quickly refilled the lower plenum.

During the reflood phase, bottom flooding of the entire core initiated, and local ECC penetration through the core to the lower plenum continued. Outside the water downflow regions, water was carried by steam to the upper regions of the core. This two-phase upflow enhanced heat transfer throughout the core. Most of the steam which vented out the top of the core was condensed in the upper plenum and hot legs by the hot leg ECC injection. The condensed steam, as well as water carried over to the upper plenum, was returned to the core with the water downflow; i.e., a circulation flow path was established.

In SCTF Test S3-13 (Run 717), hot leg ECC injection was simulated by continuous water injection into the upper plenum just above two of the eight fuel assemblies. Plots of cladding temperature shown in Figure 4.6-12 clearly indicate immediate quenching of the rods in the downflow region after the start of injection. A rapid core reflood with flooding velocities of 15 to 25 cm/s was observed.

The void fraction and heat transfer coefficients for the two-phase upflow region were well predicted using correlations developed for bottom flooding behavior; however, the correlations had to be modified to account for the high flooding rate (References J-970 and J-972).

The effects of various parameters on core thermal-hydraulics were investigated in the CCTF and SCTF tests. The results of these tests are discussed below.

- Power Distribution. Core thermal-hydraulic behavior with a typical GPWR radial power profile was similar to that with a uniform power profile. Specifically, water downflow occurred only in distinct regions adjacent to the injection location while two-phase upflow occurred over the remainder of the core. With a non-uniform power profile, core cooling in the two-phase upflow region was slightly enhanced in the high-powered bundles and slightly degraded in the low-powered bundles. Overall, core behavior was not sensitive to the power profile.

- ECC Injection Rate. Increasing the ECC injection rate increased the water downflow and core flooding rates. Consequently, core cooling in both the water downflow and two-phase upflow regions was enhanced. In a CCTF test with a 100% increase in the initial ECC injection rate into the hot legs (i.e., 5/8 vs. 7/8 injection) quench times were reduced by about 100 seconds.

- ECC Configuration. In SCTF tests with intermittent ECC injection above the tie plate, water downflow through the core occurred intermittently; consequently, core cooling in the downflow region temporarily increased and decreased. However, since the time averaged injection was the same for intermittent injection and continuous injection, overall core cooling was about the same as for continuous injection (see Figure 4.6-13).

  The SCTF tests also alternated ECC injection between different injection nozzles. In this case, water downflow alternated between local regions below the nozzle locations. Core cooling in the water downflow regions increased and decreased with the water downflow. Unlike intermittent injection, overall core cooling for alternating injection was slightly degraded relative to continuous injection.

- ECC Downflow Area. Distributing the ECC over a larger area of the core increased the water downflow region and hence the area of the core which experienced early quenching. However, distributing ECC over a wider region of the upper plenum, increased condensation in the upper plenum thereby increasing the temperature of the water downflow. As discussed below, increasing the temperature of the water downflow decreased core cooling.

- ECC Temperature. Increasing the ECC temperature decreased core cooling in the two-phase upflow region because the energy removal capacity of the water downflow was lower. Also, since circulation between the core and upper plenum is governed by the density difference between the two-phase upflow and the water downflow, increasing the temperature of the downflow reduced the flow circulation.

  Tests at SCTF covered a wide range of ECC temperatures which bounded expected PWR. In all cases, the core was adequately cooled.

- Evaluation Model versus Best-Estimate Conditions. Tests conducted in CCTF and SCTF with "best-estimate" conditions had significantly lower core power and initial cladding temperatures than the evaluation model tests. Also, all four hot leg ECC injection systems were active rather than only two (7/8 injection versus 5/8 injection). As discussed above, increasing ECC injection above the tie plate increases water downflow through the core and the core flooding rate. Due to the higher core flooding rate, and the lower core power and initial

cladding temperatures, core cooling in the two-phase upflow region was significantly improved. In SCTF tests quench times in the two-phase upflow region were reduced by 42 seconds at the core midplane relative to the evaluation model tests (53 seconds versus 95 seconds after reflood initiation). For both the best-estimate and evaluation model cases, portions of the core in the downflow regions were quenched early in the transient.

UPTF integral tests with combined ECC injection provided detailed information on thermal-hydraulic boundary conditions for the core thermal-hydraulic behavior. Significant findings from UPTF tests related to combined injection phenomena are summarized below:

- ECC delivery to the core from the upper plenum was either continuous or intermittent.
- Water downflow regions were established in portions of the core adjacent to hot legs where ECC was injected.
- Up to 70 K subcooling was observed in the water downflow region (below the tie plate).
- Full-scale strongly favored water breakthrough at the tie plate, which enhances core cooling relative to small-scale.

SCTF tests investigated the core thermal-hydraulic response to the system effects observed in UPTF tests described above.

Results of UPTF Test 18, a combined injection integral test, show similar phenomena to that calculated by TRAC-PF1/MOD1 large break LOCA analyses, with respect to multidimensional phenomena within the core region, downcomer behavior and loop behavior (Reference G-909). In general, good agreement between analysis results and findings of UPTF and SCTF/CCTF tests was obtained for phenomena such as: (1) entrainment to the broken cold leg, (2) precooling and early quenching of parts of the core during end-of-blowdown, (3) formation of water downflow and two-phase upflow regions in the core during reflood, and (4) intermittent delivery of the injected ECC water. Accordingly, the range of calculated cladding temperature histories depicted in Figure 4.6-14 is considered to envelope PWR fuel rod temperatures under licensing conditions.

For GPWRs with combined cold and hot leg ECC injection, the following behavior during a cold leg LBLOCA is expected based on test results and analyses:

- ECC injection into the hot legs flows down through the core in distinct regions. Quenching of the fuel rods in these regions initiates shortly after the accumulators start to inject.

- The ECC injected into the hot legs contributes to rapid refilling of the lower plenum and thus an early start of bottom reflood.

- At BOCREC a two-phase upflow region is established which provides relatively good core cooling.

- Intermittent hot leg ECC delivery does not have significant adverse effects on core cooling relative to continuous delivery.

- A radial power profile has almost no influence on the overall thermal-hydraulic behavior in the core region. The heat transfer in hot bundles is better than that in cold bundles during reflood in the upflow region.

- The condensation of steam in the upper plenum and hot legs as well as in cold legs reduces the differential pressure between UP and DC which supports the core water level increase.

Table 4.6-1

SUMMARY OF TEST FACILITIES RELATED TO CORE THERMAL-HYDRAULIC BEHAVIOR

Facility	Scale[2]	Number of Heated Rods[3]	Core Power (MW)	Core Area (m^2)	Core Height (m)	References
SCTF	1/21[3]	1876 (2048 Total)	9.4	0.227[4]	3.66	J-521
CCTF	1/21[3]	1824 (2048 Total)	9.4	0.222	3.66	J-052
FLECHT	1/940-1/430[3,5]	42-91 (49-100 Total)	1.4	NA[6]	3.66	E-452
FLECHT-SEASET	1/370[3]	145 (161 Total)	1.8	0.013[4]	3.66	E-454
FLECHT-SEASET	1/480[3]	145 (163 Total)	1.2	0.01	3.66	E-454
FLECHT-SEASET	1/2400[3]	21	0.2	0.002	3.66	E-454
UCLA	1/95[3]	1692[7]	0[7]	0.05	0.45	E-453
JAERI	1/1200[3]	32 (36 Total)	0.2	0.004	3.66	J-587
Semiscale	1/1600[3]	23 (25 Total)	2.0	0.003	3.66	E-451
LOBI	1/700[8]	64	5.3	0.00013	3.9	E-456, E-460
PKL	1/145[8]	314(340 Total)	2.5	0.07	3.9	E-458
REBEKA	1/193[8]	25	0.1	0.0051	3.9	E-457, E-461

Table 4.6-1

SUMMARY OF TEST FACILITIES RELATED TO
CORE THERMAL-HYDRAULIC BEHAVIOR

NOTES:

1. Facility scale is based on core flow area.
2. Total number of rods includes heated and non-heated rods.
3. Reference PWR is a Westinghouse or Japanese 3400 MWt class PWR.
4. Area shown is that without any core blockage.
5. Facility scale is based on number of heated rods.
6. The core flow areas are not available in the referenced document.
7. Core rods in UCLA facility heated by external induction heaters before tests.
8. Reference PWR is a Siemens/KWU 3900 MWt PWR.

Table 4.6-2

SUMMARY OF PARAMETER EFFECTS ON
CORE HEAT TRANSFER FOR BOTTOM FLOODING TESTS

Parameter	Parameter Variation	Effect on Overall Peak Clad Temperature	Effect on Reflood Temperature Rise
Pressure	Decrease	Increase	Increase
Core Power	Increase	Increase	Increase
Initial Temperature	Decrease	Decrease	Increase
Power/Initial Temperature Distribution	Increase (1)	Increase	Slight Decrease
Accumulator Injection Rate	Increase (2)	Decrease	Decrease
LPCI Injection Rate	Increase	Negligible	Negligible
ECC Subcooling	Increase	Slight Increase	Slight Increase
Flow Resistance	Increase	Increase	Increase
Evaluation Model versus Best-Estimate	Best Estimate	Significant Decrease	Decrease
Core Blockage	Increase	Negligible	Negligible

NOTES:

1. Increased radial power profile.

2. Increased ECC flow rate, not duration. Prolonging accumulator injection after the downcomer was filled to the cold leg elevation increased the peak clad temperature.

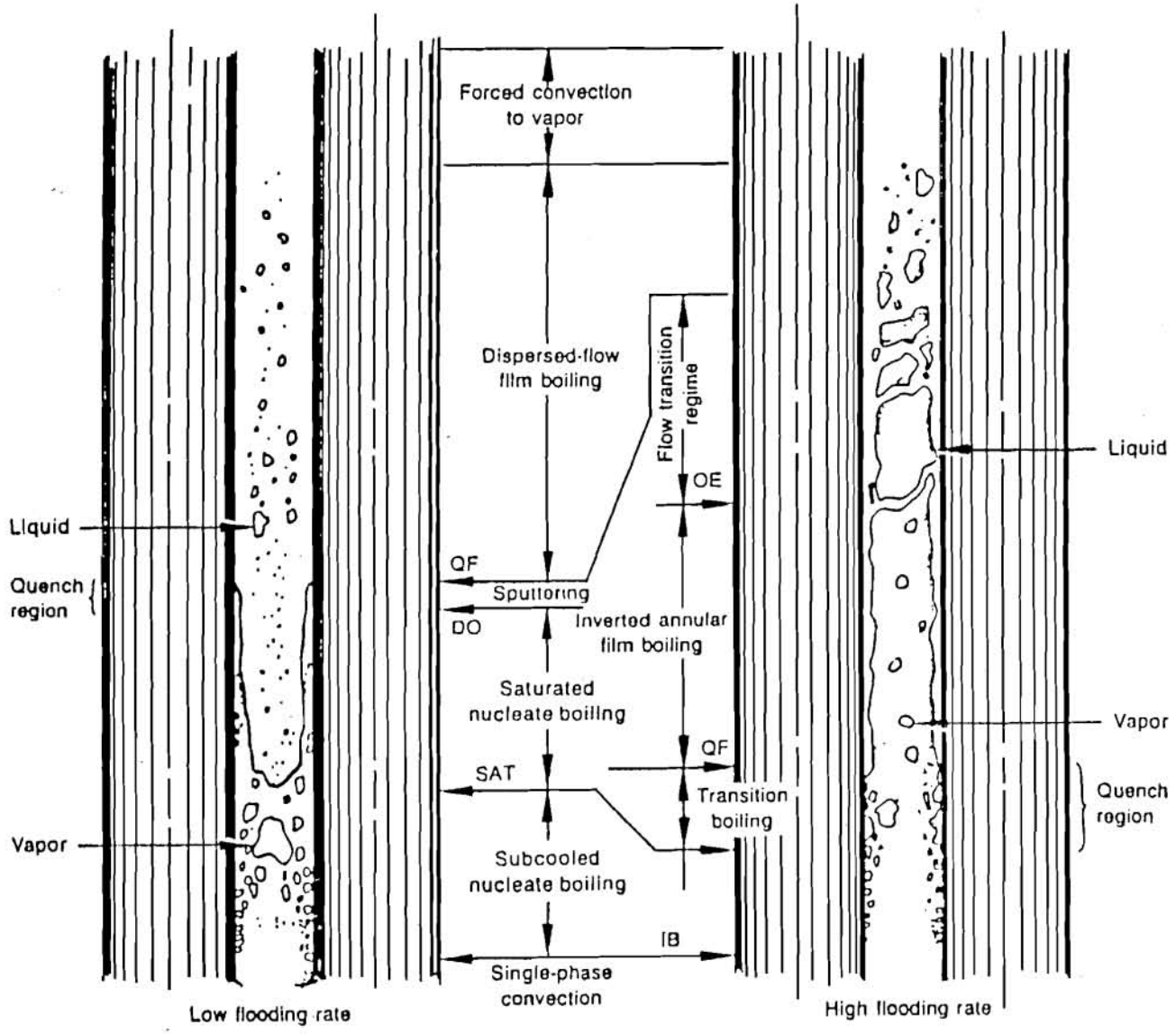

DO Dryout
OE Onset of entrainment
IB Boiling inception
QF Quench front

HEAT TRANSFER AND HYDRAULIC FLOW REGIMES
FOR BOTTOM REFLOOD
(REFERENCE E-459)

FIGURE 4.6-1

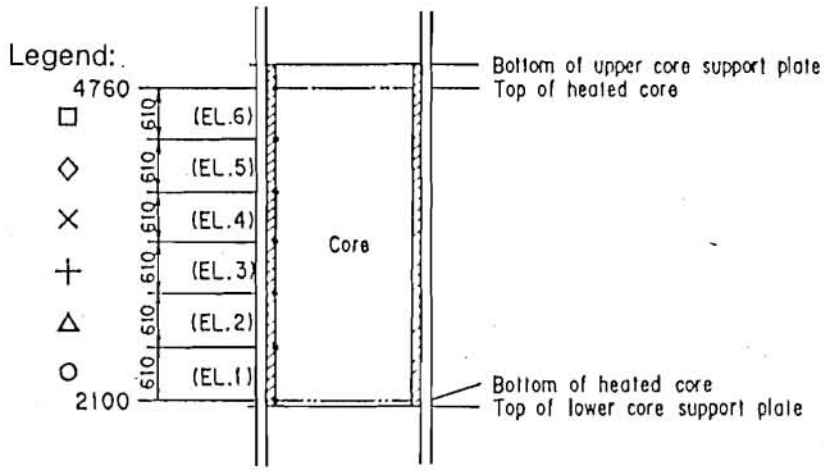

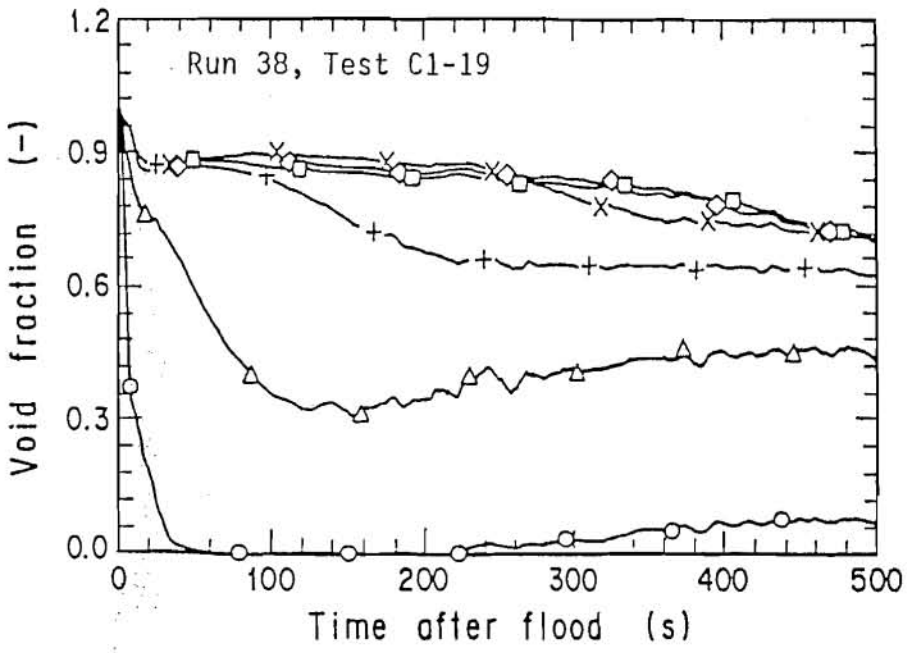

VOID FRACTION IN CORE

FIGURE 4.6-2

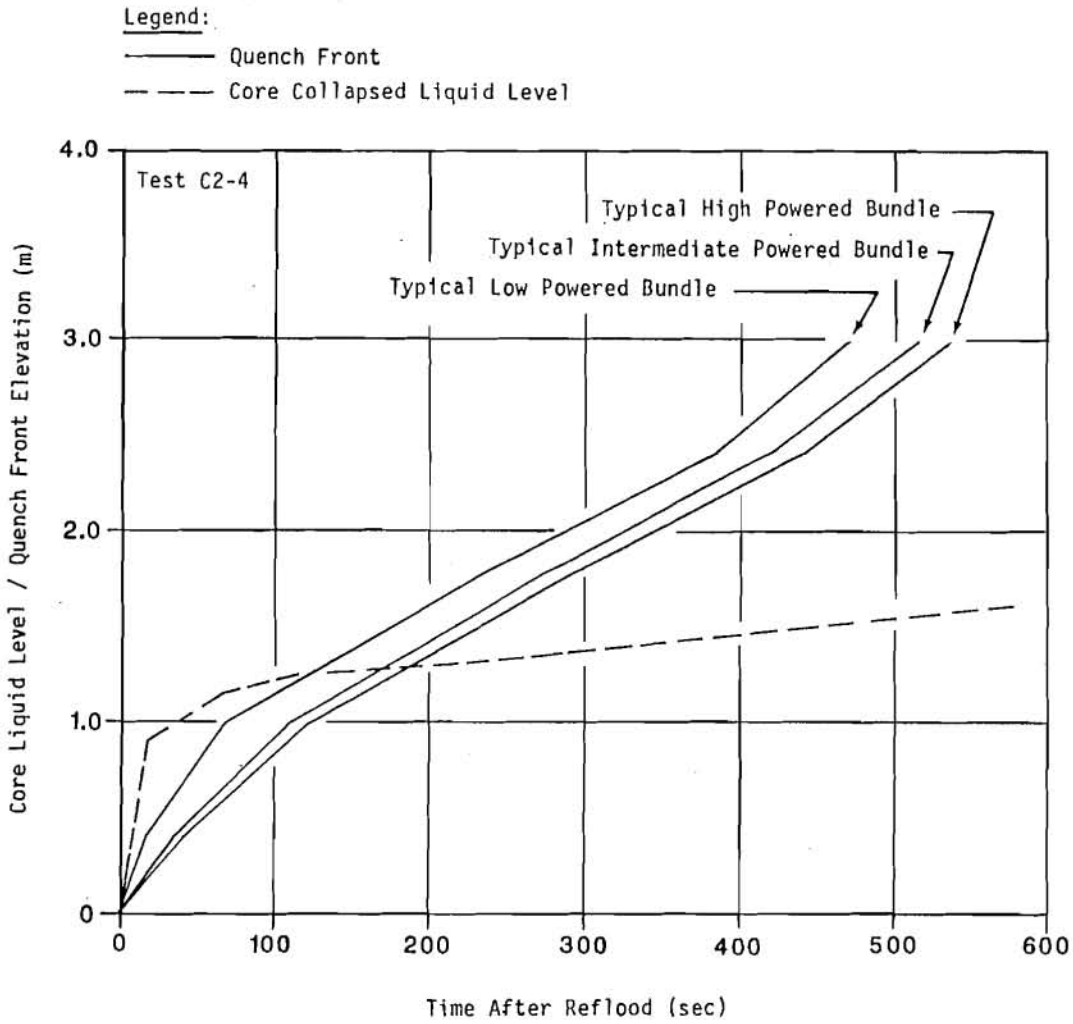

QUENCH FRONT PROPAGATION AND
CORE COLLAPSED LIQUID LEVEL

FIGURE 4.6-3

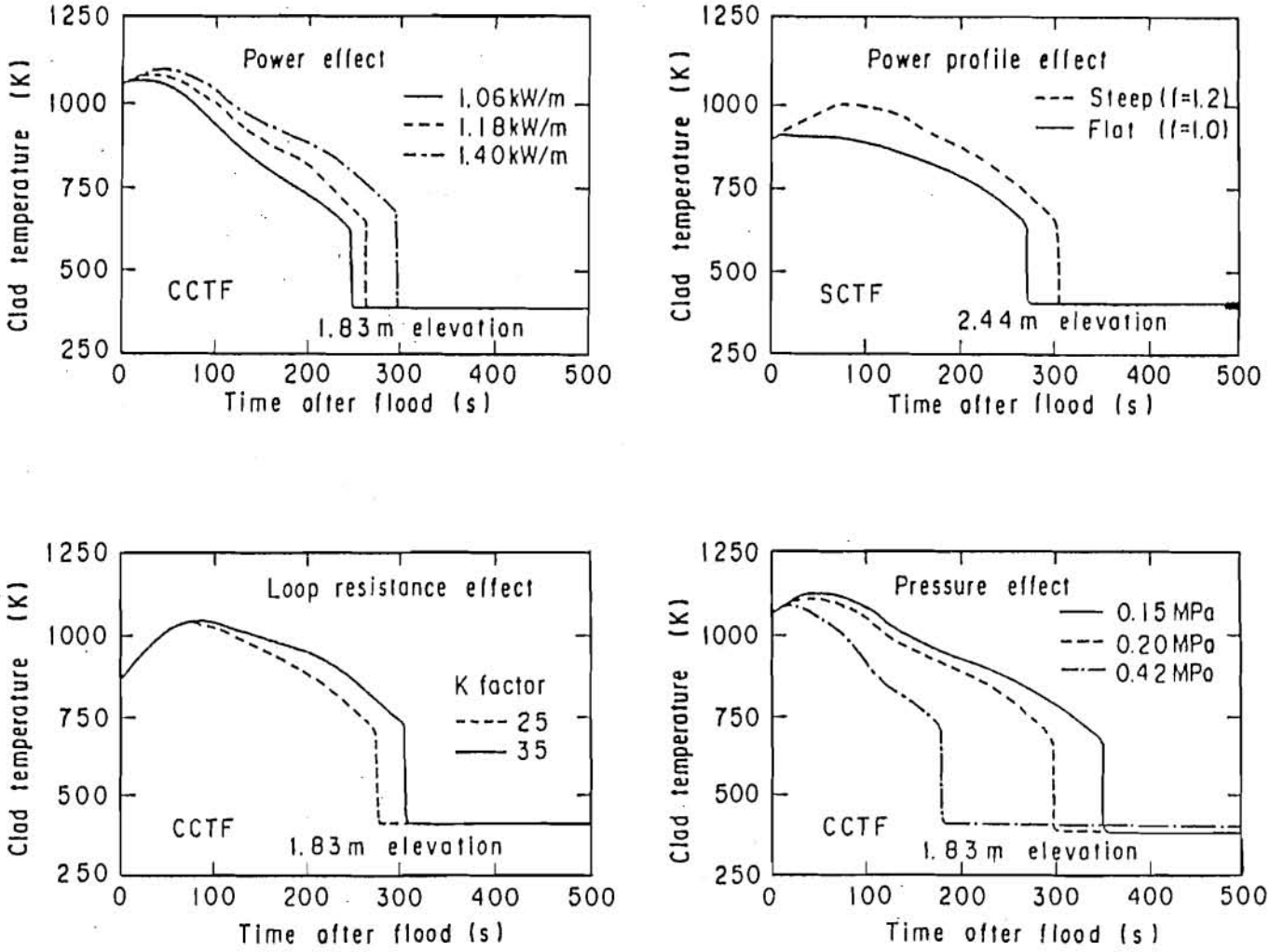

Note: Temperatures are for High Powered Rods.

PARAMETER EFFECTS ON CLAD TEMPERATURE

FIGURE 4.6-4(a)

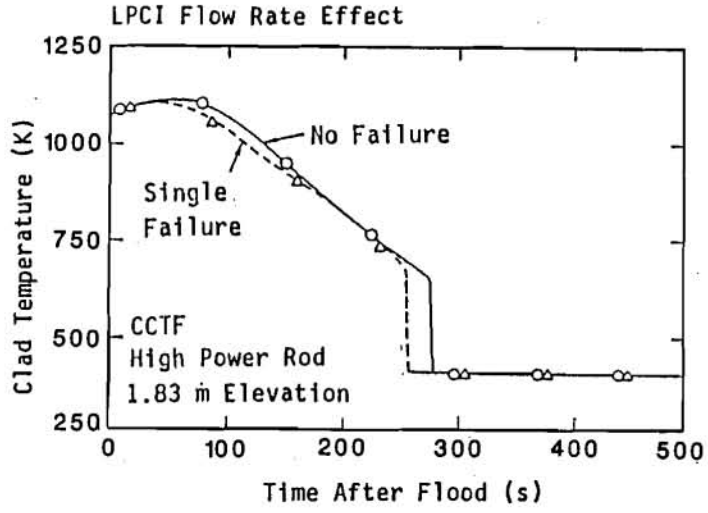

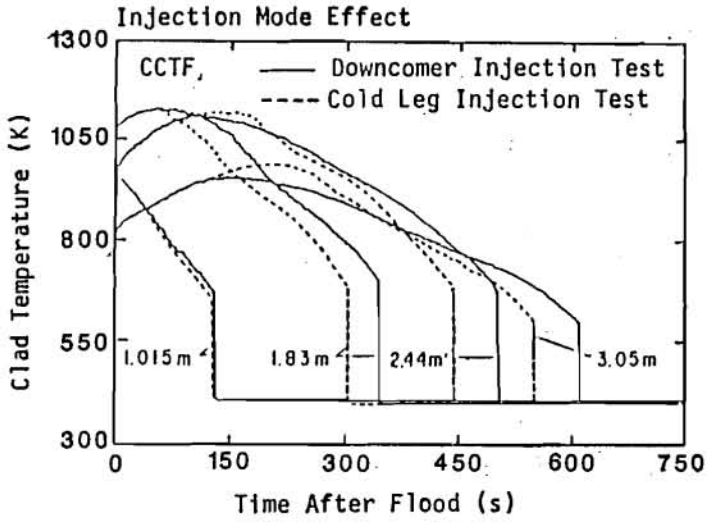

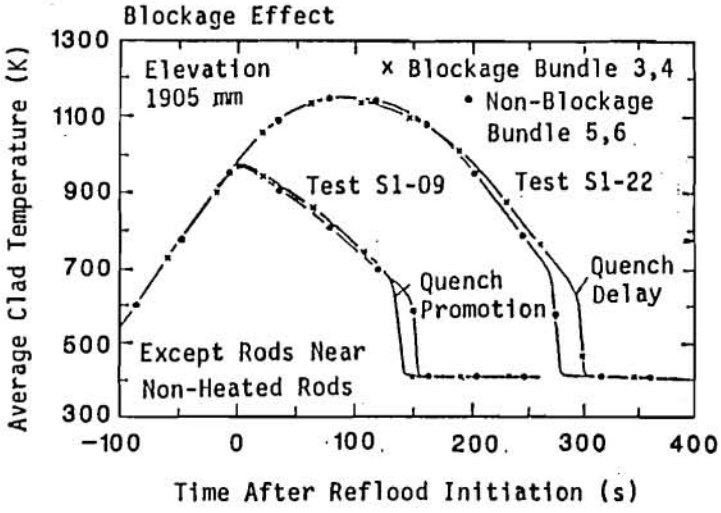

Test S1-09 - Forced Flooding, 4.5 cm/s; High LPCI Injection
Test S1-22 - Gravity Flooding, 1.4 cm/s; Low LPCI Injection

PARAMETER EFFECTS ON CLAD TEMPERATURE

FIGURE 4.6-4(b)

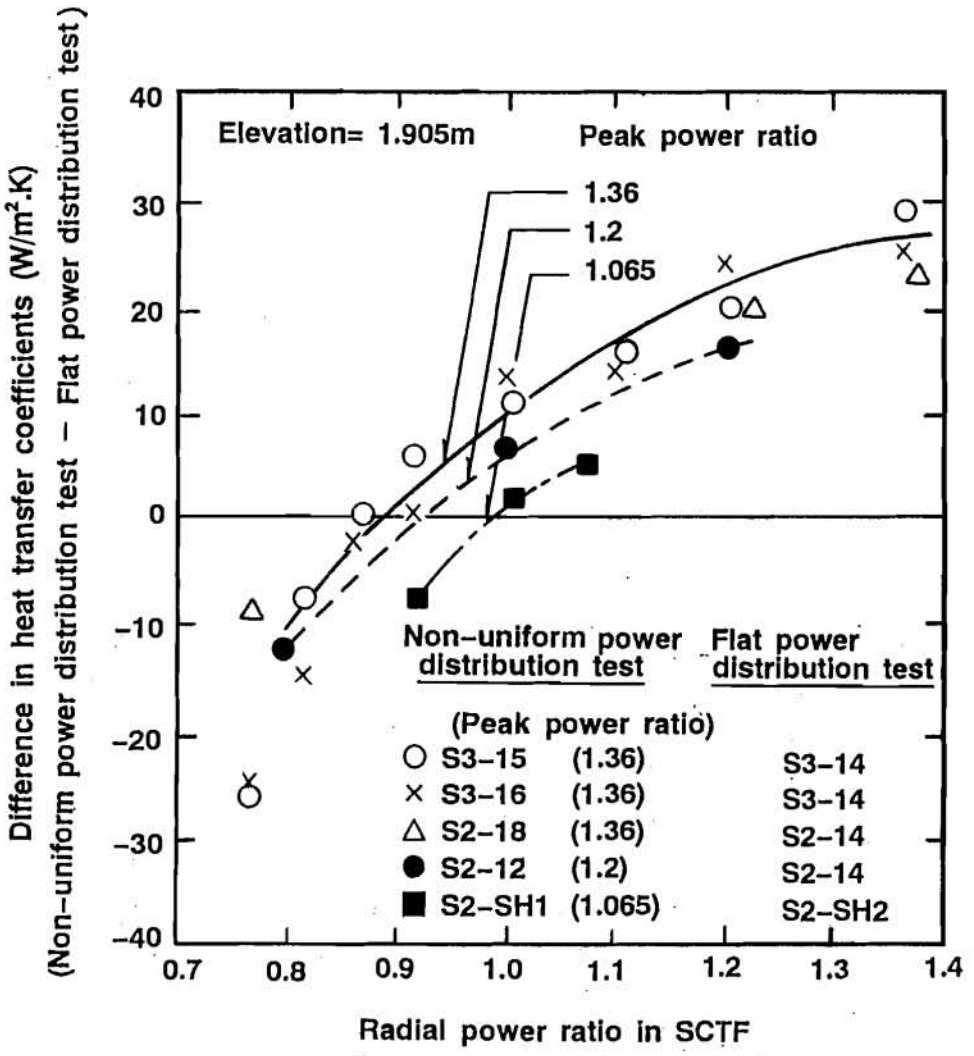

EFFECT OF PEAK POWER RATIO
ON HEAT TRANSFER COEFFICIENT IN SCTF

FIGURE 4.6-5

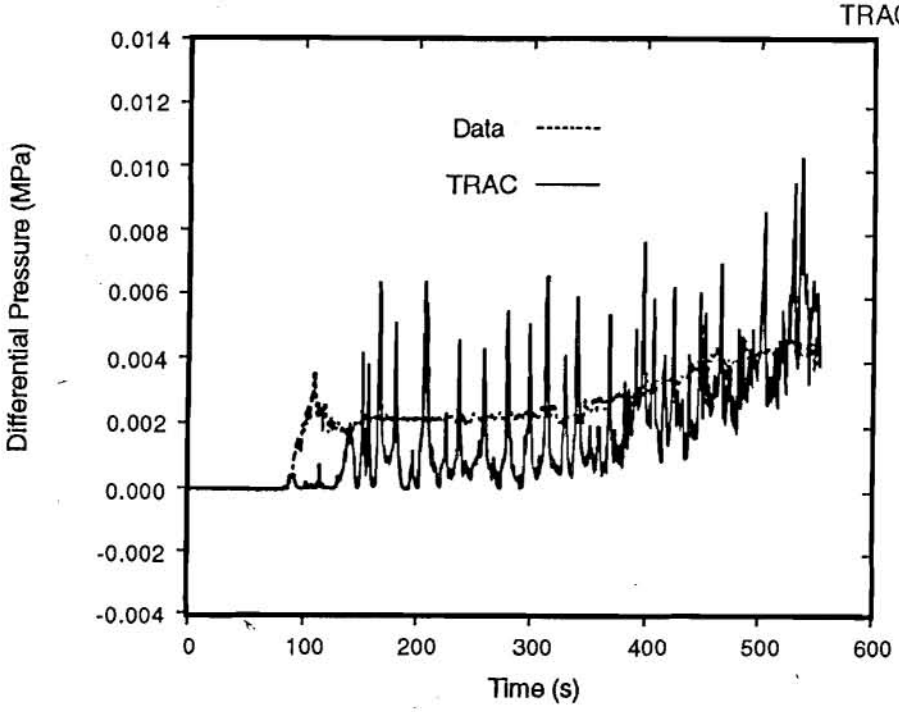

Core Upper Half ΔP Comparison

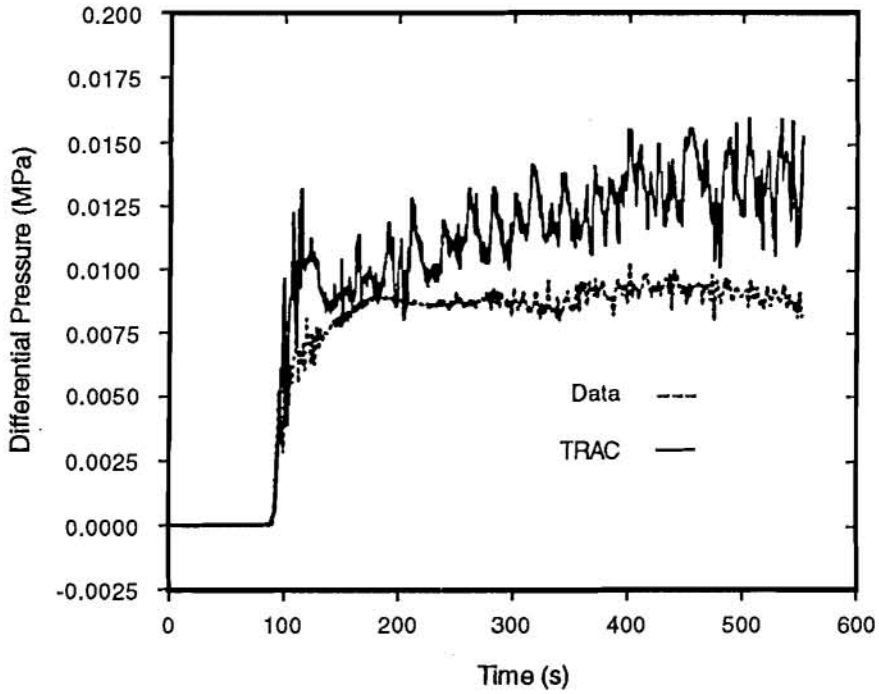

Core Lower Half ΔP Comparison

Note: CCTF Test C2-16 was a UPI Test. The "Spikes" in differential pressure indicate intermmitent penetration from the upper plenum to the core.

TRAC/DATA COMPARISON OF DIFFERENTIAL PRESSURES FOR CCTF TEST C2-16

FIGURE 4.6-6

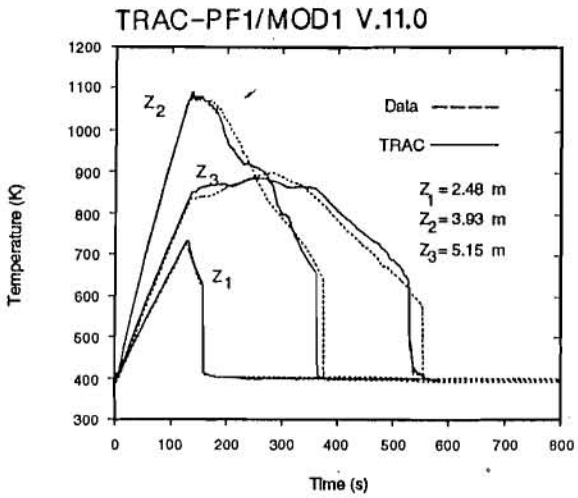

Comparison of High-Power Heater-Rod Temperatures CCTF Test C2-5

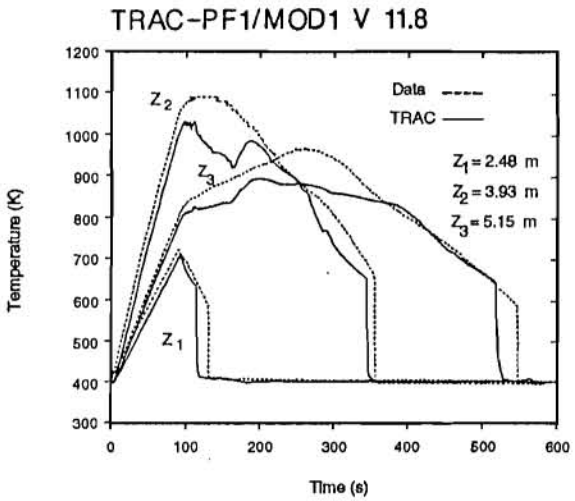

Comparison of High-Power Heater-Rod Temperatures CCTF Test C2-SH2

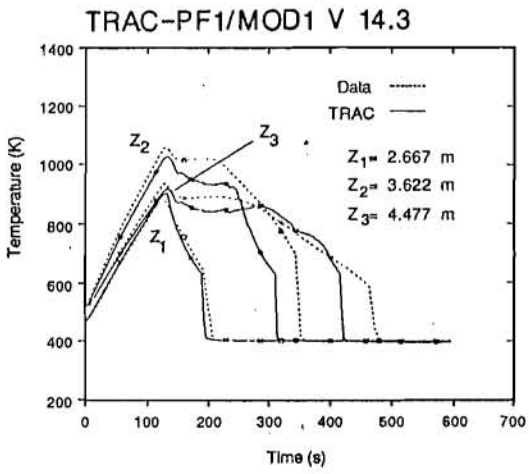

Rod Temperature Comparisons for Bundles 1-4 for SCTF Test S2-AC1

TRAC/DATA COMPARISON OF ROD TEMPERATURES FOR CCTF AND SCTF TESTS

FIGURE 4.6-7

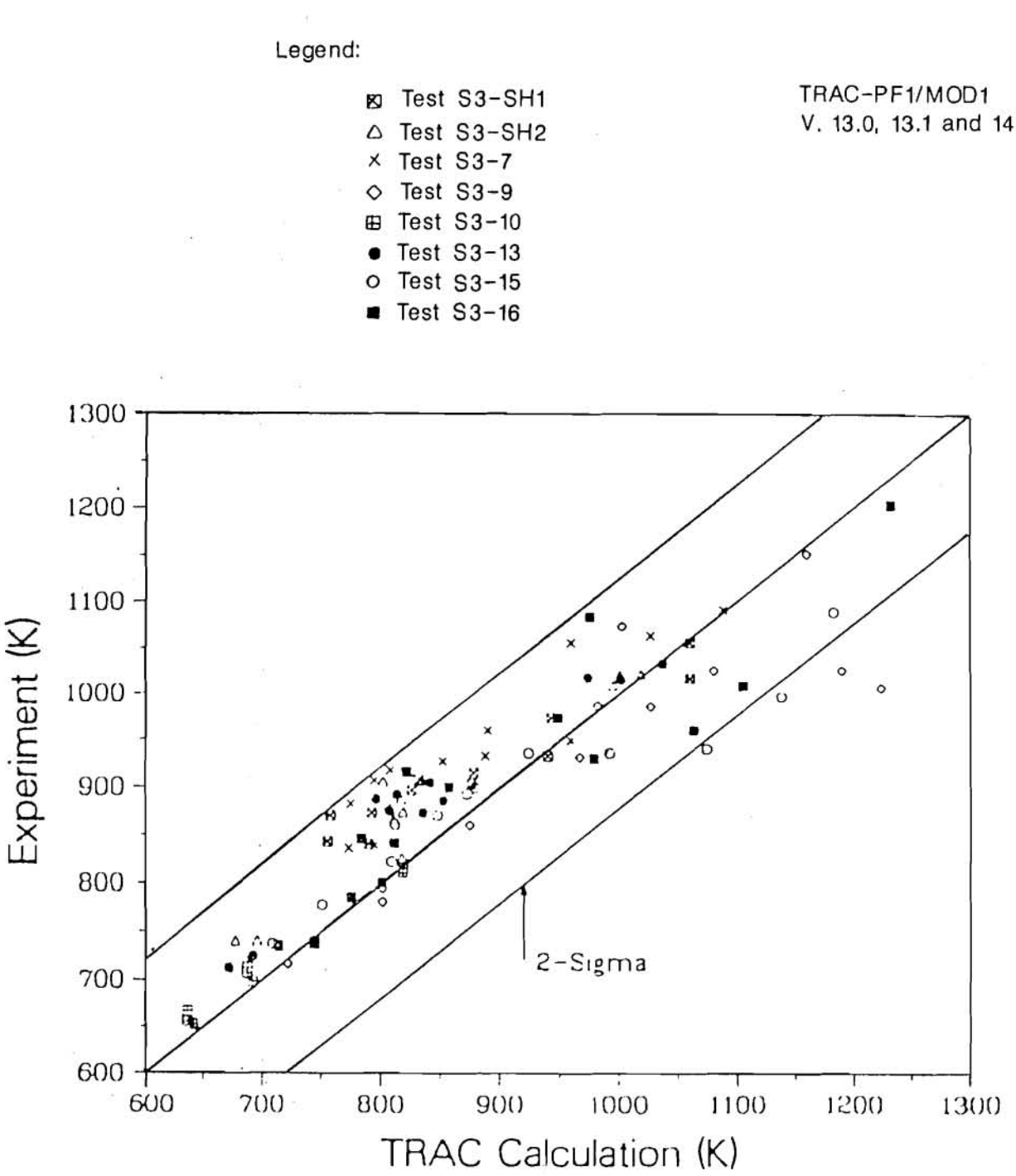

Notes: 1. The tests shown in this figure include cold leg injection tests and combined injection tests.

2. Turnaround temperature comparisons for each test are made at three heights in each of four bundles.

TRAC/DATA COMPARISON OF TURNAROUND TEMPERATURES FOR SCTF CORE-III TESTS

FIGURE 4.6-8

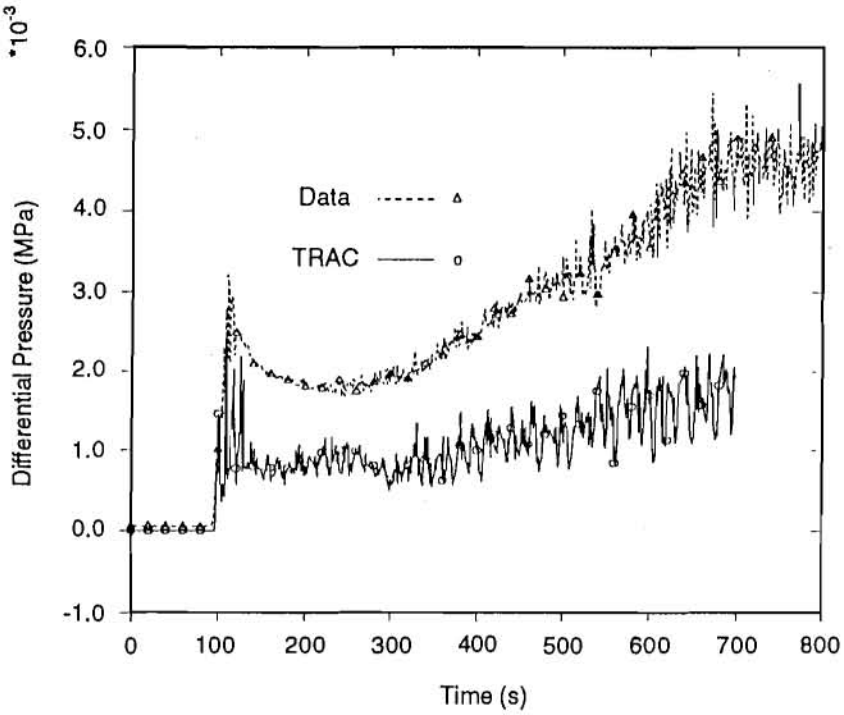

Core Upper Half ΔP

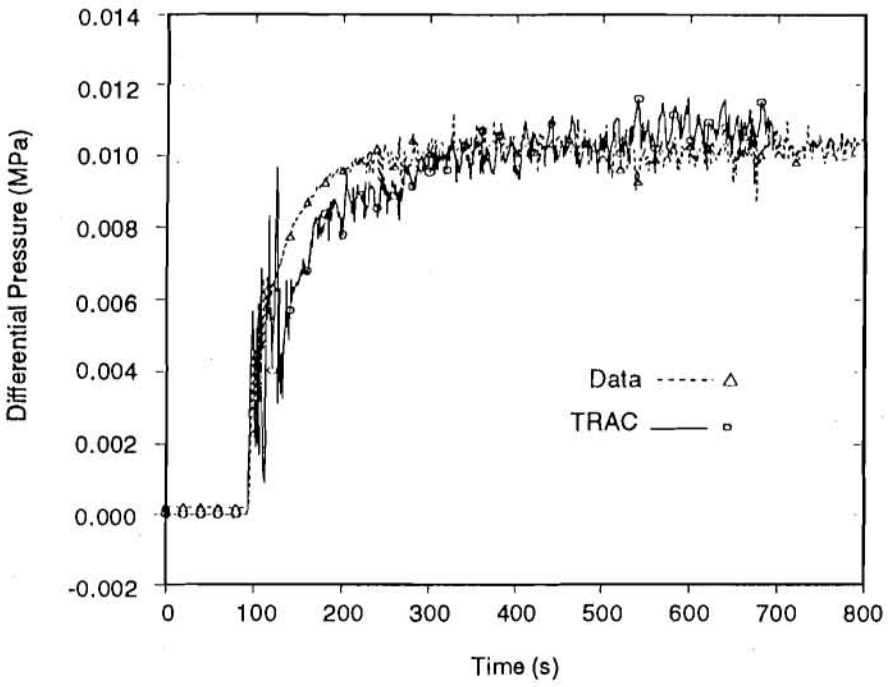

Core Lower Half ΔP

TRAC/DATA COMPARISON OF CORE DIFFERENTIAL PRESSURES FOR CCTF TEST C2-4

FIGURE 4.6-9

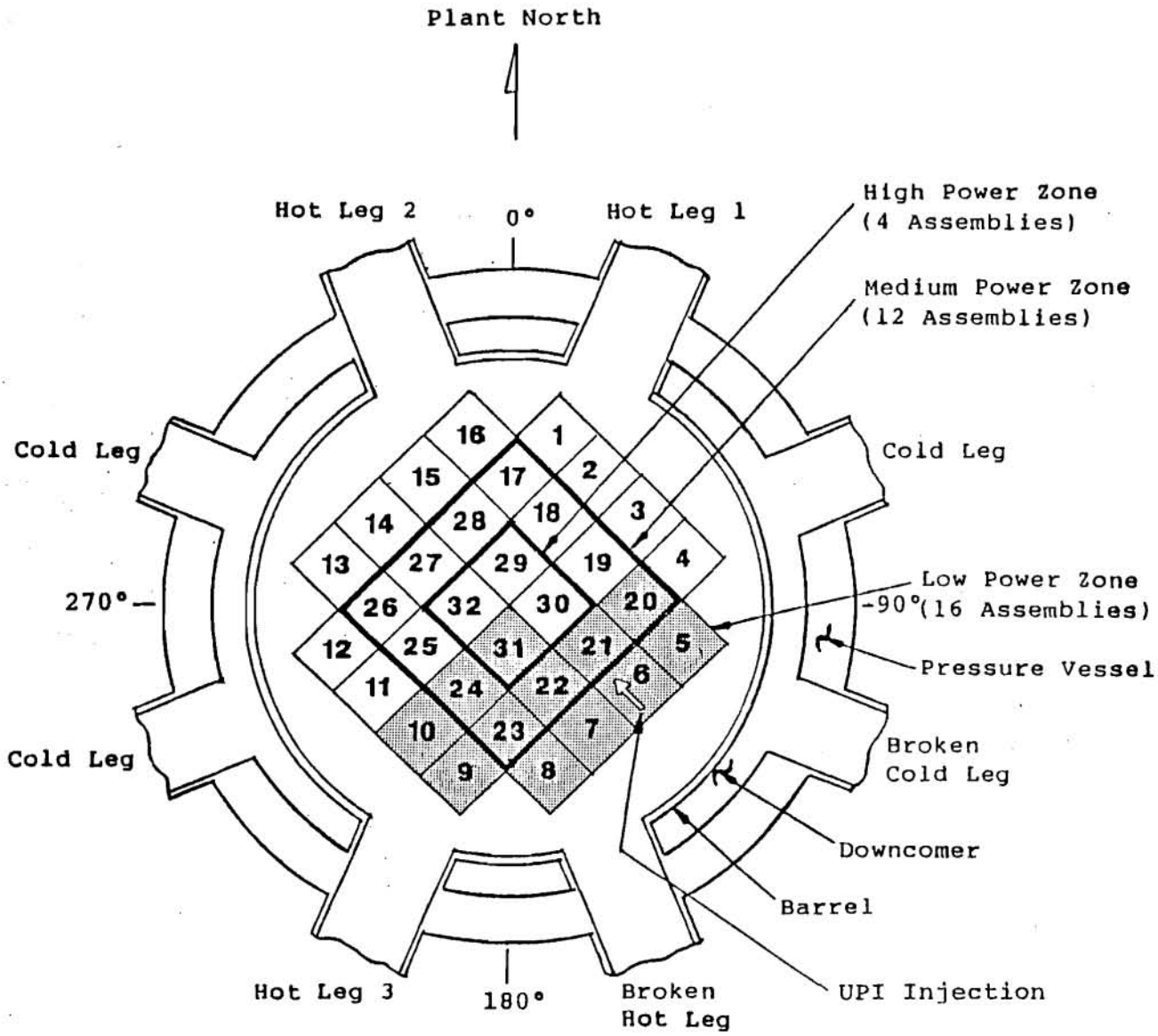

APPARENT PREFERENTIAL WATER DOWNFLOW REGION (SHADED)
INFERRED FROM CORE TEMPERATURE RESPONSE
IN CCTF-II UPI BASE CASE TEST

FIGURE 4.6-10

Notes: 1. See Figure 4.6-10 For Plan View

2. UPI - Upper Plenum Injection Base Case Test, C2-16

CLI - Reference Cold Leg Injection Test, C2-SH2

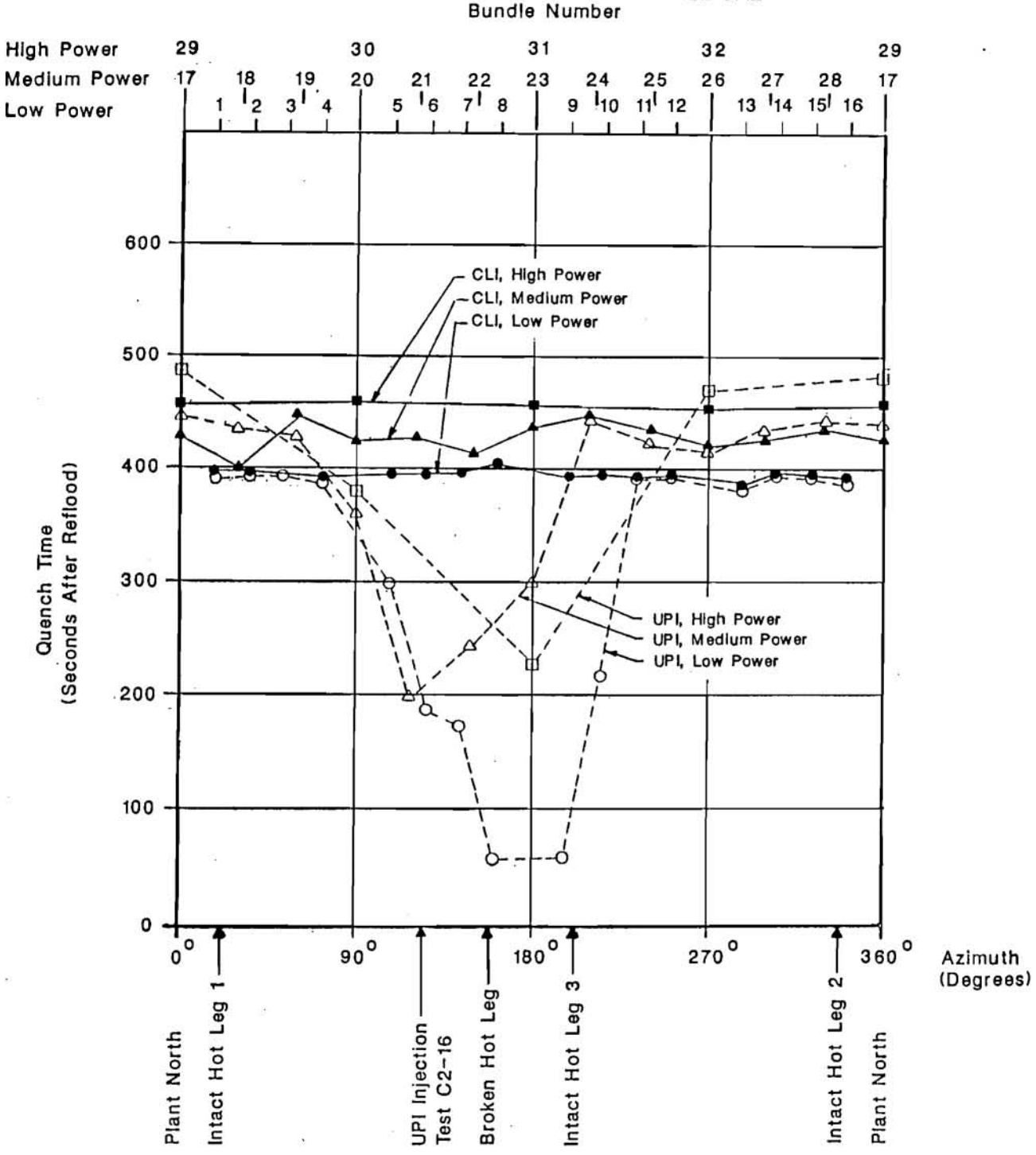

QUENCH TIMES AT 3.05 METER ELEVATION
IN CCTF UPI AND COLD LEG INJECTION TESTS

FIGURE 4.6-11

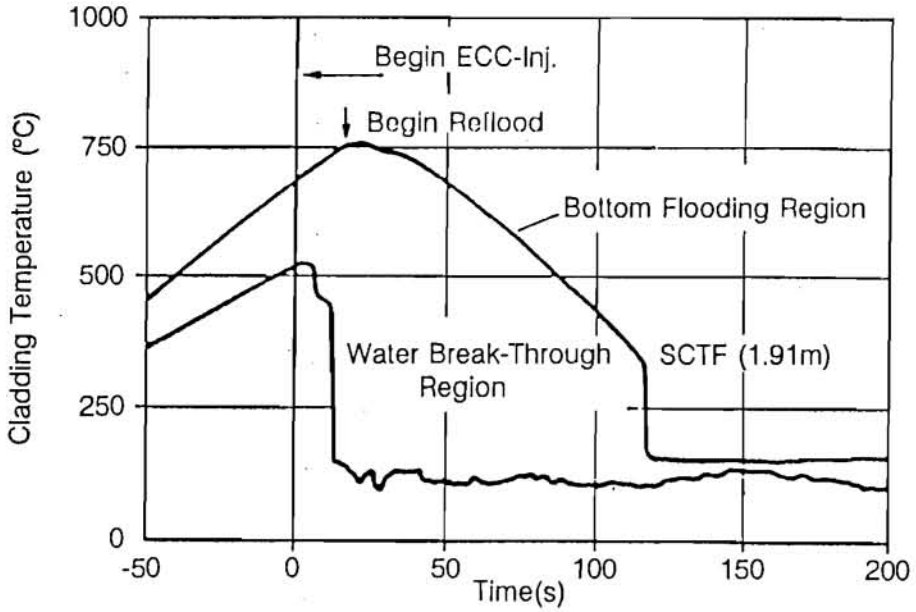

CLADDING TEMPERATURES WITH COMBINED ECC-INJECTION SCTF RUN 717

FIGURE 4.6-12

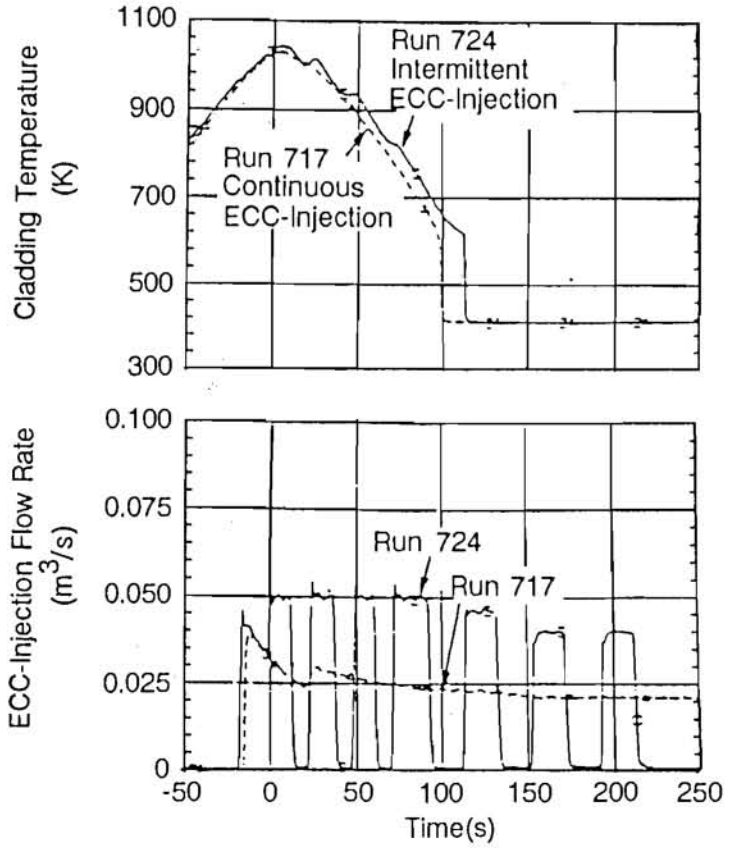

COMPARISON OF CLADDING TEMPERATURES WITH CONTINUOUS AND INTERMITTENT ECC-INJECTION SCTF RUN 717 AND RUN 724

FIGURE 4.6-13

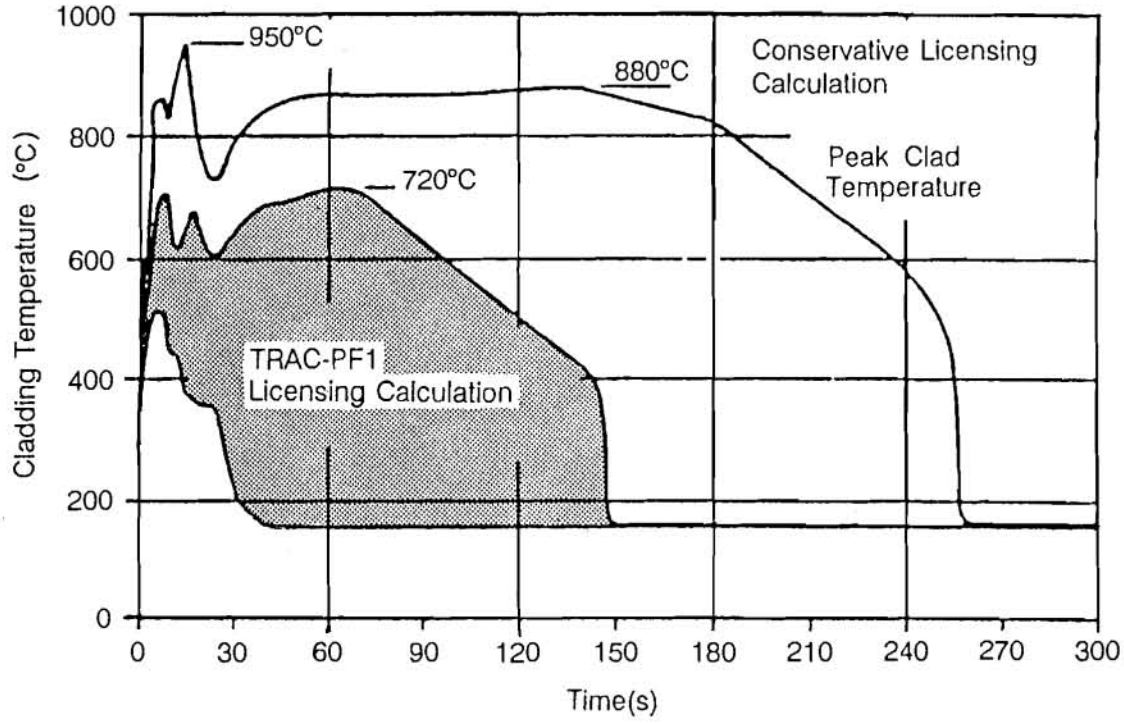

RANGE OF CLADDING TEMPERATURE HISTORIES CALCULATED WITH TRAC USING LICENSING ASSUMPTIONS COMPARED TO A CONSERVATIVE LICENSING CALCULATION

FIGURE 4.6-14

4.7 WATER DELIVERY TO AND DISTRIBUTION IN THE UPPER PLENUM

Definition of Issue and Description of Phenomena

Some PWRs have ECC systems which deliver subcooled ECC to the reactor vessel upper plenum. These include upper plenum injection (UPI) plants and combined injection plants (where ECC injected in the hot legs enters the upper plenum). During a large-break LOCA, steam or two-phase upflow from the core interacts with subcooled ECC in the upper plenum. The interaction influences ECC delivery to the core and subsequently core cooling.

Key phenomena in the upper plenum include the following:

- Steam condensation in the upper plenum by subcooled ECC, which improves core venting (i.e., decreases steam binding).
- Water accumulation, which stores water in the upper plenum and creates a hydrostatic head which contributes to the core-to-downcomer pressure drop.
- Water distribution in the upper plenum, which can influence the location of water downflow.
- Saturated/subcooled water mixing, which "dilutes" the subcooling and can influence the amount of water penetration to the core.
- Liquid entrainment and carryover into the hot legs, which removes liquid from the reactor vessel and may contribute to steam binding.
- Liquid delivery to the core, which is directly related to core cooling.

Tests in the 2D/3D Program provided improved insight on these phenomena for both UPI and combined injection.

In a UPI plant, low pressure coolant injection (LPCI) water is injected into the upper plenum. This injection is the principal source of ECC during the reflood phase of a large-break LOCA (LBLOCA). Prediction of the disposition of UPI water and, in particular, the ECC delivery to the core, is the major issue associated with this ECC system. Phenomena associated with UPI are shown in Figure 4.7-1. UPI downflow to the core may be limited by overall system behavior or the countercurrent flow limitation (CCFL) at the tie plate. This situation contributes to accumulation of UPI water in the upper plenum in the form of a two-phase mixture. Within this mixture, steam condensation is promoted. Uncondensed steam potentially carries some UPI water out of the upper plenum into the hot legs where the water either de-entrains or carries into the steam generators.

In a combined injection plant, both accumulator and pumped ECC are injected into the cold legs and hot legs of the primary loop. The hot leg injection is through nozzles (Hutze) at the bottom of the hot leg pipes aimed into the upper plenum. In this case, water delivery to the upper plenum is influenced by the steam/ECC interaction in the hot legs (i.e., countercurrent flow and condensation--see Section 4.3). Figure 4.7-2 illustrates phenomena in the upper plenum with hot leg injection. Subcooled water delivered to the upper plenum condenses steam in the upper plenum and flows down through the tie plate to the core. Condensation in the upper plenum and delivery to the core are strongly affected by the rate of ECC delivery to the upper plenum and water distribution in the upper plenum. Water delivery to the core is also affected by countercurrent flow phenomena at the tie plate.

The phenomena described above for PWRs with combined injection can also occur during a small-break LOCA (SBLOCA) in which the core uncovers at elevated pressures. However, in this case only the high pressure injection system is activated.

Importance of Issue to PWR LOCA Behavior

The pattern, flow rate, and subcooling of water delivery from the upper plenum to the core affect local core cooling in the water downflow region. Global core cooling and peak cladding temperature (PCT) are affected by the rate of reflood. Water accumulation in the upper plenum, hot legs, and steam generator inlet plena, as well as steam produced from water carried into the steam generators, increases the loop pressure drop and can potentially impede core flooding; however, steam condensation in the upper plenum improves core cooling by improving core venting capability.

Tests and Analyses that Relate to the Issue

Tests which addressed upper plenum water delivery and distribution were performed at each of the three major 2D/3D Program facilities as well as some of the ancillary facilities (ORNL, Karlstein, etc.). The tests at the ancillary facilities were performed as part of the development/calibration of the advanced instrumentation for the core/upper plenum interface. Tests outside the 2D/3D Program provided additional information, generally at small-scale. In addition, many of the 2D/3D tests were analyzed using the TRAC and ATHLET computer codes. Tests and analyses relevant for UPI and hot leg injection are listed in Tables 4.7-1 and 4.7-2, respectively.

As shown in Table 4.7-1, UPI-related separate effects tests were performed at UPTF, SCTF, the ORNL Instrument Development Loop (IDL), and Dartmouth. Integral tests were performed at both CCTF and Semiscale. Post-test analyses of each of the CCTF tests were performed using TRAC-PF1/MOD1. The UPTF test was analyzed using both TRAC-PF1/MOD2 and ATHLET.

Table 4.7-2 indicates that separate effects tests relevant to hot leg injection were performed at UPTF, SCTF, Karlstein and the University of Hannover. Combined injection integral tests were performed at each of the three 2D/3D test facilities. Integral tests with combined injection were also performed outside the 2D/3D Program at PKL and LOBI. Post-test analyses for ten of the 2D/3D tests were performed using TRAC-PF1/MOD1, TRAC-PF1/MOD2, and ATHLET.

Summary of Key Results and Conclusions from Test and Analyses

In the large-scale tests at CCTF, SCTF and UPTF, phenomena in the upper plenum and tie plate region were multidimensional. Specifically, water downflow from the upper plenum to the core occurred in discrete regions below the injection locations (i.e., UPI nozzles or hot legs). Outside these downflow regions, a two-phase mixture of steam and water flowed from the core to the upper plenum. Water accumulation in the upper plenum was also multidimensional with higher accumulation over the water downflow regions.

Discussion of the detailed results is provided in Subsection 4.7.1 for UPI and Subsection 4.7.2 for hot leg injection.

4.7.1 Upper Plenum Injection

As previously discussed, 2D/3D tests with UPI showed that delivery of water to the core occurred in a single, stable region in front of the ECC injection nozzle while outside this region a two-phase mixture of steam and water flowed upward from the core to the upper plenum. Steam and subcooled ECC mixed in the upper regions of the core and the upper plenum resulting in extensive condensation; uncondensed steam was vented out the hot legs. The lack of subcooling in the lower plenum or the hot legs during the CCTF and UPTF tests, indicated that the maximum amount of condensation took place in the upper plenum and core regions. For CCTF, virtually no subcooling was found in the core indicating that all of the condensation occurred in the upper plenum. About 80% of the condensation at UPTF occurred in the upper plenum and the remainder occurred in the core region.

The following discussion compares results from UPI and UPI-related tests at different facilities and evaluates the effect of scale. For this discussion, scale is defined relative to the core flow area; however, it should be noted that the test vessel radius may affect how readily the multidimensional phenomena are established. It should also be noted that, in integral tests with a heated core at CCTF and Semiscale, upper plenum behavior may have been influenced by system effects; the separate effects tests at UPTF, SCTF, IDL, and Dartmouth did not simulate overall system behavior.

- The size of the downflow region was predominantly a function of the facility scale. The area of the downflow region relative to the core flow area was found to decrease with increasing scale, as shown in Figure 4.7-3 (Reference U-454).

- The rate of downflow was found to be dependent upon ECC subcooling and scale for comparable (i.e., appropriately scaled) ECC injection rates. With more subcooling, the rate of water downflow constituted a larger fraction of the available water (i.e., ECC injection rate plus steam condensation rate). Subcooling above the tie plate appears to aid in downflow to the core. Scale affected downflow in that the larger scale facilities had larger downflow fractions relative to the available water as shown in Figure 4.7-4. Note that, in the CCTF tests, system effects with a heated core influenced downflow; these effects were not simulated at UPTF. However, at both CCTF and UPTF, almost all of the ECC injected in the upper plenum penetrated to the core (Reference U-454).

- Water carryover to the hot legs, and hence the potential for steam binding due to vaporization in the steam generators, was found to be influenced by scale. An increase in scale resulted in a decrease in carryover rate for similar core steam momentum fluxes as shown in Figure 4.7-5. Further, water accumulation in the hot legs occurred to a greater extent at the large-scale UPTF than at the small-scale CCTF; consequently, the portion of water carried over to the loops which

reached the steam generators was smaller at UPTF than at CCTF (Reference U-454).

- For similar gas momentum fluxes at the tie plate and ECC injection rates, the upper plenum liquid fraction was found to decrease with increasing scale as shown on Figure 4.7-6. However, it should be noted that system effects with a heated core, which were not simulated in the UPTF and ORNL tests, may affect the trend shown in Figure 4.7-6. The amount of water stored in the upper plenum at steady-state was small, ranging from about 3 seconds worth of UPI flow at UPTF to 25 seconds worth of UPI flow at SCTF. Upper plenum accumulation was also affected by the ECC injection rate. Specifically, the "no-failure" (high ECC flow) test at CCTF had an inventory that was twice that in the "single-failure" tests; however, the condensing capacity of the UPI flow exceeded the core steam flow so that the additional inventory did not hinder core venting. The water distribution across the flow area tended to be uniform except over the downflow region where more water accumulated. Overall, the differential pressure resulting from the water accumulation was a small fraction of the total loop differential pressure (Reference U-454).

The five CCTF tests were analyzed by the TRAC-PF1/MOD1 computer code at LANL (Reference U-622). In addition, LANL analyzed the UPTF test using the TRAC-PF1/MOD2 computer code (Reference U-710). For four of the five CCTF tests, the code had reasonable overall agreement with the test results, predicting multidimensional core reflood conditions, negative core-inlet flow, location of the liquid downflow, and average values for fuel rod temperatures. However, the code overpredicted the amount of UPI downflow to the core while also not predicting the core void distribution accurately. The analysis of one CCTF test (C2-AA1) did not have good overall agreement with the test, but the test conditions were not similar to a UPI plant. The TRAC analysis of the UPTF test predicted UPI downflow to the core, overall condensation of steam, and the overall break mass flow, but overpredicted liquid accumulation in the upper plenum and underpredicted the loop mass flows. Overall, the two TRAC code versions were able to predict the major trends reasonably.

With regard to expected behavior in a UPI PWR, the test results indicate water downflow from the upper plenum to the core will occur steadily and the rate of downflow will be essentially the same as the UPI flow rate. Also, most of the steam which enters the upper plenum from the core will be condensed in the upper plenum. This tends to negate the possibly detrimental effects of hot leg carryover and upper plenum accumulation.

4.7.2 Hot Leg Injection

With hot leg injection, ECC delivery to the upper plenum is influenced by the steam/ECC interaction in the hot legs. As discussed in Section 4.3.2, ECC delivery is either continuous or fluctuating. Fluctuating delivery results from periodic water accumulation in the hot legs.

In UPTF tests, water downflow to the core initiated almost immediately and only a relatively small amount of water accumulated in the upper plenum. Water downflow occurred in local regions adjacent to the hot legs where ECC was injected. Water accumulation in the upper plenum exhibited similar multidimensionality in that accumulation was higher over the downflow regions. The corresponding increase in local hydrostatic head provided the necessary driving head for water downflow. The water downflow into the core was observed to be subcooled.

Figure 4.7-7 shows the size of the downflow region for four of the UPTF separate effects tests. The figure indicates that the size of the downflow region was about 10 fuel assemblies per injection nozzle in the high pressure, SBLOCA test (Test 30); and 18-23 fuel assemblies per injection nozzle for the low pressure, LBLOCA tests (Tests 12, 20 and 26). Figure 4.7-7 also indicates that the size of the downflow region increases with increasing ECC injection rate. This trend may be attributable to an increase in injection velocity. Fluctuations in ECC delivery to the upper plenum did not affect the size or location of the downflow regions.

For the high ECC and core exit steam flows typical of an LBLOCA, 80% of the core exit steam flow was condensed in the hot legs and upper plenum by the hot leg ECC injection. Even though condensation was extensive, the water downflow to the core was substantially subcooled (~70 K); however, for conditions simulating HPI during an SBLOCA, only a portion of the core exit steam flow was condensed and the water downflow was saturated. The lack of subcooling below the tie plate indicates that the condensation efficiency in the hot legs and upper plenum was about 100%.

Finally, UPTF test results indicated ECC penetration through the tie plate at full-scale was not limited (no CCFL) over the range of expected PWR flow conditions.

Countercurrent flow phenomena at the tie plate were extensively investigated in the past, using small-scale test facilities and perforated plates up to the size of one fuel assembly (References E-931, E-932, E-471, E-933, G-901, and G-803). Typically, small-scale facilities showed behavior that was relatively homogeneous and one-dimensional, and water downflow was inhibited by CCFL even at moderate steam flows.

In the larger CCTF (1/24-scale), behavior was different. After a brief period of water accumulation following ECC initiation, water downflow to the core in a stable channel was established. There was significant upper plenum water accumulation in CCTF. The location where water downflow occurred was not precisely predictable (References J-453 through J-456).

Comparison of the UPTF results to CCFL correlations from the small-scale facilities indicates that downflow was significantly higher at the full-scale UPTF than at small-scale. This beneficial effect at large-scale is explained by the multidimensional water distribution and flow patterns; i.e., distinct breakthrough zones.

Since assessment of existing flooding correlations from literature using UPTF experimental results revealed that extrapolation to full-scale is not appropriate, a new equation was developed to correlate the tie plate countercurrent flow observed in UPTF. This new correlation is an addition to the well-known Wallis-type and Kutateladze type correlations (References G-415, G-906, and G-915). Each of the three correlations is valid for experimental facilities of a certain scale. Figure 4.7-8 shows the dimensionless gas velocity at the onset of penetration across the full range of facility scales.

An analytical model to determine water downflow rates and areas was developed by Siemens based on analyzing the pressure balance at the tie plate in the water downflow and two-phase upflow regions. This model is described in detail in Reference G-925.

Post-test analyses for several of the UPTF tests were performed using TRAC-PF1/MOD1. Review of the calculations indicates that TRAC correctly predicted fluctuating delivery from the hot legs but overpredicted the subcooling of the water delivered to the upper plenum. TRAC also did not correctly account for the horizontal momentum of the water flow into the upper plenum. Specifically, water downflow to the core and significant water accumulation in the upper plenum were predicted to occur directly below the hot legs in the TRAC calculations rather than 1 m in front of the hot legs as observed in the tests. Finally, TRAC predicted the onset of water downflow but underpredicted the rate of downflow by 20%.

For a PWR with ECC injection into hot legs it can be concluded:

- Water downflow occurs in front of the hot legs with ECC injection. Fluctuations in ECC delivery to the upper plenum result in fluctuations in water downflow to the core.

- For both the LBLOCA and SBLOCA cases, ECC injected in the hot legs penetrates through the tie plate into the core without limitation.

- In the case of an LBLOCA, more than 80% of the core exit steam flow is condensed in the upper plenum and the hot legs by the ECC injected into the hot leg and the water downflow through the tie plate is substantially subcooled.

- In the case of an SBLOCA in which the core uncovers, the condensation efficiency in the upper plenum and hot legs is close to 100% and the water downflow is saturated.

Table 4.7-1

SUMMARY OF TESTS AND ANALYSES
RELATED TO UPI PHENOMENA

Type of Test or Analysis	Facility or Analysis	Facility Scale[1]	References
UPI-Related Separate Effects Tests	UPTF: Test 20	2.1	U-454, G-411 G-020, G-220
	SCTF-II: Test S2-3 Test S2-4 Test S2-5	0.091	J-526 J-128 J-129 J-130
	ORNL IDL	0.011, 0.033	U-825
	Dartmouth	0.0091	E-465
Integral UPI Tests	CCTF-II: Test C2-AA1 Test C2-AS1 Test C2-13 Test C2-16 Test C2-18	0.091	U-412 J-047, J-245 J-049, J-247 J-061, J-259 J-064, J-262, J-452 J-066, J-264, J-453
	Semiscale	0.0017	E-011
Computer Analysis	TRAC-PF1/MOD1: CCTF Test C2-AA1 CCTF Test C2-AS1 CCTF Test C2-13 CCTF Test C2-16 CCTF Test C2-18	---	 U-622, U-626, U-627 U-622, U-629 U-622, U-634 U-622, U-636 U-622, U-637
	TRAC-PF1/MOD2: UPTF Test 20	---	 U-710
	ATHLET: UPTF Test 20	---	 G-649

NOTE:

1. The scale of the facility is based on the core flow area; the reference is a 1600 MWt Westinghouse or Japanese PWR with UPI.

Table 4.7-2

SUMMARY OF TESTS AND ANALYSES RELATED TO UPPER PLENUM WATER DELIVERY AND DISTRIBUTION WITH HOT LEG INJECTION

Type of Test or Analysis	Facility or Analysis	Facility Scale[1]	References
Separate Effects Tests Related to Hot Leg Injection	UPTF: Test 10A Test 10C Test 12 Test 13 Test 15 Test 16 Test 26C Test 30	1	G-411 G-010, G-210 G-010, G-210, U-453 G-012, G-212 G-013, G-213 G-015, G-215 G-016, G-216 G-026, G-226 G-030, G-230
	SCTF-II: Test S2-3 Test-S2-4 Test S2-5	1/24	J-526 J-128 J-129 J-130
	SCTF-III: Test S3-3 Test S3-4 Test-S3-5	1/24	J-570 J-155 J-156 J-157
	Karlstein	1/193	G-802
	University of Hannover	1/193	G-801

Table 4.7-2

SUMMARY OF TESTS AND ANALYSES RELATED TO UPPER PLENUM WATER DELIVERY AND DISTRIBUTION WITH HOT LEG INJECTION

Type of Test or Analysis	Facility or Analysis	Facility Scale[1]	References
Integral Tests with Combined Injection	UPTF: Test 3 Test 14 Test 18 Test 19 Test 28	1	G-411 G-003, G-203 G-014, G-214 G-018, G-218 G-019, G-219 G-028, G-228
	CCTF-I: Test C1-SH5	1/24	J-005, J-401
	CCTF-II: Test C2-19 Test C2-20 Test C2-21	1/24	J-067, J-454, J-455 J-068, J-456, J-557 J-069, J-456
	SCTF-I: Test S1-SH3 Test S1-SH4	1/24	J-102 J-103
	SCTF-III: Test S3-AC1 Test S3-SH2 Test S3-11 Test S3-13 Test S3-18 Test S3-19 Test S3-20 Test S3-21 Test S3-22	1/24	--- J-152 J-163, J-557 J-165 J-170, J-564 --- J-171, J-565 J-172, J-577 J-173, J-572
	PKL:	1/145	E-456, E-458
	LOBI:	1/700	E-460

Table 4.7-2

SUMMARY OF TESTS AND ANALYSES RELATED TO UPPER PLENUM WATER DELIVERY AND DISTRIBUTION WITH HOT LEG INJECTION

Type of Test or Analysis	Facility or Analysis	Facility Scale[1]	References
Computer Analyses	TRAC-PF1: SCTF Test S1-SH4	---	U-656
	TRAC-PF1/MOD1: CCTF Test C2-19 SCTF Test S3-SH1 SCTF Test S3-SH2 SCTF Test S3-5 UPTF Test 8 UPTF Test 9 UPTF Test 12 UPTF Test 13	---	U638 U-681, U-683 U-681, U-684 U-681, U-685 G-641 G-642 G-644 G-645
	ATHLET CCTF Test C2-20 SCTF Test S3-11 UPTF Test 18 UPTF Test 26	---	G-611 G-622 G-648 G-464

NOTE:

1. The scale of the facility is based on the core flow area; the reference is a 3900 MWt Siemens/KWU PWR.

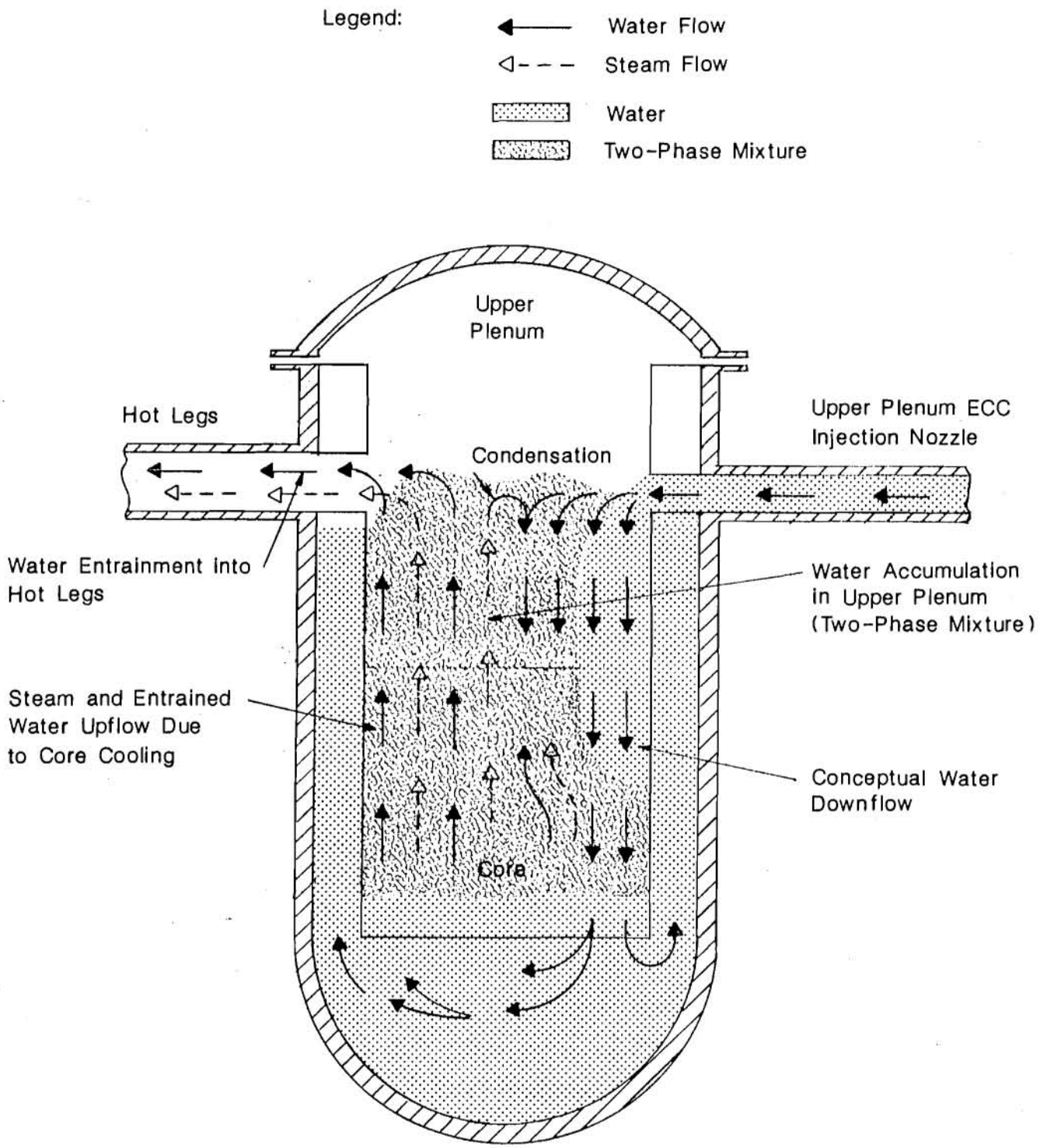

UPPER PLENUM PHENOMENA
DURING REFLOOD IN A UPI PWR

FIGURE 4.7-1

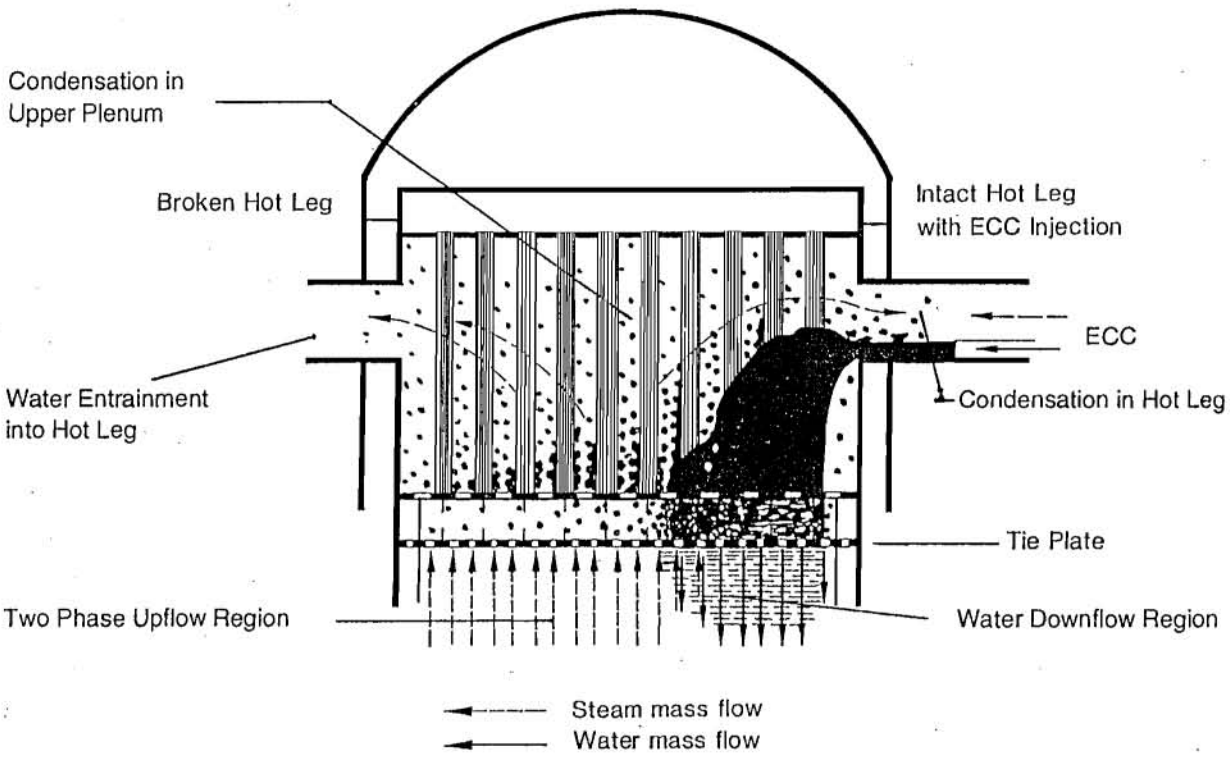

UPPER PLENUM PHENOMENA
WITH HOT LEG INJECTION

FIGURE 4.7-2

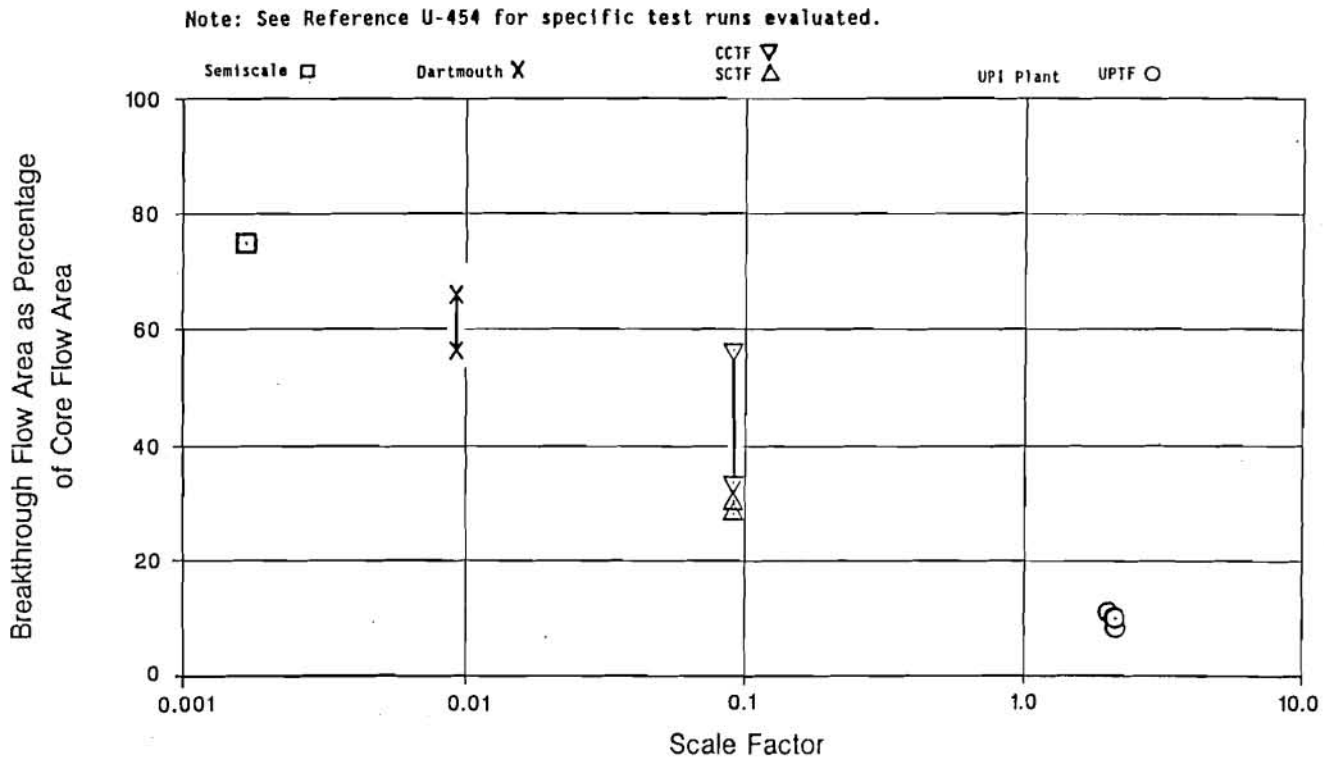

BREAKTHROUGH FLOW AREA VERSUS SCALE FACTOR
(REFERENCE U-454)

FIGURE 4.7-3

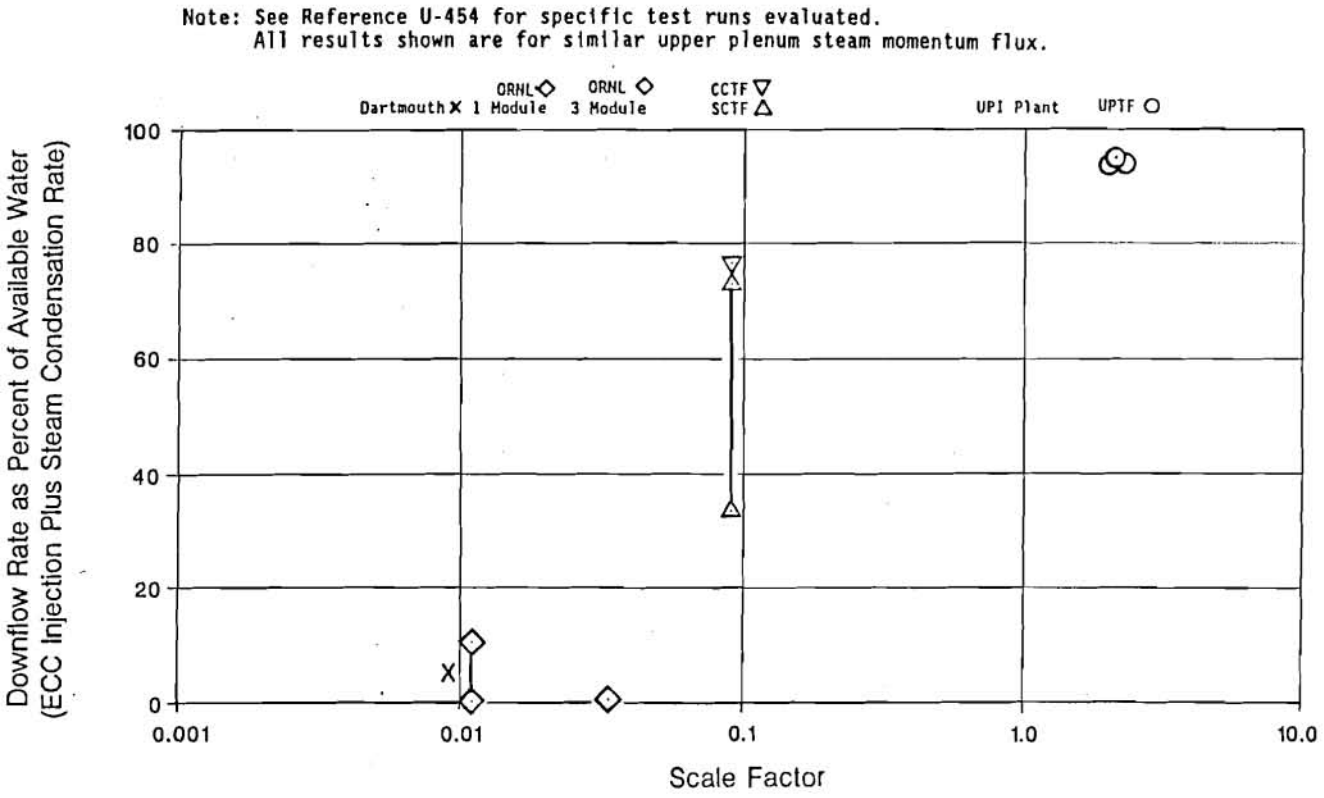

DOWNFLOW VERSUS SCALE FACTOR
(REFERENCE U-454)

FIGURE 4.7-4

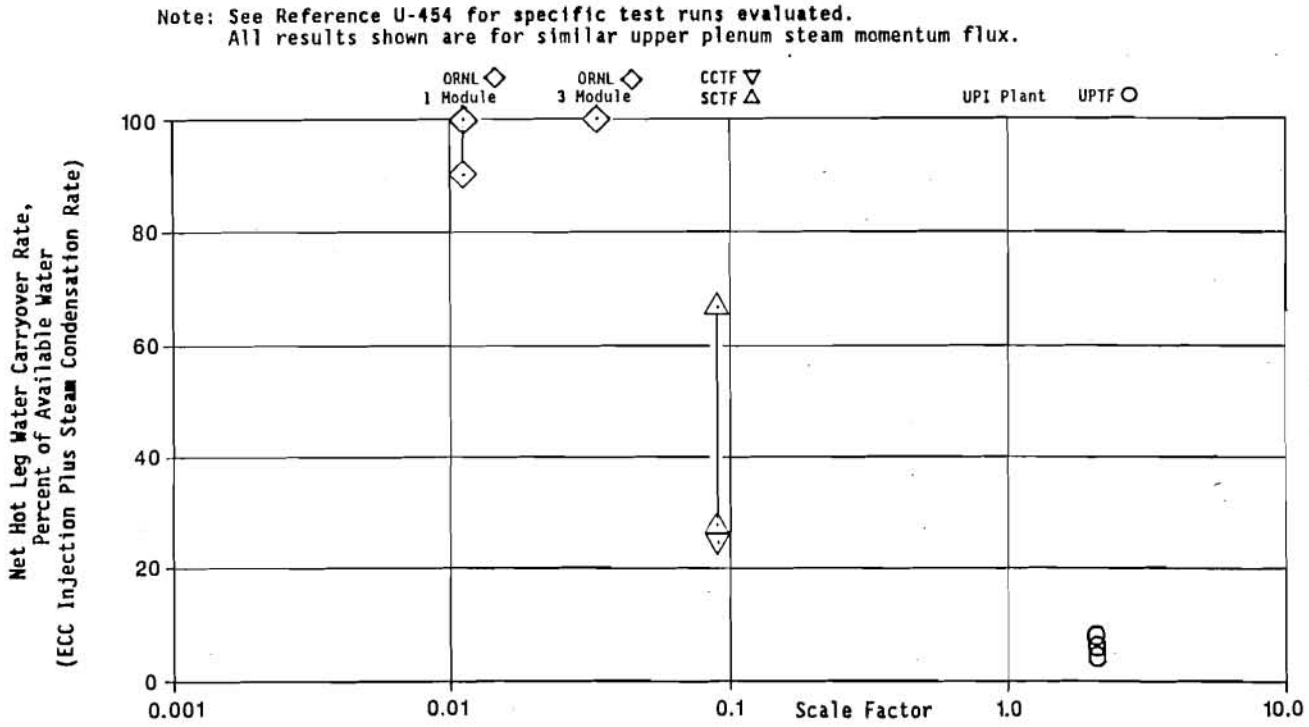

HOT LEG WATER CARRYOVER
VERSUS SCALE FACTOR
(REFERENCE U-454)

FIGURE 4.7-5

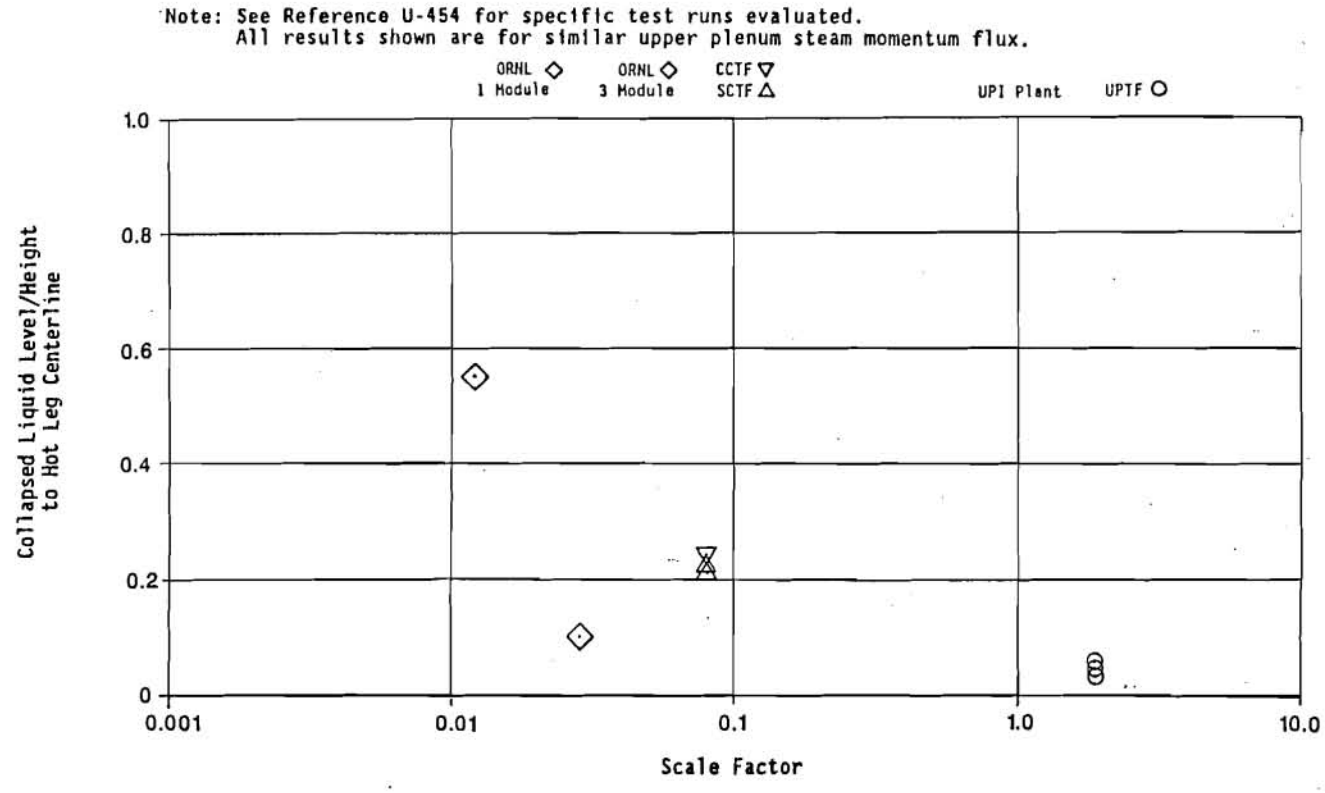

NON-DIMENSIONAL COLLAPSED LIQUID LEVEL IN UPPER PLENUM
VERSUS SCALE FACTOR
(REFERENCE U-454)

FIGURE 4.7-6

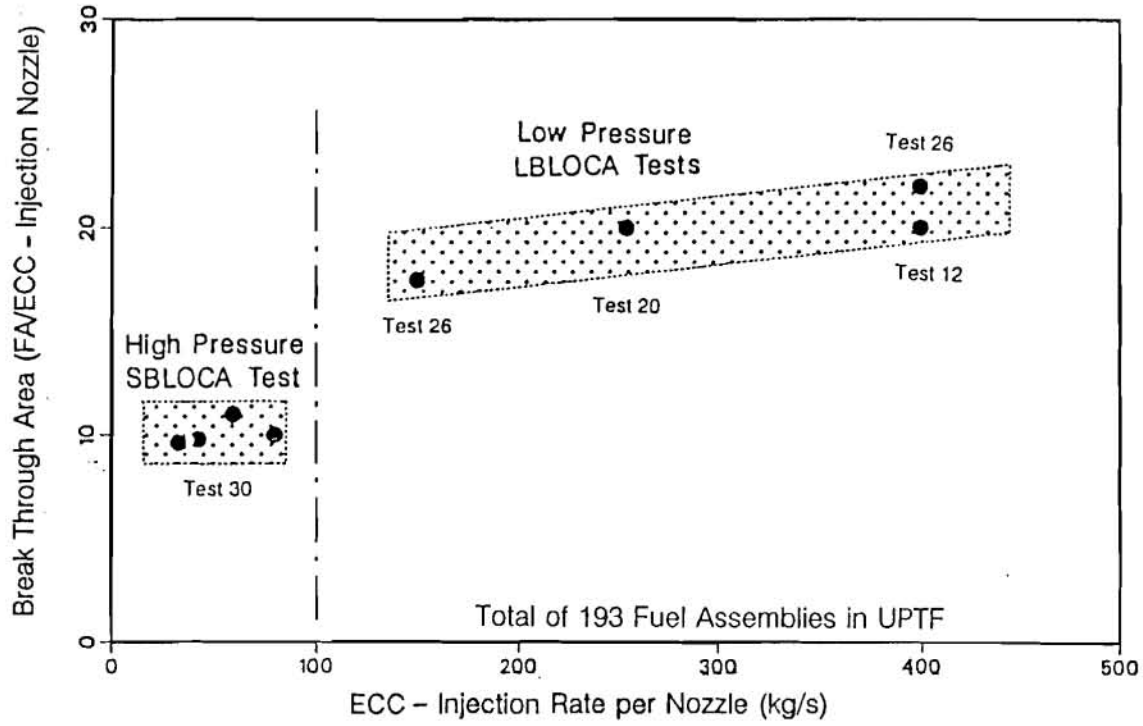

DOWNFLOW AREA VERSUS ECC-INJECTION RATE
FOR UPTF HOT LEG INJECTION TESTS

FIGURE 4.7-7

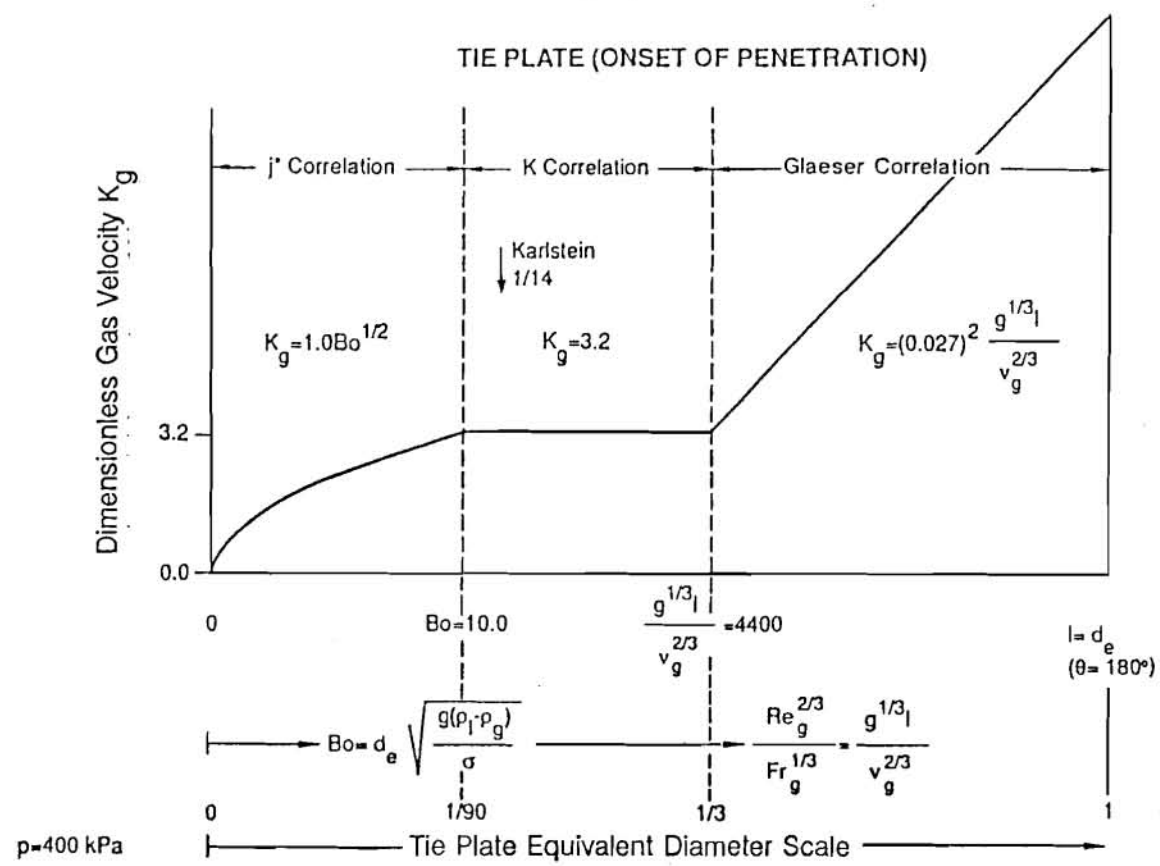

DIMENSIONLESS GAS VELOCITY VERSUS FACILITY SCALE
FOR TIE PLATE CCFL WITH HOT LEG INJECTION

FIGURE 4.7-8

4.8 WATER CARRYOVER AND STEAM BINDING WITH COLD LEG INJECTION

Definition of Issue and Description of Phenomena

Steam binding is defined as the increase in upper plenum pressure during the reflood portion of a large-break LOCA (LBLOCA) due to core steam generation and water carryover. Vaporization of liquid carryover in the reactor coolant loops (principally the steam generators) further adds to steam binding. This increase in pressure from steam binding reduces the core flooding rate and, therefore, core cooling. The phenomena associated with water carryover and steam binding are shown in Figure 4.8-1 and described below.

During the reflood phase of an LBLOCA, part of the ECC injected into the cold legs flows down the downcomer to the lower plenum and into the core. A portion of this flow is vaporized by decay heat and stored energy release in the core; the steam is vented to containment via the upper plenum and reactor coolant loops. The remainder of the core inlet water flow is either accumulated in the core or carried by the steam flow out of the core. Water carried over from the core is either de-entrained in the upper plenum, or carried over with the steam to the hot legs and steam generators.

In the upper plenum, water de-entrains due to the decrease in steam velocity corresponding to the increase in flow area relative to the core. The water which de-entrains either accumulates in the upper plenum, falls back to the core, or is re-entrained by the steam flow. Water accumulation in the upper plenum results in a two-phase mixture of steam and water. As shown in Figure 4.8-1, water which falls back to the core can be re-entrained and carried back to the upper plenum; i.e., a recirculation flow between the upper plenum and core can be established. There can also be recirculation within the upper plenum as some of the water which de-entrained in the upper plenum is re-entrained in the upper plenum.

The water carried over to the loops is either de-entrained and accumulated in the hot legs and steam generator inlet plena, or carried over to the steam generator tubes (see Figure 4.8-1). The de-entrained water accumulates in the inlet plena resulting in a two-phase mixture or drains into the hot legs where it accumulates in a stratified layer and potentially flows toward the reactor vessel (i.e., countercurrent to the two-phase flow from the upper plenum). Delivery to the upper plenum is controlled by the hot leg CCFL relationship (see Section 4.9). The water which is delivered to the upper plenum can increase the upper plenum liquid accumulation or be entrained by the steam flow back toward the steam generator inlet plena; i.e., a recirculation path can be created.

Water which is carried over to the steam generators but not de-entrained in the inlet plena is carried by the steam flow into the steam generator (SG) tubes. Since the temperature of the water on the SG secondary side is higher than saturation temperature at the post-blowdown primary side pressure, heat is transferred from the secondary side to the steam/water flow in the tubes; consequently, the water is vaporized and the steam is superheated. The flow at the SG exit is essentially single-phase steam flow. Vaporization of water in the SG's contributes to steam binding and decreases core cooling. Specifically, vaporization increases the volumetric flow rate, and therefore pressure drop, through the reactor coolant loops. This increase in intact loop differential pressure reduces the core flooding rate.

It should be noted that water carried out of the core is also vaporized in the upper plenum, hot legs, and SG inlet plena due to hot walls and structures. Because the surface area and stored energy are not as large in these regions as the SG's, the increase in the steam binding effect due to vaporization in the upper plenum, hot legs, and SG inlet plena is not as significant as the SG U-tube contribution.

Importance of Issue to PWR LOCA Behavior

As described above, water carryover and steam binding adversely affect core cooling during reflood. The magnitude of the effect is dependent on the amount of water which is carried out of the core and how the water distributes above the core. Calculations in Reference U-456 indicate the increase in peak cladding temperature (PCT) during reflood due to steam binding can be as high as 240 K (430°F).

Steam binding is not a safety concern for PWRs with combined injection because most of the steam generated in the core is condensed in the upper plenum and hot legs, and does not flow through the loops (see Sections 4.3.3 and 4.7.2).

Tests and Analyses that Relate to the Issue

Water carryover and steam binding have been investigated in transient and steady-state tests within the 2D/3D Program and elsewhere. Table 4.8-1 lists only the tests which are addressed in this evaluation. In the 2D/3D Program, tests were performed at each of the three test facilities (i.e., CCTF, SCTF, and UPTF). Steady-state tests at UPTF (Tests 10B and 29B) evaluated the effect of parametric variations in the core exit flow conditions on water de-entrainment and distribution above the core. The time history of water carryover and distribution above the core was investigated in numerous tests at CCTF and SCTF, and in transient tests at UPTF (Tests 2 and 17B). Data related to water carryover and de-entrainment in the upper plenum were also obtained from the ORNL air/water and steam/water facilities as part of the instrument development work for the 2D/3D Program. Outside the 2D/3D Program, tests were conducted at FLECHT-SEASET to investigate heat transfer from the secondary to primary sides of a SG during reflood.

The results of the UPTF tests have been evaluated in conjunction with the applicable subscale data (Reference U-456). The major results of these evaluations and comparisons are summarized below.

Post-test TRAC calculations have been performed for tests at each of the 2D/3D test facilities (see Table 4.8-1). These analyses include TRAC-PF1/MOD1 calculations of CCTF tests (References U-601 and U-621), SCTF tests (References U-641, U-661 and U-681) and UPTF Test 10B (Reference U-709). TRAC-PF1/MOD2 calculations have been performed for UPTF Tests 29B, 2 and 17 and CCTF Test C2-4 (Reference U-713). Also, as part of the developmental assessment at MOD2, post-test calculations of CCTF Test C2-SH2 and SCTF Test S3-15 were performed. The results of these analyses are summarized briefly below.

Summary of Key Results and Conclusions from Tests and Analyses

The UPTF carryover/steam binding separate effects tests (Tests 10B and 29B) investigated water accumulation and distribution above the core using several sets of constant core exit flow conditions. The test results indicated that, for each set of flow conditions, water accumulated in the upper plenum, hot legs, and SG inlet plena until equilibrium inventories were established. Water not accumulated in these regions was carried over to the SG tube regions. From the test results, MPR developed correlations which express the upper plenum, SG inlet plenum, and hot leg equilibrium inventories (nondimensionalized as liquid fractions) as functions of the flow conditions (nondimensionalized using the Wallis parameter; i.e., j^*) (Reference U-456). The observed behavior in each region including the correlations and comparisons to tests at scaled facilities, is discussed below.

- The UPTF results indicated that upper plenum inventory increases as the total core exit water flow (i.e., carryover from the core) increases; however, as steam flow increases, carryover to the reactor coolant loops increases and upper plenum inventory decreases. As shown in Figure 4.8-2, the upper plenum liquid fraction was correlated to the ratio of the dimensionless water and steam velocities. Figure 4.8-2 also shows correlations of upper plenum liquid fraction and dimensionless velocity ratio for CCTF, SCTF, and the ORNL air/water and steam/water facilities. Comparison of these correlations indicates that the data from the scaled facilities, particularly the ORNL facilities, correlate well with the UPTF data. However, CCTF tends to have slightly higher inventories for the same velocity ratio (Reference U-456).

  The above correlations are based on the total, and not the net, core exit water flow. As shown in Figure 4.8-1, the total core exit water flow includes water which de-entrains in the upper plenum and falls back to the core, countercurrent to the upward steam flow. Reference U-456 evaluated fallback (or recirculation) to the core assuming the controlling mechanism is the CCFL. For the UPTF, CCTF, and

SCTF tests, the fallback/recirculation rates were estimated using the UPTF tie plate CCFL correlation for uniform steam flow and uniform fallback. (Note, fallback was measured in the ORNL tests.) As indicated in Reference U-456, the estimated recirculation rates were higher for the CCTF-II and SCTF-II data than for the UPTF and ORNL data because the tie plate steam velocities were lower. The low steam velocities at CCTF-II and SCTF-II resulted, in part, from less restrictive (i.e., more open) tie plates. This suggests that upper plenum accumulation is influenced by the tie plate geometry (Reference U-456). Recirculation of liquid from the upper plenum to the core in CCTF and SCTF might also have been enhanced by horizontal density differences in the core causing differences in buoyancy forces. Since the simulated decay power was higher toward the center, steam generation was higher toward the center of the core and thus the fluid density was lower toward the center of the core (Reference J-536).

- The results of UPTF Tests 10B and 29B indicated that the equilibrium hot leg inventory decreases as the steam and water flows increase. Comparison of hot leg flow conditions during UPTF Tests 10B and 29B with the hot leg CCFL relationship (see Section 4.9) indicates that the two-phase velocities were above the CCFL boundary; i.e., flow to the upper plenum was prevented. The momentum interaction between the two-phase flow and the water layer in the hot leg limited the water level which could be attained. The hot leg equilibrium inventory correlation plotted the liquid fraction near the hot leg bend versus the dimensionless two-phase velocity in the hot legs (see Figure 4.8-3). (Note, the two-phase density was calculated assuming a slip ratio of two.) The correlation based on Tests 10B and 29B, which had two-phase flow from the upper plenum into the hot legs is similar to a correlation based on Test 11 which had single-phase steam flow into the hot legs. The close similarity of the relationships suggests the hot leg inventory correlation is applicable to both two-phase and steam-only flow entering the hot leg from the upper plenum (Reference U-456).

  Hot leg water accumulation at UPTF is compared to CCTF and SCTF on the basis of the liquid fraction--dimensionless two-phase velocity relationship. The CCTF tests with scaled diameter hot legs had essentially no hot leg accumulation, which is consistent with the UPTF results because the dimensionless steam velocities were very high in CCTF due to the small diameter of the pipes. The SCTF tests with a full-height, scaled-width hot leg showed stratified flow and water storage. Comparison of the results indicates that the SCTF hot leg liquid fraction increases more rapidly as the two-phase flow decreases (see Figure 4.8-3). The difference in facility behavior is consistent with the differences in hot leg cross section (Reference U-456).

- Results of the UPTF tests showed that SG inlet plenum inventory increases with both increasing steam and water flow. The water which accumulates in the inlet plenum is supported by the momentum of the two-phase flow in the inlet plenum;

hence, increasing the flows increases the momentum flux in the inlet plena and therefore the mass of water which can be supported. The equilibrium inventory correlation for the inlet plena plotted the liquid fraction versus the square of the dimensionless two-phase velocity calculated assuming homogeneous flow (see Figure 4.8-4).

SG inlet plenum accumulation at UPTF is compared to only CCTF. The SCTF inlet plenum was inadequately instrumented to allow two-phase flow behavior to be analyzed. Comparison of inlet plenum accumulation at CCTF to the UPTF correlation (see Figure 4.8-4) showed that the two appeared to be in a different regime of behavior. Specifically, the CCTF velocities are higher than the UPTF velocities. The CCTF data suggest the inlet plenum liquid fraction remains constant or decreases slightly as the dimensionless two-phase velocity increases substantially. It appears the CCTF inlet plena may be in a high steam flow regime where the inventory is determined by carryover from the inlet plena to the tube regions. The UPTF inlet plena, on the other hand, appear to be in a low steam flow regime where inventory is determined by fallback from the inlet plena to the hot legs (Reference U-456).

Transient tests at CCTF and SCTF investigated overall system behavior during reflood including thermal-hydraulic phenomena in the core and water carryover out of the core. In both facilities, water was entrained to the upper regions of the core essentially immediately after BOCREC (References U-401, U-414, U-421, U-431, and U-441). Some of the water entrained to the upper regions of the core is carried out of the core to the upper plenum and reactor coolant loops; i.e., contributes to the steam binding effect.

The CCTF and SCTF tests showed that water carryover from the core depended on the conditions at the beginning of reflood and the flooding rate. Typically, carryover was highest during the initial stages of reflood when the core flooding rate was high. When the core flooding rate decreased just prior to termination of accumulator injection, water carryover decreased significantly. Carryover increased later in reflood as the quench front progressed to the upper regions of the core. For EM conditions, the net core exit quality averaged about 90% over the duration of the transient. For BE conditions, however, the net quality at the core exit averaged about 60% indicating significant carryover (References U-414 and U-441). See Section 4.6.1 for a more detailed discussion of thermal-hydraulic behavior in the core during a LOCA.

UPTF Test 17B simulated a BE reflood transient to evaluate the time history of water accumulation above the core at full-scale. The test conditions were based on an SCTF test (Test S3-10). The net core exit steam and water flows, and a summary mass balance plot are provided in Figure 4.8-5. The mass balance plot indicates that initially the upper plenum and SG inlet plena accumulated almost all of the core exit water flow. The hot legs and SG tube regions did not accumulate appreciable

amounts of water during approximately the first 25 seconds of the transient. When the core exit water flows decreased dramatically after about 25 seconds, the upper plenum and SG inlet plenum inventories decreased, resulting in increases in the hot leg and SG tube region accumulations. During the later portion of the transient, the core exit steam flow decreased while the core exit water flow increased. The upper plenum, SG inlet plenum and hot leg inventories reflected the changes in core exit flows. At the end of the transient, the SG tube regions had accumulated about 65% of the water which exited core (Reference U-456).

Vaporization of entrained water in the SG U-tubes was investigated in tests at CCTF and FLECHT-SEASET. At both facilities, steam entered the U-tubes saturated and exited the U-tubes superheated to close to the secondary side temperature (References U-401, U-414, and E-481). This suggests all of the water was vaporized; however, at FLECHT-SEASET, measurements of the flow quality in the outlet plenum indicated that the flow in the outlet plenum was actually a non-equilibrium mixture of superheated steam and entrained water. The quality in the outlet plenum was about 97% (Reference E-481).

Post-test calculations of numerous CCTF and SCTF tests were performed using TRAC-PF1/MOD1. In CCTF analyses, water carryover from the upper plenum to the loops was generally well predicted in high power tests which had high steam flows and water carryover rates, and in low power tests which had low steam flows and negligible carryover; however, in SCTF analyses, water carryover from the upper plenum was generally underpredicted, even for tests with high steam flows. A limited number of CCTF and SCTF tests have also been analyzed using TRAC-PF1/MOD2. With the new reflood model in MOD2, more water was carried out of the core to the upper plenum; consequently, predicted carryover from the upper plenum to the loops was higher with MOD2 than MOD1. Carryover to the loops was well predicted in the SCTF calculation and overpredicted in the CCTF calculations (Reference U-713).

The ability of TRAC-PF1/MOD1 to predict water carryover/steam binding phenomena was evaluated outside the 2D/3D Program as part of the USNRC's Code Scaling, Applicability and Uncertainty (CSAU) Study. The evaluation was based on analyses of SCTF tests. The study showed that water carryover from the upper plenum to the loops was improved by increasing entrainment and interfacial shear in the core, not the upper plenum; consequently, it was concluded that prediction of carryover to the loops is dependent on calculating the flow conditions above the quench front and below the tie plate. (It should be noted that MOD2 has a new core entrainment/interfacial shear model which predicts flow conditions below the tie plate better than the old model in MOD1.) Finally, the CSAU Study estimated that TRAC-PF1/MOD1 underpredicts the reflood PCT in a four-loop Westinghouse PWR by as much as 59 K due to underprediction of steam binding (Reference U-713).

As part of the 2D/3D Program, UPTF tests have been analyzed using TRAC-PF1/MOD1 and TRAC-PF1/MOD2. Both the MOD1 and MOD2 calculations underpredicted water carryover from the core to the upper plenum. The poor prediction of carryover from the core impacted the prediction of water carryover from the upper plenum to the hot legs and SGs; specifically, carryover from the upper plenum was underpredicted. Interestingly, the upper plenum water level was, in some cases, overpredicted because the underprediction of carryover to the loops was greater than the underprediction of carryover from the core. The poor prediction of carryover from the core was attributed to the inability of the computer model of the UPTF core simulator to accurately predict flow conditions below the tie plate. Since flow conditions below the tie plate in PWR calculations are determined by the core reflood model, the results of the UPTF analyses are not considered indicative of the ability of TRAC to predict PWR LOCA behavior (Reference U-713).

A methodology for predicting transient water accumulation above the core was developed from the results of the UPTF carryover/steam binding separate effects tests and verified with UPTF transient tests (Reference U-456). This methodology was adapted for predicting transient water accumulation in US/J PWRs with cold leg injection. The predicted accumulation and distribution above the core for a 3400 MWt Class Westinghouse (W) PWR and a Combustion Engineering (CE) System 80 PWR are shown in Figure 4.8-6. The predictions are based on the core exit flow conditions of UPTF Test 17B, a BE reflood transient. Differences in water distribution above the core for UPTF Test 17B (see Figure 4.8-5) and the PWRs reflect geometrical and configurational differences (Reference U-456).

The effect of steam binding on the reflood PCT was estimated in Reference U-456 from the predicted carryover to the SG U-tubes for each of the PWRs assuming complete vaporization. A summary of this analysis which shows the maximum impact of steam binding on PCT as a function of the fraction of water carried over to the SG U-tubes is presented in Figure 4.8-7. The figure shows that, if all of the water carried out of the core reaches the SG U-tubes, the increase in PCT is about 240 K (430°F) relative to no carryover to the U-tubes. Based on the predicted carryover to the SG tube regions for US/J PWRs, the increase in the reflood PCT due to water carryover and steam binding is between 55 K and 65 K (100°F and 120°F).

Table 4.8-1

SUMMARY OF TESTS AND ANALYSES RELATED TO WATER CARRYOVER AND STEAM BINDING

Type of Test or Analysis	Facility or Analysis	Facility Scale[1]	References
Steady-state Tests	UPTF: Test 10B Test 29B	1.05	U-456, G-411 G-010, G-210 G-029, G-229
	ORNL Air/Water Facility	0.016	U-825
	ORNL Steam/Water Facility	0.0049	U-825
	FLECHT-SEASET	0.0024[2]	E-481
Transient Tests	UPTF: Test 2 Test 17B	1.05	U-456, G-411 G-002, G-202 G-017, G-217
	CCTF-I	0.047	U-401
	CCTF-II: Test C2-SH2[3] Test C2-4[3]	0.047	U-414 J-044, J-242, J-445 J-052, J-250, J-448
	SCTF-I	0.043	U-421
	SCTF-II: Test S2-SH1[3]	0.043	U-431 J-124
	SCTF-III:	0.047	U-441
Computer Analyses	TRAC-PF1/MOD1: CCTF-I CCTF-II SCTF-I SCTF-II SCTF-III UPTF Test 10B	---	 U-601 U-621 U-641 U-661 U-681 U-709
	TRAC-PF1/MOD2: CCTF Test C2-4 CCTF Test C2-SH2[4] SCTF Test S3-15[4] UPTF Test 29B UPTF Test 2 UPTF Test 17	---	 U-713 U-713 U-713 U-713 U-713 U-713

Table 4.8-1

SUMMARY OF TESTS AND ANALYSES RELATED
TO WATER CARRYOVER AND STEAM BINDING

NOTES:

1. The scale of a facility is defined relative to the core flow area of a 3400 MWt Westinghouse or Japanese PWR.

2. The scale for FLECHT-SEASET is based on the total number of steam generator U-tubes.

3. A large number of CCTF and SCTF tests covered this phenomena. These tests were selected for detailed comparison to the UPTF carryover/steam binding separate effects tests.

4. The TRAC-PF1/MOD2 calculations of these tests were performed as part of the developmental assessment of MOD2.

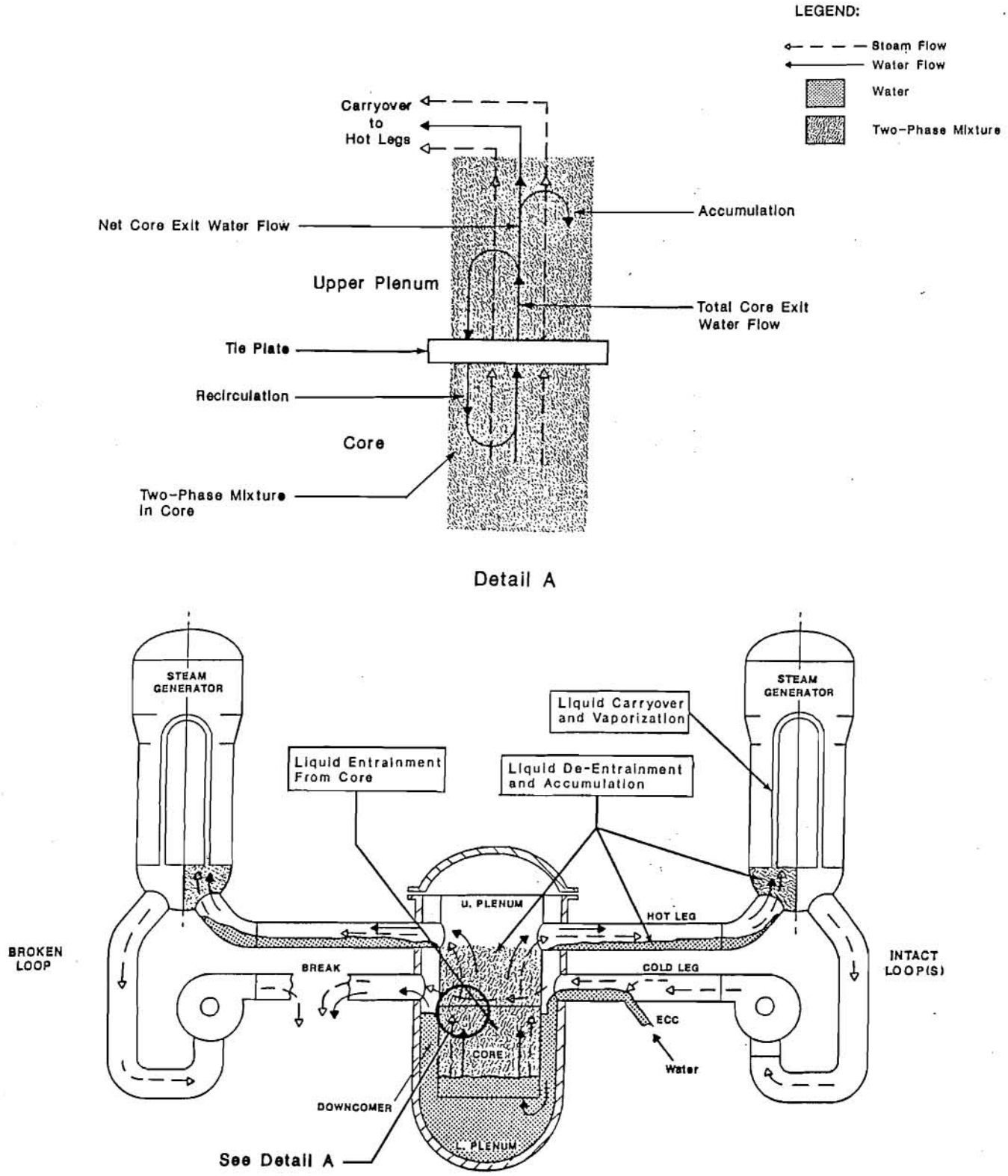

STEAM BINDING PHENOMENA
IN A PWR DURING REFLOOD

FIGURE 4.8-1

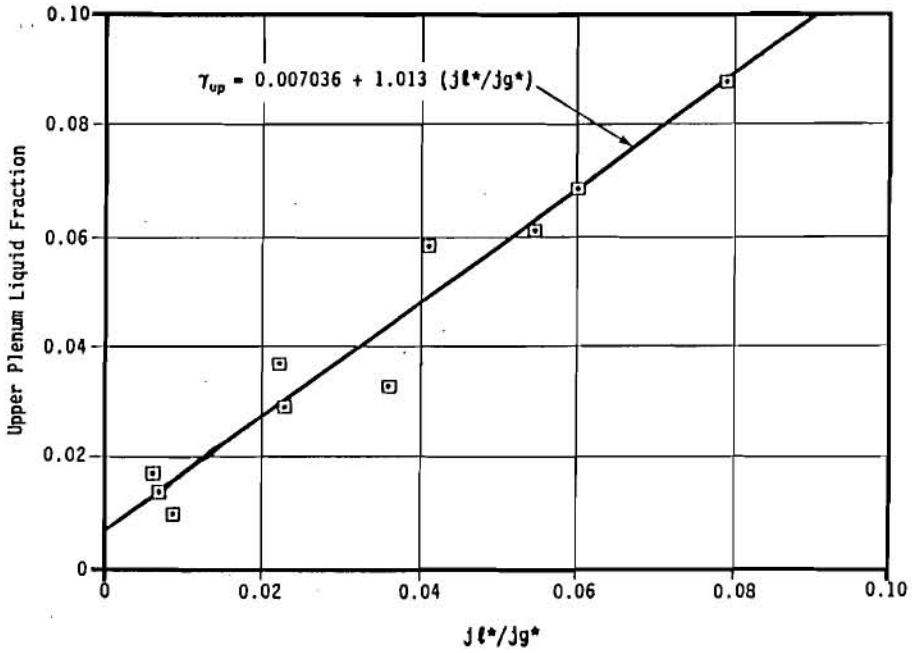

DATA FROM UPTF CARRYOVER/STEAM BINDING SEPARATE EFFECTS TESTS (10B AND 29B)

FACILITY	Equations of Least Squares Fit Lines
UPTF	γ_{up} = 0.007036 + 1.013 (jℓ*/jg*)
ORNL S/W	γ_{up} = 0.03128 + 0.8477 (jℓ*/jg*)
ORNL A/W	γ_{up} = 0.06470 + 0.8461 (jℓ*/jg*)
CCTF-II	γ_{up} = 0.02411 + 1.855 (jℓ*/jg*)
SCTF-II	γ_{up} = 0.00289 + 1.321 (jℓ*/jg*)

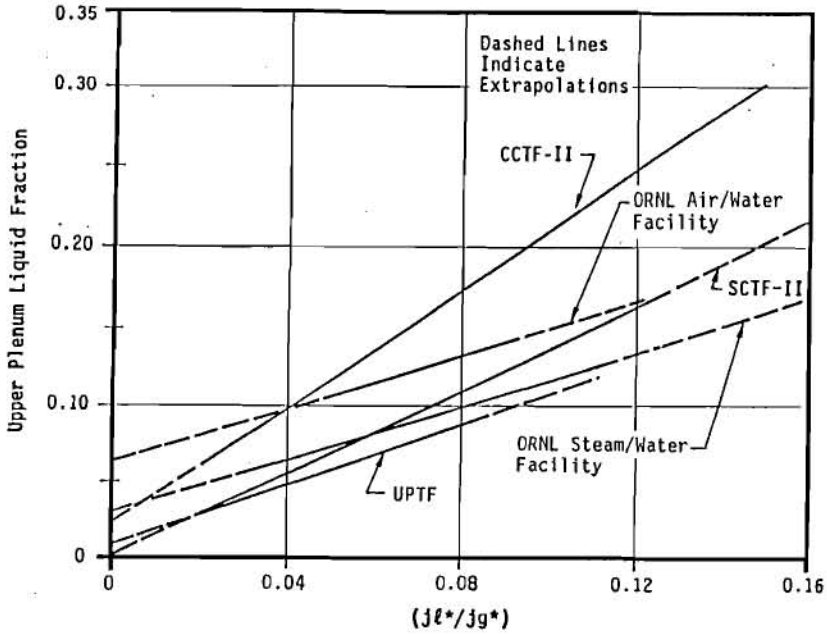

COMPARISON TO SCALED FACILITIES

Notes:

1. The liquid fraction is based on the upper plenum volume from the tie plate to the hot leg centerline.
2. The dimensionless velocities are based on the total core exit water and steam flows (see Figure 4.8-1).

UPPER PLENUM EQUILIBRIUM LIQUID INVENTORY CORRELATION FOR UPTF SEPARATE EFFECTS TESTS AND COMPARISON TO SCALED FACILITIES (REFERENCE U-456)

FIGURE 4.8-2

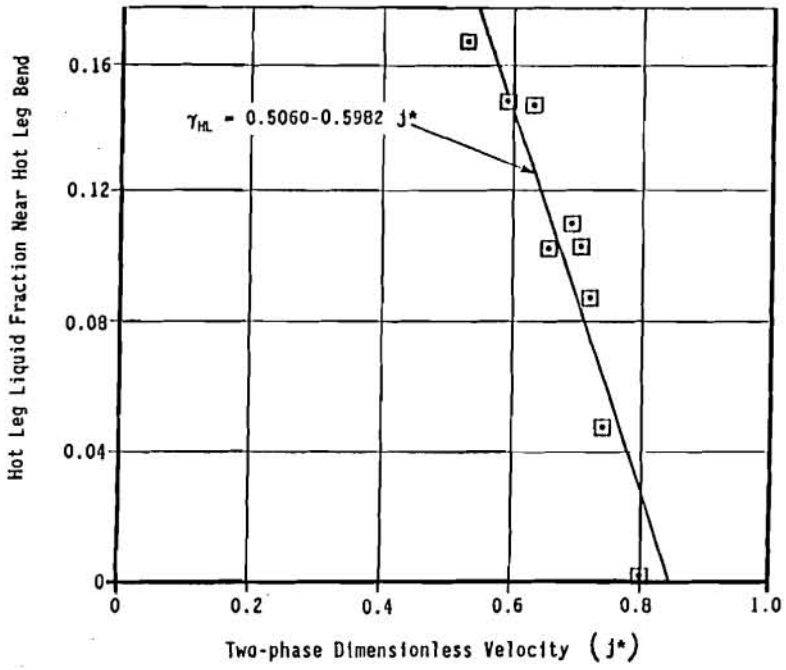

DATA FROM UPTF CARRYOVER/STEAM BINDING SEPARATE EFFECTS TESTS (10B AND 29B)

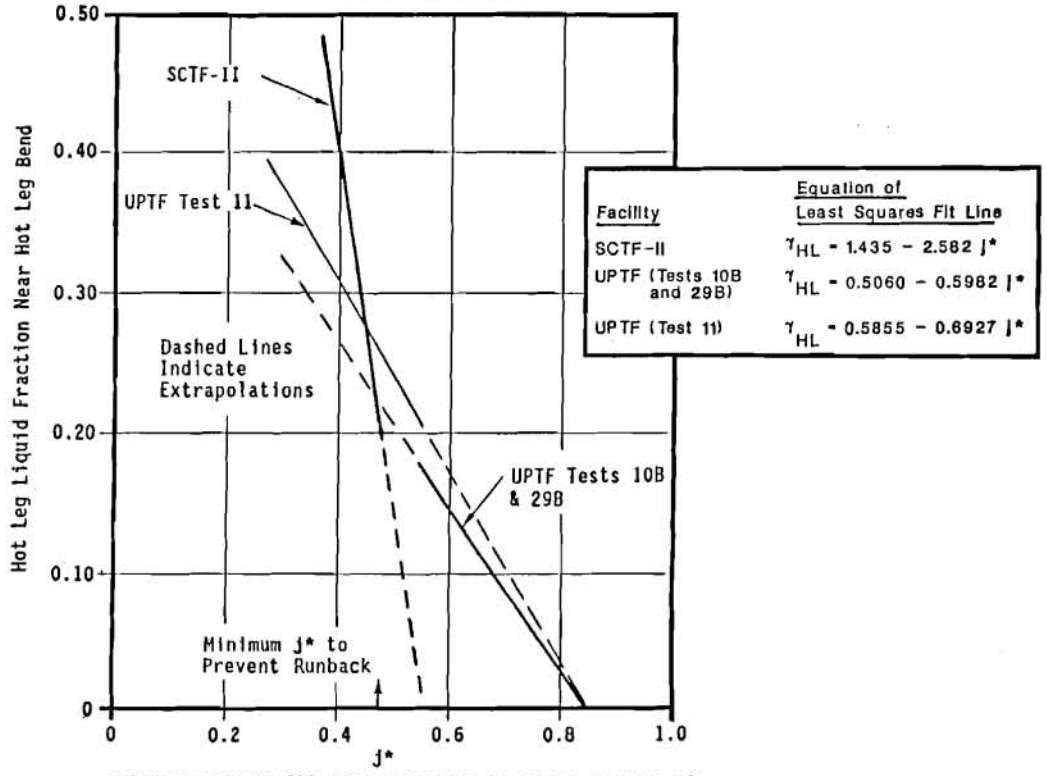

COMPARISON TO UPTF TEST 11 AND SCTF-II

Notes:
1. The liquid fraction is the average of all the loops.
2. The dimensionless two-phase velocity is calculated from the net core exit flows using the flow area and hydraulic diameter in the Hutze region. The two-phase density is calculated assuming a slip ratio of two.
3. UPTF Tests 10B and 29B are the carryover/steam binding separate effects tests.
4. UPTF Test 11 is the hot leg separate effects test (see Section 4.9).

HOT LEG EQUILIBRIUM LIQUID INVENTORY CORRELATION FROM UPTF SEPARATE EFFECTS TESTS AND COMPARISON TO OTHER UPTF TESTS AND SCTF-II (REFERENCE U-456)

FIGURE 4.8-3

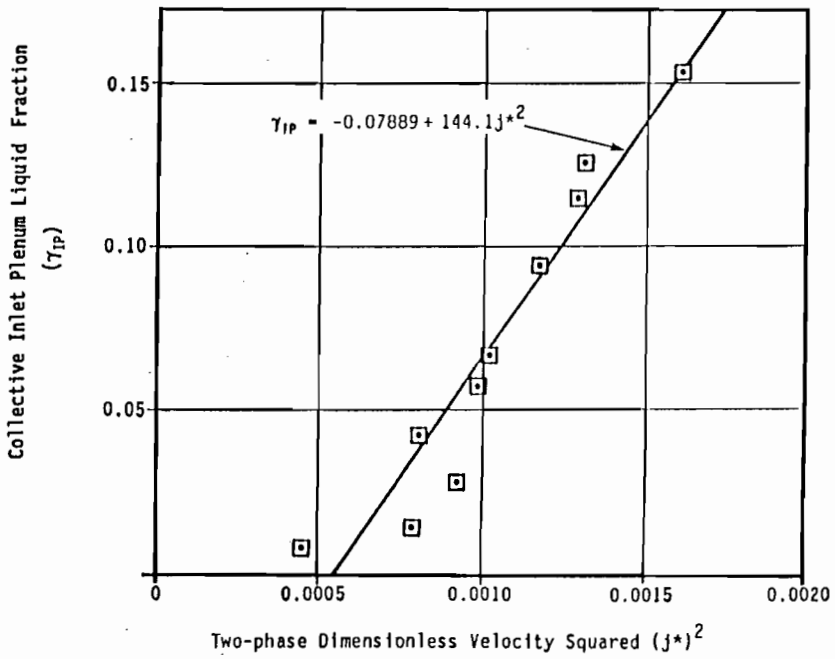

DATA FROM UPTF CARRYOVER/STEAM BINDING SEPARATE EFFECTS TESTS (10B AND 29B)

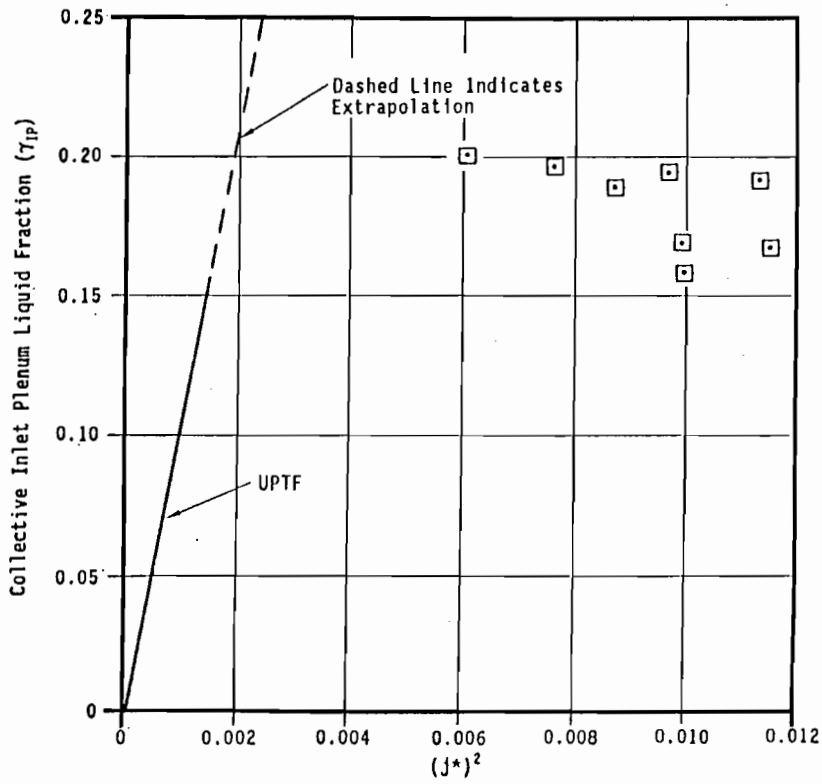

COMPARISON TO CCTF-II DATA

Notes:
1. The liquid fraction is based on the collective inlet plenum inventory and the total volume of all four SG inlet plena.
2. The dimensionless two-phase velocities are calculated from the net core exit flows using the flow area and hydraulic diameter at the top of the inlet plenum. The two-phase density is calculated assuming homogeneous flow.

SG INLET PLENUM EQUILIBRIUM LIQUID INVENTORY CORRELATION FROM UPTF SEPARATE EFFECTS TESTS AND COMPARISON TO CCTF-II DATA (REFERENCE U-456)

FIGURE 4.8-4

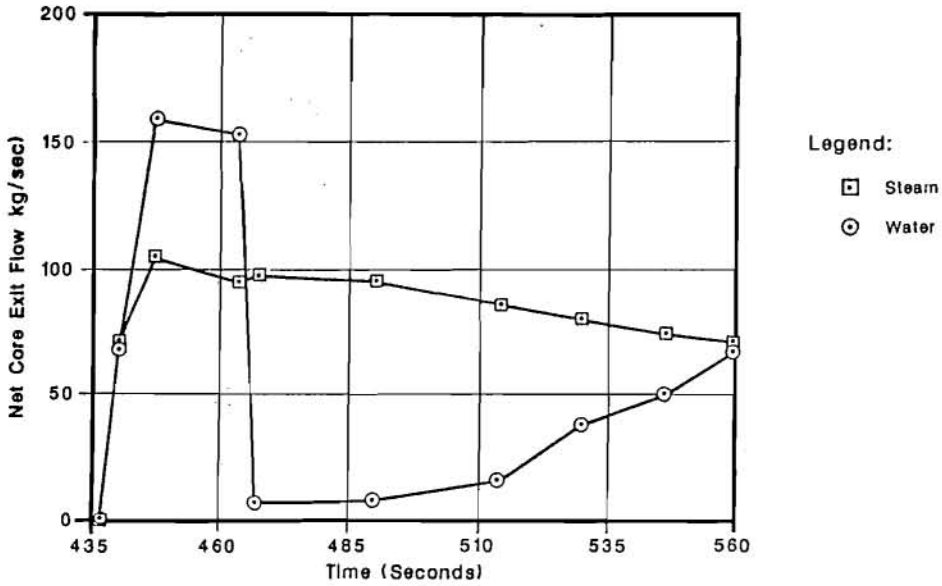

CORE EXIT FLOW CONDITIONS FOR UPTF TEST 17B

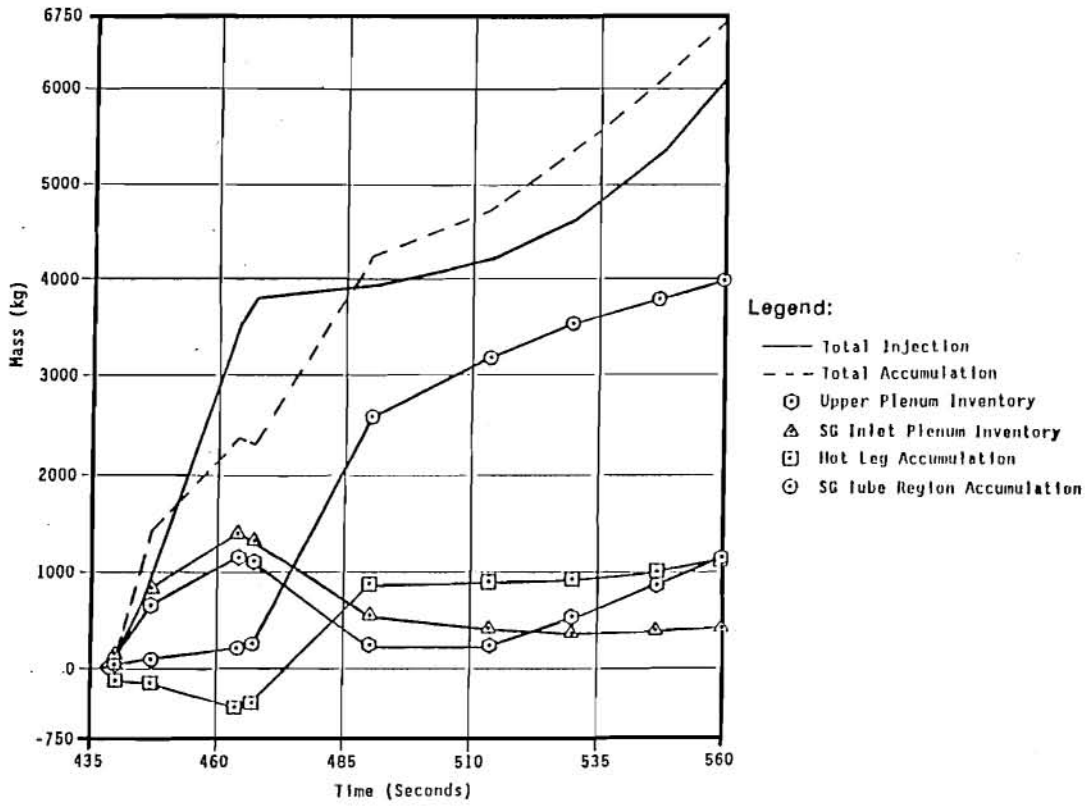

SUMMARY OF MASS BALANCE ABOVE THE CORE
UPTF TEST 17B

Note : The core exit flow conditions for UPTF Test 17B were based on SCTF Test S3-10, which simulated a best-estimate reflood transient.

BEHAVIOR FOR A BEST-ESTIMATE TRANSIENT
FOR UPTF TEST 17B
(REFERENCE U-456)

FIGURE 4.8-5

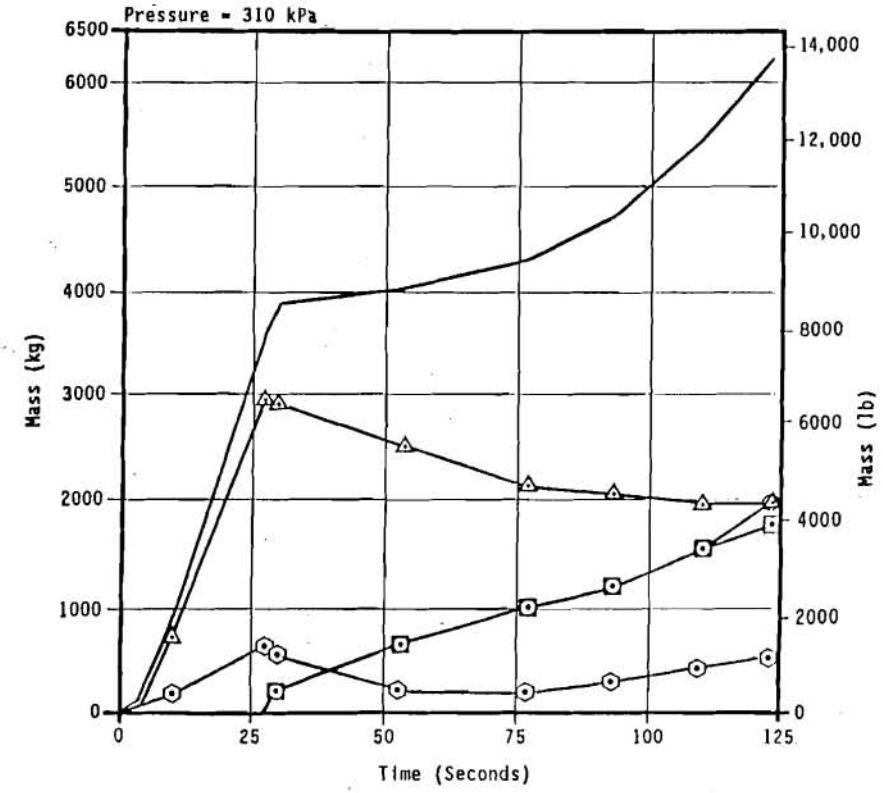

CE SYSTEM 80 PWR

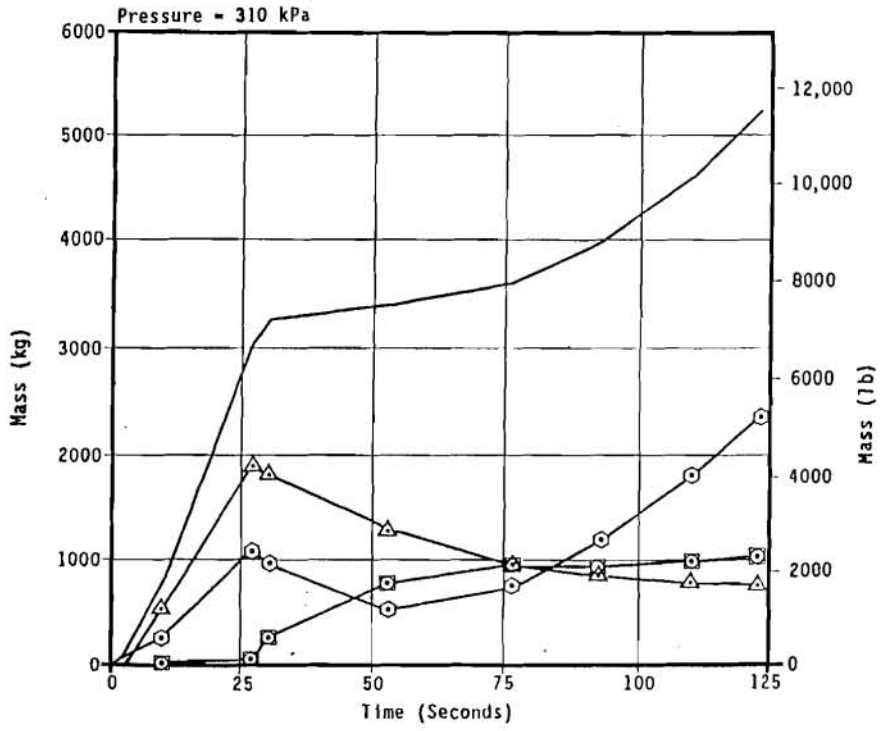

WESTINGHOUSE 3400 MWT PWR

Note: Time 0 corresponds to the beginning of core simulator water injection for UPTF Test 17B (i.e., 437 seconds) which is equivalent to BOCREC (see Figure 4.8-5).

PREDICTED WATER ACCUMULATION IN US/J PWRS FOR A BEST-ESTIMATE TRANSIENT (REFERENCE U-456)

FIGURE 4.8-6

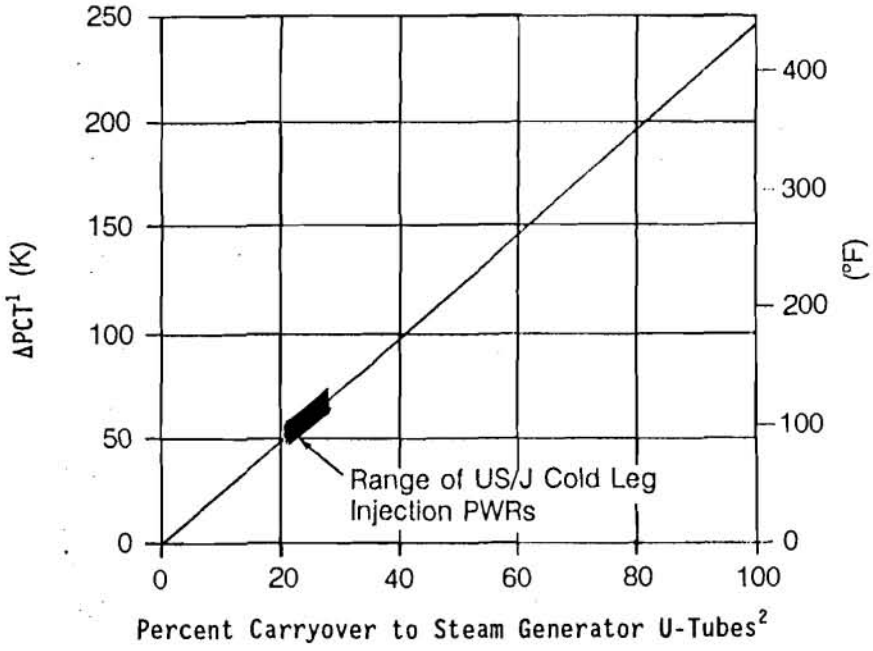

Notes:

1. Defined as the increase in peak clad temperature (PCT) relative to the PCT for no water carryover to the steam generator U-tubes.
2. Defined as the percent of water carryover from the core which reaches the steam generator U-tubes.
3. This figure shows the maximum effect of water carryover and steam binding on PCT.
4. Best-estimate behavior is based on the predicted water accumulation and distribution above the core shown in Figure 4.8-6.

EFFECT OF STEAM BINDING ON PEAK CLAD TEMPERATURE

FIGURE 4.8-7

4.9 HOT LEG COUNTERCURRENT FLOW

Definition of Issue and Description of Phenomena

The reactor safety issue associated with hot leg countercurrent flow is the characterization of the natural circulation processes which provide core cooling during a small-break LOCA (SBLOCA). In an SBLOCA heat generated in the core is transferred to water in the secondary side of the steam generators by natural circulation within the primary system. As primary system inventory decreases, natural circulation changes from single-phase (water) to two-phase (cocurrent, with water as the continuous phase) and finally to reflux condensation (Reference E-401). Hot leg countercurrent flow is applicable to the reflux condensation mode of core cooling in an SBLOCA.

Reflux condensation is the cooling mode in which steam is the continuous phase in the upper plenum and reactor coolant loops (i.e., above the core). Decay heat is removed by steam generation in the core and steam condensation in the steam generator U-tubes. As shown in Figure 4.9-1, steam condensed in the upflow leg of the U-tubes returns to the reactor vessel by flowing countercurrent to the steam flow in the hot leg. The primary system pressure during reflux condensation can be as high as 8,000 kPa (1160 psia) (Reference U-452).

Countercurrent flow can also occur in the hot legs during the reflood portion of a large break LOCA (LBLOCA). As described in Section 4.8, water de-entrained in the steam generator inlet plena drains into the hot legs. This water either accumulates in the hot legs or flows toward the reactor vessel (i.e., countercurrent to the two-phase flow from the upper plenum). The water which is delivered to the upper plenum can increase the upper plenum liquid accumulation or can be entrained by the steam flow back toward the steam generator inlet plena; i.e., a recirculation path is created. This recirculation flow of entrained water to the inlet plena mitigates the countercurrent flow and the buildup of hot leg inventory; further, it contributes to increasing the inlet plenum inventory. The net effect of countercurrent flow in the hot legs is to reduce carryover to the steam generator U-tubes, and hence reduce the steam binding effect (see Section 4.8).

Hot leg countercurrent flow is characterized by a countercurrent flow limitation (CCFL) curve, or flooding curve. The CCFL curve defines the maximum countercurrent water flow which can be achieved for a given steam flow toward the steam generator inlet plena. The countercurrent water flow can be less than the value indicated by the CCFL curve for a given steam flow if the water delivery to the hot leg from the inlet plenum is less than the maximum countercurrent flow which can be achieved; however, the countercurrent water flow cannot be greater than the value indicated by the CCFL curve.

Importance of Issue to PWR LOCA Phenomena

As indicated above, hot leg countercurrent flow is of interest primarily for characterizing natural circulation cooling processes during an SBLOCA. A principal motivation for characterizing the natural circulation cooling modes during an SBLOCA was the 1979 accident at Three Mile Island, which involved significant primary coolant inventory depletion (Reference E-401).

With regard to LBLOCA, hot leg countercurrent flow is beneficial in that it reduces PCT by reducing carryover to the steam generator U-tubes (i.e., steam binding). As discussed in Section 4.8, reduction in carryover to the U-tubes due to hot leg countercurrent flow is expected to be small, especially early in reflood; hence, the impact on reflood PCT should, likewise, be small.

Tests and Analyses that Relate to the Issue

The UPTF hot leg separate effects test (Test 11) was conducted specifically to investigate hot leg countercurrent flow at full-scale. The data from UPTF Test 11 were used to determine a CCFL correlation. This correlation is compared to CCFL curves developed from tests at other facilities, to theoretical models, and to computer analyses of UPTF Test 11. Also, the CCFL curve determined from Test 11 data is compared to the flow conditions in scaled integral tests which simulated reflux condensation. Since hot leg countercurrent flow during reflood relates to the steam binding issue, comparisons of the hot leg CCFL correlation to tests which simulated reflood are discussed in Section 4.8.

The tests and analyses considered in this evaluation of hot leg countercurrent flow and its implications for the reflux condensation mode of core cooling are listed in Table 4.9-1. A detailed comparison of the tests which investigated hot leg countercurrent flow is presented in Table 4.9-2. As shown in Table 4.9-2, while these tests encompass a wide range of pipe diameters and configurations, the UPTF data are the only data obtained at full-scale.

Summary of Key Results and Conclusions from Tests and Analyses

As previously indicated, the evaluation of the UPTF hot leg separate effects test data consisted primarily of the determination of a CCFL curve. Figure 4.9-2 presents a plot of the UPTF steam flow versus countercurrent water flow. Steam and water flow in Figure 4.9-2 are expressed as dimensionless, superficial velocity (j^*, defined in Figure 4.9-2) which is typical of countercurrent flow analyses. The data shown in the figure include only conditions with complete turnaround of water (i.e., no delivery) and partial delivery. The CCFL correlation was determined from a least squares fit of the data points with partial turnaround of the water flow; the complete turnaround points were not used because they fall above the CCFL boundary. As shown in Figure 4.9-2

the scatter of the data about the CCFL correlation is small. Also, the agreement between the 300 kPa and 1,500 kPa data is extremely good. The correlation predicts complete turnaround at $j^*_g = 0.47$.

The CCFL correlation determined from the UPTF data is compared to correlations developed from tests at subscale facilities in Figure 4.9-3. Countercurrent flow predictions calculated from these correlations are compared to the UPTF data at 1,500 kPa in Figure 4.9-4. As shown in Figure 4.9-3, the slopes of the CCFL correlations for the subscale facilities are similar to the UPTF correlation, but the y-intercepts are different. (Note that Ohnuki determined that the y-intercept of the CCFL curve depends on the length of the horizontal pipe, pipe diameter, and length of the inclined riser. The dimensions of the UPTF hot leg were used in the Ohnuki formulation to determine the y-intercept of the Ohnuki CCFL curve plotted in Figure 4.9-3.) The best agreement between the UPTF and the subscale facilities is with the Richter correlation. As shown in Figure 4.9-3, the facility used by Richter was the largest of the subscale facilities. Also, the configuration of Richter's facility and UPTF are similar.

Figure 4.9-3 also shows the CCFL curves determined using the Gardner model for pressures of 300 kPa and 1,500 kPa, the system pressures used in the UPTF testing. The Gardner model is a theoretical model in which the flooding mechanism is assumed to be unstable stationary disturbance (Reference E-941). As shown in the figure, the CCFL curves determined using the Gardner model do not compare favorably with the UPTF correlation or the correlations for the subscale facilities; hence, it appears that the assumed flooding mechanism does not reflect true countercurrent flow behavior in horizontal pipes (Reference U-904).

A previous study on modeling SBLOCA phenomena evaluated hot leg CCFL using a correlation developed by Wallis for wave instability in horizontal stratified flow (Reference E-496). The Wallis correlation relates the void fraction in the pipe with the gas velocity at which waves "break" and are propelled down the pipe (Reference E-495). Figure 4.9-5 compares the Wallis correlation to UPTF data. For the UPTF data the void fraction is based on the "hutze" region of the hot leg. As shown in Figure 4.9-5, there is reasonable agreement between the UPTF data and the Wallis correlation. This suggests that the basic approach of this correlation appears correct for scaling.

The UPTF countercurrent flow data at a pressure of 1,500 kPa (218 psia) are compared to computer analyses of UPTF Test 11 (see Figure 4.9-6). The computer analyses were performed by LANL using TRAC, by Winfrith Technology Centre using RELAP5/MOD2, and by GRS using ATHLET. Countercurrent flow behavior predicted with TRAC-PF1/MOD1 version 14.3 exhibits a "bi-stable"-type of behavior. Specifically, the code predicted either complete turnaround or complete delivery rather than a gradual CCFL boundary. MOD1 generally overpredicted the countercurrent water

flow. The analysis was repeated using different interfacial drag correlations in a pre-release version of TRAC-PF1/MOD2. The best results were obtained using a drag correlation developed by Ohnuki. As shown in Figure 4.9-6, the interfacial friction factors calculated with the Ohnuki correlation result in an improvement in the TRAC predictions. Specifically, the complete turnaround point is better predicted and the CCFL boundary is more gradual than the MOD1 predictions; however, the countercurrent water flow is still significantly overpredicted. LANL concluded that further improvements to TRAC are required to accurately predict countercurrent flow (Reference U-708).

As shown in Figure 4.9-6, RELAP5/MOD2 cycle 36.05 underpredicted the complete turnaround point by about a factor of three. This is attributed to the flow regime map used in the code. Specifically, the flow regime map does not permit stratified flow in the hot leg riser. Modification of RELAP5/MOD2 to allow stratified flow in the riser resulted in a better prediction of the test data; however, the code tended to predict either complete turnaround or complete delivery, and generally overpredicted countercurrent water flow (like TRAC-PF1/MOD1). Winfrith concluded that the modified version of RELAP5 overpredicted the countercurrent water flow because the calculated water levels were incorrect (Reference E-621). To support this conclusion, Winfrith developed an experimental computer program which uses the same correlations as RELAP5/MOD2 but "integrates the momentum equations backwards along the hot leg from the pressure vessel to the riser" (Reference E-621). The calculated hot leg water levels were more realistic than those calculated with the modified version of RELAP5/MOD2. As shown in Figure 4.9-6, the resulting countercurrent flow curve exhibits the same character as the UPTF data (i.e., a gradual CCFL boundary). This suggests that RELAP5 could predict countercurrent flow more accurately if the code calculated more realistic liquid levels in the hot leg.

Figure 4.9-6 includes the countercurrent flow behavior predicted using a full-range drift-flux model incorporated in the ATHLET computer code. GRS developed the model from the drift-flux and envelope theories (Reference G-924). As shown in Figure 4.9-6, the countercurrent flow behavior predicted by the code for the UPTF Test 11 is in close agreement with the actual test data.

In addition to the comparisons described above, the UPTF results are compared to tests at subscale facilities which simulated SBLOCAs. The facilities considered and their scales are listed in Table 4.9-1. These facilities demonstrated reflux condensation occurs without apparent hold-up due to hot leg CCFL. The conditions achieved in reflux condensation tests in the four subscale SBLOCA facilities are plotted in Figure 4.9-7. Figure 4.9-7 also shows the UPTF correlation and the data point for the UPTF conditions which simulated reflux condensation. This figure shows that although the scaled facility conditions tend to be scattered about the graph, they are all well within the CCFL boundary. The major conclusions, though, are that for all of the facilities, the observation of reflux condensation without hold-up from hot leg CCFL

is consistent with the full-scale UPTF data, and that the subscale facilities did not distort PWR hot leg behavior in a major phenomenological way (Reference U-904).

Also shown in Figure 4.9-7 is a band of "PWR conditions" which roughly envelope SBLOCA reflux condensation conditions. This figure shows that the expected PWR conditions are well within the CCFL boundary. Accordingly, uninhibited water runback to the reactor vessel is expected in a PWR during the reflux condensation portion of an SBLOCA.

Table 4.9-1

SUMMARY OF TESTS AND ANALYSES ADDRESSING
HOT LEG COUNTERCURRENT FLOW AND REFLUX CONDENSATION

Type of Test or Analysis	Facility or Analysis	Facility Scale[1]	References
Hot Leg CCFL Tests	UPTF Test 11	1.0[2,3]	U-452, U-904 G-011, G-211 G-411
	Richter	0.076[4]	E-493
	Krolweski	0.048[4]	E-491
	Ohnuki	0.0012 to 0.011[4]	J-947
	Wallis	0.0015[4]	E-495
Theoretical Model of Hot Leg CCFL	Gardner	---	E-941
Computer Analyses of UPTF Test 11	TRAC	---	U-708
	RELAP5	---	E-261
	ATHLET	---	G-924
Integral Test Simulation of Reflux Condensation	ROSA-IV	0.021[4]	E-494, E-944
	PKL	0.0069[2]	E-622, E-943
	FLECHT-SEASET	0.0033[4]	E-492
	Semiscale	0.0059[4]	E-021, E-022, E-023, E-942

NOTES:

1. For the hot leg CCFL tests, the scale of the facility is based on the hot leg flow area. For the tests which simulated reflux condensation, scale is based on core power.

2. Relative to a 3900 MWt Siemens/KWU PWR.

3. Relative to a 3400 MWt Westinghouse or Japanese PWR, the scale of UPTF is 1.0 based on the nominal hot leg area. However, when considering the reduction in flow area due to the internal injection pipe (Hutze), the scale of UPTF is 0.93.

4. Relative to a 3400 MWt Westinghouse or Japanese PWR.

Table 4.9-2

COMPARISON OF HOT LEG CCFL TESTS

Facility	Facility Scale[1]	Pipe Diameter MM (inch)	Test Conditions		Comments	Reference
			Pressure kPa (psia)	Gas Phase		
UPTF Test 11	1.0[2,3]	750 (29.5)	300 (44), 1,500 (218)	Steam	The UPTF hot leg contains an internal ECC injection pipe which reduces the flow area by about 10%.	U-452 U-904 G-011 G-211 G-411
Richter	0.076[4]	203 (8)	100 (15) to 110 (16)	Air		E-493
Krolewski	0.0048[4]	50.8 (2)	Not Available	Air	Five different pipe configurations were used. The data used in this analysis are from the experiment with the closest geometric simulation of an actual hot leg.	E-491
Ohnuki	0.0012 to 0.011[4]	25.4 (1.0) to 76.2 (3.0)	Not Available	Air Steam	These experiments varied the length and diameter of the horizontal pipe as well as the length of the inclined riser.	J-947

Table 4.9-2

COMPARISON OF HOT LEG CCFL TESTS

Facility	Facility Scale[1]	Pipe Diameter MM (inch)	Test Conditions		Comments	Reference
			Pressure kPa (psia)	Gas Phase		
Wallis	0.0015[4]	25.4 (1.0)	Not Available	Air	The pipe in these experiments is a 1"x1" rectangular pipe.	E-495

NOTES:

1. The scale of the facility is based on the hot leg flow area.

2. Relative to a 3900 MWt Siemens/KWU PWR.

3. Relative to 3400 MWt Westinghouse or Japanese PWRS, the scale of UPTF is 1.0 based on the nominal hot leg area. However, when considering the reduction in flow area due to the internal injection pipe (Hutze), the scale of UPTF is 0.93.

4. Relative to a 3400 MWt Westinghouse or Japanese PWR.

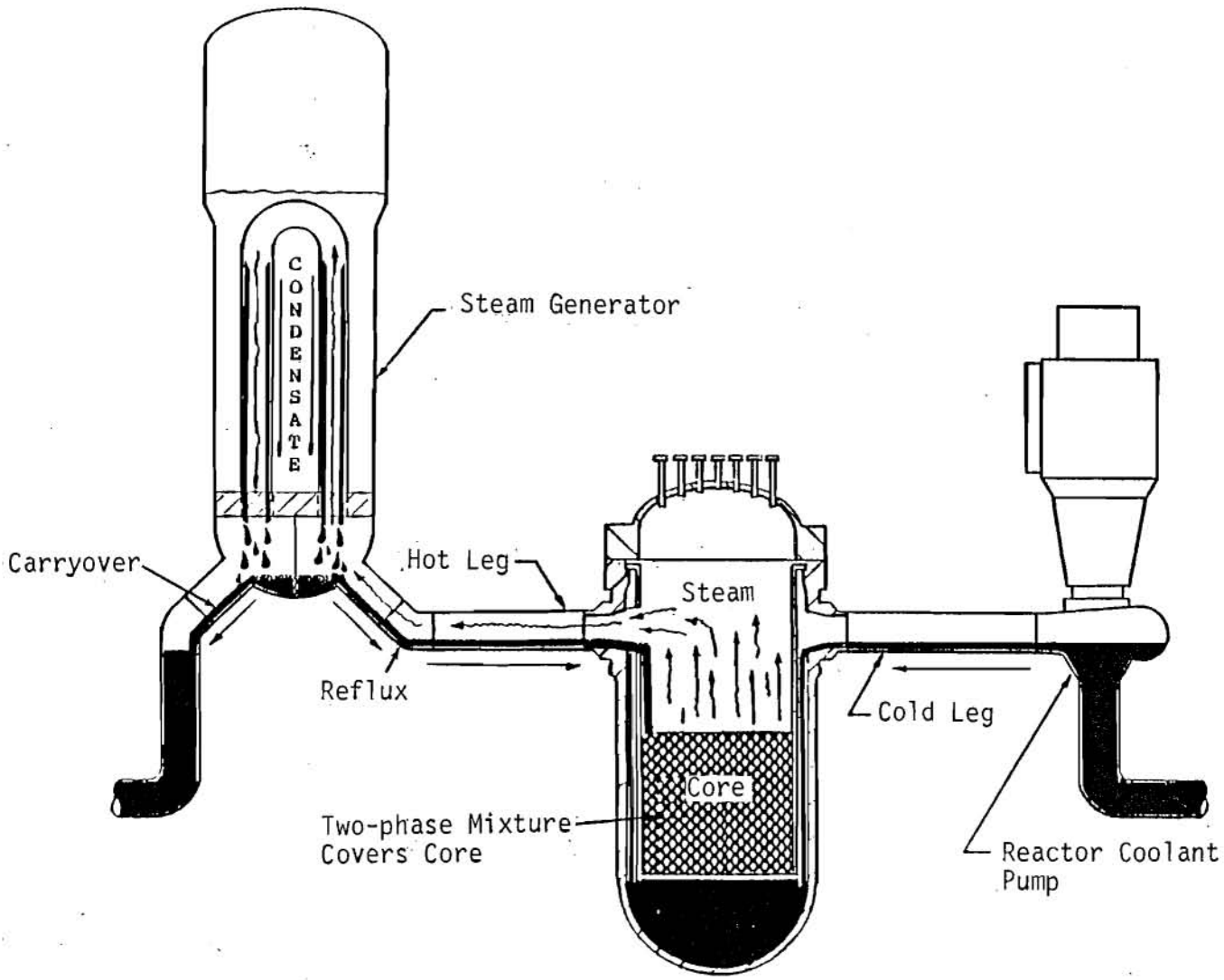

REFLUX CONDENSATION FLOW PATHS

FIGURE 4.9-1

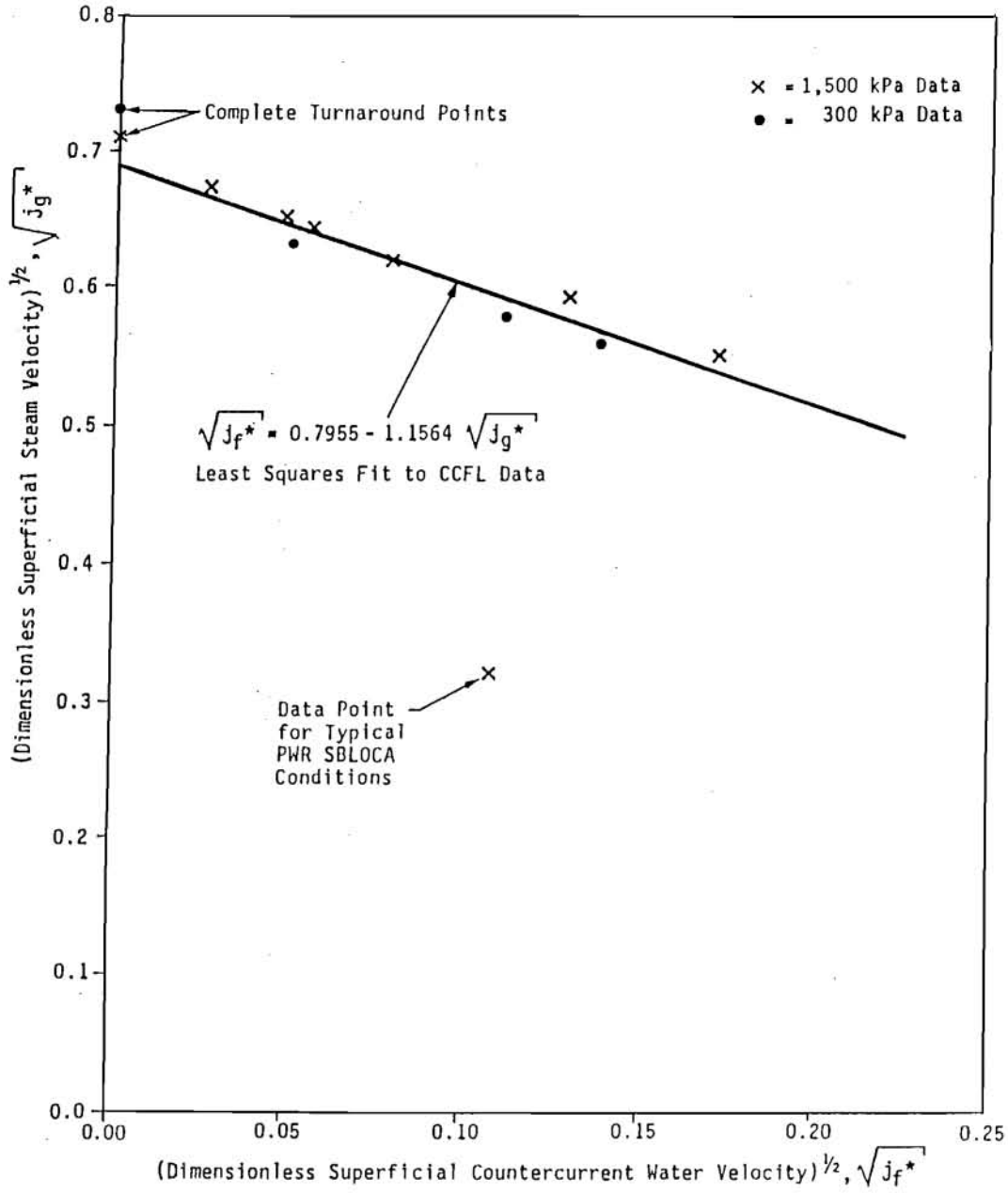

Notes: 1: The dimensionless superficial velocity, or Wallis parameter, is defined as:

$$j^* = \frac{\dot{M}}{\rho A} \sqrt{\frac{\rho}{\Delta \rho g D}}$$

2. The flow area and hydraulic diameter used to calculate the dimensionless superficial velocities are based on the "hutze" region of the hot leg. [A = 0.397m^2 (616 in^2); D = 639mm (25.2 in)]

STEAM/WATER FLOW RELATIONSHIP
FROM UPTF HOT LEG SEPARATE EFFECTS TEST
(REFERENCE U-452)

FIGURE 4.9-2

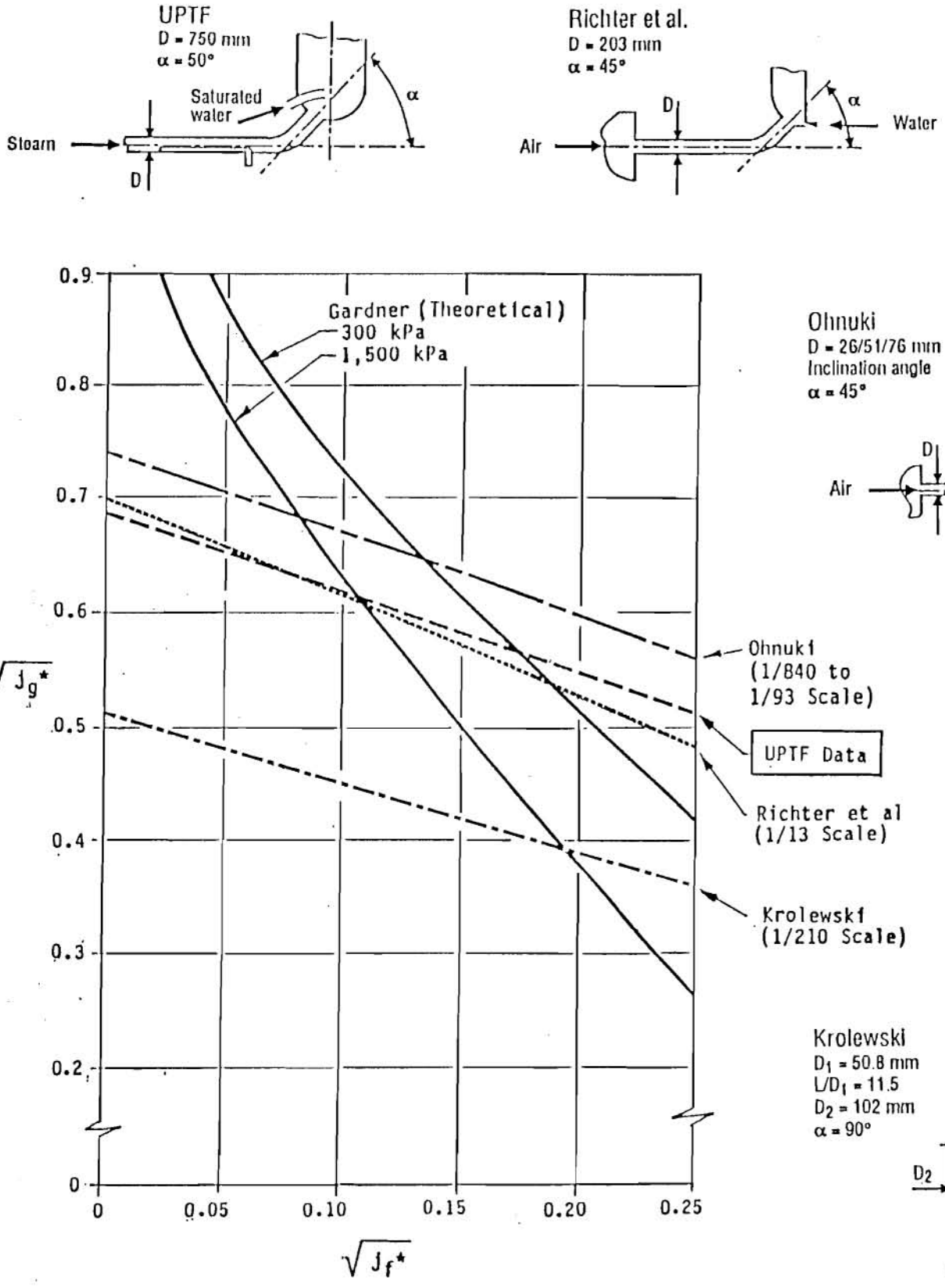

COMPARISON OF UPTF DATA TO THEORETICAL MODELS AND CORRELATIONS FROM SMALL-SCALE TESTS

FIGURE 4.9-3

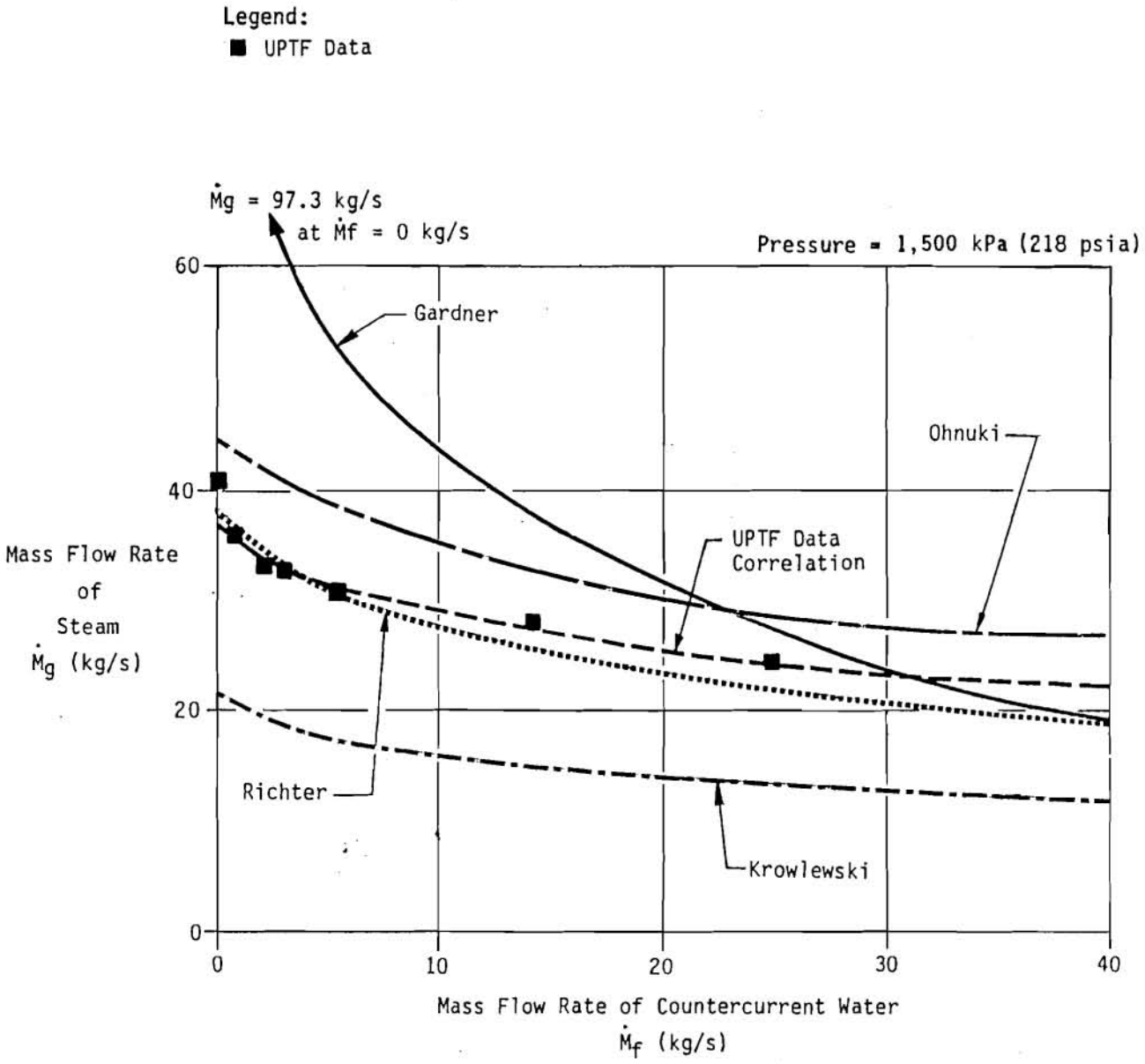

COMPARISON OF EXPERIMENTAL RESULTS
FROM UPTF TO CALCULATED PREDICTIONS OF CCFL
(REFERENCE U-452)

FIGURE 4.9-4

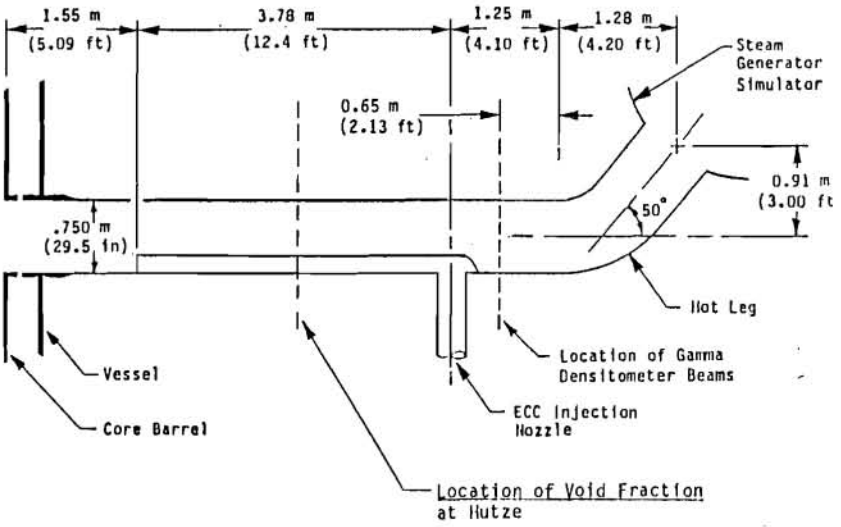

UPTF LOOP 4 HOT LEG

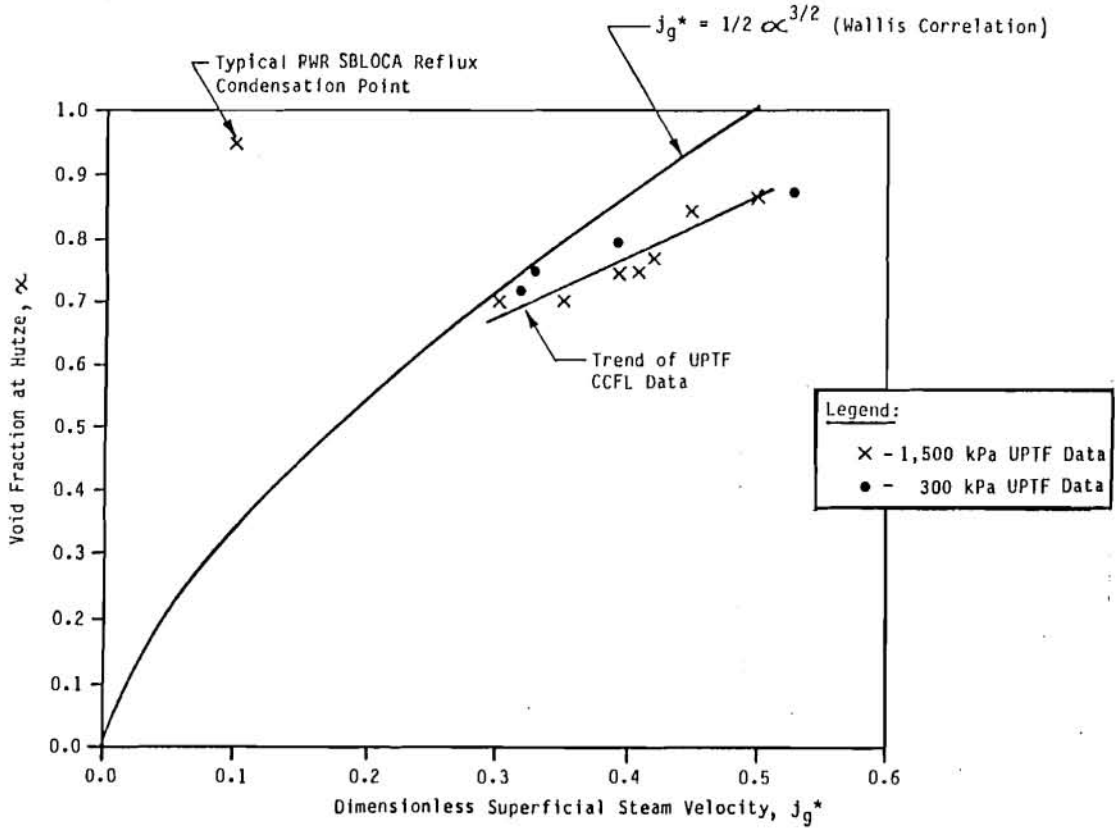

COMPARISON OF UPTF VOID FRACTION MEASUREMENTS TO WALLIS FLOODING CORRELATION (REFERENCE U-452)

FIGURE 4.9-5

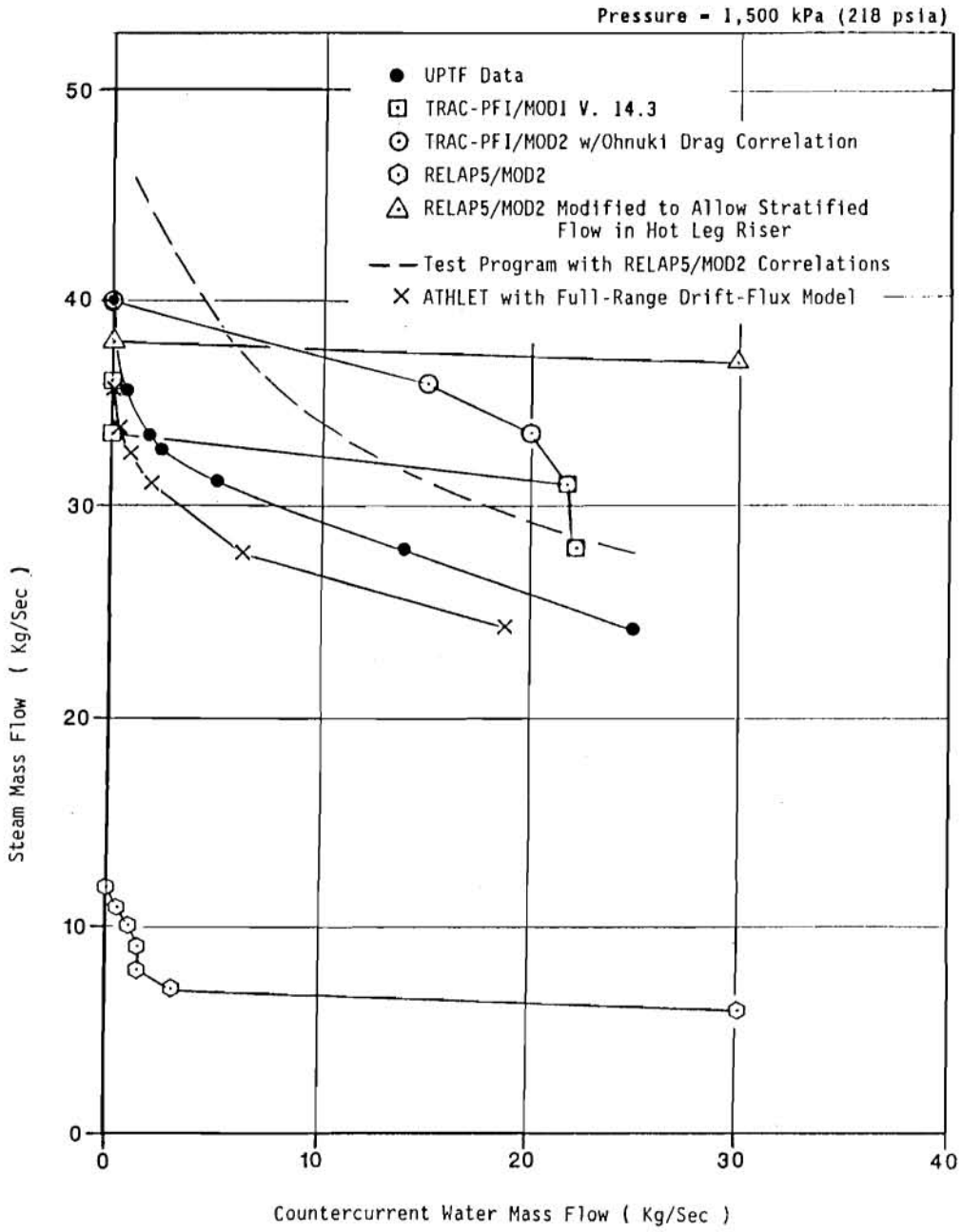

Notes: 1. The TRAC-PF1/MOD1 analysis was performed using version 14.3.

2. The TRAC-PF1/MOD2 analysis was performed using a pre-release version.

3. The RELAP5/MOD2 analyses were performed using cycle 36.05.

COMPARISON OF UPTF DATA TO COMPUTER ANALYSES

FIGURE 4.9-6

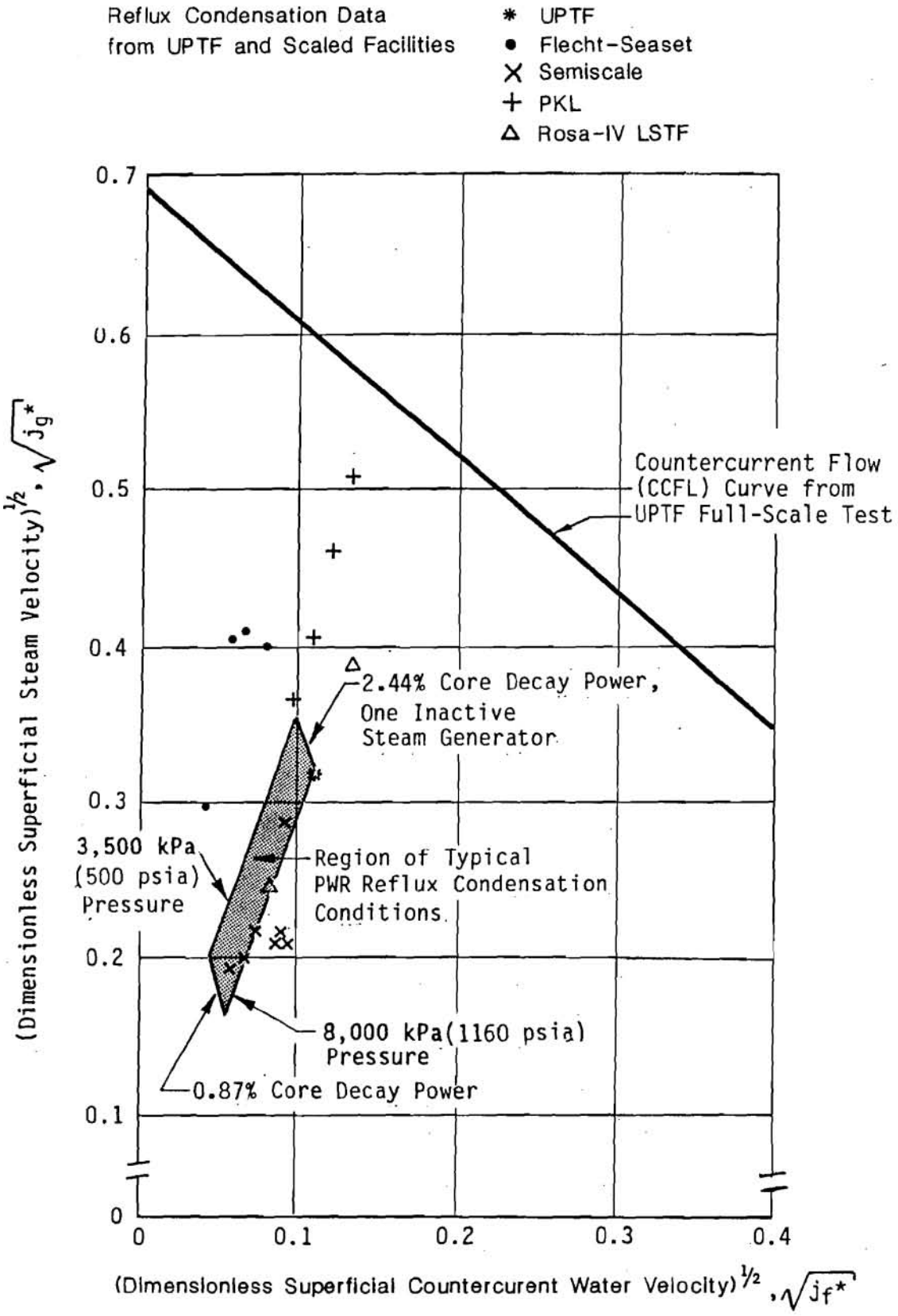

COMPARISON OF SMALL-SCALE FACILITY
REFLUX CONDENSATION EXPERIMENTAL RESULTS
TO UPTF TEST RESULTS
(REFERENCE U-452)

FIGURE 4.9-7

Section 5

BIBLIOGRAPHY

This bibliography provides a comprehensive listing of reports prepared within the 2D/3D Program and references to supporting material generated outside the 2D/3D Program. Each document is assigned a four character code consisting of a letter and a three-digit number (i.e., A-###). The letter designates the origin of the document and the number indicates the type of document. These codes are defined below.

Letter Prefixes

G	Published by FRG within the 2D/3D Program
J	Published by Japan within the 2D/3D Program
U	Published by US within the 2D/3D Program
E	External to 2D/3D Program

Numbers

001 - 200	Data Reports
201 - 400	Quick Look Reports
401 - 600	Evaluation Reports
601 - 800	Code Analysis Reports
801 - 900	Advanced Instrumentation Reports
901 - 999	Papers, Presentations, and Correspondence

NOTICE: Data generated in the 2D/3D International Program are only for use by authorized users within the restrictions of the 2D/3D Program; consequently, distribution of reports which contain 2D/3D Program test data (i.e., many of the reports listed in this bibliography) is restricted.

REPORTS AND PAPERS PUBLISHED BY FRG WITHIN 2D/3D PROGRAM

DATA REPORTS

UPTF

G-001 2D/3D Program Upper Plenum Test Facility Experimental Data Report, "Test No. 1 Fluid-Fluid Mixing Test," prepared by KWU, R 515/87/09, April 1987.

G-002 2D/3D Program Upper Plenum Test Facility Experimental Data Report, "Test No. 2 US/J PWR Integral Test with Cold Leg ECC Injection," prepared by Siemens/KWU, U9 316/88/5, April 1988.

G-003 2D/3D Program Upper Plenum Test Facility Experimental Data Report, "Test No. 3 GPWR Integral Test 5/8 Combined ECC Injection," prepared by KWU, R 515/87/14, August 1987.

G-004 2D/3D Program Upper Plenum Test Facility Experimental Data Report, "Test No. 4 US/J PWR Integral Test With Cold Leg ECC Injection," prepared by Siemens/KWU, E314/90/004, April 1990.

G-005 2D/3D Program Upper Plenum Test Facility Experimental Data Report, "Test No. 5 Downcomer Separate Effect Test," prepared by KWU, R 515/87/16, September 1987.

G-006 2D/3D Program Upper Plenum Test Facility Experimental Data Report, "Test No. 6 Downcomer Countercurrent Flow Test," prepared by Siemens/KWU, U9 316/88/18, December 1988.

G-007 2D/3D Program Upper Plenum Test Facility Experimental Data Report, "Test No. 7 Downcomer Countercurrent Flow Test," prepared by Siemens/KWU, U9 316/89/14, 1989.

G-008 2D/3D Program Upper Plenum Test Facility Experimental Data Report, "Test No. 8 Cold/Hot Leg Flow Pattern Test," prepared by Siemens/KWU, U9 316/88/12, September 1988.

G-009 2D/3D Program Upper Plenum Test Facility Experimental Data Report, "Test No. 9 Cold/Hot Leg Flow Pattern Test," prepared by Siemens/KWU, U9 316/89/5, February 1989.

G-010 2D/3D Program Upper Plenum Test Facility Experimental Data Report, "Test No. 10 Tie Plate Countercurrent Flow Test," prepared by Siemens/KWU, U9 316/88/1, February 1988.

G-011 2D/3D Program Upper Plenum Test Facility Experimental Data Report, "Test No. 11 Countercurrent Flow in PWR Hot Leg Test," prepared by KWU, R 515/87/10, May 1987.

G-012 2D/3D Program Upper Plenum Test Facility Experimental Data Report, "Test No. 12 Tie Plate Countercurrent Flow Test," prepared by KWU, R 515/86/14, November 1986.

G-013 2D/3D Program Upper Plenum Test Facility Experimental Data Report, "Test No. 13 Tie Plate Countercurrent Flow Test," prepared by KWU, U9 316/87/21, November 1987.

G-014 2D/3D Program Upper Plenum Test Facility Experimental Data Report, "Test No. 14 GPWR Integral Test with 5/8 Combined ECC Injection," prepared by Siemens/KWU, E314/90/15, September 1990.

G-015 2D/3D Program Upper Plenum Test Facility Experimental Data Report, "Test No. 15 Tie Plate Countercurrent Flow Test," prepared by Siemens/KWU, U9 316/88/17, December 1988.

G-016 2D/3D Program Upper Plenum Test Facility Experimental Data Report, "Test No. 16 Tie Plate Countercurrent Flow Test," prepared by Siemens/KWU, E314/89/21, December 1989.

G-017 2D/3D Program Upper Plenum Test Facility Experimental Data Report, "Test No. 17 US/J-PWR Integral Test with Cold Leg ECC Injection," prepared by Siemens/KWU, E314/89/18, November 1989.

G-018 2D/3D Program Upper Plenum Test Facility Experimental Data Report, "Tests No. 18 GPWR Integral Test with 5/8 Combined ECC Injection," prepared by Siemens/KWU, U9 316/89/10, June 1989.

G-019 2D/3D Program Upper Plenum Test Facility Experimental Data Report, "Test No. 19 GPWR Integral Test with 5/8 Combined ECC Injection," prepared by Siemens/KWU, U9 316/89/16, 1989.

G-020 2D/3D Program Upper Plenum Test Facility Experimental Data Report, "Test No. 20 Upper Plenum Injection Simulation Test," prepared by Siemens/KWU, U9 316/88/08, June 1988.

G-021 2D/3D Program Upper Plenum Test Facility Experimental Data Report, "Test No. 21 Downcomer Injection Test," prepared by Siemens/KWU, E314/90/17, October 1990.

G-022 2D/3D Program Upper Plenum Test Facility Experimental Data Report, "Test No. 22 Downcomer Injection Test with Vent Valves," prepared by Siemens/KWU, E314/91/007, March 1991.

G-023 2D/3D Program Upper Plenum Test Facility Experimental Data Report, "Test No. 23 Downcomer Injection Test with Vent Valves," prepared by Siemens/KWU, E314/91/001, January 1991.

G-024 2D/3D Program Upper Plenum Test Facility Experimental Data Report, "Test No. 24 Integral Test with Vent Valves," prepared by Siemens/KWU, E314/90/21, November 1990.

G-025 2D/3D Program Upper Plenum Test Facility Experimental Data Report, "Test No. 25 Downcomer/Cold Leg Steam/Water Interaction Test," prepared by Siemens/KWU, E314/90/11, August 1990.

G-026 2D/3D Program Upper Plenum Test Facility Experimental Data Report, "Test No. 26 Hot Leg Flow Pattern Test," prepared by Siemens/KWU, E314/91/005, February 1991.

G-027 2D/3D Program Upper Plenum Test Facility Experimental Data Report, "Test No. 27 Integral Test with Cold Leg Injection," prepared by Siemens/KWU, E314/90/24, September 1990.

G-028 2D/3D Program Upper Plenum Test Facility Experimental Data Report, "Test No. 28 GPWR Integral Test with 7/8 Combined ECC Injection," prepared by Siemens/KWU, E314/90/07, July 1990.

G-029 2D/3D Program Upper Plenum Test Facility Experimental Data Report, "Test No. 29 Entrainment/De-entrainment Test," prepared by Siemens/KWU, E314/90/05, June 1990.

G-030 2D/3D Program Upper Plenum Test Facility Experimental Data Report, "Test No. 30 Tie Plate Countercurrent Flow Test H-P Injection," prepared by Siemens/KWU, U9 316/89/9, April 1989.

QUICK LOOK REPORTS

G-201 2D/3D Program Upper Plenum Test Facility Quick Look Report, "Test No. 1 Fluid-Fluid Mixing Test," prepared by KWU, R 515/87/1, January 1987.

G-202 2D/3D Program Upper Plenum Test Facility Quick Look Report, "Test No. 2 US/J PWR Integral Test with Cold Leg ECC Injection," prepared by Siemens/KWU, U9 316/88/2, March 1988.

G-203 2D/3D Program Upper Plenum Test Facility Quick Look Report, "Test No. 3 GPWR Integral Test with 5/8 Combined ECC Injection," prepared by KWU, R 515/87/15, September 1987.

G-204 2D/3D Program Upper Plenum Test Facility Quick Look Report, "Test No. 4 US/J PWR Integral Test with Cold Leg ECC Injection," prepared by Siemens/KWU, E314/90/06, July 1990.

G-205 2D/3D Program Upper Plenum Test Facility Quick Look Report, "Test No. 5 Downcomer Separate Effect Test," prepared by KWU, U9 316/87/17, October 1987.

G-206 2D/3D Program Upper Plenum Test Facility Quick Look Report, "Test No. 6 Downcomer Countercurrent Flow Test," prepared by Siemens/KWU, U9 316/89/2, March 1989.

G-207 2D/3D Program Upper Plenum Test Facility Quick Look Report, "Test No. 7 Downcomer Countercurrent Flow Test," prepared by Siemens/KWU, E314/90/003, March 1990.

G-208 2D/3D Program Upper Plenum Test Facility Quick Look Report, "Test No. 8 Cold/Hot Leg Flow Pattern Test," prepared by Siemens/KWU, U9 316/88/11, September 1988.

G-209 2D/3D Program Upper Plenum Test Facility Quick Look Report, "Test No. 9 Cold/Hot Leg Flow Pattern Test," prepared by Siemens/KWU, U9 316/89/6, March 1989.

G-210 2D/3D Program Upper Plenum Test Facility Quick Look Report, "Test No. 10 Tie Plate Countercurrent Flow Test," prepared by Siemens/KWU, U9 316/88/3, 1988.

G-211 2D/3D Program Upper Plenum Test Facility Quick Look Report, "Test No. 11 Countercurrent Flow in PWR Hot Leg Test," prepared by KWU, R 515/87/08, March 1987.

G-212 2D/3D Program Upper Plenum Test Facility Quick Look Report, "Test No. 12 Tie Plate Countercurrent Flow Test," prepared by KWU, R 515/86/13, October 1986.

G-213 2D/3D Program Upper Plenum Test Facility Quick Look Report, "Test No. 13 Tie Plate Countercurrent Flow Test," prepared by KWU, U9 316/87/22, December 1987.

G-214 2D/3D Program Upper Plenum Test Facility Quick Look Report, "Test No. 14 GPWR Integral Test with 5/8 Combined ECC Injection," prepared by Siemens/KWU, E314/90/14, September 1990.

G-215 2D/3D Program Upper Plenum Test Facility Quick Look Report, "Test No. 15 Tie Plate Countercurrent Flow Test," prepared by Siemens/KWU, U9 316/89/01, February 1989.

G-216 2D/3D Program Upper Plenum Test Facility Quick Look Report, "Test No. 16 Tie Plate Countercurrent Flow Test," prepared by Siemens/KWU, E314/89/22, December 1989.

G-217 2D/3D Program Upper Plenum Test Facility Quick Look Report, "Test No. 17 US/J PWR Integral Test with Cold Leg ECC Injection," prepared by Siemens/KWU, E314/89/20, December 1989.

G-218 2D/3D Program Upper Plenum Test Facility Quick Look Report, "Test No. 18 GPWR Integral Test with 5/8 Combined ECC Injection," prepared by Siemens/KWU, U9 316/89/11, June 1989.

G-219 2D/3D Program Upper Plenum Test Facility Quick Look Report, "Test No. 19 GPWR Integral Test with 5/8 Combined ECC Injection," prepared by Siemens/KWU, U9 316/89/16, October 1989.

G-220 2D/3D Program Upper Plenum Test Facility Quick Look Report, "Test No. 20 Upper Plenum Injection Simulation Test," prepared by Siemens/KWU, U9 316/88/07, June 1988.

G-221 2D/3D Program Upper Plenum Test Facility Quick Look Report, "Test No. 21 Downcomer Injection Test," prepared by Siemens/KWU, E314/90/16, September 1990.

G-222 2D/3D Program Upper Plenum Test Facility Quick Look Report, "Test No. 22 Downcomer Injection Test with Vent Valves," prepared by Siemens/KWU, E314/91/008, March 1991.

G-223 2D/3D Program Upper Plenum Test Facility Quick Look Report, "Test No. 23 Downcomer Injection Test with Vent Valves," prepared by Siemens/KWU, E314/90/25, December 1990.

G-224 2D/3D Program Upper Plenum Test Facility Quick Look Report, "Test No. 24 Integral Test with Vent Valves," prepared by Siemens/KWU, E314/90/22, September 1990.

G-225 2D/3D Program Upper Plenum Test Facility Quick Look Report, "Test No. 25 Downcomer/Cold Leg Steam/Water Interaction Test," prepared by Siemens/KWU, E314/90/13, September 1990.

G-226 2D/3D Program Upper Plenum Test Facility Quick Look Report, "Test No. 26 Hot Leg Flow Pattern Test," prepared by Siemens/KWU, E314/91/003, February 1991.

G-227 2D/3D Program Upper Plenum Test Facility Quick Look Report, "Test No. 27 US/J PWR Integral Test with Cold Leg ECC Injection," prepared by Siemens/KWU, E314/90/26, December 1990.

G-228 2D/3D Program Upper Plenum Test Facility Quick Look Report, "Test No. 28 GPWR Integral Test with 7/8 Combined ECC Injection," prepared by Siemens/KWU, E314/90/08, September 1990.

G-229 2D/3D Program Upper Plenum Test Facility Quick Look Report, "Test No. 29 Entrainment/De-entrainment Test," prepared by Siemens/KWU, E314/90/19, November 1990.

G-230 2D/3D Program Upper Plenum Test Facility Quick Look Report, "Test No. 30 Tie Plate Countercurrent Flow Test HP-Injection," prepared by Siemens/KWU, E314/89/22, December 1989.

EVALUATION REPORTS

SCTF

G-401 Pointner, W., "Empirical Equation for the Entrainment in SCTF-III," Gesellschaft fuer Reaktorsicherheit, GRS-A-1404, January 1988.

UPTF

G-411 UPTF Summary Report (to be published).

G-412 2D/3D Program Upper Plenum Test Facility, "UPTF: Program and System Description," prepared by Siemens/KWU, U9 414/88/023, November 1988.

G-413 2D/3D Program Upper Plenum Test Facility, "Work Report: UPTF Test Instrumentation," prepared by KWU, R 515/85/23, September 1985.

G-414 Gehrmann, R., "Input to Test Objectives and Conditions for the UPTF Vent Valve Test No. 24 (Integral Test)," ASEA-Brown Boveri, ABB Technical Report No. GBRA 012023, June 6, 1989.

G-415 Glaeser, H., "Downcomer and Upper Tie Plate Countercurrent Flow in the Upper Plenum Test Facility," Gesellschaft fuer Reaktorsicherheit, GRS-A-1726, November 1990.

CODE ANALYSIS REPORTS

Karlstein Tests

G-601 Glaeser, H., and Schertel, H., "Analyses Der Karlstein-Dampf-Wasser-Gegenstromungsexperimente Mit TRAC-PF1 (11.1)," Gesellschaft fuer Reaktorsicherheit, GRS-A-1179, January 1986.

G-602 Glaeser, H., "Analysis of the Karlstein Saturated Water Tests on Steam-Water-Countercurrent Flow Using the Computer Code TRAC-PF1 (11.1, 12.5)," Gesellschaft fuer Reaktorsicherheit, GRS-A-1249, July 1986.

CCTF Tests

G-611 Krey, L.,"Post Test Calculation of CCTF Test C2-20, Run 80 with the Code System ATHLET/FLUT No. 8A," Technischer Ueberwachungs-Verein Bayern e.V., Muenchen, October 1991.

SCTF Tests

G-621 Schwarz, S., "SCTF Vent Valve Test S3-17 (Run 721) BBR Coupling Test Comparison to the TRAC Reactor Analysis," Gesellschaft fuer Reaktorsicherheit, GRS-A-1471, July 1988.

G-622 Thiele, T.H., "Post Test Calculation of SCTF S3-11 (715) using FLUT No. 6A," Pitscheider Report No. 9027, April 1990.

UPTF Tests -- Pre-test Conditioning Calculations

G-631 Schwarz, S., "UPTF - Konditionierungsrechung Fuer ABB Vent Valve Tests Datensatz, Erfahrung und Endergebnis," Gesellschaft fuer Reaktorsicherheit, GRS-A-1621, October 1989.

UPTF Test -- Post-test Analyses

G-641 Riegel, B., "Post Test Calculation of UPTF Test 8 with the Advanced Computer Code TRAC-PF1/MOD1," Gesellschaft fuer Reaktorsicherheit, GRS-A-1666, May 1990.

G-642 Riegel, B., "Post Test Calculation of UPTF Test 9 with the Advanced Computer Code TRAC-PF1/MOD1," Gesellschaft fuer Reaktorsicherheit, GRS-A-1738, December 1990.

G-643 Sonnenburg, H.G., "Analysis of UPTF 11 (Hot Leg CCF) with a Full-Range Drift Flux Model," Gesellschaft fuer Reaktorsicherheit, GRS-A-1681, June 1990.

G-644 Glaeser, H., "Post Test Calculations of UPTF Test 12 with the Advanced Computer Code TRAC-PF1/MOD1," Gesellschaft fuer Reaktorsicherheit, GRS-A-1727, November 1990.

G-645 Glaeser, H., "Post Test Calculation of UPTF Test 13 with the Advanced Computer Code TRAC-PF1/MOD1," Gesellschaft fuer Reaktorsicherheit, GRS-A-1728, November 1990.

G-646 Sonnenburg, H.G., "Analysis of UPTF - Test 26 Run 230 by ATHLET Code with Full-Range Drift Flux Model," Gesellschaft fuer Reaktorsicherheit, GRS-A-1723, October 1990.

G-647 Hora, A., and Teschendorff, V., "Post Test Calculation of UPTF Test 5B with the Computer Code FLUT," Gesellschaft fuer Reaktorsicherheit, GRS-A-1798, June 1991.

G-648 Gasteiger, H., "Post Test Calculation of UPTF Test 18 with the Code System ATHLET/FLUT," Teschnischer Ueberwachungs-Verein Bayern e.V., Muenchen, June 1991.

G-649 Thiele, T.H., "Post Test Calculation of UTPF Test No. 20 using Code System ATHLET/MOD 1.0-Cycle C," Pitscheider Report No. 9058, December 18, 1990.

G-650 Thiele, T.H., "Post Test Calculation of UPTF Test 29A using Code System ATHLET-FLUT, Version No. 8," Pitscheider Report No. 9055, November 13, 1990.

GPWR Analyses

G-661 Riegel, B., "Calculation of a Double Ended Break in the Cold Leg of the Primary Coolant Loop of a German Pressurized Water Reactor with a 5/8 Emergency Cooling Injection (Calculated with TRAC-PF1/MOD1 (Version 12.5))," Gesellschaft fuer Reaktorsicherheit, GRS-A-1322, February 1987.

G-662 Schwarz,S., "GPWR Analysis with TRAC PF1/MOD1 Version 12.5 BBR Type Reactor, 200% Cold Leg Pump Discharge Break EM-Conditions," Gesellschaft fuer Reaktorsicherheit, GRS-A-1403, January 1988.

G-663 Hrubisko, M., "Calculation of a Double Ended Break in the Hot Leg of the Primary Coolant Loop of a German Pressurized Water Reactor with a 5/8 Emergency Coolant Injection (Calculated with TRAC-PF1/MOD1 Version 12.5)," Gesellschaft fuer Reaktorsicherheit, GRS-A-1771, April 1991.

G-664 Gasteiger, H., "Calculation of a Double Ended Break in the Cold Leg of the Primary Coolant Loop of a German Pressurized Water Reactor (GPWR) with the Code System ATHLET/FLUT," Technischer Ueberwachungs-Verein Bayern e.V., Muechen, December 1990.

ADVANCED INSTRUMENTATION REPORTS

G-801 Mewes, D., Laake, H.J., and Spatz, R., "Fluid Dynamic Effects in the Area of the Tie Plate and the Spacer of the Fuel Elements Installed in Pressurized Water Reactors," Institute for Process Technology, University of Hanover, March 1985.

G-802 "Calibration of the UPTF Tie Plate Flow Module with 'Advanced Instrumentation' and Investigation of the Function from the Core Simulator Feed Back Control System with Break-Thru-Detectors," prepared by KWU, R 917/86/002, April 1986.

G-803 Hampel, G., et. al., "Final Report on the 'Advanced Instrumentation' Study-2D/3D Project," Battelle-Frankfurt Institute, BF-R-64.525.2.

G-804 "UPTF-Instrumentation Control Document," Revision 1, prepared by KWU, April 1984.

G-805 Emmerling R., "Proposal for UPTF Tie-plate Mass Flow Algorithm," KWU/R152, May 1984.

G-806 Emmerling, R., "Computer Program for the Determination of Steam/Water Mass Flow Rates through the Tie Plate," KWU, R15-85-e1021, December 1985.

G-807 Gaul, H.P., "Status of UPTF Advanced Instrumentation and Systems Failure Time History," KWU Work-Report R515/86/10, July 30, 1986.

G-808 Gaul, H.P., and Hein, K.H., "UPTF Experiment: US Advanced Instrumentation und Datenerfassungsanlage; Zusammenfassung der bearbeiteten Probleme fuer den Zeitraum- Februar 1985 - Januar 1986," Arbeits-Bericht R515/86/6, March 5, 1986.

G-809 Gaul, H.P., and Wandzilak, L., "Ueberpruefung des PFM Algorithmus mit Dummy Daten und Versuchsrechnungen," Arbeits-Bericht U9 316/88/16, September 27, 1988.

G-810 Gaul, H.P., and Schulz, N., Beschreibung der beim UPTF Pipe Flow Meter aufgetretenen Hardwareprobleme und durchgefuehrte Modifikationen an der Hardware," Arbeits-Bericht U9 316/88/10, June 20, 1988.

PAPERS, PRESENTATIONS, AND CORRESPONDENCE

Papers - Data Evaluation

G-901 Kroening, H., Hawighorst, A., and Mayinger, F., "The Influence of Flow Restrictions on the Countercurrent Flow Behavior in the Fuel-Element Top Nozzle Area," European Two-phase Flow Group Meeting, Paris-La-Defence, June 2-4, 1982.

G-902 Weiss, P., Sawitzki, M., and Winkler, F., "UPTF, a Full-scale PWR Loss-of-Coolant Accident Experiment Program," Atomkernenergie Kerntechnik Vol. 49 (1986), No. 1/2.

G-903 Hertlein, P.J., and Weiss, P.A., "UPTF Test Results - First Downcomer CCF Test," Proceedings of the Fifteenth Water Reactor Safety Information Meeting, October 26-29, 1987, NUREG/CP-0091, Volume 4, pp. 533-547.

G-904 Weiss, P.A., "UPTF Experiment - Principal Experimental Results to be used for Improved LB LOCA Understanding," Proceedings of the Sixteenth Water Reactor Safety Research Information Meeting, October 24-28, 1988, NUREG/CP-0097, Volume 4, pp. 543-555.

G-905 Weiss, P., Watzinger, H., and Hertlein, R., "UPTF Experiment - A Synopsis of Full-Scale Test Results," presented at The Third International Topical Meeting on Nuclear Power Plant Thermal-Hydraulics and Operations, Seoul, Korea, November 14-17, 1988.

G-906 Glaeser, H., "Analysis of Downcomer and Tie Plate Countercurrent Flow in the Upper Plenum Test Facility (UPTF)," presented at the Fourth International Topical Meeting on Nuclear Reactor Thermal-Hydraulics, Karlsruhe, FRG, October 10-13, 1989.

G-907 Liebert, J., and Weiss, P., "UPTF-Experiment - Effect of Full-Scale Geometry on Countercurrent Flow Behaviors in PWR Downcomer," presented at the Fourth International Topical Meeting on Nuclear Reactor Thermal-Hydraulics, Karlsruhe, FRG, October 10-13, 1989.

G-908 Weiss, P., "UPTF-Experiment - Principal Full-Scale Test Results for Enhanced Knowledge of Large Break LOCA Scenarios in PWRs," presented at the Fourth International Topical Meeting on Nuclear Reactor Thermal-Hydraulics, Karlsruhe, FRG, October 10-13, 1989.

G-909 Winkler, F., and Krebs, W., "Impact of 2D/3D Project on LOCA Licensing Analysis and Reactor Safety of PWRs," presented at the Fourth International Topical Meeting on Nuclear Reactor Thermal-Hydraulics, Karlsruhe, FRG, October 10-13, 1989.

G-910 Weiss, P., "UPTF-Experiment - Full-Scale Test on Large Break LOCA Thermal-Hydraulic Scenarios in PWR: Status & Findings," Proceedings of the Seventeenth Water Reactor Safety Research Information Meeting, October 22-25, 1989.

G-911 Emmerling, R., and Weiss, P., "UPTF-Experiment - Analysis of Flow Pattern in Pipes of Large Diameter with Subcooled Water Injection," presented at the European Two-Phase Flow Group Meeting, Paris, France, May 29-June 1, 1989.

G-912 "PWRs with Cold Leg or Combined ECC Injection -- Synopsis of Test Results," Handout G-2 from 2D/3D Coordination Meeting, Tokai-Mura, Japan, May 21-25, 1990.

G-913 Weiss, P.A., and Hertlein, R.J., "UPTF Test Results: First Three Separate Effects Tests," Nuclear Engineering and Design, Vol. 108, No. 1/2, pp. 249-263 (1988).

G-914 Weiss, P., Watzinger, H., and Hertlein, R., "UPTF Experiment: A Synopsis of Full Scale Test Results," Nuclear Engineering and Design, Vol. 122, No. 1, pp. 219-234 (1990). (Also see G-905.)

G-915 Glaeser, H., "Downcomer and Tie Plate Countercurrent Flow in the Upper Plenum Test Facility (UPTF)," Nuclear Engineering and Design, Vol. 133, pp. 259-283 (1992).

Papers - Code Analysis

G-921 Puetter, B., "50% Cold Leg Break in KWU Plant," presented at 2D/3D Coordination Meeting, Mannheim, FRG, June 18, 1985.

G-922 Plank, H., "Analyses of a Double-Ended Cold Leg Break of a 1300 MW KWU-PWR with TRAC-PF1/MOD1 (12.5)," presented at 2D/3D Analysis Meeting, Erlangen, FRG, June 5-13, 1986.

G-923 Riegel, B., Plank, H., Liesch, K., "Multidimensional Representation of GPWR Primary System in 200% LOCA Calculation," Proceedings of the Fourteenth Water Reactor Safety Information Meeting, October 27-30, 1986, NUREG/CP-0082, Volume 4, pp. 499-521.

G-924 Sonnenburg, H.G., "Analysis of UPTF Test 11 (Hot Leg CCF) with Full-Range Drift-Flux Model," Proceedings of the Fifteenth Water Reactor Safety Information Meeting, October 26-29, 1987, NUREG/CP-0091, Volume 4, pp. 585-607.

G-925 Hertlein, R., and Herr, W., "A New Model for Countercurrent Flow in the Upper Part of a PWR Core," presented at the Fourth International Topical Meeting on Nuclear Reactor Thermal-Hydraulics, Karlsruhe, FRG, October 10-13, 1989.

REPORTS AND PAPERS PUBLISHED BY JAERI WITHIN 2D/3D PROGRAM

DATA REPORTS

CCTF Core-I

J-001 "Data Report on Large Scale Reflood Test-1 -- CCTF Shakedown Test C1-SH1 (Run 005)," prepared by Japan Atomic Energy Research Institute, JAERI-Memo-8795, February 1980.

J-002 "Data Report on Large Scale Reflood Test-2 -- CCTF Shakedown Test C1-SH2 (Run 006)," prepared by Japan Atomic Energy Research Institute, JAERI-Memo-8797, February 1980.

J-003 "Data Report on Large Scale Reflood Test-3 -- CCTF Shakedown Test C1-SH3 (Run 007)," prepared by Japan Atomic Energy Research Institute, JAERI-Memo-8931, June 1980.

J-004 "Data Report on Large Scale Reflood Test-4 -- CCTF Shakedown Test C1-SH4 (Run 008)," prepared by Japan Atomic Energy Research Institute, JAERI-Memo-8932, June 1980.

J-005 "Data Report on Large Scale Reflood Test-5 -- CCTF Shakedown Test C1-SH5 (Run 009)," prepared by Japan Atomic Energy Research Institute, JAERI-Memo-8933, June 1980.

J-006 "Data Report on Large Scale Reflood Test-10 -- CCTF C1-1 (Run 010)," prepared by Japan Atomic Energy Research Institute, JAERI-Memo-9997, March 1982.

J-007 "Data Report on Large Scale Reflood Test-11 -- CCTF Test C1-2 (Run 011)," prepared by Japan Atomic Energy Research Institute, JAERI-Memo-57-156, July 1982.

J-008 "Data Report on Large Scale Reflood Test-12 -- CCTF Test C1-3 (Run 012)," prepared by Japan Atomic Energy Research Institute, JAERI-Memo-57-175, July 1982.

J-009 "Data Report on Large Scale Reflood Test-13 -- CCTF Test C1-4 (Run 013)," prepared by Japan Atomic Energy Research Institute, JAERI-Memo-57-210, August 1982.

J-010 "Data Report on Large Scale Reflood Test-14 -- CCTF Test C1-5 (Run 014)," prepared by Japan Atomic Energy Research Institute, JAERI-Memo-57-214, August 1982.

J-011 "Data Report on Large Scale Reflood Test-15 -- CCTF Test C1-6 (Run 015)," prepared by Japan Atomic Energy Research Institute, JAERI-Memo-57-239, September 1982.

J-012 "Data Report on Large Scale Reflood Test-19 -- CCTF Test C1-7 (Run 016)," prepared by Japan Atomic Energy Research Institute, JAERI-Memo-57-343, November 1982.

J-013 "Data Report on Large Scale Reflood Test-20 -- CCTF Test C1-8 (Run 017)," prepared by Japan Atomic Energy Research Institute, JAERI-Memo-57-349, November 1982.

J-014 "Data Report on Large Scale Reflood Test-27 -- CCTF Test C1-9 (Run 018)," prepared by Japan Atomic Energy Research Institute, JAERI-Memo-57-373, July 1982.

J-015 "Data Report on Large Scale Reflood Test-36 -- CCTF Test C1-10 (Run 019)," prepared by Japan Atomic Energy Research Institute, JAERI-Memo-58-063, March 1983.

J-016 "Data Report on Large Scale Reflood Test-37 -- CCTF Test C1-11 (Run 020)," prepared by Japan Atomic Energy Research Institute, JAERI-Memo-58-064, March 1983.

J-017 "Data Report on Large Scale Reflood Test-38 -- CCTF Test C1-12 (Run 021)," prepared by Japan Atomic Energy Research Institute, JAERI-Memo-58-065, March 1983.

J-018 "Data Report on Large Scale Reflood Test-53 -- CCTF Test C1-13 (Run 022)," prepared by Japan Atomic Energy Research Institute, JAERI-Memo-59-031, February 1984.

J-019 "Data Report on Large Scale Reflood Test-54 -- CCTF Test C1-14 (Run 023)," prepared by Japan Atomic Energy Research Institute, JAERI-Memo-59-032, February 1984.

J-020 "Data Report on Large Scale Reflood Test 55 -- CCTF Test C1-15 (Run 024)," prepared by Japan Atomic Energy Research Institute, JAERI-Memo-59-033, February 1984.

J-021 "Data Report on Large Scale Reflood Test-56 -- CCTF Test C1-16 (Run 025)," prepared by Japan Atomic Energy Research Institute, JAERI-Memo-59-034, February 1984.

J-022 "Data Report on Large Scale Reflood Test-57 -- CCTF Test C1-17 (Run 036)," prepared by Japan Atomic Energy Research Institute, JAERI-Memo-59-035, February 1984.

J-023 "Data Report on Large Scale Reflood Test-58 -- CCTF Test C1-18 (Run 037)," prepared by Japan Atomic Energy Research Institute, JAERI-Memo-59-036, February 1984.

J-024 "Data Report on Large Scale Reflood Test-59 -- CCTF Test C1-19 (Run 038)," prepared by Japan Atomic Energy Research Institute, JAERI-Memo-59-037, February 1984.

J-025 "Data Report on Large Scale Reflood Test-60 -- CCTF Test C1-20 (Run 039)," prepared by Japan Atomic Energy Research Institute, JAERI-Memo-59-038, February 1984.

J-026 "Data Report on Large Scale Reflood Test-61 -- CCTF Test C1-21 (Run 040)," prepared by Japan Atomic Energy Research Institute, JAERI-Memo-59-039, February 1984.

J-027 "Data of CCTF Test C1-11 (Run 20), C1-19 (Run 38), and C1-20 (Run 039): Spool Piece Data," prepared by Japan Atomic Energy Research Institute, January 17, 1983.

J-028 "Data Report on Large Scale Reflood Test-62 -- CCTF Test C1-22 (Run 041)," prepared by Japan Atomic Energy Research Institute, JAERI-Memo-59-040, March 1984.

CCTF Core-II

J-041 "Data Report on Large Scale Reflood Test-40 -- CCTF Core-II Test C2-AC1 (Run 051)," prepared by Japan Atomic Energy Research Institute, JAERI-Memo-58-150 May 1983.

J-042 "Data Report on Large Scale Reflood Test-41 -- CCTF Core-II Test C2-AC2 (Run 052)," prepared by Japan Atomic Energy Research Institute, JAERI-Memo-58-154, May 1983.

J-043 "Data Report on Large Scale Reflood Test-42 -- CCTF Core-II Shakedown Test C2-SH1 (Run 053)," prepared by Japan Atomic Energy Research Institute, JAERI-Memo-58-166, May 1983.

J-044 "Data Report on Large Scale Reflood Test-43 -- CCTF Core-II Shakedown Test C2-SH2 (Run 054)," prepared by Japan Atomic Energy Research Institute, JAERI-Memo-58-155, May 1983.

J-045 "Data Report on Large Scale Reflood Test-44 -- CCTF Test C2-1 (Run 055)," prepared by Japan Atomic Energy Research Institute, JAERI-Memo-58-156, May 1983.

J-046 "Data Report on Large Scale Reflood Test-45 -- CCTF Core-II Test C2-2 (Run 056)," prepared by Japan Atomic Energy Research Institute, JAERI-Memo-58-157, May 1983.

J-047 "Data Report on Large Scale Reflood Test-77 -- CCTF Core-II Test C2-AA1 (Run 057)," prepared by Japan Atomic Energy Research Institute, JAERI-Memo-59-445, February 1985.

J-048 "Data Report on Large Scale Reflood Test-78 -- CCTF Core-II Test C2-AA2 (Run 058)," prepared by Japan Atomic Energy Research Institute, JAERI-Memo-59-446, February 1985.

J-049 "Data Report on Large Scale Reflood Test-79 -- CCTF Core-II Test C2-AS1 (Run 059)," prepared by Japan Atomic Energy Research Institute, JAERI-Memo-59-447, February 1985.

J-050 "Data Report on Large Scale Reflood Test-80 -- CCTF Core-II Test C2-AS2 (Run 060)," prepared by Japan Atomic Energy Research Institute, JAERI-Memo-59-448, February 1985.

J-051 "Data Report on Large Scale Reflood Test-81 -- CCTF Core-II Test C2-3 (Run 061)," prepared by Japan Atomic Energy Research Institute, JAERI-Memo-59-449, February 1985.

J-052 "Data Report on Large Scale Reflood Test-82 -- CCTF Core-II Test C2-4 (Run 062)," prepared by Japan Atomic Energy Research Institute, JAERI-Memo-59-450, February 1985.

J-053 "Data Report on Large Scale Reflood Test-83 -- CCTF Core-II Test C2-5 (Run 063)," prepared by Japan Atomic Energy Research Institute, JAERI-Memo-59-451, February 1985.

J-054 "Data Report on Large Scale Reflood Test-84 -- CCTF Core-II Test C2-6 (Run 064)," prepared by Japan Atomic Energy Research Institute, JAERI-Memo-59-452, February 1985.

J-055 "Data Report on Large Scale Reflood Test-85 -- CCTF Core-II Test C2-7 (Run 065)," prepared by Japan Atomic Energy Research Institute, JAERI-Memo-59-467, February 1985.

J-056 "Data Report on Large Scale Reflood Test-86 -- CCTF Core-II Test C2-8 (Run 067)," prepared by Japan Atomic Energy Research Institute, JAERI-Memo-59-453, February 1985.

J-057 "Data Report on Large Scale Reflood Test-87 -- CCTF Core-II Test C2-9 (Run 068)," prepared by Japan Atomic Energy Research Institute, JAERI-Memo-59-454, February 1985.

J-058 "Data Report on Large Scale Reflood Test-88 -- CCTF Core-II Test C2-10 (Run 069)," prepared by Japan Atomic Energy Research Institute, JAERI-Memo-59-455, February 1985.

J-059 "Data Report on Large Scale Reflood Test-89 -- CCTF Core-II Test C2-11 (Run 070)," prepared by Japan Atomic Energy Research Institute, JAERI-Memo-60-011, February 1985.

J-060 "Data Report on Large Scale Reflood Test-95 -- CCTF Core-II Test C2-12 (Run 071)," prepared by Japan Atomic Energy Research Institute, JAERI-Memo-60-172, July 1985.

J-061 "Data Report on Large Scale Reflood Test-96 -- CCTF Core-II Test C2-13 (Run 072)," prepared by Japan Atomic Energy Research Institute, JAERI-Memo-60-157, July 1985.

J-062 "Data Report on Large Scale Reflood Test-97 -- CCTF Core-II Test C2-14 (Run 074)," prepared by Japan Atomic Energy Research Institute, JAERI-Memo-60-173, July 1985.

J-063 "Data Report on Large Scale Reflood Test-98 -- CCTF Core-II Test C2-15 (Run 075)," prepared by Japan Atomic Energy Research Institute, JAERI-Memo-60-191, August 1985.

J-064 "Data Report on Large Scale Reflood Test-99 -- CCTF Core-II Test C2-16 (Run 076)," prepared by Japan Atomic Energy Research Institute, JAERI-Memo-60-158, February 1985.

J-065 "Data Report on Large Scale Reflood Test-100 -- CCTF Core-II Test C2-17 (Run 077)," prepared by Japan Atomic Energy Research Institute, JAERI-Memo-61-143, April 1986.

J-066 "Data Report on Large Scale Reflood Test-101 -- CCTF Core-II Test C2-18 (Run 078)," prepared by Japan Atomic Energy Research Institute, JAERI-Memo-60-223, August 1985.

J-067 "Data Report on Large Scale Reflood Test-128 -- CCTF Core-II Test C2-19 (Run 079)," prepared by Japan Atomic Energy Research Institute, JAERI-Memo-63-081, March 1988.

J-068 "Data Report on Large Scale Reflood Test-129 -- CCTF Core-II Test C2-20 (Run 080)," prepared by Japan Atomic Energy Research Institute, JAERI-Memo-63-082, March 1988.

J-069 "Data Report on Large Scale Reflood Test-130 -- CCTF Core-II Test C2-21 (Run 081)," prepared by Japan Atomic Energy Research Institute, JAERI-Memo-63-083, March 1988.

J-070 "Data Report on Major Experimental Results from CCTF Tests," prepared by Japan Atomic Energy Research Institute, JAERI-Memo-01-014.

SCTF Core-I

J-081 "Data Report on Large Scale Reflood Test-6 -- SCTF Test S1-SH1 (Run 505)," prepared by Japan Atomic Energy Research Institute, JAERI-Memo-9939, February 1982.

J-082 "Data Report on Large Scale Reflood Test-7 -- SCTF Test S1-SH2 (Run 506)," prepared by Japan Atomic Energy Research Institute, JAERI-Memo-9975, March 1982.

J-083 "Data Report on Large Scale Reflood Test-8 -- SCTF Test S1-01 (Run 507)," prepared by Japan Atomic Energy Research Institute, JAERI-Memo-9976, March 1982.

J-084 "Data Report on Large Scale Reflood Test-9 -- SCTF Test S1-02 (Run 508)," prepared by Japan Atomic Energy Research Institute, JAERI-Memo-9977, March 1982.

J-085 "Data Report on Large Scale Reflood Test-16 -- SCTF Test S1-03 (Run 509)," prepared by Japan Atomic Energy Research Institute, JAERI-Memo-57-318, November 1982.

J-086 "Data Report on Large Scale Reflood Test-17 -- SCTF Test S1-04 (Run 510)," prepared by Japan Atomic Energy Research Institute, JAERI-Memo-57-319, November 1982.

J-087 "Data Report on Large Scale Reflood Test-18 -- SCTF Test S1-05 (Run 511)," prepared by Japan Atomic Energy Research Institute, JAERI-Memo-57-320, November 1982.

J-088 "Data Report on Large Scale Reflood Test-21 -- SCTF Test S1-06 (Run 512)," prepared by Japan Atomic Energy Research Institute, JAERI-Memo-57-350, November 1982.

J-089 "Data Report on Large Scale Reflood Test-22 -- SCTF Test S1-07 (Run 513)," prepared by Japan Atomic Energy Research Institute, JAERI-Memo-57-351, November 1982.

J-090 "Data Report on Large Scale Reflood Test-23 -- SCTF Test S1-08 (Run 514)," prepared by Japan Atomic Energy Research Institute, JAERI-Memo-57-354, November 1982.

J-091 "Data Report on Large Scale Reflood Test-24 -- SCTF Test S1-09 (Run 515)," prepared by Japan Atomic Energy Research Institute, JAERI-Memo-57-355, November 1982.

J-092 "Data Report on Large Scale Reflood Test-25 -- SCTF Test S1-10 (Run 516)," prepared by Japan Atomic Energy Research Institute, JAERI-Memo-57-365, December 1982.

J-093 "Data Report on Large Scale Reflood Test-26 -- SCTF Test S1-11 (Run 517)," prepared by Japan Atomic Energy Research Institute, JAERI-Memo-57-372, December 1982.

J-094 "Data Report on Large Scale Reflood Test-28 -- SCTF Test S1-12 (Run 518)," prepared by Japan Atomic Energy Research Institute, JAERI-Memo-57-380, December 1982.

J-095 "Data Report on Large Scale Reflood Test-33 -- SCTF Test S1-13 (Run 519)," prepared by Japan Atomic Energy Research Institute, JAERI-Memo-57-401, December 1982.

J-096 "Data Report on Large Scale Reflood Test-29 -- SCTF Test S1-14 (Run 520)," prepared by Japan Atomic Energy Research Institute, JAERI-Memo-57-381, December 1982.

J-097 "Data Report on Large Scale Reflood Test-30 -- SCTF Test S1-15 (Run 521)," prepared by Japan Atomic Energy Research Institute, JAERI-Memo-57-382, December 1982.

J-098 "Data Report on Large Scale Reflood Test-31 -- SCTF Test S1-16 (Run 522)," prepared by Japan Atomic Energy Research Institute, JAERI-Memo-57-384, December 1982.

J-099 "Data Report on Large Scale Reflood Test-32 -- SCTF Test S1-17 (Run 523)," prepared by Japan Atomic Energy Research Institute, JAERI-Memo-57-385, December 1982.

J-100 "Data Report on Large Scale Reflood Test-34 -- SCTF Test S1-18 (Run 524)," prepared by Japan Atomic Energy Research Institute, JAERI-Memo-57-402, December 1982.

J-101 "Data Report on Large Scale Reflood Test-35 -- SCTF Test S1-19 (Run 525)," prepared by Japan Atomic Energy Research Institute, JAERI-Memo-57-403, December 1982.

J-102 "Data Report on Large Scale Reflood Test-46 -- SCTF Test S1-SH3 (Run 528)," prepared by Japan Atomic Energy Research Institute, JAERI-Memo-58-296, September 1983.

J-103 "Data Report on Large Scale Reflood Test-47 -- SCTF Test S1-SH4 (Run 529)," prepared by Japan Atomic Energy Research Institute, JAERI-Memo-58-297, September 1983.

J-104 "Data Report on Large Scale Reflood Test-48 -- SCTF Test S1-20 (Run 530)," prepared by Japan Atomic Energy Research Institute, JAERI-Memo-58-298, September 1983.

J-105 "Data Report on Large Scale Reflood Test-49 -- SCTF Test S1-21 (Run 531)," prepared by Japan Atomic Energy Research Institute, JAERI-Memo-58-311, September 1983.

J-106 "Data Report on Large Scale Reflood Test-50 -- SCTF Test S1-22 (Run 532)," prepared by Japan Atomic Energy Research Institute, JAERI-Memo-58-299, September 1983.

J-107 "Data Report on Large Scale Reflood Test-51 -- SCTF Test S1-23 (Run 536)," prepared by Japan Atomic Energy Research Institute, JAERI-Memo-58-300, September 1983.

J-108 "Data Report on Large Scale Reflood Test-52 -- SCTF Test S1-24 (Run 537)," prepared by Japan Atomic Energy Research Institute, JAERI-Memo-58-301, September 1983.

SCTF Core-II

J-121 "Data Report on Large Scale Reflood Test-63 -- SCTF Test S2-AC1 (Run 601)," prepared by Japan Atomic Energy Research Institute, JAERI-Memo-59-280, September 1984.

J-122 "Data Report on Large Scale Reflood Test-64 -- SCTF Test S2-AC2 (Run 602)," prepared by Japan Atomic Energy Research Institute, JAERI-Memo-59-281, September 1984.

J-123 "Data Report on Large Scale Reflood Test-65 -- SCTF Test S2-AC3 (Run 603)," prepared by Japan Atomic Energy Research Institute, JAERI-Memo-59-286, September 1984.

J-124 "Data Report on Large Scale Reflood Test-66 -- SCTF Test S2-SH1 (Run 604)," prepared by Japan Atomic Energy Research Institute, JAERI-Memo-59-282, September 1984.

J-125 "Data Report on Large Scale Reflood Test-67 -- SCTF Test S2-SH2 (Run 605)," prepared by Japan Atomic Energy Research Institute, JAERI-Memo-59-287, September 1984.

J-126 "Data Report on Large Scale Reflood Test-68 -- SCTF Test S2-01 (Run 606)," prepared by Japan Atomic Energy Research Institute, JAERI-Memo-59-288, September 1984.

J-127 "Data Report on Large Scale Reflood Test-69 -- SCTF Test S2-02 (Run 607)," prepared by Japan Atomic Energy Research Institute, JAERI-Memo-59-283, September 1984.

J-128 "Data Report on Large Scale Reflood Test-70 -- SCTF Test S2-03 (Run 608)," prepared by Japan Atomic Energy Research Institute, JAERI-Memo-59-432, January 1985.

J-129 "Data Report on Large Scale Reflood Test-71 -- SCTF Test S2-04 (Run 609)," prepared by Japan Atomic Energy Research Institute, JAERI-Memo-59-433, January 1985.

J-130 "Data Report on Large Scale Reflood Test-72 -- SCTF Test S2-05 (Run 610)," prepared by Japan Atomic Energy Research Institute, JAERI-Memo-59-434, February 1985.

J-131 "Data Report on Large Scale Reflood Test-73 -- SCTF Test S2-06 (Run 611)," prepared by Japan Atomic Energy Research Institute, JAERI-Memo-59-435, February 1985.

J-132 "Data Report on Large Scale Reflood Test-74 -- SCTF Test S2-07 (Run 612)," prepared by Japan Atomic Energy Research Institute, JAERI-Memo-59-436, February 1985.

J-133 "Data Report on Large Scale Reflood Test-75 -- SCTF Test S2-08 (Run 613)," prepared by Japan Atomic Energy Research Institute, JAERI-Memo-59-437, February 1985.

J-134 "Data Report on Large Scale Reflood Test-76 -- SCTF Test S2-09 (Run 614)," prepared by Japan Atomic Energy Research Institute, JAERI-Memo-59-438, February 1985.

J-135 "Data Report on Large Scale Reflood Test-90 -- SCTF Test S2-10 (Run 615)," prepared by Japan Atomic Energy Research Institute, JAERI-Memo-60-110, May 1985.

J-136 "Data Report on Large Scale Reflood Test-91 -- SCTF Test S2-11 (Run 616)," prepared by Japan Atomic Energy Research Institute, JAERI-Memo-60-111, May 1985.

J-137 "Data Report on Large Scale Reflood Test-92 -- SCTF Test S2-12 (Run 617)," prepared by Japan Atomic Energy Research Institute, JAERI-Memo-60-112, May 1985.

J-138 "Data Report on Large Scale Reflood Test-93 -- SCTF Test S2-13 (Run 618)," prepared by Japan Atomic Energy Research Institute, JAERI-Memo-60-113, May 1985.

J-139 "Data Report on Large Scale Reflood Test-94 - SCTF Test S2-14 (Run 619)," prepared by Japan Atomic Energy Research Institute, JAERI-Memo-60-114, May 1985.

J-140 "Data Report on Large Scale Reflood Test-99 -- SCTF Test S2-15 (Run 620)," prepared by Japan Atomic Energy Research Institute, JAERI-Memo-60-258, October 1985.

J-141 "Data Report on Large Scale Reflood Test-100 -- SCTF Test S2-16 (Run 621)," prepared by Japan Atomic Energy Research Institute, JAERI-Memo-60-259, October 1985.

J-142 "Data Report on Large Scale Reflood Test-101 -- SCTF Test S2-17 (Run 622)," prepared by Japan Atomic Energy Research Institute, JAERI-Memo-60-260, October 1985.

J-143 "Data Report on Large Scale Reflood Test-102 -- SCTF Test S2-18 (Run 623)," prepared by Japan Atomic Energy Research Institute, JAERI-Memo-60-268, October 1985.

J-144 "Data Report on Large Scale Reflood Test-103 -- SCTF Test S2-19 (Run 624)," prepared by Japan Atomic Energy Research Institute, JAERI-Memo-60-269, October 1985.

J-145 "Data Report on Large Scale Reflood Test-104 -- SCTF Test S2-21 (Run 626)," prepared by Japan Atomic Energy Research Institute, JAERI-Memo-60-270, October 1985.

SCTF Core-III

J-151 "Data Report on Large Scale Reflood Test-105 -- SCTF Test S3-SHI (Run 703)," prepared by Japan Atomic Energy Research Institute, JAERI-Memo-62-115, March 1987.

J-152 "Data Report on Large Scale Reflood Test-106 -- SCTF Test S3-SH2 (Run 704)," prepared by Japan Atomic Energy Research Institute, JAERI-Memo-62-116, March 1987.

J-153 "Data Report on Large Scale Reflood Test-107 -- SCTF Test S3-01 (Run 705)," prepared by Japan Atomic Energy Research Institute, JAERI-Memo-62-117, March 1987.

J-154 "Data Report on Large Scale Reflood Test-108 -- SCTF Test S3-02 (Run 706)," prepared by Japan Atomic Energy Research Institute, JAERI-Memo-62-118, March 1987.

J-155 "Data Report on Large Scale Reflood Test-109 -- SCTF Test S3-03 (Run 707)," prepared by Japan Atomic Energy Research Institute, JAERI-Memo-62-119, March 1987.

J-156 "Data Report on Large Scale Reflood Test-110 -- SCTF Test S3-04 (Run 708)," prepared by Japan Atomic Energy Research Institute, JAERI-Memo-62-120, March 1987.

J-157 "Data Report on Large Scale Reflood Test-111 -- SCTF Test S3-05 (Run 709)," prepared by Japan Atomic Energy Research Institute, JAERI-Memo-62-121, March 1987.

J-158 "Data Report on Large Scale Reflood Test-112 -- SCTF Test S3-06 (Run 710)," prepared by Japan Atomic Energy Research Institute, JAERI-Memo-62-122, March 1987.

J-159 "Data Report on Large Scale Reflood Test-113 -- SCTF Test S3-07 (Run 711)," prepared by Japan Atomic Energy Research Institute, JAERI-Memo-62-123, March 1987.

J-160 "Data Report on Large Scale Reflood Test-114 -- SCTF Test S3-08 (Run 712)," prepared by Japan Atomic Energy Research Institute, JAERI-Memo-62-124, March 1987.

J-161 "Data Report on Large Scale Reflood Test-115 -- SCTF Test S3-09 (Run 713)," prepared by Japan Atomic Energy Research Institute, JAERI-Memo-62-125, March 1987.

J-162 "Data Report on Large Scale Reflood Test-116 -- SCTF Test S3-10 (Run 714)," prepared by Japan Atomic Energy Research Institute, JAERI-Memo-62-126, March 1987.

J-163 "Data Report on Large Scale Reflood Test-117 -- SCTF Test S3-11 (Run 715)," prepared by Japan Atomic Energy Research Institute, JAERI-Memo-63-076, March 1988.

J-164 "Data Report on Large Scale Reflood Test-118 -- SCTF Test S3-12 (Run 716)," prepared by Japan Atomic Energy Research Institute, JAERI-Memo-63-233, June 1988.

J-165 "Data Report on Large Scale Reflood Test-119 -- SCTF Test S3-13 (Run 717)," prepared by Japan Atomic Energy Research Institute, JAERI-Memo-63-077, March 1988.

J-166 "Data Report on Large Scale Reflood Test-120 -- SCTF Test S3-14 (Run 718)," prepared by Japan Atomic Energy Research Institute, JAERI-Memo-62-335, September 1987.

J-167 "Data Report on Large Scale Reflood Test-121 -- SCTF Test S3-15 (Run 719)," prepared by Japan Atomic Energy Research Institute, JAERI-Memo-62-330, September 1987.

J-168 "Data Report on Large Scale Reflood Test-122 -- SCTF Test S3-16 (Run 720)," prepared by Japan Atomic Energy Research Institute, JAERI-Memo-63-078, March 1988.

J-169 "Data Report on Large Scale Reflood Test-123 -- SCTF Test S3-17 (Run 721)," prepared by Japan Atomic Energy Research Institute, JAERI-Memo-63-079, March 1988.

J-170 "Data Report on Large Scale Reflood Test-124 -- SCTF Test S3-18 (Run 722)," prepared by Japan Atomic Energy Research Institute, JAERI-Memo-63-234, June 1988.

J-171 "Data Report on Large Scale Reflood Test-126 -- SCTF Test S3-20 (Run 724)," prepared by Japan Atomic Energy Research Institute, JAERI-Memo-63-080, March 1988.

J-172 "Data Report on Large Scale Reflood Test-127 -- SCTF Test S3-21 (Run 725)," prepared by Japan Atomic Energy Research Institute, JAERI-Memo-01-397, November 1989.

J-173 "Data Report on Large Scale Reflood Test-128 -- SCTF Test S3-22 (Run 726)," prepared by Japan Atomic Energy Research Institute, JAERI-Memo-01-065, March 1989.

QUICK LOOK REPORTS

CCTF Core-I

J-201 "Quick Look Report on Large Scale Reflood Test, Shakedown Test 1 -- CCTF Test C1-SH1 (Run 005)," prepared by Japan Atomic Energy Research Institute, JAERI-Memo-8641, January 1979.

J-202 "Quick Look Report on Large Scale Reflood Test, Shakedown Test 3 -- CCTF Test C1-SH3 (Run 007)," prepared by Japan Atomic Energy Research Institute, JAERI-Memo-8930, June 1980.

J-203 "Quick Look Report on Large Scale Reflood Test, Shakedown Test 4 -- CCTF Test C1-SH4 (Run 008)," prepared by Japan Atomic Energy Research Institute, JAERI-Memo-9149, October 1980.

J-204 "Quick Look Report on Large Scale Reflood Test-1 -- CCTF Test C1-1 (Run 010)," prepared by Japan Atomic Energy Research Institute, JAERI-Memo-8453, August, 1979.

J-205 "Quick Look Report on Large Scale Reflood Test-2 -- CCTF Test C1-2 (Run 011)," prepared by Japan Atomic Energy Research Institute, JAERI-Memo-8530, October 1979.

J-206 "Quick Look Report on Large Scale Reflood Test-3 -- CCTF Test C1-3 (Run 012)," prepared by Japan Atomic Energy Research Institute, JAERI-Memo-8538, November 1979.

J-207 "Quick Look Report on Large Scale Reflood Test-4 -- CCTF Test C1-4 (Run 013)," prepared by Japan Atomic Energy Research Institute, JAERI-Memo-8685, February 1980.

J-208 "Quick Look Report on Large Scale Reflood Test-5 -- CCTF Test C1-5 (Run 014)," prepared by Japan Atomic Energy Research Institute, JAERI-Memo-8696, February 1980.

J-209 "Quick Look Report on Large Scale Reflood Test-6 -- CCTF Test C1-6 (Run 015)," prepared by Japan Atomic Energy Research Institute, JAERI-Memo-8990, July 1980.

J-210 "Quick Look Report on Large Scale Reflood Test-7 -- CCTF Test C1-7 (Run 016)," prepared by Japan Atomic Energy Research Institute, JAERI-Memo-8991, July 1980.

J-211 "Quick Look Report on Large Scale Reflood Test-8 -- CCTF Test C1-8 (Run 017)," prepared by Japan Atomic Energy Research Institute, JAERI-Memo-8992, July 1980.

J-212 "Quick Look Report on Large Scale Reflood Test-9 -- CCTF Test C1-9 (Run 018)," prepared by Japan Atomic Energy Research Institute, JAERI-Memo-9125, September 1980.

J-213 "Quick Look Report on Large Scale Reflood Test-10 -- CCTF Test C1-10 (Run 019)," prepared by Japan Atomic Energy Research Institute, JAERI-Memo-9207, November 1980.

J-214 "Quick Look Report on Large Scale Reflood Test-11 -- CCTF Test C1-11 (Run 020)," prepared by Japan Atomic Energy Research Institute, JAERI-Memo-9208, November 1980.

J-215 "Quick Look Report on Large Scale Reflood Test-12 -- CCTF Test C1-12 (Run 021)," prepared by Japan Atomic Energy Research Institute, JAERI-Memo-9270, January 1981.

J-216 "Quick Look Report on Large Scale Reflood Test-13 -- CCTF Test C1-13 (Run 022)," prepared by Japan Atomic Energy Research Institute, JAERI-Memo-9282, January 1981.

J-217 "Quick Look Report on Large Scale Reflood Test-14 -- CCTF Test C1-14 (Run 023)," prepared by Japan Atomic Energy Research Institute, JAERI-Memo-9305, February 1981.

J-218 "Quick Look Report on Large Scale Reflood Test-15 -- CCTF Test C1-15 (Run 024)," prepared by Japan Atomic Energy Research Institute, JAERI-Memo-9329, February 1981.

J-219 "Quick Look Report on Large Scale Reflood Test-16 -- CCTF Test C1-16 (Run 025)," prepared by Japan Atomic Energy Research Institute, JAERI-Memo-9349, March 1981.

J-220 "Quick Look Report on Large Scale Reflood Test-18 -- CCTF Test C1-17 (Run 036)," prepared by Japan Atomic Energy Research Institute, JAERI-Memo-9712, October 1981.

J-221 "Quick Look Report on Large Scale Reflood Test-19 -- CCTF Test C1-18 (Run 037)," prepared by Japan Atomic Energy Research Institute, JAERI-Memo-9713, October 1981.

J-222 "Quick Look Report on Large Scale Reflood Test-23 -- CCTF Test C1-19 (Run 038)," prepared by Japan Atomic Energy Research Institute, JAERI-Memo- 9767, November 1981.

J-223 "Quick Look Report on Large Scale Reflood Test-24 -- CCTF Test C1-20 (Run 039)," prepared by Japan Atomic Energy Research Institute, JAERI-Memo-9768, November 1981.

J-224 "Quick Look Report on Large Scale Reflood Test-29 -- CCTF Test C1-21 (Run 040)," prepared by Japan Atomic Energy Research Institute, JAERI-Memo-9903, January 1982.

J-225 "Quick Look Report on Large Scale Reflood Test-30 -- CCTF Test C1-22 (Run 041)," prepared by Japan Atomic Energy Research Institute, JAERI Memo 9904, February 1982.

CCTF Core-II

J-241 "Quick Look Report on Large Scale Core-II Reflood Test, First Shakedown Test C2-SH1 (Run 53)," prepared by Japan Atomic Energy Research Institute, JAERI-Memo-57-397, December 1982.

J-242 "Quick Look Report on CCTF Core-II Reflood Test, Second Shakedown Test, C2-SH2 (Run 54)," prepared by Japan Atomic Energy Research Institute, JAERI-Memo-57-391, December 1982.

J-243 "Quick Look Report on CCTF Core-II Reflood Test C2-1 (Run 55)," prepared by Japan Atomic Energy Research Institute, JAERI-Memo-57-392, December 1982.

J-244 "Quick Look Report on CCTF Core-II Reflood Test C2-2 (Run 56)," prepared by Japan Atomic Energy Research Institute, JAERI-Memo-57-393, December 1982.

J-245 "Quick Look Report on CCTF Core-II Reflood Test C2-AA1 (Run 57) -- Investigation of the Reflood Phenomena Under Upper Plenum Injection Condition," prepared by Japan Atomic Energy Research Institute, JAERI-Memo-58-415, November, 1983.

J-246 "Quick Look Report on CCTF Core-II Reflood Test C2-AA2 (Run 58) -- Investigation of Downcomer Injection Effects," prepared by Japan Atomic Energy Research Institute, JAERI-Memo-58-386, October 1983.

J-247 "Quick Look Report on CCTF Core-II Reflood Test, C2-AS1 (Run 59) -- Investigation on the Reflood Phenomena Under Upper Plenum Injection Condition," prepared by Japan Atomic Energy Research Institute, JAERI-Memo-58-416, November 1983.

J-248 "Quick Look Report on CCTF Core-II Reflood Test C2-AS2 (Run 60) -- Effect of Vent Valve Type ECCS.1," prepared by Japan Atomic Energy Research Institute, JAERI-Memo-58-459, January 1984.

J-249 "Quick Look Report on CCTF Core-II Reflood Test C2-3 (Run 61) -- Investigation of Initial Downcomer Water Accumulation Rate Effects," prepared by Japan Atomic Energy Research Institute, JAERI-Memo-58-460, January 1984.

J-250 "Quick Look Report on CCTF Core-II Reflood Test C2-4 (Run 62) -- Investigation of Reproducibility," prepared by Japan Atomic Energy Research Institute, JAERI-Memo-58-479, January 1984.

J-251 "Quick Look Report on CCTF Core-II Reflood Test, C2-5 (Run 63) -- Investigation of the Reflood Phenomena Under Low Power Condition," prepared by Japan Atomic Energy Research Institute, JAERI-Memo-59-046, February 1984.

J-252 "Quick Look Report on CCTF Core-II Reflood Test, C2-6 (Run 64) -- Effect of Radial Power Profile," prepared by Japan Atomic Energy Research Institute, JAERI-Memo-59-012, February 1984.

J-253 "Quick Look Report on CCTF Core-II Reflood Test, C2-7 (Run 65) -- Calibration Test," prepared by Japan Atomic Energy Research Institute, JAERI-Memo-59-047, February 1984.

J-254 "Quick Look Report on CCTF Core-II Reflood Test, C2-8 (Run 67) --Effect of Systems Pressure," prepared by Japan Atomic Energy Research Institute, JAERI-Memo-59-028, February 1984.

J-255 "Quick Look Report on CCTF Core-II Reflood Test C2-9 (Run 68) -- Effect of LPCI Flow Rate," prepared by Japan Atomic Energy Research Institute, JAERI-Memo-59-048, February 1984.

J-256 "Quick Look Report on CCTF Core-II Reflood Test C2-10 (Run 69) -- Effect of Vent Valve Type ECCS 2," prepared by Japan Atomic Energy Research Institute, JAERI-Memo-59-029, February 1984.

J-257 "Quick Look Report on CCTF Core-II Reflood Test C2-11 (Run 70) -- Investigation of the End-of-Bypass and Refill Phenomena Under the Condition of Loop Isolations," prepared by Japan Atomic Energy Research Institute, JAERI Memo-59-013, February 1984.

J-258 "Quick Look Report on CCTF Core-II Reflood Test C2-12 (Run 71) -- Best Estimate Reflood Experiment," prepared by Japan Atomic Energy Research Institute, JAERI Memo-59-326, October 1984.

J-259 "Quick Look Report on CCTF Core-II Reflood Test, C2-13 (Run 72) -- Investigation of the Reflood Phenomena for No LPCI Pump Failure Simulation Upper Plenum Injection Test," prepared by Japan Atomic Energy Research Institute, JAERI-Memo-59-416, January 1985.

J-260 "Quick Look Report on CCTF Core-II Reflood Test C2-14 (Run 74) -- Investigation of the Refill Phenomena and Its Effect on the Reflooding Behavior," prepared by Japan Atomic Energy Research Institute, JAERI-Memo-59-352, October 1984.

J-261 "Quick Look Report on CCTF Core-II Reflood Test C2-15 (Run 75) -- Investigation of FLECHT-SET Coupling Test Results," prepared by Japan Atomic Energy Research Institute, JAERI-Memo-60-255, September 1985.

J-262 "Quick Look Report on CCTF Core-II Reflood Test C2-16 (Run 76) -- Effect of Asymmetric Upper Plenum Injection on Reflood Phenomena," prepared by Japan Atomic Energy Research Institute, JAERI-Memo-60-142, June 1985.

J-263 "Quick Look Report on CCTF Core-II Reflood Test C2-17 (Run 77) -- Investigation of the Refill Phenomena with Core Reversal Steam Flow," prepared by Japan Atomic Energy Research Institute, JAERI- Memo-61-136, May 1986.

J-264 "Quick Look Report on CCTF Core-II Reflood Test C2-18 (Run 78) -- Best Estimated Refill/Reflood Upper Plenum Injection Test," prepared by Japan Atomic Energy Research Institute, JAERI-Memo-60-372, December 1985.

SCTF Core-I

J-281 "Quick Look Report on Large Scale Reflood Test-17 -- SCTF Test S1-SH1 (Run 505)," prepared by Japan Atomic Energy Research Institute, JAERI-Memo-9702, September 1981.

J-282 "Quick Look Report on Large Scale Reflood Test-20 -- SCTF Test S1-SH2 (Run 506)," prepared by Japan Atomic Energy Research Institute, JAERI-Memo-9732, October 1981.

J-283 "Quick Look Report on Large Scale Reflood Test-22 -- SCTF Test S1-02 (Run 508)," prepared by Japan Atomic Energy Research Institute, JAERI-Memo-9734, November 1981.

J-284 "Quick Look Report on Large Scale Reflood Test-25 -- SCTF Test S1-03 (Run 509)," prepared by Japan Atomic Energy Research Institute, JAERI-Memo-9803, November 1981.

J-285 "Quick Look Report on Large Scale Reflood Test-26 -- SCTF Test S1-04 (Run 510), prepared by Japan Atomic Energy Research Institute, JAERI-Memo-9804, November 1981.

J-286 "Quick Look Report on Large Scale Reflood Test-27 -- SCTF Test S1-05 (Run 511)," prepared by Japan Atomic Energy Research Institute, JAERI-Memo-9805, November 1981.

J-287 "Quick Look Report on Large Scale Reflood Test-28 -- SCTF Test S1-06 (Run 512)," prepared by Japan Atomic Energy Research Institute, JAERI-Memo-9806, November 1981.

J-288 "Quick Look Report on Large Scale Reflood Test-31 -- SCTF Test S1-07 (Run 513)," prepared by Japan Atomic Energy Research Institute, JAERI-Memo-57-176, July 1982.

J-289 "Quick Look Report on Large Scale Reflood Test-32 -- SCTF Test S1-08 (Run 514)," prepared by Japan Atomic Energy Research Institute, JAERI-Memo-57-177, July 1982.

J-290 "Quick Look Report on Large Scale Reflood Test-33 -- SCTF Test S1-09 (Run 515)," prepared by Japan Atomic Energy Research Institute, JAERI-Memo-57-178, July 1982.

J-291 "Quick Look Report on Large Scale Reflood Test 34 -- SCTF Test S1-10 (Run 516)," prepared by Japan Atomic Energy Research Institute, JAERI-Memo-57-179, July 1982.

J-292 "Quick Look Report on Large Scale Reflood Test-35 -- SCTF Test S1-11 (Run 517)," prepared by Japan Atomic Energy Research Institute, JAERI-Memo-57-180, July 1982.

EVALUATION REPORTS

CCTF Core-I

J-401 "Evaluation Report on CCTF Core-I Reflood Test C1-SH5 (Run 009) -- Investigation of the PKL Coupling Test," prepared by Japan Atomic Energy Research Institute, JAERI-Memo-9965, February 1982.

J-402 "Evaluation Report on CCTF Core-I Reflood Test C1-1 (Run 010) -- Investigation of the Loop Flow Resistance Effect," prepared by Japan Atomic Energy Research Institute, JAERI-Memo-9966, February 1982 (publicly released as JAERI-M-83-140, September 1983).

J-403 "Evaluation Report on CCTF Core-I Reflood Tests C1-2 (Run 11) and C1-11 (Run 20) -- Reproducibility Test," prepared by Japan Atomic Energy Research Institute, JAERI-Memo-57-048, March 1982.

J-404 "Evaluation Report on CCTF Core-I Reflood Tests C1-2 (Run 11) and C1-11 (Run 20) -- Effect of the Installment of the Baffle Plates in the Control Rod Guide Tubes and the Spool Piece in the Primary Loops," prepared by Japan Atomic Energy Research Institute, JAERI-M-83-094, June 1983.

J-405 "Evaluation Report on CCTF Core-I Reflood Tests C1-2 (Run 11) and C1-3 (Run 12) -- Effects of Initial Downcomer Wall Temperature on System Behavior of a PWR during Reflood Phase of a Loss-Of-Coolant Accident," prepared by Japan Atomic Energy Research Institute, JAERI-Memo-9925, January 1982.

J-406 "Evaluation Report on CCTF Core-I Reflood Tests C1-2 (Run 11) and C1-3 (Run 12) -- Effects of Initial Superheat of the Downcomer Wall," prepared by Japan Atomic Energy Research Institute, JAERI-M-83-090, June 1983.

J-407 "Evaluation Report on CCTF Core-I Reflood Test C1-4 (Run 13) and C1-15 (Run 24) -- Investigation of the Refill Simulation and the Nitrogen Injection Effects," prepared by Japan Atomic Energy Research Institute, JAERI-Memo-9967, February 1982 (publicly released as JAERI-M-83-121, August 1983).

J-408 "Evaluation Report on CCTF Core-I Reflood Test C1-5 (Run 14) -- Overall System Thermo-Hydrodynamic Behavior Observed in the Base Case Test," prepared by Japan Atomic Energy Research Institute, JAERI-Memo-57-051, March, 1982 (publicly released as JAERI-M-83-207, February 1983).

J-409 "Evaluation Report on CCTF Core-I Reflood Tests C1-5 (Run 14), C1-10 (Run 19) and C1-12 (Run 21) -- Effects of Containment Pressure on System Behaviors During Reflood Phase of a LOCA," prepared by Japan Atomic Energy Research Institute, JAERI-Memo-57-013, February 1982 (publicly released as JAERI-M-83-091, June 1983).

J-410 "Evaluation Report on CCTF Core-I Reflood Tests C1-5 (Run 14), C1-17 (Run 36) and C1-20 (Run 39) -- Core Thermo-Hydrodynamics and Thermally Multidimensional Effects On It," prepared by Japan Atomic Energy Research Institute, JAERI-Memo-57-052, March 1982.

J-411 "Evaluation Report on CCTF Core-I Reflood Tests C1-6 (Run 15), C1-9 (Run 18), C1-11 (Run 20) and C1-13 (Run 22) -- Effects of ECC Water Injection Rate," prepared by Japan Atomic Energy Research Institute, JAERI-Memo-57-018, March 1982 (publicly released as JAERI-M-83-044).

J-412 "Evaluation Report on CCTF Core-I Reflood Tests C1-7 (Run 16) and C1-14 (Run 23) -- Effects of Initial Clad Temperature," prepared by Japan Atomic Energy Research Institute, JAERI-Memo-9953, February 1982 (publicly released as JAERI-M-83-026).

J-413 "Evaluation Report on CCTF Core-I Reflood Tests C1-18 (Run 37) and C1-8 (Run 17) -- Investigation of the Effect of Water Remaining in the Loop Seal Section on Reflood Behavior," prepared by Japan Atomic Energy Research Institute, JAERI-Memo-9996, February 1982 (publicly released as JAERI-M-83-115, July 1983).

J-414 "Evaluation Report on CCTF Core-I Reflood Tests C1-16 (Run 25), C1-21 (Run 40) and C1-22 (Run 41) -- Comparison of the FLECHT-SET Test Results With The FLECHT Coupling Test Results," prepared by Japan Atomic Energy Research Institute, JAERI-Memo-57-014, March 1982 (publicly released as JAERI-M-83-065, May 1983).

J-415 "Evaluation Report on CCTF Core-I Reflood Tests C1-17 (Run 36) and C1-20 (Run 39)," prepared by Japan Atomic Energy Research Institute, JAERI-M-83-028, February 1983.

J-416 "Evaluation Report on CCTF Core-I Reflood Test C1-19 (Run 38) -- Experimental Assessment of the Evaluation Model For the Safety Analysis on the Reflood Phase of a PWR LOCA," prepared by Japan Atomic Energy Research Institute, JAERI-Memo-57-053, March, 1982 (publicly released as JAERI-M-83-029, February 1983).

J-417 "Development of the Model for the Mass Balance Calculation of the CCTF Test -- The Estimation of the Core Inlet Mass Flow Rate," prepared by Japan Atomic Energy Research Institute, JAERI-Memo-9936, January 1982.

J-418 "Analysis Report on CCTF Core-I Reflood Tests," prepared by Japan Atomic Energy Research Institute, JAERI-Memo-57-057, March 1982.

J-419 "Large Scale Reflood Test With Cylindrical Core Test Facility (CCTF) -- Core-I FY 1979 Tests," prepared by Japan Atomic Energy Research Institute, JAERI-Memo-82-002, March 1982.

J-420 "CCTF Core-I Test Results," prepared by Japan Atomic Energy Research Institute, JAERI-M-82-073, July 1982.

J-421 "Findings in CCTF Core-I Test," prepared by Japan Atomic Energy Research Institute, JAERI-Memo-58-050, February 1983.

J-422 "Results of Downcomer CCFL Experiment," prepared by Japan Atomic Energy Research Institute, JAERI-Memo-59-245, August 1984.

CCTF Core-II

J-441 "Evaluation of CCTF Core-II Acceptance Test-1 (Run 051)," prepared by Japan Atomic Energy Research Institute, JAERI-Memo-57-275, October 1982.

J-442 "Evaluation Report on CCTF Core-II Reflood Tests C2-AC1 (Run 51) and C2-4 (Run 62) -- Effect of Initial Clad Temperature," prepared by Japan Atomic Energy Research Institute, JAERI-M-84-026, February 1984.

J-443 "Evaluation of CCTF Core-II Acceptance Test 2 (Run 052)," prepared by Japan Atomic Energy Research Institute, JAERI-Memo-57-375, November 1982.

J-444 "Evaluation of CCTF Core-II Second Acceptance Test C2-AC2 (Run 052) -- Investigation of Difference in Reflooding Behaviors Between Core-I and Core-II Facilities," prepared by Japan Atomic Energy Research Institute, JAERI-M-84-036, March 1984.

J-445 "Evaluation Report on CCTF Core-II Reflood Test Second Shakedown Test C2-SH2 (Run 54) -- Effect of Core Supplied Power on Reflood Phenomena," prepared by Japan Atomic Energy Research Institute, JAERI-M-85-025, March 1985.

J-446 "Evaluation Report on CCTF Core-II Reflood Test C2-AA2 (Run 58) -- Investigation of Downcomer Injection Effects," prepared by Japan Atomic Energy Research Institute, JAERI-M-89-227, January 1990.

J-447 "Evaluation Report on CCTF Core-II Reflood Test C2-3 (Run 61) -- Investigation of Initial Downcomer Water Accumulation Velocity Effects," prepared by Japan Atomic Energy Research Institute, JAERI-M-86-185, January 1987.

J-448 "Evaluation Report on CCTF Core-II Reflood Test C2-4 (Run 62) -- Investigation of Reproducibility," prepared by Japan Atomic Energy Research Institute, JAERI-M-85-026, March 1985.

J-449 "Evaluation Report on CCTF Core-II Reflood Test C2-6 (Run 64) -- Effect of Radial Power Profile," prepared by Japan Atomic Energy Research Institute, JAERI-M-85-027, March 1985.

J-450 "Evaluation Report on CCTF Core-II Reflood Test C2-8 (Run 67) -- Effect System Pressure," prepared by Japan Atomic Energy Research Institute, JAERI-M-87-001, January 1987.

J-451 "Evaluation Report on CCTF Core-II Reflood Test C2-9 (Run 68) -- Effect of LPCI Flow Rate," prepared by Japan Atomic Energy Research Institute, JAERI-M-87-002, February 1987.

J-452 "Evaluation Report on CCTF Core-II Reflood Test C2-16 (Run 76) -- Effect of Asymmetric Upper Plenum Injection on Reflood Phenomena," prepared by Japan Atomic Energy Research, JAERI-M-87-051, March 1987.

J-453 "Evaluation Report on CCTF Core-II Reflood Test C2-18 (Run 78) --Best Estimate Refill/Reflood Upper Plenum Injection Test," prepared by Japan Atomic Energy Research Institute, JAERI-M-87-052, March 1987.

J-454 "Evaluation Report on CCTF Core-II Reflood Test C2-19 (Run 79) -- Combined Injection Mode Under EM Condition," prepared by Japan Atomic Energy Research Institute, JAERI-Memo-62-334, September 1987.

J-455 Pointner, W., "Study on Effects of Combined Injection (EM Conditions) on Reflood Phenomena (Test C2-19/Run 79)," Japan Atomic Energy Research Institute, JAERI-Memo-62-294, August 1987.

J-456 "Evaluation Report on CCTF Core-II Reflood Tests C2-20 (Run 80) and C2-21 (Run 81) -- BE Condition & Effect of Hot Leg ECC Flow Rate Under Combined Injection Mode," prepared by Japan Atomic Energy Research Institute, JAERI-Memo-63-267, July 1988.

J-457 "Analysis Report on Large Scale Reflood Tests with Cylindrical Core Test Facility -- Tests in FY 1983," prepared by Japan Atomic Energy Research Institute, JAERI-Memo-60-108.

J-458 "Analysis Report on Large Scale Reflood Tests with Cylindrical Core Test Facility -- Tests in FY 1984," prepared by Japan Atomic Energy Research Institute, JAERI-Memo-60-403.

J-459 "Analysis Report on CCTF Reflood Test," prepared by Japan Atomic Energy Research Institute, JAERI-Memo-61-059.

SCTF Core-I

J-481 "Design of Slab Core Test Facility (SCTF) in Large Scale Reflood Test Program. Part I: Core-I," prepared by Japan Atomic Energy Research Institute, JAERI-Memo-9701, September 1981 (publicly released as JAERI-M-83-080, June 1983).

J-482 "System Pressure Effects on Reflooding Phenomena Observed in the SCTF Core-I Forced Flooding Effects," prepared by Japan Atomic Energy Research Institute, JAERI-Memo-9729, October 1981 (publicly released as JAERI-M-83-079, June 1983).

J-483 "Dispersed Flow and Corresponding Phenomena in SCTF Observed with High-Speed Camera," prepared by Japan Atomic Energy Research Institute, JAERI-M-9971, February 1982.

J-484 "Effects of Core Inlet Water Subcooling on Reflooding Phenomena Under Forced Flooding in SCTF Core-I Tests," prepared by Japan Atomic Energy Research Institute, JAERI-Memo-9972, February 1982 (publicly released as JAERI-M-83-122, August 1983).

J-485 "Effect of Upper Plenum Water Accumulation on Reflooding Phenomena Under Forced Flooding in SCTF Core-I Tests," prepared by Japan Atomic Energy Research Institute, JAERI-Memo-9973, February 1982 (publicly released as JAERI-M-83-114, July 1983).

J-486 "SCTF Core-I Tests Results: System Pressure Effects on Reflooding Phenomena," prepared by Japan Atomic Energy Research Institute, JAERI-M-82-075, July 1982.

J-487 "Examination of Repeatability in Reflood Phenomena Under Forced Flooding in SCTF Core-I Tests," prepared by Japan Atomic Energy Research Institute, JAERI-Memo-57-251, September 1982 (publicly released as JAERI-M-083-237, January 1984).

J-488 "Core Thermal Behavior Under Forced Feed Flooding in SCTF Core-I Tests," prepared by Japan Atomic Energy Research Institute, JAERI-Memo-57-270, October 1982.

J-489 "Heat Transfer Enhancement Due to Chimney Effect in Reflood Phase," prepared by Japan Atomic Energy Research Institute, JAERI-Memo-57-297, October 1982.

J-490 "Effect of LPCI Water Injection Rate on Carryover Characteristics During Reflood," prepared by Japan Atomic Energy Research Institute, JAERI-Memo-58-035, February 1983.

J-491 "Droplets Flow and Heat Transfer at Top Region of Core In Reflood Phase," prepared by Japan Atomic Energy Research Institute, JAERI-M-83-022, February 1983.

J-492 "Evaluation of Cross Flow Velocity Across Rod Bundles During Reflood Phase in SCTF Core-I Forced Feed Flooding Tests," prepared by Japan Atomic Energy Research Institute, JAERI-Memo-58-443, December 1983.

J-493 "Effects of Upper Plenum Injection on Thermo-Hydrodynamic Behavior Under Refill and Reflood Phases of a PWR-LOCA," prepared by Japan Atomic Energy Research Institute, JAERI-Memo-59-052, February 1984 (publicly released as JAERI-M-84-221, December 1984).

J-494 "Cold Leg Injection Reflood Test Results in the SCTF Core-I Under Constant System Pressure," prepared by Japan Atomic Energy Research Institute, JAERI-Memo-59-053, February 1984 (publicly released as JAERI-M-90-129, August 1990).

J-495 "Characteristics of Lower Plenum Injection Reflood Tests in SCTF Core-I," prepared by Japan Atomic Energy Research Institute, JAERI-Memo-59-051, March 1984 (publicly released as JAERI-M-84-223, December 1984).

J-496 "Examination of Refill Simulation Test Results in SCTF Core-I," prepared by Japan Atomic Energy Research Institute, JAERI-Memo-60-098, April 1985.

J-497 "Effects of Core Inlet Water Mass Flow Rate on Reflooding Phenomena in the Forced Feed SCTF Core-I Tests," prepared by Japan Atomic Energy Research Institute, JAERI-Memo-61-024, February 1986 (publicly released as JAERI-M-88-166, September 1988).

J-498 "Effects of Radial Core Power Profile on Core Thermo-Hydraulic Behavior during Reflood Phase in SCTF Core-I Forced Feed Tests," prepared by Japan Atomic Energy Research Institute, JAERI-M-91-093, June 1991.

SCTF Core-II

J-521 "Design of Slab Core Test Facility (SCTF) in Large Scale Reflood Test Program, Part II: Core-II," prepared by Japan Atomic Energy Research Institute, JAERI-Memo-59-396, December 1984.

J-522 "Effects of Radial Power Profile on Two-Dimensional Thermal-Hydraulic Behavior in Core in SCTF Core-II Cold Leg Injection Tests," prepared by Japan Atomic Energy Research Institute, JAERI-Memo-59-415, January 1985.

J-523 "Study on ECC Injection Modes in Reflood Tests with SCTF Core-II Comparison between Gravity and Forced Feeds," prepared by Japan Atomic Energy Research Institute, JAERI-Memo-61-115, March 1985 (publicly released as JAERI-M-91-001, February 1991).

J-524 "Development of SCTF Cold Leg Injection Test Method for Eliminating U-Tube Oscillation During the Initial Period," prepared by Japan Atomic Energy Research Institute, JAERI-Memo-60-145, June 1984 (publicly released as JAERI-M-90-107, July 1990).

J-525 "Two Dimensional Thermal-Hydraulic Behavior in Core in SCTF Core-II Cold Leg Injection Tests (Radial Power Profile Test Results)," prepared by Japan Atomic Energy Research Institute, JAERI-M-85-106, July 1985.

J-526 "Evaluation of SCTF Core-II Tests with Upward Steam Flow and Upper Plenum Water Injection," prepared by Japan Atomic Energy Research Institute, JAERI-Memo-60-287, October 1985.

J-527 "Data Reduction and Analysis Procedures in SCTF Core-II," prepared by Japan Atomic Energy Research Institute, JAERI-Memo-60-393, January 1986.

J-528 "Two-Dimensional Thermal-Hydraulic Behavior in Core in SCTF Core-II Forced Feed Reflood Tests (Effects of Radial Power and Temperature Distributions)," prepared by Japan Atomic Energy Research Institute, JAERI, Memo-60-395, January 1986 (publicly released as JAERI-M-86-195, January 1987).

J-529 "Comparison of Facility Characteristics Between SCTF Core-I and Core-II," prepared by Japan Atomic Energy Research Institute, JAERI-Memo-61-018, February 1986 (publicly released as JAERI-M-90-130, August 1990).

J-530 "Large Scale Reflood Test Results with Slab Core Test Facility (SCTF): Core-II Tests in FY 1984," prepared by Japan Atomic Energy Research Institute, JAERI-Memo-61-058.

J-531 "Reflood Behavior at Low Initial Clad Temperature in Slab Core Test Facility Core-II," prepared by Japan Atomic Energy Research Institute, JAERI-Memo-61-066, March, 1986 (publicly released as JAERI-M-90-106, July 1990).

J-532 "Analysis of SCTF/CCTF Counterpart Test Results," prepared by Japan Atomic Energy Research Institute, JAERI-Memo-61-114, March 1986 (publicly released as JAERI-M-90-083, June 1990).

J-533 "Effects of System Pressure on Two-Dimensional Thermal-Hydraulic Behavior in Core in SCTF Core-II Reflood Tests." prepared by Japan Atomic Energy Research Institute, JAERI-Memo-61-265, August 1986.

J-534 "Evaluation Report on SCTF Core-II Test S2-19 (Effect of LPCI Flow Rate on Core Thermal Hydraulic Behavior During Reflood in a PWR)," prepared by Japan Atomic Energy Research Institute, JAERI-Memo-01-078, March 1989.

J-535 "Evaluation Report on SCTF Core-II Test S2-08 (Effect of Core Inlet Subcooling on Thermal-Hydraulic Behavior Including Two-Dimensional Behavior in Pressure Vessel during Reflood in a PWR)," prepared by Japan Atomic Energy Research Institute, JAERI-Memo-01-058, March 1989 (publicly released as JAERI-M-90-236, January 1991).

J-536 "Analysis Report on SCTF Core-I and II Reflood Test," prepared by Japan Atomic Energy Research Institute, JAERI-Memo-01-348.

J-537 "Evaluation Report on SCTF Core-II Test S2-19 (Quantitative Evaluation of Relation Between Degree of Heat Transfer Enhancement Due to Radial Power Distribution and Amount of Increase of Upward Liquid Flow Rate During Reflood in PWR-LOCA)," prepared by Japan Atomic Energy Research Institute, JAERI-M-91-033, March 1991.

SCTF Core-III

J-551 "Design of Slab Core Test Facility (SCTF) in Large Scale Reflood Test Program, Part III: Core-III," prepared by Japan Atomic Energy Research Institute, JAERI-Memo-62-110, March 1987.

J-552 "Analysis Report on Large Scale Reflood Tests with Core-III of the Slab Core Test Facility -- Test in FY 1985," prepared by Japan Atomic Energy Research Institute, JAERI-Memo-61-197.

J-553 "Evaluation Report on SCTF Core-III Test S3-SH1 (Overall Thermal-Hydraulic Characteristics Under Combined Injection Mode for German-Type PWR)," prepared by Japan Atomic Energy Research Institute, JAERI-Memo-62-093, March 1987.

J-554 "Evaluation Report on SCTF Core-III Test S3-06 (Effect of Radial Power Distribution on Thermal-Hydraulic Characteristics Under Combined Injection Mode German PWR)," prepared by Japan Atomic Energy Research Institute, JAERI-Memo-62-111, March 1987 (publicly released as JAERI-M-88-213, October 1988).

J-555 Pointner, W., "Method for the Determination of the Steam Injection Rates to the UPTF Core Simulator for SCTF/UPTF Coupling Tests," Japan Atomic Energy Research Institute, JAERI-Memo-62-293, August 1987.

J-556 "Analysis Report on Large Scale Reflood Tests with Core-III of Slab Core Test Facility -- Test in FY 1986," prepared by Japan Atomic Energy Research Institute, JAERI-Memo-62-295.

J-557 Pointner, W., "System Behavior for the Refill/Reflood Phase During a Combined Injection Test With Conditions in SCTF and CCTF -- Comparison between SCTF Test S3-11 (Run 715) and CCTF Test C2-20 (Run 80)," Japan Atomic Energy Research Institute, JAERI-Memo-62-296, August 1987.

J-558 "Evaluation Report on SCTF Core-III Tests S3-14, S3-15 and S3-16 (Effect of Radial Power Profile Shape on Two Dimensional Thermal Hydraulic Behavior)," prepared by Japan Atomic Energy Research Institute, JAERI-Memo-62-329, September 1987 (publicly released as JAERI-M-88-060, March 1988).

J-559 "Evaluation Report on SCTF-III Test S3-SH2 (Observed Reflood Phenomena in S3-SH2 Test Under Combined Injection Mode for German Type PWR)," prepared by Japan Atomic Energy Research Institute, JAERI-Memo-62-344, October 1987.

J-560 Pointner, W., "Empirical Core Model for CCTF and SCTF," Japan Atomic Energy Research Institute, JAERI-Memo-63-068, March 1988.

J-561 "Evaluation Report on SCTF Core-III Tests S3-7 and S3-8 (Investigation of Tie Plate Water Temperature Distribution Effects on Water Break-through and Core Cooling During Reflooding)," prepared by Japan Atomic Energy Research Institute, JAERI-Memo-63-070, March 1988 (publicly released as JAERI-M-90-035, March 1990).

J-562 "Evaluation Report on SCTF-III Test S3-12 (Observed Reflood Phenomena in Test S3-12 Under Combined Injection Mode for German-Type PWR," prepared by Japan Atomic Energy Research Institute, JAERI-Memo-63-071, March 1988.

J-563 "Evaluation Report on SCTF-III Test S3-13 (Observed Reflood Phenomena in Test S3-13 Under Combined Injection Mode For German-Type PWR)," prepared by Japan Atomic Energy Research Institute, JAERI-Memo-63-072, March 1988.

J-564 "Evaluation Report on the SCTF-III Test S3-18 (Observed Reflood Phenomena in Test S3-18 Under Combined Injection Mode for German-Type PWR)," prepared by Japan Atomic Energy Research Institute, JAERI-Memo-63-073, March 1988.

J-565 "Evaluation Report on SCTF Core-III Test S3-20 (Investigation of Water Break Through and Core Cooling Behaviors Under Intermittent ECC Water Delivery," prepared by Japan Atomic Energy Research Institute, JAERI-Memo-63-074, March 1988 (publicly released as JAERI-M-90-080, May 1990).

J-566 "Evaluation Report on SCTF Core-III Test S3-01 (Effect of Water Sealing at Bottom of Downcomer on Thermal-Hydraulic Behavior in Pressure Vessel in a PWR with Combined Injection Type ECCS)," prepared by Japan Atomic Energy Research Institute, JAERI-Memo-63-230, June 1988.

J-567 "Evaluation Report on SCTF Core-III Test S3-02 (Effect of Water Temperature Falling Into Core on Core Thermal-Hydraulic Behavior in a PWR With Combined Injection Type ECCS)," prepared by Japan Atomic Energy Research Institute, JAERI, Memo-63-231, June 1988.

J-568 "Evaluation Report on SCTF Core-III Test S3-17 (Investigation of Thermo-Hydrodynamic Behavior During Reflood Phase of LOCA in a PWR with Vent Valves)," prepared by Japan Atomic Energy Research Institute, JAERI-Memo-63-232, June 1988 (publicly released as JAERI-M-90-036, March 1990).

J-569 "Evaluation Report on SCTF Core-III Test S3-SH1 (Effect of Hot Leg Injection on Core Thermal-Hydraulics With Combined Injection Type ECCS)," prepared by Japan Atomic Energy Research Institute, JAERI-M-88-125, July 1988.

J-570 "Evaluation Report on SCTF-III Test S3-3, S3-4 and S3-5 Countercurrent Flow Limitation Phenomenon in Full-Radius Core," prepared by Japan Atomic Energy Research Institute, JAERI-Memo-01-028, January 1989.

J-571 "Study on Flow Circulation Phenomena in Pressure Vessel During Reflood Phase of PWR with Combined-Injection Type ECCS Under Cold-Leg-Large-Break LOCA," prepared by Japan Atomic Energy Research Institute, JAERI-Memo-01-015, February 1989.

J-572 "Evaluation Report on SCTF Core-III Test S3-22 (Investigation of Water Break-through and Core Cooling Behaviors under Alternate ECC Water Delivery from Hot Legs to Upper Plenum during Reflooding in PWRs with Combined-Injection Type ECCS," prepared by Japan Atomic Energy Institute, JAERI-Memo-01-077 (publicly released as JAERI-M-91-104, July 1991).

J-573 "Evaluation Report on SCTF-III Test S3-10: Reflood Phenomena Under Best Estimate Conditions," prepared by Japan Atomic Energy Research Institute, JAERI-Memo-01-086, March 1989.

J-574 "Experimental Study on In-Core Reflood Behavior Under Combined Injection of ECC Water," prepared by Japan Atomic Energy Research Institute, JAERI-Memo-63-467, January 1989.

J-575 "Evaluation Report on SCTF Core-III Test S3-9: Investigation of Reflooding Behavior Under An Evaluation Model Condition in PWRs with Cold-Leg-Injection-Type ECCS," prepared by Japan Atomic Energy Research Institute, JAERI-Memo-01-251, July 1989 (publicly released as JAERI-M-90-046).

J-576 "Evaluation Report on SCTF-III Test S3-11: Observed Reflood Phenomena Under BE Condition of Combined ECC Injection Mode For German Type PWR," prepared by Japan Atomic Energy Research Institute, JAERI-Memo-01-263, August 1989.

J-577 "Evaluation Report on SCTF-III Test S3-21: Observed Reflood Phenomena in Test S3-21 Under Combined ECC Injection Mode," prepared by Japan Atomic Energy Research Institute, JAERI-Memo-02-069, March 1990.

J-578 "Evaluation Report on SCTF Core-III Test S3-9 (Investigation of CCTF Coupling Test Results Under An Evaluation Model Condition in PWRs With Cold-Leg-Injection-Type ECCS)," prepared by Japan Atomic Energy Research Institute, JAERI-M-90-046, March 1990.

Other JAERI Facilities

J-581 "Evaluation of the Pressure Difference across the Core during PWR-LOCA Reflood Phase," prepared by Japan Atomic Energy Research Institute, JAERI-M-8168, March 1979.

J-582 "Experimental Results of the Effective Water Head in Downcomer during Reflood Phase of a PWR LOCA," prepared by Japan Atomic Energy Research Institute, JAERI-M-8978, August 1980.

J-583 "Preliminary Analysis of the Effect of the Grid Spacers on the Reflood Heat Transfer," prepared by Japan Atomic Energy Research Institute, JAERI-M-9992, February 1982.

J-584 "Quench Model for Lower Temperature than Thermo-Hydrodynamic Maximum Liquid Superheat," prepared by Japan Atomic Energy Research Institute, JAERI-M-10000, March 1982.

J-585 "The Characteristics of Cross Flow in a Rod Bundle," prepared by Japan Atomic Energy Research Institute, JAERI-M-82-003, March 1982.

J-586 "Study of the Thermo-Hydrodynamic Phenomena in the Nuclear Core during Reflood Phase," prepared by Japan Atomic Energy Research Institute, JAERI-M-83-032, March 1983.

J-587 "Report on Reflood Experiment of Grid Spacer Effect," prepared by Japan Atomic Energy Research Institute, JAERI-M-84-131, July 1984.

J-588 "Thermal-Hydraulic Evaluation Study of the Effectiveness of Emergency Core Cooling System for Light Water Reactors," prepared by Japan Atomic Energy Research Institute, JAERI-M-85-122, August 1985.

J-589 "Cross Flow Resistance in Air-Water Two-Phase Flow in Rod Bundle," prepared by Japan Atomic Energy Research Institute, JAERI-M-86-184, January 1987.

J-590 "Study on Thermo-Hydraulic Behavior during Reflood Phase of a PWR-LOCA," prepared by Japan Atomic Energy Research Institute, JAERI-M-88-262, January 1989.

J-591 "Estimation of Shear Stress in Counter-Current Gas-Liquid Annular Two-Phase Flow," prepared by Japan Atomic Energy Research Institute, JAERI-M-90-215, January 1991.

CODE ANALYSIS REPORTS

CCTF

J-601 "Assessment of TRAC-PD2 Reflood Core Thermal-Hydraulic Model by CCTF Test C1-16," prepared by Japan Atomic Energy Research Institute, JAERI-M-82-166, November 1982.

J-602 "Assessment of Core Thermo-Hydrodynamic Models of REFLA-1D with CCTF Data," prepared by Japan Atomic Energy Research Institute, JAERI-M-83-103, June 1983.

J-603 "Analysis of TRAC-PD2 Prediction for the Cylindrical Core Test Facility Evaluation-Model Test C1-19 (Run 38)," prepared by Japan Atomic Energy Research Institute, JAERI-M-84-041, March 1979.

J-604 "Assessment of TRAC-PF1 Predictive Capability for the Thermal-Hydraulic Behaviors along a Primary Loop during the Reflood Phase of a PWR-LOCA," prepared by Japan Atomic Energy Research Institute, JAERI-M-84-042, March 1984.

J-605 "Assessment of REFLA Local Power Effect Model with CCTF Data," prepared by Japan Atomic Energy Research Institute, JAERI-M-84-246, February 1985.

J-606 "Analysis of TRAC-PF1 Calculated Core Heat Transfer for CCTF Test C1-5 (Run 14)," prepared by Japan Atomic Energy Research Institute, JAERI-M-85-117, August 1985.

J-607 "Assessment of TRAC-PF1/MOD1 Code for Cylindrical Core Test Facility Base Case Test C2-4," prepared by Japan Atomic Energy Research Institute, JAERI-Memo-01-007, February 1989.

J-608 Pointner, W., "Comparison Between a TRAC GPWR Calculation and a CCTF Test With Combined Injection and EM Boundary Conditions for the Reflood Phase of a German PWR-LOCA," Japan Atomic Energy Research Institute, JAERI-Memo-62-292, August 1987.

J-609 "Assessment of TRAC-PF1/MOD1 Code for Core Thermal Hydraulic Behavior during Reflood with CCTF and SCTF Data," prepared by Japan Atomic Energy Research Institute, JAERI-Memo-01-009, February 1989.

SCTF

J-611 "Computer Codes HeatT and HeatQ for Heat Transfer Analysis in SCTF," prepared by Japan Atomic Energy Research Institute, JAERI-Memo-9867, January 1982.

J-612 "Comparison Between SCTF Tests S1-SH2, S1-01, S1-02, and S1-04 and the TRAC Post-Test Predictions," prepared by Japan Atomic Energy Research Institute, JAERI-Memo-58-339, September 1983.

J-613 "COBRA/TRAC Analysis of Two-Dimensional Thermal-Hydraulic Behavior in SCTF Reflood Tests," prepared by Japan Atomic Energy Research Institute, JAERI-Memo-60-219, August, 1985 (publicly released as JAERI-M-86-196, January 1987).

J-614 "Predictability of REFLA Core Model for SCTF Data," prepared by Japan Atomic Energy Research Institute, JAERI-87-163, October 1987.

J-615 "Assessment of TRAC-PF1/MOD1 Code for Thermal Hydraulic Behavior Including Two-Dimensional Behavior In Pressure Vessel During Reflood in Slab Core Test Facility," prepared by Japan Atomic Energy Research Institute, JAERI-Memo-01-006, February 1989.

Other

J-621 "REFLA-1D/MODE 1: A Computer Program for Reflood Thermo-Hydrodynamic Analysis during PWR-LOCA User's Manual," prepared by Japan Atomic Energy Research Institute, JAERI-M-9286, January 1981.

J-622 "REFLAP/REFLA (Mod 0): A System Reflooding Analysis Computer Program," prepared by Japan Atomic Energy Research Institute, JAERI-M-9397, March 1981.

J-623 "One-dimensional System Analysis Code for Reflood Phase during LOCA," prepared by Japan Atomic Energy Research Institute, JAERI-M-9780, November 1981.

J-624 "Improvement of Core Mass Balance Calculation in REFLA-1D/MODE1," prepared by Japan Atomic Energy Research Institute, JAERI-M-82-099, August 1982.

J-625 "Investigation of Reflood Models by Coupling REFLA-1D and Multi-loop System Model," prepared by Japan Atomic Energy Research Institute, JAERI-M-83-147, September 1983.

J-626 "REFLA-1D/MODE3: A Computer Code for Reflood Thermo-Hydrodynamic Analysis during PWR-LOCA. User's Manual," prepared by Japan Atomic Energy Research Institute, JAERI-M-84-243, February 1985.

J-627 "Updating of Best Evaluation Codes Fiscal Year 1984 Work Report," prepared by Japan Atomic Energy Research Institute, JAERI-Memo-60-394, December 1985.

J-628 "User's Manual of the REFLA-1D/MODE4 Reflood Thermo-Hydrodynamic Analysis Code: Incorporation of Local Power Effect Model and Fuel Temperature Profile Effect Model into REFLA-1D," prepared by Japan Atomic Energy Research Institute, JAERI-M-85-210, January 1986.

J-629 "Assessment of TRAC-PF1/MOD1 for Countercurrent, Annular and Stratified Flows," prepared by Japan Atomic Energy Research Institute, JAERI-M-85-219, January 1986 (this is the public release of a LANL 2D/3D Technical Note -- see U-704).

J-630 "Improvement of TRAC-PF1 Code with JAERI's Reflood Model of REFLA-1D Code, prepared by Japan Atomic Energy Research Institute, JAERI-Memo-02-009 February 1990.

J-631 "Implementation of an Implicit Method Into Heat Conduction Calculation of TRAC-PF1/MOD1 Code," prepared by Japan Atomic Energy Research Institute, JAERI-Memo-01-008, February 1989 (publicly released as JAERI-M-90-122, August 1990).

ADVANCED INSTRUMENTATION REPORTS

J-801 "Data Processing of Advanced Two-Phase Flow Instrumentation In Slab Core Test Facility (SCTF) Core-I," prepared by Japan Atomic Energy Research Institute, JAERI-Memo-9802, November 1981.

J-802 "Evaluation of Advanced Two-Phase Flow Instrumentation In SCTF Core-I," prepared by Japan Atomic Energy Research Institute, JAERI-Memo-57-206, August 1982 (publicly released as JAERI-M-84-065, March 1984).

PAPERS, PRESENTATIONS, AND CORRESPONDENCE

Papers - Data Evaluation

J-901 Murao, Y., Sudo, Y., and Iguchi, T., "Topics on Hydrodynamic Models of PWR Reflood Phenomena," presented at the Japan - US Seminar on Two-Phase Flow Dynamics, Kobe, Japan, July 31 - August 3, 1979.

J-902 Sudo, Y., "Estimation of Average Void Fraction in Vertical Two-Phase Flow Channel Under Low Liquid Velocity," Journal of Nuclear Science & Technology, Vol. 17, No. 1 (January 1980).

J-903 Sudo, U., "Film Boiling Heat Transfer during Reflood Phase in Postulated PWR Loss-of-Coolant Accident," Journal of Nuclear Science and Technology, Vol. 17, No. 7, pp. 516-530 (July 1980).

J-904 Murao, Y., Sudoh, T., and Sugimoto, J., "Experimental and Analytical Modeling of the Reflood-Phase during PWR-LOCA," presented at the Nineteenth National Heat Transfer Conference, Orlando, FL, USA, July 27-30, 1980.

J-905 Hirano, K., Murao, Y.,"Large Scale Reflood Test," Nippon Genshiryoku Gakkai-Shi, Vol. 22, No. 10, pp. 681-686 (October 1980).

J-906 Murao, Y., and Sugimoto, J., "Correlation of Heat Transfer Coefficient for Saturated Film Boiling During Reflood Phase Prior to Quenching," Journal of Nuclear Science and Technology, Vol. 18, No. 4, pp. 275-284 (April 1981).

J-907 Sudo, Y., and Akimoto, H., "Downcomer Effective Water Head during Reflood in Postulated PWR LOCA," Journal of Nuclear Science and Technolgy, Vol. 19, No. 1 (January 1982).

J-908 Osakabe, M., and Adachi, H., "Characteristic of Two-Phase Slanting Flow in Rod Bundle," Journal of Nuclear Science and Technology, Vol. 19, No. 6, pp. 504-506 (June 1982).

J-909 Okubo, T., and Murao, Y., "Effects of ECC Water Injection Rate on Reflood Phase during LOCA," Journal of Nuclear Science and Technology, Vol. 19, No. 7, pp. 593-595 (July 1982).

J-910 Murao, Y., and Iguchi, T., "Experimental Modeling of Core Hydrodynamics during Reflood Phase of LOCA," Journal of Nuclear Science and Technology, Vol. 19, No. 8, pp. 613-627, (August 1982).

J-911 Murao, Y., Akimoto, H., Sudoh, T., and Okubo, T., "Experimental Study of System Behavior during Reflood Phase of PWR-LOCA using CCTF," Journal of Nuclear Science and Technology, Vol. 19, No. 9, pp. 705-719 (September 1982).

J-912 Murao, Y., Sudoh, T., Iguchi, T., et al, "Findings in CCTF Core-I Test," Proceedings of the Tenth Water Reactor Safety Information Meeting, October 12-15, 1982, NUREG/CP-0041, Vol. 1, pp. 275-286.

J-913 Adachi, H., Sudo, Y., Sobajima, M., et al, "SCTF Core-I Reflood Test Results," presented at the Tenth Water Reactor Safety Information Meeting, October 12-15, 1982, NUREG/CP-0041, Vol. 1, pp. 287-306.

J-914 Sobajima, M., and Ohnuki, A., "Carryover Characteristic during Reflood Process in Large Scale Separate Effects Tests," Nuclear Engineering and Design, Vol. 74, No. 2, pp. 165-171 (February 1983).

J-915 Ohnuki, A., and Sobajima, M., "Mass Effluent Rate Out of Core during Reflood," Journal of Nuclear Science and Technology, Vol. 20, No. 3, pp. 267-269 (March 1983).

J-916 Sudo, Y., and Osakabe, M., "Effects of Partial Flow Blockage on Core Heat Transfer in Forced-Feed Reflood Tests," Journal of Nuclear Science and Technology, Vol. 20, No. 4, pp. 322-332 (April 1983).

J-917 Iguchi, T., and Murao, Y., "Water Accumulation Phenomena in Upper Plenum during Reflood Phase of PWR-LOCA by Using CCTF Data," Journal of Nuclear Science and Technology, Vol. 20, No. 6, pp. 453-466 (June 1983).

J-918 Osakabe, M., and Sudo, Y., "Heat Transfer Calculation of Simulated Heater Rods throughout Reflood Phase in Postulated PWR-LOCA Experiments," Journal of Nuclear Science and Technology, Vol. 20, No. 7, pp. 559-570 (July 1983).

J-919 Abe, Y., Sudo, Y., and Osakabe, M., "Experimental Study of Upper Core Quench in PWR Reflood Phase," Journal of Nuclear Science and Technology, Vol. 20, No. 7, pp. 571-583 (July 1983).

J-920 Sugimoto, J., and Murao, Y., "Experimental Study of Effect of Initial Clad Temperature on Reflood Phenomena during PWR-LOCA," Journal of Nuclear Science and Technology, Vol. 20, No. 8, pp. 645-657 (August 1983).

J-921 Iguchi, T., Okubo, T., and Murao, Y., "Visual Study of Flow Behavior in Upper Plenum during Simulated Reflood Phase of PWR-LOCA," Journal of Nuclear Science and Technology, Vol. 20, No. 8, pp. 698-700 (August 1983).

J-922 Sudo, Y., and Ohnuki, A., "Mechanism of Falling Water Limitation in Two-Phase Counter Flow through Single Hole Vertical Channel," Nippon Kikai Gakkai Ronbunshu, B. Hen, Vol. 49, No. 444, pp. 1685-1694 (August 1983).

J-923 Iwamura, T., Osakabe, M., and Sudo, Y., "Effects of Radial Core Power Profile on Core Thermo-Hydraulic Behavior during Reflood Phase in PWR-LOCAs," Journal of Nuclear Science and Technology, Vol. 20, No. 9, pp. 743-751 (September 1983).

J-924 Adachi, H., Sobajima, M., Iwamura, T., et al, "SCTF Core-I Reflood Test Results," Proceedings of the Eleventh Water Reactor Safety Research Information Meeting, October 14-24, 1983, NUREG/CP-0048, Vol. 2, pp. 277-296.

J-925 Murao, Y., Iguchi, T., Sugimoto, J., et al, "Status of CCTF Test Program," Proceedings of the Eleventh Water Reactor Safety Research Information Meeting, October 14-24, 1983, NUREG/CP-0048, Vol. 2, pp. 257-276.

J-926 Sudo, Y., "Parameter Effects on Downcomer Penetration of ECC Water in PWR-LOCA," Journal of Nuclear Science and Technology, Vol. 21, No. 1, pp. 32-41 (January 1984).

J-927 Osakabe, M., and Sudo, Y., "Analysis of Saturated Film Boiling Heat Transfer in Reflood Phase of PWR-LOCA: Turbulent Boundary Layer Model," Journal of Nuclear Science and Technology, Vol. 21, No. 2, pp. 115-125 (February 1984).

J-928 Sugimoto, J., and Murao, Y., "Effect of Grid Spacers on Reflood Heat Transfer in PWR-LOCA," Journal of Nuclear Science and Technology, Vol. 21, No. 2, pp. 103-114 (February 1984).

J-929 Akimoto, H., Iguchi, T., and Murao, Y., "Pressure Drop Through Broken Cold Leg during Reflood Phase of Loss-of-Coolant Accident of Pressurized Water Reactor," Journal of Nuclear Science and Technology, Vol. 21, No. 6, pp. 450-465 (June 1984).

J-930 Murao, Y., "Quench Front Movement during Reflood Phase," Proceedings of the First International Workshop on Fundamental Aspects of Post-Dryout Heat Transfer, April 2-4, 1984, Salt Lake City, UT, USA, NUREG/CP-0060, pp. 103-117.

J-931 Sudo, Y., and Ohnuki, A., "Mechanism of Falling Water Limitation under Counter-Current Flow through a Vertical Flow Path," Bull, JSME, Vol. 27, No. 226, pp. 708-715 (April 1984).

J-932 Murao, Y., Adachi, H., and Iguchi, T., "Status of CCTF/SCTF Test Program," Proceedings of the Twelfth Water Reactor Safety Research Information Meeting, October 23-26, 1984, NUREG/CP-0058, Vol. 2, pp. 342-372.

J-933 Murao, T., Iguchi, T., Okabe, K., et al, "Results of CCTF Upper Plenum Injection Tests," Proceedings of the Twelfth Water Reactor Safety Research Information Meeting, October 23-26, 1984, NUREG/CP-0058, Vol. 2, pp. 306-341.

J-934 Okabe, K., and Murao, Y., "Swelling Model of Two-Phase Mixture in Lower Plenum at End of Blowdown Phase of PWR-LOCA," Journal of Nuclear Science and Technology, Vol. 21, No. 12, pp. 919-930 (December 1984).

J-935 Okubo, T., and Murao, Y., "Experimental Study of ECC Water Injection Rate Effects on Reflood Phase of PWR-LOCA," Journal of Nuclear Science and Technology, Vol. 22, No. 2, pp. 93-108 (February 1985).

J-936 Akimoto, H., Tanaka, Y., Kozawa, Y., et al., "Oscillatory Flows Induced by Direct Contact Condensation of Flowing Steam with Injected Water," Journal of Nuclear Science and Technology, Vol. 22, 1985, pp. 269-283 (April 1985).

J-937 Sobajima, M., and Adachi, H., "Coolability Study on Two-Bundle Scale Flow Blockage in the Reflood Process," Nuclear Engineering and Design, Vol. 86, No. 3, pp. 345-355 (June 1985).

J-938 Iwamura, T., and Adachi, H., "Initial Thermal-Hydraulic Behaviors under Simultaneous ECC Water Injection into Cold Leg and Upper Plenum in a PWR LOCA," Journal of Nuclear Science and Technology, Vol. 22, No. 6, pp. 451-460 (June 1985).

J-939 Akimoto, H., Iguchi, T., and Murao, Y., "Core Radial Power Profile Effect on System and Core Cooling Behavior during Reflood Phase of PWR-LOCA with CCTF Data," Journal of Nuclear Science and Technology, Vol. 22, No. 7, pp. 538-550 (July 1985).

J-940 Iguchi, T., and Murao, Y., "Experimental Study on Reflood Behavior in PWR with Upper Plenum Injection Type ECCS by Using CCTF," Journal of Nuclear Science and Technology, Vol. 22, No. 8, pp. 637-652 (August 1985).

J-941 Sobajima, M., "Experimental Modeling of Steam-Water Countercurrent Flow Limit for Perforated Plates," Journal of Nuclear Science and Technology, Vol. 22, No. 9, pp. 723-732, (September 1985).

J-942 Murao, Y., Iguchi, T., Sugimoto, J., et al, "Results of CCTF Tests," Proceedings of the Thirteenth Water Reactor Safety Research Information Meeting, October 22-25, 1985, NUREG/CP-0072, Vol. 4, pp. 289-314.

J-943 Iwamura, T., Sobajima, M., Adachi, H., et al, "Results of SCTF Reflood Tests," Proceedings of the Thirteenth Water Reactor Safety Research Information Meeting, October 22-25, 1985, NUREG/CP-0072, Vol. 4, pp. 315-330.

J-944 Sugimoto, J., Okubo, T., and Murao, Y., "Heat Transfer Enhancement due to Water Accumulation near Grid Spacers during Reflood," Proceedings of the Third International Topical Meeting on Reactor Thermal Hydraulics, Newport, RI, USA, October 15-18, 1985.

J-945 Murao, Y., Fujiki, K., and Akimoto, H., "Experimental Assessment of Evaluation Model for Safety Analysis on Reflood Phase of PWR-LOCA," Journal of Nuclear Science and Technology, Vol. 22, No. 11, pp. 890-902 (November 1985).

J-946 Iwamura, T., Adachi, H., and Sobajima, M., "Experimental Study of Two-Dimensional Thermal-Hydraulic Behavior in Core during Reflood Phase of PWR LOCA," Journal of Nuclear Science and Technolgoy, Vol. 23, No. 2, pp. 123-135 (February 1986).

J-947 Ohnuki, A., "Experimental Study of Countercurrent Two-Phase Flow in Horizontal Tube Connected to Inclined Riser," Journal of Nuclear Science and Technology, Vol. 23, No. 3, pp. 219-232 (March 1986).

J-948 Adachi, H., Iwamura, T., Ohnuki, A., et al, "Recent Study on Two-Dimensional Thermal-Hydraulic Behavior in PWR Core During the Reflood Phase of LOCA with the Slab Core Test Facility (SCTF)," Proceedings of the Second International Topical Meeting on Nuclear Power Plant Thermal Hydraulics and Operations, Tokyo, Japan, April 15-17, 1986.

J-949 Sobajima, M., Adachi, H., Iwamura, T., and Ohnuki, A., "Two Dimensional Fall Back Flow and Core Cooling in the Slab Core Test Facility (SCTF)," Proceedings of the Second International Topical Meeting on Nuclear Power Plant Thermal Hydraulics and Operations, Tokyo, Japan, April 15-17, 1986.

J-950 Iguchi, T., Murao, Y., Akimoto, H., et al, "Assessment of Current Safety Evaluation Analysis on the Reflood Phase during a LOCA in a PWR with the Cold Leg Injection Type ECCS: 1) System Behavior, and 2) Thermal-hydraulic Behavior in the Core," Proceedings of the Second International Topical Meeting on Nuclear Power Plant Thermal Hydraulics and Operations, Tokyo, Japan, April 15-17, 1986.

J-951 Abe, Y., Sobajima, M. and Murao, Y., "Experimental Study of Effects of Upward Steam Flow Rate on Quench Propagation by Falling Water Film," Journal of Nuclear Science and Technology, Vol. 23, No. 5, pp. 415-432 (May 1986).

J-952 Iwamura, T., Adachi, H., and Sobajima, M., "Air-Water Two-Phase Cross Flow Resistance in Rod Bundle," Journal of Nuclear Science and Technology, Vol. 23, No. 7, pp. 658-660 (July 1986).

J-953 Iwamura, T., Adachi, H., Sobajima, M. et al, "Heat Transfer Enhancement in SCTF Tests," Proceedings of the Fourteenth Water Reactor Safety Research Information Meeting, October 27-31, 1986, NUREG/CP-0082, Vol. 4, pp. 429-444.

J-954 Iguchi, T., Murao, T., Sugimoto, J., et al, "Summary of CCTF Test Results," Proceedings of the Fourteenth Water Reactor Safety Research Information Meeting, October 27-31, 1986, NUREG/CP-0082, Vol. 4, pp. 387-406.

J-955 Akimoto, H., Iguchi, T., and Murao, Y., "System Pressure Effect on System and Core Cooling Behavior during Reflood Phase of PWR LOCA," Journal of Nuclear Science and Technology, Vol. 24, No. 4, pp. 276-288 (April 1987).

J-956 Ohnuki, A., and Adachi, H., "Limitation of Countercurrent Gas-Liquid Flow in a Horizontal Flow Path Connected to an Inclined Flow Path: Prediction of Gas Velocity on Initiation of Liquid Penetration," Nippon Kikai Gakkai Ronbunshu, B. Hen, Vol. 53, No. 490, pp. 1685-1690 (June 1987).

J-957 Okubo, T., Iguchi, T., and Murao, Y., "Experimental Study of Initial Downcomer Water Accumulation Velocity Effects on Reflood Phase of PWR-LOCA," Journal of Nuclear Science and Technology, Vol. 24, No. 7, pp. 573-579 (July 1987).

J-958 Ohnuki, A., Adachi, H., and Murao, Y., "Scale Effects on Countercurrent Gas-Liquid Flow in Horizontal Tube Connected to Inclined Riser," Proceedings from ANS National Heat Transfer Conference, Pittsburgh, PA, USA, August 9-12, 1987. (Also see J-966.)

J-959 Adachi, H., Iguchi, T., Iwamura, T., et al, "Multi-dimensional Effect Found in SCTF Reflood Tests for US/J PWR," Proceedings of the Fifteenth Water Reactor Safety Information Research Meeting, October 26-30, 1987, NUREG/CP-0091, Vol. 4, pp. 549-558.

J-960 Murao, Y., Iguchi, T., Sugimoto, J., et al, "Reflooding Phenomena of German PWR Estimated from CCTF (Cylindrical Core Test Facility), SCTF (Slab Core Test Facility), and UPTF (Upper Plenum Test Facility) Results," Proceedings of the Fifteenth Water Reactor Safety Research Information Meeting, October 26-30, 1987, Vol. 4 Addenda.

J-961 Okabe, K., and Murao, Y., "Hydrodynamics of ECC Water Bypass and Refill of Lower Plenum at PWR-LOCA," Journal of Nuclear Science and Technology, Vol. 24, No. 10, pp. 785-797 (October 1987).

J-962 Iguchi, T., and Murao, Y., "Effect of Decay Heat Level on Reflood Phenomena during PWR-LOCA," Journal of Nuclear Science and Technology, Vol. 24, No. 10, pp. 821-831 (October 1987).

J-963 Iguchi, T., Murao, Y., Akimoto, H., et al, "Assessment of Current Safety Evaluation Analysis on Reflood Behavior during PWR-LOCA by Using CCTF Data," Journal of Nuclear Science and Technology, Vol. 24, No. 11, pp. 887-896 (November 1987).

J-964 Akimoto, H., Iguchi, T., and Murao, Y., "Effect of Pressure Drop through Broken Cold Leg on Thermal Hydraulic Behavior during Reflood Phase of PWR-LOCA," Journal of Nuclear Science and Technology, Vol. 25, No. 1, pp. 45-55 (January 1988).

J-965 Iguchi, T., and Murao, Y., "Effect of Asymmetric Upper Plenum Injection on Reflood Behavior," Journal of Nuclear Science and Technology, Vol. 25, No. 4, pp. 350-358 (April 1988).

J-966 Ohnuki, A., Adachi, H., and Murao, Y., "Scale Effects on Countercurrent Gas-Liquid Flow in a Horizontal Tube Connected to an Inclined Riser," Nuclear Engineering and Design, Vol. 107. No. 3, pp. 283-294 (May 1988). (Also see J-958.)

J-967 Iguchi, T., Iwamura, T., Akimoto, H., et al, "SCTF-III Test Plan and Recent SCTF-III Test Results," Nuclear Engineering and Design, Vol. 108, No. 1/2, pp. 241-247 (June 1988).

J-968 Iguchi, T., Murao, Y., and Sugimoto, J., "Summary of CCTF Test Results -- Assessment of Current Safety Evaluation Analysis on Reflood Behavior during a LOCA in a PWR with Cold-Leg-Injection-Type ECCS," Nuclear Engineering and Design, Vol. 108, No. 1/2, pp. 233-239 (June 1988).

J-969 Iguchi, T., Okubo, T., and Murao, Y., "Effect of Loop Seal on Reflood Phenomena in PWR," Journal of Nuclear Science and Technology, Vol. 25, No. 6, pp. 520-527 (June 1988).

J-970 Iguchi, T., Adachi, H., Sugimoto, J., et al, "Recent Results of Analytical Study on SCTF-III Tests for Reflood Phenomena of PWR with Combined-Injection-Type ECCS under Cold-Leg-Large-Break LOCA," Proceedings of the Sixteenth Water Reactor Safety Research Information Meeting, October 24-27, 1988, NUREG/CP-0097, Vol. 4, pp. 557-581.

J-971 Iwamura, T., Iguchi, T., Adachi, H., and Murao, Y., "Quantitative Evaluation of Heat Transfer Enhancement due to Radial Power Distribution during Reflood Phase of PWR-LOCA," Journal of Nuclear Science and Technology, Vol. 26, No. 4, pp. 428-440 (April 1989).

J-972 Murao, Y., Iguchi, T., Adachi, H., et al, "Multi-Dimensional Thermal-Hydraulics in Pressure Vessel during Reflood Phase of a PWR-LOCA," Proceedings of the Fourth International Topical Meeting on Nuclear Reactor Thermal-Hydraulics (NURETH-4), Karlsruhe, FRG, October 1989.

J-973 Okubo, T., Iguchi, T., and Murao, Y., "Experimental Study of Reflooding Behavior in PWRs under Downcomer Injection," Journal of Nuclear Science and Technology, Vol. 27, No. 1, pp. 30-44 (January 1990).

J-974 Ohnuki, A., Akimoto, H., and Murao, Y., "Effect of Liquid Flow Rate on Film Boiling Heat Transfer during Reflood in Rod Bundle," Journal of Nuclear Science and Technology, Vol. 27, No. 6, pp. 535-546 (June 1990).

J-975 Iguchi, T., "Void Fraction in Simulated PWR Fuel Bundle during Reflood Phase," Journal of Nuclear Science and Technology, Vol. 18, No. 12, pp. 957-968 (December 1981).

Papers - Code Analysis

J-981 Murao, Y., "Analytical Study of Thermo-Hydrodynamic Behavior of Reflood-Phase during LOCA," Journal of Nuclear Science and Technology, Vol. 16, No. 11, pp. 802-817 (November 1979).

J-982 Murao, Y., Sugimoto, J., Okubo, T., et al, "Reflood Code Development Work in JAERI," Proceedings of the Eleventh Water Reactor Safety Research Information Meeting, October 11-24, 1983, NUREG/CP-0048, Vol. 1, pp. 137-149.

J-983 Murao, Y., "Reflood Analysis Code REFLA," Proceedings of the First International Workshop on Fundamental Aspects of Post-Dryout Heat Transfer, Salt Lake City, UT, USA, April 2-4, 1984, NUREG/CP-0060, pp. 56-67.

J-984 Okubo, T., and Murao, Y., "Assessment of Core Thermo-Hydrodynamic Models of REFLA-1D Code with CCTF Data for Reflood Phase of PWR-LOCA," Journal of Nuclear Science and Technology, Vol. 22, No. 12, pp. 983-994 (December 1985).

J-985 Akimoto, H., "Analysis of TRAC-PF1 Calculated Core Heat Transfer for CCTF Test C1-5 (Run 14)," Nuclear Engineering and Design, Vol. 88, pp. 215-227 (1985).

J-986 Sugimoto, J., Sudoh, T., and Murao, Y., "Analytical Study of Thermal Response Similarity between Simulated Fuel Rods and Nuclear Fuel Rods during Reflood Phase of PWR-LOCA," Journal of Nuclear Science and Technology, Vol. 23, No. 4, pp. 315-325 (April 1986).

J-987 Murao, Y., Iguchi, T., Adachi, H., et al, "Development of Reflood Model at JAERI," Proceedings of the Fourteenth Water Reactor Safety Research Information Meeting, October 27-31, 1986, NUREG/CP-0082, Vol. 4, pp. 445-458.

J-988 Akimoto, H., Iwamura, T., Ohnuki, A., et al, "Status of J-TRAC Code Development," Proceedings of the Fourteenth Water Reactor Safety Research Information Meeting, October 27-31, 1986, NUREG/CP-0082, Vol. 5, pp. 381-394.

J-989 Iguchi, T., Murao, Y., and Akimoto, H., "Assessment of Core Radial Profile Effect Model for REFLA Code by Using CCTF Data," Journal of Nuclear Science and Technology, Vol. 24, No. 7, pp. 536-546 (July 1987).

J-990 Murao, Y., "Status of Development of Thermal-Hydraulic Reactor Transient Analysis Code J-TRAC and Future Plan," Proceedings of the Fourth Seminar on Software Development in Nuclear Energy Research," Tokai, Ibaraki, Japan, September 9-10, 1987, JAERI-M-87-199, pp. 18-48.

J-991 Murao, Y., and Hojo, T., "Numerical Simulation of Reflooding Behavior in Tight-Lattice Rod Bundles," Nuclear Technology Vol. 80, No. 1, pp. 83-92 (January 1988).

J-992 Hojo, T., Iguchi, T., and Murao, Y., "Application of REFLA Core Model to Safety Evaluation Code," Journal of Nuclear Science and Technology, Vol. 25, No. 2, pp. 190-197 (February 1988).

J-993 Murao, Y., "Status of ICAP Activities in Japan," Proceedings of the Sixteenth Water Reactor Safety Research Information Meeting, October 24-27, 1988, NUREG/CP-0097, Vol. 4, pp. 199-218.

J-994 Akimoto, J., Ohnuki, A., Kikuta, M., et al, "Assessment of J-TRAC Code with CCTF/SCTF Test Data," Proceedings of the Sixteenth Water Reactor Safety Research Information Meeting, October 24-27, 1988, NUREG/CP-0097, Vol. 4, pp. 583-606.

J-995 Okubo, T., Sugimoto, J., Iguchi, T., and Murao, Y., "Developmental Assessment of REFLA-1DS Code with Data from CCTF Tests for Reflood Phase of LOCA in PWRs with Cold-Leg-Injection Type ECCS," Proceedings of the Fourth International Topical Meeting on Nuclear Reactor Thermal Hydraulics (NURETH-4), Karlsruhe, FRG, October 10-13, 1989, Vol. 1, pp. 190-195.

J-996 Murao, Y., Akimoto, H., Iguchi, T., et al, "Code Improvements Based on Results from the 2D/3D and ICAP Activities," Proceedings of the Seventeenth Water Reactor Safety Research Information Meeting, October 23-25, 1989, NUREG/CP-0105, Vol. 3, pp. 159-186.

J-997 Asaka, H., Murao, Y., and Kukita, Y., "Assessment of TRAC-PF1 Condensation Heat Transfer Model for Analysis of ECC Water Injection Transients," Journal of Nuclear Science and Technology, Vol. 26, No. 11, pp. 1045-1057 (November 1989).

REPORTS AND PAPERS PUBLISHED BY US WITHIN 2D/3D PROGRAM

EVALUATION REPORTS

CCTF Core-I

U-401 "Research Information Report on the Results of the Core-I Test Series at the Japan Atomic Energy Research Institute Cylindrical Core Test Facility," prepared by MPR Associates, MPR-863, Revision 1, October 1985.

CCTF Core-II

U-411 "Literature Survey of Emergency Core Cooling Tests Related to Upper Plenum Injection," prepared by MPR Associates, Revision 1, December 18, 1985.

U-412 "CCTF-II Research Information Report for Tests Related to Upper Plenum Injection (UPI)," prepared by MPR Associates, MPR-933, March 1987.

U-413 "Evaluation of Thermal Hydraulic Behavior in the CCTF-II Best Estimate Reflood Test," prepared by MPR Associates, Revision 1, April 20, 1987.

U-414 "Research Information Report for the Cylindrical Core Test Facility (CCTF) Core-II Test Series (Excluding Tests Involving Upper Plenum Injection)," prepared by MPR Associates, MPR-934, April 1988.

SCTF Core-I

U-421 "Research Information Report on the Results of the Core-I Test Series at the Japan Atomic Energy Research Institute Slab Core Test Facility," prepared by MPR Associates, MPR-918, April 1988.

SCTF Core-II

U-431 "Research Information Report on the Slab Core Test Facility (SCTF) Core-II Test Series," prepared by MPR Associates, MPR-1115, July 1989.

SCTF Core-III

U-441 "Research Information Report on the Slab Core Test Facility (SCTF) Core-III Test Series," prepared by MPR Associates, MPR-1263, September 1992.

UPTF

U-451 "Upper Plenum Injection (UPI) of Emergency Core Coolant (ECC) -- Previous Tests and Analyses, and Capabilities of the Upper Plenum Test Facility (UPTF) to Perform UPI Tests," prepared by MPR Associates, September 13, 1985.

U-452 "Summary of Results from the UPTF Hot Leg Separate Effects Test, Comparison to Scaled Tests and Application to U.S. Pressurized Water Reactors," prepared by MPR Associates, MPR-1024, Revision 1, December 1987.

U-453 "Evaluation of the UPTF Entrainment/De-entrainment Test," Revision 1, prepared by MPR Associates, April 1, 1988.

U-454 "Summary of Results from the UPTF Upper Plenum Injection (UPI) Separate Effects Test, Comparison to Previous Scaled Tests and Application to U.S. Pressurized Water Reactors," prepared jointly by MPR Associates and Siemens (UB KWU) December 1988.

U-455 "Summary of Results from the UPTF Downcomer Separate Effects Tests, Comparison to Previous Scaled Tests and Application to U.S. Pressurized Water Reactors," prepared by MPR Associates, MPR-1163, July 1990.

U-456 "Summary of Results from the UPTF Carryover/Steam Binding Separate Effects Tests, Comparison to Previous Scaled Tests and Application to U.S. Pressurized Water Reactors," prepared by MPR Associates, MPR-1213, October 1990.

U-457 Theofanous, T.G., and Yan, H., "A Unified Interpretation of One- Fifth to Full Scale Thermal Mixing Experiments Related to Pressurized Thermal Shock," University of California at Santa Barbara, NUREG/CR-5677, April 1991.

U-458 "Summary of Results from the UPTF Cold Leg Flow Regime Separate Effects Tests, Comparison to Previous Scaled Tests and Application to U.S. Pressurized Water Reactors," prepared by MPR Associates, MPR-1208, October 1992.

U-459 "Evaluation of Accumulator Nitrogen Discharge During a PWR Large Break LOCA," prepared by MPR Associates, MPR-1331, September 1992.

U-460 "Summary of Results from the UPTF Downcomer Injection/Vent Valve Separate Effects Tests, Comparison to Previous Scaled Tests and Application to U.S. Pressurized Water Reactors," prepared by MPR Associates, MPR-1329, September 1992.

CODE ANALYSIS REPORTS

CCTF Core-I

U-601 Motley, F., "Research Information Report Results From TRAC Analysis Of Cylindrical Core Test Facility Core-I Test Series," Los Alamos National Laboratory, LA-2D/3D-TN-86-10, July 1986.

U-602 Okubo, T., and Fujita, R.K., "Summary of Analysis of TRAC-PD2 Post Test Calculations for CCTF Core-I Parametric Effects Test," Los Alamos National Laboratory, LA-2D/3D-TN-82-5, February 1982.

U-603 Ireland, J.R., "Cylindrical Core Test Facility (CCTF) Posttest Sensitivity Analysis of Test C1-1 (Run 10) Using TRAC-PD2," Los Alamos National Laboratory, LA-UR-80-1999, July 1980.

U-604 Motley, F., "TRAC Analysis of CCTF Base Case C1-5 (Run 14) with a Multidimensional Model," Los Alamos National Laboratory, LA-2D/3D-TN-81-29, September 1981.

U-605 Okubo, T., "Analysis of a TRAC-PD2 Post-test Calculation of CCTF Test C1-5 (Run 14)," Los Alamos National Laboratory, LA-2D/3D-TN-81-26, October 1981.

U-606 Fujita, R.K., "TRAC-PD2 Post-Test Analysis of CCTF Test C1-5 (Run 14)," Los Alamos National Laboratory, LA-2D/3D-TN-81-27, October 1981.

U-607 Okubo, T., "An Analysis of a TRAC-PD2 Post-Test Calculation of CCTF Test C1-6 (Run 15)," Los Alamos National Laboratory, LA-2D/3D-TN-81-34, October 1981.

U-608 Okubo, T., "An Analysis of a TRAC-PD2 Code Calculation for CCTF Test C1-6 (Run 15)," Los Alamos National Laboratory, LA-2D/3D-TN-82-8, March 1982.

U-609 Fujita, R.K., "TRAC-PD2 Post Test Analysis of CCTF Test C1-10 (Run 19)," Los Alamos National Laboratory, LA-2D/3D-TN-81-30, October 1981.

U-610 Brown, T., and Williams, K.A., "TRAC-PD2 Post Test Analysis of CCTF Test C1-11 (Run 20)," Los Alamos National Laboratory, LA-2D/3D-TN-81-11, January 1981.

U-611 Fujita, R.K., "Analysis of CCTF Core-I Test C1-11 (Run 20)," Los Alamos National Laboratory, LA-2D/3D-TN-81-13, April 1981.

U-612 Fujita, R.K., "TRAC-PD2 Post Test Analysis of CCTF Test C1-12 (Run 21)," Los Alamos National Laboratory, LA-2D/3D-TN-81-31, October 1981.

U-613 Sugimoto, J., "TRAC-PD2 Reflood Code Assessment for CCTF Test C1-16," Los Alamos National Laboratory, LA-2D/3D-TN-81-9, February 1981.

U-614 Motley, F., "TRAC-PD2 Post Test Analysis of the CCTF Evaluation Model Test C1-19 (Run 38)," Los Alamos National Laboratory, LA-2D/3D-TN-82-7, March 1982.

U-615 Akimoto, H., "Analysis of TRAC-PD2 and CCTF Results for the Cylindrical Core Test Facility Evaluation Model Test C1-19 (Run 38)," Los Alamos National Laboratory, LA-2D/3D-TN-82-9, September 1982.

U-616 Motley, F., "TRAC-PD2 Analysis of CCTF Multidimensional Test 11 (C1-20, Run 39)," Los Alamos National Laboratory, LA-2D/3D-TN-81-28, October 1981.

U-617 Fujita, R.K., "Data Analysis of CCTF Core-I Base Case and Selected Parametric Effects Tests," Los Alamos National Laboratory, LA-2D/3D-TN-81-16, April 1981.

U-618 Williams, K.A., "Double Blind Pretest Prediction of the CCTF Core-I Evaluation Model Test Using TRAC-PD2," Los Alamos National Laboratory LA-2D/3D-TN-81-12, March 1981.

CCTF Core-II

U-621 Crowley, C.J., Cappiello, M.W., and Boyack, B.E., "Summary Report of TRAC-PF1 Assessment Against the CCTF Core-II Data," Los Alamos National Laboratory, LA-CP-89-17, February 1989.

U-622 Cappiello, M.W., Stumpf, H.J., and Boyack, B.E., "CCTF Core-II Upper Plenum Injection Summary," Los Alamos National Laboratory, LA-2D/3D-TN-86-16, March 1987.

U-623 Kotas, J.F., "TRAC-PF1 Calculation of CCTF Core-II Acceptance Test-1 (C2-AC1, Run 51)," Los Alamos National Laboratory, LA-2D/3D-TN-83-10, September 1983.

U-624 Motley, F., "TRAC-PF1 Calculation of CCTF Core-II Base Case (C2-SH1, Run 53)," prepared by Los Alamos National Laboratory, LA-2D/3D-TN-83-12, September 1983.

U-625 Crowley, C.J. and Rothe, P.H., "TRAC-PF1 Calculation of CCTF Core-II Reflood Test 54 (C2-SH2)," Los Alamos National Laboratory, LA-2D/3D-TN-86-2, March 1986.

U-626 Boyack, B.E., "TRAC-PF1/MOD1 Analysis of CCTF UPI Test C2-AA1 (Run 57)," Los Alamos National Laboratory, LA-2D/3D-TN-86-6, April 1986.

U-627 Roberts, M., "TRAC-PF1/MOD1 Upper Plenum Nodalization Studies of CCTF UPI Test C2-AA1 (Run 57)," Los Alamos National Laboratory, LA-2D/3D-TN-86-14, March 1986.

U-628 Siebe, D.A. and Boyer, B., "The Analysis of CCTF Run 58 with TRAC PF1/MOD1," Los Alamos National Laboratory, LA-2D/3D-TN-86-19.

U-629 Cappiello, M., "CCTF Run 59 TRAC-PF1/MOD1 Analysis," Los Alamos National Laboratory, LA-2D/3D-TN-85-1, January 1985.

U-630 Kotas, J.F., "The Effect of the Radial Power Upon the Reflood Phase of a Loss-of-Coolant Accident: A TRAC Analysis of CCTF Test C2-5 (Run 63) and CCTF Test C2-6 (Run 64)," Los Alamos National Laboratory, LA-2D/3D-TN-84-6, September 1984.

U-631 Slater, C.E., "TRAC-PF1 Calculation of CCTF Core-II Reflood Test C2-10 (Run 69)," Los Alamos National Laboratory, LA-2D/3D-TN-85-7, September 1984.

U-632 Crowley, C.J., Fanning, M.W., and Rothe, P.H., "TRAC-PF1 Calculation of CCTF Core-II Refill Test 70," Los Alamos National Laboratory, LA-2D/3D-TN-85-14, December 1985.

U-633 Stumpf, H.J. and Wiilcutt, G.J., "CCTF Run 71 TRAC-PF1/MOD1 Analysis," Los Alamos National Laboratory, LA-2D/3D-TN-86-8, May 1986.

U-634 Cappiello, M.W., "TRAC-PF1/MOD1 Analysis of CCTF No-Failure UPI Test C2-13 (Run-72)," Los Alamos National Laboratory, LA-2D/3D-TN-86-7, July 1986.

U-635 Crowley, C.J. and Rothe, P.H., "TRAC-PF1 Calculation of CCTF Core-II Reflood Test 75 (C2-15)," Los Alamos National Laboratory, LA-2D/3D-TN-86-1, April 1986.

U-636 Stumpf, H.J., "CCTF Run 76 TRAC-PF1/MOD1 Analysis," Los Alamos National Laboratory, LA-2D/3D-TN-86-6, April 1986.

U-637 Stumpf, H.J., "CCTF Run 78 TRAC-PF1/MOD1 Analysis," Los Alamos National Laboratory, LA-2D/3D-TN-86-5, May 1986.

U-638 Cappiello, M.W., "TRAC-PF1/MOD1 Analysis of CCTF Combined Injection Test Run 79," Los Alamos National Laboratory, LA-2D/3D-TN-86-20.

SCTF Core-I

U-641 Williams, K.A., "Research Information Report on the TRAC Analysis and Experimental Results of the Core-I Test Series at the Japan Atomic Energy Research Institute Slab Core Test Facility," prepared by Los Alamos National Laboratory, LA-CP-88-52,
March 1988.

U-642 Smith, S., "SCTF Steam Supply Design Analysis with TRAC," Los Alamos National Laboratory, NUREG/CR-1946, May 1981.

U-643 Smith, S., "A Parametric Study of the Effect of Material Properties on the Calculated Rod Heatup Rate for the SCTF," Los Alamos National Laboratory, LA-2D/3D-TN-81-21, June 1981.

U-644 Smith, S., "Revision of the TRAC Calculational Model for the SCTF," Los Alamos National Laboratory, LA-2D/3D-TN-81-17, October 1981.

U-645 Smith, S., "TRAC Analysis of the SCTF High Pressure Shakedown Test: Run 506," Los Alamos National Laboratory, LA-2D/3D-TN-81-22, October 1981.

U-646 Smith, S., "TRAC Analysis of the SCTF Base Case Test Run 507," Los Alamos National Laboratory, LA-2D/3D-TN-81-23, October 1981.

U-647 Smith, S., "TRAC Analysis of the SCTF Low Pressure Test: Run 508," Los Alamos National Laboratory, LA-2D/3D-TN-81-24, October 1981.

U-648 Smith, S., "TRAC Analysis of the SCTF High Subcooling Test: Run 510," Los Alamos National Laboratory, LA-2D/3D-TN-81-25, December 1981.

U-649 Fujita, R.K., "TRAC-PD2 Analysis of SCTF Power-Effects Tests," Los Alamos National Laboratory, LA-2D/3D-TN-82-3, March 1982.

U-650 Fujita, R.K., "TRAC-PD2 Analysis of SCTF Peak Core Power-Effects Tests," Los Alamos National Laboratory, LA-2D/3D-TN-82-5, March 1982.

U-651 Sudo, Y., "Analysis of TRAC and SCTF Results for System Pressure Effects Tests Under Forced Flooding: Runs 506, 507 and 508," Los Alamos National Laboratory, NUREG/CR-2622 (LA-2D/3D-TN-81-33; LA-9258-MS) March 1982.

U-652 Smith, S., "TRAC Analysis of the SCTF Forced Flooding ECC Injection Rate Tests: Runs 507, 511 and 515," Los Alamos National Laboratory, LA-2D/3D-TN-82-04, September 1982.

U-653 Smith, S., "Analysis of the SCTF FLECHT Counterpart Test Using TRAC-PF1," Los Alamos National Laboratory, LA-2D/3D-TN-83-02, January 1983.

U-654 Gilbert, J.S. and Williams, K.A., "Rod Bundle Cross-Flow Study," Los Alamos National Laboratory, LA-2D/3D-TN-83-13, September 1983.

U-655 Osakabe, M., Gilbert, J.S., and Fujita, R.K., "TRAC-PD2 Analysis of Radial Core Pressure Loss During Reflood for Test S1-08," Los Alamos National Laboratory, LA-2D/3D-TN-83-16, December 1983.

U-656 Lin, J.C., "TRAC-PF1 Calculation of SCTF Core-I Combined Injection Test: Run 529," Los Alamos National Laboratory, LA-2D/3D-TN-84-7, November 1984.

SCTF Core-II

U-661 Shire, P.R., Gilbert, J.S., and Lin, J.C., "SCTF Core-II TRAC-PF1/MOD1 Analysis Summary," Los Alamos National Laboratory, LA-CP-89-113, May 1, 1989.

U-662 Gilbert, J.S., "TRAC-PF1/MOD1 Calculation of SCTF Core-II Test S2-SH1 (Run 604)," Los Alamos National Laboratory, LA-2D/3D-TN-85-6, March 1985.

U-663 Shire, P.R. and Boyack, B.E, "Upper-Plenum Studies of SCTF Run 605," Los Alamos National Laboratory, LA-2D/3D-TN-86-15, August 1986.

U-664 Shire, P.R., "TRAC-PF1/MOD1 Re-Analysis of SCTF Core-II Test S2-SH2 (Run 605)," Los Alamos National Laboratory, LA-CP-87-103, December 1986.

U-665 Lin, J.C., "TRAC-PF1/MOD1 Calculation of SCTF Core-II Supply Test S2-03 (Run 608)," Los Alamos National Laboratory, LA-2D/3D-TN-85-13, July 1985.

U-666 Abe, Y., Lin, J.C., and Gilbert, J., "TRAC-PF1/MOD1 Calculation of SCTF Core-II Steam Supply Test S2-05 (Run 610)," Los Alamos National Laboratory, LA-2D/3D-TN-85-9, July 1985.

U-667 Gilbert, J.S., "TRAC-PF1/MOD1 Calculation of SCTF Core-II Test S2-06 (Run 611)," Los Alamos National Laboratory, LA-2D/3D-TN-86-9, March 1986.

U-668 Lin, J.C., "TRAC-PF1/MOD1 Calculation of SCTF Core-II FLECHT-SET Coupling Test S2-08 (Run 613)," Los Alamos National Laboratory, LA-2D/3D-TN-85-2, February 1985.

U-669 Gilbert, J.S., "TRAC-PF1/MOD1 Calculation of SCTF Core-II Test S2-09 (Run 614)," Los Alamos National Laboratory, LA-2D/3D-TN-85-4, March 1985.

U-670 Gilbert, J.S., "TRAC-PF1/MOD1 Calculation of SCTF Core-II Test S2-12 (Run 617)," Los Alamos National Laboratory, LA-2D/3D-TN-86-13, March 1987.

SCTF Core-III

U-681 Boyack, B.E., Shire, P.R., and Harmony, S.C., "TRAC-PF1/MOD1 Code Assessment Summary Report for SCTF Core-III," by Los Alamos National Laboratory, LA-CP-90-71, February 1990.

U-682 Gilbert, J.S., "TRAC-PF1/MOD1 Calculation of Operational Study No. 1," Los Alamos National Laboratory, LA-CP-87-112.

U-683 Harmony, S.C. and Boyack, B.E., "A Posttest Analysis of SCTF Run 703 Using TRAC-PF1/MOD1," Los Alamos National Laboratory, (to be issued).

U-684 Mascheroni, P.L. and Boyack, B.E., A Posttest Analysis of SCTF Run 704 Using TRAC-PF1/MOD1," Los Alamos National Laboratory, LA-CP-88-131, June 1988.

U-685 Harmony, S.C., "TRAC-PF1/MOD1 Analysis of SCTF Test S3-5 (Run 709)," Los Alamos National Laboratory, (to be issued).

U-686 Shire, P.R., "TRAC-PF1/MOD1 Analysis of SCTF Core-III Test S3-9 (Run 713)," Los Alamos National Laboratory, LA-CP-88-11, January 1988.

U-687 Harmony, S.C. and Boyack, B.E., "A Posttest Analysis of SCTF Run 714 Using TRAC-PF1/MOD1," Los Alamos National Laboratory, LA-CP-88-234, September 1988.

U-688 Boyack, B.E., "A Posttest Assessment of TRAC-PF1/MOD1 and TRAC-PF1/MOD2 Using SCTF Core-III Run 719 (Test S3-15)," Los Alamos National Laboratory, LA-CP-90-27, January 1990.

U-689 Rhee, G., "A Posttest Analysis of SCTF Run 720 Using TRAC-PF1/MOD1," Los Alamos National Laboratory, (to be issued).

UPTF

U-701 Cappiello, M.W., "TRAC-PF1 Calculations of a UPTF Intact Loop during ECC Injection," Los Alamos National Laboratory, LA-2D/3D-TN-81-20, May 1981.

U-702 Cappiello, M. "GPWR and UPTF Intact Loop Calculations -- Assessment of UPTF Alternative Loop Configurations," Los Alamos National Laboratory, LA-2D/3D-TN-82-2, January 1982.

U-703 Cappiello, M. "An Analysis of the UPTF Base Case with TRAC-PF1/MOD1," Los Alamos National Laboratory, LA-2D/3D-TN-85-8, July 1985.

U-704 Ohnuki, A. and Cappiello, M.W., "Assessment of TRAC-PF1/MOD1 for Countercurrent-Annular and Stratified Flows," Los Alamos National Laboratory, LA-2D/3D-TN-85-3, September 1985 (publicly released as a JAERI-M Report -- see J-629).

U-705 Dotson, P., "UPTF Downcomer Pretest Analysis," Los Alamos National Laboratory, LA-2D/3D-TN-85-10, October 1985.

U-706 Dotson, P., "Small-Break LOCA TRAC Pretest Calculation," Los Alamos National Laboratory, LA-2D/3D-TN-86-4, December 1986.

U-707 Hedstrom, J., and Cappiello, M.W., "Results of a Pretest Analysis of the UPTF US/Japanese Integral Test," Los Alamos National Laboratory, LA-2D/3D-TN-86-17, March 1987.

U-708 Cappiello, M., "Posttest Analysis of the Upper Plenum Test Facility Small-Break Loss-of-Coolant Accident Test with TRAC-PF1/MOD1 and MOD2," Los Alamos National Laboratory, LA-CP-88-154, July 1988.

U-709 Stumpf, H.J., "Posttest Analysis of UPTF Test 10B Using TRAC-PF1/MOD1," Los Alamos National Laboratory, LA-CP-90-1, January 1990.

U-710 Shire, P.R., "TRAC-PF1/MOD2 Analysis of UPTF Test 20 Upper Plenum Injection in a Two-Loop PWR," Los Alamos National Laboratory, LA-CP-90-2, January 1990.

U-711 Siebe, D.A., and Stumpf, H.J., "Posttest Analysis of the Upper Plenum Test Facility Downcomer Separate Effects Tests with TRAC- PF1/MOD2," Los Alamos National Laboratory, LA-CP-90-299, July 1990.

U-712 Stumpf, H.J., "Posttest Analysis of UPTF Test 08 Using TRAC-PF1/MOD2," Los Alamos National Laboratory, LA-CP-90-373, September 6, 1990.

U-713 Siebe, D.A., and Stumpf, H.J., "Assessment of the Ability of TRAC-PF1/MOD1 and TRAC-PF1/MOD2 to Predict Phenomena Related to Steam Binding," Los Alamos National Laboratory, LA-CP-92-79, March 1992.

U-714 Mullen, E. M., Stumpf, H. J. and Siebe, D. A., "Summary of Cold-Leg Flow Phenomena Observed in UPTF and CCTF Tests and TRAC Posttest Analyses," Los Alamos National Laboratory, LA-CP-91-332, September 1991.

U-715 Mullen, E. M., Stumpf, H. J., and Siebe, D. A., "Summary of Downcomer Injection Phenomena for UPTF and TRAC Post-test Analysis," Los Alamos National Laboratory, LA-CP-92-188, May 1992.

U-716 Siebe, D.A., and Stumpf, H.J., "An Assessment of TRAC-PF1/MOD2 against Data from the Upper Plenum Test Facility for Accumulator Nitrogen Surge," Los Alamos National Laboratory, LA-CP-92-408, November 1992.

US/J PWRs

U-721 Ireland, J. and Liles, D., "A TRAC-PD2 Analysis of a Large-Break Loss-of-Coolant Accident in a Reference US PWR, "Los Alamos National Laboratory, LA-2D/3D-TN-81-10, March 1981.

U-722 Fujita, R.K., Motely, F., and Williams, K.A., "TRAC-PF1 Analysis of a Best-Estimate Large-Break LOCA in Westinghouse PWR with Four Loops and 17 x 17 Fuel," Los Alamos National Laboratory, LA-2D/3D-TN-83-4, September 1983.

U-723 Spore, J.W. and Cappiello, M.W., "TRAC-PF1/MOD1 Analysis of a 200% Cold-Leg Break in a US/Japanese PWR with Four Loops and 15x15 Fuel," Los Alamos National Laboratory, LA-2D/3D-TN-85-11, November 1985.

U-724 Coddington, P. and Motely, F., "TRAC-PF1/MOD1 Analysis of a Minimum Safeguards Large Break Loss-of-Coolant Accident in a 4-Loop PWR with 17 x 17 Fuel," Los Alamos National Laboratory, LA-2D/3D-TN-86-3, August 1986.

U-725 Gido, R.G. and Cappiello, M.W., "TRAC-PF1/MOD1 Analysis of a 200% Cold-Leg Break in a Babcock & Wilcox Lowered Loop Plant," Los Alamos National Laboratory, LA-2D/3D-TN-86-12, October 1986.

U-726 Shire, P.R and Spore, J.W., "TRAC-PF1/MOD1 Analysis of a Minimum Safeguards Large-Break LOCA in a US/Japanese PWR with Four Loops and 15 x 15 Fuel," Los Alamos National Laboratory, LA-CP-87-61, April 1987.

U-727 Gruen, G.E. and Fisher, J.E., "TRAC PF1/MOD1 US/Japanese PWR Conservative LOCA Prediction," EGG Idaho, NUREG/CR-4965 (EGG-2513), November 1987.

GPWRs

U-741 Motley, F. and Cappiello, M., "TRAC-PD2 Hot Leg Sensitivity Study," Los Alamos National Laboratory, LA-2D/3D-TN-81-1, February 1981.

U-742 Motley, F., "Review of the TRAC Calculated GPWR Upper Plenum/Core Flow Conditions to Aid in the Design of UPTF," Los Alamos National Laboratory, LA-2D/3D-TN-81-19, May 1981.

U-743 Motley, F., and Williams K.A., "TRAC-PD2 Calculation of a Double-Ended Cold-Leg Break in a Reference German PWR," Los Alamos National Laboratory, LA-2D/3D-TN-81-32, January 1981.

U-744 Motley, F., "TRAC-PF1 Calculation of a Reference German PWR at the Initiation of ECC Injection," Los Alamos National Laboratory, LA-2D/3D-TN-81-8, February 1981.

U-745 Cappiello, M.W., "TRAC-PF1 Sensitivity Studies of a GPWR Intact Loop During ECC Injection," Los Alamos National Laboratory, LA-2D/3D-TN-81-18, May 1981.

U-746 Cappiello, M.W., and Hrubisko, M., "GPWR-1982 TRAC-PF1 Input Deck Description," Los Alamos National Laboratory, LA-2D/3D-TN-82-10, December 1982.

U-747 Cappiello, M.W., "GPWR-1982 TRAC-PF1 Base Case Results," Los Alamos National Laboratory, LA-2D/3D-TN-83-6, February 1983.

U-748 Cappiello, M.W., and Vojtek, I., "TRAC-PF1 Analysis of a 200% Hot Leg Break in a German PWR," Los Alamos National Laboratory, LA-2D/3D-TN-83-8, August 1983.

ADVANCED INSTRUMENTATION REPORTS

Evaluation of Instrument Performance

U-801 "Program Plan for Correction of US Instrument Degradation or Failure in the Upper Plenum Test Facility (UPTF) in the Federal Republic of Germany," prepared by the Nuclear Regulatory Commission, NUREG-1284, July 1987.

U-802 "Insights Derived from USNRC Advanced Instrumentation in CCTF and SCTF," prepared by MPR Associates, MPR-1035, December 1987.

U-803 Fullmer, K.S., "Review of INEL SCTF Instrumentation," EGG Idaho, EGG-3D-6370, November 1983.

U-804 Fullmer, K.S., "Review of INEL CCTF Instrumentation," EGG Idaho, EGG-3D-6544, April 1984.

U-805 Fullmer, K.S., "Review of INEL CCTF-II Instrumentation," EGG Idaho, EGG-3D-6981, September 1985.

U-806 Fullmer, K.S., "Review of INEL SCTF Core-II Instrumentation," EGG Idaho, EGG-3D-6982, September 1985.

U-807 Hardy, J.E. and Herskovitz, M.B., "Assessment of the Adequacy of ORNL Instrumentation in Reflood Test Facilities," Oak Ridge National Laboratory, NUREG/CR-3651, (ORNL/TM-9067), April 1985.

U-808 Hardy, J.E., et.al., "ORNL Instrumentation Performance for Slab Core Test Facility (SCTF) - Core 1 Reflood Test Facility," Oak Ridge National Laboratory, NUREG/CR-3286 (ORNL/TM-8762), November 1983.

U-809 "ORNL Instrumentation Performance for Slab Core Test Facility Runs 604, 608 and 613," prepared by Oak Ridge National Laboratory, ORNL/NRC/LTR-85/19, June 1985.

U-810 "Performance of ORNL Instrumentation in Cylindrical Core Test Facility - Core-II (CCTF-II) for Runs 075, 076 and 079," prepared by Oak Ridge National Laboratory, ORNL/NRC/LTR-85/18, June 1985.

U-811 Morgan, K.A., "SCTF I Uncertainty Analysis," EGG Idaho, EGG-CAAD-5398, September 1981.

U-812 Morgan, K.A., "CCTF I Uncertainty Analysis," EGG Idaho, EGG-CAAD-5704, December 1981.

U-813 Lassahn, G.D., "BMFT UPTF Advanced Instrumentation Uncertainty Analysis Report," EGG Idaho, EGG-3D-6751, February 1985.

Instrument Interpretation in Two-Phase Flow

U-821 "Review and Evaluation of ORNL Instrument Development Loop Data and Formulation of a Mass Flow Rate Calculation Scheme," prepared by MPR Associates, March 1983.

U-822 "A Study of Special Effects Around a Tie Plate Turbine Meter in Two-Phase Upflow," prepared by MPR Associates, MPR-826, June 1984.

U-823 "Evaluation of a Steady State Mass Flow Rate Calculation Method Using ORNL Instrument Development Loop Transient Data," prepared by MPR Associates, MPR-859, January 1985.

U-824 Hardy, J.E., "Mass Flow Measurements Under PWR Reflood Conditions in a Downcomer and at a Core Barrel Vent Valve Location," Oak Ridge National Laboratory, NUREG/CR-2710 (ORNL/TM-8331), 1982.

U-825 Thomas, D.G. and Combs, S.K., "Measurement of Two-Phase Flow at the Core/Upper Plenum Interface for a PWR Geometry Under Simulated Reflood Conditions, Oak Ridge National Laboratory, NUREG/CR-3138 (ORNL/TM-8204), 1983.

U-826 Lassahn, G.D., "Mass Flow Estimation Using Subroutines DRPOF4 and EMDOT4," EGG Idaho, EGG-3D-6305, July 1983.

Film and Impedance Probes

U-831 Eads, B.G., et.al., "Advanced Instrumentation for Reflood Studies Program Quarterly Progress Report (October-December 1977)," Oak Ridge National Laboratory, ORNL/NUREG/TM-202, 1977.

U-832 Moorhead, A.J., et.al., "Fabrication of Sensors for High-Temperature Steam Instrumentation Systems," Oak Ridge National Laboratory, NUREG/CR-1359 (ORNL/NUREG-65), 1980.

U-833 Hardy, J.E., et.al., "Transient Testing of an In-core Impedance Flow Sensor in a 9-Rod Heated Bundle," Oak Ridge National Laboratory, ORNL/NUREG/TM-389, 1981

U-834 Hardy, J.E and Hylton, J.O., "Electrical Impedance String Probes for Two-Phase Void and Velocity Measurements," Oak Ridge National Laboratory, ORNL/NUREG/TM-8172, 1982.

Turbine Meters

U-841 "CCTF-II Operation and Maintenance Manual - Turbine Flowmeter Measurement System," Measurements Incorporated OM-236-1, July 1981.

U-842 Jensen, M.F., "Turbine Flowmeter System Tests," EGG Idaho, EGG-3D-5372, March 1981.

Drag Discs

U-846 "CCTF Operation and Maintenance Manual-Instrumented Spool Piece and Downcomer Drag Disk Flow Measurement Systems," prepared by EGG Idaho, EGG-3D-5105, March 1980.

U-847 "UPTF Drag Disk Transducer Test Report," EGG Idaho, EGG-3D-6980, July 1985.

Gamma Densitometers

U-851 "SCTF Operation and Maintenance Manual Single-Beam Density Measurement Systems," prepared by EGG Idaho, EGG-3D-5179, January 1981.

U-852 Rohrdanz, R.F., "Prototype Test Report for the SCTF Single Beam Density Measuring Systems," EGG Idaho, EGG-3D-5457, June 1981.

U-853 Grimesey, R.A. and Tomberlin, T.A., "Radiation Shielding Calculations for UPTF Gammaray Densitometer," EGG Idaho, EGG-PHYS-6201, March 1983.

U-854 Menkhaus, D.E., "BMFT UPTF Densitometer System Test Report," EGG Idaho, EGG-RTH-7075, November 1985.

Liquid Level Detectors/Fluid Distribution Grid

U-861 "CCTF Operation and Maintenance Manual -- Conductivity Liquid Level Measurement System (CLLMS)," EGG Idaho, EGG-3D-5046, December 1979.

U-862 "Optical Liquid-Level Detector Two-Phase Flow Test Report," EGG Idaho, EGG-3D-4523, May 1981.

Spool Pieces and Pipe Flowmeters

U-866 "SCTF Operation and Maintenance Manual -- Cold Leg and Vent Pipe Instrumented Spool Pieces and Downcomer Drag Disk Flow Measurement Systems," prepared by EGG Idaho, EGG-3D-5177, March 1981.

U-867 "SCTF Operation and Maintenance Manual -- Hot Leg Spool Piece Flow Measurement System," prepared by EGG Idaho, EGG-3D-5178, March 1981.

U-868 Cornell, J.A., "Two-Phase Flow Testing of SCTF Hot Leg Spool Piece Data Analysis Report," EGG Idaho, EGG-3D-5416, April 1981.

Velocimeters

U-871 "CCTF-II Operation and Maintenance Manual -- Cooled Velocimeter Flow Measurement System," prepared by EGG Idaho, EGG-3D-5809, April 1982.

U-872 Menkhaus, D.E., "CCTF-II Cooled Velocimeter Probe Performance Test Report," EGG Idaho, EGG-3D-5511, December 1981.

Video Probes

U-876 "CCTF-II Operation and Maintenance Manual -- Video Probe Systems," prepared by EGG Idaho, EGG-3D-5772, April 1982.

PAPERS, PRESENTATIONS, AND CORRESPONDENCE

Papers - Data Evaluation

U-901 Zuber, N., "Proposed UPTF Thermal Mixing Experiments," presented at the 2D/3D Coordination Meeting, Mannheim, FRG, June 1985.

U-902 Theofanous, T.G., Iyer, K., Nourbakhsh, H.P., and Shabana, E., "Scaling of Thermal Mixing Phenomena from 1/5 to Full-Scale Test Facilities," Proceedings of the Fourteenth Water Reactor Safety Information Meeting, October 27 - 31, 1986, Vol. 4, pp. 363-386.

U-903 Naff, S.A., "UPTF-Experiment Core Simulator Entrainment/De-entrainment Test 10C," Handout G-5 from 2D/3D Coordination Meeting, Mannheim, FRG, May 1987.

U-904 Damerell, P.S., Ehrich, N.E., and Wolfe, K.A., "Use of Full-Scale UPTF Data to Evaluate Scaling of Downcomer (ECC Bypass) and Hot Leg Two-Phase Flow Phenomena," Proceedings of the Fifteenth Water Reactor Safety Research Information Meeting, October 26-29, 1987, NUREG/CP-0091, Vol. 4, pp. 143-165.

U-905 Rhee, G., Damerell, P., and Simons, J., "Use of 2D/3D Data to Scale Up Liquid Carryover/De-entrainment (Steam Binding) Behavior to a PWR," Proceedings of the Sixteenth Water Reactor Safety Research Information Meeting, October 24-27, 1988, NUREG/CP-0097, Vol, 4, pp. 485-509.

U-906 Russell, A., Damerell, P., Ahrens, G., and Weiss, P., "UPTF Upper Plenum Injection (UPI) Test Results and Application to PWR," Proceedings of the Sixteenth Water Reactor Safety Research Information Meeting, October 24-27, 1988, NUREG/CP-0097, Vol. 4, pp. 511-531.

Papers - Code Analysis

U-911 Coddington, P., "The Effect of Accumulator Nitrogen on the Reflood of a PWR Core during a Large Break LOCA," presented at the IAEA Specialists Meeting on Fuel Behavior under Accident Conditions and Acceptance Criteria, Warsaw, Poland, September 30 - October 4, 1985.

Papers - Instrumentation

U-921 Eads, G.B., et al., "Development of In-Vessel Reflood Instrumentation at ORNL," Meeting of the Japanese Nuclear Society, Osaka, Japan, March 26-28, 1979.

U-922 Combs, S.K., and Hardy, J.E., "An Experimental Investigation of Flow Monitoring Instrument in the Upper Plenum of an Air-Water Reflood Test Facility," Symposium on Polyphase Flow and Transport Technology, ASME Centennial Meeting, San Francisco, CA, August 12-15, 1980.

U-923 Zabriskie, W.L., et al., "Instrumentation Development for Low Range, Long Line Differential Pressure Measurements," ISA Transactions, Vol. 20, No. 4, pp. 61-75 (1981).

U-924 Hardy, J.E., and Hylton, J.O., "Electrical Impedance String Probes for Two-Phase Void and Velocity Measurements," International Journal of Multiphase Flow, October 1984.

U-925 Hardy, J.E., et al., "Measurement of Two-Phase Flow Momentum with Force Transducers," presented at International Symposium on Gas-Liquid Two-Phase Flows, ASME Winter Annual Meeting, Dallas, Texas, November 1990, CONF-901109-1.

Correspondence

U-931 "US Input to Definition of Test Objectives and Conditions for UPTF Fluid-Fluid Mixing Test (Test No. 1 in Matrix and Sequence)," enclosure to MPR letter from P. Damerell to L. Shotkin (USNRC), February 14, 1986.

U-932 "US Input to Definition of Test Objectives and Conditions for the Third UPTF Cold Leg Injection Integral Test No. 27," enclosure to MPR letter from P. Damerell to G. Rhee (USNRC), February 3, 1989.

REPORTS AND PAPERS EXTERNAL TO 2D/3D PROGRAM

DATA REPORTS

ECC Delivery Depressurization

E-001 Crowley, C.J., et al., "1/5 Scale Countercurrent Flow Data Presentation and Discussion," Creare, NUREG/CR-2106 (Creare TN-333), November 1981.

E-002 Crowley C.,J., et al., "Downcomer Effects in a 1/15 Scale PWR Geometry - Experimental Data Report," Creare, NUREG-0281, May 1977.

E-003 Crowley, C.J., and Sam, R.G., "Experimental Data Report for Flashing Transients," Creare, NUREG/CR-2060 (Creare TN-330), February 1982.

E-004 Cudnik, R.A., et al., "Topical Report on Penetration Behavior in a 1/15 Scale Model of a Four-Loop Pressurized Water Reactor," Battelle Columbus Labs, BMI-NUREG-1973, June 1977.

Upper Plenum Injection

E-011 "Experimental Data Report for Semiscale Mod-1 Tests S-05-6 and S-05-7 (Alternate ECC Injection Tests)," prepared by EGG Idaho, TREE-NUREG-1055, June 1977.

Hot Leg Countercurrent Flow/Reflux Condenser Mode

E-021 "Experiment Data Report for Semiscale Mod-2A Natural Circulation Tests S-NC-2B, S-NC-3 and S-NC-4B," prepared by EGG Idaho, NUREG/CR-2454, December 1981

E-022 "Experiment Data Report for Semiscale Mod-2A Natural Circulation Tests S-NC-5 and S-NC-6," prepared by EGG Idaho, NUREG/CR-2501, January 1982.

E-023 "Experimental Operating Specification, Natural Circulation Test Series, Semiscale Mod-2A," prepared by EGG Idaho, EGG-SEMI-5427, April 1981.

Accumulator Nitrogen Discharge

E-031 Denham, M.K. and Dore, P., "ISP-25, Boundary Conditions and Experimental Procedure for ACHILLES Run A1B105," AEEW, SESD Note 495, September 1988.

EVALUATION REPORTS

General

E-401 "Compendium of ECCS Research for Realistic LOCA Analysis," NUREG-1230, December 1988.

ECC Delivery during Depressurization

E-411 Beckner, W.D. et al., "Analysis of ECC Bypass Data," USNRC, NUREG-0573, July 1979.

E-412 Beckner, W.D., et al., "PWR Lower Plenum Refill Research Results," USNRC Research Information Letter No. 128, December 8, 1981.

E-413 "A Preliminary Study of Annulus ECC Flow Oscillations," Creare, NP-839, Research Project 347-1, August 1978.

E-414 Crowley, C.J., et al., "An Evaluation of ECC Penetration Using Two Scaling Parameters," Creare, Creare TN-233, Septernber 1976.

E-415 Rothe, P.H., "Technical Summary Attachment to ECC Bypass RIL Volume I: Review of Findings," Creare, NUREG/CR-0885, Vol. 1 (Creare TN-296, Vol. 1), July 1979.

E-416 Crowley, C.J., Wei, S., Murrary, J.G., Rothe, P.H., and McKenna, S.A., "Technical Summary Attachment to ECC Bypass RIL Volume II: Technical Appendices," Creare, NUREG/CR-0885, Vol. 2 (Creare TN-296, Vol. 2), July 1979.

E-417 Crowley, C.J., and Sam, R.G., "Experimental Facility and Preliminary Results for Flashing Transients at 1/5 Scale," Creare, Creare TM-707, July 1980.

E-418 Crowley, C.J., Wei, S. and Rothe, P.H., "Analysis of Flashing Transient Effects During Refill," Creare, NUREG/CR-1765, March 1981.

E-419 Crowley, C.J., "Summary of Refill Effects Studies with Flashing and ECC Interactions," Creare, NUREG/CR-2058, November 1981.

E-420 Carbiener, W.A., et al., "Steam-Water Mixing an System Hydrodynamics Program; Task 4; Quarterly Progress Report; January 1, 1977 - March 31, 1977," Battelle Columbus Labs, BMI-NUREG-1972, May 1977.

E-421 Segev, A. and Collier, R.P., "Development of a Mechanistic Model for ECC Penetration in a PWR Downcomer," Battelle Columbus Labs, NUREG/CR-1426, June 1980.

E-422 Segev, A. and Collier, R.P., "Application of Battelle's Mechanistic Model to Lower Plenum Refill," Battelle Columbus Labs, NUREG/CR-2030, March 1981.

Loop Behavior

E-431 Brodrick, J.R., Burchill, W.E., and Lowe, P.A., "1/5 Scale Intact Loop Post-LOCA Steam Relief Tests," Combustion Engineering, CENPD-63, Revision 1, March 1973.

E-432 Burchill, W.E., Lowe, P.A., and Brodrick, J.R., "Steam-Water Mixing Test Program Task D: Formal Report for Task B and Final Report for the Steam Relief Phases of the Test Program," Combustion Engineering, AEC-COO-2244-1 (CENPD-101), October 1973.

E-433 Rothe, P.H., Wallis, G.B., and Thrall, D.E., "Cold Leg Flow Oscillations," Creare Inc., EPRI NP-282, November 1976.

E-434 Crowley, C.J., Sam, R.G. and Rothe, P.H., "Summary Report: Hot Leg ECC Flow Reversal Experiments," Creare R & D, Creare TM-870, 1982.

E-435 Lilly, G.P., Stephens, A.G. and Hochreiter, L.E., "Mixing of Emergency Core Cooling Water with Steam: 1/14 Scale Testing Phase," Westinghouse Electric Corporation, WCAP-8307 (EPRI Program 294-2), January 1975.

E-436 Lilly, G.P. and Hochreiter, L.E., "Mixing of Emergency Core Cooling Water with Steam: 1/3 Scale Test and Summary," Westinghouse Electric Corporation, WCAP-8423 (EPRI Program 294-2), June 1975.

Fluid/Fluid Mixing

E-441 Theofanous, T., et. al, "Decay of Buoyancy Driven Stratified Layers with Application to PTS," Purdue University, NUREG/CR-3700, February 1984.

Core Thermal-Hydraulic Behavior

E-451 Bruestle, H.R., et. al., "Thermal-Hydraulic Analysis of the Semiscale Mod-1 Reflood Test Series (Gravity Feed Tests)," Idaho National Engineering Laboratory, TREE-NUREG-1010, January 1977.

E-452 Cadek, F.F., et. al., "PWR FLECHT Final Report Supplement," Westinghouse Electric Corporation, WCAP-7931, October 1972.

E-453 Catton, I., and Toman, W.I., "Multidimensional Thermal-Hydraulic Reflood Phenomena in a 1692-Rod Slab Core," EPRI-NP-2392, 1982.

E-454 Conway, C.E., et. al., "PWR FLECHT Separate Effects and Systems Effects Test (SEASET), Program Plan," Westinghouse Electric Corporation, WCAP-9183, November 1977.

E-455 DeJarlais, G. and Ishii, M., "Inverted Annular Flow Experimental Study," Argonne National Laboratory, NUREG/CR-4277.

E-456 Addobo, C., Piplies, L. and Riebold, W. L., "LOBI-MOD 2: Facility Description and Specification for OECD-CNI International Standard Problem No. 18 (ISP-18): Volume 1 - Geometrical Configuration of the Test Facility," CEC Communication No. 4010, July 1983.

E-457 Erbacher, F. J., Neitzel, H. J., and Wiehr, K., "Cladding Deformation and Emergency Core Cooling of a Pressurized Water Reactor in a LOCA," Summary Description of the REBEKA Program, KfK-4781, August 1990.

E-458 Kremin, H., et. al., "Transientenuntersuchungen in der PKL-Anlage (PKL III A) Abschlussbericht, Band 2: Beschreibung der Versuchsanlage," Siemens/KWU, U9 414/89/018, September 1989.

E-459 Arrieta, L. and Yadigaroglu, G., "Analytical Model for Bottom Reflooding Heat Transfer in Light Water Reactors (The UCFLOOD Code)," University of California, EPRI NP-756, August 1978.

E-460 "LOBI-MOD2: Research Program A Final Report," CEC Communication No. 4333, October 1990.

E-461 Wiehr, K., "REBEKA-Buendelversuche: Untersuchungen zur Wechselwirkung Zwischen aufblaehenden Zirkaloy-Huellen und einsetzender Notkuehlung," Abschlussbericht, KfK-4407, May 1988.

E-462 Costigan, G., "Visualization of Single Tube Reflooding Experiments by Dynamic Neutron Radiography," Harwell Report, AERE-R12118, 1986.

Upper Plenum Injection

E-465 Barathan, D., et. al., "An Investigation of the Distribution and Entrainment of ECC Water Injection into the Upper Plenum," Thayer School of Engineering, Dartmouth College, NUREG/CR-1078, January 1980.

Tie Plate Countercurrent Flow

E-471 Jones, D.D., "Subcooled Countercurrent Flow Limiting Characteristics of the Upper Region of a BWR Fuel Bundle," General Electric Company, Nuclear Systems Products Division, NEDG-NUREG-23549, 1977.

Steam Binding

E-481 Howard, R.C. and Hochreiter, L.E., "PWR FLECHT SEASET Steam Generator Separate Effects Task Data Analysis and Evaluation Report: NRC/EPRI/Westinghouse Report No. 9," Westinghouse Electric Corporation, NUREG/CR-1534 (EPRI NP-1461; WCAP-9724), February 1982.

Hot Leg Countercurrent Flow/Reflux Condenser Mode

E-491 Krolewski, S.M., "Flooding Limits in a Simulated Nuclear Reactor Hot Leg," Massachusetts Institute of Technology, Submission as Part of Requirement for a B.Sc., 1980.

E-492 "PWR FLECHT-SEASET Systems Effects, Natural Circulation and Reflux Condensation," prepared by Westinghouse Electric Corporation, NUREG/CR-3654 (EPRI NP-3497; WCAP-10415), August 1984.

E-493 Richter, H.J., Wallis, G.B., Carter, K.H. and Murphy, S.L., "Deentrainment and Countercurrent Air-water Flow in a Model PWR Hot Leg," Thayer School of Engineering, September 1978.

E-494 "ROSA-IV Large Scale Test Facility (LSTF) System Description," JAERI-M 84-237, January 1985.

E-495 Wallis, G.B., "Flooding in Stratified Gas-Liquid Flow," Dartmouth College Report No. 27327-9, August 1970.

E-496 Zuber, N., "Problems in Modeling of Small Break LOCA," US Nuclear Regulatory Commission, NUREG-0724, October 1980.

Vent Valves

E-501 "Ueberstromvorrichtungen, Funktionssicherheit in der ersten Blowdown-Phase," FE-report Nr. 902-J 32 A (83), BMFT Research Program 150 376.

PWRs

E-511 Combustion Engineering System 80 Preliminary Safety Analysis Report (CESSAR), Docket STN-50-470.

E-512 Trojan Nuclear Plant Final Safety Analysis Report, Docket 50344-38.

E-513 Crystal River Unit 3 Final Safety Analysis Report, Docket 50-302.

E-514 Genkai Nuclear Plant Units 3 and 4 Final Safety Analysis Report.

E-515 Tomari Nuclear Plant Units 1 and 2 Safety Analysis Report.

CODE ANALYSIS REPORTS

General

E-601 Taylor, D.D., Shamway, R.W., and Singer, G.L., "TRAC-BD1/MOD1: An Advanced Best Estimate Computer Program for Boiling Water Reactor Transient Analysis," EG&G Idaho, NUREG/CR-3633 (EGG-2294), April 1984.

E-602 Boyack, B.E., Stumpf, H.J. and Lime, J.F., "TRAC User's Guide," Los Alamos National Laboratory NUREG/CR-4442 (LA-10590-M), November 1985.

E-603 "TRAC-PF1/MOD1: An Advanced Best-Estimate Computer Program for Pressurized Water Reactor Thermal-Hydraulic Analysis," Los Alamos National Laboratory, NUREG/CR-3858, July 1986.

E-604 "TRAC-PF1/MOD1 Correlations and Models," prepared by Los Alamos National Laboratory, NUREG/CR-5069 (LA-11208-MS), December 1988.

E-605 "TRAC-PF1/MOD2 Code Manual: User's Guide," prepared by Los Alamos National Laboratory, NUREG/CR-5673, Vol. 2, July 1992.

E-606 "TRAC-PF1/MOD2 Code Manual: Theory," prepared by Los Alamos National Laboratory, NUREG/CR-5673, Vol. 1, (to be published).

E-607 "TRAC-PF1/MOD2 Code Manual: Programmer's Guide," prepared by Los Alamos National Laboratory, NUREG/CR-5673, Vol. 3, July 1992.

E-608 "TRAC-PF1/MOD2 Code Manual: Developmental Assessments," prepared by Los Alamos National Laboratory, NUREG/CR-5673, Vol. 4, (to be published).

E-609 "Quantifying Reactor Safety Margins: Application of Code Scaling, Applicability, and Uncertainty Evaluation Methodology to a Large-Break, Loss-of-Coolant," Idaho National Engineering Laboratory, NUREG/CR-5249, December 1989.

ECC Delivery During Depressurization

E-611 Rohatgi, U.S., et al., "Bias in Peak Clad Temperature Predictions Due to Uncertainties in Modeling of ECC Bypass and Dissolved Non-condensible Gas Phenomena," Brookhaven National Laboratory, NUREG/CR-5254, September 1990.

Hot Leg Countercurrent Flow/Reflux Condenser Mode

E-621 Dillistone, M.J., "Analysis of the UPTF Separate Effects Test 11 (Steam-Water Countercurrent Flow in the Broken Loop Hot Leg) Using RELAP5/MOD2," Winfrith Technology Centre, AEEW-M2555, August 1989 (also published as NUREG/IA-0071, June 1992).

E-622 Thompson, S.L. and Kmetyk, L.N., "RELAP5 Assessment: PKL Natural Circulation Tests," Sandia National Laboratories, NUREG/CR-3100 (SAND82-2902), January 1983.

PAPERS, PRESENTATIONS, AND CORRESPONDENCE

ECC Delivery During Depressurization

E-901 Alb, G.P., and Chambre, P.L., "Correlations for the Penetration of ECC Water in a Model of a PWR Downcomer Annulus," Nuclear Engineering and Design, 53, pp. 237-248 (1979).

E-902 Bankoff, S.G. and Lee, S.C., "A Brief Review of Countercurrent Flooding Models Applicable to PWR Geometries," Nuclear Safety, 26, 139-152 (1985).

E-903 Segev, A.; Flanigan, L.J.; Kurth, R.E. and Collier, R.P., "Countercurrent Steam Condensation and its Application to ECC Penetration," presented at the 19th National Heat Transfer Conference, Orlando, Florida, July 1980.

E-904 Simpson, H.C. and Rooney, D.H., "Further Studies of Non-Equilibrium During Refilling a PWR," University of Strathclyde Glasgow, Scotland, UK, presented at European Two-Phase Flow Group Meeting, Zurich, Switzerland, June 1983.

Loop Behavior

E-911 Aoki, S., Inoue, A., Kozawa, Y., and Akimoto, H., "Direct Contact Condensation of Flowing Steam onto Injected Water," Proceedings of the Sixth International Heat and Mass Transfer Conference, Toronto, Ontario August 1978, Volume 6, pp. 107-112.

E-912 Aya, L. and Nariai, H., "Threshold of Pressure and Fluid Oscillations Induced by Injection of Subcooled Water into Steam Flow in Horizontal Pipe," Proceedings of ASME-JSME Thermal Engineering Joint Conference, Vol. 3, pp. 417-424, 1983.

E-913 Block, J.A., "Condensation-Driven Fluid Motions," International Journal of Multiphase Flow, Volume 6, pp. 113-129 (1980).

E-914 Daly, B.J. and Harlow, F.H., "A Model of Countercurrent Steam-Water Flow in Large Horizontal Pipes," Nuclear Science and Engineering, Vol. 77, pp. 273-284 (1981).

E-915 Nariai, H. and Aya, I., "Fluid and Pressure Oscillations Occurring at Direct Contact Condensation of Steam Flow with Cold Water," Nuclear Engineering and Design, Vol. 95, pp. 35-45 (1986).

E-916 Rothe, P.H.; Wallis, G.B. and Block J.A., "Cold Leg ECC Flow Oscillations," presented at Symposium on Thermal and Hydraulic Aspects of Nuclear Reactor Safety, Vol. 1: Light Water Reactors, pp. 133-150, 1977.

Fluid/Fluid Mixing

E-921 Iyer, K., Gherson, P. and Theofanous, T.G., "Purdue's One-half Scale HPI Mixing Test Program," Proceedings of the Second Nuclear Thermal-Hydraulics Meeting of the Annual ANS Meeting, New Orleans, LA, USA, June 3 - 7, 1984, pp. 859 - 861.

E-922 Iyer, K. and Theofanous, T.G., "Decay of Buoyancy Driven Stratified Layers with Applications to PTS: Reactor Predictions," Proceedings from the National Heat Transfer Conference, Denver, CO, USA, August 4 - 7, 1985.

E-923 Iyer, K. and Theofanous, T.G., "Flooding-Limited Thermal Mixing: The Case of High-Fr Injection," presented at the Third International Topical Meeting on Reactor Thermal Hydraulics, Newport, RI, USA, October 15 - 18, 1985.

E-925 Theofanous, T. and Iyer, K., "Mixing Phenomena of Interest to SBLOCA's," presented at Specialists Meeting on Small-break LOCA Analyses in LWRs, Pisa, Italy, June 23-27, 1985.

E-926 Theofanous, T.G. and Nourbakhsh, "PWR Downcomer Fluid Temperature Transients due to High Pressure Injection at Stagnated Loop Flow," Proceedings of the Joint NRC/ANS Meeting on Basic Thermal Hydraulic Mechanisms in LWR Analysis, September 14 - 15, 1982, Bethesda, MD, USA, NUREG/CP-0043, pp. 583 - 612.

Tie Plate Countercurrent Flow

E-931 Bankoff, S.G., Tankin, R.S., Yuen, M.C. and Hsieh, C.L., "Countercurrent Flow of Air/Water and Steam/Water through a Horizontal Perforated Plate," International Journal of Heat Mass Transfer, Vol. 24, No. 8, pp. 1381-1395 (1981).

E-932 Dilber, I. and Bankoff, S.G., "Countercurrent Flow Limits for Steam and Cold Water through a Horizontal Perforated Plate with Vertical Jet Injection," International Journal of Heat Mass Transfer, Vol. 28, No. 12, pp. 2382-2385 (1985).

E-933 Kutateladze, S.S., "Elements of the Hydrodynamics of Gas-Liquid Systems, Fluid Mechanics," Soviet Research, Vol. 1, No. 4 (1972).

E-934 Naitoh, M., Chino, K. and Kawabe, R., "Restrictive Effect of Ascending Steam on Falling Water during Top Spray Emergency Core Cooling," Journal of Nuclear Science and Technology, Vol. 15, No. 11, pp. 806-815 (November 1978).

Hot Leg Countercurrent Flow/Reflux Condenser Mode

E-941 Gardner, G.C., "Flooded Countercurrent Two-Phase Flow in Horizontal Tubes and Channels," International Journal of Multiphase Flow, Vol. 9, No. 4, pp. 367-382 (1983).

E-942 Larson, T.K., et. al., "Scaling Criteria and an Assessment of Semiscale Mod-3 Scaling for Small-Break Loss-of-Coolant Transients," presented at the Joint NRC/ANS Meeting on Basic Thermal-Hydraulic Mechanisms in LWR Analysis, Bethesda, MD, September 14-15, 1982.

E-943 Mandl, R.M. and Weiss, P.A., "PKL Tests on Energy Transfer Mechanisms during Small-Break LOCAs," Nuclear Safety, Vol. 23, No. 2 (March-April 1982).

E-944 Tasaka, K., et. al., "The Results of 5% Small-Break LOCA Tests and Natural Circulation Tests at the ROSA-IV LSTF," Proceedings of the Fourteenth Water Reactor Safety Research Information Meeting, October 27-31, 1986, NUREG/CP-0082, Vol. 4, pp. 177-197.

Section 6

ABBREVIATIONS AND ACRONYMS

ABB	-	ASEA Brown Boveri
ACC	-	Accumulators
ATHLET	-	Code for Analysis of Thermal-Hydraulics of Leaks and Transients
B&W	-	Babcock & Wilcox
BBR	-	Brown Boveri Reaktor (now ASEA Brown Boveri or ABB)
BCL	-	Broken Cold Leg
BE	-	Best-estimate
BMFT	-	Bundesministerium fuer Forschung und Technologie (Federal Ministry for Research and Technology)
BOCREC	-	Bottom of Core Recovery
BTD	-	Breakthrough Detector
CCFL	-	Countercurrent Flow Limitation
CCTF	-	Cylindrical Core Test Facility
CE	-	Combustion Engineering (now ABB-CE)
CI	-	Combined Injection
CL	-	Cold Leg
CLI	-	Cold Leg Injection
CS	-	Core Simulator (UPTF)

CSAU	-	Code Scaling, Applicability, and Uncertainty Study
DAS	-	Data Acquisition System
DB	-	Drag Body
DC	-	Downcomer
DCI	-	Downcomer Injection
DP	-	Differential Pressure
ECC	-	Emergency Core Coolant
ECCS	-	Emergency Core Coolant System or Emergency Core Cooling System
EM	-	Evaluation Model
EOB	-	End-of-Blowdown
FA	-	Fuel Assembly
FASS	-	Fast Automatic Shutdown System (UPTF)
FDG	-	Fluid Distribution Grid
FLECHT-SEASET	-	Full-length Emergency Cooling Heat Transfer Separate Effects and Systems Effects Test
FRG	-	Federal Republic of Germany
GKM	-	Grosskraftwerk Mannheim
GPWR	-	German Pressurized Water Reactor
GRS	-	Gesellschaft fuer Anlagen- und Reaktorsicherheit (Company for Plant and Reactor Safety); formerly Gesellschaft fuer Reaktorsicherheit (Company for Reactor Safety)
HL	-	Hot Leg
HLI	-	Hot Leg Injection

HPCI	-	High Pressure Coolant Injection
HPI	-	High Pressure Injection
HPIS	-	High Pressure Injection System
HPSI	-	High Pressure Safety Injection
IDL	-	Instrument Development Loop
INEL	-	Idaho National Engineering Laboratory
J	-	Japan
JAERI	-	Japan Atomic Energy Research Institute
KWU	-	Kraftwerk Union (now a division of Siemens)
LANL	-	Los Alamos National Laboratory
LBLOCA	-	Large Break Loss-of-Coolant Accident
LLD	-	Liquid Level Detector
LOBI	-	Loop of Blowdown Investigation
LOCA	-	Loss-of-Coolant Accident
LOFT	-	Loss of Fluid Test
LPCI	-	Low Pressure Coolant Injection
LPI	-	Low Pressure Injection
LPIS	-	Low Pressure Injection System
MK	-	Muehlheim Kaerlich PWR
MPR	-	MPR Associates
ORNL	-	Oak Ridge National Laboratory
PCT	-	Peak Cladding Temperature

PKL	-	Primarkreislaufe (Primary Coolant Loop - KWU Test Facility)
PTS	-	Pressurized Thermal Shock
PWR	-	Pressurized Water Reactor
REFLA	-	Reflood Analysis (Code)
RELAP	-	Reactor Leak and Analysis Program (Code)
ROSA	-	Rig of Safety Assessment
SBLOCA	-	Small Break Loss-of-Coolant Accident
SCTF	-	Slab Core Test Facility
SG	-	Steam Generator
SGIP	-	Steam Generator Simulator Inlet Plena
SGS	-	Steam Generator Simulator
SGTR	-	Steam Generator Simulator Tube Regions
TRAC	-	Transient Reactor Analysis Code
TUM	-	Technische Universitaet Muenchen (Technical University of Munich)
TV	-	Test Vessel
UCSP	-	Upper Core Support Plate
UK	-	United Kingdom
UP	-	Upper Plenum
UPI	-	Upper Plenum Injection
UPTF	-	Upper Plenum Test Facility
US	-	United States

USNRC	-	United States Nuclear Regulatory Commission
VV	-	Vent Valve
W	-	Westinghouse Electric Corporation
W/S	-	Ratio of Core Simulator Water and Steam Injection Rates (UPTF)

Section 7

NOMENCLATURE

A	Flow Area
C_p	Heat Capacity
D	Diameter
D_H	Hydraulic Diameter
	D_H = 4 (flow area/wetted perimeter)
Fr	Froude Number
	$Fr = V/(gD)^{1/2}$
g	Gravitational Acceleration
h	Enthalpy
$H_{v,top}$	Downcomer Top Void Height (Level Reduction Below Cold Leg due to Entrainment)
j	Velocity
j^*	Wallis Parameter (or Dimensionless Velocity)

$$j^* = \left[\frac{\dot{M}}{\rho A}\right] \left[\frac{\rho}{(\rho_L - \rho_G) g D_H}\right]^{1/2} \quad \textit{for single-phase flow}$$

$$j^* = \left[\frac{\dot{M}}{\rho_{TP} A}\right] \left[\frac{\rho_{TP}}{(\rho_L - \rho_{TP}) g D_H}\right]^{1/2} \quad \textit{for two-phase flow}$$

K^* Kutateladze Number

$$K^* = \left[\frac{\dot{M}}{\rho A}\right] \left[\frac{\rho^2}{g\sigma (\rho_L - \rho_g)}\right]^{1/4}$$

$\dot{M}$ Mass Flow

Re Reynolds Number

$$Re = \frac{D_H V \rho}{\mu}$$

R_T Thermodynamic Ratio

$$R_T = \frac{\dot{M}_{ECC}\, Cp\, (T_{sat} - T_{ECC})}{\dot{M}_{stm}\, (h_{stm} - h_f)}$$

S Slip Ratio for Liquid/Gas Cocurrent Flow (S=1 for Homogeneous Flow)

T Temperature

V Velocity

α Void Fraction

γ Liquid Fraction

ρ Density

ρ_{TP} Two-phase Density

$$\rho_{TP} = \frac{\rho_L \left[1 + S\left(\dot{M}_L/\dot{M}_g\right)\right]}{(\rho_L/\rho_G) + S\left(\dot{M}_L/\dot{M}_G\right)}$$

μ Viscosity

Subscripts

ECC	Emergency Core Coolant
f	Liquid Phase
g	Gas Phase
G	Gas Phase
HL	Hot Leg
IP	Inlet Plenum
l	Liquid Phase
L	Liquid Phase
S	Steam
Sat	Saturated
STM	Steam
UP	Upper Plenum
W	Water

Appendix A

BRIEF DESCRIPTION OF TEST FACILITIES, INSTRUMENTATION AND TESTS CONDUCTED

A.1 CYLINDRICAL CORE TEST FACILITY (CCTF)

A.1.1 Facility Description

CCTF was a full-height, 1/21-scale model of the primary coolant system of an 1,100 MWe four-loop PWR. The facility simulated the overall primary system response and the in-core thermal hydraulic behavior during the refill and reflood phases of a large cold leg break LOCA. The reference reactors for CCTF were the Trojan reactor in the USA (4-loop PWR with cold leg injection ECCS, 1,130 MWe) for major parts and the Ohi-1 reactor in Japan (4-loop PWR with cold leg injection ECCS, 1,175 MWe) for certain other aspects.

Facility Layout

Figures A.1-1 and A.1-2 depict the major components of the facility. They included a pressure vessel with simulated core, four primary piping loops (three intact and one broken) with steam generators and pump simulators, and two tanks attached to the ends of the broken loop to simulate containment. Vertical dimensions and locations of system components were as close as practicable to the corresponding dimensions and locations in the reference reactor. Flow areas were typically scaled based on the nominal core flow area scaling ratio (1/21). The maximum operating pressure of major components of CCTF was 600 kPa.

Electrically-heated rods were used in the core to simulate nuclear fuel rods. A total of 1,824 heated rods were installed. The maximum electrical power supplied to the heated rods was 10 MW. This power could simulate the decay heat during the refill and reflood phases of an LBLOCA.

In CCTF, ECC injection nozzles were located in the cold legs, hot legs, upper plenum, downcomer, and lower plenum to simulate ECC systems of cold leg injection, combined injection, upper plenum injection, and downcomer injection PWRs. Also, vent valves were installed in the core barrel to simulate B&W PWRs with vent valves.

Auxiliary systems included the drain system from pressure vessel and containment tanks, and the steam injection system to upper plenum.

Main Components

The main components and subsystems of CCTF are discussed briefly below.

Pressure Vessel - Figure A.1-3 shows the CCTF pressure vessel. The cylindrical pressure vessel was full-height (about 10 m) with a scaled diameter (1.3 m). The pressure vessel housed the downcomer annulus, lower plenum, core, and upper plenum. The core barrel separated the core and upper plenum from the downcomer. The pressure vessel wall was made of carbon steel clad with stainless steel. The pressure vessel wall thickness was 90 mm. Electrical resistance heaters were used on the outer surface of the pressure vessel wall to preheat the wall before a test, to accurately simulate transient heat release from the pressure vessel wall which occurs during a PWR LOCA. Except for the addition of an upper ring containing an upper plenum injection header and additional instrumentation nozzles, the CCTF-II vessel was the same as that used in CCTF-I.

The CCTF core contained 32, 8 x 8 bundles (see Figure A.1-4), each containing 57 heated rods and seven nonheated rods (total of 1,824 heated rods and 224 nonheated rods). As shown in Figure A.1-5, the heated rods were fabricated with an Inconel cladding, Nichrome heater element, and boron nitride or magnesium oxide insulators. All heated rods had an outer diameter of 10.7 mm, a heated length of 3.66 m, and chopped-cosine axial power profile. These dimensions were identical to the corresponding dimensions of PWR fuel rods. The clad thickness, 1 mm, was thicker than that of fuel rods, because of the requirement for thermocouple attachment. The heat capacity of the heated rods was approximately 40% larger than that of nuclear fuel rods.

The nonheated rods simulated the guide thimble tubes and instrument thimble tubes in PWR fuel assemblies. They were either stainless steel pipes or solid bars with an outer diameter of 13.8 mm. The heated rods and nonheated rods were held in their radial positions by grid spacers located at six elevations. A grid spacer was a lattice structure of stainless steel plates 0.4 mm and 0.8 mm thick, and 40 mm high. No special device (e.g., mixing promoter) was attached on the grid spacer. The rod pitch was 14.3 mm which is identical to the reference PWR.

Figure A.1-4 shows the three (high, medium, and low) power zones of the electrically-heated core. The radial power distribution of the core was controlled by setting the power supplied to each zone. In CCTF-I, each bundle included rods with three different power densities. In CCTF-II, all heated rods in each bundle were provided with the same power density. The axial power profile was the same in all rods with an axial peaking factor (ratio of maximum to average power) of 1.49 for CCTF-I and 1.40 for CCTF-II.

As shown in Figure A.1-3, the core/upper plenum boundary included an upper core support plate and end box tie plate. These plates were perforated plates with appropriately-scaled flow areas. Plugging devices were installed on the tie plate in CCTF-II to better simulate the reference PWR geometry.

The upper plenum internals modeled those used in the reference Westinghouse plant; in particular, control rod drive structures and support columns. Although the CCTF upper plenum internals were full height, the horizontal dimensions were 8/15 of those of the Westinghouse plant to allow individual upper plenum internal structures to be placed over the individual 8 x 8 heated rod bundles in the CCTF core. This approach created a more uniform and realistic flow distribution than using reactor-typical, larger size upper plenum internal structures. The detailed shape and arrangement of the upper plenum internals were different between CCTF-I and CCTF-II. The arrangement of the upper plenum internals for CCTF-II is shown in Figure A.1-4. The arrangement was determined to simulate the horizontal flow resistance distribution in the reference PWRs. Baffle plates were inserted into the control rod guide tubes to increase the flow resistance.

In CCTF-II, four vent valves, located in the barrel between the upper plenum and downcomer annulus, modeled the vent valves in a B&W reactor vessel. These vent valves simulated the flow area, flow resistance, and opening and closing differential pressures of actual vent valves. For CCTF-II tests simulating B&W reactors, these vent valves were free to open; for all other tests the valves were locked shut.

The downcomer annulus surrounded the core barrel. The flow area of the downcomer was scaled larger than the 1/21-scaling ratio to avoid excessive hot wall effects which would lead to an unrealistically low effective downcomer driving head. To simulate the effective downcomer driving head more realistically, the baffle area of the PWR was included in the CCTF downcomer. The possible deficiencies of the enlarged downcomer annulus are reduction in the rate of increase of the downcomer water level, reduction of heat release from the downcomer wall per unit flow area, and reduction of the azimuthal steam flow velocity in comparison to that in PWR. The effect of the reduction in the rate of increase of the downcomer water level on the reflood behavior was investigated with a special purpose test, and confirmed to be minimal. The heat release from the downcomer wall was simulated as discussed above. The effect of the reduced azimuthal steam velocity on the reflood behavior was not investigated experimentally; however, using CCTF and UPTF data, it was analyzed as shown in Section 3.1.2.1.

Primary Loops and Containment Tanks - Four full-length primary loops were connected to the central pressure vessel (see Figures A.1-1 and A.1-2). Three of the loops were intact; that is, they allowed flow from the pressure vessel upper plenum, through the hot leg, steam generator, crossover leg, pump simulator, and cold leg to

the pressure vessel downcomer. The fourth loop simulated a full-size, double-ended, offset cold leg break about two meters from the vessel wall. Both ends of the broken loop were connected to the containment simulator. The pipe flow area was scaled from the PWR by the ratio of core flow areas; the inside diameter was 0.155 m.

Each hot leg connected the upper plenum and the inlet plenum of the steam generator simulator. Each had a riser part as well as a horizontal portion. The angle and height of the riser were based on the reference PWR.

Two steam generator simulators (SGSs) were installed in CCTF. They were U-tube and shell type heat exchangers. Each of the steam generator vessels was shared by two loops (a vertical plate divided each steam generator in half) so each loop essentially had, in effect, its own steam generator. The number of U-tubes was reduced per the core flow area scaling ratio. The CCTF U-tubes were the same diameter but 25% shorter than the U-tubes in the reference PWRs. During a test, the secondary sides of the SGs contained high pressure saturated water (540 K and 5300 kPa) to simulate heat transfer from the secondary sides. These conditions corresponded to those on the secondary side of the steam generator in a PWR during the reflood portion of a LOCA. There was no flow on the secondary side of the steam generators during the tests.

Each crossover leg connected the steam generator outlet plenum to a pump simulator. The crossover piping included a loop seal, the same height as in the reference PWR.

Each pump simulator consisted of a casing and vane simulator to simulate countercurrent flow limitation phenomena, and an orifice plate to simulate flow resistance. The flow resistance was varied using orifice plates with different diameter holes. The orifice plate typically used simulated the locked rotor flow resistance of a reactor coolant loop.

The configuration of CCTF simulated a 200% cold leg break. The break point was simulated with two fast-opening break valves located at the two ends of the broken loop. Two interconnected tanks (containment tank simulators), one attached to each of the two ends of the break, simulated the PWR containment (see Figures A.1-1 and A.1-2). On the tank connected to the broken loop hot leg, a pressure control system maintained pressure at a preselected value by venting steam, as needed, to the atmosphere. On the tank connected to the broken loop cold leg, an internal steam/water separator allowed for measurement of the water flow rate form the downcomer to the break.

ECC Injection System - In CCTF-I, the ECCS included two water supply tanks: the pressurized accumulator (ACC) tank, capable of providing water at a high flow rate for a short duration; and the low pressure coolant injection (LPCI) tank, capable of

providing water at a lower flow rate for a longer duration. Each tank could supply water to either the lower plenum or to the four cold legs through the ECC nozzles (ECC ports).

The ECC water in the ACC tank was supplied to the primary loops by nitrogen pressurization, as in the reference PWR. The water flow rate was adjusted with the pressure in the ACC tank and the flow resistance of the piping. ECC water in the LPCI tank was pumped into the primary loop with the LPCI pumps; control valves were used to adjust the flow rate.

The ECC piping entered the top of the cold leg at a 45 degree angle, as in the reference PWR. To simulate the velocity of the ECC, the flow area of the end of the piping was adjusted by inserting a throttling device.

In CCTF-II two pressurized tanks were added, with ECCS piping to the upper plenum injection header, the downcomer, and the hot legs. One tank stored cold water, while the other stored hot water. Each tank was pressurized with steam. Control valves were used to adjust the flow from each tank in order to control the ECC temperature and total flow rate.

The upper plenum, downcomer, and hot leg injection nozzles were also newly installed in CCTF-II. These nozzles were used to investigate alternative ECCS configurations. The design and location of each of these nozzles is described briefly below.

- The upper plenum injection (UPI) nozzles were vertical pipes with a horizontal discharge at the hot leg elevation. In PWRs with UPI, the ECC injection nozzles are located in the upper plenum wall at the hot leg elevation. To simulate the impingement of ECC on control rod guide tubes expected in PWRs with UPI, the discharge end of the pipes faced the simulated guide tubes.

- Two LPCI injection nozzles were located in the downcomer wall at the cold leg elevation. Thermal shields were not installed in the nozzles.

- An ECC injection nozzle was added to each of the four hot legs for simulation of combined injection PWRs. The geometry of the injection pipe internal to the hot leg (i.e., the hutze) was representative of Siemens/KWU PWRs.

Control and Instrumentation

Process Control System - The time-dependent variables were controlled with a computer during a typical CCTF test; these included power supplied to heated rods, ECC flow rate, and ECC temperature. Pressure in Containment Tank-2 was maintained constant. The test initiation time and the sequence of events (e.g., power decay initiation and ECC injection initiation) were also controlled with the computer.

To ensure the integrity of the heated rods, the maximum clad temperature was monitored during the tests. If the temperature exceeded the maximum allowable, power was reduced to 80%. If the clad temperature continued to increase after the power reduction, power was shut off. This procedure and the test termination procedure were also performed by the computer.

Instrumentation - CCTF instrumentation consisted of over 1,600 sensors, including both conventional devices (e.g., pressure transducers and thermocouples) provided by JAERI, and advanced two-phase flow instrumentation developed by the USNRC and their contractors for the 2D/3D Program.

Conventional instrumentation provided by JAERI included approximately 700 thermocouples attached to rod clad surfaces throughout the core, and an additional 100 thermocouples which measured fluid, steam, and wall temperatures near and in the core. Other thermocouples, flow meters, and pressure and differential pressure sensors, located throughout the test facility, provided information on fluid conditions, flow rates, liquid levels, and pressure distribution. In addition to these instruments, JAERI provided television cameras and film cameras (both moving and still) mounted at viewing windows in the hot and cold legs. These cameras provided visual data to aid in interpretation of the test results.

Advanced instrumentation provided by USNRC primarily monitored local two-phase fluid conditions. The advanced instrumentation included fluid distribution grid/liquid level detectors (FDG/LLD), turbine meters, impedance probes, film probes, and spool pieces.

A.1.2 Catalog of Tests

CCTF testing was performed in two phases:

- CCTF-I, 1979 - 1981
- CCTF-II, 1982 - 1985

Table A.1-1 lists the CCTF tests, classified first by the injection configuration being simulated (cold leg injection, combined injection, downcomer injection, or upper plenum injection) and then further classified by test objective.

The base case tests for cold leg injection were conducted under the typical test conditions which were chosen from the safety evaluation analysis of the reference reactor. It was intended through the test results to investigate and understand the basic overall reflood behavior with cold leg injection. Parameter effect tests for cold leg injection were performed to investigate the effect of various parameters (i.e., pressure, power, ECC flow rate, etc.) on reflood behavior. The range of parameters tested covered the conditions at reflood initiation expected in the safety evaluation analysis and the conditions expected in a best-estimate analysis. Special purpose tests for cold leg injection were performed to investigate the reflood behavior under EM and BE conditions, the refill behavior, and loop seal effect.

For combined injection ECCS, the refill-reflood tests were performed under EM and BE conditions; only one parameter test for ECC flow was performed. For upper plenum injection, four reflood tests and one refill-reflood test were performed. Parameter effect tests included: ECC injection location, ECC flow and core power. For downcomer injection, three reflood tests were performed with closed and open vent valves.

Table A.1-1

CCTF AND SCTF TESTS

Group	Test Objective	Test/Run Number[1]	Description [2]	Comments
Cold Leg Injection Parameter Effects	Base Case	C1-5/14	CCTF-I Base Case	
		C2-SH1/53	CCTF-II Base Case	Same as CCTF-I EM test (C1-19)
		C2-4/62[3]	CCTF-II Base Case/ Repeatability	
		S1-1/507	SCTF-I Forced Feed Base Case	
		S1-10/516[3]	SCTF-I Forced Feed Base Case/Repeatability	
		S1-12/518	SCTF-I Gravity Feed Base Case	Lower plenum injection
		S1-14/520	SCTF-I Gravity Feed Base Case	Cold leg injection
		S2-10/615	SCTF-II Forced Feed Base Case	
		S2-SH1/604	SCTF-II Gravity Feed Base Case	Cold leg injection
	Effect of Pressure	C1-10/19	Low pressure	Compare to C1-5
		C1-12/21	High Pressure	Compare to C1-5
		C2-8/67	Low Pressure	Compare to C2-4
		C2-1/55	High Pressure	Compare to C2-4
		S1-2/508	Forced Feed, Low Pressure	Compare to S1-1
		S1-SH2/506	Forced Feed, High Pressure	Compare to S1-1
		S2-2/607	Gravity Feed, Low Pressure	Compare to S2-SH1
		S2-1/606[3]	Gravity Feed, High Pressure, Steep Q, Steep T	Compare to S2-6
	Effect of Core Power	C2-SH2/54	Low Power	Initial Power = 7.9 MW; compare to C2-4
		C2-5/63	Low Power	Initial Power = 7.1 MW; compare to C2-4
		S1-6/512	Forced Feed, High Power	Compare to S1-1
	Effect of Initial Clad Temperature	C1-7/16	High Clad Temperature	Maximum clad temperature = 973 K at beginning of core recovery; compare to C1-5
		C1-14/23	High Clad Temperature	Maximum clad temperature = 1073 K at beginning of core recovery; compare to C1-5
		C2-AC1/52	Low Clad Temperature	Compare to C2-4
		S2-AC3/603[3]	Gravity Feed, BE, Low Clad Temperature	Compare to S2-9 for effect of clad temperature at BE conditions

Table A.1-1

CCTF AND SCTF TESTS

Group	Test Objective	Test/Run Number[1]	Description [2]	Comments
Cold Leg Injection Parameter Effects (Continued)	Effect of Power/ Temperature Distribution	C2-5/63 C2-6/64	Steep Q Flat Q	
		S1-7/513	Forced Feed, Flat Q	Test terminated due to computer failure; repeated as S1-11
		S1-11/517 S1-8/514	Forced Feed, Flat Q Forced Feed, Steep Q	Repeat of S1-7
		S2-17/622 S2-16/621 S2-SH2/605 S2-1/606[3] S2-6/611 S2-7/612[3]	Forced Feed, Flat Q, Flat T Forced Feed, Steep Q, Steep T Gravity Feed, Flat Q, Flat T Gravity Feed, High Pressure, Steep Q, Steep T Gravity Feed, Steep Q, Steep T Radial Power Distribution Like CCTF Test C2-5	
		S3-14/718 S3-15/719 S3-16/720	Flat Q Slant Q Steep Q	
	Combined Effects of Power/ Temperature Distribution and UCSP Liquid Level Distribution	S2-14/619[3]	Forced Feed, Flat Q, Flat T, Flat Liquid Level	Counterpart to CCTF-II Test C2-6; Compare to S2-17 for liquid level distribution
		S2-12/617	Forced Feed, Steep Q, Steep T, Flat Liquid Level	Compare to S2-16 for liquid level distribution
		S2-15/620	Forced Feed, Steep Q, Flat T, Flat Liquid Level	
		S2-21/626	Forced Feed, Flat Q, Steep T, Flat Liquid Level	

Table A.1-1

CCTF AND SCTF TESTS

Group	Test Objective	Test/Run Number[1]	Description [2]	Comments
Cold Leg Injection Parameter Effects (Continued)	Effect of ECC Flow Rate	C1-2/11[3]	Low ACC Flow Rate/No Upper Plenum Guide Tube Internals	Compare to C1-5
		C1-11/20	Low ACC Flow Rate/ Repeatability	Compare to C1-5
		C1-6/15	High LPCI Flow Rate	Compare to C1-5
		C1-9/18	Low LPCI Flow Rate	Compare to C1-5
		C1-13/22	Short ACC Flow Duration	Comapre to C1-5
		C2-9/68	High LPCI Flow Rate	Compare to C2-SH2
		S1-SH1/505	Forced Feed, High Flow Rate	
		S1-5/511	Forced Feed, Low LPCI Flow Rate	
		S1-9/515	Forced Feed, High ACC and LPCI Flow Rate	
		S1-16/522	Gravity Feed, Low ACC Flow Rate	
		S1-17/523	Gravity Feed, Low ACC and LPCI Flow Rates	
		S1-21/531	Gravity Feed, Low LPCI Flow Rate	
		S1-22/532	Gravity Feed, No ACC Injection, Low LPCI Flow Rate	
		S2-11/616	Forced Feed, High ACC Flow Rate	Compare to S2-10
		S2-19/624	Forced Feed, High LPCI Flow Rate	Compare to S2-10
		S2-AC1/601	Gravity Feed, High ACC Flow Rate	Compare to S2-SH1
		S2-AC2/602	Gravity Feed, Short ACC Flow Duration	Compare to S2-SH1
		S2-AC3/603[3]	Gravity Feed, Low and Long ACC Flow Rate	Compare to S2-SH1
	Effect of ECC Temperature	S1-4/510	Forced Feed, Low ECC Temperature	Compare to S1-1
		S1-15/521	Gravity Feed, High ACC Temperature (Saturated)	Compare to S1-14
		S1-18/542[3]	Refill, High ACC Temperature (Saturated)	Compare to S1-19
		S2-8/613	Gravity Feed, Low ECC Temperature	Compare to S1-SH1
	Effect of Downcomer Wall Temperature	C1-2/11[3]	High Downcomer Wall Temperature	
		C1-3/12	Low Downcomer Wall Temperature	
	Effect of Loop Flow Resistance	C1-SH4/8	High Loop Flow Resistance, High ECC Temperature	Cold leg injection scoping test; compare to C1-2
		C1-1/10	High Loop Flow Resistance, Low ECC Temperature	Compare to C1-2

Table A.1-1

CCTF AND SCTF TESTS

Group	Test Objective	Test/Run Number[1]	Description [2]	Comments
Cold Leg Injection Parameter Effects (Continued)	Effect of Downcomer Water Accumulation Rate	C2-3/61	High Rate of Downcomer Water Accumulation	Compare to C2-4
	Effect of UCSP Liquid Level	S1-3/509	Low UCSP Liquid Level	Compare to S1-1
Cold Leg Injection Special Purpose Tests	Evaluation Model (EM) Tests	C1-19/38	Evaluation Model	Same as CCTF-II base case (C2-SH1); compare to C1-5
		S3-9/713	Evaluation Model Integral Test	Compare to S3-10
	Best Estimate (BE) Tests	C2-12/71	Best Estimate	Compare to C2-4
		S2-9/614	Gravity Feed, Best Estimate	Compare to S2-SH1
		S3-10/714	Best Estimate Integral Test	Compare to S3-9
	Refill Tests	C1-SH1/5 C1-4/13 C1-15/24	Refill, No Core Power Refill/Reflood Refill/Reflood Nitrogen Injection	
		C2-2/56 C2-14/74 C2-17/77 C2-11/70	Refill Refill/Reflood Refill/Reflood, Steam Injection Refill, Blocked Loops	No reflood simulation
		S1-19/525 S1-18/524[3]	Refill Refill, High ACC Temperature (Saturated)	
	Effect of Asymmetric Power/Temperature Distribution	C1-17/36 C1-20/39	Asymmetric Core Power Asymmetric Core Temperature	Compare to C1-5
	Effect of Water in Loop Seal	C1-8/17 C1-18/37	Loop Seal Filling Loop Seal Filling	Test terminated early due to high clad temperature; repeated as C1-18. Repeat of C1-8; compare to C1-5
	Effect of Forced vs. Gravity Feed	S1-12/518	Gravity Feed, Lower Plenum Injection	Compare to S1-14
	Evaluation of SCTF Gravity Feed Oscillations	S1-23/536 S1-24/537	Low ACC Flow Rate, Long ACC Duration Gradual Reduction from ACC Flow Rate to LPCI Flow Rate	

Table A.1-1

CCTF AND SCTF TESTS

Group	Test Objective	Test/Run Number[1]	Description [2]	Comments
Cold Leg Injection Special Purpose Test (Continued)	Facility Coupling Tests	C1-16/25	Counterpart to FLECHT-SET Test 3105B	
		C1-21/40	Counterpart to FLECHT-SET Test 2714B	
		C1-22/41	Counterpart to FLECHT-SET Test 3420B	
		C2-AC2/52	Counterpart to FLECHT-SET Test 2714B and CCTF-I Test C1-21	
		C2-15/75	Counterpart to FLECHT-SET Test 2714B	
		S1-13/519	Counterpart of FLECHT-SEASET Test 43716C	
		S2-7/612[3]	Radial Power Distribution Like CCTF Test C2-5	Cold leg injection
		S2-14/619[3]	Forced Feed, Flat Q, Flat T, Flat Liquid Level; Counterpart to CCTF-II Test C2-6.	
		S2-18/623	Counterpart to CCTF-II Test C2-5	Forced feed
Other Cold Leg Injection Tests	Repeatability Tests	C1-11/20[3]	Low ACC Flow Rate/Repeatability	
		C2-4/62[3]	CCTF-II Base Case/Repeatability	Compare to C2-SH1
		S1-10/516[3]	SCTF-I Forced Feed Base Case/Repeatability	Compare to S1-1
		S2-13/618	SCTF-I/II Repeatability	Compare to S1-1
	Miscellaneous	C1-SH2/6	Low Power, Flat Power Profile, High Pressure, LP Injection	Low power and LP injection scoping test
		C1-SH3/7	Low Power, Non-Flat Power Profile, High Pressure, LP Injection	Steep Q and LP injection scoping test
		S1-20/530	Effect of Closed Vent Valve Line	Vent valve line was inadvertently left open on previous SCTF-I tests (S1-14/520 to S1-17/523)
		S1-14/520[3]	Effect of Open Vent Line	

Table A.1-1

CCTF AND SCTF TESTS

Group	Test Objective	Test/Run Number[1]	Description [2]	Comments
Combined Injection Separate Effects Tests	CCFL Evaluation	S2-3/608	Steam Injection, Saturated ECC, No Core Power	Water injected into upper plenum
		S2-4/609	Steam Injection, Saturated ECC, Core Power On	Water injected into upper plenum
		S2-5/610	Steam Injection, Subcooled ECC, Core Power On	Water injected into upper plenum
		S3-3/707	Uniform Subcooled Water	
		S3-4/708	Local Subcooled Water	
		S3-5/709	Distributed Subcooled Water	
	Core Cooling Evaluation	S3-SH1/703	Core Cooling Base Case	
		S3-1/705	Lower Plenum Water Level Effect	
		S3-2/706	Subcooling Effect	
		S3-6/710	Power Distribution Effect	
		S3-7/711	ECC Location Effect	
		S3-8/712	ECC Location Changing Effect	
		S3-12/716	High Power, High Clad Temperature	
		S3-AC2/702	Core Cooling BE	
Combined Injection Integral Tests	Effect of Injection Configuration	C2-21/81	7/8 Injection (4 Hot Legs, 3 Cold Legs)	Compare to C2-19 (5/8 injection: 2HL, 3CL) for effect of ECC flow rate to hot legs
		S3-13/717[3]	Continuous UP Injection	
		S3-20/724	Intermittent UP Injection	
		S3-22/726	Alternate UP Injection	
	Effect of ECC Temperature	S1-SH3/528	Saturated ECC	
		S1-SH4/529	Subcooled ECC	
		S3-18/722	High Injection Temperature	Compare to S3-13
	Effect of Core Power and Clad Temperature	S3-19/723	Low Pressure, High Power, High Clad Temperature	Failed test
		S3-21/725	Low Pressure, High Power, High Injection Temperature	Compare to S3-13
	Evaluation Model (EM) Tests	C2-19/79	5/8 Injection (2 Hot Legs, 3 Cold Legs)	
		S3-SH2/704	EM Orientation	
		S3-13/717[3]	EM	Compare to S3-11
	Best Estimate (BE) Tests	C2-20/80 [3]	BE	Compare to C2-19
		S3-AC1/701	BE Orientation	
		S3-11/715	BE	Compare to S3-13

Table A.1-1

CCTF AND SCTF TESTS

Group	Test Objective	Test/Run Number[1]	Description [2]	Comments
Combined Injection Special Purpose Tests	Facility Coupling Tests	C1-SH5/9	Counterpart to PKL Test K7A	
		C2-20/80 [3]	Counterpart to PKL	
Upper Plenum Injection Tests	Base Case	C2-16/76	Asymmetric (One Port) Injection	
	Parameter Effects	C2-AS1/59	Symmetric (Two Port) Injection	
		C2-13/72	Symmetric (Two Port) Injection, High UPI Flow Rate	
		C2-AA1/57	Symmetric (Two Port) Injection, High Power, Very High HPI Flow Rate	
		C2-18/78	UPI Best Estimate/Refill	
Downcomer Injection Tests	Parameter Effects	C2-AA2/58	Vent Valves Closed	
		C2-AS2/60	Vent Valves Open	
		C2-10/69	Vent Valves Open, Loops Blocked	
		S3-17/721	Vent Valve Test	
Mass Balance Calibration Test	Verification of Mass Flow Measurements	C2-7/65	Mass Balance Calibration	

NOTES:

1. Test number identifies facility and test series:

   C1 = CCTF Core-I
   C2 = CCTF Core-II
   S1 = SCTF Core-I
   S2 = SCTF Core-II
   S3 = SCTF Core-III

2. The following abbreviations are used in the test descriptions:

   BE = Best estimate
   EM = Evaluation model
   IT = Integral test
   Flat Q = Flat power profile
   Slant Q = Slant power profile
   Steep Q = Steep power profile
   Flat T = Flat initial clad temperature profile
   Steep T = Steep initial clad temperature profile
   ACC = Accumulator
   ECC = Emergency core coolant

3. Test is listed twice in the table because it can be used to evaluate more than one effect.

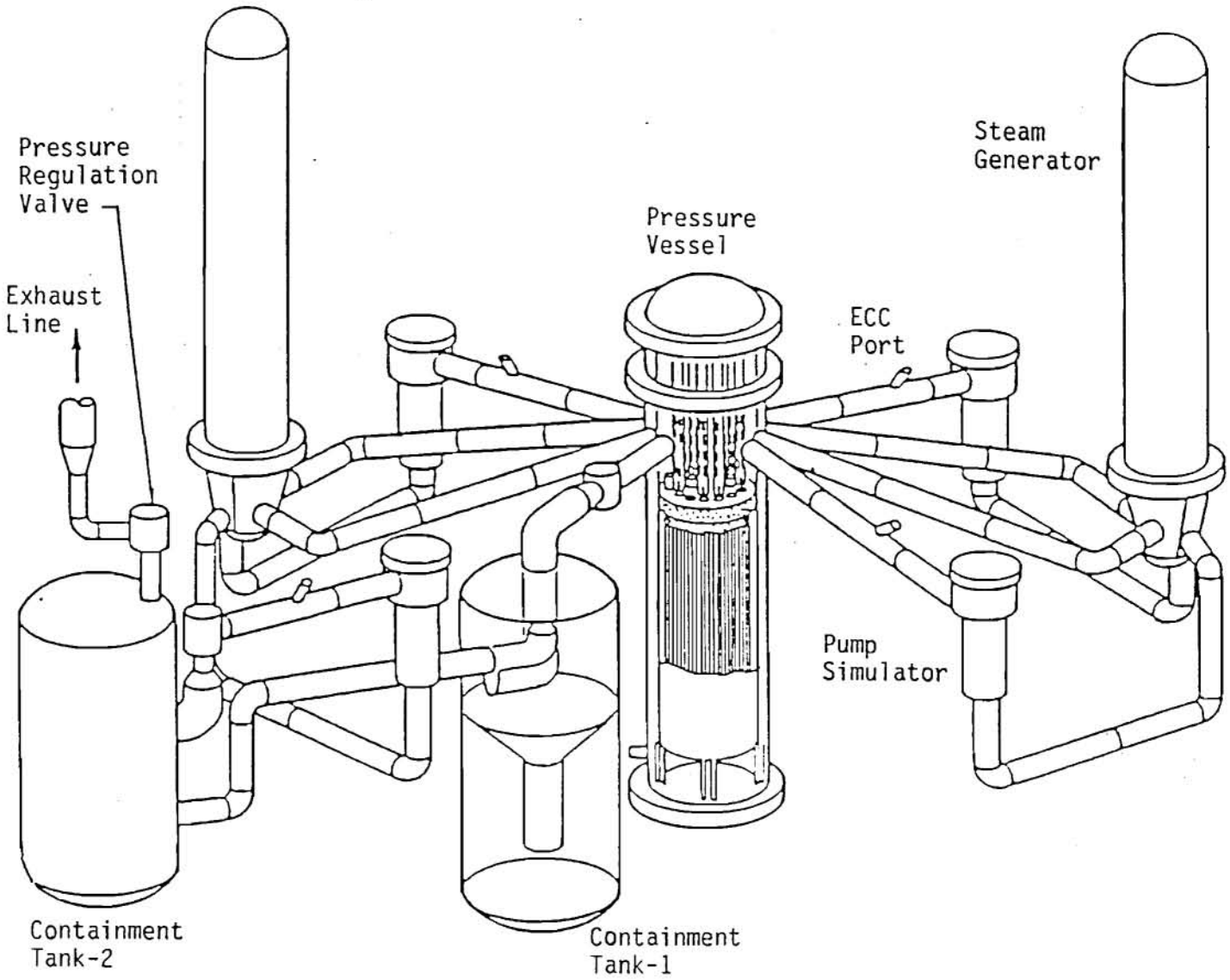

CYLINDRICAL CORE TEST FACILITY
(CCTF)

FIGURE A.1-1

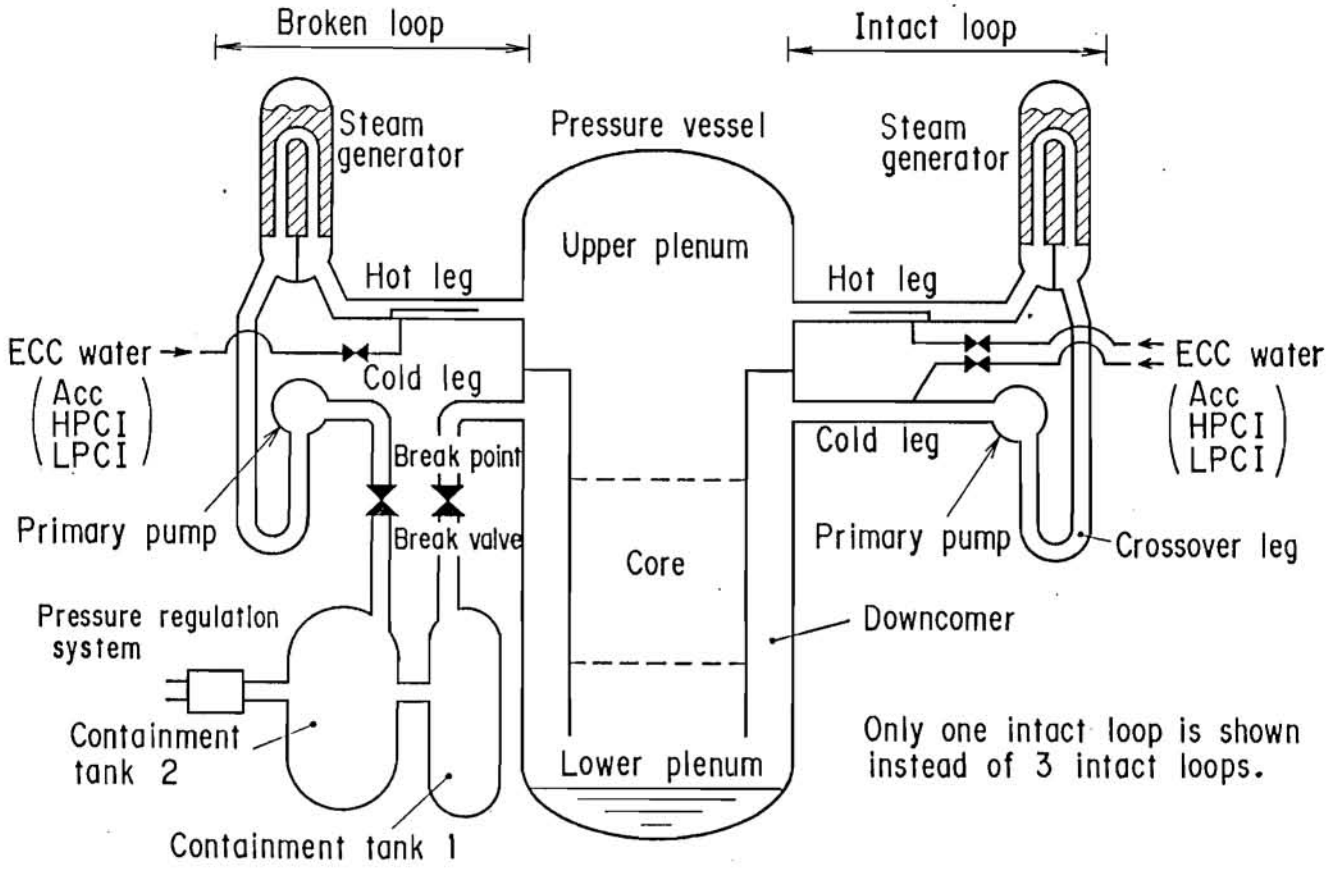

SCHEMATIC DIAGRAM OF CCTF MAIN PARTS

FIGURE A.1-2

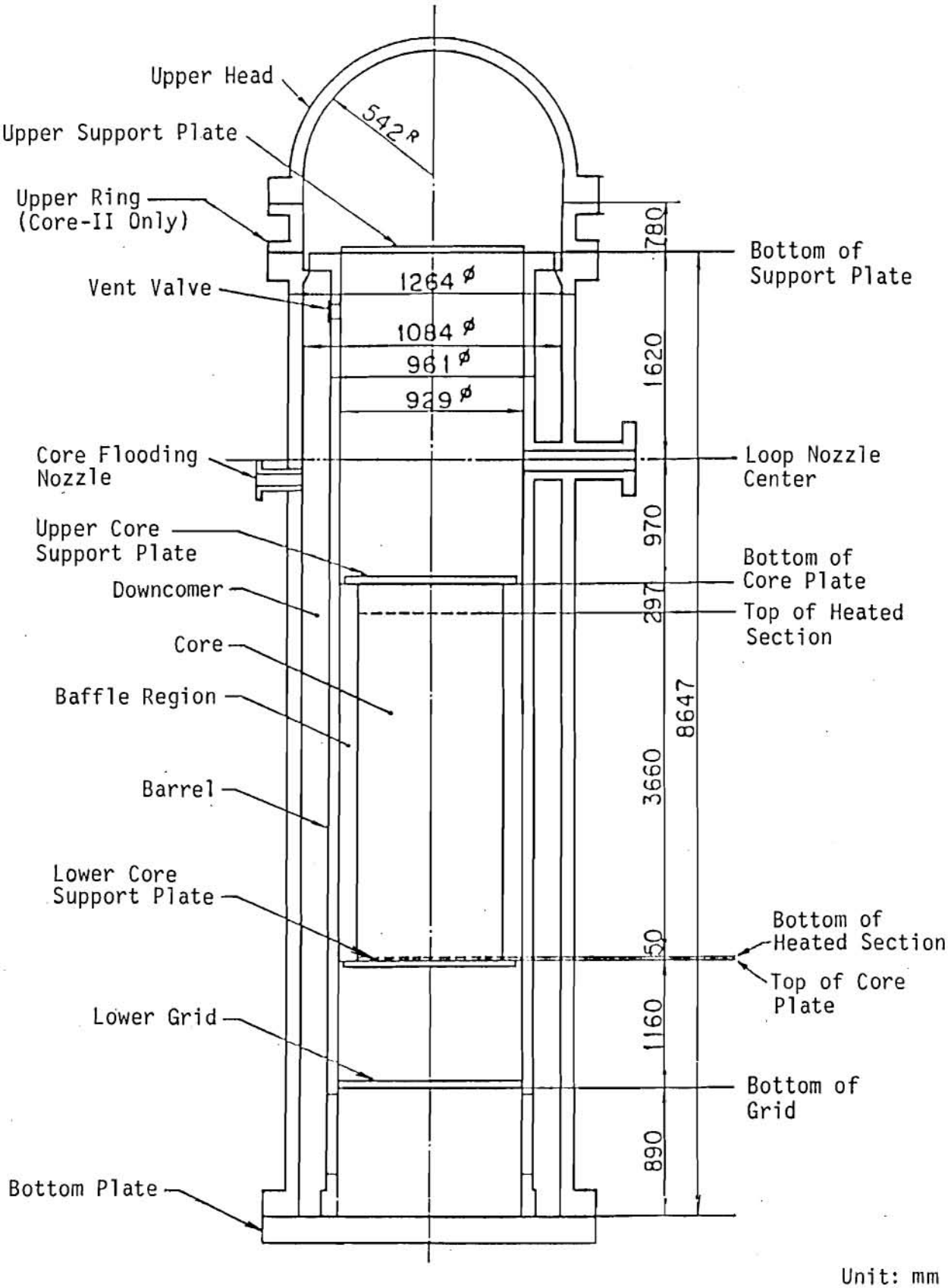

VERTICAL CROSS SECTION OF
CCTF CORE-II PRESSURE VESSEL

FIGURE A.1-3

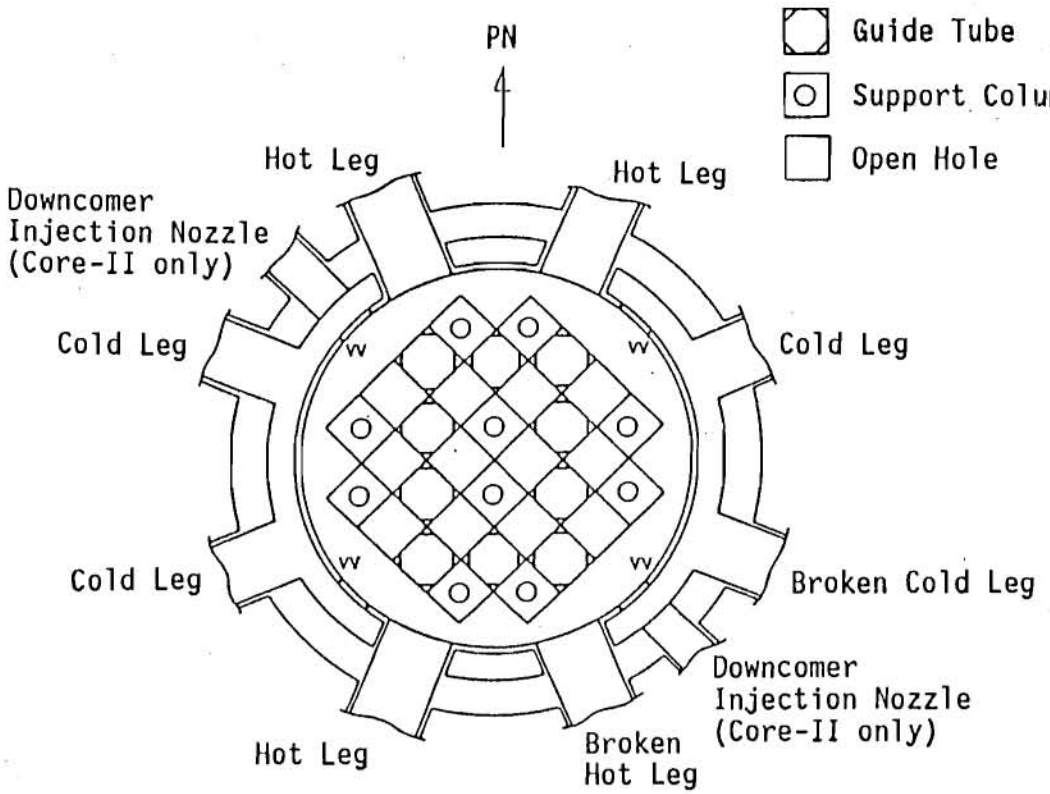

UPPER PLENUM

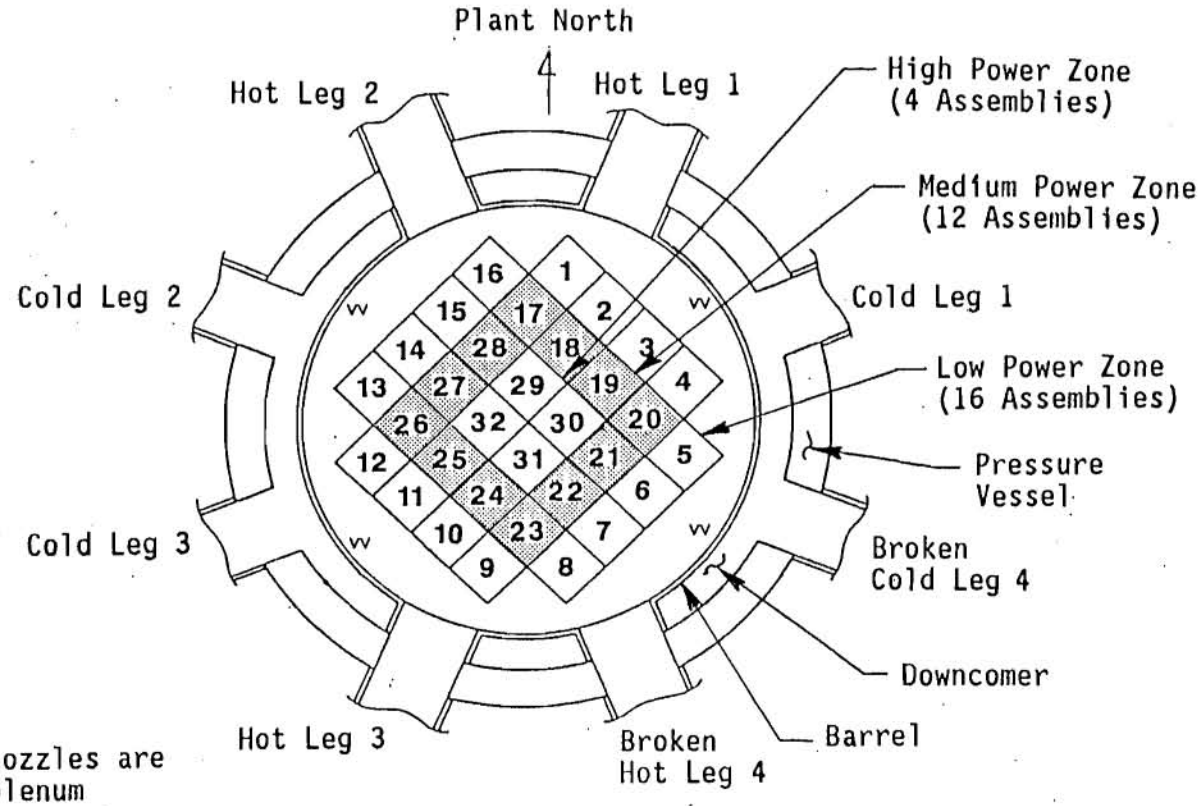

CORE (See Note)

Note:

Primary loop nozzles are at the upper plenum elevation, but are shown on the core cross section for reference.

CCTF PRESSURE VESSEL HORIZONTAL CROSS SECTIONS

FIGURE A.1-4

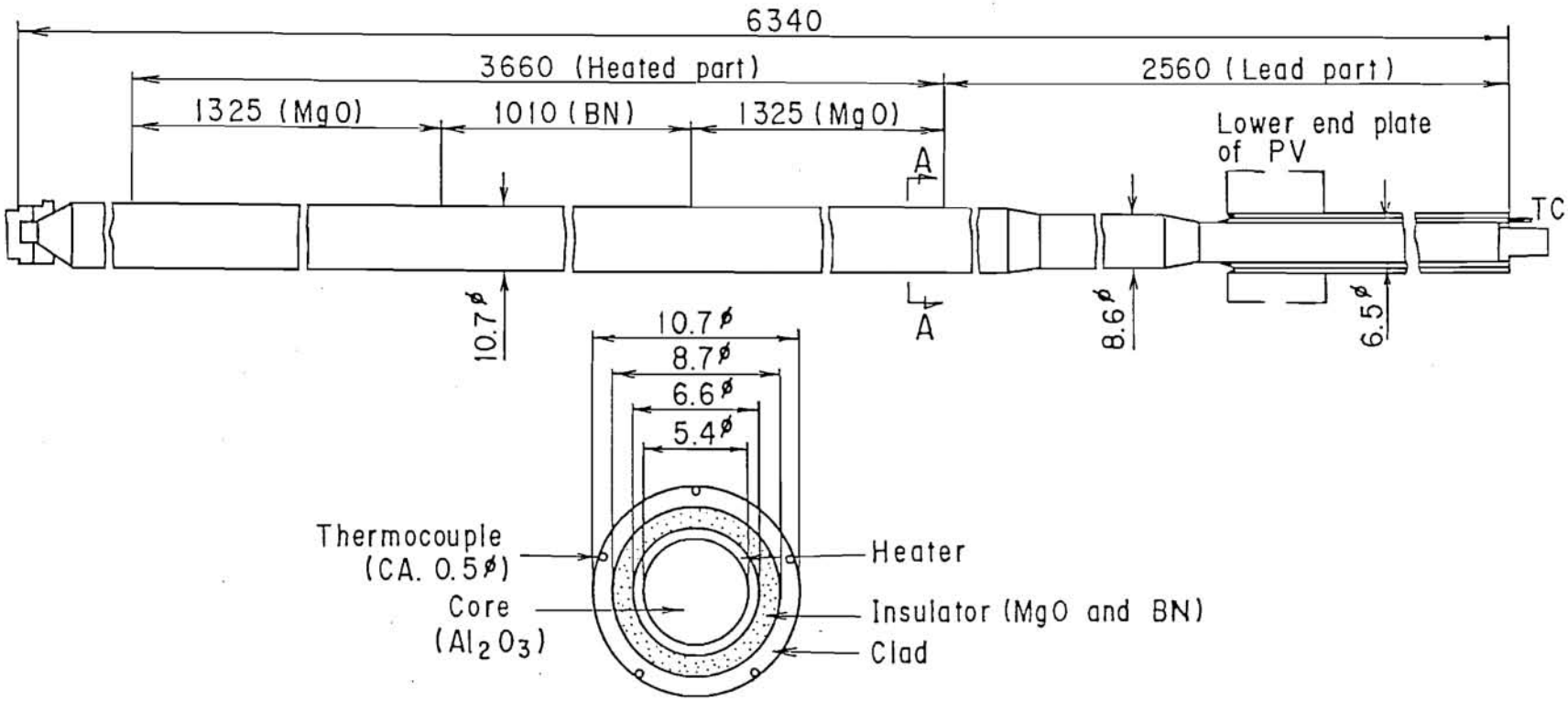

Section A-A

Unit: mm

CCTF HEATER ROD GEOMETRY

FIGURE A.1-5

A.2 SLAB CORE TEST FACILITY (SCTF)

A.2.1 Facility Description

SCTF was a full-height, full radius, 1/21-scale model of a sector of an 1,100 MWe four-loop PWR pressure vessel. The primary objective of the SCTF test program was to study two-dimensional thermal-hydraulic behavior within the reactor vessel during the refill and reflood phase of a large break LOCA in a PWR. While the pressure vessel was simulated in detail, only a crude loop simulation was used. The most significant feature of SCTF was that it contained a full-height heated core with realistic rod diameters and spacing and a core lateral extent of over 1.8 m (the core radius of the largest PWRs). This large core lateral extent provided the capability to examine multi-dimensional effects.

Facility Layout

Figure A.2-1 depicts the major components in the facility. They included a pressure vessel with a simulated core, a hot leg, a steam/water separator, an intact cold leg with a pump simulator, a broken cold leg, and two tanks attached to the ends of the broken loop to simulate containment. Vertical dimensions of system components were close to the corresponding dimensions in the reference PWR. Typically flow areas were based on the nominal core flow area scaling ratio (1/21). Maximum operating pressure of major components of SCTF was 600 kPa.

Electrically-heated rods were used in the simulated core to simulate nuclear fuel rods. A total of 1,872 heated rods were installed. The maximum electrical power supplied to the heated rods was 10 MW. This power could simulate the decay heat during the refill and reflood phases of an LBLOCA.

In SCTF, ECC injection nozzles were located in the cold leg, hot leg, upper plenum, and lower plenum to simulate core boundary conditions under ECC systems of cold leg injection, combined injection, upper plenum injection, and downcomer injection PWRs. Also, a special loop which connected the upper plenum and downcomer was used to simulate PWRs with vent valves in the core barrel.

Auxiliary systems included drain system from the pressure vessel and containment tanks, steam injection system to the upper plenum and steam/water separator, and water extraction system from the upper plenum.

Main Components

Pressure Vessel - Figure A.2-2 shows the SCTF pressure vessel. The vessel housed a downcomer, lower plenum, core, and upper plenum. The vessel simulated a radial slice of a PWR from the center (Bundle 1 in Figure A.2-2) to the periphery

(downcomer). Heights of components within the pressure vessel were about the same as those in the reference PWR.

As shown in Figure A.2-3, the core consisted of eight simulated fuel bundles arranged in a row (i.e., a slab geometry). For SCTF-I and II, each bundle contained 234 electrically-heated rods and 22 nonheated rods arranged in a 16 x 16 array (a total of 1,872 heated rods and 176 nonheated rods). In SCTF-III, the number of heated rods per bundle was increased from 234 to 236. All heated rods had an outer diameter of 10.7 mm, and a heated length of 3.6 m. These dimensions were identical to the corresponding dimensions of PWR fuel rods. The clad thickness, 1 mm, was thicker than that of fuel rods because of requirement for thermocouple attachment. The heat capacity of the heated rods was approximately 30% higher than that of nuclear fuel rods (to be filled in by JAERI; note, basis should be consistent with page 4.6-3).

The nonheated rods simulated the guide thimble tubes and instrument thimble tubes in PWR fuel assemblies. They were either stainless steel pipes or solid bars with an outer diameter of 13.8 mm. The heated rods and nonheated rods were held in their radial positions by grid spacers located at six elevations. The rod pitch was 14.3 mm which is identical to the reference PWR. In SCTF-I only, two of the fuel bundles (Bundles 3 and 4) contained flow blockage sleeves (60% blockage) at the mid-elevation to simulate the effect of ballooned fuel cladding.

Power to each bundle was individually adjustable to permit simulation of a radial power distribution. The axial power profile in all rods was a chopped cosine with an axial peaking factor (ratio of maximum to average power) of 1.4.

Honeycomb insulator panels surrounded the core, the upper plenum and the upper part of the lower plenum, to reduce the heat release from the SCTF vessel wall, which would not occur in PWRs (see Figure A.2-2). In SCTF-I, the surface next to the core was discontinuous as there were numerous panels. In SCTF-II and SCTF-III, the panels were covered by a continuous plate to provide a smooth surface facing the core and upper plenum.

Located above the core were the end boxes and the upper core support plate. Appropriate hydraulic resistance simulators were included to model the cross-flow resistance of the fuel rod tips at the top of the core and the axial flow resistance of the control rods when they are inserted.

A full-height core baffle region simulated the volume between the core and the core barrel in the reference reactor (see Figure A.2-2). In SCTF-II, the flow path at the bottom of the core baffle region was blocked to prevent water from flowing up into the core baffle region. In SCTF-III, the flow paths at the side of the core baffle region were also blocked.

The full-height downcomer was a rectangular channel. Flow area in the downcomer was adjustable (using a filler) to simulate the flow area for different reactor designs (e.g., US/Japanese or German). Provisions were made for blocking the bottom of the downcomer to conduct forced flooding tests (see Section A.2.2). In addition, a U-shaped pipe connected the top of the downcomer directly to the upper plenum to allow simulation of PWRs with vent valves in the core barrel (i.e., B&W PWRs).

The lower and upper plena of the pressure vessel were volume-scaled from the reference PWR, using the powered-rod ratio as a scale factor. This approach resulted in a realistic-height upper plenum and slightly shorter lower plenum (see Figure A.2-2). The upper plenum internals consisted of control rod guide tubes, support columns, orifice plates, and open holes (see Figure A.2-3). As in CCTF, the radius of each internal was scaled down from that of the reference reactor by a factor of 8/15, to give a more realistic flow path simulation (SCTF-I and II only). Full-size internals representative of a German PWR were used in SCTF-III.

Hot leg and cold leg nozzles were located at elevations that match the nozzle elevations in the reference PWR as closely as possible; however, because of space restrictions, the broken cold leg and the intact cold leg nozzles were located slightly below the hot leg penetration to avoid interference between the nozzles and the hot leg penetration in the downcomer (Figure A.2-2).

Since the focus of SCTF-III was the combined injection GPWR, several changes were made to the components in the pressure vessel to better simulate the German Siemens/KWU PWR. The significant changes were the following:

- The filler used in the downcomer in SCTF-I and SCTF-II was removed to simulate the larger downcomer flow area in the German PWR (GPWR).
- The baffle region was isolated from the core.
- Although the total number of rods remained the same, the number of heated rods per bundle was increased slightly from 234 to 236. The nonheated rod arrangement was changed to better simulate German fuel bundles.
- The SCTF-III components comprising the core/upper plenum interface (end boxes and upper core support plate) were representative of those in the reference GPWR.
- In the SCTF-III upper plenum, internal structures simulated the GPWR at full-scale. The support columns of SCTF-III were split and mounted in a staggered arrangement to achieve the desired flow simulation (see Figure A.2-4).

Primary Loops and Containment Tanks - The primary flow loops were simulated using a simplified system consisting of a single hot leg, a steam/water separator, an intact cold leg, and a broken cold leg.

The hot leg connected the upper plenum to the steam/water separator. The SCTF hot leg included a riser part like PWR hot legs. Hot leg flow area was scaled from the total flow area of four PWR hot legs, but the length was shortened. The cross section of the hot leg was an elongated circle of full height.

A steam/water separator located at the end of the hot leg simulated the hydraulic behavior of a steam generator. It housed a simulated inlet plenum and a tank for steam/water separation (see Figure A.2-2). Between the inlet plenum and the tank was a perforated plate which simulated the tubesheet of a steam generator. In the separation tank, entrained water was separated from the steam flow and measured. Steam could be injected into the separation tank to simulate vaporization of water in the U-tubes of a steam generator.

The intact cold leg connected the steam/water separator with the upper portion of the downcomer. The flow area was scaled from the flow area for three PWR cold legs; the cross section was circular. A pump simulator and loop seal were provided in the intact cold leg. An orifice plate was used to obtain proper flow resistance in the pump simulator.

The broken cold leg was simulated with two pipes, which connected the downcomer to Containment Tank-I and the steam/water separator to Containment Tank-II. The two containment tanks were the same tanks used for CCTF.

ECC Injection System - The SCTF ECCS consisted of an accumulator and a low pressure injection system. The injection ports for these systems were located in the lower plenum, downcomer, broken cold leg, hot leg, and intact cold leg between the pump simulator and pressure vessel. Additionally, injection and extraction systems provided and/or removed ECC using special nozzles located just above the upper core support plate.

Control and Instrumentation

Process Control System - The time-dependent variables were controlled with a computer during a typical SCTF test; these included power supplied to heated rods, ECC flow rate, and ECC temperature. Pressure in Containment Tank-II was maintained constant. The test initiation time and the sequence of events (e.g., power decay initiation and ECC injection initiation) were also controlled with the computer.

Instrumentation - SCTF was instrumented with over 1,500 sensors which included both conventional devices (e.g., pressure transducers, thermocouples) and advanced two-phase flow instrumentation. JAERI provided most of the conventional instruments, including approximately 700 thermocouples attached to rod clad surfaces throughout the core to measure the clad temperatures of heated rods. An additional 192 thermocouples were used to measure fluid, steam, and wall temperatures near and in the core. Other thermocouples, flow meters, pressure, and differential pressure sensors were located throughout the test facility and provided data which was used to determine fluid conditions, flow rates, liquid levels, and pressure distributions. In addition, viewing windows in the pressure vessel and loops permitted the use of television cameras and film cameras (both moving and still) to provide visual data which assisted in interpreting the test results.

A variety of advanced two-phase instrumentation was supplied to SCTF by the USNRC. The advanced instrumentation included fluid distribution grid/liquid level detectors (FDG/LLD), turbine meters, impedance probes, film probes, and spool pieces.

A.2.2 Catalog of Tests

SCTF testing was performed in three phases:

- SCTF-I, 1981 - 1983
- SCTF-II, 1983 - 1985
- SCTF-III 1986 - 1987

Table A.1-1 lists the SCTF tests, classified first by the injection configuration being simulated (cold leg injection, combined injection, downcomer injection, or upper plenum injection) and then by test objective.

The base case tests for cold leg injection were performed to investigate the two-dimensional thermal-hydraulics in the pressure vessel during reflood. Parameter effects tests for cold leg injection were performed to investigate the effect of various parameters (e.g., power distribution, rod temperature distribution, upper plenum liquid level, etc.) on two-dimensional thermal-hydraulics. Special purpose tests for cold leg injection were performed to investigate the two-dimensional thermal-hydraulic behavior under both evaluation model (EM) and best-estimate (BE) conditions. Two-dimensional thermal-hydraulics during the refill phase were also investigated.

For combined injection PWRs, the refill-reflood tests were performed under both EM and BE conditions. Additionally, seven integral tests simulating the refill-reflood phases and eight separate effect tests simulating the reflood phase were performed to study

parametric effects. In the CCFL evaluation tests, steam upflow was established in the core and water was injected into the upper plenum to investigate the CCFL characteristics at the tie plate with a full-scale radius.

SCTF tests for cold leg injection were performed using two modes of ECC injection: gravity feed and forced feed. In the gravity feed mode, ECC injected into the cold leg flowed, by gravity, down the downcomer and into the core. In the forced feed mode, the ECC was injected directly into the lower plenum by isolating the downcomer from the lower plenum; i.e., the water was forced into the core. The forced feed tests investigated core cooling behavior using defined boundary conditions at the core inlet. The gravity feed tests included the effect of downcomer water head on the two-dimensional core cooling behavior. By comparing the results of gravity feed and forced feed tests with similar flooding rates, it was concluded that there was no major difference between experimental results in both modes.

In the SCTF tests with gravity feed mode for cold leg injection ECCS, the amplitude of U-tube oscillations between the core and the downcomer was atypically large and the flooding rate was atypically high during the early transient, when the ECC injection flow rate was scaled proportional to the core flow area. This oscillatory behavior obscured the two-dimensional thermal-hydraulic behavior, which was the focus of the SCTF tests. However, by reducing the ECC injection rate early in the transient, the oscillatory behavior was suppressed, the core flooding rate was more typical, and two-dimensional thermal-hydraulic behavior could be readily discerned; consequently, most SCTF gravity feed tests were performed with a reduced ECC flow.

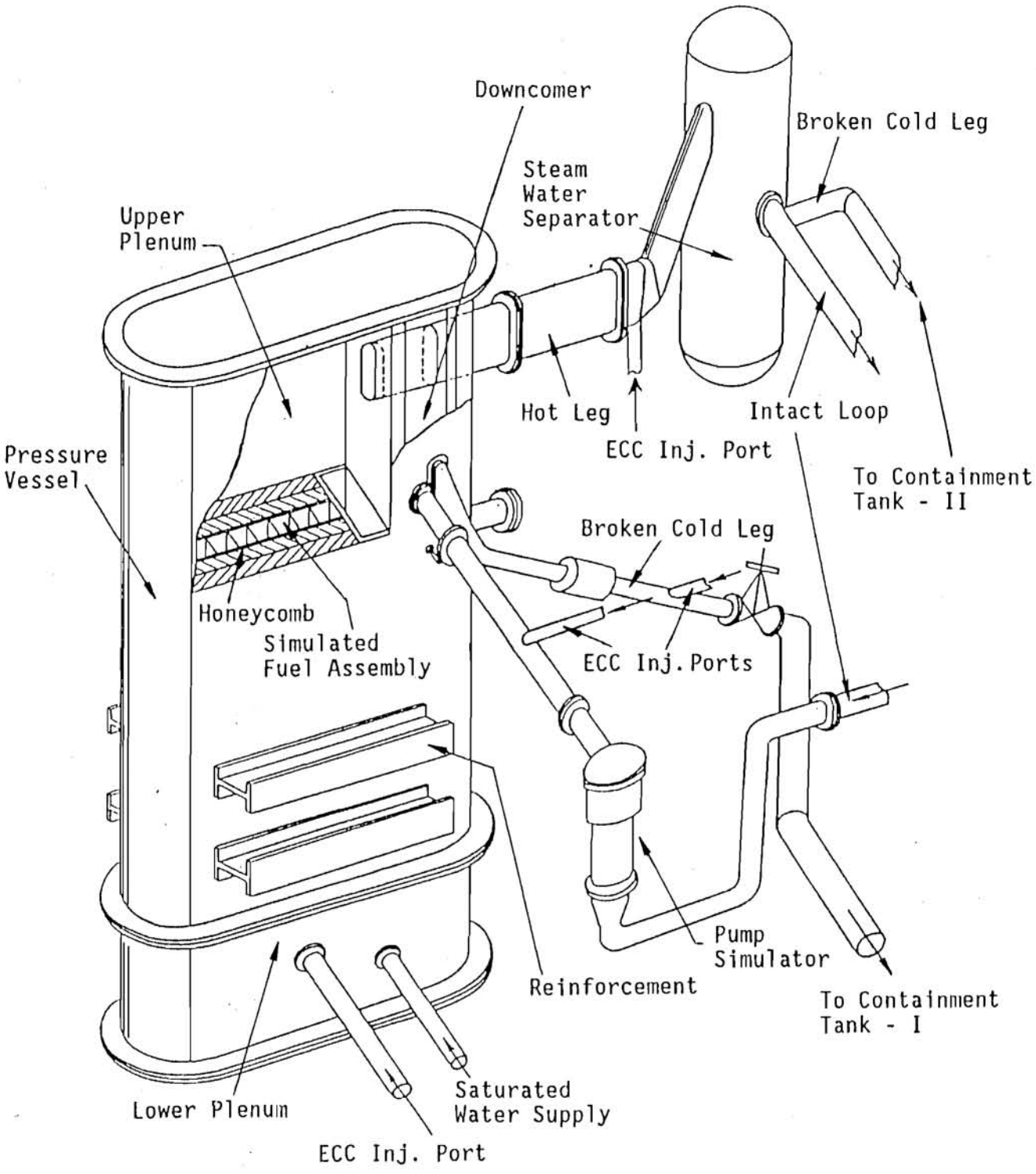

OVERVIEW OF SLAB CORE TEST FACILITY

FIGURE A.2-1

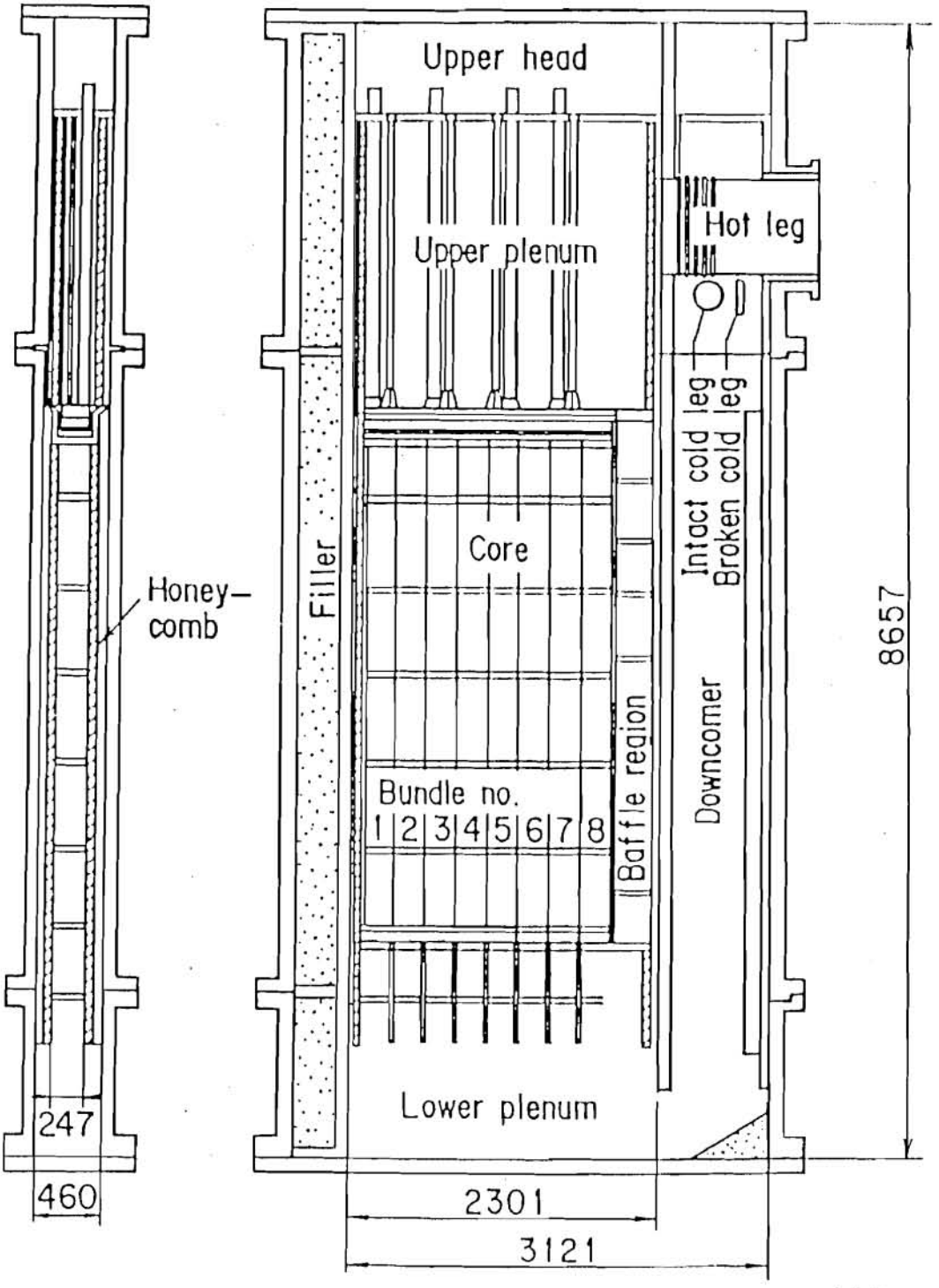

VERTICAL CROSS SECTION
OF SCTF CORE-II PRESSURE VESSEL

FIGURE A.2-2

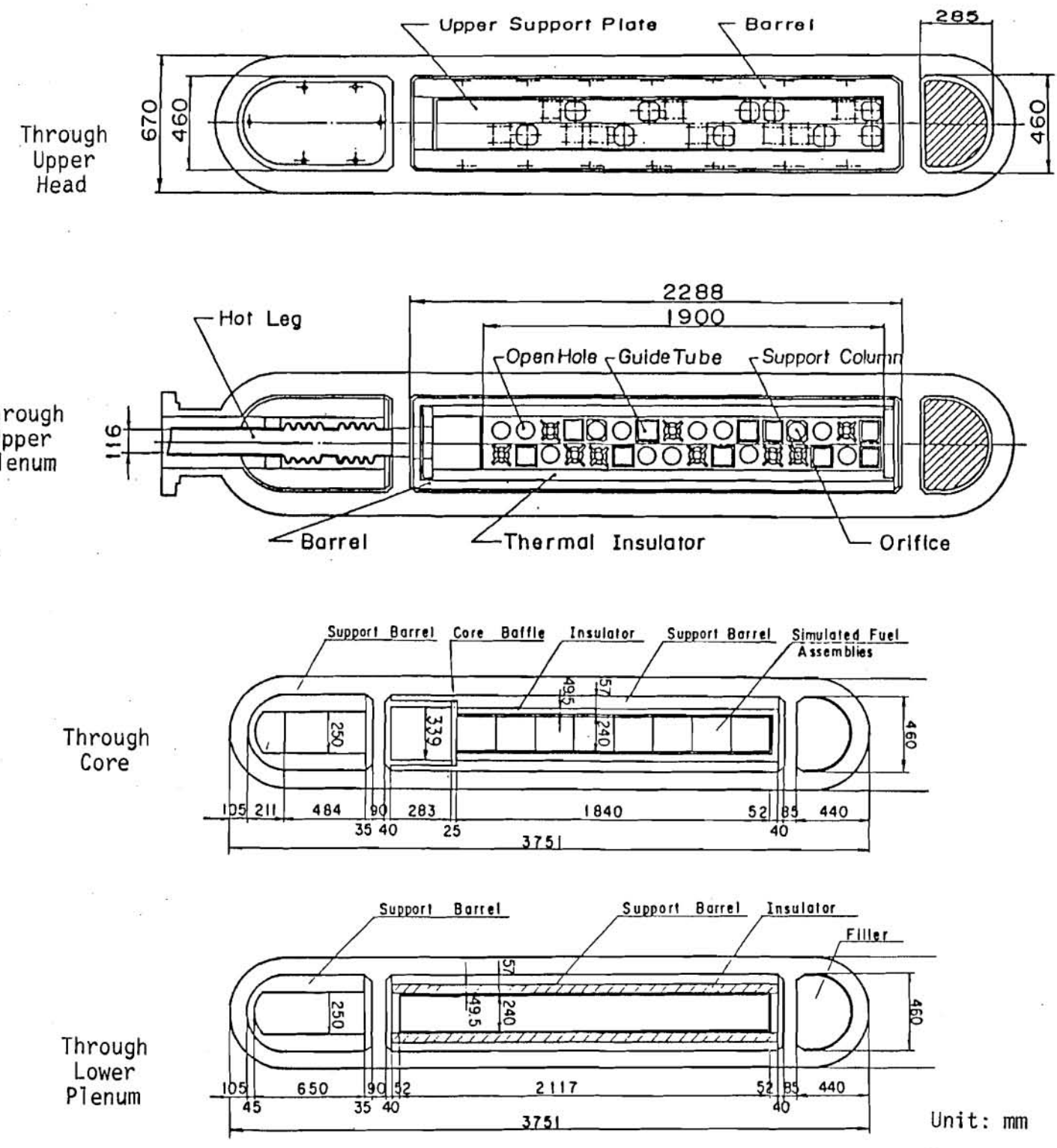

HORIZONTAL CROSS SECTIONS OF THE SCTF CORE-I AND -II PRESSURE VESSEL AT FOUR ELEVATIONS

FIGURE A.2-3

A.3 UPPER PLENUM TEST FACILITY (UPTF)

A.3.1 Facility Description

The UPTF was originally designed to investigate multidimensional behavior of water and steam during the end-of-blowdown, refill, and reflood phases of an LBLOCA in a PWR. The areas of investigation were defined to be the upper plenum, the downcomer, and the reactor coolant pipes connected to the test vessel.

Based on the results of risk assessment studies performed in the seventies and early eighties, additional provisions were made to investigate safety issues related to small break scenarios. Valuable data could be generated regarding these issues although the operational pressure of UPTF was limited to about 1900 kPa and the component simulators, as described below, were optimized for LBLOCA conditions.

The UPTF was built on the site of the large coal-fired power plant GKM in Mannheim, FRG. This location was chosen to readily supply the substantial demands for steam, water, and electricity for UPTF testing. The UPTF was integrated in the supply and disposal systems of the power plant.

Facility Layout

The UPTF represented a typical pressurized water reactor of 1300 MWe power class (GPWR) as designed by Siemens/KWU. The reference plant was the power plant Grafenrheinfeld located in southern Germany. The primary system of the Grafenrheinfeld plant consists of a reactor pressure vessel and four primary coolant loops each containing an U-tube steam generator and a primary coolant pump.

The UPTF was a mockup of the primary coolant system at full-scale (see Figures A.3-1 and A.3-2). In an early phase of 2D/3D Program definition it became obvious that a full-scale core would not be representable with electrically-heated fuel rods for technical and economical reasons. It therefore was decided to replace the core by a core simulator which produced flow conditions at the core/upper plenum interface similar to those generated by a heated core. The core simulator injected steam and water below the tie plate to simulate steam generation and liquid entrainment in a heated core. The overall mass balance was maintained by extraction of water from the bottom of the test vessel.

Steam generators and main reactor coolant pumps were also replaced by simulators. Both of the simulators were designed to preserve the volumes, flow resistances, and key elevations of the reference plant. The steam generator simulators were equipped with feedback systems to simulate evaporation of water carried to the steam generator

tubes during the reflood portion of an LBLOCA. The pump simulators were adjustable throttle valves and could simulate the flow resistance of spinning or locked reactor coolant pumps in the low pressure phases of LOCA.

The break of a main coolant pipe was simulated by large fast-opening valves. The break location could be varied from hot leg to cold leg. Break size could be varied from full offset break (200% of the loop flow area) to 25% of loop flow area. Smaller break sizes for SBLOCA conditions could be simulated as needed by bypassing the large break valves.

The break was connected to a containment simulator. The back pressure could be controlled in the range of 250 kPa to 600 kPa, which covers the conditions of containment designs relevant for reactor systems evaluated in the 2D/3D Program.

The ECC systems were replaced by large accumulators connected to the ECC injection ports. ECC injection was performed using control valves and was adjustable to simulate the ECC injection characteristics of the system designs used in the three participating countries.

In some system areas, provisions were made to account for reactor designs other than the reference plant; these are noted separately in the component descriptions below.

Main Components

The main components and subsystems of UPTF are briefly discussed below. The discussion covers both configuration and function.

Test Vessel - The UPTF test vessel (see Figure A.3-3) was a full-scale representation of the reference plant reactor pressure vessel. The main dimensions were identical to those of the reference plant except for the vessel wall thickness which was reduced according to the lower design pressure of UPTF.

The upper plenum structures consisting of upper core support columns, and upper core support plate, as well as control rod guide tubes were identical to those in the reference plant.

To facilitate instrument line routing from the upper plenum out of the test vessel, a ring was installed between the upper flange of the test vessel and the upper head. The ring was equipped with penetration nozzles for the instrumentation lines of upper plenum instruments. For the instruments installed in the lower part of the test vessel and downcomer, penetration nozzles were provided over the length of the test vessel.

The downcomer width was compromised between US/J and German design. The UPTF downcomer width was 250 mm compared to 315 mm for the reference PWR. The lower core structure consisting of core barrel, core shroud, intermediate core support, and core was identical to the reference reactor except for the core, which is replaced by the core simulator, and the vent valves installed in the core barrel to simulate ABB (BBR)/B&W design. Also, for ABB (BBR)/B&W plant simulation, two ECC injection ports were provided for downcomer ECC injection.

The steam/water supply lines for the 17 individual core simulator injection zones penetrate through the lower head of the test vessel.

Core Simulator - The core simulator was designed to create steam/water flow conditions at the core/upper plenum interface (i.e., the tie plate area) similar to those expected for the low pressure phases of a LOCA. This was achieved by controlled injection of water and steam according to preprogrammed values or to algorithms providing feedback from measured conditions.

The upper part of the core simulator consisted of 193 dummy fuel assemblies, about 1 m in length, geometrically simulating fuel assemblies in the reference plant. The dummy fuel assemblies were not heated and severed as flow conditioners for the two-phase flow at core exit.

Below each of the dummy fuel assemblies was a nozzle capable of injecting steam and water flow (see Figure A.3-4). The core cross section was divided into 17 injection zones (see Figure A.3-5) which could be individually controlled to produce flow distributions. Different power profiles could be simulated as well as core responses to water breakthrough caused by hot leg ECC injection.

For separate effects tests, preprogrammed steam and water mass flow rates were injected into the test vessel via the core simulator creating clearly-defined boundary conditions. In integral tests, baseline injection mass flow rates for steam and water were based on PWR LOCA analyses and subscale tests. Feedback control systems provided realistic system response for these cases when the boundary conditions significantly deviated from the reference values. The boundary conditions relevant for core thermal-hydraulic behavior were the core bottom flooding rate and, in case of hot leg ECC injection, local water breakthrough from the upper plenum into the core. The algorithms applied for feedback flow condition were derived from a large number of SCTF and CCTF tests. For proper feedback from rapid changes of boundary conditions, the control valves of the core simulator injection systems have a specified travel time of 0.7 s for 100% stroke.

Two-phase flow exiting the core in a reactor would be produced by boiling and entrainment in the core. In UPTF this process is simulated by controlled injection of

water and steam from external sources, and the mass injected has to be extracted from the system to keep the correct mass balance. The injection mass flow rates were measured, and the same amount of water mass was drained from the lower plenum of the test vessel by the controlled drainage system.

Steam Generator Simulators and Water Separators - In the low pressure phases of an LBLOCA the steam generators act as flow resistances for the steam flowing from the upper plenum to the downcomer via the intact loops. In addition, the hot fluid on the secondary side of the steam generator is a heat source. Steam production due to water entering the tubes on the primary side can significantly affect the differential pressure between upper plenum and downcomer. Steam generator simulators were installed in the three intact coolant loops of UPTF to simulate the behavior of real steam generators during refill and reflood phases of an LBLOCA.

Proper inflow conditions were obtained by maintaining inflow orientation as well as cross section and height of the reference steam generator inlet plenum. The U-tube bundle was replaced by an assembly of two-stage, cyclone steam/water separators which had a similar flow area and the flow resistance (see Figure A.3-6). The overall volume and overflow height were retained by the loop configuration.

The evaporation of water entering the heat exchange area was simulated by steam injection into the dome of the steam generator simulator. This could be performed in a preprogrammed way (transient or constant) or automatically controlled by a feedback system based on measured conditions. In separate effects tests, preprogrammed steam generator simulator steam injection was used as a clearly-defined boundary condition. In integral tests, the feedback system was used to obtain a simulation of the real steam generator, to evaluate the system effects on the emergency core cooling process. Two different modes of operation are distinguished by the steam generator simulator feedback system:

- Dispersed water flow entering the steam generator tube regions.
- Water plug flow entering the steam generator tube regions.

Water droplets carried by steam flow to the steam generator simulators were separated by the cyclone separators, measured and drained from the system. The same amount of steam as the water separated was injected to the dome of the steam generator simulator.

If a water plug entering the steam generator simulator was detected by the measurement systems, large quantities of steam were injected according to algorithms developed at the Technical University of Munich. The resulting pressure increase in the loop drove the water plug back to the hot leg and into the upper plenum.

Steam/water separators were installed close to the break valves. Break mass flow rates entering the separators were split into single-phase water and steam flows. Water was separated by two-stage cyclones, measured and drained to the water collecting tank (see Figure A.3-6). Steam flow was measured by orifices and vented to the containment simulator where it was condensed.

The steam/water separator on the hot leg side could be used as a steam generator simulator for tests simulating LOCAs with break sizes smaller than 200% of the loop flow area. The overall design was similar to that of the steam generator simulators but the number of cyclones was increased according to higher mass flow rates expected in the broken loop in case of a full offset break of a main coolant pipe.

Pump Simulators - In UPTF, pump simulators, which model the volume, and key internal heights of the reactor coolant pump for the reference reactor, were installed in the intact loops as well as the broken loop. The flow resistance of the pump simulators was adjustable and was preset according to the test requirements (see Figure A.3-7). The pressure drop coefficient could be varied over a wide range. For separate effects tests requiring no flow in the primary coolant piping, the loops were completely blocked by the pump simulators.

Containment Simulator - The containment simulator was designed as a pressure suppression/control system simulating large, dry containment conditions.

The containment simulator consisted of a large vessel (1500 m^3) which was divided into a dry well (500 m^3) and a wet well (1000 m^3). The steam flow from the primary system entered the containment simulator at the top of the dry well and flowed via 14 downcomers into the water inventory of the wet well where it condensed (see Figure A.3-8).

Nitrogen was mixed with steam in the downcomers to reduce dynamic effects of steam condensation in the wet well, so that the overall pressure oscillations were limited to 20 kPa.

When pressure in the primary coolant system dropped below the specified containment pressure, a backflow of steam was provided. An auxiliary steam supply system provided controlled injection of up to 300 kgs/s to maintain the containment pressure at its specified value. In case of rapid transients, a set of safety valves prevented excessive pressure spikes and overpressurization of the containment simulator.

Containment pressure was controlled by the central computer where the desired conditions were programmed. The range of simulated containment pressures was from 250 kPa to 600 kPa, which covered US/J and FRG PWR containment designs to be simulated in the 2D/3D Program.

ECC Injection System - Accumulator and low pressure ECC injection systems of actual PWRs were replaced in UPTF by large accumulators and control systems able to simulate the characteristics of various ECC system designs. Eight ECC injection ports were provided in the primary loop piping: four in the hot legs and four in the cold legs. In addition, two downcomer injection ports were provided for simulation of ECC concepts as used, for instance, by B&W or ABB (BBR).

The ECC water in UPTF was contained in four large storage tanks pressurized by steam. During discharge of water, the pressure in the storage tanks was maintained by steam from the steam supply system. Two of the ECC storage tanks could also be used for nitrogen storage for simulation of nitrogen discharge from the accumulators at the end of accumulator injection typical for US/J PWR designs.

ECC was fed from the storage tanks to a common header and distributed to the injection ports. Flow to each injection port was individually controlled (see Figure A.3-9). To simulate dissolved nitrogen in accumulator ECC, nitrogen could be added to the ECC water close to the injection ports.

For proper flow conditioning, the ECC piping within one meter of the injection port was identical to that in the reference plant. The cold leg ECC port cross section was adjusted by inserts to consider the different cross sections of the injection ports of US/J PWRs and GPWRs. ECC water in the tanks and piping could be preheated to 120°C using steam nozzles in the tanks and a recirculation system. For simulation of structural heat, the water and ECC piping close to the injection could be heated up to 160°C.

Control and Instrumentation

Process Control System - The process control system consisted of several computers and control loops to establish time-dependent test boundary conditions and provide feedback to active test facility subsystems.

The overall process was controlled by control computer P1 (SIEMENS microcomputer SMP). Test initiation, time-dependent boundary conditions, as well as the shutdown procedure, were stored in, and controlled by, the P1 computer.

For test initiation, the opening times and opening sequence of the break valves, and the start of core simulator steam and water injection, steam generator simulator injection and ECC injection were controlled in a preprogrammed way. During the test, time-dependent boundary conditions such as core simulator steam and water injection rates, ECC injection rates, steam generator simulator steam injection rates, and containment pressure were also controlled by control computer P1. Core simulator and steam generator simulator injection rates could be automatically controlled by feedback systems as described below.

For integral tests which were to simulate realistic PWR system behavior, the basic steam and water injection rates were predetermined and stored in control computer P1. If, during the test, certain measured conditions deviated from pre-calculated values, the injection rates could be adjusted. Algorithms for the variation of core response to different bottom flooding rates or local water breakthrough from the upper plenum (in the case of hot leg ECC injection), which were developed based on SCTF and CCTF tests, were stored in control computer P2 (SIEMENS microcomputer MMC).

In addition, P2 controlled the fast, automatic shutdown system (FASS) which would terminate tests if test conditions exceeded design limits.

Steam generator feedback systems were controlled by computer (SIEMENS PC 16-20) for each of the intact loop steam generator simulators. The on-line simulation of steam production considered the amount of water entering the heat transfer area as well as the flow pattern, as previously discussed.

Instrumentation and Data Acquisition Systems (DAS) - UPTF instrumentation was divided into operation instrumentation and test instrumentation. Operation instrumentation was used to control boundary conditions for test operation. Test instrumentation was used to measure processes and phenomena investigated in the tests. Test instrumentation such as thermocouples and pressure transducers were called conventional instrumentation. In addition, specialized and complex two-phase flow instrumentation (called advanced instrumentation) was developed and supplied to UPTF by USNRC. These instruments are:

- Tie plate flow modules to specially determine mass flow rates at the core/upper plenum interface.
- Breakthrough detectors to measure water downflow from upper plenum to core.
- Pipe flowmeters to determine hot leg and broken cold leg mass flow rates.
- Purged DP transducers to measure upper plenum water inventory at several locations.
- FDG/LLD optical sensors to distinguish water- and steam-filled volumes.
- Turbine meters to measure velocities.

The signals from the instrument sensors were conditioned and stored by the data acquisition systems, which also was provided by USNRC. There were two independent systems in UPTF. The stand-alone DAS (HP-A600 computer) collected and stored the digital data from the 705 channels of the FDG/LLD systems. The main DAS was based on a VAX 11/750 computer. A total of 938 analog channels, 15

channels for the γ-densitometers of the pipe flowmeters, and 210 analog auxiliary and spare channels were installed in the main DAS.

According to the band width desired (5 Hz), the general data sampling rate for UPTF instrumentation was 25 Hz. For pipe flowmeter absolute pressure, pipe flowmeter drag rake force, and tie plate drag body force a sampling rate of 150 Hz was chosen.

Facility Load Monitoring System - To record the load history of critical test facility components, an independent monitoring system was installed. In tests where extraordinary loads were expected, the system also was used to supervise the test performance and, if necessary, terminate the test before the integrity of facility components was jeopardized.

The monitoring system consisted of a data acquisition system which collected and stored the data from the various sensors. The following instruments are installed on selected facility components or supports.

- Four pressure taps
- Thirteen force meters
- Thirty strain gages
- Eight acceleration meters
- Nine displacement meters

A.3.2 Catalog of Tests

The UPTF test program was designed to cover a wide range of phenomena, parameters, and PWR ECC system designs. The UPTF test matrix is summarized below by region of the primary system and phenomena of interest. The basic test conditions are summarized in Table A.3-1.

- Downcomer Behavior during End-of-Blowdown Tests - This group of tests investigated countercurrent flow in the downcomer during the end-of-blowdown phase of an LBLOCA; ECC systems simulated included cold leg injection and downcomer injection.
- Downcomer Behavior during Reflood Tests - These tests evaluated water entrainment from the downcomer during the reflood phase of an LBLOCA; both cold leg and downcomer ECC injection systems were simulated.

- Tie Plate and Upper Plenum Behavior Tests - This test group investigated full-scale countercurrent flow at the tie plate for ECC delivered to the upper plenum and steam or two-phase upflow from the core. Upper plenum water accumulation was also investigated in these tests.

- Upper Plenum/Hot Leg De-entrainment Tests - These tests investigated entrainment/de-entrainment and accumulation of water upstream of the steam generator tubes (i.e., in the upper plenum, hot legs, and steam generator inlet plena) during reflood.

- Loop Behavior Tests - This group of tests investigated the development of flow patterns, particularly stratified flow and plug flow, for various ECC and steam or two-phase mass flow rates.

- Separate Effects Tests with Vent Valves - The test group evaluated the effect of vent valves on downcomer countercurrent flow during EOB, and water entrainment from the downcomer during reflood.

- Small Break LOCA Separate Effects Tests - These tests investigated the following phenomena related to SBLOCAs.

  - Fluid-fluid mixing in the cold leg and downcomer at elevated temperature (i.e., pressurized thermal shock).

  - Steam/water countercurrent flow in the hot legs for the reflux-condenser mode of core cooling during an SBLOCA.

  - Steam/water countercurrent flow at the tie plate with high pressure ECC injection into the hot legs when the system is at an elevated pressure.

- Integral Tests - Integral tests simulated overall system behavior during the EOB, refill, and reflood phases of an LBLOCA. Specific ECCS concepts simulated included:

  - Cold leg injection.

  - Combined injection.

  - Cold leg/downcomer injection with vent valves.

Table A.3-1

UPTF TESTS

Group	Test Objective	Test Numbers	Run Numbers	Basic Test Conditions[1]
Downcomer Behavior during End-of-Blowdown	Downcomer CCFL and ECC Bypass	4A	174	CLI; transient depressurization from 1200 kPa; loops open
		5A	063	CLI; transient depressurization from 1800 kPa; loops blocked
		5B	062	CLI; steady-state CS steam injection; loops blocked
		6	131, 132, 133, 135, 136	CLI; ECC saturated; steady-state CS steam injection; loops blocked
		7	200, 201, 202, 203	CLI; ECC saturated; steady-state CS steam injection; loops blocked
		21A	272	DCI; ECC subcooled; steady-state CS steam injection; loops blocked
		21B	274	DCI; ECC saturated; steady-state CS steam injection; loops blocked
Downcomer Behavior during Reflood	Downcomer Entrainment	25A	242	CLI; DC wall superheated; steady-state SGS steam injection; loops open
		25B	241	CLI; DC wall saturated; steady-state SGS steam injection; loops open
		21D	171	DCI; DC wall saturated; steady-state SGS steam injection; loops open
Tie Plate and Upper Plenum Behavior Tests	Simultaneous Two-Phase Upflow and Water Downflow; Breakthrough at Tie Plate; Upper Plenum Pool Formation	20	090	UPI; ECC subcooled; CS steam and water injection; no SGS steam injection
		10A	080	HLI; ECC saturated; CS steam injection; no SGS steam injection
		12	014	HLI; ECC subcooled; CS steam injection; no SGS steam injection
		13	071	HLI; ECC subcooled; CS steam and water injection (W/S=4); no SGS steam injection
		26C	232	HLI; ECC subcooled; CS steam and water injection (W/S=10); no SGS steam injection
		15A	123	HLI; ECC subcooled; CS steam and water injection (hysteresis); no SGS steam injection
		15B	127	HLI; ECC subcooled; CS steam and water injection (W/S=4); auto SGS steam injection[2]
		16A	181	HLI; ECC subcooled; CS steam and water injection (W/S=1.7); auto SGS steam injection[2]
		16B	184	HLI; ECC subcooled; CS steam and water injection (W/S=2.7); auto SGS steam injection[2]
Upper Plenum/Hot Leg De-entrainment Tests	Tie Plate CCFL; Entrainment to Upper Plenum, Hot Legs and SG	10C	082	Steady-state CS steam and water injection; loops blocked
		10B	081	Steady-state CS steam and water injection; loops open
		29	210, 211, 212	Steady-state CS steam and water injection; loops open

Table A.3-1

UPTF TESTS

Group	Test Objective	Test Numbers	Run Numbers	Basic Test Conditions[1]
Loop Behavior Tests	Flow Pattern in Hot Legs	8A	112 (2nd portion)	HLI; ECC subcooled; CS steam injection; auto SGS steam injection[2]; low loop flow resistance
		8B	111	HLI; ECC subcooled; CS steam injection; auto SGS steam injection[2]; high loop flow resistance
		26B	231	HLI; ECC subcooled; CS steam injection; no SGS steam injection
		26A	230	HLI; ECC saturated; CS steam injection; no SGS steam injection
	Flow Pattern in Cold Legs	8A	112 (1st portion)	CLI; ECC subcooled; CS steam injection; no SG simulation; low loop flow resistance
		8B	111	CLI; ECC subcooled; CS steam injection; no SG simulation; high loop flow resistance
	Flow Pattern in Hot and Cold Legs	9A	056	CI; ECC subcooled; CS steam and water injection; auto SGS steam injection[2]; low loop flow resistance
		9B	059	CI; ECC subcooled; CS steam and water injection; auto SGS steam injection[2]; high loop flow resistance
Vent Valve Separate Effects Tests	Downcomer CCFL and ECC Bypass during End-of-Blowdown	22A	280 (1st portion)	DCI; ECC subcooled; steady-state CS steam injection; loops blocked; W free
		22B	281, 283	DCI; ECC saturated; steady-state CS steam injection; loops blocked; W free
		22Bs	285	DCI; ECC saturated; steady-state CS steam injection; loops blocked; W free; TS
		22C	282	DCI; ECC saturated; steady-state CS steam injection; loops blocked; W free
		22Cs	284	DCI; ECC saturated; steady-state CS steam injection; loops blocked; W free; TS
	Flow Phenomena in Downcomer, Loops and Upper Plenum during Reflood	21C	273, 275	DCI; ECC subcooled; steady-state CS steam and water injection; loops open; W blocked
		22A	280 (2nd portion)	DCI; ECC subcooled; steady-state CS steam and water injection; loops blocked; W free
		23B	290	DCI; ECC subcooled; steady-state SGS steam injection; loops blocked; W free; TS
		23A	291	DCI; ECC subcooled; steady-state CS steam and water injection; loops open; W free; TS

Table A.3-1

UPTF TESTS

Group	Test Objective	Test Numbers	Run Numbers	Basic Test Conditions[1]
SBLOCA Separate Effects Tests	Fluid-Fluid Mixing in Cold Leg and Downcomer	1	020, 021, 023, 025, 026	CLI; ECC subcooled; primary system filled with warm water
	Hot Leg CCFL	11	030-034, 036-045	Steady-state CS steam injection; water injection into inlet plenum of broken hot leg steam/water separator; intact loops blocked
	Behavior in Hot Leg and Upper Plenum with HPI	30	141, 142	HLI; ECC subcooled; system pressure = 1500 kPa
Cold Leg ECC Injection Integral Test	System Behavior during a Simulated LOCA Transient	27A 27B 2 4B 17B 17A	256 255 101 177 151 151	CLI; BE refill/reflood simulation; nitrogen discharge from ACC CLI; BE reflood simulation; high loop flow resistance CLI; EM reflood simulation CLI; BE reflood simulation; moderate loop flow resistance CLI; BE reflood simulation; low loop flow resistance No ECC injection; BE reflood simulation; low loop flow resistance
Combined ECC Injection Integral Tests[3]	System Behavior during a Simulated LOCA Transient	3 18 28 19 14	C5 169 262 192 221	CI; cold leg break – break size = 2A; EM refill/reflood simulation CI; cold leg break – break size = 2A; EM refill/reflood simulation CI; cold leg break – break size = 2A; BE refill/reflood simulation CI; cold leg break – break size = 0.5A; EM refill/reflood simulation CI; hot leg break – break size = 2A; EM refill/reflood simulation
Downcomer/ Cold Leg ECC Injection with Vent Valves Integral Test	System Behavior during a Simulated LOCA Transient	24	302, 304	DCI and CLI; cold leg break; EM refill/reflood simulation; TS

Table A.3-1

UPTF TESTS

NOTES:

1. The following abbreviations are used in the test conditions:

CI	Combined ECC injection
CLI	Cold leg ECC injection
DCI	Downcomer ECC injection
HLI	Hot leg ECC injection
UPI	Upper plenum ECC injection
ACC	Accumulators
BE	Best estimate
CS	Core simulator
EM	Evaluation model
SGS	Steam generator simulator
TS	Thermal sleeves installed in downcomer ECC injection nozzles
VV	Vent valves
W/S	Ratio of core simulator water and steam injection rates

2. "Auto SGS steam injection" indicates that the SGS feedback control system was activated to automatically inject steam based on the water flow into the SGS.

3. Break size is defined relative to the cross-sectional area of the reactor coolant piping (A).

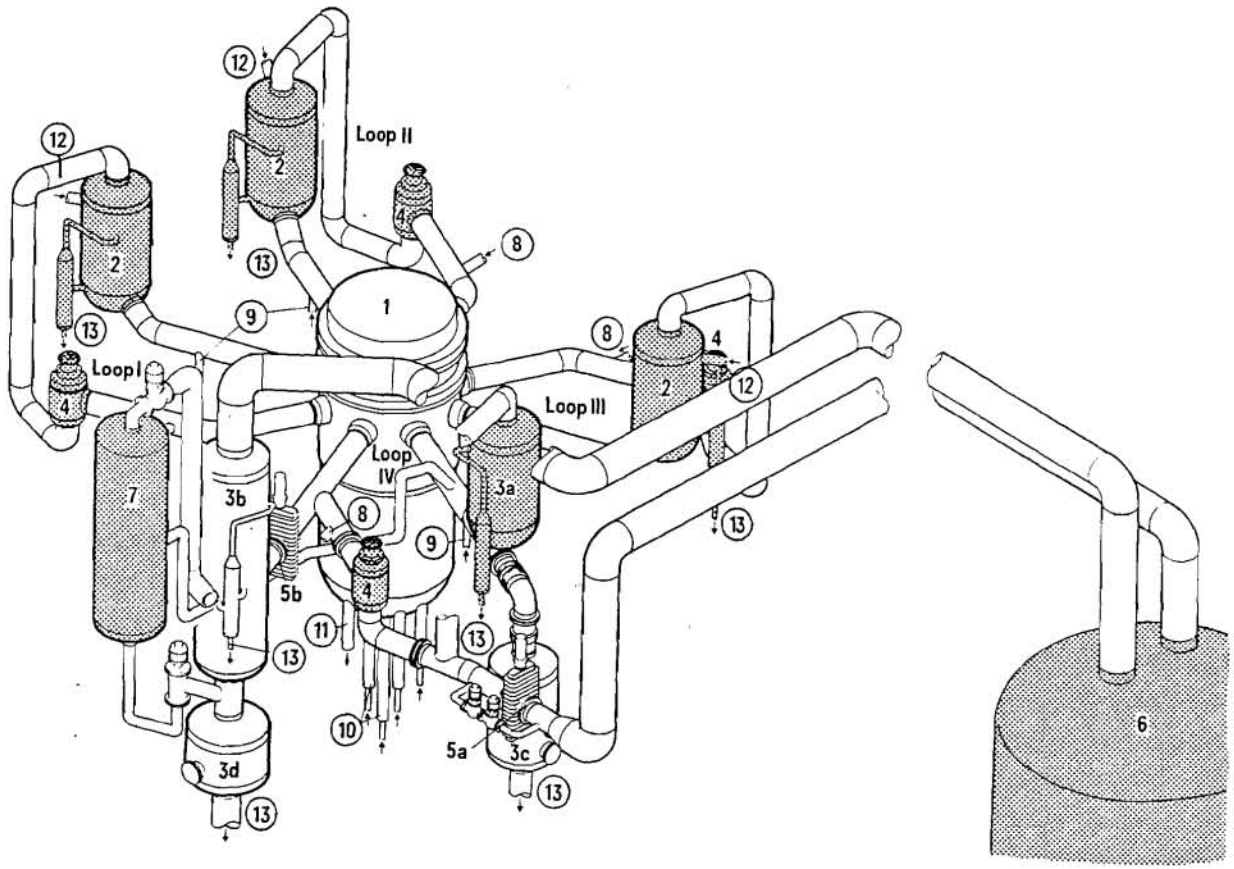

1 Test Vessel
2 Steam Generator Simulator (Intact Loop)
3a Steam Generator Simulator/ Water Separator (Broken Loop Hot Leg)
3b Water Separator (Broken Loop Cold Leg)
3c Drainage Vessel for Hot Leg
3d Drainage Vessel for Cold Leg
4 Pump Simulator
5a Break Valve (Hot Leg)
5b Break Valve (Cold Leg)
6 Containment Simulator
(7) Surgeline-Nozzle
(8) ECC-Injection Nozzles (Cold Leg)
(9) ECC-Injection Nozzles (Hot Leg)
(10) Core Simulator Injection Nozzle
(11) TV-Drainage Nozzle
(12) Steam Injection Nozzle
(13) Drainage Nozzle
Simulator

UPTF PRIMARY SYSTEM

FIGURE A.3-1

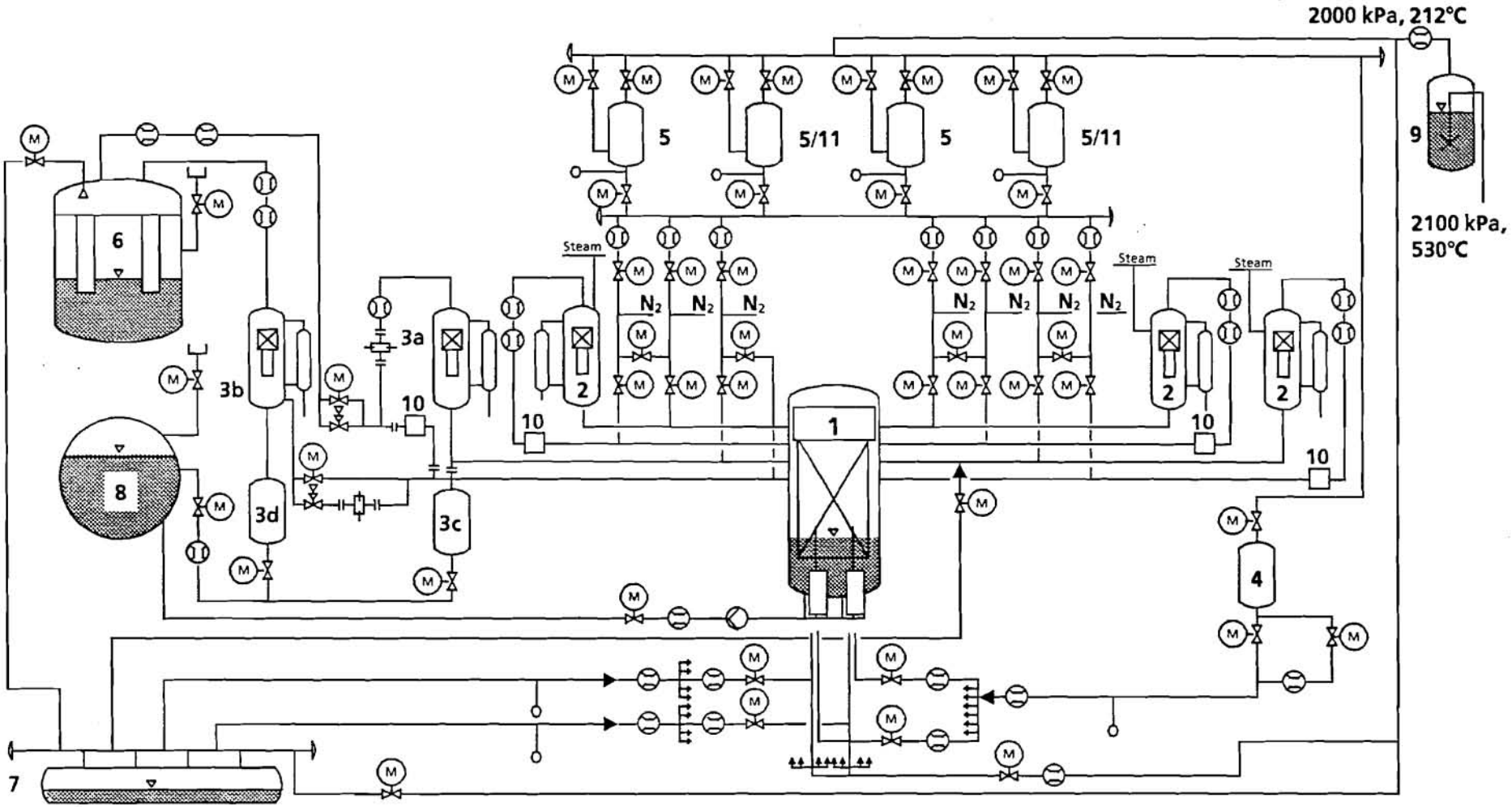

1 Test Vessel
2 Steam Generator Simulator (Intact Loop)
3a Steam Generator Simulator/Water Separator (Broken Loop Hot Leg)
3b Water Separator (Broken Loop Cold Leg)
3c Drainage Vessel for Hot Leg
3d Drainage Vessel for Cold Leg
4 Hot Water Storage Tank
5 Accumulator
6 Containment Simulator
7 Steam Storage Tank
8 Water Collecting Tank
9 Steam Cooler
10 Pump Simulator
11 N_2-Tank
O Sample

UPTF FLOW DIAGRAM

FIGURE A.3-2

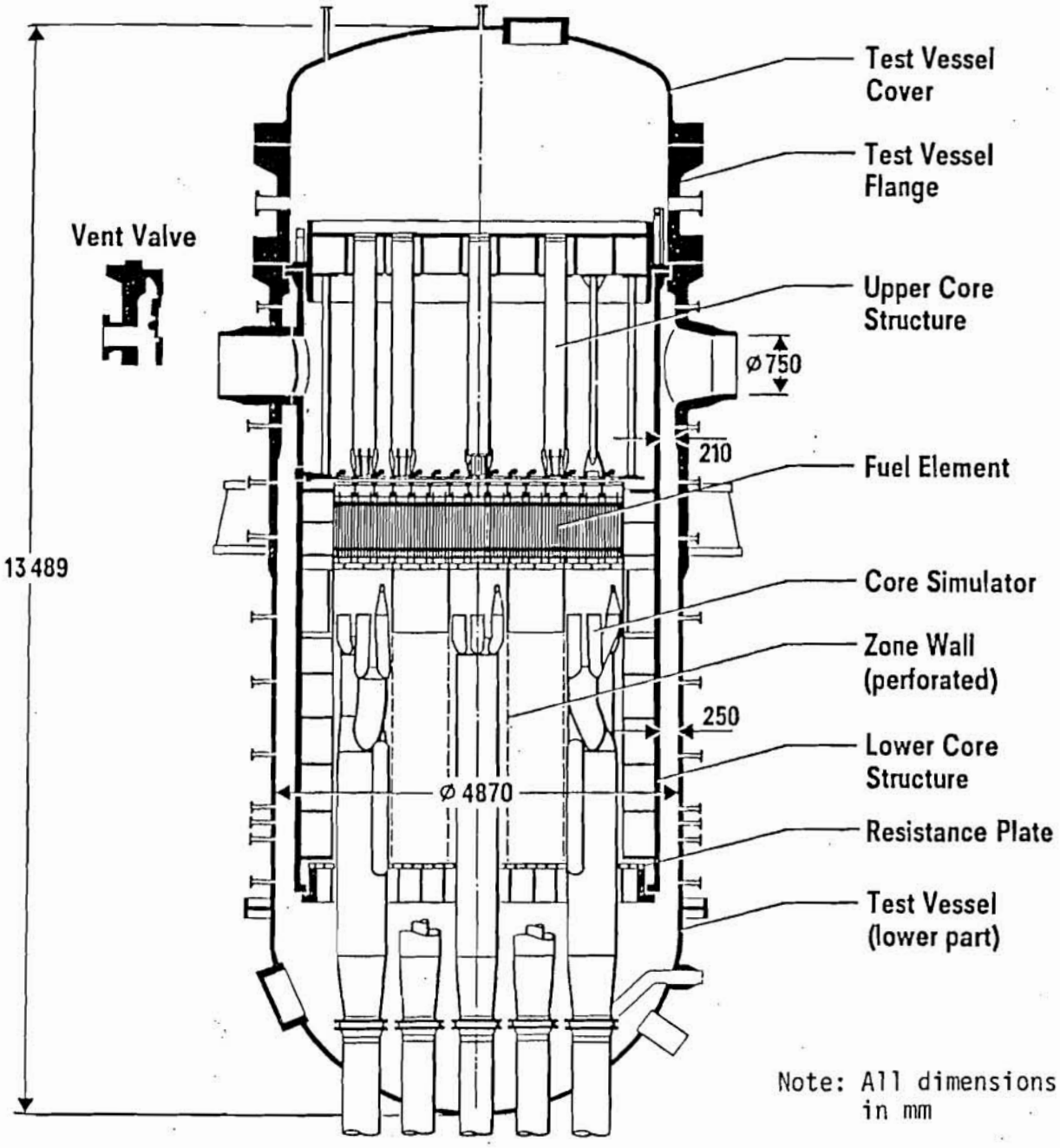

UPTF TEST VESSEL

FIGURE A.3-3

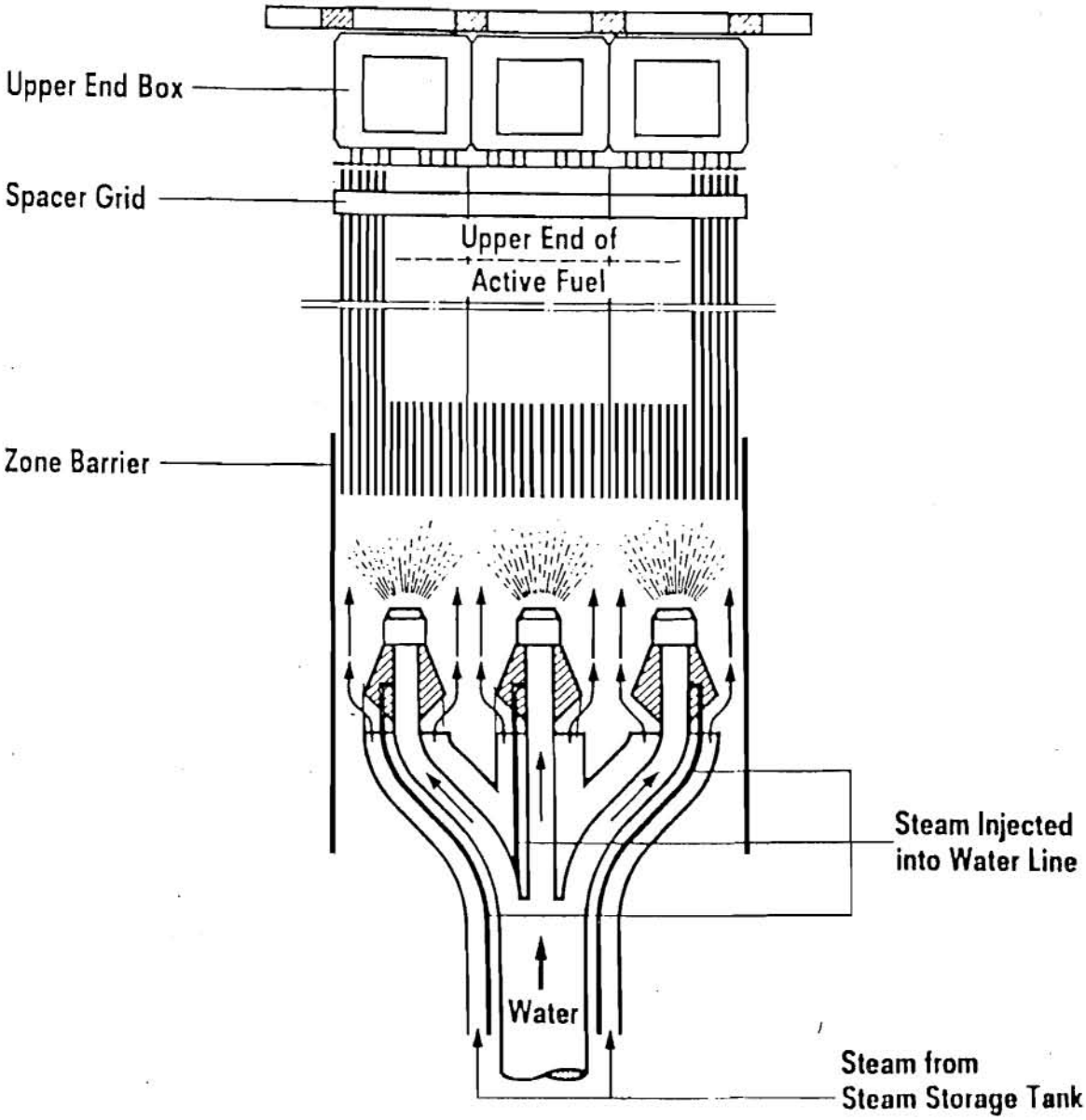

UPTF CORE SIMULATOR INJECTION SYSTEM

FIGURE A.3-4

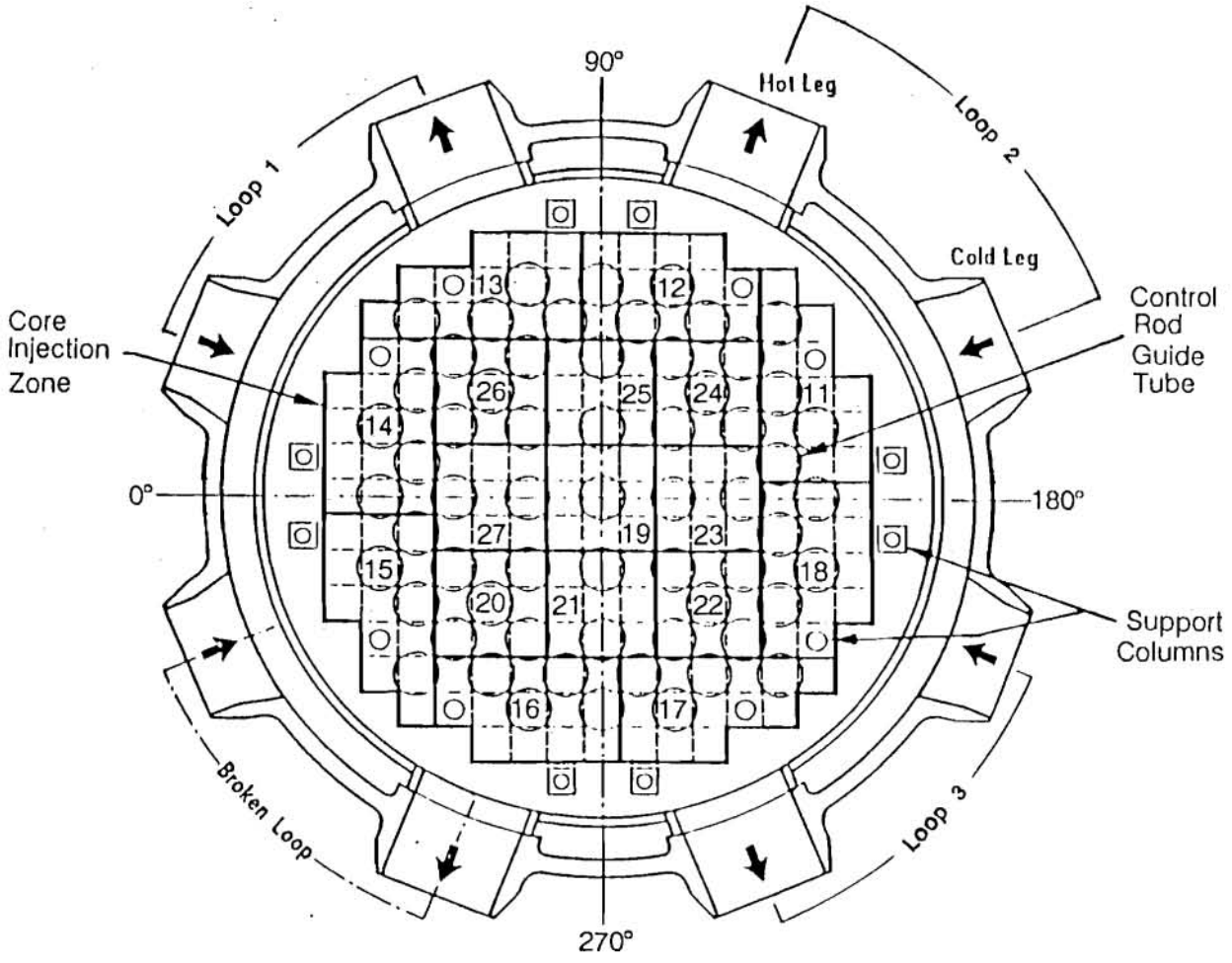

UPTF CORE/UPPER PLENUM INTERFACE

FIGURE A.3-5

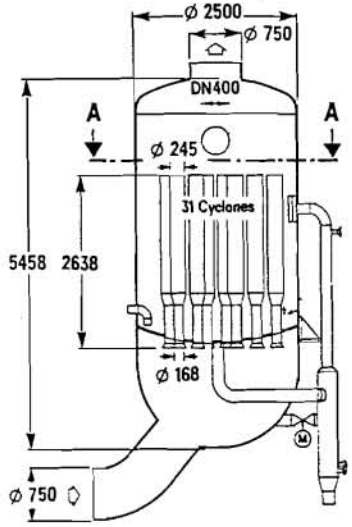

Section A – A

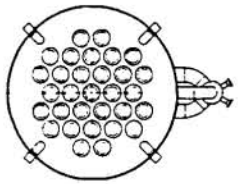

Steam generator simulator
of intact loops

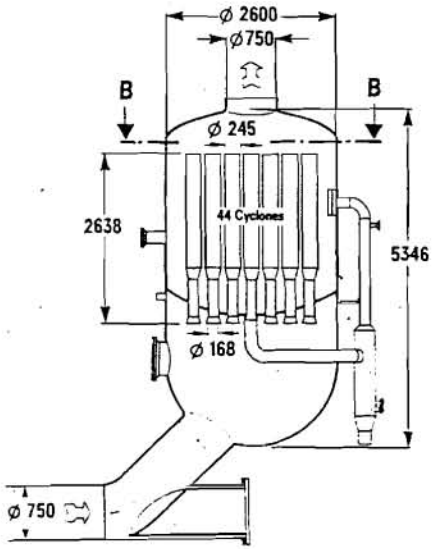

Section B - B

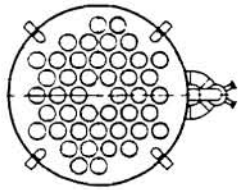

Steam generator simulator
(water separator)
of broken loop hot leg

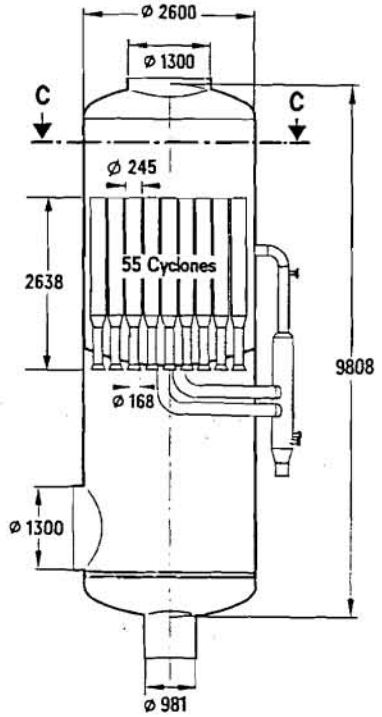

Section C - C

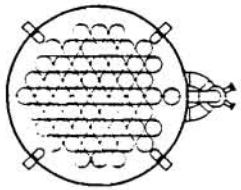

Water separator of
broken loop cold leg

Note: All dimensions in mm

UPTF STEAM GENERATOR SIMULATORS AND WATER SEPARATORS

FIGURE A.3-6

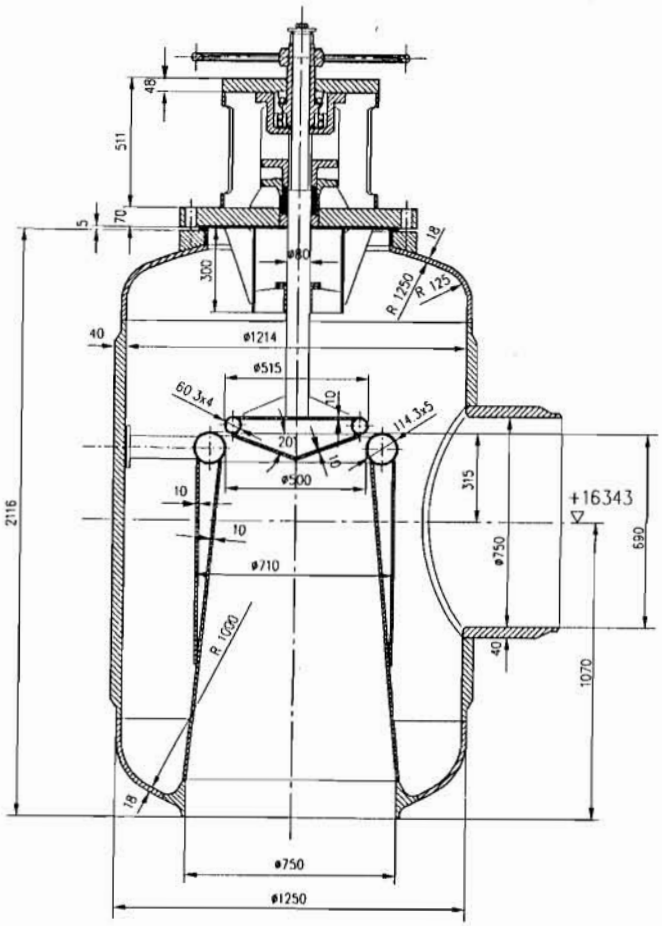

UPTF PUMP SIMULATOR

FIGURE A.3-7

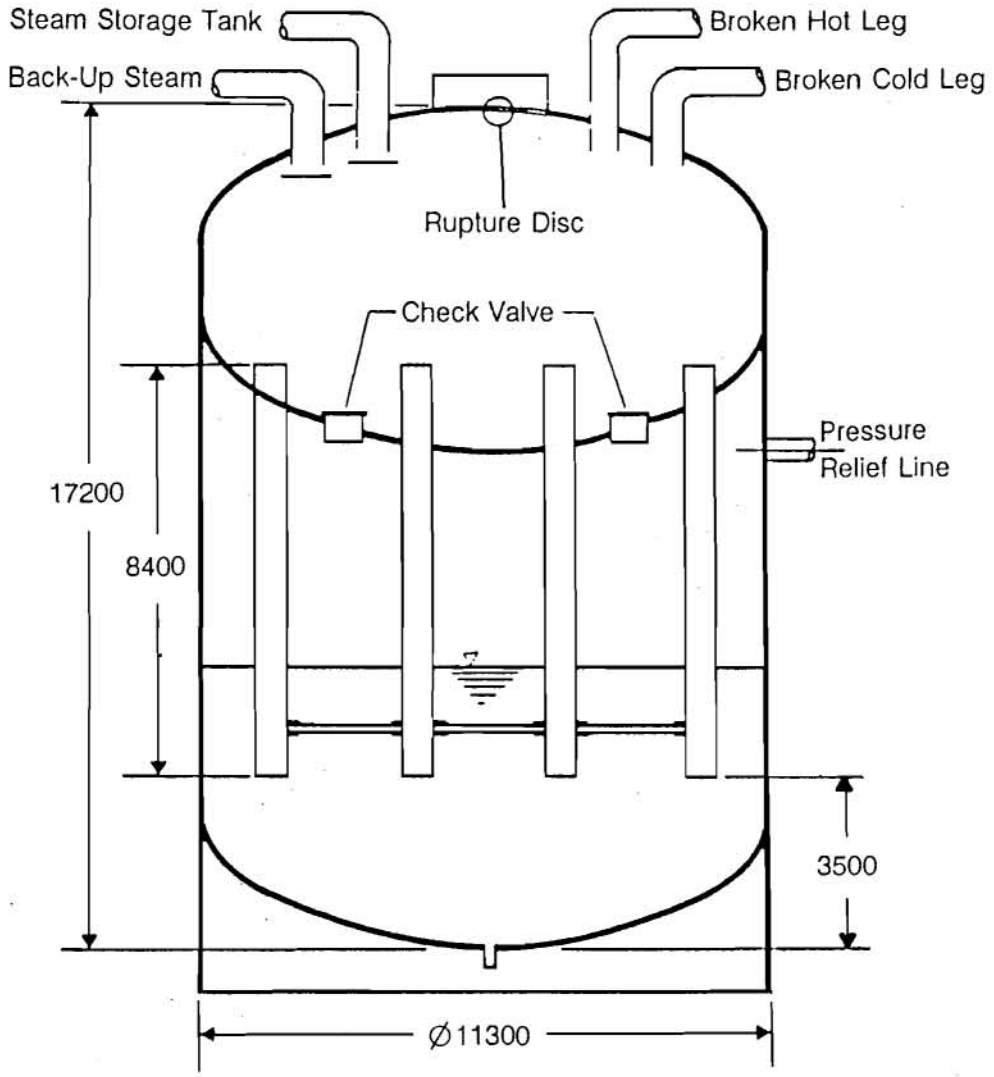

Note: All dimensions in mm

UPTF CONTAINMENT SIMULATOR

FIGURE A.3-8

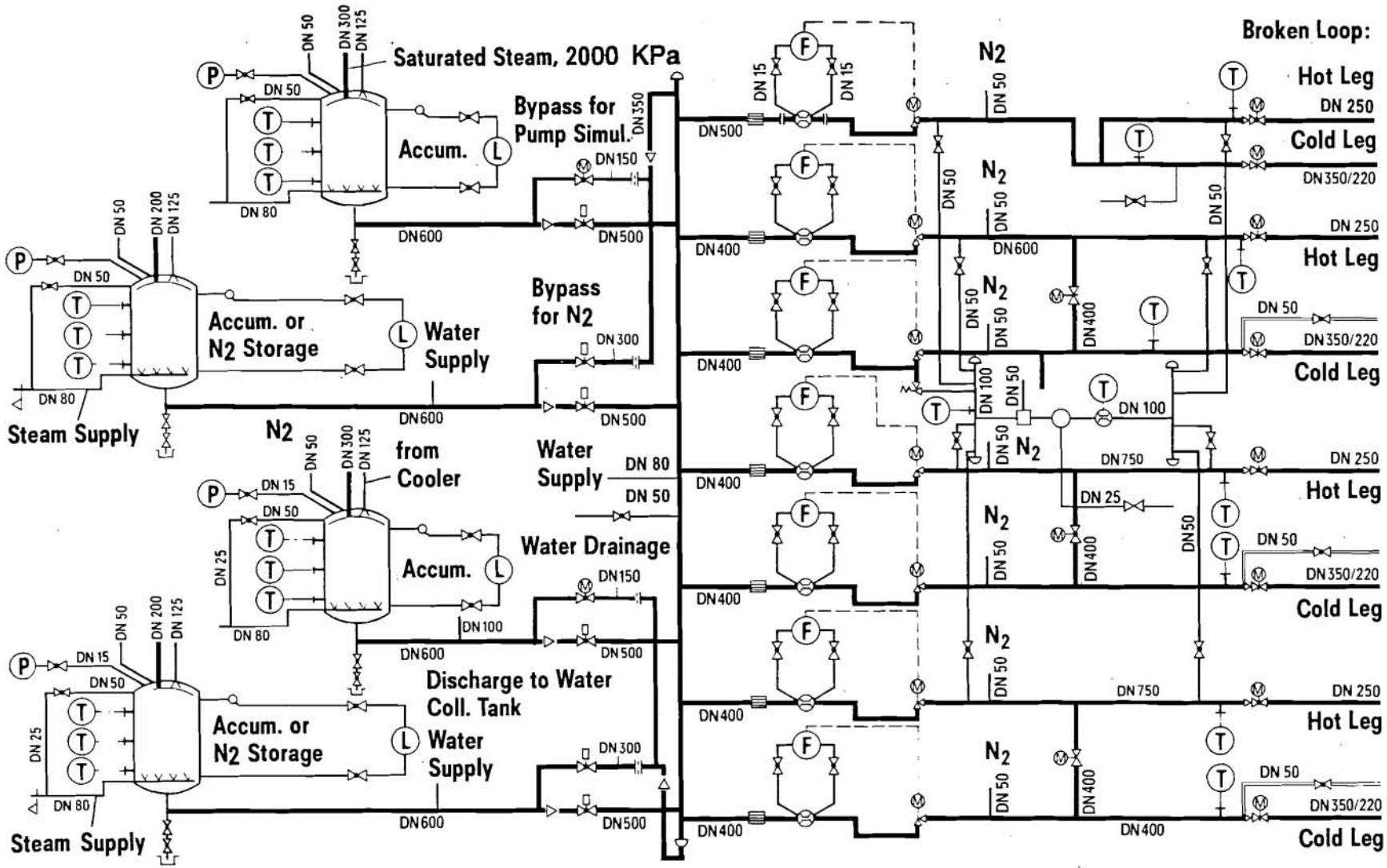

F = Flow Rate Measurement
T = Temperature Measurement
P = Pressure Measurement
L = Water Level Measurement

UPTF ECC INJECTION SYSTEM FLOW DIAGRAM

FIGURE A.3-9

Appendix B

TRAC COMPUTER CODE DESCRIPTION AND LIST OF ANALYSES

As part of the USNRC contribution to the 2D/3D Program, the Transient Reactor Analysis Code (TRAC), developed by Los Alamos National Laboratory (LANL), was provided to the other participants in the program. In addition, LANL carried out an analytical support program using TRAC under the direction of the USNRC. Selected TRAC calculations were also carried out by the other program participants.

The objectives of the analytical support program were to utilize TRAC to: support design of the test facilities, determine prototypical initial and boundary conditions to be used in tests, and to evaluate the predictive capability of TRAC by comparing code predictions to test data.

In an effort (Reference E-609) separate from the 2D/3D Program, the USNRC developed a methodology to evaluate thermal-hydraulic code scaling, applicability and uncertainty. This methodology was demonstrated by applying it to the use of TRAC-PF1/MOD1 v 14.3 for a cold-leg LBLOCA in a Westinghouse 4-loop PWR. Data from the 2D/3D Program were used extensively in evaluating reflood heat transfer, ECC delivery/bypass during the end-of-blowdown, and water carryover/steam binding.

B.1 EVOLUTION OF TRAC AND DESCRIPTION OF TRAC-PF1/MOD1 AND TRAC-PF1/MOD2

At the beginning of the 2D/3D Program, TRAC was an experimental code for reactor safety analysis. Concurrent with the 2D/3D Program, TRAC was developed into a sophisticated and mature computer code for the analysis of thermal-hydraulic transients in reactor systems. The use of TRAC as a part of the 2D/3D Program contributed significantly to its development as code experience and data from the 2D/3D Program were continually fed back to the code developers. The 2D/3D Program provided the best and most complete set of experimental data for assessing TRAC against large-break LOCA (LBLOCA) phenomena. TRAC has gone through several major releases with a number of versions of each release. The last code version used as part of the 2D/3D Program was TRAC-PF1/MOD2, v 5.3, which was released in June 1990.

TRAC has been developed at LANL under the sponsorship of the USNRC. A preliminary TRAC version consisting of only one-dimensional components was completed in December 1976. Although this version was not released publicly nor documented formally, it was used in TRAC-P1 development and formed the basis for the one-dimensional loop component modules. The first publicly-released version, TRAC-P1, was completed in December 1977.

TRAC-P1 was designed primarily for analysis of LBLOCAs in PWRs. It could be applied directly to many analyses ranging from blowdowns in simple pipes to integral LOCA tests in multiloop facilities. A refined version, TRAC-P1A, was released to the National Energy Software Center in May 1979. Although it treated the same class of problems, TRAC-P1A was more efficient than TRAC-P1 and incorporated improved hydrodynamic and heat transfer models. TRAC-PD2 (released in April, 1981) contained improvements in reflood heat transfer models and numerical solution methods. Although TRAC-PD2 was an LBLOCA code, it was applied successfully to small-break problems and to the Three Mile Island transient.

TRAC-PF1 was designed to improve the ability of TRAC-PD2 to handle small-break LOCAs and other transients. TRAC-PF1 used a full two-fluid model with two-step numerics in the one-dimensional components. The two-fluid model, in conjunction with a stratified-flow regime, handled countercurrent flow better than the drift-flux model used previously. The two-step numerics allowed large time steps for slow transients. A one-dimensional core component permitted simpler calculations, although the three-dimensional vessel option was retained. A non-condensible gas field was added to the one- and the three-dimensional hydrodynamics. Significant improvements were also made to the trip logic and the input. TRAC-PFI was released publicly in July 1981.

TRAC-PF1/MOD1 (Reference E-603) provided full balance-of-plant modeling through the addition of a general capability to model plant control systems. The steam generator model was improved and a special turbine component was added. The physical models were also modified, with the condensation model containing the most significant changes. Wall heat transfer in the condensation and film-boiling regimes was improved. Finally, the motion equations were modified to include momentum transport by phase change, and to preserve momentum conservation in the three-dimensional vessel. TRAC-PF1/MOD1 was released in April, 1986.

TRAC-PF1/MOD2 was released in June 1990. It contains several improvements including a generalized heat structure capability with fully implicit axial conduction, improved constitutive models, better heat-transfer and drag correlations, an improved reflood model, and several additional refinements for a variety of components. These upgrades are discussed in more detail below.

TRAC-PF1/MOD1 is described in References E-602, E-603 and E-604, and TRAC-PF1/MOD2 is described in References E-605, E-606, E-607 and E-608. Key characteristics of the TRAC-PF1/MOD1 and TRAC-PF1/MOD2 are summarized below.

- Variable-Dimensional Fluid Dynamics. A one-dimensional or three-dimensional (r,θ,z) flow calculation can be used within the reactor vessel. Flow within the loop components is treated one-dimensionally. Three-dimensional modeling provides explicit calculations of multidimensional flow patterns inside the reactor vessel that are important in determining ECC penetration during blowdown. Multidimensional core flow effects, upper plenum pool formation, and core penetration during reflood can be treated directly.

- Nonhomogeneous, Nonequilibrium Modeling. A full two-fluid (six-equation) hydrodynamic model describes the steam-water flow, thereby allowing important phenomena such as countercurrent flow to be treated explicitly. A stratified flow regime is included in the one-dimensional hydrodynamics. A seventh field equation (mass balance) describes a noncondensible gas field, and an eighth field equation tracks solutes in the liquid.

- Flow-Regime-Dependent Constitutive Equation Package. The thermal-hydraulic equations describe the transfer of mass, energy, and momentum between the steam-water phases and the interaction of these phases with the heat flow from the system structures. Because these interactions are dependent on the flow topology, a flow-regime-dependent constitutive equation package has been incorporated into the code.

- Consistent Analysis of Entire Accident Sequences. An important TRAC feature is its ability to address entire accident sequences, including computation of initial conditions, with a consistent and continuous calculation. For example, the code models the blowdown, refill, and reflood phases of a LOCA. This modeling eliminates the need to perform calculations using different codes to analyze a single accident. In addition, a steady-state solution capability provides self-consistent initial conditions for subsequent transient calculations.

- Component and Functional Modularity. TRAC is completely modular by component. The components in a calculation are specified through input data. Available components allow the user to model a wide range of PWR designs or experimental configurations. This feature also allows component modules to be improved, modified, or added without disturbing the remainder of the code. TRAC component modules currently include accumulators, breaks and fills, heat structures, pipes, plenums, pressurizers, pumps, steam generators, tees, turbines, valves, and vessels with associated internals (downcomer, core, upper plenum, etc.).

  TRAC is also modular by function; that is, major aspects of the calculations are performed in separate modules. For example, the basic one-dimensional hydrodynamics solution algorithm, the wall-temperature field solution algorithm and other functions are performed in separate routines that can be accessed by all component modules. This modularity allows the code to be upgraded readily as improved correlations and test information become available.

- Comprehensive Heat-Transfer Capability. TRAC-PF1/MOD2 incorporates detailed heat-transfer analyses of the vessel and the loop components. Included is a two-dimensional (r,z) treatment of fuel-rod heat conduction with dynamic fine-mesh rezoning to resolve both bottom-flood and falling-film quench fronts. The heat transfer from the fuel rods and other system structures is calculated using flow regime-dependent heat-transfer coefficients obtained from a generalized boiling curve based on a combination of local conditions and history effects.

Changes from TRAC-PF1/MOD1 to TRAC-PF1/MOD2

Several improvements were made between the MOD1 and MOD2 versions of TRAC-PF1. These improvements are listed below.

- The MOD2 models and correlations (Reference E-606) are more defensible.

- MOD2 runs faster than MOD1. Depending on the type of transient and the noding, it will run between 1.2 and 10.0 times faster than MOD1.

- The improved post-CHF heat transfer and interfacial models in MOD2 accurately simulate separate-effects tests.

- MOD2 has an improved reflood model based on mechanistic and defensible models.

- There are improved constitutive models in MOD2 for downcomer penetration, upper plenum de-entrainment, hot/cold leg ECC injection, vertical stratification in the vessel component, and condensation and evaporation in the presence of noncondensibles.

- Generalized heat structure capability in MOD2 allows the user to accurately model complicated configurations.

- An improved valve model based on experimental data for partially closed valves was implemented in MOD2.

- Improved vessel numerics that eliminate mass errors even at large time step sizes that can occur in small breaks or operational transients were included in MOD2.

- An offtake model is available in MOD2 to accurately represent small breaks in the bottom, top, or side of a pipe.

- The American Nuclear Society (ANS) 1979 Decay Heat Standard was implemented as a default model in MOD2.

- A countercurrent flow limitation (CCFL) model was implemented in both the one-dimensional and three-dimensional components in MOD2.

- An improved subcooled boiling model based on published correlations was implemented in MOD2.

- The momentum solution was forced to be conserving in MOD2.

- The external thermocouple model developed by the United Kingdom Atomic Energy Authority (UKAEA) was implemented in MOD2.

- The fully implicit axial conduction solution developed by the Japan Atomic Energy Research Institute (JAERI) was implemented in MOD2.

B.2 CATALOG OF ANALYSES

Within the 2D/3D Program, an extensive code analysis program was performed using TRAC. The analyses are listed in the following subsections according to the facility (i.e., PWR or test facility).

B.2.1 PWR Analyses

A total of 18 PWR and related calculations were performed in the 2D/3D Program. These calculations included both evaluation model (EM) and best-estimate (BE) analyses of US/J type PWRs and GPWRs. The analyses are listed in Table B.2-1.

B.2.2 CCTF Analyses

TRAC analyses of CCTF tests included nine tests from Core-I and 20 tests from Core-II. The tests analyzed covered several different ECCS configurations including cold leg injection, downcomer injection, combined injection and upper plenum injection. The analyses are listed in Tables B.2-2 (Core-I) and B.2-3 (Core-II).

B.2.3 SCTF Analyses

Calculations of SCTF tests included tests from each of the three test series; specifically, 13 tests from Core-I, 12 tests from Core-II, and 10 tests from Core-III. The tests analyzed included both integral and separate effects tests, as well as several different ECCS configurations. The analyses are listed in Tables B.2-4 (Core-I), B.2-5 (Core-II), and B.2-6 (Core-III).

B.2.4 UPTF Analyses

A total of 19 UPTF tests were analyzed using TRAC. The tests analyzed included separate effects tests which focused on thermal-hydraulic behavior in specific regions of the primary system (i.e., upper plenum, hot legs, cold legs or downcomer), as well as several integral tests. The analyses are listed in Table B.2-7.

Table B.2-1

TRAC PWR AND RELATED CALCULATIONS

(Note: The most recent calculations are listed first for each PWR type.)

PWR Type	Report Title	Source	Reference	TRAC Version
US/J	TRAC-PF1/MOD1 US/Japanese PWR Conservative LOCA Prediction	INEL	U-727	PF1/MOD1 v. 14.3
US/J	TRAC-PF1/MOD1 Analysis of a Minimum-Safeguards Large-Break LOCA in a US/Japanese PWR with Four Loops and 15x15 Fuel	LANL	U-726	PF1/MOD1 v. 12.2
US/J	TRAC-PF1/MOD1 Analysis of a 200% Cold Leg Break in a US/Japanese PWR with Four Loops and 15x15 Fuel	LANL	U-723	PF1/MOD1 [1]
US/J	TRAC-PF1/MOD1 Analysis of a Minimum-safeguards Large-break Loss-of-Coolant Accident in a 4-loop PWR with 17x17 Fuel	LANL	U-724	PF1/MOD1 [1]

Table B.2-1

TRAC PWR AND RELATED CALCULATIONS

(Note: The most recent calculations are listed first for each PWR type.)

PWR Type	Report Title	Source	Reference	TRAC Version
US/J	TRAC-PF1 Analysis of a Best-estimate Large-break LOCA in a Westinghouse PWR with Four Loops and 17x17 Fuel	LANL	U-722	TRAC-PF1
US/J	A TRAC-PD2 Analysis of a Large-Break Loss-of-Coolant Accident in a Reference US PWR	LANL	U-721	PD2
GPWR	Calculation of a Double Ended Break in the Cold Leg of the Primary Coolant Loop of a German Pressurized Water Reactor with a 5/8 Emergency Cooling Injection	GRS	G-661	PF1/MOD1 v. 12.5
GPWR	Calculation of a Double Ended Break in the Hot Leg of the Primary Coolant Loop of a German Pressurized Water Reactor with a 5/8 Emergency Coolant Injection	GRS	G-663	PF1/MOD1 v. 12.5

Table B.2-1

TRAC PWR AND RELATED CALCULATIONS

(Note: The most recent calculations are listed first for each PWR type.)

PWR Type	Report Title	Source	Reference	TRAC Version
GPWR	TRAC-PF1 Analysis of a 200% Hot-leg Break in a German PWR	LANL	U-748	PF1/MOD1 v. 8.2
GPWR	Comparison Between a TRAC GPWR Calculation and a CCTF Test with Combined Injection and EM Boundary Conditions for the Reflood Phase of a German PWR-LOCA	JAERI	J-608	PF1/MOD1 [1]
GPWR	GPWR-1982 TRAC-PF1 Base Case Results	LANL	U-747	PF1, PF1/MOD1
GPWR	A TRAC-PF1 Calculation of a Reference German PWR at the Initiation of ECC Injection	LANL	U-744	PF1
GPWR	GPWR-1982 TRAC-PF1 Input Deck Description	LANL	U-746	PF1
GPWR	TRAC-PD2 Calculation of a Double-Ended Cold-Leg Break in a Reference German PWR	LANL	U-743	PD2

Table B.2-1

TRAC PWR AND RELATED CALCULATIONS

(Note: The most recent calculations are listed first for each PWR type.)

PWR Type	Report Title	Source	Reference	TRAC Version
BBR	GPWR Analysis with TRAC-PF1/MOD1 Version 12.5 BBR Type Reactor, 200% Cold Leg Pump Discharge Break EM-Condition	GRS	G-662	PF1/MOD1 v. 12.5
B&W	TRAC-PF1/MOD1 Analysis of a 200% Cold Leg Break in a Babcock & Wilcox Lowered-loop Plant	LANL	U-725	PF1/MOD1 v. 11.1

NOTE:

1. Code version not documented in report.

Table B.2-2

TRAC ANALYSES OF CCTF CORE-I TESTS

Test/Run Number	Description	Reference	TRAC Version
C1-01/10	Loop K-factor	U-603	PD2
C1-05/14	Base case	U-602 U-604 U-605 U-606 U-617	PD2
C1-05/14	Base case	J-985	PF1/M0D1 v. 8.2
C1-06/15	ECC flow	U-602 U-607 U-617	PD2
C1-10/19	System pressure	U-602 U-609 U-617	PD2
C1-11/20	Reproducibility	U-610 U-611	PD2
C1-12/21	System effect	U-602 U-612 U-617	PD2
C1-16/25	FLECHT coupling	U-613	PD2
C1-16/25	FLECHT coupling	J-601	PD2
C1-19/38	EM	U-614 U-615 U-618	PD2
C-1-19/38	EM	J-603 J-604	PD2
C1-20/39	Multidimensional effect	U-616	PD2
Summary	--	U-601	--

Table B.2-3

TRAC ANALYSES OF CCTF CORE-II TESTS

Test/Run Number	Description	Reference	TRAC Version
C2-AC1/51	Low temperature	U-623	PF1/MOD1 v. 9.9
C2-SH1/53	Base case	U-624	PF1/MOD1 v. 8.1
C2-SH2/54	Low power	U-625	PF1/MOD1 v. 11.8
C2-1/55	High pressure	J-609	PF1/MOD1 v. 12.5
C2-AA1/57	UPI, high power	U-626 U-627	PF1/MOD1 v. 12.5
C2-AA2/58	Downcomer injection	U-628	PF1/MOD1 v. 12.7
C2-AS1/59	UPI, single failure	U-629	PF1/MOD1 v. 11
C2-4/62	Base case	J-607 J-609	PF1/MOD1 v. 12.5
C2-4/62	Base case	U-714	PF1/MOD2 v. 5.3
C2-5/63	Low power	J-609	PF1/MOD1 v. 12.5
C2-5/63	Low power, steep profile	U-630	PF1/MOD1 v. 11.0
C2-6/64	Low power, flat profile	U-630	PF1/MOD1 v. 10.3
C2-8/67	Low pressure	J-609	PF1/MOD1 v. 12.5
C2-10/69	Vent valves	U-631	PF1/MOD1 v. 12.7
C2-11/70	Refill	U-632	PF1/MOD1 v. 11.0
C2-12/71	Best estimate	J-609	PF1/MOD1 v. 12.5
C2-12/71	Best estimate	U-633	PF1/MOD1 v. 12.3
C2-13/72	UPI, symmetric	U-634	PF1/MOD1 v. 12.1
C2-15/75	FLECHT coupling	U-635	PF1/MOD1 v. 11.2
C2-16/76	UPI, asymmetric	U-636	PF1/MOD1 v. 12.3

Table B.2-3

TRAC ANALYSES OF CCTF CORE-II TESTS

Test/Run Number	Description	Reference	TRAC Version
C2-18/78	UPI best estimate	U-637	PF1/MOD1 v. 12.3
C2-19/79	Combined injection	U-638	PF1/MOD1 v. 11.5
C2-20/80	Combined injection	J-997	PF1/MOD1 v. 12.5
Summary	Non-UPI tests	U-621	---
Summary (UPI)	All UPI tests	U-622	---

Table B.2-4

TRAC ANALYSES OF SCTF CORE-I TESTS

Test/Run Number	Description	Reference	TRAC Version
S1-SH2/506	High pressure	U-645 U-651 J-612	PD2
S1-01/507	Base-case	U-646 U-651 U-649 U-652 J-612	PD2
S1-02/508	Low pressure	U-647 U-651 J-612	PD2
S1-04/510	High subcooling	U-648 J-612	PD2
S1-05/511	Low LPCI	U-652	PD2
S1-06/512	High power	---	PD2
S1-07/513	Flat power	U-649	PD2
S1-08/514	Steep power	U-649 U-655	PD2
S1-09/515	High ECC	U-652	PD2
S1-10/516	Base case	U-648	PD2
S1-11/517	Flat power	---	PD2
S1-13/519	SCTF/CCTF/FLECHT-SEASET coupling	U-653	PD2, PF1
S1-SH4/529	Combined injection	U-656	PF1
Summary	---	U-641	---

Table B.2-5

TRAC ANALYSES OF SCTF CORE-II TESTS

Test/Run Number	Description	Reference	TRAC Version
S2-AC1/601	Acceptance test	U-661	PF1/MOD1 v. 14.3
S2-AC2/602	Acceptance test	U-661	PF1/MOD1 v. 14.3
S2-SH1/604	Base case	U-662	PF1/MOD1 v. 12.0
S2-SH2/605	Flat power profile	U-663 U-664	PF1/MOD1 v. 12.7
S2-03/608	Steam supply, UPI	U-665	PF1/MOD1 v. 12.0
S2-05/610	Steam supply, UPI	U-666	PF1/MOD1 v. 12.0
S2-06/611	Steep power and temp profiles	U-667	PF1/MOD1 v. 12.0
S2-08/613	FLECHT coupling	U-668	PF1/MOD1 v. 12.0
S2-09/614	Low stored energy	U-669	PF1/MOD1 v. 12.0
S2-12/617	Steep power profile	U-670	PF1/MOD1 v. 12.0
S2-14/619	Flat power	J-609 J-615	PF1/MOD1 v. 12.5
S2-16/621	Steep power	J-615	PF1/MOD1 v. 12.5
Summary	---	U-661	---

Table B.2-6

TRAC ANALYSES OF SCTF CORE-III TESTS

Test/Run Number	Description	Reference	TRAC Version
S3-SH1/703	GPWR core cooling	U-683	PF1/MOD1 v. 14.3
S3-SH2/704	GPWR EM integral	U-684	PF1/MOD1 v. 14.3
S3-05/709	CCFL, nonuniform	U-685	PF1/MOD1 v. 14.3
S3-07/711	GPWR core cooling	U-681	PF1/MOD1 v. 14.3
S3-09/713	US/J EM integral	U-686	PF1/MOD1 v. 13.1
S3-10/714	US/J BE integral	U-687	PF1/MOD1 v. 13.0
S3-13/717	GPWR EM integral	U-681	PF1/MOD1 v. 14.3
S3-15/719	Inclined power profile	U-688	PF1/MOD1 v. 14.3
S3-16/720	Steep power profile	U-689	PF1/MOD1 v. 14.3
Summary	--	U-681	--

Table B.2-7

TRAC ANALYSES OF UPTF TESTS

Test Number (Run No. or Phase)	Description	Reference	TRAC Version
2	US/J PWR integral reflood	U-713 U-714	PF1/MOD1 v. 5.3
4 (Phase A)	US/J PWR integral refill	U-711	PF1/MOD1 v. 5.3
5 (Phase A)	Downcomer transient refill	U-711	PF1/MOD1 v. 5.3
6 (Run 133)	Downcomer countercurrent flow	E-611 U-711	PF1/MOD1 v. 12.5 PF1/MOD2 v. 5.3
7 (Runs 200 & 201)	Downcomer countercurrent flow	U-711	PF1/MOD2 v. 5.3
8 (Phases A & B)	Cold/Hot leg flow pattern	G-641 U-712 U-714	PF1/MOD1 v. 13.0, 14.3 PF1/MOD2 v. 5.3
9 (Phase A)	Cold/Hot leg flow pattern	G-642	PF1/MOD1 v. 13.0
10 (Phase B)	Entrainment/De-entrainment	U-709	PF1/MOD1 v. 14.3
11	Hot leg countercurrent flow	U-708	PF1/MOD1 v. 14.3 PF1/MOD2 prelim.
12 (Run 014)	Tie plate countercurrent flow	G-644	PF1/MOD1 v. 12.5, 12.8, 14.4
13 (Run 071)	Tie plate countercurrent flow	G-645	PF1/MOD1 v. 12.5, 12.8, 14.3
17 (Phase B)	US/J PWR integral reflood	U-713 U-714	PF1/MOD2 v. 5.3
20	Upper Plenum Injection	U-710	PF1/MOD2 prelim.
21 (Phases A &B)	Downcomer injection	U-715	PF1/MOD2 v. 5.3

Table B.2-7

TRAC ANALYSES OF UPTF TESTS

Test Number (Run No. or Phase)	Description	Reference	TRAC Version
22 (Phase A)	Downcomer injection/ vent valves -- refill	U-715	PF1/MOD2 v. 5.3
23 (Phase B)	Downcomer injection/ vent valves -- reflood	U-715	PF1/MOD2 v. 5.3
25 (Phases A & B)	Downcomer/Cold leg reflood	U-714	PF1/MOD2 v. 5.3 + error corr.
27 (Phases A & B)	US/J PWR integral refill/reflood	U-716	PF1/MOD2 v. 5.3
29 (Phase B)	Entrainment/De-entrainment	U-713	PF1/MOD2 v. 5.3

Gesellschaft für Anlagen- und Reaktorsicherheit (GRS) mbH

Schwertnergasse 1
50667 Köln
Telefon (02 21) 20 68-0
Telefax (02 21) 20 68 442
Telex 2 214 123 grs d

Forschungsgelände
85748 Garching b.München
Telefon (0 89) 3 20 04-0
Telefax (0 89) 3 20 04 299
Telex 5 215 110 grs md

Kurfürstendamm 200
10719 Berlin
Telefon (0 30) 88 41 89-0
Telefax (0 30) 88 23 655

GRS - 101 Reactor Safety Issues Resolved by the 2D/3D Program

ISBN 3-923875-51-7